

Wednesday

Hot Topic Session: Molecular Imaging and Radionuclide Therapy for Prostate Cancer

Wednesday, Dec. 2 7:15AM - 8:15AM Location: E451A



FDA Discussions may include off-label uses.

Participants

Uwe Haberkorn, MD, Heidelberg, Germany, (uwe.haberkorn@med.uni-heidelberg.de) (*Moderator*) Nothing to Disclose Eric M. Rohren, MD, PhD, Houston, TX (*Moderator*) Nothing to Disclose

Alexander Drzezga, MD, Cologne, Germany (*Moderator*) Research Grant, Eli Lilly and Company; Speakers Bureau, Siemens AG; Speakers Bureau, General Electric Company; Speakers Bureau, Piramal Enterprises Limited; Research Consultant, Eli Lilly and Company; Research Consultant, Piramal Enterprises Limited; ; ; ; ; ;

ABSTRACT

Radium-223 is a recently approved therapy for treatment of bone metastases in patients with metastatic prostate carcinoma. As an alpha-emitting radioisotope, radium has the potential to be a powerful therapy for treatment of a variety of skeletal malignancies. In this presentation, the use of radium-223 in the treatment of prostate cancer will be reviewed through a case-based format. Future directions in radium-223 therapy will be discussed.

URL

Sub-Events

SPSH40A Ra-223 Therapy for Skeletal Metastases from Prostate Cancer

Participants

Eric M. Rohren, MD, PhD, Houston, TX (Presenter) Nothing to Disclose

LEARNING OBJECTIVES

1) Review the chemical and physical features of radium-223 dichloride. 2) Discuss the clinical utility of radium-223 therapy. 3) Understand the technique for radium-223 administration. 4) Review the anticipated outcomes of radium-223 therapy through case-based review.

ABSTRACT

Radium-223 is a recently approved therapy for treatment of bone metastases in patients with metastatic prostate carcinoma. As an alpha-emitting radioisotope, radium has the potential to be a powerful therapy for treatment of a variety of skeletal malignancies.

URL

Honored Educators

Presenters or authors on this event have been recognized as RSNA Honored Educators for participating in multiple qualifying educational activities. Honored Educators are invested in furthering the profession of radiology by delivering high-quality educational content in their field of study. Learn how you can become an honored educator by visiting the website at: https://www.rsna.org/Honored-Educator-Award/

Eric M. Rohren, MD, PhD - 2015 Honored Educator

SPSH40B Comparison of Ga-68 and F-18 Labeled Small Molecule PSMA Tracers for Prostate Cancer Imaging

Participants Carsten Kobe, Cologne, Germany (*Presenter*) Nothing to Disclose

LEARNING OBJECTIVES

1) Understand the concept of PSMA PET-imaging in the diagnosis of prostate cancer in general and in comparison to conventional methods. 2) Learn about the currently available alternatives for radiolableling of PSMA-tracers, e.g. 68-Gallium and 18F-Fluoride and their characteristics. 3) Gain insights from first comparative studies about the clinical value of the available tracers with regard to their sensitivity, specificity and practicability.

SPSH40C PSMA Ligands for Imaging and Therapy of Prostate Cancer

Participants

Uwe Haberkorn, MD, Heidelberg, Germany (Presenter) Nothing to Disclose

LEARNING OBJECTIVES

1) Understand the background and pharmacokinetics of PSMA ligands for PET/CT. 2) Estimate the value of PSMA-based imaging in comparison to choline-based imaging. 3) Assess the value of PSMA-targeting for diagnosis and therapy. 4) Estimate the effects and side effects of endoradiotherapy with PSMA ligands

ABSTRACT

The second second

I ne prostate-specific membrane antigen (PSMA) is frequently over-expressed in prostate cancer (PCa) which led to the development of several PSMA-targeting molecules are for the detection and therapy of metastatic castration resistant prostate cancer (mCRPC). In a first diagnostic study 82.8% of 319 patients investigated with 68Ga-PSMAHBED-PET/CT at least one lesion indicative for PCa was detected. Amongst lesions investigated by histology, 30 were false-negative in 68Ga-PSMAHBED-PET/CT, all other lesions (n=416) were diagnosed true-positive or -negative. Fifty of 116 patients available for follow-up received a local treatment after 68Ga-PSMAHBED-PET/CT. A comparison of the 68Ga-PSMA-ligand with 18F-fluoromethylcholine PET/CT revealed 78 PC-suspicious lesions in 32 patients using 68Ga-PSMA-PET/CT and 56 lesions in 26 patients using Choline-PET/CT (significant with p=0.04). All lesions detected by 18F-fluoromethylcholine-PET/CT were also seen by 68Ga-PSMA-PET/CT. Since the ligand bound to PSMA is internalized, the target may also be used for endoradiotherapy. We used a small molecule inhibitor of PSMA MIP-1095 for therapy in 25 men with final stage mCRPC. PSA values decreased by >50% in 60.7% of the men treated. 84.6 % of men with bone pain showed complete or moderate reduction in pain. Hematological toxicities were mild. 25% of men treated had a transient slight to moderate dry mouth. No adverse effects on renal function were observed. In order to increase the therapeutic flexibilty a theranostic PSMA ligand coupled to DOTA was synthesized which allows coupling to Ga-68 for diagnostic use or to Lu-177 or Ac-225 for therapy. Initial experience in 30 patients shows promising results concerning antitumor activity with mild side effects.

URL

Controversy Session: 'My Back Hurts': Fluoroscopy or CT-guided Intervention?

Wednesday, Dec. 2 7:15AM - 8:15AM Location: E451B

CT IR

AMA PRA Category 1 Credit ™: 1.00 ARRT Category A+ Credit: 1.00

FDA Discussions may include off-label uses.

Participants

Walter S. Bartynski, MD, Charleston, SC (Moderator) Nothing to Disclose

LEARNING OBJECTIVES

1) Identify various etiologies of low back pain and neck pain that may be amenable to image-guided pain injections. 2) Develop a pain management plan utilizing image-guided injections. 3) Assess what imaging findings and clinical symptoms are appropriate for image-guided pain injections. 4) Discuss the advantages and disadvantages of CT versus fluoroscopically guided pain injections.

Sub-Events

SPSC40A For Fluoroscopic Injection Procedures

Participants

Lubdha M. Shah, MD, Salt Lake Cty, UT, (lubdha.shah@hsc.utah.edu) (Presenter) Nothing to Disclose

LEARNING OBJECTIVES

View learning objectives under main course title.

ABSTRACT

URL

SPSC40B CT Injection Procedures

Participants

Peter G. Kranz, MD, Durham, NC, (peter.kranz@duke.edu) (*Presenter*) Research Consultant, Cephalogics, LLC; Research Consultant, Biogen Idec Inc

LEARNING OBJECTIVES

View learning objectives under main course title.

URL

ASRT@RSNA 2015: Face Transplantation and Surgical Planning

Wednesday, Dec. 2 8:00AM - 9:00AM Location: N230

HN

AMA PRA Category 1 Credit [™]: 1.00 ARRT Category A+ Credit: 1.00

Participants

Frank J. Rybicki III, MD, PhD, Ottawa, ON (Presenter) Research Grant, Toshiba Corporation;

LEARNING OBJECTIVES

1) To describe the principles of face transplantation from a surgical perspective. 2) Protocols for evaluation of bony structures, including 3D printed models. 3) Pre- and post- face transplantation vasucular imaging to define and follow-up the vascular anastomoses. 4) Detail insights of transplantation biology enable by 320-detector row CT.

ABSTRACT

Face transplantation is now accepted as the only option to restore form and function in patients with severe facial deformity. The transplanted tissue comes from an organ donor and is called an "allograft". The allograft tissues can include bone, regions of forehead, eyelid, nose, lips, chin, and cheeks. Surgical planning uses CT, MR, and 3D printed models typically printed from CT images. For all steps, the radiology technologist plays a critical role working in concert with the radiologists and surgeons. Bone is shown in 3d reformatted images and 3D printed models. The vascular anastomosis is the most critical aspect for successful engraftment. CT angiography (CTA) noninvasively images vessels for anastomoses. Patients typically have altered vascular anatomy of the external carotid circulation because of the injury and/or lesions that require face transplantation. Both arterial and venous mapping is required. Post-operatively, both CTA and MRA are used to evaluate patients for surveillance and when potential complications arise. Volumetric rendering of all relevant structures is important in surveillance and can be achieved by 3D printing soft tissue structures. Post-operative CTA has yielded insights to the vascular physiology and pathology of tissue transplantation.

NR

ER

RSNA/ESR Emergency Symposium: CNS Emergencies (An Interactive Session)

Wednesday, Dec. 2 8:30AM - 10:00AM Location: S402AB

AMA PRA Category 1 Credits ™: 1.50 ARRT Category A+ Credits: 1.50

FDA Discussions may include off-label uses.

Participants

Ronald J. Zagoria, MD, San Francisco, CA, (ron.zagoria@ucsf.edu) (*Moderator*) Nothing to Disclose Andras Palko, MD, PhD, Szeged, Hungary (*Moderator*) Medical Advisory Board, Affidea Group;

Sub-Events

MSSR41A CNS Trauma and Neurovascular Injury

Participants

Howard A. Rowley, MD, Madison, WI, (hrowley@uwhealth.org) (*Presenter*) Research Consultant, Bracco Group; Research Consultant, Guerbet SA; Research Consultant, General Electric Company; Consultant, F. Hoffmann-La Roche Ltd; Consultant, W.L. Gore & Associates, Inc; Consultant, Lundbeck Group; ; ; ; ; ;

LEARNING OBJECTIVES

1) To be familiar with traumatic brain injury demographics and classification schemes. 2) Be able to apply appropriateness criteria for head trauma imaging in children and adults. 3) Identify key imaging patterns and pitfalls in the evaluation of brain and neurovascular trauma.

ABSTRACT

This lecture on CNS Trauma and Neurovascular Injury is divided into 4 parts: Part 1 will briefly review traumatic brain injury (TBI) demographics and the most common TBI classification schemes; Part 2 will discuss the current imaging approach to acute TBI in clinical practice. Part 3 will illustrate the imaging manifestations of the different injuries located in the extra-axial space (e.g., scalp and skull injury; epidural, subdural, subarachnoid and intraventricular collections), and the intra-axial space (e.g., dysautoregulation, contusion, hematoma, penetrating TBI, axonal injury, fat emboli). Part 4 will review traumatic neurovascular injuries and fracture patterns correlated with high risk of vascular injury.

MSSR41B CNS Non-Traumatic Emergencies

Participants

Marion Smits, MD, PhD, Rotterdam, Netherlands, (marion.smits@erasmusmc.nl) (Presenter) Nothing to Disclose

LEARNING OBJECTIVES

1) To know the modalities (CT/MRI) and protocols for non-traumatic neurological emergencies. 2) To know and diagnose the main non-traumatic neurological vascular and non-vascular emergencies. 3) To be aware of the pitfalls and limitations of clinical presentation and imaging findings in non-traumatic neurological emergencies.

ABSTRACT

Neurological emergencies are often associated with high morbidity and mortality, and thus require prompt diagnostic and therapeutic action. Non-traumatic emergencies may however have a subacute onset, and radiological signs may be subtle, which can lead to delay in diagnosis and treatment. Since clinical features are often nonspecific, the radiologist may be the first to point the clinician in the direction of the correct diagnosis. It is therefore of great importance that the radiologist is aware of and familiar with the various imaging findings, on both computed tomography (CT) and magnetic resonance imaging (MRI), of non-traumatic neurological emergencies. These include vascular, infectious and inflammatory diseases. Commonly encountered emergencies are ischaemic and haemorrhage stroke, venous thrombosis, arterial dissection, abscess, acute disseminated encephalomyelitis (ADEM), and encephalitis. Radiological findings in rarer diseases may mimic those in the more commonly occurring diseases, but need to be correctly interpreted as therapeutic strategies and prognosis may be entirely different. Such entities include for instance posterior reversible encephalopathy syndrome (PRES), reversible cerebral vasoconstriction syndrome, Susac's syndrome, and status epilepticus. Furthermore, initial findings of (impending) complications of brain disease, such as hydrocephalus and herniation of brain structures, may be subtle, while early recognition allows for prompt and adequate intervention. Finally, diagnostic and therapeutic interventions performed in an emergency setting may interfere with the diagnosis and interpretation of clinical and imaging findings. Associated limitations and pitfalls therefore need to be recognised to avoid false negative or false positive diagnosis respectively.

MSSR41C Interactive Case Discussion

Participants

Howard A. Rowley, MD, Madison, WI (*Presenter*) Research Consultant, Bracco Group; Research Consultant, Guerbet SA; Research Consultant, General Electric Company; Consultant, F. Hoffmann-La Roche Ltd; Consultant, W.L. Gore & Associates, Inc; Consultant, Lundbeck Group; ;;;;;

Marion Smits, MD, PhD, Rotterdam, Netherlands, (marion.smits@erasmusmc.nl) (Presenter) Nothing to Disclose

LEARNING OBJECTIVES

1) To review traumatic brain injury (TBI) and non-traumatic neurological emergencies. 2) To describe imaging manifestations of TBI and non-traumatic neurological emergencies. 3) To understand the clinical implications of radiological imaging findings in TBI and

non-traumatic neurological emergencies. 4) To know the state-of-the-art radiological imaging options for the assessment of acute TBI and non-traumatic neurological emergencies.

ABSTRACT

This interactive case discussion builds on the two previous lectures in this session, on traumatic and non-traumatic neurological emergencies respectively. Both lecturers will take the audience through several clinical cases, highlighting and emphasizing important issues from their lectures, such that the previously presented theory is placed in a clinical context. Preferably, the participants will have attended the two prior lectures, to optimally benefit from and participate in this interactive case discussion.

Medical Physics 2.0: Mammography

Wednesday, Dec. 2 8:30AM - 10:00AM Location: N226

BR DM PH

AMA PRA Category 1 Credits ™: 1.50 ARRT Category A+ Credits: 1.50

Participants

Ehsan Samei, PhD, Durham, NC (*Director*) Nothing to Disclose Douglas E. Pfeiffer, MS, Boulder, CO (*Director*) Nothing to Disclose

Sub-Events

RC521A Mammography Perspective

Participants

Douglas E. Pfeiffer, MS, Boulder, CO (Presenter) Nothing to Disclose

LEARNING OBJECTIVES

1) Understand the history and development of mammographic imaging equipment. 2) Understand the impact of equipment development on testing protocols. 3) Understand the impact of equipment development on regulation.

ABSTRACT

Mammographic imaging has undergone tremendous change since its inception. Rapid development from screen-film imaging to nearly universal acceptance of digital imaging has required a shift in testing methodology. This talk will briefly introduce the developments that have taken place and discuss the impact that this development has had on testing and regulation.

RC521B Mammography 1.0

Participants

Melissa C. Martin, MS, Gardena, CA (*Presenter*) Nothing to Disclose Eric A. Berns, PhD, Denver, CO (*Presenter*) Nothing to Disclose

LEARNING OBJECTIVES

1) Current requirements for Quality Control for Hologic Digital Mammography Units. 2) Current requirements for Quality Control for General Electric Digital Mammography Units. 3) Current requirements for Quality Control for Fuji Computed Radiography for Mammography Units. 4) Current requirements for Quality Control for Printers used with Digital Mammography Units. 5) Current requirements for Quality Control for Printers used with Digital Mammography Units. 5) Current requirements for Quality Control for Monitors used with Digital Mammography Units.

Active Handout: Melissa Carol Martin

http://abstract.rsna.org/uploads/2015/13010862/rc521b.pdf

RC521C Mammography 2.0

Participants

Andrew Karellas, PhD, Worcester, MA (Presenter) Research collaboration, Koning Corporation

LEARNING OBJECTIVES

1) To provide an overview of how the Medical Physicist can prepare for the future of clinical mammography physics. 2) To provide a landscape of mammography imaging technologies. 3) To describe methods of image quality metrics, dose reduction, and quality control in relation to mammography technologies. 4) To describe the future roles of the Medical Physicist in clinical mammography physics.

Pearls and Pitfalls in MSK Radiology

Wednesday, Dec. 2 8:30AM - 10:00AM Location: N227

MK MR

AMA PRA Category 1 Credits ™: 1.50 ARRT Category A+ Credits: 1.50

Participants

Sub-Events

RC551A MRI of Arthroplasty: How to Do It

Participants

Hollis G. Potter, MD, New York, NY (Presenter) Research support, General Electric Company

LEARNING OBJECTIVES

1) To become familiar with different patterns of abnormal synovial response around implants. 2) To become familiar with protocols using standardized and newer sequences which optimize tissue contrast and provide accurate diagnosis.

ABSTRACT

MRI characteristics of adverse local tissue reactions, periprosthetic infection, and component loosening will be reviewed. Characteristics of osteolysis will also be discussed, as well as additional complications of joint arthroplasty.

Active Handout:Hollis G. Potter

http://abstract.rsna.org/uploads/2015/15001917/Active RC551A.pdf

RC551B MRI of Bone Marrow: What's Normal What's Not?

Participants

Miriam A. Bredella, MD, Boston, MA, (mbredella@mgh.harvard.edu) (Presenter) Nothing to Disclose

LEARNING OBJECTIVES

1) Differentiate normal variations in MRI appearance of bone marrow from malignant marrow infiltrative disorders. 2) Become familiar with the MRI appearance of age-related and post-treatment changes of bone marrow.

ABSTRACT

MRI characteristics of normal bone marrow will be reviewed, including changes related to aging and therapy. Imaging examples of benign and malignant disorders affecting bone marrow will be reviewed including pitfalls in MRI interpretation of bone marrow.

RC551C Tumors and Tumor-like Lesions of the Musculoskeletal System: Pearls and Pitfalls for the General Radiologist

Participants

Behrang Amini, MD, PhD, Houston, TX, (bamini@mdanderson.org) (Presenter) Nothing to Disclose

LEARNING OBJECTIVES

1) Become familiar with the imaging appearance of common and uncommon presentations of benign and malignant musculoskeletal lesions. 2) Know how to manage indeterminate focal bone and soft tissue abnormalities.

ABSTRACT

Radiologists are often challenged by the overlap in the imaging appearance of benign and malignant musculoskeletal lesions. The imaging appearance of challenging bone and soft tissue lesions will be reviewed. Suggestions will be made for management with the aim of balancing patient safety with the burden of further investigation or intervention.

High Resolution CT of Diffuse Lung Disease: Read Cases with the Experts (An Interactive Session)

Wednesday, Dec. 2 8:30AM - 10:00AM Location: N228



AMA PRA Category 1 Credits ™: 1.50 ARRT Category A+ Credits: 1.50

Participants

Georgeann McGuinness, MD, New York, NY (*Moderator*) Nothing to Disclose Brett M. Elicker, MD, San Francisco, CA, (brett.elicker@ucsf.edu) (*Presenter*) Nothing to Disclose Daria Manos, MD, FRCPC, Halifax, NS, (daria.manos@nshealth.ca) (*Presenter*) Nothing to Disclose Sharyn L. MacDonald, MBChB, Christchurch, New Zealand (*Presenter*) Nothing to Disclose Georgeann McGuinness, MD, New York, NY (*Presenter*) Nothing to Disclose

LEARNING OBJECTIVES

1)Understand the applications and limitations of HRCT in detecting and characterizing diffuse lung disease through the discussion of expert analysis of unknown cases. 2) Apply correct usage of the HRCT lexicon to specific findings, to better elucidate pathophysiology and to refine differential considerations, by observing experts in HRCT approach unknown cases. 3) Develop diagnosis and management algorithms by working through problematic cases with the expert discussants. Please bring your charged mobile wireless device (phone, tablet or laptop) to participate.

ABSTRACT

Bladder, the Forgotten Organ: Role of CT, MRI, and PET in Diagnosis, Staging, and Surveillance of Cancer

Wednesday, Dec. 2 8:30AM - 10:00AM Location: N229



AMA PRA Category 1 Credits ™: 1.50 ARRT Category A+ Credits: 1.50

Participants

Stuart G. Silverman, MD, Brookline, MA, (sgsilverman@partners.org) (*Coordinator*) Author, Wolters Kluwer nv Andrew B. Rosenkrantz, MD, New York, NY (*Presenter*) Nothing to Disclose Homer A. Macapinlac, MD, Houston, TX (*Presenter*) Nothing to Disclose

LEARNING OBJECTIVES

1) Learn the latest developments on the role of CT, MRI, and PET/CT in the detection, diagnosis, staging, and surveillance of patients with bladder cancer. 2) Learn currently recommended CT, MRI, and PET/CT techniques and protocols and how to implement them in clinical practice. 3) Learn how to interpret CT, MRI, and PET/CT scans of the bladder with an emphasis on case review and diagnostic pitfalls.

ABSTRACT

The urinary bladder is the most common site of malignancy of the urinary tract and is imaged by radiologists on many abdominal imaging exams. However, historically the bladder has been a 'forgotten' organ and thought to be largely the purview of the urologist due to the central role that cystoscopy has played in both the diagnosis and local staging of bladder cancer. Recent advances in CT, MRI, and PET have emerged that now allow radiologists to play an important role in the detection, diagnosis, staging, and surveillance of patients with or suspected of having bladder cancer. This course will detail these advances and explain how, when, and why radiologists should be using these three modalities in clinical practice today. Using illustrative case examples, advances in knowledge such as how CT urography can be used to detect bladder cancer, how MR urography can be used to distinguish muscle-invasive from superficial tumors and evaluate the upper tracts, and how PET/CT (and the newly introduced PET/MRI) can be used to stage and follow patients. With additional advances in low dose CT, emerging MRI techniques, and novel PET agents, radiology will play an increasingly vital role in the care of patients with bladder cancer in the future.

Digital Information Security and Medical Imaging Equipment: Threats, Vulnerabilities and Best Practices

Wednesday, Dec. 2 8:30AM - 10:00AM Location: S403B

IN PH SQ

AMA PRA Category 1 Credits ™: 1.50 ARRT Category A+ Credits: 1.50

Participants

Sub-Events

RC523A Medical Device Security in a Connected World

Participants

Kevin McDonald, Rochester, MN, (mcdonald.kevin@mayo.edu) (Presenter) Nothing to Disclose

LEARNING OBJECTIVES

1) Understand the changing environment of network and internet connected devices and software. 2) Be aware of the motivations and tatics of current threat actors. 3) Understand common security issues found in medical devices. 4) Know simple actions that can decrease risk.

ABSTRACT

Medical devices are increasingly becoming dependent on technology and network connectivity, at a time that the electronic environment is becoming more dangerous. Because of this medical devices and systems can become easy targets for attackers attempting to access PHI, disrupt patient care or even harm a patient. When tested, these devices have been shown to have multiple vulnerabilities. These vulnerabilities range from hardcoded passwords, publically available service passwords and no encryption of patient data. Because of this institutions using these devices need to work with their vendors to improve the security of medical devices and take actions themselves to help protect their environment and patients.

RC523B Knowing if Your Imaging Systems are Secure and Keeping Them That Way

Participants

J. Anthony Seibert, PhD, Sacramento, CA, (jaseibert@ucdavis.edu) (Presenter) Nothing to Disclose

LEARNING OBJECTIVES

1) Understand the vulnerabilities of imaging system modalities to security and privacy breeches. 2) Determine ways to protect and secure imaging systems from internal and external threats. 3) Describe institutional best-practices to maintain protection yet provide necessary accessibility for imaging modalities.

RC523C The US Government and Medical Device Security

Participants Kevin Hemsley, Idaho Falls, ID (*Presenter*) Nothing to Disclose

LEARNING OBJECTIVES

1) What are industrial control systems (ICS) and how do they play in the field. 2) What is the role and capabilities of ICS-CERT (Industrial Control Systems Cyber Emergency Response Team). 3) What is some steps that can be taken to protect ICSs.

Mobile Computing for Decision Support and Learning While You Work (Hands-on)

Wednesday, Dec. 2 8:30AM - 10:00AM Location: S401AB

IN

AMA PRA Category 1 Credits ™: 1.50 ARRT Category A+ Credits: 1.50

Participants

Michael P. D'Alessandro, MD, Iowa City, IA, (michael-dalessandro@uiowa.edu) (*Presenter*) Nothing to Disclose Jeffrey R. Galvin, MD, Baltimore, MD (*Presenter*) Nothing to Disclose James J. Choi, MD, West Des Moines, IA (*Presenter*) Nothing to Disclose

LEARNING OBJECTIVES

1) Learn to perform decision support on a mobile device at the point-of-care to answer questions that arise during clinical work and thus tie learning to practice and receive point-of care CME for it. 2) Learn to read Ebooks and educational apps on a mobile device.3) Learn to stay up-to-date with radiology journals and society news on a mobile device.4) Learn to manage a library of journal articles on a mobile device.5) Learn to view podcasts and vodcasts on a mobile device. 6) Learn to maintain a learning portfolio and learning network on a mobile device.

ABSTRACT

Acquiring and maintaining competency in the practice of radiology requires a program of continuous learning. This continuous learning would be most effectively performed during clinical work, when it has the greatest potential for modifying physicians' knowledge, attitudes, and behaviors as well as positively affecting patients' care, outcomes, and lives. The advent of mobile computing, and the rich assortment of authoritative radiology resources it allows easy access to, now allows this dream to become reality. This course will be a hands-on, state-of-the-art review that will teach the radiologist how to use mobile computing to perform continuous learning while you work. The Apple iOS, Google Android and Microsoft Windows Phone platforms will be covered. Participants will be encouraged to bring their own mobile phone or tablet to the course and will be asked before the course to download into their mobile device several free apps that will be demonstrated, so they can follow along during the session. These free apps are listed on the course handout at http://www.radiologyebooks.com/rsna.html

URL

http://www.radiologyebooks.com/rsna.html

Active Handout: Michael Patrick D'Alessandro

http://abstract.rsna.org/uploads/2015/13013317/RCA41.pdf

RCB41

Hands-on Introduction to Social Media (Hands-on)

Wednesday, Dec. 2 8:30AM - 10:00AM Location: S401CD

IN

AMA PRA Category 1 Credits ™: 1.50 ARRT Category A+ Credit: 0

Participants

C. Matthew Hawkins, MD, Decatur, GA, (matt.hawkins@emory.edu) (*Presenter*) Nothing to Disclose Safwan Halabi, MD, Stanford, CA (*Presenter*) Nothing to Disclose Neil U Lall, MD, Cincinnati, OH (*Presenter*) Nothing to Disclose Tirath Y. Patel, MD, Toledo, OH (*Presenter*) Nothing to Disclose Amy L. Kotsenas, MD, Rochester, MN (*Presenter*) Nothing to Disclose

LEARNING OBJECTIVES

1) Appreciate the professional relevance of social media for radiologists. 2) Understand the differences between Facebook pages and personal accounts. 3) Better grasp how hospitals and groups can use Facebook to connect with patients. 4) Setup and use a Twitter account. 5) Understand the purpose of hashtags, lists, and DMs. 6) Get acquainted with other radiologists and radiology organizations on Twitter. 7) Evaluate enterprise solutions for managing multiple social media accounts for larger groups and organizations. 8) Understand how to safely /securely communicate via social media while maintaining HIPAA requirements.

URL

http://bit.ly/RSNASocialMediaIntro

Active Handout:Safwan Halabi

http://abstract.rsna.org/uploads/2015/11035017/RCB41.pdf

Dialogue with The Joint Commission: New Diagnostic Imaging Standards for CT and MR

Wednesday, Dec. 2 8:30AM - 10:00AM Location: S404AB



AMA PRA Category 1 Credits ™: 1.50 ARRT Category A+ Credits: 1.50

Participants

Ehsan Samei, PhD, Durham, NC (*Director*) Nothing to Disclose Ehsan Samei, PhD, Durham, NC (*Moderator*) Nothing to Disclose Ehsan Samei, PhD, Durham, NC (*Presenter*) Nothing to Disclose Alec J. Megibow, MD, MPH, New York, NY (*Presenter*) Consultant, Bracco Group Richard C. Semelka, MD, Chapel Hill, NC, (richsem@med.unc.edu) (*Presenter*) Research support, Siemens AG.; Consultant, Guerbet SA. Fergus V. Coakley, MD, Lake Oswego, OR (*Presenter*) Nothing to Disclose

Andrea D. Browne, PhD, Oakbrook Terrace, IL (*Presenter*) Nothing to Disclose

LEARNING OBJECTIVES

1) Describe areas addressed by the new and revised imaging standards. 2) Understand why The Joint Commission made changes to and/or revised the diagnostic imaging standards. 3) Describe how compliance with the new and revised imaging standards will be evaluated during the on-site survey. 4) Describe ways to demonstrate compliance with the new and revised imaging standards to promote patient safety and patient care.

ABSTRACT

This presentation will provide an overview of the new and revised diagnostic imaging standards. These new standards impact both Ambulatory Care and Hospital diagnostic imaging customers of the Joint Commission. Topics to be covered include: Background on the new and revised diagnostic imaging standards; an overview of the new and revised diagnostic imaging standards; a description of how compliance with the new and revised diagnostic imaging standards will be evaluated during the on-site survey. It will also provide practical insights and suggestions regarding implementation of the new and revised diagnostic imaging standards to promote patient safety and improve patient care in Joint Commission accredited organizations.

Musculoskeletal Series: Current Trends in Musculoskeletal Imaging

Wednesday, Dec. 2 8:30AM - 12:00PM Location: E451B



ARRT Category A+ Credits: 4.00 AMA PRA Category 1 Credits ™: 3.25

FDA Discussions may include off-label uses.

Participants

Mark D. Murphey, MD, Reston, VA, (MMurphey@acr.org) (*Moderator*) Nothing to Disclose Christine B. Chung, MD, San Diego, CA (*Moderator*) Nothing to Disclose

Sub-Events

RC504-01 Imaging Diagnosis of Atypical Infection

Wednesday, Dec. 2 8:30AM - 8:55AM Location: E451B

Participants

Mark D. Murphey, MD, Reston, VA (Presenter) Nothing to Disclose

LEARNING OBJECTIVES

1) Identify the typical imaging features suggesting atypical musculoskeletal infection. 2) Understand the pathological basis for the imaging patterns of atypical musculoskeletal infection. 3) Detect imaging features that allow differentiation of atypical musculoskeletal infection.

Honored Educators

Presenters or authors on this event have been recognized as RSNA Honored Educators for participating in multiple qualifying educational activities. Honored Educators are invested in furthering the profession of radiology by delivering high-quality educational content in their field of study. Learn how you can become an honored educator by visiting the website at: https://www.rsna.org/Honored-Educator-Award/

Mark D. Murphey, MD - 2015 Honored Educator

RC504-02 MRI of Total Knee Arthroplasty: Synovial Patterns Predictive of Disease

Wednesday, Dec. 2 8:55AM - 9:05AM Location: E451B

Participants

Angela E. Li, MBBS, MMed, New York, NY (*Presenter*) Nothing to Disclose Darryl B. Sneag, MD, Chestnut Hill, MA (*Abstract Co-Author*) Nothing to Disclose Harry G. Greditzer IV, MD, New York, NY (*Abstract Co-Author*) Nothing to Disclose Christine C. Johnson, MD, New York, NY (*Abstract Co-Author*) Nothing to Disclose Kara Fields, New York, NY (*Abstract Co-Author*) Nothing to Disclose Douglas E. Padgett, MD, New York, NY (*Abstract Co-Author*) Consultant, Stryker Corporation; Theodore T. Miller, MD, New York, NY (*Abstract Co-Author*) Nothing to Disclose Hollis G. Potter, MD, New York, NY (*Abstract Co-Author*) Research support, General Electric Company

PURPOSE

To determine the sensitivity and specificity of various synovial appearances on MRI in patients with a painful total knee arthroplasty (TKA).

METHOD AND MATERIALS

With IRB approval, 101 consecutive patients who had knee MRI within 1 year prior to revision TKA were identified from our hospital registry of retrieved TKA implants. All MR scans were performed on a 1.5T magnet. Axial, coronal and sagittal PD, sagittal inversion recovery and MAVRIC PD MR images were retrospectively reviewed blinded to the ultimate diagnoses and the cases were categorized by the appearance of the synovium as one of the following: bulky hypertrophied synovium (suggestive of particle induced synovitis), lamellated and hyperintense (suggestive of infection), globally thickened and contracted (suggestive of arthrofibrosis), and mildly thickened with a homogenous effusion (suggestive of non-specific synovitis). The MR appearances were then compared with operative reports, microbiology, and pathology reports.

RESULTS

Bulky hypertrophied synovium had 69% sensitivity, 89% specificity and 94% PPV for particle induced synovitis with implant particles seen at histopathology, and 98 % sensitivity, 78% specificity and 75% PPV for an operative diagnosis of aseptic loosening, severe polyethylene wear, or osteolysis. Lamellated synovitis had 85% sensitivity, 99% specificity and 94% PPV for infection. A contracted and globally thickened synovium had 75% sensitivity, 98% specificity and 60% PPV for arthrofibrosis. A mildly thickened synovial appearance had 63% sensitivity, 93% specificity, and 79% PPV for stiffness, instability, and nonspecific pain as the reason for revision TKA.

CONCLUSION

In patients with a painful TKA, MRI appearance of the synovium can be used to differentiate between cases of particle induced wear, infection, arthrofibrosis and non-specific synovitis.

CLINICAL RELEVANCE/APPLICATION

MRI is predictive of various synovial pathologic conditions in TKA and may be valuable in the diagnostic workup of patients with a painful TKA.

RC504-03 The Value of Simultaneous 18F-FDG-PET/MRI for the Detection of Spondylodiscitis: A Feasibility Study

Wednesday, Dec. 2 9:05AM - 9:15AM Location: E451B

Participants

Benjamin Friedrich, Leipzig, Germany (*Abstract Co-Author*) Nothing to Disclose Jeanette Fahnert, Leipzig, Germany (*Abstract Co-Author*) Nothing to Disclose Sandra Purz, MD, Leipzig, Germany (*Abstract Co-Author*) Nothing to Disclose Jens Gulow, Leipzig, Germany (*Abstract Co-Author*) Nothing to Disclose Thomas K. Kahn, MD, Leipzig, Germany (*Abstract Co-Author*) Nothing to Disclose Henryk Barthel, Leipzig, Germany (*Abstract Co-Author*) Consultant, Siemens AG Consultant, The Piramal Group Travel support, Siemens AG Travel support, The Piramal Group Speaker, Siemens AG Speaker, The Piramal Group Osama Sabri, MD, Leipzig, Germany (*Abstract Co-Author*) Research Consultant, The Piramal Group; Research Consultant, Siemens AG; Patrick Stumpp, MD, Leipzig, Germany (*Presenter*) Nothing to Disclose

PURPOSE

The diagnosis of infectious spondylodiscitis is often challenging. Alterations seen in MRI are quite sensitive, but lack specificity and the distinction from osteochondrosis is often difficult. The aim of the present study was to assess the diagnostic value of simultaneous 18F-FDG-PET/MRI in cases of suspected spondylodiscitis.

METHOD AND MATERIALS

In a prospective study 25 patients with suspected spondylodiscitis were enrolled. All patients underwent a simultaneous whole spine simultaneous 18F-FDG-PET/MRI scan including standard MRI sequences with-/-out contrast. Image datasets were evaluated by two radiological residents with 1-5 years experience and one board certified nuclear medicine physician independently and finally in consensus. For all suspected spinal discs as well as a healthy disc SUVmean and SUVmax were determined. The diagnostic certainty of MRI data was evaluated on a five-point Likert Scale. The consensus decision was dichotomized into spondylodiscitis - no spondylodiscitis.

RESULTS

The inter-rater agreement between the two radiologists in regard of the MRI scans was moderate with a weighted κ =0.67 and an absolute diagnostic certainty in just 10%. With addition of the PET data, the agreement between the radiologists rose to κ =0.95 and an absolute diagnostic certainty in 50%. In one case the diagnosis changed due to the additional PET data. The final histological analysis was in all cases identical with the imaging diagnosis. There was a strong correlation between the SUVmax ratio of healthy/sick disc and the 5-point MRI rating with a R2=0.52; p<0.001. In a ROC analysis a SUVmax ratio of 2.89 had a 100% specificity and sensitivity with an AUC of 1 for the correct diagnosis. Neither level of CRP nor leukocyte count could show a significant correlation to the spondylodiscitis diagnosis.

CONCLUSION

Simultaneous 18F-FDG-PET/MRI for the detection of Spondylodiscitis seems to be feasable and is increasing the diagnostic certainty in an often challenging imaging diagnosis.

CLINICAL RELEVANCE/APPLICATION

18F-FDG-PET/MRI can be safely used for the detection of Spondylodiscitis.

RC504-04 Assessing the Effect of Football Play on Knee Articular Cartilage Using Delayed Gadolinium-Enhanced MRI of Cartilage (dGEMRIC)

Wednesday, Dec. 2 9:15AM - 9:25AM Location: E451B

Participants

Wenbo Wei, Columbus, OH (*Presenter*) Nothing to Disclose Becky Lathrop, Columbus, OH (*Abstract Co-Author*) Nothing to Disclose Guang Jia, PhD, Baton Rouge, LA (*Abstract Co-Author*) Nothing to Disclose David Flanigan, MD, Columbus, OH (*Abstract Co-Author*) Consultant, Vericel; Consultant, Smith & Nephew plc Ajit M. Chaudhari, PhD, Columbus, OH (*Abstract Co-Author*) Nothing to Disclose Michael V. Knopp, MD, PhD, Columbus, OH (*Abstract Co-Author*) Nothing to Disclose Alan Rogers, MD, Columbus, OH (*Abstract Co-Author*) Nothing to Disclose Jason E. Payne, MD, Columbus, OH (*Abstract Co-Author*) Nothing to Disclose

PURPOSE

Articular cartilage injuries are very common among NFL players. In retired NFL players, early onset of OA was found to be three times higher than the general population. Delayed gadolinium-enhanced MRI of cartilage (dGEMRIC) has been shown to quantify regional variations of glycosaminoglycan (GAG) concentrations within the cartilage. The goal of this pilot study is to determine the cumulative effects of multiple years of play on cartilage microarchitecture assessed by GAG concentration variation using dGEMRIC.

METHOD AND MATERIALS

The MR images of both of each athlete's knee joints were acquired using an 8-channel knee coil at a 3T system (Achieva, Philips). dGEMRIC was performed at pre- and post-contrast injection periods using a set of five fast field echo pulse sequences with multiple flip angles (4, 8, 12, 16, 20 degrees). Sagittal slices were obtained with the imaging parameters as TR/TE = 6.3/3.2 ms, resolution = 0.37×0.37 mm², slice thickness = 4 mm, NSA = 2. The contrast agent Magnevist was injected intravenously at a standard dose of 0.2 mmol/kg body weight. To help the contrast efficiently diffuse into the cartilage, subjects were instructed to perform joint movement for 100 minutes. The total procedure time was around 3.5 hours.

RESULTS

Except the MTP of the right knee at the pre-season, subjects with more years of football play retained relatively higher volume of contrast at all cartilage compartments in both pre- and post-season. At the pre-season and post-season, one year collegiate football players presented pre-season with 0.116 mM and initial post session with 0.117 mM average contrast concentration. In players with more years of experience, the measurements were elevated to 0.139 mM and 0.140 mM, respectively, both with a 20% increase. The p-value generated from student t-test did not present any significant difference at the pre-season which is probably due to the limited sample size.

CONCLUSION

In conclusion, playing collegiate football for a longer period of time may lead to microstructural alterations, like GAG concentration changes within the knee cartilage. The decreased GAG concentration may be indicative of a higher risk factor for articular cartilage degradation and potential development of OA.

CLINICAL RELEVANCE/APPLICATION

dGEMRIC can be a quantitative imaging technique to identify micro-architectural changes in cartilage health that are not observed with standard cartilage MR sequences.

RC504-05 Use of Combined Dynamic and Quantitative MRI to Investigate the Influence of Cartilage Contact on Cartilage Morphology, Composition, and Ultra-Structure

Wednesday, Dec. 2 9:25AM - 9:35AM Location: E451B

Participants

Jarred Kaiser, Madison, WI (*Abstract Co-Author*) Nothing to Disclose Fang Liu, Madison, WI (*Abstract Co-Author*) Nothing to Disclose Darryl Thelen, Madison, WI (*Abstract Co-Author*) Nothing to Disclose Richard Kijowski, MD, Madison, WI (*Presenter*) Nothing to Disclose

PURPOSE

To investigate the relationship between cartilage contact and cartilage morphology, composition, and ultra-structure using combined dynamic and quantitative MRI.

METHOD AND MATERIALS

Four young asymptomatic volunteers underwent combined dynamic and static MRI on a 3.0T scanner. Dynamic SPGR images were continuously acquired while the subjects actively flexed and extended their knee at 0.5 Hz for 5 minutes in a custom-made loading device. Static 3D-FSE and mcDESPOT bi-component T2 mapping sequences were also performed. Reconstructed kinematics were used to compute tibia contact maps which were defined as the maximum depth of penetration of the tibia cartilage mesh into the femoral cartilage mesh through the flexion-extension cycle. 3D-FSE was used to create tibia cartilage thickness maps, while mcDESPOT was used to create tibia cartilage single-component T2 relaxation time (T2) maps and cartilage fast relaxing water fraction (FF) maps, the latter of which is thought to represent water bound to proteoglycan. The maps were sub-divided into 10 equal-sized regions of interest (ROI) on the medial and lateral tibia. ROI-based Pearson correlation analysis was performed between cartilage contact and cartilage quantitative MRI parameters.

RESULTS

Cartilage contact was greater on the medial tibia than the lateral tibia for all subjects with larger areas of positive penetration of the tibia cartilage mesh into the femoral cartilage mesh and greater maximum depth of penetration. Higher FF values were also noted in the medial tibia in all subjects, while no visible differences in the cartilage thickness and cartilage T2 maps between the medial and lateral tibia could be identified. The degree of cartilage contact was positively correlated with cartilage thickness (r=0.341, p=0.001) and cartilage FF (r=0.417, p<0.001) and negatively correlated with cartilage T2 (r=-0.211, p=0.04).

CONCLUSION

Cartilage is a tissue well-adapted to withstand higher compressive forces with areas exposed to greater contact being thicker and having lower T2 (likely reflecting a thicker radial zone comprised of perpendicularly oriented collagen fibers) and higher FF (likely reflecting greater proteoglycan content).

CLINICAL RELEVANCE/APPLICATION

Combined dynamic and quantitative MRI may be useful for investigating how biomechanical factors within the knee joint influence normal cartilage physiology and cartilage degeneration in patients with osteoarthritis.

RC504-06 Functional Cartilage Imaging in Clinical Practice

Wednesday, Dec. 2 9:35AM - 10:00AM Location: E451B

Participants

Christine B. Chung, MD, San Diego, CA (Presenter) Nothing to Disclose

LEARNING OBJECTIVES

1) Emphasize the biochemical composition of articular cartilage and its relationship to intrinsic MR property. 2) Describe the normal morphologic and quantitative MR signature of articular cartilage on various pulse sequences. 3) Describe MR and clinical cartilage grading systems. 4) Identify indications and appropriate MR protocols for cartilage evaluation, including primary chondral/ osteochondral evaluation versus cartilage evaluation as a surrogate for meniscal function.

RC504-07 Osteochondral Injuries

Wednesday, Dec. 2 10:10AM - 10:30AM Location: E451B

Carol L. Andrews, MD, Pittsburgh, PA (Presenter) Author, Reed Elsevier; Author, Informa PLC

LEARNING OBJECTIVES

1) Describe the findings of imaging of acute bone injury including radiography and MRI. 2) Recognize the bone and marrow changes see on MRI in osteopenia and hyperemia. 3) Identify the imaging findings of osteonecrosis. 4) Accurately describe the entity typically referred to as "osteochondral lesion".

RC504-08 Grade 1 Cartilage Lesions in the Knee are Precursors of More Severe Cartilage Damage - Data from the Osteoarthritis Initiative

Wednesday, Dec. 2 10:30AM - 10:40AM Location: E451B

Participants

Benedikt J. Schwaiger, MD, San Francisco, CA (*Presenter*) Nothing to Disclose Alexandra S. Gersing, MD, San Francisco, CA (*Abstract Co-Author*) Nothing to Disclose John Mbapte Wamba, MD, San Francisco, CA (*Abstract Co-Author*) Nothing to Disclose Michael C. Nevitt, PhD, San Francisco, CA (*Abstract Co-Author*) Nothing to Disclose Charles E. McCulloch, San Francisco, CA (*Abstract Co-Author*) Instructor, F. Hoffmann-La Roche Ltd Expert Witness, Mallinckrodt plc Consultant, Mallinckrodt plc Thomas M. Link, MD, PhD, San Francisco, CA (*Abstract Co-Author*) Research funded, General Electric Company; Research funded,

Thomas M. Link, MD, PhD, San Francisco, CA (*Abstract Co-Author*) Research funded, General Electric Company; Research funded, InSightec Ltd; Royalties, Springer Science+Business Media Deutschland GmbH; Research Consultant, Pfizer Inc;

PURPOSE

The significance of MR cartilage signal abnormalities with or without cartilage swelling (grade 1 lesions) is not well understood and previous reports in the literature are inconclusive. Purpose of our study was therefore to assess the natural evolution of different types of grade 1 cartilage lesions (G1CL) in subjects without radiographic evidence of knee osteoarthritis (OA) over 48 months in comparison to matched controls without lesions.

METHOD AND MATERIALS

Subjects from the Osteoarthritis Initiative (n=59; age 56.6±8.3; 56% women) with G1CL diagnosed on 3T MRIs of the right knee but without focal defects of cartilage and without radiographic evidence of OA (KL scores 0-1) were frequency matched for age, sex, baseline KL and BMI with 52 controls without any cartilage lesion (age 54.8±6.5; 58% women). Individual G1CL (n=76) on intermediate-weighted fast spine echo sequences were categorized into 4 subgrades: A=hypointense, B=inhomogeneous, C=hyperintense, D=hyperintense with swelling. After 48 months progression of cartilage and subchondral bone marrow changes was assessed. Fisher's exact test was used for group and subgrade comparisons.

RESULTS

At baseline G1CL were detected significantly more frequently in the patellofemoral than in the tibiofemoral joint (48 vs. 28, P=0.022), and subgrades A or B were more frequent than C or D (n=65 vs. 11, P<0.001). Across compartments, G1CL progressed in 48-67% to focal cartilage lesions, while only 2-6% of controls showed incidental focal lesions (patella: 48 vs. 6%, P<0.001; trochlea: 52 vs. 2%, P<0.001; medial femur: 67 vs. 2%, P<0.001; lateral femur: 50 vs. 2%, P=0.011; medial tibia: 50 vs. 2%, P<0.001; lateral tibia: 47 vs. 6%, P<0.001). No significant differences in progression were found between G1CL subgrades (P>0.05). Incidental bone marrow abnormalities were associated with G1CL lesions in the patella (39 vs. 2% in the controls, P<0.001), trochlea (36 vs. 2%, P<0.001) and lateral tibia (47 vs. 2%, P<0.001).

CONCLUSION

G1CL are precursors of more severe structural cartilage abnormalities. Reporting these signal abnormalities is therefore crucial to identify patients at risk for progressive cartilage degeneration and may impact patient management.

CLINICAL RELEVANCE/APPLICATION

Grade 1 cartilage lesions often progress to more severe cartilage degeneration, and diagnosis therefore may have an impact on patient management, including life style changes and cartilage repair.

RC504-09 MR Bone Morphometry Predicts Biomechanical Property

Wednesday, Dec. 2 10:40AM - 10:50AM Location: E451B

Participants

Betty Tran, San Diego, CA (*Abstract Co-Author*) Nothing to Disclose Sheronda Statum, San Diego, CA (*Abstract Co-Author*) Nothing to Disclose Reni Biswas, San Diego, CA (*Abstract Co-Author*) Nothing to Disclose Kyu-Sung Kwack, MD, PhD, Suwon, Korea, Republic Of (*Abstract Co-Author*) Nothing to Disclose Robert Healey, San Diego, CA (*Abstract Co-Author*) Nothing to Disclose Won C. Bae, PhD, San Diego, CA (*Presenter*) Nothing to Disclose Christine B. Chung, MD, San Diego, CA (*Abstract Co-Author*) Nothing to Disclose

PURPOSE

Subchondral trabecular bone is often involved during knee injury and joint degeneration. MR evaluation of articular cartilage, as well as subchondral bone, would be useful clinically. Purpose of this study was to determine if MR morphometric measures of subchondral trabecular bone correlates with shear biomechanical failure.

METHOD AND MATERIALS

Nine 8.5-mm diameter osteochondral cores were harvested (Fig.A) from tibial plateau of cadaveric donors (age range 60 to 86 years old) and imaged at 3T (Fig.C) using 3D spoiled gradient echo without fat suppression at 200 micron isotropic resolution. Cores were cut axially, while recording force and displacement to determine shear energy (Fig.B). MR data was cropped to 1-mm thickness near each cut location, region of interest was selected to exclude artifacts, and standard bone morphometric analysis was performed (Fig C). Total of 19 cut locations were analyzed.

RESULTS

From MR data, 3D structure of trabeculae could be discerned (Fig.C). Many of morphometric measures, including bone volume fraction, trabecular thickness, and structure model index, correlated significantly with biomechanical shear energy (Fig.D), suggesting that higher density, thicker, and plate-like properties of the trabeculae correlated with higher shear energy needed to cut through the sample.

CONCLUSION

High resolution MRI is a useful modality not only for soft tissue evaluation, but also for quantitative evaluation of trabecular bone, which may serve as a surrogate for bone strength.

CLINICAL RELEVANCE/APPLICATION

This study has implications for evaluation of human bone structure using non-ionizing MRI modality, with applications for conditions such as subchondral bone insufficiency fracture.

RC504-10 The Role of Mechanical Stress on the Vascularization of Subchondral Bone in the Femoral Head: A DCE-MRI Study

Wednesday, Dec. 2 10:50AM - 11:00AM Location: E451B

Participants

Jean-Francois Budzik, MD,PhD, Lille, France (*Presenter*) Nothing to Disclose Guillaume Lefebvre, MD, Lille, France (*Abstract Co-Author*) Nothing to Disclose Helene Behal, Lille, France (*Abstract Co-Author*) Nothing to Disclose Sebastien Verclytte, MD, Marcq en Baroeul, France (*Abstract Co-Author*) Nothing to Disclose Pierre Hardouin, Boulogne-Sur-Mer, France (*Abstract Co-Author*) Nothing to Disclose Anne Cotten, MD, Lille, France (*Abstract Co-Author*) Nothing to Disclose

PURPOSE

To assess the normal perfusion pattern of subchondral bone in the femoral head with Dynamic Contrast Enhanced (DCE)-MRI and to study the influence of mechanical stress.

METHOD AND MATERIALS

This prospective study was approved by our Institutional Review Board. Informed Consent was obtained. DCE-MRI of the right hip was performed in sixty adults (32 women, 28 men) between April and September 2014. Mean age was 37.5 (±12.5). Regions of interest (ROI) were deposed in the center and in subchondral areas of the femoral head. Semi-quantitative and pharmacokinetic parameters were calculated. Perfusion parameters were compared between ROIs using a linear mixed model. Associations of each perfusion parameter with age, sex, body mass index (BMI) were studied using analysis of covariance models; age and sex were systematically introduced into models.

RESULTS

Semi-quantitative and pharmacokinetic parameters were different between the center of the femoral head and supero-lateral, antero-superior and posterior subchondral zones ($p \le 0.028$). Parameters in the inferior zone differed from those of the supero-lateral and antero-superior zones ($p \le 0.029$).BMI was negatively correlated with Time To Peak in all zones ($p \le 0.041$). BMI was positively correlated with Ktrans and Ve values in all zones except the inferior ($p \le 0.035$). Ve values were inferior in women in every zone ($p \le 0.039$).Ktrans and Ve values were negatively correlated with age in posterior and inferior zones ($p \le 0.039$).

CONCLUSION

This study demonstrates that the perfusion of subchondral bone is not homogeneous within the femoral head. Our results suggest that mechanical stress influences the microvascular properties of subchondral bone marrow.

CLINICAL RELEVANCE/APPLICATION

The proposed role of mechanical stress on the microvascularization of subchondral bone offers new opportunities in osteoarthritis research.

RC504-11 Metatarsophalangeal Joint Instability

Wednesday, Dec. 2 11:00AM - 11:25AM Location: E451B

Participants

Hilary R. Umans, MD, Ardsley, NY (Presenter) Nothing to Disclose

LEARNING OBJECTIVES

Overview of lesser metatarsophalangeal joint (MPJ) plantar plate (PP) and capsular degeneration and tear and discuss how it relates to MPJ instability Lesser MPJ Anatomy Symptoms / Exam MPJ region pain Sub-metatarsal Tenderness, esp plantar lateral base toe proximal phalanx Webspace Toe deformity Deviation, esp tibial +/- splaying 2nd-3rd toes Hyperextension at MPJ Etiology of PP and Capsular ligament degeneration + tear Chronic stress >> common than acute trauma Hyperextension + Axial loading high heels Crowding narrow toebox HAV + 2nd metatarsal (MT) protrusion Synovitis stretches MPJ capsule, leading to laxity and MPJ instability degeneration at the phalangeal insertion of the MPJ PP Traumatic tear less common PP tear pattern esp 2nd toe MPJ esp lateral insertion Frequent assoc'd tear of the lateral capsule Clinical grading MPJ instability Vertical stress test Digital Purchase Paper pull-out test Toe deformity Deviation, splaying, hyperextension Natural history: worsening deformity and dysfunction Imaging MRI Without vs with IV gadolinium Bright T2 signal defect at insertion +/- enhancement Enhancing defect +/- corresponding bright T2 signal defect Normal midline Hi Signal zone up to 2.5 mm Elongation = pathologic US Tear = hypoechoic defect at insertion Normal midline hypoechoic zone = 2.5mm Widens with degeneration + tear MRI vs US MRI Static exam Global Overview Can evaluate the capsule More easily DDx b/t pericapsular reactive soft tissue thickening (fibrosis +/or edema) + web space neuroma US Dynamic exam Assess focal tenderness + MPJ instability Technically challenging / learning curve Image incrementally from medial - lateral insertion DDx pericapsular fibrosis from webspace neuroma US Pitfalls Mostly anisotropy due to non-parallel imaging Can mistake midline hypoechoic zone for tear Limitations Sensitive, Not specific Difficult to differentiate degeneration vs tear MPJ capsule

cannot be evaluated Tx Options Conservative measures Taping Padding Rest NSAIDs Avoid steroid injection near the plantar plate insertion Surgery 2 approved surgical devices / approaches for repair of the PP via a doral incision Mini-Scorpion Device Incorporates Weil osteotomy with Plantar Plate repair Limited favorable outcomes Hat-trick System No osteotomy Unilateral or Bilateral Recently approved

ABSTRACT

Active Handout: Hilary Ruth Umans

http://abstract.rsna.org/uploads/2015/15001725/RC504-11.pdf

RC504-12 Chronic Wrist Symptoms in Correlation with Abnormal Scapholunate Joint Kinematics in Four-Dimensional CT Examinations: Initial Clinical Experience

Wednesday, Dec. 2 11:25AM - 11:35AM Location: E451B

Participants

Nima Hafezi Nejad, MD, MPH, Baltimore, MD (*Abstract Co-Author*) Nothing to Disclose John N. Morelli, MD, Baltimore, MD (*Abstract Co-Author*) Nothing to Disclose Uma Thakur, MD, Watchung, NJ (*Abstract Co-Author*) Nothing to Disclose Scott D. Lifchez, MD, Baltimore, MD (*Abstract Co-Author*) Nothing to Disclose Kenneth R. Means JR, MD, Baltimore, MD (*Abstract Co-Author*) Speakers Bureau, Auxilium Pharmaceuticals, Inc Faculty, Integra LifeSciences Holdings Corporation Jaimie Shores, MD, Baltimore, MD (*Abstract Co-Author*) Consultant, AxoGen, Inc Stockholder, MDConnectME Shadpour Demehri, MD, Baltimore, MD (*Presenter*) Research support, General Electric Company; Researcher, Carestream Health, Inc; Consultant, Toshiba Corporation

PURPOSE

Using Four Dimensional CT scan (4D-CT) we aimed at showing abnormal kinematics of Scapholunate (SL) interval in symptomatic wrists with inconclusive radiographic findings, compared to 4D-CT examinations of asymptomatic contralateral wrists.

METHOD AND MATERIALS

This is an IRB approved, HIPPA complaint, retrospective study of wrist 4D-CT scans of patients who were referred for further evaluation of chronic wrist pain (> 3 months). In all, 12 symptomatic wrists (11 subjects) with chronic symptoms and inconclusive radiographs and 10 asymptomatic contralateral wrists were scanned using 4D-CT. SL interval was measured during three wrist motions: relaxed to clenched fist, flexion to extension, and radial to ulnar deviation. Change in SL interval measurements after each motion was recorded using double-oblique multiplanar reformation technique.

RESULTS

We extracted the normal limits of SL interval during active motion in symptomatic and asymptomatic wrists. While the SL interval is expected to be smaller than 1 mm in asymptomatic wrists (except for the clenched fist: 0.51 - 1.34 mm), symptomatic wrists present with SL interval of larger than 1 mm. In fact in clenched fists (2.53 ± 1.19 mm), or during extension (2.54 ± 1.48 mm) or ulnar deviation (2.06 ± 1.12 mm), average expected SL interval in symptomatic wrists is more than 2 mms. No change in SL interval measurements was detected during all the three wrist motions in asymptomatic contralateral wrists. In contrast, SL intervals increased while moving from relaxed to clenched (0.70; 0.24 - 1.16 mm; p = 0.01), from flexion to extension (1.04; 0.26 - 1.81 mm; p = 0.01) and from radial to ulnar deviation (0.48; - 0.03 - 1.00 mm; p = 0.06). There was a moderate correlation between SL interval change and presence/absence of symptoms (Spearman Rho: 0.45 - 0.65)

CONCLUSION

Compared to asymptomatic wrists, SL interval measurements significantly increase during active motion in symptomatic wrists with inconclusive plain radiographs using 4D-CT examination.

CLINICAL RELEVANCE/APPLICATION

4D CT of the wrist is suitable and clinically feasible to detect subtle motion abnormality suggestive of SLIL insufficiency in patients with chronic wrist pain. This study shows how SL motion abnormalities is associated with presence of symptoms. Moreover, it reports different SL interval limits that are expected in asymptomatic and symptomatic wrists.

RC504-13 Dynamic Ultrasound of Upper Extremity

Wednesday, Dec. 2 11:35AM - 12:00PM Location: E451B

Participants Mary M. Chiavaras, MD, PhD, Ancaster, ON (*Presenter*) Nothing to Disclose

LEARNING OBJECTIVES

To understand indications, learn technique, and review associated anatomy for dynamic ultrasound imaging of the shoulder, elbow, wrist, and hand.

Neuroradiology Series: Brain Tumors

Wednesday, Dec. 2 8:30AM - 12:00PM Location: E451A

NR BQ MR

AMA PRA Category 1 Credits ™: 3.25 ARRT Category A+ Credits: 3.50

Participants

Rivka R. Colen, MD, Houston, TX, (rcolen@mdanderson.org) (*Moderator*) Nothing to Disclose James G. Smirniotopoulos, MD, Bethesda, MD (*Moderator*) Nothing to Disclose

Sub-Events

RC505-01 Beyond Enhancement and Histology: Molecular Markers for Diagnosis

Wednesday, Dec. 2 8:30AM - 8:55AM Location: E451A

Participants James G. Smirniotopoulos, MD, Bethesda, MD (*Presenter*) Nothing to Disclose

Active Handout: James G. Smirniotopoulos

http://abstract.rsna.org/uploads/2015/15000013/RC505-01 Smirniotopoulos(1).pdf

RC505-03 Radiogenomics Defines Key Genomic Network Driving GBM Invasion

Wednesday, Dec. 2 9:05AM - 9:15AM Location: E451A

Participants

Rivka R. Colen, MD, Houston, TX (*Presenter*) Nothing to Disclose Markus Luedi, Houston, TX (*Abstract Co-Author*) Nothing to Disclose Sanjay K. Singh, Houston, TX (*Abstract Co-Author*) Nothing to Disclose Islam S. Hassan, MBBCh, Houston, TX (*Abstract Co-Author*) Nothing to Disclose Joy Gummin, Houston, TX (*Abstract Co-Author*) Nothing to Disclose Erik P. Sulman, MD, PhD, Houston, TX (*Abstract Co-Author*) Nothing to Disclose Frederick F. Lang, MD, Houston, TX (*Abstract Co-Author*) Nothing to Disclose Pascal O. Zinn, MD, Boston, MA (*Abstract Co-Author*) Nothing to Disclose

PURPOSE

Clinical care and outcome in Glioblastoma (GBM) remains challenging due to the tumor's invasive grwoth. To establish personalized treatment options in GBM, discovery of genetic mechanisms essential for the tumor's invasion is needed. We have previously described radiogenomic approaches to diagnose gene networks non invasively by analyzing genomic data from TCGA. The purpose of the current reseach is to identify a genetic network that drives GBM invasion and can be targeted specifically.

METHOD AND MATERIALS

Using Kaplan-Meier statistics, the data of the two independent databases TCGA and REMBRANDT were used to validate the genetic netowork's impact on clinical outcome. The genes' staus was assessed in a panel of human glioma stem cells (GSCs) and conventional proneural, classical and mesenchymal GBM cell lines using RT-PCR. Differentiation potential (Tuj1+ve, S100A+ve, and GFAP+ve), self-renewal (limiting dilution assays), invasion (Boyden chamber) and proliferation (BrdU) were assessed. Gain (lentiviral vectors) and loss (SMARTchoice Inducible shRNA) of function experiments were performed. Orthotopic xenograft models (nude mice) were used to characterize the genes impact in vivo. Potential FDA approved therapeutics were identified using connectivity map.

RESULTS

Texture analysis based on radiogenomics significantly predicted the genes responsible for invasion of GBM in a non-invasive manner. Invasion in both, in vitro and in vivo was significantly decreased upun downregulation of this gene network. Transcriptome microarray analysis showed that an upregulation of the described genes results in class switching from proneural to mesenchymal subtypes. Cmap derived therapeutics could significantly inhibit the gene network's activity and hence invasion.

CONCLUSION

The describend genes could be essential drivers of molecular subtypes and invasion in GBM. The therapeutics defined with cmap offer a targetted therapy to adress these key features of GBM pathogenesis. Noninvasive radiogenomics-based identification of tumor subgroups and potential treatment approaches can significantly contribute to personalized therapy.

CLINICAL RELEVANCE/APPLICATION

The described gene network seems to be key for GBM pathogenesis. Noninvasive, radiogenomics-based subgroup identification and specific novel treatment approaches can significantly contribution to personalized GBM therapy.

RC505-04 Radiogenomic Analysis of TCGA/TCIA Diffuse Lower Grade Gliomas by Molecular Subtype

Wednesday, Dec. 2 9:15AM - 9:25AM Location: E451A

Participants Chad A. Holder, MD, Atlanta, GA (*Presenter*) Nothing to Disclose Laila M. Poisson, Detroit, MI (*Abstract Co-Author*) Nothing to Disclose Lee Cooper, Atlanta, GA (*Abstract Co-Author*) Nothing to Disclose

Erich Huang, PhD, Bethesda, MD (Abstract Co-Author) Nothing to Disclose James Y. Chen, MD, San Diego, CA (Abstract Co-Author) Research Consultant, EBM Technologies, Inc Research Consultant, Banyan Biomarkers, Inc Scott N. Hwang, MD, PhD, Memphis, TN (Abstract Co-Author) Nothing to Disclose Sugoto Mukherjee, MD, Charlottesville, VA (Abstract Co-Author) Nothing to Disclose Leo J. Wolansky, MD, Cleveland, OH (Abstract Co-Author) Nothing to Disclose Brent D. Griffith, MD, Detroit, MI (Abstract Co-Author) Nothing to Disclose Kristen W. Yeom, MD, Palo Alto, CA (Abstract Co-Author) Nothing to Disclose Michael Iv, MD, Stanford, CA (Abstract Co-Author) Nothing to Disclose Max Wintermark, MD, Lausanne, Switzerland (Abstract Co-Author) Advisory Board, General Electric Company; Rivka R. Colen, MD, Houston, TX (Abstract Co-Author) Nothing to Disclose Rajan Jain, MD, Northville, MI (Abstract Co-Author) Nothing to Disclose Justin Kirby, Bethesda, MD (Abstract Co-Author) Stockholder, Myriad Genetics, Inc John B. Freymann, BS, Rockville, MD (Abstract Co-Author) Nothing to Disclose Daniel L. Rubin, MD, MS, Palo Alto, CA (Abstract Co-Author) Nothing to Disclose C. Carl Jaffe, MD, Boston, MA (Abstract Co-Author) Nothing to Disclose Daniel J. Brat, MD, PhD, Atlanta, GA (Abstract Co-Author) Nothing to Disclose Adam E. Flanders, MD, Penn Valley, PA (Abstract Co-Author) Nothing to Disclose

PURPOSE

To investigate relationships between imaging phenotype and genetic classification of LGGs in the TCGA/TCIA database, we analyzed semi-quantitative MR features and IDH/1p19q classifications.

METHOD AND MATERIALS

Pre-operative MRIs of 72 TCGA/TCIA LGGs were reviewed by 3 neuroradiologists blinded to molecular status, using the VASARI LGG feature-set (standardized set of 26 MRI features). Data were compiled across 3 readers to define a single measure per sample. Clinical and molecular classifications were obtained from the LGG-AWG marker paper (TCGA Research Network.NEJM;2015, in press). Associations with histology, WHO grade and molecular type were assessed by Fisher's exact test (categorical features) and ANOVA/t-test (continuous features).

RESULTS

Of 70 tumors with IDH/1p19q classification, 16 were IDHmut-codel, 34 were IDHmut-non-codel, and 19 were IDHwt. IDHmut-codel tumors were preferentially centered in the frontal lobes (75%, FET p=0.026). IDHmut-non-codel tumors tended to arise in frontal (41%) and temporal lobes (41%), while IDHwt tumors did not show preference. Nonenhancing tumor margins were more well-defined for IDHmut LGGs (56% and 76% were well-defined) than for IDHwt tumors (32%, FET p=0.027). 66% of LGGs had an enhancing region, but this was not associated with molecular class (FET p=0.286), although enhancement was more likely in grade III than grade II (FET, p=0.043). 23% of these grade II/III tumors had MRI evidence of necrosis, with presence equally likely in any of the 3 molecular classes (FET p=0.931); however, 5/16 (31%) of LGGs with necrosis on MRI were grade II. IDHwt tumors tended to be smaller than IDHmut tumors (23.0 cm2 vs 39.7cm2, respectively, for maximal area, t-test p<0.001). Further differences were found in T1/FLAIR ratio (FET p=0.030), T2/FLAIR signal crossing the midline (FET p=0.007), and presence of hemorrhage (FET p=0.009), cysts (FET p=0.006), or satellites (FET p=0.030).

CONCLUSION

Review showed differential MR features between LGG molecular classes. IDHwt LGGs had association with aggressive features (e.g., small dimension with poorly-defined non-contrast-enhanced borders). Lack of association with necrosis or presence of an enhancing region suggests that the IDHwt class is not simply underdiagnosed GBM. An investigation of imaging profiles that align with molecular type or define further subclasses is underway.

CLINICAL RELEVANCE/APPLICATION

Differential MR features exist between LGG molecular classes.

Honored Educators

Presenters or authors on this event have been recognized as RSNA Honored Educators for participating in multiple qualifying educational activities. Honored Educators are invested in furthering the profession of radiology by delivering high-quality educational content in their field of study. Learn how you can become an honored educator by visiting the website at: https://www.rsna.org/Honored-Educator-Award/

Daniel L. Rubin, MD, MS - 2012 Honored Educator Daniel L. Rubin, MD, MS - 2013 Honored Educator

RC505-05 The Triple-Negative Low-Grade Glioma: MR Imaging Correlates of Aggressive Molecular Phenotype

Wednesday, Dec. 2 9:25AM - 9:35AM Location: E451A

Participants

Javier Villanueva Meyer, MD, San Francisco, CA (*Presenter*) Nothing to Disclose Byung Se Choi, MD, Seongnam-Si, Korea, Republic Of (*Abstract Co-Author*) Nothing to Disclose Matthew Wood, San Francisco, CA (*Abstract Co-Author*) Nothing to Disclose Tarik Tihan, San Francisco, CA (*Abstract Co-Author*) Nothing to Disclose Soonmee Cha, MD, San Francisco, CA (*Abstract Co-Author*) Nothing to Disclose

PURPOSE

Low-grade gliomas (LGGs) are a heterogeneous group of tumors with distinct clinical behavior and prognosis. One strategy to improve their characterization is with molecular biomarkers: P53, IDH 1/2, and 1p19q. These objective markers correlate with histologic classification and clinical outcomes. Specifically, the absence of IDH1/2 mutation or 1p19q deletion have been identified as indicative of a poor prognosis. The purpose of our study was to determine MR imaging parameters that can discriminate a, recently-described, aggressive subtype of LGG that is characterized by an absence of all three of these genetic alterations.

METHOD AND MATERIALS

A retrospective review of our medical records from 2010 to 2014 yielded 105 cases of pathologically-confirmed LGG that had molecular testing for P53 mutation, IDH1/2 mutation, and 1p/19q deletion. The MR imaging characteristics including tumor location, volume, infiltration pattern, cortical involvement, hemorrhage, contrast-enhancement, and quantitative diffusion and perfusion were assessed. Additionally, clinical data of patient treatment, disease course, and survival was collected.

RESULTS

There were 24 diffuse astrocytomas (23%), 36 oligoastrocytomas (34%) and 45 oligodendrogliomas (43%). P53 mutation was found in 21 (20%), IDH1/2 mutation was found in 70 (67%), and 1p19q deletion was found in 45 (43%). Thirteen cases (12%) did not have any of these genetic alterations. Triple-negative tumors showed a lower incidence of cortical involvement (p<0.05) and lower mean and minimum apparent diffusion coefficient (ADC) values (1.25 vs 1.45x10^-3 mm^2/s; 0.89 vs 1.09x10^-3 mm^2/s, p<0.01). Multiple logistic regression analysis showed low ADC value as an independent predictor of triple-negative LGG. With a cut-off of 1.0x10^-3 mm^2/s, ADC value provides a 73% sensitivity and a 72% specificity with an odds ratio of 7.0 (p<0.01). In cases with available clinical follow-up, triple-negative LGGs were found to have disease progression within 2 years in 50% compared to 16% in the non-triple-negative cohort.

CONCLUSION

Triple-negative LGGs are a clinically and biologically aggressive phenotype that exhibit lower mean ADC values and lack of cortical involvement on MR imaging.

CLINICAL RELEVANCE/APPLICATION

MR imaging features can be used alongside molecular biomarkers to assess the aggressiveness and prognosis of LGGs and subsequently may provide a means of guiding management as patient-tailored therapy.

RC505-06 Do Macrocyclic Gadolinium Based Contrast Agents(GBCA) Deposit Gd in Normal Brain Tissue in Patients Receiving Contrast Enhanced MRI?

Wednesday, Dec. 2 9:35AM - 9:45AM Location: E451A

Participants

Nozomu Murata, MD, PhD, Seattle, WA (*Presenter*) Nothing to Disclose Luis F Gonzalez-Cuyar, MD, Seattle, WA (*Abstract Co-Author*) Nothing to Disclose Kiyoko Murata, MD,PhD, Tokyo, Japan (*Abstract Co-Author*) Nothing to Disclose Corinne L. Fligner, MD, Seattle, WA (*Abstract Co-Author*) Nothing to Disclose Russell Dills, PhD, Seattle, WA (*Abstract Co-Author*) Nothing to Disclose Daniel S. Hippe, MS, Seattle, WA (*Abstract Co-Author*) Research Grant, Koninklijke Philips NV; Research Grant, General Electric Company Kenneth R. Maravilla, MD, Seattle, WA (*Abstract Co-Author*) Nothing to Disclose

PURPOSE

Based on T1 shortening on noncontrast MR, recent studies have suggested that small amounts of gadolinium(Gd) may accumulate in brain even in patients with normal renal function. Recently McDonald confirmed Gd deposition in postmortem human brain tissue. To date, studies have shown Gd brain deposition only with Group 1 linear agents. The purpose of this study was to determine whether Gd is deposited in brain among patients receiving more stable macrocyclic agents using postmortem tissue analysis with inductively coupled plasma mass spectrometry (ICP-MS).

METHOD AND MATERIALS

This study was approved by the IRB. Brain tissue was collected at autopsy from decedents with available medical records that document past history of MRIs with or without GBCA exposure. Decedents with no prior MRI or only nonGd MRI served as controls. Tissue samples were collected from white matter, putamen, globus pallidus, caudate nucleus, pons and dentate nucleus and analyzed for Gd using ICP-MS. Bone tissue from rib was also analyzed as a reference tissue in each case. Results were correlated with types of agent received, cumulative dose, time since dosing and clinical and laboratory data.

RESULTS

Among 21 cases obtained to date, 15 cases with normal renal function received 1 or more GBCA exposures and 6 cases had no exposure. ICP-MS showed measurable amounts of Gd deposition (range 0.003-3.54ng/mg) in all 15 cases receiving GBCA.A subset of these ,4 cases received only a macrocyclic GBCA(1 Gadavist ; 3 ProHance) with doses ranging from 10 to 126 ml and Gd was also detected in all macrocyclic cases (0.006-0.188 ng/mg). Gd in brain was detected after only a single dose and deposition was present among all brain regions sampled. Gd deposition in rib was also positive in all 15 cases and showed significantly higher levels than brain in each case. By comparison there was no detectable Gd in any control cases.

CONCLUSION

Gd deposition occurs in normal brain tissue in patients with normal renal function with a past history of GBCA exposure even in those receiving only macrocyclic agents. The clinical significance remains undetermined and we are pursuing further investigation.

CLINICAL RELEVANCE/APPLICATION

Gd deposition is present in normal brain tissue after only one dose even with macrocyclis agents. This important observation needs further investigation to determine potential toxic effects.

Handout:Nozomu Murata

http://abstract.rsna.org/uploads/2015/15004555/RSNA2015 RC505-06WF.pptx

RC505-07 Post-therapy Brain Tumors: Imaging Pitfalls and Strategy

Wednesday, Dec. 2 9:45AM - 10:10AM Location: E451A

Soonmee Cha, MD, San Francisco, CA (Presenter) Nothing to Disclose

LEARNING OBJECTIVES

1) Discuss biologic and pathologic complexity of post-therapy brain tumors. 2) Present latest advances in imaging methods to differentiate recurrent tumor and treatment effect. 3) Review strengths and pitfalls of imaging post-therapy brain tumors. 4) Describe imaging strategy to improve diagnosis and management of patients with treated brain tumor.

RC505-08 Directions, Protons and Flows - Practical Advanced Brain Tumor Imaging

Wednesday, Dec. 2 10:30AM - 10:55AM Location: E451A

Participants

Jeffrey L. Sunshine, MD, PhD, Pepper Pike, OH (*Presenter*) Research support, Siemens AG Travel support, Siemens AG Travel support, Koninklijke Philips NV Travel support, Sectra AB Travel support, Allscripts Healthcare Solutions, Inc

RC505-10 A Multiparametric Voxel-level Model for Prediction of Cellularity in Glioblastoma

Wednesday, Dec. 2 11:05AM - 11:15AM Location: E451A

Participants

Peter Chang, MD, Bronx, NY (*Presenter*) Nothing to Disclose Daniel S. Chow, MD, New York, NY (*Abstract Co-Author*) Nothing to Disclose Timothy Ung, New York City, NY (*Abstract Co-Author*) Nothing to Disclose Jennifer Soun, MD, New York, NY (*Abstract Co-Author*) Nothing to Disclose Christopher G. Filippi, MD, Grand Isle, VT (*Abstract Co-Author*) Research Consultant, Regeneron Pharmaceuticals, Inc; Research Consultant, Syntactx Angela Lignelli-Dipple, MD, New York, NY (*Abstract Co-Author*) Nothing to Disclose Peter Canoll, New York City, NY (*Abstract Co-Author*) Nothing to Disclose Lawrence H. Schwartz, MD, New York, NY (*Abstract Co-Author*) Committee member, Celgene Corporation; Committee member, Novartis AG; Committee member, ICON plc; Committee member, BioClinica, Inc

PURPOSE

To create a robust multiparametric model for prediction of cellular density in glioblastoma (GBM) using voxel-by-voxel analysis of T1W-postcontrast, FLAIR and ADC intensity values calibrated to biopsy-proven histopathologic data.

METHOD AND MATERIALS

As part of an IRB-approved protocol, MR-localized biopsies of GBM patients were obtained from both contrast-enhancing tumor (CE) and nonenhancing (nCE) peritumoral edema using Brainlab referenced to T1W-postcontrast images. Total cell counts were obtained after HandE slide preparation scanned at 400x magnification. FLAIR and ADC data were interpolated and coregistered to the reference T1W volume using affine transformation and a mutual information cost function. For each biopsy site, corresponding mean intensity was obtained on T1W-postcontrast, FLAIR and ADC sequences. Univariate linear regression was used to determine correlation between cell count and intensity for each MR sequence. Two multivariate linear regression models, one each for CE and nCE regions, were used to combine data from each MR sequence into a robust model for tumor cellularity.

RESULTS

A total of 58 biopsy sites were obtained. Overall, cellularity demonstrated moderate linear correlation with T1W-postcontrast (r = 0.76), FLAIR (r = 0.62) and ADC (r = 0.64, within nCE region only). Multiple linear regression combining all three variables yielded a model highly predictive of cellularity, both within the nCE (r = 0.93) and CE (r = 0.76) region. Within the nCE region, the model weighted ADC (p = 0.0072) and FLAIR (p = 0.058) more significantly than T1W (p = 0.83), as determined by analysis of variance (ANOVA). Within the CE region, T1W (p < 0.001) and FLAIR (p = 0.12) were weighted more significantly than ADC (p = 0.21).

CONCLUSION

A multiparametric model combining T1W-postcontrast, FLAIR and ADC values strongly predicts cell counts in GBM, notably with correlation >90% in the nCE region. By applying this model at each voxel within the tumor volume, a noninvasive map of cellular density can be generated.

CLINICAL RELEVANCE/APPLICATION

Cellularity maps of the peritumoral region in GBM localize tumor microinvasion and may be used as a tool to guide extended surgical resection or biopsy and to assess infiltrative tumor burden.

RC505-11 Receiver Operating Characteristic (ROC) and Logistic Fit Analysis for Detecting Brain Tumor Based on OEF Measurements Obtain by PET and MR

Wednesday, Dec. 2 11:15AM - 11:25AM Location: E451A

Participants

Parinaz Massoumzadeh, PhD, Saint Louis, MO (*Presenter*) Nothing to Disclose Jonathan E. McConathy, MD, PhD, Saint Louis, MO (*Abstract Co-Author*) Research Consultant, Eli Lilly and Company; Research Consultant, Blue Earth Diagnostics Ltd; Research Consultant, Siemens AG; Research support, GlaxoSmithKline plc Andrei Vlassenko, MD, PhD, Saint Louis, MO (*Abstract Co-Author*) Nothing to Disclose Yi Su, PhD, Saint Louis, MO (*Abstract Co-Author*) Nothing to Disclose Hongyu An, DSc, Chapel Hill, NC (*Abstract Co-Author*) Nothing to Disclose Charles F. Hildebolt, DDS, PhD, Saint Louis, MO (*Abstract Co-Author*) Nothing to Disclose Daniel S. Marcus, PhD, Saint Louis, MO (*Abstract Co-Author*) Nothing to Disclose Tammie S. Benzinger, MD, PhD, Saint Louis, MO (*Abstract Co-Author*) Nothing to Disclose Tammie S. Benzinger, MD, PhD, Saint Louis, MO (*Abstract Co-Author*) Research Grant, Eli Lilly and Company; Investigator, Eli Lilly and Company; Investigator, F. Hoffmann-La Roche Ltd; Receiver operating characteristic (ROC) curve and logistic fit analysis for detecting brain tumors using cerebral oxygen extraction fraction (OEF) measurement obtained by [15]O positron emission tomography (PET) and oxygen sensitive magnetic resonance (MR) imaging.

METHOD AND MATERIALS

30 participants (20 with brain tumors) were recruited. MRI included standard clinical sequences plus OEF-MR1; a two-dimensional multi-echo gradient spin echo sequence. Concurrent with the MR acquisition, subjects with brain tumors underwent PET scanning, which included 2 sets of 3 scans with serial inhalation of air with 40-75 mCi [15]O labeled carbon monoxide , 40-75 mCi [15]O labeled oxygen , and injection of 25-50 mCi [15]O labeled water. MR and PET data were post-processed off line and registered to the anatomic T1 pre-and post-contrast images. Regions of interest were drawn based upon contrast-enhancing tumor areas, contra-lateral normal white matter (NWM), and normal gray matter (NGM) Ratios of OEF (rOEF) were obtained for lesions compared to normal tissue. Statistical analyses, including Bland-Altman plot, ROC, and logistic fit, were performed.

RESULTS

Bivariate analyses results are: between two rOEF-PET measurements of all selected regions R=0.92 and P <0.0001, and tumor type R=0.68 and p<0.0001; and similarly betweenr rOEF-MR and rOEF-PET all selected regions R=0.3 and P <0.0413, and tumor type R=0.39 and p<0.173. Based on Bland-Altman analysis both MR and PET methods of obtaining OEF are in agreement (the measurements lie within range ± 1.96 xSD). However, the coefficient obtain for rOEF-MR covers much larger range which may not not be clinically acceptable. Area under ROC curve (AUC) has much higher value for PET (0.95) than MR (0.58).

CONCLUSION

Both MR and [15]O PET can measure OEF in brain tumors and in peritumoral edema. Variable OEF measurements for tumor and edema may be implication for tumor grade and prognosis. BOLD MR fails in regions with signal loss on SWI or T2*. Area under ROC Curve (AUC) has much higher value for PET (0.95) than MR (0.58). Based on logistic fit probablity of distinguing tumor with PET is much higher than MR.

CLINICAL RELEVANCE/APPLICATION

Both MR and PET techniques have tremendous potential and may offer new insight into the underlying physiology of brain tumors and their response to therapy without requiring radiation or injected contrast. BOLD MR fails in regions with signal loss on SWI or T2*.

RC505-12 What Does the Black Box Tell us? Risk and Benefit of Ferumoxytol as an MRI Contrast Agent

Wednesday, Dec. 2 11:25AM - 11:35AM Location: E451A

Participants

Csanad G. Varallyay, MD, PhD, Portland, OR (*Presenter*) Nothing to Disclose Rochelle Fu, Portland, OR (*Abstract Co-Author*) Nothing to Disclose Joao Prola Netto, MD, Portland, OR (*Abstract Co-Author*) Nothing to Disclose Edward Neuwelt, MD, Portland, OR (*Abstract Co-Author*) Nothing to Disclose

PURPOSE

Ferumoxytol, an ultrasmall iron oxide nanoparticle (USPIO) has been marketed as Feraheme® for iron replacement therapy in patients with chronic kidney disease. Due to its magnetic properties, and long plasma half-life, ferumoxytol uniquely allows MR imaging of the intravascular space early after injection, which is beneficial for high-resolution blood volume mapping of brain lesions. Delayed (24h) ferumoxytol enhancement may help in differential diagnosis. As of March 30, 2015, the FDA added a boxed warning to Feraheme® package insert, which strengthens existing warnings regarding potential fatal and serious hypersensitivity reactions including anaphylaxis, even in patients who received Feraheme® previously. It emphasizes the importance of trained personnel, monitoring at least 30 min post injection to properly treat hypersensitivity reactions.

METHOD AND MATERIALS

Our institution has been actively doing imaging research with ferumoxytol for over 10 years. In this study we evaluated early adverse events (occurring within 1 day), potentially related to ferumoxytol administration hypersensitivity, and qualitatively compared it with published data.

RESULTS

At the time writing this abstract we have analyzed a total of 553 ferumoxytol infusions in 298 patients and have not recorded any severe (grade 3, 4 or 5) hypersensitivity reactions occurring within 1 day. Early grade 1 and 2 reactions, were present, such as nausea/vomiting (5.1%), hypertension (3.3%), pruritus (1.3%). In published data, the frequency of severe hypersensitivity of Feraheme® was equivalent to ionic iodinated contrast media, and about 10x higher than gadolinium MR contrast agents and nonionic iodinated contrast agents.

CONCLUSION

Our results suggest less frequent severe hypersensitivity reactions compared to published data, and it may be due to the difference in patient population. A detailed toxicity evaluation of our data is in progress. The intended purpose of change in labeling by the addition of the boxed warning is to strengthen the warnings in the label and to mitigate the risk of serious hypersensitivity reactions including anaphylaxis in order to enhance patient safety.

CLINICAL RELEVANCE/APPLICATION

Ferumoxytol remains safe for MRI in the vast majority of patients, with a very small risk of serious adverse event, and personnel should be prepared to treat such reactions if they were to occur.

RC505-13 Moving Towards Quantitative Brain Tumor Imaging

Wednesday, Dec. 2 11:35AM - 12:00PM Location: E451A

Thomas L. Chenevert, PhD, Ann Arbor, MI (Presenter) Consultant, Koninklijke Philips NV

GI

СТ

Gastrointestinal Series: Advances in Abdominal CT

Wednesday, Dec. 2 8:30AM - 12:00PM Location: E350

AMA PRA Category 1 Credits ™: 3.25 ARRT Category A+ Credits: 4.00

FDA Discussions may include off-label uses.

Participants

Daniele Marin, MD, Cary, NC (*Moderator*) Nothing to Disclose Avinash R. Kambadakone, MD, Boston, MA (*Moderator*) Nothing to Disclose Ravi K. Kaza, MD, Ann Arbor, MI (*Moderator*) Nothing to Disclose

Sub-Events

RC509-01 Radiation Dose Reduction in CT

Wednesday, Dec. 2 8:30AM - 8:50AM Location: E350

Participants

Amy K. Hara, MD, Scottsdale, AZ (Presenter) Royalties, General Electric Company;

LEARNING OBJECTIVES

1) Compare advantages and disadvanatages of various techniques to reduce radiation dose for abdominal CT. 2) Describe how iterative reconstruction techniques work and how they can improve image quality of low dose exams. 3) Develop a strategy to implement low dose techniques in clinical practice.

Honored Educators

Presenters or authors on this event have been recognized as RSNA Honored Educators for participating in multiple qualifying educational activities. Honored Educators are invested in furthering the profession of radiology by delivering high-quality educational content in their field of study. Learn how you can become an honored educator by visiting the website at: https://www.rsna.org/Honored-Educator-Award/

Amy K. Hara, MD - 2015 Honored Educator

RC509-02 Intra-Patient Comparison of Standard, BMI-based and Attenuation-based Tube Voltage Selection in Abdominal MDCT: Effect on Dose and Image Quality Parameters

Wednesday, Dec. 2 8:50AM - 9:00AM Location: E350

Participants

Faezeh Sodagari, MD, Chicago, IL (*Presenter*) Grant, Siemens AG Adeel R. Seyal, MD, Chicago, IL (*Abstract Co-Author*) Grant, Siemens AG Atilla Arslanoglu, MD, Chicago, IL (*Abstract Co-Author*) Grant, Siemens AG Fernanda D. Gonzalez Guindalini, MD, Chicago, IL (*Abstract Co-Author*) Nothing to Disclose Vahid Yaghmai, MD, Chicago, IL (*Abstract Co-Author*) Nothing to Disclose

PURPOSE

Intra-patient comparison of abdominal MDCT radiation dose and image quality parameters when using attenuation-based automated tube voltage selection versus standard and BMI-based selections .

METHOD AND MATERIALS

This study was IRB approved and HIPAA compliant. Abdominal MDCT scans of fifty patients who had been imaged with both standard protocol (120 kV and filtered-back-projection reconstruction algorithm) and new protocol (automated kV selection and iterative reconstruction) were compared. Data was also analyzed based on BMI-based kV selection (100 kV if BMI <25 kg/m2). Radiation dose, image noise (subcutaneous fat), SNR (aorta and liver) and CNR (aorta and liver) were recorded. P<0.05 was considered significant.

RESULTS

Patient mean BMI was comparable between the two studies (24.6 kg/m2 for first study and 24.7 kg/m2 for second study; P=0.77). With automated tube voltage selection protocol, 43/50 (86%) were scanned with 100 kV, 5/50 (10%) with 120kV and 2/50 (4%) with 140kV. BMI for 100kV group ranged between 17.8 and 29.925 kg/m2. Sixteen patients scanned with 100kV had BMI \ge 25 kg/m2 would have been utilized as cut-off point for 100kV san, 30% fewer patients would have been scanned with 100kV (28 vs 43). Compared with standard protocol, CDTIvol, DLP, and effective dose decreased 17.2%, 20% and 20.4%, respectively, in 43 patients that were automatically selected for 100kV scan. Image noise decreased by 21.7% (P<0.001) while CNR and SNR of liver and aorta increased >24% (P<0.001).

CONCLUSION

Attenuation-based automated tube voltage selection results in lower tube voltage in significantly higher number of patients, compared with standard and BMI-based selections. Image quality parameters improve with combination of lower tube voltage selection and iterative reconstruction.

CLINICAL RELEVANCE/APPLICATION

Attenuation-based automated tube voltage selection results in significantly higher number of patients imaged with lower dose

compared with BMI-selection.

Honored Educators

Presenters or authors on this event have been recognized as RSNA Honored Educators for participating in multiple qualifying educational activities. Honored Educators are invested in furthering the profession of radiology by delivering high-quality educational content in their field of study. Learn how you can become an honored educator by visiting the website at: https://www.rsna.org/Honored-Educator-Award/

Vahid Yaghmai, MD - 2012 Honored Educator Vahid Yaghmai, MD - 2015 Honored Educator

RC509-03 Oral Contrast Media Concentration Selection for Low kVp/keV CT Scanning

Wednesday, Dec. 2 9:00AM - 9:10AM Location: E350

Participants

Manuel Patino, MD, Boston, MA (*Presenter*) Nothing to Disclose Diana Murcia, MD, Boston, MA (*Abstract Co-Author*) Nothing to Disclose Andrea Prochowski Iamurri, MD, Boston, MA (*Abstract Co-Author*) Nothing to Disclose Yasir Andrabi, MD, MPH, Boston, MA (*Abstract Co-Author*) Nothing to Disclose Avinash R. Kambadakone, MD, Boston, MA (*Abstract Co-Author*) Nothing to Disclose Dushyant V. Sahani, MD, Boston, MA (*Abstract Co-Author*) Research Grant, General Electric Company; Research Consultant, Allena Pharmaceuticals, Inc

PURPOSE

Oral contrast media is commonly used for abdominal CT. Clinical implementation of low-kVp/DECT imaging demands adjustments in OCM concentration. The purpose of our study is to evaluate the impact of low X-ray energy (kVp/keV) on OCM using phantom and clinical data, and to assess optimal OCM concentrations for low-energy diagnostic CT scans

METHOD AND MATERIALS

Anthropomorphic CT colo phantom study: Four OCM solutions were used as follows: Water, Gastrografin® (Bracco dx, 9mg/ml), Iohexol (GE healthcare, 12mg/ml), and Barium Sulfate (Readi-CAT® 2.0%). Each solution was diluted with water to obtain 75, 50, and 25% of the standard dose of OCM for adults. The phantom was filled up serially with 400 ml of each OCM solution, from the lowest to the standard OCM concentration, and scanned on ssDECT scanner (Discovery-CT750 HD, GE Healthcare) on SECT (80, 100 and 120 kVp, and 250mA) and DECT modes (140/80 kVp and 375 mA). VMC (40, 50, 60, and 70keV) images were generated yielding a total of 91 image datasets (39 on SECT, and 52 on DECT). Three ROIs were placed at 3 locations in colonic lumen to measure HU, SD and CNR. Clinical study: GI tract attenuation was measured in 50 consecutive patients with standard-dose, positive (barium and iodine) OCM in both SECT and DECT. Multiple ROIs were placed in different locations of the GI tract on 120-SECT and DECT-low keV images to measure HU. Statistical analysis was conducted with pair student t-test

RESULTS

Colonic attenuation in 120kVp-scans with standard OCM dose ranges between 261 and 303 HU. There was an inverse correlation between OCM HU and kVp/keV, irrespective of OCM concentration, increasing HU 2X on low-kVp and 5X on low-keV images (p<0.05). There was 5% drop in CNR with low-kVp but 15% increase with low-keV for all OCM's. Clinical abdomen CT exams mirrored phantom results. Optimal OCM dilutions for 100/80kVp scans were: Gastrografin® 75/75%, Iohexol 75/75% and Barium 75/50%. OCM dilutions of 25-50% were optimal on 40-70keV scans

CONCLUSION

Low kVp/keV scans increase GI tract attenuation, enabling OCM dose concentration reduction for diagnostic exams

CLINICAL RELEVANCE/APPLICATION

OCM-customization provides opportunity to optimize IQ, and decrease OCM-related artifacts, allowing better assessment of GI and, adjacent, extra-intestinal pathologies on low X-ray energy CT scans. It might also contribute to reduce radiation dose, associated with tube current modulation

Honored Educators

Presenters or authors on this event have been recognized as RSNA Honored Educators for participating in multiple qualifying educational activities. Honored Educators are invested in furthering the profession of radiology by delivering high-quality educational content in their field of study. Learn how you can become an honored educator by visiting the website at: https://www.rsna.org/Honored-Educator-Award/

Dushyant V. Sahani, MD - 2012 Honored Educator Dushyant V. Sahani, MD - 2015 Honored Educator

RC509-04 Intravenous Contrast Issues

Wednesday, Dec. 2 9:10AM - 9:30AM Location: E350

Participants

John R. Leyendecker, MD, Dallas, TX (Presenter) Nothing to Disclose

LEARNING OBJECTIVES

1) To understand the risks of intravenous administration of iodinated CT contrast media. 2) To be familiar with the latest information on the use of iodinated CT contrast media in the setting of renal impairment. 3) To be familiar with potential future developments in intravenous CT contrast agents.

RC509-05 The Application of Spectral CT in Reducing Contrast Medium Dosage in Abdominal CT: Comparison between the Lower Contrast Injection Protocol (350mgl/kg)

Participants

Lei Yuxin, MMed, Xianyang City, China (*Presenter*) Nothing to Disclose Xiaoxia Chen, MMed, Xianyang City, China (*Abstract Co-Author*) Nothing to Disclose Ma Chunling, MMed, Xianyang City, China (*Abstract Co-Author*) Nothing to Disclose Zhanli Ren, Xianyang, China (*Abstract Co-Author*) Nothing to Disclose Qi Yang, Xianyang, China (*Abstract Co-Author*) Nothing to Disclose Tian Xin, MMed, Xianyang City, China (*Abstract Co-Author*) Nothing to Disclose Qiang Tian, Xian, China (*Abstract Co-Author*) Nothing to Disclose

PURPOSE

To evaluate the feasibility of using spectral CT in contrast-enhanced abdominal scans to reduce the total dosage of contrast medium while maintaining image quality.

METHOD AND MATERIALS

Prospectively randomized 44 contrast-enhanced abdominal CT patients to 2 groups: group A (n=22) using spectral CT with 350mgI/kg contrast injection protocol; group B (n=22) with the conventional 120kVp with 500mgI/kg. The injection rate was adjusted to have the total injection time of 25s for both groups. For the 120kVp scan, tube current (m A) was automatically adjusted to achieve noise index (NI) of 10, and for spectral CT, a m A was selected based on the average of the min and max m A from the 120kVp m A table for NI=10. CT dose index (CTDI) and effective dose were recorded. CT number and standard deviation (SD) of the abdominal aorta in arterial phase (AP), portal vein in venous phase (VP), liver parenchyma and erector spinae on the 120kVp images and 60keV spectral CT images were measured to calculate contrast-noise-ratio (CNR). Measurements were compared with t-test.

RESULTS

The body mass index between 2 groups showed no difference (p>0.05). For the 60keV spectral CT images, CT number and CNR were ($359.00\pm53.21HU$, 51.52 ± 12.56) for abdominal aorta and ($185.32\pm22.90HU$, 20.63 ± 6.19) for portal vein. These values were higher than the respective values of ($306.03\pm46.36HU$, 44.52 ± 13.43) and ($149.25\pm19.66HU$, 15.11 ± 3.65) for the 120kVp images. The SD values in erector spinae of the spectral CT images were $5.88\pm0.99HU$ in AP and $6.05\pm0.99HU$ in VP, statistically the same as those of the 120kVp images ($5.90\pm1.43HU$ in AP and $5.85\pm0.73HU$ in VP) (P>0.05). The CTDI and effective dose were ($14.28\pm2.61mGy$, $6.63\pm1.21mSv$) for spectral CT and ($13.55\pm4.73mGy$, $6.23\pm2.08mSv$) for 120kVp CT with no difference (p>0.05). On the other hand, group A with spectral CT achieved 30% contrast dose reduction at 350mgI/kg compared with the conventional 120kVp group.

CONCLUSION

Compared with the conventional 120kVp CT, spectral CT can reduce the total contrast dosage by 30% and at the same time improves the vessel contrast enhancement and CNR without radiation dose increase.

CLINICAL RELEVANCE/APPLICATION

Spectral CT can reduce the total contrast dosage by 30% and improves vessel enhancement and CNR without radiation dose increase.

RC509-06 Dual-Energy CT and Virtual Monoenergetic Reconstructions: Utility of Novel and Basic Algorithms in Assessment of Intestinal Wall Enhancement and Applications for Acute Intestinal Ischemia

Wednesday, Dec. 2 9:40AM - 9:50AM Location: E350

Participants

Pedro Lourenco, MD, Vancouver, BC (*Presenter*) Nothing to Disclose Ryan Rawski, BSc, MSc, Vancouver, BC (*Abstract Co-Author*) Nothing to Disclose Patrick D. McLaughlin, FFRRCSI, Cork, Ireland (*Abstract Co-Author*) Speaker, Siemens AG Tim O'Connell, MD, Meng, Vancouver, BC (*Abstract Co-Author*) President, Resolve Radiologic Ltd; Speake, Siemens AG Savvas Nicolaou, MD, Vancouver, BC (*Abstract Co-Author*) Institutional research agreement, Siemens AG

PURPOSE

Acute bowel ischemia and infarction are devastating abdominal emergencies, with reported mortality rates up to 93%. CT sensitivity for detection of acute bowel ischemia is poor, in particular in the diagnosis of early bowel ischemia, and CT findings are often non-specific. Virtual monoenergetic reconstructions allow for optimized enhancement and evaluation of bowel wall for signs of ischemia and infarction. The basic algorithm has limited utility given high noise and signal to noise. Here, we evaluate the utility of a novel (VMI+) and the basic (VMI) virtual monoenergetic algorithms in acute bowel ischemia.

METHOD AND MATERIALS

18 patients with pathologically confirmed bowel ischemia or infarction presented to a quaternary hospital. Abdominal DECT (100 and 140 keV) were obtained at the time of presentation. Axial series were reconstructed with VMI+ and VMI software application (Monoenergetic Basic and Plus, Dual Energy, Siemens) and evaluated for improved noise reduction, and the reconstructions were compared with virtual 120-keV series that blended spectral information from high and low keV datasets. Images were considered to lie within the sweet spot if noise level was < 40 HU.

RESULTS

Utilizing the novel algorithm broadened the sweet spot of diagnostically acceptable monoenergetic keV levels by 416%. With VMI+, the mean diagnostic range was 57-190 keV (SD 9.3 and 0.0, respectively), whereas using VMI, mean diagnostic range was 69-101 keV (SD 3.9 and 13.0, respectively). SNR and CNR were also significantly improved utilizing the VMI+ technique, by 107 and 76%, respectively. CNR utilizing the VMI+ algorithm at 50, 100 and 150 keV was 4.90 (SD 1.44) 3.18 (SD 1.44) 1.26 (SD 0.71), respectively, while VMI algorithm CNR was significantly inferior, at 2.39 (SD 0.92), 1.54 (SD 0.61) and 0.35 (SD 0.18). Intestinal wall enhancement was maximized at 40 keV, given the maximal CNR (5.18 SD 1.42), which allows for optimal assessment of bowel wall at this level, albeit tolerating lower SNR.

CONCLUSION

The "sweet spot" for virtual monoenergetic reconstructions was significantly increased when utilizing the VMI+ algorithm, with a diagnostic keV range increased by approximately 400%. SNR and CNR also demonstrate marked improvement by 107 and 76%, respectively, with VMI+ over VMI.

CLINICAL RELEVANCE/APPLICATION

The VMI+ reconstructions are markedly superior to the basic VMI algorithm, and are useful in assessing bowel wall enhancement.

RC509-07 Patient Size-independent Monoenergetic Imaging for Detection Hypervascular Liver Tumors: Impact of a Second-generation Monoenergetic Algorithm

Wednesday, Dec. 2 9:50AM - 10:00AM Location: E350

Participants

Daniele Marin, MD, Cary, NC (*Presenter*) Nothing to Disclose Juan Carlos Ramirez-Giraldo, PhD, Malvern, PA (*Abstract Co-Author*) Employee, Siemens AG Sonia Gupta, MD, Newark, DE (*Abstract Co-Author*) Nothing to Disclose Sandra Stinnett, MS, MPH, Durham, NC (*Abstract Co-Author*) Nothing to Disclose Rendon C. Nelson, MD, Durham, NC (*Abstract Co-Author*) Consultant, General Electric Company Consultant, Nemoto Kyorindo Co, Ltd Consultant, VoxelMetrix, LLC Research support, Bracco Group Research support, Becton, Dickinson and Company Speakers Bureau, Siemens AG Royalties, Wolters Kluwer nv Ehsan Samei, PhD, Durham, NC (*Abstract Co-Author*) Nothing to Disclose Achille Mileto, MD, Durham, NC (*Abstract Co-Author*) Nothing to Disclose Wanyi Fu, BEng, Durham, NC (*Abstract Co-Author*) Nothing to Disclose

PURPOSE

To investigate the impact of a novel monoenergetic reconstruction algorithm on the conspicuity of hypervascular liver tumors during dual-energy CT (DECT) of the liver.

METHOD AND MATERIALS

This retrospective, single-center HIPAA-compliant study was IRB-approved and informed patient consent was waived. Fifty-nine patients (35 men, 24 women) with 47 hypervascular liver tumors underwent DECT (80/Sn140 kVp) in the late hepatic arterial phase, with a dual-source CT system (Siemen Definition Flash). Datasets at energy levels ranging from 40 to 100 keV were reconstructed using first and second-generation monoenergetic algorithms (Syngo DE Monoenergetic and Monoenergetic Plus, respectively). Noise and tumor-to-liver contrast-to-noise ratio (CNR) were calculated and compared among different reconstructed datasets. The effect of patient's effective diameter on lesion CNR was also assessed. P-values were obtained for paired difference using generalized estimating equations (GEE) to account for multiple lesions per patient.

RESULTS

Noise was significantly lower and tumor-to-liver CNR significantly higher between 40 and 60 keV energies using a second- compared to a first-generation monoenergetic algorithm (P <.001 for all comparisons). The highest tumor-to-liver CNR was achieved using the second-generation monoenergetic algorithm at 40 keV, with an approximately 25% improvement in CNR compared to a first-generation algorithm at the optimal energy of 70 keV (Mean [SD] = 4.99 [1.70] vs. 3.80 [2.40]; P <.001). Our data showed that patient body size did not significantly affect the selection of the optimal monoenergetic level using the second-generation monoenergetic algorithm. This is in contrast with the significant impact of body size in the selection of the optimal energy level with the first-generation algorithm.

CONCLUSION

The second-generation monoenergetic algorithm significantly improves the conspicuity of hypervascular liver tumors compared to a first-generation algorithm, while simultaneously decreasing the variability introduced by patient's body weight in selecting the optimal monoenergetic level.

CLINICAL RELEVANCE/APPLICATION

A second-generation monoenergetic algorithm improves the conspicuity of hypervascular liver tumors and may streamline the workflow of DECT by decreasing the variability related to patient's body size.

RC509-08 Dual Energy CT

Wednesday, Dec. 2 10:10AM - 10:30AM Location: E350

Participants Alvin C. Silva, MD, Scottsdale, AZ (*Presenter*) Nothing to Disclose

LEARNING OBJECTIVES

1) Discuss the basic principles and different approaches for Dual-Energy CT. 2) Review common Dual-Energy CT post-processing displays. 3) Describe strategies for implementing Dual-Energy CT in clinical practice.

ABSTRACT

RC509-09 Variability and Effect of Degree of Enhancement on CT Attenuation Measurements in Virtual Unenhanced Images Generated from Fast Kilovoltage Switching Dual-energy CT Using Iodine Material Suppression Algorithm

Wednesday, Dec. 2 10:30AM - 10:40AM Location: E350

Participants Evan A. Raff, MD, Los Angeles, CA (*Abstract Co-Author*) Nothing to Disclose Ravi K. Kaza, MD, Ann Arbor, MI (*Presenter*) Nothing to Disclose Mahmoud M. Al-Hawary, MD, Ann Arbor, MI (*Abstract Co-Author*) Nothing to Disclose Matthew S. Davenport, MD, Cincinnati, OH (*Abstract Co-Author*) Book contract, Wolters Kluwer nv; Book contract, Reed Elsevier; Katherine E. Maturen, MD, Ann Arbor, MI (*Abstract Co-Author*) Consultant, GlaxoSmithKline plc; Medical Advisory Board, GlaxoSmithKline plc

Amit Pandya, MD, Ann Arbor, MI (Abstract Co-Author) Nothing to Disclose

Joel F. Platt, MD, Superior Township, MI (Abstract Co-Author) Nothing to Disclose

PURPOSE

To determine the rate and magnitude of CT number discrepancies between true unenhanced images (TUE) and virtual unenhanced images (VUE) generated from a fast kilovoltage switching dual-energy CT scanner using iodine material suppression algorithm.

METHOD AND MATERIALS

In this IRB-approved HIPAA-compliant retrospective cohort study, 21 multi-phasic abdominal CT examinations (unenhanced, corticomedullary [CM], nephrographic [NG]) obtained on a fast kilovoltage switching dual-energy CT scanner (GE, Milwaukee, WI) were reviewed. VUE images were generated from both dual-energy post-contrast phases using Material Suppressed Iodine (MSI) algorithm. CT numbers were measured on the matched TUE, VUE, and post-contrast images at predefined locations in the liver, pancreas, spleen, left kidney, main portal vein, aorta, and erector spinae muscle. 725 regions of interest were placed at 145 locations. The correlation between VUE and TUE CT numbers was assessed with Pearson's correlation coefficient. Absolute CT number discrepancies and 95% confidence intervals (CI) were calculated for each VUE and TUE comparison. The effect of phase of enhancement on CT number discrepancies was assessed with ANOVA.

RESULTS

Overall, VUE and TUE measurements were not significantly different (p=0.29), and there was a very strong correlation between VUE and TUE CT numbers in both post-contrast phases (CM: r=0.91, NG: r=0.93, p<0.001). The mean difference between TUE and VUE images was 1 HU (95% CI: -7 to +9 HU) for CM phase imaging and 2 HU (95% CI: -6 to +10 HU) for NG phase imaging. Discrepancies \geq 5 HU occurred 36 times (25%, 36/145) in the CM phase and 33 times (23%, 33/145) in the NG phase. Discrepancies \geq 10 HU were rare in both phases (n=4 [CM], n=2 [NG]). Inter-phase VUE imaging differed by a mean of 0.7 HU (95% CI: -7 to +8 HU) between the CM and NG phases in the same subject, with 26 discrepancies \geq 5 HU (18%, 26/145) and 3 discrepancies \geq 10 HU (2%, 3/145). There was no significant correlation between the degree of enhancement and the magnitude of VUE-TUE discrepancies (r = 0.23).

CONCLUSION

CT numbers on VUE images generated from fast kilovoltage switching dual-energy CT scans have a very strong positive correlation to TUE CT numbers and are similar on a population level, but vary on a per-patient level.

CLINICAL RELEVANCE/APPLICATION

Discrepancies in TUE and VUE measurements of 5-9 HU are common and may affect enhancement calculations that rely on VUE data.

Honored Educators

Presenters or authors on this event have been recognized as RSNA Honored Educators for participating in multiple qualifying educational activities. Honored Educators are invested in furthering the profession of radiology by delivering high-quality educational content in their field of study. Learn how you can become an honored educator by visiting the website at: https://www.rsna.org/Honored-Educator-Award/

Katherine E. Maturen, MD - 2014 Honored Educator

RC509-10 Optimization of CT Protocol Using Integrated Automated Protocol Selection Software (GSI Assist) in Single-source Rapid Kilovoltage-switching Spectral CT: The Effect on Radiation Dose

Wednesday, Dec. 2 10:40AM - 10:50AM Location: E350

Participants

Amir Borhani, MD, Pittsburgh, PA (*Abstract Co-Author*) Nothing to Disclose Alessandro Furlan, MD, Pittsburgh, PA (*Abstract Co-Author*) Author, Reed Elsevier; Research Grant, General Electric Company Mark A. Sparrow, MD, Pittsburgh, PA (*Presenter*) Nothing to Disclose Matthew H. Kulzer, MD, Pittsburgh, PA (*Abstract Co-Author*) Nothing to Disclose Mitchell E. Tublin, MD, Pittsburgh, PA (*Abstract Co-Author*) Nothing to Disclose Negar Iranpour, MD, Pittsburgh, PA (*Abstract Co-Author*) Nothing to Disclose

PURPOSE

GSI Assist (GE®) is an automated software which helps with selection of optimal dual-energy CT (DECT) scan parameters based on patient's size and desired level of noise. This software uses scout-based attenuation characteristics to select an appropriate preset that will match (within 20%) the dose of a single-kvp CT scan (SECT). The purpose of this study is to evaluate the radiation dose when using GSI Assist for abdominal CT protocols and to compare the radiation dose of DECT with matched SECT.

METHOD AND MATERIALS

113 consecutive patients who underwent dual-energy CT of the abdomen, using a single source rapid kvp-switching DECT scanner (HD750 GE), were retrospectively reviewed. 43 patients (56 CT examinations) had matched SECT examinations (with comparable noise index, similar collimation, similar body part, and similar phase of contrast) within 2 years. The body part scanned, phase of study, absorbed dose (CTDIvol), dose-length product (DLP), effective dose (ED; using conversion factor of 0.015), body mass index (BMI), and weight were recorded for each scan. CTDIvol, DLP, and ED were compared between matched SECT and DECT examinations using paired t-test. Effect of weight, BMI, and phase of imaging on DECT radiation dose was also evaluated using linear regression analysis and Bland-Altman plot.

RESULTS

Mean CTDIvol and ED were 10.98 mGy (4.26-26.4; SD=5.95) and 7.68 mSv (2.1-21.2; SD=4.2) for DECT as compared to 11.6 mGy

(3.3-25.2; SD=7) and 7.9 mSv (1.7-20.6; SD=4.9) for matched SECT studies, respectively. These values were not statistically different (p=0.4 and 0.7, respectively). DECT radiation dose had significant correlation with patient's weight (R²=0.55; p<0.001) and BMI (R²=0.72; p<0.001), similar to SECT. Although DECT dose to patients with extreme weights (<65kg or >130kg) and extreme BMI (<18 or >30) was slightly higher, the correlation was not statistically significant (R² of 0.15 and 0.07, respectively).

CONCLUSION

There was no statistical difference between radiation dose of DECT and single-kvp CT when an automated software (GSI Assist) was used for optimal protocol selection. The average radiation dose from DECT was well below ACR reference level.

CLINICAL RELEVANCE/APPLICATION

Automated protocol selection software (GSI Assist) allows choosing the optimal abdominal CT technique on single-source dualenergy CT while maintaining the dose at the level of single-kvp CT dose.

RC509-11 Advances in Oncologic Imaging

Wednesday, Dec. 2 10:50AM - 11:10AM Location: E350

Participants

Meghan G. Lubner, MD, Madison, WI, (mgsaur@yahoo.com) (*Presenter*) Grant, General Electric Company; Grant, NeuWave Medical, Inc; Grant, Koninklijke Philips NV

LEARNING OBJECTIVES

1) Briefly define established size-related oncologic response criteria used in CT. 2) Discuss application of volumetric assessment of tumor burden at diagnosis and in assessing response to therapy. 3) Briefly describe selected examples of response assessment criteria looking at other tumor imaging characteristics such as tumor attenuation or enhancement in addition to size. 4) Examine CT tumor texture analysis as an additional tool to evaluate tumor heterogeneity at baseline and during therapy.

ABSTRACT

Honored Educators

Presenters or authors on this event have been recognized as RSNA Honored Educators for participating in multiple qualifying educational activities. Honored Educators are invested in furthering the profession of radiology by delivering high-quality educational content in their field of study. Learn how you can become an honored educator by visiting the website at: https://www.rsna.org/Honored-Educator-Award/

Meghan G. Lubner, MD - 2014 Honored Educator Meghan G. Lubner, MD - 2015 Honored Educator

RC509-12 Texture Characteristics and Mutational Status of Primary Colorectal Cancer

Wednesday, Dec. 2 11:10AM - 11:20AM Location: E350

Participants

Cinthia Cruz, MD, Boston, MA (Presenter) Nothing to Disclose

Synho Do, PhD, Boston, MA (Abstract Co-Author) Nothing to Disclose

James H. Thrall, MD, Boston, MA (*Abstract Co-Author*) Board Member, Mobile Aspects, Inc; Board Member, WorldCare International Inc; Consultant, WorldCare International Inc; Shareholder, Antares Pharma, Inc; Shareholder, iBio, Inc; Shareholder, Peregrine Pharmaceuticals, Inc

Debra A. Gervais, MD, Chestnut Hill, MA (Abstract Co-Author) Nothing to Disclose

PURPOSE

To determine whether there is an association between texture energy of primary lesions of colorectal cancer and their mutational status.

METHOD AND MATERIALS

A total of 24 cases were included. The most frequent mutations [single nucleotide polymorphisms (SNP)] found in a previous study with a cohort of 713 subjects of our institution, were analyzed. Five wild type (WT) tumors, 5 BRAF, 5 KRAS, 4 TP53 and 4 NRAS mutant (M) primary tumors were delineated and extracted from the pretreatment portal-venous phase 5mm slice thickness contrast enhanced CTs, creating a mask. For each phenotype we concatenated acquired texture energy measurements (TEV) for each slice of tumor to form a matrix (N by 9), where N is the number of slices. We computed more than 2000 pixels for each slice and, pixel spacing was normalized to 0.5 mm. Matrixes were used for statistical analysis. Texture analysis was performed using software developed by the laboratory of medical imaging and computation from our institution which includes normalization, filtering, and calculation of texture energy in the primary tumors. Nine different texture energies were compared between genotypes using student T tests, Fisher's Exact Test was used to assess for statistical significance.

RESULTS

Significant differences were found on WT: M texture energy values (TEV)-3,4,5,8 and 9 at 59: 65, 41:47, 30: 37, 63: 72 and 31: 39 (p= 0.005, 0.002 and <0.001 for the latter); on WT: KRAS on TEV-4,5,8 and 9 at 41: 46(p<0.001), 30: 39 (p<0.001), 63: 71 (p=0.003) and 31: 38 (p<0.001). WT: NRAS was significantly different for all TEV-1 through 9(p<0.001), at 724: 838 (16%), 268: 315(17%), 58: 77(33%), 40: 54(35%), 30:40 (31%), 303: 381(26%), 189: 236(25%), 63:78 (24%) and 31:44 (39%). NRAS was most significantly associated with TEVs greater than 16% of WT tumors (p<0.001).

CONCLUSION

Wild type tumors, KRAS and NRAS mutants were found to have distinct texture energy patterns compared with other tumors. WT showed significantly lower texture energy values than mutant tumors. NRAS was most significantly associated to high energy values relative to WT.

Known associations of single nucleotide polymorphisms and clinical and imaging features play a pivotal role in treatment of colorectal cancer. Texture energy analysis is another tool for characterizing tumors using imaging data that can help us to guide genetic-driven biopsies and possibly treatments.

Honored Educators

Presenters or authors on this event have been recognized as RSNA Honored Educators for participating in multiple qualifying educational activities. Honored Educators are invested in furthering the profession of radiology by delivering high-quality educational content in their field of study. Learn how you can become an honored educator by visiting the website at: https://www.rsna.org/Honored-Educator-Award/

Debra A. Gervais, MD - 2012 Honored Educator

RC509-13 N-Staging in Primary Rectal Cancer: Can CT-Perfusion Differentiate between Malignant and Non-Malignant Pelvic Lymph Nodes? Preliminary Results from a Prospective, Blinded Feasibility Study Comparing CT-Perfusion Findings to Histopathology.

Wednesday, Dec. 2 11:20AM - 11:30AM Location: E350

Participants

Zahra Kassam, MD, London, ON (*Presenter*) Nothing to Disclose Kyle Burgers, London, ON (*Abstract Co-Author*) Nothing to Disclose Joanna Walsh, London, ON (*Abstract Co-Author*) Nothing to Disclose Errol E. Stewart, PhD, London, ON (*Abstract Co-Author*) Nothing to Disclose Pavlo Ohorodnyk, MD, London, ON (*Abstract Co-Author*) Nothing to Disclose Barbara J. Fisher, MD, London, ON (*Abstract Co-Author*) Nothing to Disclose Ting-Yim Lee, MSc, PhD, London, ON (*Abstract Co-Author*) Research Grant, General Electric Company Royalties, General Electric Company

PURPOSE

To determine whether CT-Perfusion has the potential to distinguish between malignant and non-malignant lymph nodes in patients with primary rectal cancer.

METHOD AND MATERIALS

18 patients with rectal cancer were evaluated preoperatively with CT-perfusion (CT-P). Dynamic CT-P of the pelvis was performed following IV contrast injection. All visible pelvic lymph nodes were categorized qualitatively by the radiologist as being positive or negative for malignancy. Wherever possible, the inguinal lymph nodes of each patient were used as internal negative controls. Analysis of the lymph nodes included: (1) Visual CT interpretation by the radiologist, (2) CT-Perfusion, and (3) Histopathology (standard of reference). The visual and CT-Perfusion analysis were done independently, by different reviewers. The lymph nodes were assessed for blood flow, blood volume, mean transit time and capillary permeability. Patients with T2 disease were treated surgically with total mesorectal excision (TME); while those with T3/4 or node-positive disease underwent neoadjuvant therapy, followed by repeat CT-P.The nodes within the TME specimen were organized into perirectal zones according to a pre-established regional lymph node map. Ultrastaging of the lymph nodes was performed at 2 mm sections. The pathologist was blinded to the imaging and perfusion results.

RESULTS

Visual interpretation yielded 100 abnormal and 68 normal nodes; sensitivity was 1.0 and specificity was 0.33.CT-P demonstrated a pattern of peripheral perfusion in malignant nodes, while reactive nodes demonstrated homogeneous perfusion. Overall blood flow in non-malignant nodes was significantly higher than in malignant nodes (p<0.000). Analysis revealed 31 abnormal and 104 normal nodes (some nodes could not be evaluated due to motion artifact). Sensitivity was 1.0 and specificity increased to 0.87. The lower size limit for technical lymph node evaluation by CT-P was 3.2 mm.

CONCLUSION

CT-Perfusion shows early promise in N-staging of primary rectal cancer, even in nodes <5 mm. Qualitative N-staging by conventional CT could potentially overstage disease.

CLINICAL RELEVANCE/APPLICATION

Accurate N-staging of small nodes by conventional imaging methods can be challenging. Early results suggest that N-staging by CT-Perfusion has the potential to positively impact patient management, in the settings of (1) Initial diagnosis, (2) Response to therapy, and (3) Assessment of recurrence.

RC509-14 Dual Energy CT Utilization in Clinical Practice: Impact on Workflow and Radiation Doses

Wednesday, Dec. 2 11:30AM - 11:40AM Location: E350

Participants

Yasir Andrabi, MD, MPH, Boston, MA (*Abstract Co-Author*) Nothing to Disclose Manuel Patino, MD, Boston, MA (*Abstract Co-Author*) Nothing to Disclose Rani S. Sewatkar, MBBS, Edison, NJ (*Abstract Co-Author*) Nothing to Disclose Andrea Prochowski Iamurri, MD, Boston, MA (*Abstract Co-Author*) Nothing to Disclose Farhad Mehrkhani, MD, Boston, MA (*Abstract Co-Author*) Nothing to Disclose Avinash R. Kambadakone, MD, Boston, MA (*Abstract Co-Author*) Nothing to Disclose Dushyant V. Sahani, MD, Boston, MA (*Presenter*) Research Grant, General Electric Company; Research Consultant, Allena Pharmaceuticals, Inc

PURPOSE

The growing demand for dual energy (DE) CT has introduced workflow challenges and radiation dose concerns. Therefore we studied the impact of increased DE CT utilization on the CT workflow and radiation doses of cancer FU exams performed in last 2 years.

METHOD AND MATERIALS

In this IRB approved retrospective analysis, 20,325 cancer FU CT exams (age=61.6 years, weight=76.8 kg) performed between Dec 2012 - Mar 2015 on 5 of our scanners (GE Healthcare=3, Siemens=2) were included. Two GE scanners (Discovery CT750 HD) have DE capability and iterative reconstruction algorithms (IRT; ASIR) and remaining 1 is a single energy (SE) scanner (Light Speed Pro) with FBP algorithm. Both Siemens scanners have IRTs (SAFIRE); DE is present on one scanner (Flash). Exams were stratified into 3 groups: Group1: DE exams (DE-GE, DE-Siemens), Group2: SE-FBP and Group3: SE-IRT (ASIR,SAFIRE). Radiation doses were retrieved and compared between different groups and National Averages.

RESULTS

The DE CT constituted 41% of all cancer FU exams (DE-GE=8089, DE-Siemens=208) compared to 59% SE exams (SE-FBP=2075; SE-ASiR=6647; SE-SAFIRE=3306). Three fold increases in DE CT utilization was noted (21% in 2012 and 67% in 2015) with an overall slight increase in the total number of CT exams performed on these scanners. The radiation doses for DE CT exams were substantially (47%) lower than National averages (DIR). Doses were comparable to SE-FBP exams (CTDI(mGy); Group1=10.6 (DE-GE=12.1, DE-Siemens=9.2); Group2=12.4;p>0.05) and nearly 13% higher than SE-IRT scans (Group3=9.3mGy(SE-ASiR=9.6,SE-SAFIRE=8.9); p<0.05). A16% reduction in DE-CT doses were noted in 2015 compared to 2012.

CONCLUSION

There is a threefold increase in the utilization of DE-CT exams for cancer FU exams from last 2 years. DE-CT radiation doses are substantially (47%) lower than national averages, comparable to our institutional SE-FBP cancer FU exams and 13% higher than our SE-IRT scans. There is also a 16% reduction in DE-CT doses from 2012.

CLINICAL RELEVANCE/APPLICATION

There is an increase in DE-CT utilization due to its growing clinical applications. These exams have different acquizition and postprocessing demands, thus, raising work flow and radiation dose concerns. Our study indicates that DE CT exams do not interfere with the work flow and the radiation doses are also in the acceptable range for diagnostic CT exams.

Honored Educators

Presenters or authors on this event have been recognized as RSNA Honored Educators for participating in multiple qualifying educational activities. Honored Educators are invested in furthering the profession of radiology by delivering high-quality educational content in their field of study. Learn how you can become an honored educator by visiting the website at: https://www.rsna.org/Honored-Educator-Award/

Dushyant V. Sahani, MD - 2012 Honored Educator Dushyant V. Sahani, MD - 2015 Honored Educator

RC509-15 CT Workflow Issues

Wednesday, Dec. 2 11:40AM - 12:00PM Location: E350

Participants

Dushyant V. Sahani, MD, Boston, MA (*Presenter*) Research Grant, General Electric Company; Research Consultant, Allena Pharmaceuticals, Inc

Honored Educators

Presenters or authors on this event have been recognized as RSNA Honored Educators for participating in multiple qualifying educational activities. Honored Educators are invested in furthering the profession of radiology by delivering high-quality educational content in their field of study. Learn how you can become an honored educator by visiting the website at: https://www.rsna.org/Honored-Educator-Award/

Dushyant V. Sahani, MD - 2012 Honored Educator Dushyant V. Sahani, MD - 2015 Honored Educator Second and Third Trimester Obstetrical Ultrasound (An Interactive Session)

Wednesday, Dec. 2 8:30AM - 10:00AM Location: E450B

GU OB US

AMA PRA Category 1 Credits ™: 1.50 ARRT Category A+ Credits: 1.50

Participants

LEARNING OBJECTIVES

Please bring your charged mobile wireless device (phone, tablet or laptop) to participate.

Sub-Events

RC510A 3D Ultrasound in Obstetrics

Participants Beryl R. Benacerraf, MD, Brookline, MA (*Presenter*) Nothing to Disclose

LEARNING OBJECTIVES

1) To learn the principles of 3D sonography and the applications for fetal scanning. To evaluate clinical situations where 3D scanning is helpful and where it is not useful beyond the 2D examination. 2) To see examples of fetal malformations scanned in 3D using surface rendering and multiplanar reconstruction. 3) To learn how to use volume scanning to dramatically reduce scan time and improve you scanning efficiency by rescanning stored volumes of complete fetal anatomy.

ABSTRACT

Three-dimensional (3D) ultrasound allows us to acquire a volume and display any plane of section within that volume regardless of the scanning orientation. The ability to display a 3D image of any type or plane has been one of the most powerful recent advances in sonography, particularly in the field of obstetrics and gynecology. In imaging of the fetus, 3D ultrasound is advantageous in demonstrating many types of fetal defects and dysmorphologic facial features using surface rendering. The fetal brain is also one of the areas where 3D ultrasound has been most helpful, since the reconstruction of the third non-scanning plane is crucial in demonstrating planes of section not previously visible sonographically. The corpus callosum is an example of one area not readily imaginable in standard imaging planes. The fetal sutures are also easy to image with 3D, which is particularly helpful in fetuses with suspected craniosynostosis. 3D ultrasound is key for imaging fetal skeletal abnormalities, providing additional information on affected fetuses as compared to 2D. Evaluation of the spine using 3D has been helpful to determine the level of spina bifida, thus providing crucial information regarding prognosis. Evaluation of the fetal heart is an intense area of research interest, and the heart can be imaged in realtime 3D (4D) using a method called STIC. This method provides the ability to obtain a full volume of the beating heart to evaluate in detail off line with or without color Doppler and while it is beating.Volume imaging is also key in improving efficiency of the ultrasound department. The entire fetus can be imaged easily by acquiring and archiving a few volumes. This way, the patient can spend far less time in the ultrasound room and the entire scan can be done remotely and virtually using the stored volumes. This techniques reduces operator dependency usually associated with 2D ultrasound.

RC510B Fetal Genitourinary Anomalies

Participants

Roya Sohaey, MD, Portland, OR (Presenter) Nothing to Disclose

LEARNING OBJECTIVES

1) Apply the Urinary Tract Dilation classification system to fetal imaging practice. 2) Develop an anatomic approach for differential diagnosis of urinary tract obstruction. 3) Develop an understanding of which cases would benefit from fetal MR.

ABSTRACT

By the conclusion of this course, the participant will be able to apply the prenatal UrinaryTract Dilation (UTD) classification system for diagnosis and follow-up planning. The learner will develop an anatomic approach towards differential diagnosis for obstructive causes of UTD, renal cystic dysplasia and complex genitourinary anomalies. In addition, a fetal sex-based approach for analysis of complex lower tract anomalies will be discussed. The course will demonstrate how fetal MR is useful as a problem solving tool in certain complex cases. The lecture is didactic and case-based in format.

RC510C Placenta

Participants Sara M. Durfee, MD, Boston, MA (*Presenter*) Nothing to Disclose

LEARNING OBJECTIVES

1) Identify the cause of vaginal bleeding in patients with placental abnormalities that include placenta previa and placental abruption. 2) Describe the sonographic features of placenta accreta. 3) Define trophotropism and describe how this process leads to both normal and abnormal placentation.

ABSTRACT

After this presentation, the participant will understand how the normal placenta develops and how factors such as trophotropism lead to placental abnormalities. Specific abnormalities such as placenta previa, placental abruption and placenta accreta will be

addressed in detail. In addition, first trimester abnormalities such as the chorionic bump and subchorionic hematomas will be discussed. The presenter will describe the sonographic appearance of succenturiate lobe, circumvallate placenta and sonolucencies within the placenta and will comment on placental masses.

Trauma Imaging Pitfalls

Wednesday, Dec. 2 8:30AM - 10:00AM Location: E353C

ER

AMA PRA Category 1 Credits ™: 1.50 ARRT Category A+ Credits: 1.50

Participants

Sub-Events

RC508A Chest Trauma Imaging Pitfalls

Participants

Felipe Munera, MD, Miami, FL, (fmunera@med.miami.edu) (Presenter) Nothing to Disclose

LEARNING OBJECTIVES

1) Review the MDCT findings of Aortic Diaphragmatic injuries. 2) Describe potential diagnostic pitfalls and mimics aortic and diaphragmatic injuries.

ABSTRACT

Thoracic injuries are the third most common injuries in blunt trauma. The purpose of this lecture is not an exhaustive review of all the potential traumatic thoracic injuries but rather to focus on two areas of particular concern, acute traumatic aortic injury and diaphragmatic injuries. Key imaging findings and potential pitfalls in recognizing blunt and penetrating traumatic injuries to the diaphragm and thoracic aorta will be discussed. Diagnosing aortic and diaphragmatic injuries each present unique challenges. Recognition of traumatic aortic and diaphragmatic injuries is important to allow for timely treatment, as delays in diagnosis can lead to increased morbidity and mortality.

RC508B Abdominal Trauma Imaging Pitfalls

Participants

Michael N. Patlas, MD, FRCPC, Hamilton, ON, (patlas@hhsc.ca) (Presenter) Nothing to Disclose

LEARNING OBJECTIVES

1)To discuss common pitfalls in interpretation of cases of blunt and penetrating abdominal trauma. 2)To analyze factors leading to errors. 3)To discuss advantages of different phases of imaging and multiplanar reconstructions (MPRs) for detection of traumatic injuries.

ABSTRACT

MDCT have led to a paradigm shift in the management of abdominal injuries minimizing the role of laparotomy. To this end, an awareness of pitfalls of MDCT detection of these injuries is of increasing importance. Bowel and mesenteric injuries are uncommon. Delayed diagnosis of bowel and mesenteric injuries may result in disastrous complications and high mortality rates. This presentation will focus on imaging pearls and pitfalls in detection of blunt and penetrating bowel and mesenteric injuries. The presentation will also cover pitfalls in diagnosis of pancreatic, biliary, adrenal and ureteric injuries.

RC508C Pelvic Trauma Imaging Pitfalls

Participants

Guillermo P. Sangster, MD, Shreveport, LA, (gsangs@lsuhsc.edu) (Presenter) Nothing to Disclose

LEARNING OBJECTIVES

1) Discuss potential imaging pitfalls and mimics that may be misinterpreted as traumatic pelvic injuries. 2) Substantiate the advantages of Multidetector computed tomography (MDCT) for the screening of stable patients suspected to have traumatic pelvic injuries. 3) Differentiate intra and extraperitoneal pelvic injuries in patients suffering blunt and penetrating trauma.

ABSTRACT

Pelvis traumatic injuries range from benign to life threatening conditions. MDCT is the imaging modality of choice for evaluation of hemodynamically stable patients with pelvic trauma. This live activity demonstrates the benefits of MDCT in the detection and preoperative planning of patients sustaining pelvic injuries. Subtle signs should be recognized for timely diagnosis, and familiarity with potential mimics is key to avoid unnecessary procedures.

RC508D Extremity Trauma Imaging Pitfalls

Participants

O. Clark West, MD, Houston, TX (Presenter) Nothing to Disclose

LEARNING OBJECTIVES

1) Identify extremity injuries that are difficult detect on screening radiographs. 2) Illustrate search patterns that may improve detection of easily missed injuries. 3) Design clinical pathways using advanced imaging and/or follow-up radiography to detect radiographically occult injuries.

ABSTRACT

Take home messages: •Posterior shoulder dislocation: narrow gleno-humeral joint, loss of parallel articular surfaces, fixed internal rotation on multiple views andtrough impaction fracture. •Supracondylar fracture: anterior humeral line should intersect middle 50% of capitellum on well positioned lateral view. •Monteggia fracture-dislocation: radio-capitellar line should intersect the capitellum in ALL projections •Proximal radius- Vertical head fracture (external oblique view) - Impacted neck fracture - Flipped radial head fracture-dislocation • Galeazzi fracture-dislocation - beware ascribing DRUJ dislocation to poor positioning of lateral radiograph. For trauma, obtain 3 views of joints: •Axillary view of shoulder • External oblique of elbow • Wrist 4 view: PA, lateral, external oblique and "Scaphoid" view (ulnar deviated PA view) • Pearl for the day: watch for the least obvious of multiple injuries

Handout:O. Clark West

http://abstract.rsna.org/uploads/2015/15003347/WestOC_Trauma Imaging Pitfalls Upper Extremity_RSNA 2015 Handout.pdf

Changing the Way Radiologists Work: How and Why We Need to Embrace a Culture of Safety

Wednesday, Dec. 2 8:30AM - 10:00AM Location: E351

HP SQ

AMA PRA Category 1 Credits ™: 1.50 ARRT Category A+ Credits: 1.50

Participants

Kimberly E. Applegate, MD, MS, Zionsville, IN, (keapple@emory.edu) (*Coordinator*) Nothing to Disclose Kimberly E. Applegate, MD, MS, Zionsville, IN, (keapple@emory.edu) (*Moderator*) Nothing to Disclose Giles W. Boland, MD, Boston, MA (*Presenter*) Principal, Radiology Consulting Group; Royalties, Reed Elsevier Nabile M. Safdar, MD, Alpharetta, GA (*Presenter*) Shareholder, Montage Healthcare Solutions, Inc;

LEARNING OBJECTIVES

1) To describe how technology can accelerate an existing culture of safety in radiology. 2) To assess the risks of poor technology implementations when there is a weak safety culture. 3) To identify the highest impact opportunities for improving safety in one's practice through technology. 4) To assess the maturity of one's informatics infrastructure to support a safety program.

Vascular Series: CT Angiography: New Techniques and Their Application

Wednesday, Dec. 2 8:30AM - 12:00PM Location: E352

VA CT

AMA PRA Category 1 Credits ™: 3.25 ARRT Category A+ Credits: 4.00

FDA Discussions may include off-label uses.

Participants

Dominik Fleischmann, MD, Palo Alto, CA (Moderator) Research support, Siemens AG;

Handout:Dominik Fleischmann

http://abstract.rsna.org/uploads/2015/15003239/Fleischmann_RSNA2015_Contrast.pdf

Sub-Events

RC512-01 Iterative Image Reconstruction

Wednesday, Dec. 2 8:30AM - 8:55AM Location: E352

Participants

Norbert J. Pelc, ScD, Stanford, CA (*Presenter*) Research support, General Electric Company; Research support, Koninklijke Philips NV; Consultant, Varian Medical Systems, Inc; Consultant, NanoX; Scientific Advisory Board, RefleXion Medical Inc; Scientific Advisory Board, Prismatic Sensors AB; Medical Advisory Board, OurCrowd, LP;

LEARNING OBJECTIVES

1) Understand the basic concepts behind iterative reconstruction algorithms. 2) Understand the differences between these methods and conventional reconstruction. 3) Appreciate the potential advantages and disadvantages of iterative methods.

ABSTRACT

For many decades, essentially all CT images have been reconstructed using an "analytic" algorithm, such as filtered backprojection. These methods are computationally efficient, allowing fast image reconstruction, and if the raw data are of high quality the images can be exact. As the dose is reduced or if there are deterministic errors in the data, analytic reconstruction may produce lower image quality than may be possible. Iterative reconstruction methods can build in knowledge of measurement noise and other errors and yield higher image quality. They can produce lower noise images in low dose settings and in some cases higher spatial resolution. Iterative methods are generally nonlinear, meaning that the image quality depends on the object being scanned. They also produce images whose properties are "non-stationary", meaning that the image quality can vary significantly across the image. Understanding these allows the user to best evaluate their performance and appropriately use them in clinical settings.

RC512-02 Impact of Iterative Reconstruction and Improved Spatial Resolution in CT Angiography (CTA) of Fenestrated Stent Grafts

Wednesday, Dec. 2 8:55AM - 9:05AM Location: E352

Participants

Terri J. Vrtiska, MD, Rochester, MN (*Presenter*) Nothing to Disclose Juan Montoya, Rochester, MN (*Abstract Co-Author*) Nothing to Disclose Thanila A. Macedo, MD, Rochester, MN (*Abstract Co-Author*) Nothing to Disclose Thomas A. Foley, MD, Rochester, MN (*Abstract Co-Author*) Nothing to Disclose Ying Huang, MD,PhD, Rochester, MN (*Abstract Co-Author*) Nothing to Disclose Nikkole Weber, Rochester, MN (*Abstract Co-Author*) Nothing to Disclose Cynthia H. McCollough, PhD, Rochester, MN (*Abstract Co-Author*) Research Grant, Siemens AG Joel G. Fletcher, MD, Rochester, MN (*Abstract Co-Author*) Grant, Siemens AG; ;

PURPOSE

To determine if improved spatial resolution and advanced model iterative reconstruction (IR) could improve confidence or reduce artifacts at CTA in patients with fenestrated stent grafts (FSGs).

METHOD AND MATERIALS

Patients with FSGs underwent 2 CTA exams, one using a CT system with IR and improved spatial resolution (System A: Somatom Force, Siemens), and the other without IR (System B: Somatom Definition Flash or Sensation 64, Siemens). A kV selection/chart and identical slice thickness were used for both exams. Anonymized images from each system were reviewed by a 2 radiologists in side-by-side comparison, with readers specifying preference and rationale. In a separate session, readers evaluated each artery with a stent for stenosis (0=none to 3=>80%) and intraluminal artifacts (0=none to 4=non-diagnostic). Occlusion, in-stent neointimal hyperplasia, and kinks were also noted (present vs. not). Confidence for each parameter was recorded (0=uncertain to 9=completely confident). Slice-specific CTDIvol at the proximal portion of each artery was recorded from the DICOM header.

RESULTS

21 pts with FSGs having 73 vessels with stents (14 Celiac, 18 SMA, 41 renal) underwent CTA on both CT systems. System A used lower tube potentials across the study cohort. The slice-specific CTDIvol with System A was lower (mean diff -13%). In 86% (36/42) of side by side comparisons, System A was preferred due to better in-stent visualization (n=8), less noise (n=22), and fewer artifacts (n=14). System B was preferred in 5 cases with increased metal artifacts but lower slice-specific radiation dose. When in-slice radiation dose of System A was \geq 10% lower than System B, mean intraluminal artifacts scores were lower for System A (1.8 vs. 2.1, p<0.01) and confidence for in-stent stenosis was higher (7.2 vs. 6.5, p<0.002). Otherwise, there was no

difference in artifact score, stenosis, occlusion, kink or artifact (p>0.34), except that System B had a higher confidence for neointimal hyperplasia (7.6 vs. 6.8, p=0.02).

CONCLUSION

Improved spatial resolution and IR were visually preferred in unblinded comparisons, and resulted in higher confidence for in-stent visualization at lower relative doses.

CLINICAL RELEVANCE/APPLICATION

Improved spatial resolution and IR can improve confidence and reduce stent-related artifacts at lower dose levels, which facilitates surveillance in patients with fenestrated endografts.

RC512-03 Assessment of Adamkiewicz Artery Using Low Dose Multi-detector Computed Tomography with Novel Iterative Model-based Reconstruction Technique

Wednesday, Dec. 2 9:05AM - 9:15AM Location: E352

Participants

Tae Hyun Nam, Seongnam-Si, Korea, Republic Of (*Presenter*) Nothing to Disclose Eun Ju Chun, MD, PhD, Seongnam-Si, Korea, Republic Of (*Abstract Co-Author*) Nothing to Disclose Hyo Jin Kim, Seoul, Korea, Republic Of (*Abstract Co-Author*) Nothing to Disclose Bon Seoung Gu, Seongnam, Korea, Republic Of (*Abstract Co-Author*) Nothing to Disclose Soon Ahn Kwon, Seongnam-si, Korea, Republic Of (*Abstract Co-Author*) Nothing to Disclose Gwan Hong Min, Seongnam-si, Korea, Republic Of (*Abstract Co-Author*) Nothing to Disclose

PURPOSE

To compare the visualization of the Adamkiewicz artery (AKA) on multi-detector computed tomography (MDCT) with novel iterative model-based reconstruction (IMR) in comparison to the iterative reconstruction (iDOSE) and filtered back projection (FBP) when the low dose CT protocol was applied.

METHOD AND MATERIALS

Forty patients (male 65.0%, mean age 65±16 years) with aortic aneurysm or dissection who underwent 256-slice MDCT with low dose CT protocol (100 kVp and 20 mA) were enrolled. Acquired raw data were reconstructed by using FBP, median level of iDOSE (iDOSE4) and IMR, and analyzed blindly by two observers. In the quantitative analysis, the signal-to-noise ratio (SNR) of the aorta and contrast-to-noise ratio (CNR) of the anterior spinal artery relative to the spinal cord were measured on multi-planar reformatted images. In qualitative analysis, the visualization of the AKA and its continuity with the intercostal or the lumbar artery were evaluated by using a four-point scale (1, poor to 4, excellent). The visualization scale of 3 or 4 was considered assessable. The one-way analysis of variance was used to evaluate the image quality of three reconstruction algorithm.

RESULTS

The interobserver agreement was good for SNR (k=0.94) and fair for CNR (k=0.73). In qualitative analysis, both SNR and CNR of IMR (SNR, 29.4 \pm 7.3; CNR, 4.8 \pm 1.7) were significantly higher than iDOSE (SNR, 20.3 \pm 6.2; CNR, 3.7 \pm 1.4) and FBP (SNR, 14.3 \pm 3.1, CNR, 3.2 \pm 1.2) (P<.05 for all comparisons). The visualization of AKA was also significantly better in IMR (3.7 \pm 0.5) from than iDOSE (3.0 \pm 0.9) and FBP (2.5 \pm 0.7) (p-value <.05). The prevalence of the assessable AKA was highest in IMR (87.5%) followed by iDOSE (70.0%) and FBP (42.5%) (p<0.05).

CONCLUSION

IMR algorithm led to improving the visualization of the AKA compared to the use of iDOSE and FBP when the low dose CT protocol was applied.

CLINICAL RELEVANCE/APPLICATION

Presurgical localization of the AKA is very important for protecting the spinal cord injury. As compared to iDOSE and FBP, novel IMR algorithm is helpful for evaluation of the AKA.

RC512-04 CT-angiography (CTA) with Low kV and Low Contrast Medium Volume Using a 256 Multi Detector CT Scanner (MDCT) in the Evaluation of Abdominal Aorta Disease: Diagnostic Efficacy and Radiation Dose Reduct

Wednesday, Dec. 2 9:15AM - 9:25AM Location: E352

Participants

Cammillo R. Talei Franzesi, Milan, Italy (*Presenter*) Nothing to Disclose Davide Ippolito, MD, Monza, Italy (*Abstract Co-Author*) Nothing to Disclose Davide Fior, MD, Monza, Italy (*Abstract Co-Author*) Nothing to Disclose Pietro A. Bonaffini, MD, Monza, Italy (*Abstract Co-Author*) Nothing to Disclose Maria V. Schiavone, MD, Monza, Italy (*Abstract Co-Author*) Nothing to Disclose Sandro Sironi, MD, Monza, Italy (*Abstract Co-Author*) Nothing to Disclose

PURPOSE

To reduce the radiation dose exposure and the contrast medium volume by using low-kV setting CT-angiography (CTA) protocol, in the evaluation of abdominal aorta disease.

METHOD AND MATERIALS

From January 2013 to December 2014, 60 patients (23 women and 37 men; mean age 64.2 years; range, 34-83 years) with abdominal aorta disease were prospectively enrolled in our study. All patients underwent 256 MDCT scan examination of abdominal aorta (Brilliance-iCT, Philips, NL). Thirty-four patients were evaluated using low-dose radiation protocol (100 kV; automated tube current modulation) and low-contrast volume (30 mL; 4 mL/s; 350 mgI/mL). Twenty-six patients, as control group, underwent standard CTA protocol (120 kV; automated tube current modulation), with 80 mL of contrast medium volume. Intravessels density

measurements (HU) were performed manually drawing a region of interest (ROI) in the lumen of abdominal aorta, renal arteries and common iliac arteries. The radiation dose exposure (dose-length product, DLP; CT dose index, CTDIvol) and the signal-to-noise-ratio (SNR) were calculated. The obtained data were then compared between the two groups and statistically analysed.

RESULTS

All exams reached high diagnostic quality, permitting to correctly visualize and evaluate the lumen and wall of the main aortic branches. In the study group higher density measurements were observed as compared to control group, in abdominal aorta (mean attenuation value 332 HU vs 318 HU), renal arteries (341 HU vs 305 HU) and common iliac arteries (324 HU vs 311 HU). No significant noise increase was observed in the study group (mean signal to noise ratio, SNR 14.3) in comparison to control group (SNR 18.2). A significant (p<0.05) reduction in radiation dose exposure was achieved using low-kV protocol (DLP 335 mGy*cm, CTDIvol 5.8 mGy), as compared to control group (DLP 973 mGy*cm; CTDIvol 19.4 mGy), with an overall radiation dose reduction of 65%.

CONCLUSION

Low kV protocol with low contrast medium volume allows reducing the radiation dose exposure, preserving the renal function, in the evaluation of patients with abdominal vascular disease.

CLINICAL RELEVANCE/APPLICATION

Low-kV protocol with low contrast media volume reduces the radiation exposure, preserving renal function and providing an effective tool for the evaluation of patients with abdominal vascular disease.

RC512-05 Impact of Noise-Optimized Virtual Monochromatic Imaging at Third-Generation Dual-Source Dual-Energy CT Angiography of the Lower Extremity Run-off

Wednesday, Dec. 2 9:25AM - 9:35AM Location: E352

Participants

Julian L. Wichmann, MD, Charleston, SC (*Presenter*) Nothing to Disclose
Matthew R. Gillott, MD, Charleston, SC (*Abstract Co-Author*) Nothing to Disclose
Carlo N. De Cecco, MD, PhD, Charleston, SC (*Abstract Co-Author*) Nothing to Disclose
Akos Varga-Szemes, MD, PhD, Charleston, SC (*Abstract Co-Author*) Nothing to Disclose
Thomas J. Vogl, MD, PhD, Frankfurt, Germany (*Abstract Co-Author*) Nothing to Disclose
U. Joseph Schoepf, MD, Charleston, SC (*Abstract Co-Author*) Research Grant, Bracco Group; Research Grant, Bayer AG; Research Grant, General Electric Company; Research Grant, Siemens AG; Research support, Bayer AG; ;
Ricardo Yamada, MD, Charleston, SC (*Abstract Co-Author*) Nothing to Disclose
Marcelo Guimaraes, Charleston, SC (*Abstract Co-Author*) Nothing to Disclose
Marcelo Guimaraes, Charleston, SC (*Abstract Co-Author*) Nothing to Disclose
Gonsultant, Terumo Corporation; Patent holder, Cook Group Incorporated ; Consultant, Baylis Medical
Company; Consultant, Terumo Corporation; Patent holder, Cook Group Incorporated
Stefanie Mangold, MD, Charleston, SC (*Abstract Co-Author*) Nothing to Disclose
Giuseppe Muscogiuri, MD, Charleston, SC (*Abstract Co-Author*) Nothing to Disclose
Stephen R. Fuller, Charleston, SC (*Abstract Co-Author*) Nothing to Disclose
Christian Canstein, Charleston, SC (*Abstract Co-Author*) Nothing to Disclose

PURPOSE

To assess the impact of a noise-optimized image-based virtual monochromatic imaging algorithm (VMI+) on objective and subjective image quality at third-generation dual-source dual-energy CT angiography (CTA) of the lower extremity run-off.

METHOD AND MATERIALS

We retrospectively evaluated dual-energy CTA studies of the lower extremity run-off in 48 patients (32 male, 16 female; mean age 63.3 \pm 13.8 years) performed on a third-generation dual-source CT system. Images were reconstructed with standard linear blending (F_0.5) representing 120-kVp polychromatic acquisition, VMI+ and traditional monochromatic (VMI) algorithms at 40-120 keV energy levels in 10-keV increments. Vascular attenuation and image noise in 18 run-off artery segments were measured; signal-to-noise ratio (SNR) and contrast-to-noise ratio (CNR) were calculated. Two observers used five-point scales to subjectively evaluate vascular attenuation and image noise.

RESULTS

Objective image quality metrics peaked in the 40 and 50 keV VMI+ series (SNR: 20.2 ± 10.7 and 19.0 ± 9.5 , respectively; CNR: 18.5 \pm 10.3 and 16.8 \pm 9.1, respectively) and were significantly (all P <0.0001) higher compared to the corresponding 40 and 50 keV VMI series (SNR: 8.7 \pm 4.1 and 10.8 \pm 5.0; CNR: 8.0 \pm 4.0 and 9.6 \pm 4.9) and the standard linearly-blended F_0.5 datasets (SNR: 10.7 \pm 4.4; CNR: 8.3 \pm 4.1). Subjective assessment of attenuation was highest for the 40 and 50 keV VMI and VMI+ image series (range, 4.84-4.91), both superior to F_0.5 (4.07; P <0.0001). Corresponding subjective noise assessment was superior for 50 keV VMI+ (4.71; all P <0.0001) compared to corresponding VMI (2.60) and F_0.5 (4.11).

CONCLUSION

Image reconstruction with VMI+ at low keV levels (40-50 keV) improves objective and subjective image quality compared to traditional VMI and standard linear blending reconstructions at dual-energy CTA of the lower extremity run-off.

CLINICAL RELEVANCE/APPLICATION

Improved image quality using VMI+ may improve evaluation and diagnosis in lower extremity run-off dual-energy CTA cases with suboptimal vascular opacification and potentially facilitate reduction of iodine load.

RC512-06 Salvage of Suboptimal CT Angiographic Studies Using Virtual Monoenergetic Images from Novel Spectral Detector CT Scanner

Wednesday, Dec. 2 9:35AM - 9:45AM Location: E352

Majid Chalian, MD, Cleveland Heights, OH (*Abstract Co-Author*) Nothing to Disclose Mojgan Hojjati, MD, Cleveland, OH (*Abstract Co-Author*) Nothing to Disclose Amar Dhanantwari, PhD, Highland Heights, OH (*Abstract Co-Author*) Employee, Koninklijke Philips NV Prabhakar Rajiah, MD, FRCR, Cleveland, OH (*Abstract Co-Author*) Institutional Research Grant, Koninklijke Philips NV

PURPOSE

To evaluate the ability of spectral detector CT (SDCT), a novel dual-layer technology to salvage suboptimal CT angiographic studies utilizing retrospectively generated virtual monoenergetic images.

METHOD AND MATERIALS

This study included 17 patients who had CTA on SDCT prototype (Philips Healthcare, Cleveland, OH, USA) and had a suboptimal study, defined as aortic attenuation < 200 HU. Monochromatic image sets were generated at 40, 50, 60, 70, 80 kev. Attenuation, noise, SNR and CNR were measured at ascending aorta (AA), descending aorta (DA), aortic root (AR), LAD, and left ventricle (LV). Subjective evaluation of vascular enhancement, image noise and overall image quality were graded on a 5-point scale (1- Non diagnostic, 5- excellent) by cardiac imager. From the monoenergetic reconstructions, an ideal set was chosen, defined as the highest energy that provided a mean attenuation value of > 200 HU, while maintaining good image quality. At this ideal energy level, attenuation, noise, SNR and subjective image quality were compared to standard 120 kVp polyenergetic study. Paired t-test was used for analysis of quantitative variables. Qualitative analysis was done using Chi-square test.

RESULTS

Mean attenuation in the conventional images was 175.9+/-55.9 HU, 188.9+/-70.4 HU, 178.2+/-67.1 HU, 164.6+/-60.1 HU, and 153.3+/-86.1 HU in the AA, DA, AR, LV, and LAD, respectively. With monochromatic images, there was improved attenuation at 40, 50, 60, 70, 80 keV levels (p value < 0.001 for all) in all pateints. 50 keV image provided the best subjective image quality (4.1 vs. 1.5 on conventional images, p=0.017). Attenuation (175.9+/-55.9 vs. 334.7+/-126.8 HU, p<0.001), SNR (10.5+/-9.0 vs. 18.2+/-14.2, p<0.001) and CNR (16.0+/-13.9 vs. 25.4+/-20.2, p=0.001) of AA was significantly higher at 50 keV as compared to the conventional polychromatic images. Similar trends were seen in other structures. Attenuation, CNR, and SNR increased for 46.5%, 37.5%, and 41.5% at 50 keV compared to conventional 120 keV.

CONCLUSION

All suboptimal CTAs were salvaged using low monoenergetic reconstruction. At the optimal monoenergetic level, the attenuation, SNR, CNR and image quality were significantly higher than that of conventional polychromatic image.

CLINICAL RELEVANCE/APPLICATION

Suboptimal angiographic studies can be salvaged using SDCT, thus obviating the need for additional contrast and radiation.

Honored Educators

Presenters or authors on this event have been recognized as RSNA Honored Educators for participating in multiple qualifying educational activities. Honored Educators are invested in furthering the profession of radiology by delivering high-quality educational content in their field of study. Learn how you can become an honored educator by visiting the website at: https://www.rsna.org/Honored-Educator-Award/

Prabhakar Rajiah, MD, FRCR - 2014 Honored Educator

RC512-07 Dual-energy and Low kVp CTA

Wednesday, Dec. 2 9:45AM - 10:10AM Location: E352

Participants

Thomas Henzler, MD, Mannheim, Germany, (thomas.henzler@medma.uni-heidelberg.de) (Presenter) Nothing to Disclose

LEARNING OBJECTIVES

1) The lecture will review the technical background behind dual-energy CT and primarily acquired low kVp single energy CT angiography. 2) Advantages and disadvantages between dual energy CT angiography and low kVp CT angiography are discussed. 3) Practical advices for different CTA protocols are given. 4) The clinical impact of the techniques regarding radiation dose reduction as well as contrast medium reduction will be discussed.

RC512-08 Implications for Contrast Medium Delivery

Wednesday, Dec. 2 10:20AM - 10:45AM Location: E352

Participants

Dominik Fleischmann, MD, Palo Alto, CA (Presenter) Research support, Siemens AG;

LEARNING OBJECTIVES

1) Physics of kVp dependent attenuation of x-rays (see previous lecture). 2) Physiologic principles (rules) of early artrial enhancement following intravenous contrast medium injection. 3) Potential limitations and disadvantages of low-contrast protocols in clinical practice.

ABSTRACT

Advances x-ray tubes technology allow the routine use of lower kVp settings for CT data acquisition. Lower kVp increases the xray attenuation of iodine relative to soft tissues, with the potential to either increase vascular opacification for the same contrast medium volume, or decrease the total contrast medium volume while maintaining image contrast.Judicious selection and modification of contrast medium injection parameters requires not only a basic understanding of the physics of kVp-dependent x-ray attenuation of x-rays (see previos presentation in this course), but also a fundamental understanding or early arterial contrast dynamics, and the potential limitations of reducing contrast medium volume for a given cardiovascular CT exam.CONTRAST PHYSIOLOGY: early arterial contrast medium dynamics can be summarized by four basic rules describing arterial opacification as a function of intravenous contrast administration:(1) Arterial enhancement is proportional to the contrast medium injection rate (iodine / second) (2) Arterial enhancement also increases in a cumulative fashion with a longer injection duration(3) The main physiologic parameter controlling the strength of arterial enhancement is cardiac output(4) For large (runoff) or diseased (aneurysms) vasular territories, the contrast medium transit time within a vascular territory has to be accounted for.LIMITATIONS OF REDUCING CONTRAST MEDIUM VOLUME: While theoretically the contrast/noise ratio may be unchanged when a low kVp / low contrast medium volume protocol is used, such calculations are based on well opacified large vessels, where the high vascular attenuation suggests that an increase in image noise can be tolerated. However, relevant vascular features are often displayed in less attenuated small vessels or vascular borders which are affected by partial volume, and both, 3D visualization and quantitative measurements may in fact be less accurate.Any study-design aimed at assessing a low-contrast medium volume protocol thus requires a rigorous design that proves equal or better image quality. Furthermore - since low-contrast medium volume protocols are inherently justified by the perceived harm of intravenous contrast use - a study design also needs to demonstrate that a new low-dose protocol in fact reduces harm in the population of interest.

RC512-09 Low Contrast Media Volume for CTA of the Aorta: Individualized Protocols Adapted to the Tube Voltage

Wednesday, Dec. 2 10:45AM - 10:55AM Location: E352

Participants

Kai Higashigaito, Zurich, Switzerland (*Presenter*) Nothing to Disclose Tabea Schmid-Rueegger, Zurich, Switzerland (*Abstract Co-Author*) Nothing to Disclose Gilbert Puippe, Zurich, Switzerland (*Abstract Co-Author*) Nothing to Disclose Fabian Morsbach, Zurich, Switzerland (*Abstract Co-Author*) Nothing to Disclose Thomas Pfamatter, MD, Zurich, Switzerland (*Abstract Co-Author*) Nothing to Disclose Hatem Alkadhi, MD, Zurich, Switzerland (*Abstract Co-Author*) Nothing to Disclose Daniela B. Husarik, MD, Zurich, Switzerland (*Abstract Co-Author*) Nothing to Disclose

PURPOSE

To investigate into tube voltage-adapted contrast media (CM) volume reduction protocols for CT-angiography (CTA) of the aorta using automated attenuation-based tube voltage selection (ATVS).

METHOD AND MATERIALS

In this prospective, IRB approved study, 190 patients (69.6±11.3 years) undergoing thoracoabdominal CTA with ATVS (ref.kVp=110, ref.mAs=130) on a 192-slice dual-source CT were included. Intravenous contrast media (CM) volume was adapted based on iodine attenuation curves derived from a phantom study and depending on automatically selected tube voltages (range: 80-110kVp at 10kVp intervals). CM volume and injection rate decreased at a maintained bolus length from 110kVp (68 ml@3.6 ml/s) to 80kVp (33 ml@1.8 ml/s). Subjective image quality was assessed by three blinded, independent readers. Objective image quality (aortic attenuation and contrast-to-noise ratio [CNR]) was determined. Volume CT-dose-index (CTDIvol) and size-specific dose estimates (SSDE) were recorded. Cohen's kappa was calculated to evaluate inter-reader agreements. Linear regression was used to assess relationships between selected tube voltage and aortic attenuation/CNR.

RESULTS

62 Patients were imaged at 80kVp, 84 at 90kVp, 33 at 100kVp and 11 at 110kVp. Agreements between the three readers were good for subjective image quality ($\kappa = 0.691$). Diagnostic image quality was achieved in 96.9% of scans. Scans at 80kVp showed mean aortic attenuation of 330±54HU, at 90 kVp 325±54HU, at 100kVp 336±74HU and at 110kVp 387±62HU. CNR values were as follows: 80kVp 15±3, 90kVp 15±4, 100kVp 14±4 and 110kVp 15±4. Linear regression analysis showed no significant correlation between selected tube voltage and mean aortic attenuation (p = 0.108) and between selected tube voltage and CNR (p=0.795). Mean CTDI was 3.50±0.83mGy and mean SSDE was 4.08±0.72mGy.

CONCLUSION

Individualized adaptation of the CM volume and injection rate to automatically selected tube voltages using ATVS allows for a reduction of CM in CTA of the aorta, while maintaining a constant and diagnostic image quality.

CLINICAL RELEVANCE/APPLICATION

Contrast media can be reduced in an individualized fashion according to the automatically selected tube voltage for CTA of the aorta.

RC512-10 Low Iodine-dose Abdominal CT Angiography Using Low Energy (keV) Images from ssDECT

Wednesday, Dec. 2 10:55AM - 11:05AM Location: E352

Participants

Manuel Patino, MD, Boston, MA (*Presenter*) Nothing to Disclose Andrea Prochowski Iamurri, MD, Boston, MA (*Abstract Co-Author*) Nothing to Disclose Diana Murcia, MD, Boston, MA (*Abstract Co-Author*) Nothing to Disclose Yasir Andrabi, MD, MPH, Boston, MA (*Abstract Co-Author*) Nothing to Disclose Farhad Mehrkhani, MD, Boston, MA (*Abstract Co-Author*) Nothing to Disclose Rodrigo Canellas, MD, Boston, MA (*Abstract Co-Author*) Nothing to Disclose Mukta D. Agrawal, MBBS, MD, Arlington, MA (*Abstract Co-Author*) Nothing to Disclose Dushyant V. Sahani, MD, Boston, MA (*Abstract Co-Author*) Research Grant, General Electric Company; Research Consultant, Allena Pharmaceuticals, Inc

PURPOSE

To assess the performance of abdominal angiography with ssDECT using standard- (33 to 35g), low- (21 to 24g) and ultra-low-(16g) iodine dose, compared to SECT angiography with standard-iodine dose. Second, to determine the energy level (keV) for optimal assessment of vascular structures.

METHOD AND MATERIALS

This IRB approved clinical trial was designed in three phases. A total of 105 patients with AAA, scheduled for a follow-up CTA were

enrolled. Each subject had a standard-iodine dose CTA. The follow-up CTA was performed on a ssDECT scanner (Discovery CT750 HD; GE Healthcare), with DECT mode and Iodixanol (GE Healthcare) as follows: Phase 1) 35 patients were scanned with standard-iodine dose (33 to 35g). Phase 2) 64 patients were scanned with 30%-reduced iodine dose (21-24g). Phase 3: 10 patients were scanned with 55%-reduced iodine dose (16g). Virtual monochromatic images (VMC) (40, 50, 60 and 70keV) were generated from arterial-phase DECT images. Two experienced-radiologists evaluated the VMC images for image quality, diagnostic keV-range, optimal keV for vascular assessment, and vascular evaluation. Aortic attenuation was measured and contrast-to-noise-ratio (CNR) was calculated from SECT and VMC images. CTDIvol and DLP were measured and recorded. Statistical analysis was conducted with pair student t-test.

RESULTS

Standard, low and ultra-low-dose DE-CTA exams were rated as high diagnostic quality by the readers (IQ=4.5, 4.2 and 4, respectively). VMC (40 to 70 keV) images were rated diagnostic, and 40 to 50keV were rated optimal for vascular evaluation for all 3 groups. Compared to SE-CTA images, intravascular attenuation and CNR on 40-50keV DECT images were higher at standard (3X/35%), low (2X/30%) and ultra-low (2X/20%) iodine dose (p<0.001). Both readers detected 18/18 endoleaks on the DECT scans. Radiation dose was 20-30% lower on DE-CTA, compared to SE-CTA (p<0.05).

CONCLUSION

DECT increases intravascular attenuation and CNR enabling substantial iodine dose reduction, compared to SECT. Ultra-low iodine dose DE-CTA is feasible without reduction in diagnostic quality.

CLINICAL RELEVANCE/APPLICATION

DECT allows substantial reduction of iodine dose for CT angiography while rendering high quality images, providing an opportunity to decrease contrast media related renal risks, especially in older patients. These results can be applied to other vascular regions.

Honored Educators

Presenters or authors on this event have been recognized as RSNA Honored Educators for participating in multiple qualifying educational activities. Honored Educators are invested in furthering the profession of radiology by delivering high-quality educational content in their field of study. Learn how you can become an honored educator by visiting the website at: https://www.rsna.org/Honored-Educator-Award/

Dushyant V. Sahani, MD - 2012 Honored Educator Dushyant V. Sahani, MD - 2015 Honored Educator

RC512-11 Diagnostic Value of 70 kVp Time-resolved 4D Bone Subtracted CT Angiography with 80 cm -z-axis Coverage in Addition to Static High-pitch CT Angiography: Diagnostic Confidence and Impact on Patient Management

Wednesday, Dec. 2 11:05AM - 11:15AM Location: E352

Participants

Holger Haubenreisser, Mannheim, Germany (*Presenter*) Speaker, Siemens AG; Speaker, Bayer AG Amir Bigdeli, Ludwigshafen, Germany (*Abstract Co-Author*) Nothing to Disclose Mathias Meyer, Mannheim, Germany (*Abstract Co-Author*) Nothing to Disclose Philipp Riffel, MD, Mannheim, Germany (*Abstract Co-Author*) Nothing to Disclose Stefan O. Schoenberg, MD, PhD, Mannheim , Germany (*Abstract Co-Author*) Institutional research agreement, Siemens AG Thomas Henzler, MD, Mannheim, Germany (*Abstract Co-Author*) Nothing to Disclose

PURPOSE

To prospectively investigate the diagnostic value of time-resolved CT angiography 4D bone subtracted datasets with 80 cm z-axis coverage in addition to static CT angiography in patients with lower limb peripheral arterial occlusive disease (PAOD).

METHOD AND MATERIALS

40 (mean age:71.7yrs;24men) patients with suspected lower limb PAOD underwent a combined CTA protocol consisting of a highpitch-CTA run-off study starting from the abdominal aorta as well as a time-resolved-CTA of the lower limbs over 80cm (60s total scan time (8x3s, 6x6s); 70kV; 20ml iomeprol400). In addition to the time-resolved series, time-resolved bone subtracted maximumintensity-projections were generated for each examination. Each of seven lower leg artery segments was rated with regard to contrast and diagnostic confidence (3-point scale) for stenosis assessment. In addition, two radiologists and one vascular surgeon assessed the time-resolved examination regarding additional information leading to changes in patient management.

RESULTS

Compared to the static high-pitch-CTA, time-resolved-CTA datasets with peak contrast enhancement showed significantly higher contrast and CNR in all lower limb vessel segments (p<0.05). Diagnostic confidence was rated higher for time-resolved studies when compared to the standard static high-pitch CTA studies (median: time-resolved-CTA: 3[range 2-3]; high-pitch: 2[1-3]). Clinically relevant findings with subsequent impact on patient management that were only visible in the time-resolved-CTA studies were found in 7 of 40 patients, including complete vessel occlusion that was mimicked by extensive calcification.

CONCLUSION

Compared to static high-pitch-CTA, time-resolved-CTA improves arterial contrast enhancement and provides higher diagnostic confidence in patients with suspected lower limb PAOD. Compared to static high-pitch run-off studies, time-resolved studies CTA acquisitions lead to a higher number of clinically important findings that directly influenced patient management.

CLINICAL RELEVANCE/APPLICATION

Adding 70 kVp dynamic CTA examinations to standard static run-off CTA improves diagnostic confidence while retaining low iodine loads, potentially influencing patient management.

RC512-12 Perfusion-based Assessment of Disease Activity in Untreated and Treated Patients with Aortitis and Chronic Periaortitis: Correlation with CT-morphological, Clinical and Serological Data

Participants

Georg Bier, MD, Tubingen, Germany (*Presenter*) Nothing to Disclose Jorg Henes, MD, Tubingen, Germany (*Abstract Co-Author*) Nothing to Disclose Carolin Eulenbruch, Tubingen, Germany (*Abstract Co-Author*) Nothing to Disclose Theodoros Xenitidis, Tuebingen, Germany (*Abstract Co-Author*) Nothing to Disclose Konstantin Nikolaou, MD, Tuebingen, Germany (*Abstract Co-Author*) Speakers Bureau, Siemens AG Speakers Bureau, Bracco Group Speakers Bureau, Bayer AG Marius Horger, MD, Tuebingen, Germany (*Abstract Co-Author*) Nothing to Disclose

PURPOSE

To evaluate the role of CT perfusion-based assessment of inflammatory activity in patients with treated and untreated aortitis and chronic periaortitis (A/CP) and to compare results with those of clinical and serological markers.

METHOD AND MATERIALS

35 patients (20 female, 15 male) with aortitis/chronic periaortitis (A/CP) and clinical symptoms were examined by whole-body contrast-enhanced computed tomography (CECT) and subsequently by segmental volume perfusion-CT (VPCT) for assessment of the degree of vascularization of A/CP as surrogate marker for inflammatoric activity. Blood flow (BF), blood volume (BV), volume transfer constant (k-trans), time to peak (TTP) and mean transit time (MTT) were determined and the thickness of the increased connective tissue formation was measured. Imaging data was subsequently correlated with clinical symptoms as well as with acute phase inflammatory parameters (C-reactive protein/CRP, erythrocyte sedimentation rate/ESR and leukocyte number).

RESULTS

21/35 patients were untreated, 14/35 had previous of ongoing immunosuppression. The interobserver agreement was good (0.78) for all VPCT parameters. Average values of perfusion parameters were higher in untreated patients, but remained also abnormally elevated in treated patients. Good agreement was found between perfusion data and CRP as well as ESR in aortitis (treated and untreated; p < 0.05) and in untreated patients with periaortitis (p < 0.05).

CONCLUSION

Perfusion-CT parameters in untreated aortitis and periaortitis show good correlation with serological markers with respect to disease activity assessment. In treated periaortitis, however, correlations with serological markers were week or inexistent suggesting an increased rolve for (perfusion-based) imaging.

CLINICAL RELEVANCE/APPLICATION

For the first time the use of a new imaging technique for diagnosis and assessment of disease activity in patients with treated and untreated aortitis and periaortitis is reported. The weak correlation of VPCT with serological parameters in treated periaortitis patients suggests a potentially increased role for VPCT displaying serologically 'occult' disease activity.

RC512-13 Regional Mapping of Aortic Wall Stress Employing Deformable, Motion-Coherent Modeling based on ECG-gated CT Angiography: Exploratory Investigation with Pathodynamic Correlation in a TAVR Population

Wednesday, Dec. 2 11:25AM - 11:35AM Location: E352

Participants Achille Mileto, MD, Durham, NC (*Presenter*) Nothing to Disclose Tobias Heye, MD, Basel, Switzerland (*Abstract Co-Author*) Nothing to Disclose Daniele Marin, MD, Cary, NC (*Abstract Co-Author*) Nothing to Disclose Daniel Boll, Basel, Switzerland (*Abstract Co-Author*) Nothing to Disclose

PURPOSE

To investigate the clinical feasibility of employing deformable, motion-coherent modeling for regional mapping of aortic wall stress in a transaortic valve replacement (TAVR) population undergoing ECG-gated MDCT angiography.

METHOD AND MATERIALS

For this IRB-approved, HIPAA-compliant prospective study we employed thoracic ECG-gated dual-source MDCT angiography (CTA) datasets from 250 consecutive patients (150 men,100 women; mean age, 79.0 ± 9.1 years), who prospectively underwent CTA and echocardiography on the same day. Deformable, motion coherent modeling of aortic wall stress was performed using the PhyZiodynamic framework. The complex aortic motion was dissected into three types of aortic wall translocation, namely longitudinal strain, axial strain, and axial deformation by utilizing exported four-dimensional coordinates for seven anatomic locations, using the Matlab environment.

RESULTS

One hundred fifty-four patients were categorized as having severe aortic stenosis with a mean flow rate of 4.7 ± 0.6 mL/s; 96 patients were categorized with mild to moderate aortic stenosis with a mean flow rate of 3.5 ± 0.6 mL/s. Inverse correlation between heart rate and longitudinal strain (R2= 0.79), as well as longitudinal (R2= 0.95) and axial strain (R2= 0.31) was noted. In contrast, a significant trend towards an increase in axial deformation was observed with progressive increase in heart rate (P<.001). These findings indicated that shorter R-R interval may limit aortic motion in the longitudinal and axial planes due to inherent aortic wall rigidity. Increased aortic blood flow in the ascending aorta led to significantly greater longitudinal strain throughout the cardiac contraction cycle (P<.001), whereas increasing aortic valve areas led to significantly increased magnitudes in axial deformation (P<.001). Longitudinal strain propagating through the aortic wall was predominantly dependent upon the pressure gradients within the aorta. Axial deformation was dependent on the magnitude of passing blood volume.

CONCLUSION

Our study demonstrates the clinical feasibility of deformable, motion-coherent modeling based on ECG-gated MDCT angiography

acquisition for regional mapping aortic wall stress.

CLINICAL RELEVANCE/APPLICATION

Regional mapping of aortic wall stress may provide more objective information on quiescent landing zones suitable for deploying aortic prosthetic grafts, as well as providing insights on atherosclerotic changes of aortic wall.

RC512-14 Post Processing, Workflow and Interpretation

Wednesday, Dec. 2 11:35AM - 12:00PM Location: E352

Participants

Karin E. Dill, MD, Evanston, IL (Presenter) Nothing to Disclose

LEARNING OBJECTIVES

1) Understand the newest post processing techniques currently available for CT angiography. 2) Describe patient-centric imaging and workflow tools which optimize patient care.

ABSTRACT

Rapid evolution of imaging post-processing tools allows for continued advancement in the ability to manipulate data for image interpretation. The newest CTA post processing software will be demonstrated, leading to improved diagnostic capability. Efficient workflow algorithms will be reviewed which center around the patient, bringing multidisciplinary teams together in the workup, diagnosis and treatment of those seeking care. An emphasis will be placed on imaging guidelines which will ultimately be linked to decision support for reimbursement.

Interventional Series: Peripheral and Visceral Occlusive Disease

Wednesday, Dec. 2 8:30AM - 12:00PM Location: E353A

VA IR AMA PRA Category 1 Credits ™: 3.25 ARRT Category A+ Credits: 4.00

FDA Discussions may include off-label uses.

Participants

Parag J. Patel, MD, Milwaukee, WI (*Moderator*) Consultant, Medtronic, Inc; Consultant, C. R. Bard, Inc; Consultant, Penumbra, Inc; Jonathan M. Lorenz, MD, Chicago, IL (*Moderator*) Nothing to Disclose

LEARNING OBJECTIVES

1) Describe pros and cons of intervention for median arcuate ligament compression on the celiac axis. 2) Explain the use of radial artery access. 3) Outline 3 recommendations for endovascular treatment of peripheral vascular disease. 4) Describe current status of true percutaneous endovascular repair of abdominal aortic aneurysms. 5) Describe 2 vascular compression syndromes.

Sub-Events

RC514-01 Radial Artery Access. Why? When? How?

Wednesday, Dec. 2 8:30AM - 9:00AM Location: E353A

Participants

Marcelo Guimaraes, Charleston, SC (*Presenter*) Consultant, Cook Group Incorporated ; Consultant, Baylis Medical Company; Consultant, Terumo Corporation; Patent holder, Cook Group Incorporated

LEARNING OBJECTIVES

View learning objectives under main course title.

RC514-03 Morphological Predictors of Optimal Recanalization Strategy for Long-segment Chronic Total Occlusions of the Femoropopliteal Arteries

Wednesday, Dec. 2 9:10AM - 9:20AM Location: E353A

Participants

Jungong Zhao, MD, Shanghai, China (Presenter) Nothing to Disclose

PURPOSE

To investigate the morphological characteristics of long-segment chronic total occlusions of the femoropopliteal arteries (LFP-CTOs) as predictors of the optimal recanalization strategy.

METHOD AND MATERIALS

We retrospectively evaluated the morphological characteristics of 102 CTOs (74 patients) treated with antegrade and/or retrograde recanalization using contrast enhanced-magnetic resonance / computed tomography angiography and digital subtraction angiography imaging results. Proximal morphology, lesion length, calcification, proximal branching, collateral circulation, runoff vessels, and concomitant arterial occlusion were used as predictors for univariate analysis. Multivariate logistic regression analysis was performed to identify independent predictors of successful angioplasty and recanalization.

RESULTS

Antegrade and retrograde recanalization were successful in 82 and 10 CTOs, respectively (total success rate, 90.2%). The antegrade approach was frequently used for wire crossing and had a shorter mean procedure time than the retrograde approach (90.7 \pm 35.3 min vs. 185.5 \pm 41.2 min, P < 0.001). Multivariate analysis revealed that concomitant artery occlusion [odds ratio (OR): 0.299; 95% confidence interval (CI): 0.103-0.868; P=0.026) was a lower likelihood technical success; flush occlusion (OR: 41.795; 95% CI: 4.567-382.517; P<0.001) and large collateral (OR: 14.829; 95% CI: 1.350-162.898; P=0.027) were predictors of retrograde recanalization. During follow-up, sustained ABI improvement was founded in 79.3% limbs, and the binary restenosis rate was 40.2% in antegrade group and 50.0% in retrograde group (P > 0.05), but the flush occlusion (OR: 3.736; 95% CI: 1.152 - 12.119; P=0.028) was associated with a significantly higher likelihood of binary restenosis.

CONCLUSION

We recommend that LFP-CTOs with concomitant occlusion should be treated with bypass surgery, whereas flush occlusions and those with large collateral circulation should be managed with retrograde recanalization earlier if antegrade approach fails.

CLINICAL RELEVANCE/APPLICATION

Morphological characteristics of long-segment chronic total occlusions of femoropopliteal arteries can help predict the optimal strategy for endovascular recanalization.

RC514-04 Trends in Use of Vascular Ultrasound and Noninvasive Physiologic Testing for Peripheral Arterial Disease: Are These Tests Being Overused?

Wednesday, Dec. 2 9:20AM - 9:30AM Location: E353A

Participants

David C. Levin, MD, Philadelphia, PA (Presenter) Consultant, HealthHelp, LLC; Board of Directors, Outpatient Imaging Affiliates, LLC

Laurence Parker, PhD, Philadelphia, PA (*Abstract Co-Author*) Nothing to Disclose Geoffrey A. Gardiner JR, MD, Philadelphia, PA (*Abstract Co-Author*) Nothing to Disclose Vijay M. Rao, MD, Philadelphia, PA (*Abstract Co-Author*) Nothing to Disclose

PURPOSE

The U.S Preventive Services Task force has never supported routine screening for peripheral arterial disease (PAD). There is no need to treat asymptomatic (or even many symptomatic) patients and studies suggest only very modest recent growth in PAD incidence. For these reasons, our goal was to assess recent trends in the use of ultrasound (US) and noninvasive physiologic tests (NPTs), the most common tests used to screen for and initially diagnose PAD.

METHOD AND MATERIALS

The nationwide Medicare Part B databases for 2001 through 2013 were used. The 2 CPT codes for extremity arterial US and the 3 codes for extremity NPTs were selected. Procedure volume trends were evaluated. Medicare's physician speciality codes were used to determine which specialists were doing the studies. Utilization rates per 1000 were calculated.

RESULTS

Total Medicare volume of extremity arterial US was 396,734 in 2001, increasing every year thereafter to 818,272 in 2013 (+106%). The US utilization rate per 1000 was 11.7 in 2001, rising to 21.9 in 2013 (+87%). NPT volume increased from 716,005 in 2001 to a peak of 1,362,789 in 2010, then dropped to 1,278,145 in 2013 (+79% vs 2001)). The NPT rate per 1000 increased from 21.0 to a peak of 38.7 in 2010, then dropped to 34.3 in 2013 (+63% vs 2001). The 3 highest volume specialties in arterial US in 2013 were surgery (258,104 - up 108% vs 2001), radiology (210,477 - up 93% vs 2001) and cardiology (187,275 - up 267% vs 2001). The 3 highest volume specialties in NPTs in 2013 were surgery (444,623 - up 35% vs 2001), cardiology (267,005 - up 206% vs 2001), and primary care (229,215 - up 208% vs 2001). The overall rate of use of these 2 major kinds of tests for PAD increased from 32.7 per 1000 in 2001 to 56.2 in 2013 (+72%).

CONCLUSION

Use of both US and NPTs for possible PAD grew rapidly from 2001 to 2013. Growth was especially high among surgeons and cardiologists. There is no apparent medical rationale for the increasing utilization of these tests for PAD. The rapid growth in use of both US and NPTs raises concern about overuse, especially given the fact that surgeons and cardiologists are in a position to self-refer.

CLINICAL RELEVANCE/APPLICATION

n/a

RC514-05 Update on Recommendations for Endovascular Treatment of PVD in 2015-This Is What to Do and Why to Do It

Wednesday, Dec. 2 9:30AM - 10:00AM Location: E353A

Participants

Martin A. Funovics, MD, Vienna, Austria (Presenter) Nothing to Disclose

LEARNING OBJECTIVES

View learning objectives under main course title.

RC514-06 EVAR: True Percutaneous Devices? When?

Wednesday, Dec. 2 10:00AM - 10:30AM Location: E353A

Participants

Parag J. Patel, MD, Milwaukee, WI (Presenter) Consultant, Medtronic, Inc; Consultant, C. R. Bard, Inc; Consultant, Penumbra, Inc;

LEARNING OBJECTIVES

View learning objectives under main course title.

RC514-07 Automated Quantification of Muscle Perfusion Using contrast Enhanced Ultrasound: Initial in Vitro and in Vivo Evaluation of Lower Limb Perfusion

Wednesday, Dec. 2 10:30AM - 10:40AM Location: E353A

Participants

Wing Keung t. Cheung, London, United Kingdom (*Abstract Co-Author*) Nothing to Disclose Katherine t. Williams, London, United Kingdom (*Abstract Co-Author*) Nothing to Disclose Kirsten t. Chrstensen-Jeffries, London, United Kingdom (*Abstract Co-Author*) Nothing to Disclose Brahman Dharmarajah, MBBS, MRCS, London, United Kingdom (*Presenter*) Nothing to Disclose Robert J. Eckersley, PhD, London, United Kingdom (*Abstract Co-Author*) Nothing to Disclose Alun Davies, FRCR, London, United Kingdom (*Abstract Co-Author*) Nothing to Disclose Mengxing Tang, London, United Kingdom (*Abstract Co-Author*) Nothing to Disclose

PURPOSE

An accurate and automated technique for quantification of tissue microperfusion is desirable for a wide-range of clinical applications including atherosclerotic and diabetic peripheral vascular disease. Existing studies evaluating peripheral vascular disease still use qualitative visual assessment and studies quantifying contrast ultrasound signals have limited outcomes. In this study, we develop a pixel-based automated bubble detection algorithm capable of separating contrast signals from both tissue signal and noise thus generating a quantitative surrogate measure of muscle blood flow.

METHOD AND MATERIALS

Quantification of contrast signal at varying dilutions of microbubble was performed within an in-vitro phantom to develop the

automated bubble detection algorithm. After ethical approval and informed consent, the in-vivo study evaluated muscle perfusion of the right calf before and after physical exercise in 5 healthy volunteers. Imaging was acquired using a Phillips iU-22 ultrasound platform with a L9-3 linear probe. Offline blinded image analysis was performed using an average of 5 regions of interest placed over the muscle bulk. Surface area ratio of bubble pixel intensity to background signal was calculated as a surrogate of muscle microperfusion which was compared before and after exercise.

RESULTS

The In vitro study demonstrated a good agreement between known bubble concentrations and quantification measures generated by the algorithm (R=0.94). For in vivo data the quantification results were calculated using the algorithm and compared before and after subject exercise. Initial analysis showed that the average blood volume in the calf muscle increased by 48% after exercise (P<0.004).

CONCLUSION

The automated bubble detection algoritm has shown to be a promising tool for detecting and quantifying microbubble signals representing muscle microperfusion both in vitro and in vivo.

CLINICAL RELEVANCE/APPLICATION

Contrast enhanced ultrsound may provide a novel imaging technique for assessment of lower limb muscle microperfusion. This novel imaging biomarker may provide valuable information in diagnosis and treatment response in lower limb peripheral vascular disease.

RC514-08 Twins Study: Role of Femoral Ultrasound Examination in Predicting Cardiovascular Risk

Wednesday, Dec. 2 10:40AM - 10:50AM Location: E353A

Participants

Pierleone Lucatelli, MD, Roma, Italy (*Abstract Co-Author*) Nothing to Disclose Carlo Cirelli, Rome, Italy (*Abstract Co-Author*) Nothing to Disclose Renato Argiro, Rome, Italy (*Presenter*) Nothing to Disclose Beatrice Sacconi, MD, Rome, Italy (*Abstract Co-Author*) Nothing to Disclose Riccardo Rosati, Rome, Italy (*Abstract Co-Author*) Nothing to Disclose Fabrizio Fanelli, MD, Rome, Italy (*Abstract Co-Author*) Nothing to Disclose Carlo Catalano, MD, Rome, Italy (*Abstract Co-Author*) Nothing to Disclose

PURPOSE

Compare Common-Femoral-Artery (CFA) and Common-Carotid-Artery (CCA) Echo-Color-Doppler examination in predicting the cardiovascular risk in a sample of apparently healthy twins recruited from the Italian Twin Registry.

METHOD AND MATERIALS

The multicenter study included 322 twins (59.9% female) aged 20-78 years (52.1 \pm 15.3). Subjects underwent Echo-Color-Doppler examination of CCA and CFA. Mean IMT in both right and left sides of the CCA or CFA was recorded. Mean values were compared by Student's t test for paired data and by robust regression model to take account of the dependence of twin data within pairs and of confounders (age and gender). Plaques (thickening \geq 1.5 mm over IMT) prevalence and composition (calcific, fibro-lipidic, mixed) in the two regions were estimated and compared by chi-squared test or logistic regression for clustered observation.

RESULTS

A significant difference (P<0.01) between mean CCA-IMT and mean CFA-IMT was detected ($0.70\pm0.20 \text{ vs } 0.73\pm0.24\text{ mm}$), although mean difference between the two traits was relatively small ($0.03\pm0.17\text{mm}$). Plaque prevalence was significantly higher in CFA compared to CCA (40.7% vs 30.4%). This result was confirmed even when only lipid plaque(33.6% in CCA and 24.5% in CFA) was considered and when age and gender were incorporated in the analysis. Isolated plaque prevalence was 18.3% for CCA and 8.1% for CFA. 51.2% of the sample had at least a plaque in both traits.

CONCLUSION

Echo-Color-Doppler identifies more plaques in CFA than in CCA, with prevalent fibro-lipidid composition. Femoral Echo-Color-Doppler should be introduced as part of screening protocols in order to assess the cardiovascular risk.

CLINICAL RELEVANCE/APPLICATION

Echo-Color-Doppler identifies more plaques in CFA than in CCA therefore Femoral Echo-Color-Doppler should be introduced as part of screening protocols in order to assess the cardiovascular risk.

RC514-09 Ultrasound Assessment of the Posterior Circumflex Humeral Artery in Elite Volleyball Players: Aneurysm Prevalence, Anatomy, Branching Pattern and Vessel Characteristics

Wednesday, Dec. 2 10:50AM - 11:00AM Location: E353A

Participants

Daan van de Pol, MD, Amsterdam, Netherlands (*Presenter*) Nothing to Disclose Mario Maas, MD, PhD, Utrecht, Netherlands (*Abstract Co-Author*) Nothing to Disclose Aart Terpstra, Amsterdam, Netherlands (*Abstract Co-Author*) Nothing to Disclose Marja Pannekoek-Hekman, Amsterdam, Netherlands (*Abstract Co-Author*) Nothing to Disclose Paul Kuijer, PhD, Amsterdam, Netherlands (*Abstract Co-Author*) Nothing to Disclose R. Nils Planken, MD,PhD, Amsterdam, Netherlands (*Abstract Co-Author*) Nothing to Disclose

PURPOSE

Elite overhead athletes, like volleyball players, are at risk of finger ischemia due to arterial emboli originating from an injured and degenerated proximal posterior circumflex humeral artery (PCHA) in the dominant shoulder. Ultrasound (US) is the first line imaging modality for assessment of the PCHA in symptomatic athletes. However, identification and assessment of the PCHA is cumbersome in the hands of inexperienced ultrasonographists, partially due to anatomical variations and the nearby originating and resembling

deep brachial artery (DBA). The purpose of this study is (1) to determine the prevalence of PCHA aneurysms in elite volleyball players and (2) to describe PCHA and DBA characteristics that can be used for accurate identification and assessment of the PCHA.

METHOD AND MATERIALS

From January 2014 until July 2014, two experienced ultrasonographists completed the standardized PCHA US-protocol in 286 elite volleyball players. Assessment included determination of PCHA aneurysms (defined as segmental vessel dilatation \geq 150%), anatomy/branching pattern, and PCHA and DBA vessel characteristics: course and diameter.

RESULTS

The PCHA was identified in 100% of volleyball players (n=286) and the DBA in 96% (n=276). An aneurysm of the PCHA was detected in 4.1% of the volleyball players (n=12) with a mean diameter of 5.9mm \pm 1.7 and was significantly larger compared to non-dilated PCHA vessel segments (p<0.01). The mean non-dilated PCHA and DBA diameters were 3.8mm \pm 0.5 (95%CI 3.7-3.8) and 2.3mm \pm 0.5 (95%CI 2.2-2.3), respectively. The PCHA originated directly from the axillary artery in 82% (n=235) and the DBA in 70% (n=200). PCHA anatomical variations included a common trunk with the DBA (n=24), common trunk with a different artery than the DBA (n=21) and a common trunk with two other arteries (n=3). The PCHA showed a tortuous course towards the humerus in 100% of the cases. The DBA showed a straight course parallel to the axillary artery in 100% of the cases.

CONCLUSION

The prevalence of PCHA aneurysms was 4.1% in our study cohort of 286 elite volleyball players. The reported PCHA and DBA vessel characteristics provide clear guidance for identification and assessment of the PCHA.

CLINICAL RELEVANCE/APPLICATION

One in twenty-five elite volleyball players showed a PCHA aneurysm on ultrasound. We provide PCHA characteristics and diameters that can be used as reference values (normal vs. aneurysmatic) for clinical assessment and research.

RC514-10 Compressive Vascular Syndromes

Wednesday, Dec. 2 11:00AM - 11:30AM Location: E353A

Participants Lindsay S. Machan, MD, Vancouver, BC (*Presenter*) Nothing to Disclose

LEARNING OBJECTIVES

View learning objectives under main course title.

RC514-11 Median Arcuate Ligament Syndrome

Wednesday, Dec. 2 11:30AM - 12:00PM Location: E353A

Participants

Jonathan M. Lorenz, MD, Chicago, IL (Presenter) Nothing to Disclose

LEARNING OBJECTIVES

View learning objecitves under main course title.

Body MRI: Technical Challenges (An Interactive Session)

Wednesday, Dec. 2 8:30AM - 10:00AM Location: E353B

MR

AMA PRA Category 1 Credits ™: 1.50 ARRT Category A+ Credits: 1.50

FDA Discussions may include off-label uses.

Participants

Sub-Events

RC529A Motion Control Techniques in Body MRI

Participants

Hersh Chandarana, MD, New York, NY (*Presenter*) Equipment support, Siemens AG; Software support, Siemens AG; Consultant, Bayer, AG;

LEARNING OBJECTIVES

1) Understand basic concepts of k-space and acquisition time. 2) Discuss various methods to accelerate acquisition by k-space undersampling. 3) Discuss motion robust acquisition schemes including non-Cartesian k-space sampling.

ABSTRACT

ABSTRACT: Assessment of multiple post-contrast phases after gadolinium contrast injection is essential for lesion detection and characterization, and thus is a routine component of abdominopelvic MRI. Contrast-enhanced multiphase MR examination is usually performed using a T1-weighted fat-saturated 3D volumetric interpolated sequence with Cartesian k-space sampling in a breath-hold. However, this method is sensitive to respiratory motion and can result in suboptimal images in patients who cannot adequately breath-hold. Techniques to overcome this major limitation include rapid imaging to decrease acquisition time and motion robust acquisition schemes. Concept of acquisition time and k-space will be discussed followed by discussion of techniques to perform rapid and motion robust imaging.

RC529B Which Contrast Agent Should I Use?

Participants

Matthew S. Davenport, MD, Cincinnati, OH, (matdaven@med.umich.edu) (*Presenter*) Book contract, Wolters Kluwer nv; Book contract, Reed Elsevier;

LEARNING OBJECTIVES

1) Review common gadolinium-based contrast agents (GBCA). 2) Understand the strengths and weaknesses of various GBCA. 3) Learn the incidence and significance of various risks associated with GBCA administration.

ABSTRACT

This presentation will review the strengths and weaknesses of a variety of modern gadolinium-based contrast agents. Controversies, risks, and benefits will be presented. Practice optimization with respect to selection of a GBCA formulary will be discussed.

RC529C Optimizing Diffusion-Weighted Imaging at 1.5 and 3T

Participants

Dow-Mu Koh, MD, FRCR, Sutton, United Kingdom (Presenter) Nothing to Disclose

LEARNING OBJECTIVES

1) To understand how to get the best body diffusion-weighted MRI at 1.5T and 3.0T by optimizing image signal-to-noise and minimizing image artefacts. 2) To appreciate the additional challenges of body diffusion-weighted MRI at 3.0T. 3. To review newer imaging techniques that can be applied at 3.0T to improve body diffusion-weighted MRI including combinatorial fat suppression schemes, image-based shimming, reduced field-of-view acquisitions and readout-segmented echo-planar imaging techniques.

ABSTRACT

Body diffusion-weighted MRI (DWI) is now widely applied for disease evaluation, especially in oncology. DWI is relatively quick and easy to perform using single-shot echo-planar imaging (EPI) technique. However, imaging optimisation is important to ensure that high quality images are consistently attained. At both 1.5T and 3.0T, parameter optimization is necessary to maximize signal-to-noise (such as by reducing echo-times, using coarser matrix, thicker partition thickness, multiple signal averages) of the acquired images and to minimize potential artefacts (e.g. motion, chemical shift, eddy currents, Nyquist ghosting, susceptibility and G-noise) that will degrade image quality. Although body DWI is generally more robust at 1.5T, recent advances at 3.0T allow high quality DWI images to be obtained, including whole body studies. Imaging at 3.0T has the advantage of higher image signal-to-noise; but is more prone to artefacts arising from chemical shift (suboptimal fat suppression), susceptibility effects and image distortion. Hence, meticulous optimisation of fat suppression (e.g. using combinatorial fat suppression schemes) and avoidance of regions with high susceptibility effects are important. More recently, the introduction of image-based shimming has helped to improve DWI quality at 3.0T, particular for large field-of-view imaging. Image distortion and susceptibility artifacts can be reduced using read-out segmented EPI techniques. The higher signal-to-noise at 3.0T also allows for high spatial resolution reduced field-of-view techniques to be applied.At 3.0T, there is also an opportuity to perform DWI studies on a hybrid PET-MRI system. To maximise

information gained from such studies, protocol design and clinical workflow are important.

Breast Imaging: Politics and Practice

Wednesday, Dec. 2 8:30AM - 10:00AM Location: E450A

BR

AMA PRA Category 1 Credits ™: 1.50 ARRT Category A+ Credits: 1.50

Participants

LEARNING OBJECTIVES

1) To understand the basis for the evidence supporting screening mammography as it is currently practiced in the US, and how changes to that paradigm based on risk or density lack the same level of rigorous scientific support. 2) To understand the issue of overdiagnosis of breast cancer through screening and why the estimates of the rate of this phenomenon vary so widely and how we might actually resolve this controversy. 3) To understand why the study of screening for breast cancer in high risk women with MRI and US is not readily generalizable to average risk women and the risks we take if we do apply these technologies more broadly.

Sub-Events

RC515A Current Controversies

Participants

Etta D. Pisano, MD, Charleston, SC (*Presenter*) Founder, NextRay, Inc CEO, NextRay, Inc Research Grant, Koning Corporation Research Grant, Koninklijke Philips NV Research Grant, Zumatek, Inc Research Grant, FUJIFILM Holdings Corporation Equipment support, Siemens AG Research Grant, Siemens AG Equipment support, Koninklijke Philips NV Research Grant, Koninklijke Philips NV

LEARNING OBJECTIVES

1) To understand the basis for the evidence supporting screening mammography as it is currently practiced in the US, and how changes to that paradigm based on risk or density lack the same level of rigorous scientific support. 2) To understand the issue of overdiagnosis of breast cancer through screening and why the estimates of the rate of this phenomenon vary so widely and how we might actually resolve this controversy. 3) To understand why the study of screening for breast cancer in high risk women with MRI and US is not readily generalizable to average risk women and the risks we take if we do apply these technologies more broadly.

RC515B Economic Challenges

Participants

Geraldine B. McGinty, MD, MBA, New York, NY (Presenter) Nothing to Disclose

LEARNING OBJECTIVES

1) Understand the funfdamentals of healthcare payment policy as they impact breast imaging. 2) Understand recent developments in payment policy for breast imaging. 3) Understand possible future direction of payment policy for breast imaging.

RC515C Breast Density

Participants

Jennifer A. Harvey, MD, Charlottesville, VA, (jharvey@virginia.edu) (*Presenter*) Researcher, Hologic, Inc; Researcher, VuCOMP, Inc; Researcher, Matakina Technology Limited; Shareholder, Matakina Te

LEARNING OBJECTIVES

1) Be familiar with the grassroots political efforts of women with dense breast tissue. 2) Understand imaging options for women with dense tissue. 3) Understand implications of breast cancer risk due to breast density.

ABSTRACT

The sensitivity of mammography is reduced in women with dense breast tissue. Women with extremely dense breasts are more likley to present with an interval palpable cancer between screening exams (17 times more likely in one study). Althoug this is a known limitation, somen undergoing regular screening that develop an interval cancer may feel disinfranchised from mammography. Grassroots efforts have initiated 'density laws' in at least 19 states, and a federal law may ultimately be passed. These laws vary, but informing women of their density is a uniform component. Many laws also mandate discussion of offering additional screening. The efficacy and cost of additional imaging is controversial as is the methodd in which to identify and apply these ancillary tests. Women with high breast density are also at about 4 fold increased risk for developing breast cancer compared with women with fatty breasts, emphasizing that the need to provide better screening strategies may potentially improve overall breast cancer mortality.

Mobile Computing Devices

Wednesday, Dec. 2 8:30AM - 10:00AM Location: S404CD

IN SQ

AMA PRA Category 1 Credits ™: 3.25 ARRT Category A+ Credits: 3.50

Participants

David S. Hirschorn, MD, Staten Island, NY, (hirschorn.david@mgh.harvard.edu) (*Moderator*) Nothing to Disclose Asim F. Choudhri, MD, Memphis, TN (*Moderator*) Nothing to Disclose George L. Shih, MD, MS, New York, NY (*Moderator*) Consultant, Image Safely, Inc; Stockholder, Image Safely, Inc; Consultant, Angular Health, Inc; Stockholder, Angular Health, Inc;

Sub-Events

RC554A Introduction

Participants

David S. Hirschorn, MD, Staten Island, NY (Presenter) Nothing to Disclose

RC554B Platforms and Security

Participants

George L. Shih, MD, MS, New York, NY (*Presenter*) Consultant, Image Safely, Inc; Stockholder, Image Safely, Inc; Consultant, Angular Health, Inc; Stockholder, Angular Health, Inc;

LEARNING OBJECTIVES

1) Mobile Health: Discuss mobile healthcare trends and evolution involving Apple iOS and Google Android, with specific focus on mobile health apps and platforms, including Apple HealthKit and Apple ResearchKit. 2) Mobile Security: Provide basic understanding of different security concerns in mobile health and discuss options in the healthcare setting.

ABSTRACT

Mobile healthcare devices of all shapes and sizes are now ubiquitous in clinical setting. Radiologists and other providers are leveraging mobile solutions in their clinical workflow. The major mobile platforms provide distinct advantages for both app developers and end users (ie, clinicians and patients) in the healthcare setting. Both iOS and Android platforms have development toolkits that allow for health-related apps. Apple has released HealthKit and ResearchKit, which are more medically focused, and several apps are already available which leverage these new capabilities. A major EHR vendor, EPIC, now has the ability to directly communicate and with a patient's iPhone with bi-directional data-sharing. Wearable devices, such as the Apple iWatch, and other third party mobile health devices are also discussed. The wearable and portable devices will continue to accelerate the shift to mobile healthcare.Mobile devices will need to have the same or enhanced security compared with traditional computers because of increased portability and the Bring Your Own Device (BYOD) phenomenon where clinicians are increasingly using their personal devices for work. Managing enterprise mobile security on a wide range of work and personal mobile devices will remain challenging although can be alleviated by using Mobile Device Manager software which can deploy updates and enforce security policies. Shared mobile devices for patients in the clinical setting may also present similar challenges.

ABSTRACT

Mobile healthcare devices of all shapes and sizes are now ubiquitous in clinical setting. Radiologists and other providers are leveraging mobile solutions in their clinical workflow. The major mobile platforms provide distinct advantages for both app developers and end users (ie, clinicians and patients) in the healthcare setting. The two main platforms for tablet mobile devices are Apple iOS and the Google Android. Mobile devices will need to have the same or enhanced security compared with traditional computers because of increased portability and the Bring Your Own Device (BYOD) phenomenon where clinicians are increasingly using their personal devices for work. Managing enterprise mobile security on a wide range of work and personal mobile devices will remain challenging although can be alleviated by using Mobile Device Manager software which can deploy updates and enforce security policies. Shared mobile devices for patients in the clinical setting may also present similar challenges.

RC554C Apps, Bandwidth, and Integration

Participants

Asim F. Choudhri, MD, Memphis, TN (Presenter) Nothing to Disclose

LEARNING OBJECTIVES

1) To have an understanding of available applications available for mobile medical imaging, including native clients, web clients, and virtual desktop/terminal server approaches. 2) To have an understanding of bandwidth concerns in mobile medical imaging, including device data handling, network speeds, and possible bandwidth cost issues. 3) To have an understanding of possible clinical implementations of mobile medical imaging within radiology departments and in health care networks overall.

ABSTRACT

Applications: There are several vastly different approaches to mobile viewing of medical images. Native clients are programs written using a software development kit for a given platform. These clients can retrieve data from remote servers and view locally stored image data. Web clients are web-based programs which are often (but not always) platform independent. They will typically access remotely stored data which may be stored in a local cache but is usually not permanently stored on the mobile device. Virtual desktop/terminal server software allows a mobile device to access a remote computer or server. The remote server handles all

higher level processing and data storage, minimizing the processing requirements of the mobile device but possibly straining bandwidth limitations. Examples of several applications using each of these approaches will be presented, with a discussion of pros and cons for each method as it pertains to an individual user and as it pertains to widespread implementation within a healthcare network. Bandwidth: Viewing medical images may require transfer of datasets that are tens or hundreds of megabytes in size. This provides a special challenge for mobile devices which typically receive data via wireless communication. If using a cellular network, network bandwidth can be a limiting factor (as can data transfer costs). File compression can reduce the size of files, however requires data processing power and may involve compromises in image quality. Once data is on a device, image processing may overwhelm its processing capabilities compared with dedicated PACS workstations. We will discuss both network and device bandwidth concerns as it relates to mobile medical imaging, and possible solutions for overcoming obstacles. Integration into a healthcare system: Mobile review of medical imaging is a tool which has potential to significantly change health care delivery, but the specifics for implementation are unclear. After a device platform has been selected, security protocols established, and bandwidth concerns solved, each institution will need to determine what role this technology will play. Possibilities include radiology residents (or even faculty) consulting with subspecialty faculty, surgeons and interventionalists triaging patients for procedures and for procedure planning, however these approaches are simply extensions of existing practices. New frontiers in consultation will be discussed, including an example involving mobile imaging review in a multidisciplinary stroke team. Guidance will also be provided regarding training and establishing institutional "standard operating procedures" documents. The current state of medical-legal concerns and risk management strategies will also be discussed.

RC554D Displays and Quality Assurance

Participants

David S. Hirschorn, MD, Staten Island, NY (Presenter) Nothing to Disclose

LEARNING OBJECTIVES

1) Discuss ranges of spatial and contrast resolution for medical imaging. 2) Explore options for calibration and quality assurance. 3) Understand the impact of ambient light and viewing distance and angle on medical image display.

ABSTRACT

Mobile devices have significantly smaller displays than desktop or even laptop computers to make them lighter and more easily transported. They are also designed for shorter viewing distances which require smaller pixels. The smaller total display size tends to reduce the number of pixels, while the smaller pixel size tends to increase the number of pixels. On balance, these displays typically have considerably fewer pixels than their stationary counterparts. Nonetheless, even desktop displays typically have less resolution than the original image size of a radiograph which is typically about 5 megapixel (MP) for a chest radiograph. And both types of displays have more resolution than a single CT image, which is 0.25 MP. Since these devices do allow zooming and panning, they may be suitable for image interpretation under controlled circumstances. The main purpose of the DICOM Part 14 Grayscale Display Function is to ensure that contrast is preserved across the range of shades of gray from black to white, particularly at the edges where uncalibrated displays tend to fall off. With desktop displays this can be measured with a photometer, either external or built-in, and graphics adapter adjustments can be made to make the display conformant. Mobile devices typically do not offer this degree of adjustability. This requires a different approach to DICOM curve conformance, and a reasonable alternative is to present the user with a visual challenge to identify low contrast targets placed randomly on the display. If the user can find them and tap on them, then the display may be considered compliant, and if not, then the display should not be relied upon.

Case-based Review of Pediatric Radiology (An Interactive Session)

Wednesday, Dec. 2 8:30AM - 10:00AM Location: S406A

CH GI GU OB PD

AMA PRA Category 1 Credits ™: 1.50 ARRT Category A+ Credits: 1.50

Participants

Sudha A. Anupindi, MD, Philadelphia, PA (Director) Nothing to Disclose

LEARNING OBJECTIVES

1) To apply a systematic approach in the evaluation of pediatric diseases. 2) To identify essential imaging features of various pediatric congenital, musculoskeletal, abdominal and neurological diseases using a multimodality approach. 3) To understand and develop best imaging practice for various pediatric diseases.

ABSTRACT

To apply a systematic approach in the evaluation of pediatric diseases To identify essential imaging features of various pediatric congenital, musculoskeletal, abdominal and neurological diseases using a multimodality approach To understand and develop best imaging practice for various pediatric diseases

Sub-Events

MSCP41A Fetal Thoracic and Abdominal Anomalies

Participants Christopher I. Cassady, MD, Houston, TX (*Presenter*) Nothing to Disclose

LEARNING OBJECTIVES

View learning objectives under main course title.

MSCP41B Pediatric Abdominopelvic Tumors

Participants

M. Beth McCarville, MD, Memphis, TN (Presenter) Support, General Electric Company

LEARNING OBJECTIVES

View learning objectives under main course title.

MSCP41C Congenital Disorders of the Genitourinary Tract

Participants Tracy N. Kilborn, MBChB, Cape Town, South Africa (*Presenter*) Nothing to Disclose

LEARNING OBJECTIVES

View learning objectives under main course title.

Next Generation IT to Improve Quality and Safety

Wednesday, Dec. 2 8:30AM - 10:00AM Location: S405AB



AMA PRA Category 1 Credits ™: 1.50 ARRT Category A+ Credit: .50

Participants

Ramin Khorasani, MD, Roxbury Crossing, MA (Moderator) Consultant, Medicalis Corp

ABSTRACT

Improving healthcare system performance is a major national focus. An important element of performance improvement in healthcare is national adoption and meaningful use of interoperable health information technology tools, supported by federal regulations as part of Health Information technology and Economic Health Act (HITECH). Radiology has been a leader in adoption of health IT tools and solutions. In this session, we will review some key, next generation health IT requirements to improve quality of care and patient safety while reducing waste. The speakers will use case example to demonstrate how health IT tools can be used to improve access to imaging, improve appropriateness of imaging ordering, improving radiology report value, enhance communication of critical test results, and enable appropriate follow up imaging and care coordination for patients.

Sub-Events

RC553A Improving Access and Appropriateness

Participants

Keith D. Hentel, MD, MS, New York, NY, (keh9003@med.cornell.edu) (Presenter) Nothing to Disclose

LEARNING OBJECTIVES

1) Understand avialable technologies available for improving access to imaging practices. 2) Understand available technologies for improving appropriateness of imaging performed.

RC553B Improving Value of Radiology Reports

Participants

Ross W. Filice, MD, Washington, DC, (ross.w.filice@gunet.georgetown.edu) (Presenter) Nothing to Disclose

RC553C Improving Communication of Critical Results and Follow-up Recommendations

Participants

Ramin Khorasani, MD, Roxbury Crossing, MA (Presenter) Consultant, Medicalis Corp

Sinonasal and Orbital Imaging

Wednesday, Dec. 2 8:30AM - 10:00AM Location: S406B

HN NR

AMA PRA Category 1 Credits ™: 1.50 ARRT Category A+ Credits: 1.50

Participants

Sub-Events

RC506A Sinonasal Inflammatory Disease

Participants

Rebecca S. Cornelius, MD, Cincinnati, OH (*Presenter*) Stockholder, Gilead Sciences, Inc; Stockholder, HCP, Inc; Stockholder, CVS Health Corporation; Stockholder, 3M Company; Spouse, Stockholder, Gilead Sciences, Inc; Spouse, Stockholder, HCP, Inc; Spouse, Stockholder, CVS Health Corporation; Spouse, Stockholder, 3M Company; Spouse, Stockholder, Celgene Corporation; Spouse, Stockholder, E. I. du Pont de Nemours & Company

LEARNING OBJECTIVES

1) Recognize imaging findings in chronic rhinosinusitis. 2) Recognize imaging findings of orbital and intracranial complications of sinonasal inflammatory disease. 3) Differentiate between types of fungal sinus disease.

Active Handout:Rebecca Sue Cornelius

http://abstract.rsna.org/uploads/2015/15001949/Active RC506A.pdf

RC506B Sinonasal Tumors

Participants

Ilona M. Schmalfuss, MD, Gainesville, FL, (schmai@radiology.ufl.edu) (Presenter) Nothing to Disclose

LEARNING OBJECTIVES

1) Describe differentiating imaging features between the different sinonasal tumors. 2) Discuss extension patterns of sinonasal malignancies. 3) Outline critical areas of involvement that impact treatment of sinonasal tumors.

RC506C Orbital Differential Diagnosis

Participants

Michelle A. Michel, MD, Milwaukee, WI (Presenter) Nothing to Disclose

LEARNING OBJECTIVES

1) Recommend optimal imaging modality for evaluating diverse pathology of orbit. 2) Discuss approach to orbital lesion diagnosis based upon patters of disease, patient demographics, and presenting symptoms. 3) Recognize orbital pathologies occurring in key differential diagnoses.

ABSTRACT

Sinonasal Inflammatory DiseaseRhinosinusitis is one of the most commonly diagnosed diseases in the United States, affecting >16% of the US population annually. There are acute, subacute and chronic forms defined by duration. Imaging is indicated in patients with chronic disease. Complications of rhinosinusitis include spread into adjacent superficial tissues, orbital extension and intracranial extension. Types of sinusitis will be defined, characteristics of chronic disease and fungal disease discussed and imaging examples of complications reviewed.Sinonasal TumorsSinonasal tumors (benign and malignant) present with non-specific symptoms such as nasal obstruction or drainage, leading to work up with CT. Associated facial, oral, ocular, or central nervous system symptoms should raise the concern for an advanced, often malignant tumor and evaluated with MRI. Distinguishing imaging features will be presented for the different sinonasal tumors to facilitate the correct diagnosis, prevent complications, determine the extent of the tumor, and provide accurate staging for optimal treatment planning purposes and imroyed patient prognosis.Orbital Differential DiagnosisOrbital pathology is diverse and lesions can appear similar on imaging. There are differential diagnoses (DDx) to understand that aid in making an accurate diagnosis. Clinical information should also be correlated with imaging findings. The DDx's that will be discussed include: intraocular lesions, ocular calcification, optic nerve-sheath complex lesions, intraconal lesions, extraocular muscle enlargement, infiltrative lesions, and lacrimal gland lesions. Although there are a large number of pathologies that can affect the orbit, knowledge of these key differential diagnoses, patterns of disease, and clinical features can be very helpful to the imager in distinguishing these lesions.

Active Handout: Michelle A. Michel

http://abstract.rsna.org/uploads/2015/15001951/RC506C-Active.pdf

Radiomics Mini-Course: Promise and Challenges

Wednesday, Dec. 2 8:30AM - 10:00AM Location: S502AB

BQ PH

AMA PRA Category 1 Credits ™: 1.50 ARRT Category A+ Credits: 1.50

Participants

Sandy Napel, PhD, Stanford, CA (*Director*) Medical Advisory Board, Fovia, Inc; Consultant, Carestream Health, Inc; Scientific Advisor, EchoPixel, Inc

Sub-Events

RC525A An Overview of Radiomics

Participants

Maryellen L. Giger, PhD, Chicago, IL (*Presenter*) Stockholder, Hologic, Inc; Shareholder, Quantitative Insights, Inc; Royalties, Hologic, Inc; Royalties, General Electric Company; Royalties, MEDIAN Technologies; Royalties, Riverain Technologies, LLC; Royalties, Mitsubishi Corporation; Royalties, Toshiba Corporation; Researcher, Koninklijke Philips NV; Researcher, U-Systems, Inc

LEARNING OBJECTIVES

1) Understand the meaning of radiomics relative to computer-aided diagnosis and quantitative imaging. 2) Learn about the current state-of-the-art in radiomics. 3) Appreciate the existing and future potential role of radiomics with other -omics data and within precision medicine.

ABSTRACT

RC525B From Radiomics to Radiogenomics

Participants

Hugo Aerts, PhD, Boston, MA (Presenter) Nothing to Disclose

LEARNING OBJECTIVES

1) Understand the motivation for integrating imaging with genomic and clinical data. 2) Learn about the methodology for quantitative radiomic analysis Example biomarker quantification studies in Radiomics and Imaging-Genomics (Radiogenomics).

ABSTRACT

RC525C Challenges for Radiomics and Radiogenomics

Participants

Karen Drukker, PhD, Chicago, IL, (kdrukker@uchicago.edu) (Presenter) Nothing to Disclose

LEARNING OBJECTIVES

1) Recognizing potential pitfalls along the radiomics/radiogenomics pipeline. 2) Understanding the crucial role of statistics in the design and evaluation of radiomics/radiogenomics phenotypes and systems.

ABSTRACT

Handout:Karen Drukker

http://abstract.rsna.org/uploads/2015/15003209/referencesCited.docx

Radiogenomics of Lung Cancer-Changing Landscape and Challenges

Wednesday, Dec. 2 8:30AM - 10:00AM Location: S403A

CH BQ OI

AMA PRA Category 1 Credits ™: 1.50 ARRT Category A+ Credits: 1.50

Participants Sub-Events

RC518A Lung Cancer in the Radiogenomic Era-Implications for Imaging

Participants

Lawrence H. Schwartz, MD, New York, NY (*Presenter*) Committee member, Celgene Corporation; Committee member, Novartis AG; Committee member, ICON plc; Committee member, BioClinica, Inc

LEARNING OBJECTIVES

1) To understand the clinical needs for Radiogenomic Imaging in Lung Cancer. 2) To understand what imaging modalities and quantification techniques can be used in Radiogenomic Imaging in Lung cancer. 3) To illustrate examples of successes and failures in Radiogenomic Imaging approaches in Lung Cancer.

RC518B Qualitative Assessments of Lung Cancer for Radiogenomic Analysis

Participants

Hyun-Ju Lee, MD, PhD, Seoul, Korea, Republic Of (Presenter) Nothing to Disclose

LEARNING OBJECTIVES

1) To introduce the results of correlation between imaging features and genetic phenotypes of lung cancer. 2) To describe the implications of imaging traits on pathology, patient prognosis, and genetics. 3) To introduce the role of qualitative assessment for the next step high-throughput quantitative feature selection.

ABSTRACT

```
RC518C Quantitative Assessment in Lung Cancer Radiogenomics-Reproducibility and Reliability
```

Participants

Binsheng Zhao, DSc, New York, NY (*Presenter*) License agreement, Varian Medical Systems, Inc; License agreement, Keosys SAS; License agreement, Hinacom Software and Technology, Ltd; License agreement, ImBio, LLC; License agreement, AG Mednet, Inc

LEARNING OBJECTIVES

1) Familiarize the audience with quantitative image features that can be computed to characterize tumors. 2) Discuss reproducibility and reliability of image features due to, repeat CT scans, CT acquisition and reconstruction techniques, tumor segmentations.

ABSTRACT

The way tumors look on radiological images may also reveal their underlying cancer gene expressions. Tumor imaging phenotypes can be characterized not only qualitatively by the radiologist's eyeballing, but also quantitatively by computer through image feature analysis. Radiogenomics promises the ability to assess cancer genotype though the tumor's imaging phenotype. However, to date, little attention has been paid to the sensitivity of image features to repeat scans, imaging acquisition techniques, reconstruction parameters and tumor segmentations. This refresher course will first familiarize the audience with quantitative image features that can be computed to characterize tumor size, shape, edge and density texture statistics. Both phantom and in-vivo studies will be introduced to explain how repeat CT scans and CT imaging acquisition and reconstruction techniques affect the assessment of quantitative image features in lung cancer Radiogenomics studies. Last but not least, the effects of image segmentation on feature calculations will be addressed.

Using IHE Profiles to Plan for Medical Imaging

Wednesday, Dec. 2 8:30AM - 10:00AM Location: S501ABC

IN

AMA PRA Category 1 Credits ™: 1.50 ARRT Category A+ Credits: 1.50

Participants

David S. Mendelson, MD, Larchmont, NY (*Moderator*) Spouse, Employee, Novartis AG; Advisory Board, Nuance Communications, Inc; Advisory Board, General Electric Company; Advisory Board, Toshiba Corporation Kinson Ho, Waterloo, ON, (kinson.ho@agfa.com) (*Presenter*) Employee, Agfa-Gevaert Group David A. Clunie, MBBS, Bangor, PA (*Presenter*) Owner, PixelMed Publishing LLC Christopher Lindop, Waukesha, WI (*Presenter*) Employee, General Electric Company Donald Dennison, Waterloo, ON, (don@dondennison.com) (*Presenter*) Nothing to Disclose

LEARNING OBJECTIVES

1) Value of IHE with content and vendor neutral integration. 2) How content neutral clinical information is managed with a Vendor Neutral Archive (VNA). 3) Planning for a Vendor Neutral Archive (VNA) or expand upon an existing VNA system to support both imaging and non-imaging content and systems. 4) The benefit of using IHE Imaging profiles for cross-enterprise and cross-community image sharing".

ABSTRACT

Integrating the Healthcare Enterprise (IHE) is a joint initiative of healthcare professionals and industry vendors to improve the way clinical systems in healthcare share information. IHE promotes the coordinated use of established standards such as webservices, DICOM and HL7 to address specific clinical need in support of optimal patient care. Established in 1997, the IHE Radiology Committee, a development domain of IHE, has profiled the clinical use cases to develop a framework of interoperability, known as the IHE Integration Profiles. Integration Profiles are developed specifically to be 'Vendor Neutral'. The first Integration Profile developed by IHE is known as Scheduled Workflow. It specifies how imaging departmental workflow can operate seamlessly between vendors. The Integration Profiles are maintained and published by IHE in the IHE Technical Framework. With the introduction of Cross-Enterprise Document Sharing (XDS) in 2005, IHE has extended the definition of 'Neutral' to include non-imaging content storage in healthcare. This course will specifically deliver and review the IHE Integration Profiles developed by IHE Radiology and the other IHE domain committees profile which can be used by healthcare professionals and the industry for the interoperability specification, procurement and installation of a 'Content' Vendor Neutral Archive (VNA).

RC516

Career Development for Women Radiologists and Radiation Oncologists (In Conjunction with the American Association for Women Radiologists)

Wednesday, Dec. 2 8:30AM - 10:00AM Location: S504AB

LM OT

AMA PRA Category 1 Credits ™: 1.50 ARRT Category A+ Credit: 0

Participants

Susan J. Ackerman, MD, Charleston, SC (Moderator) Nothing to Disclose

Sub-Events

RC516A Residency - What Does It Take?

Participants

Rachel M. Nelson, MD, Charleston, SC (Presenter) Nothing to Disclose

LEARNING OBJECTIVES

1) Early identification of the key skills and resources needed to excel in a radiology residency. 2) Application of these skills and resources to build a solid foundation in radiology. 3) Utilization of this foundation to balance clinical duties and continuing education with involvement in non-academic pursuits.

ABSTRACT

Navigating a radiology residency is a daunting task, especially in the beginning. By building a solid foundation, each resident will have the basic skill sets and access to the resources needed to excel. Basic fund of knowledge, early mentorship, and effective communication are key aspects of a strong foundation. Residents can then build on this foundation through residency balancing both continuing education in the more complex realms of radiology as well as involvement in research, national organizations or the local community.

RC516B Climbing the Ladder - Challenges and Opportunity

Participants

Madelene C. Lewis, MD, Charleston, SC, (lewism@musc.edu) (Presenter) Nothing to Disclose

LEARNING OBJECTIVES

1) Identify opportunities to ascend the ladder to promotion and leadership roles. 2) Develop strategies to overcome common challenges in building a successful academic career. 3) Formulate a plan to effectively climb the ladder.

ABSTRACT

Climbing the ladder is not an easy task, and along the way you will encounter many challenges and opportunities. However, there are skill sets and practical tips that are useful in turning challenges into opportunities as well as capitalizing on opportunities. Mentorship is invaluable for navigating your climb up the ladder. Mentors can serve as a sounding board and give honest feedback based on their experiences and perspective. Networking is also an effective method for getting in the door and helping with the ascent up. In today's competitive and accelerated world, those looking to advance their careers need to be proactive, develop a plan, and embrace learning new leadership skills.

RC516C Challenges of Private Practice - How to Be Successful

Participants

Beatriz E. Amendola, MD, Coral Gables, FL, (dramendola@gmail.com) (Presenter) Speakers Bureau, Varian Medical Systems, Inc

LEARNING OBJECTIVES

1) After this presentation, the participant will be able to identify practical points to help them succeed in developing a private practice, in the field of Radiaiton Oncology. 2) Define polcies to develop a successful practice. 3) Develop resource management with vendors and staff.

ABSTRACT

This presentation will be based on my personal experience of more than 15 years in the private practice of Radiation Oncology, mostly as a solo-practice. The reason I decided to go into private practice, after many years of academia it was my desire to be independent and be able to provide the best quality of medical care for my pratients the way I wanted. Develop a team of excellence is the main ingredient; followed by the ability to provide them with the appropriate technical tools, if possible 'state-ofthe-art' or even better, offer the most advanced technology available. Innovative research and emphazise the patient and their family needs in fighting their disease are keys to success. Support of frends and family is essential in this endevour.

RC516D Women at the Top - Do's and Don'ts

Participants Carol M. Rumack, MD, Aurora, CO, (carol.rumack@ucdenver.edu) (*Presenter*) Nothing to Disclose

LEARNING OBJECTIVES

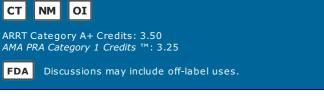
1) Learn actions and habits that will help you perform well at a high level in an organization. 2) Learn actions and planning strategy that will help you get your new ideas across in a competitive environment. 3) Learn actions that may be risky to your career.

ABSTRACT

What to do and what not to do at the top levels of an organization are different than just being a team player for one of those leaders. My goals are to teach specific actions that you can use to perform well and to make as many as possible into habits so that you become a reliable and trusted colleague who is listened to for good ideas. How to prepare yourself so that you are ready accept new challenges? It may be your chance to succeed where others hesitate to go! How can you build a support system of other leaders? How do you plan for your ideas to succeed with their support in a top level meeting? In a leadership position there are risky actions that may destroy your credibility. What should you not be doing? Is it ok to be too cautious to speak? Why does not being visible can help undermine your success?

Nuclear Medicine Series: Non-FDG PET Radiotracers in Oncology

Wednesday, Dec. 2 8:30AM - 12:00PM Location: S505AB



Participants

Hossein Jadvar, MD, PhD, Los Angeles, CA, (jadvar@med.usc.edu) (*Moderator*) Nothing to Disclose David A. Mankoff, MD, PhD, Philadelphia, PA (*Moderator*) Speaker, Koninklijke Philips NV; Consultant, General Electric Company

Sub-Events

RC511-01 Proliferation Imaging: FLT/PET in Oncology

Wednesday, Dec. 2 8:30AM - 9:00AM Location: S505AB

Participants

David A. Mankoff, MD, PhD, Philadelphia, PA (Presenter) Speaker, Koninklijke Philips NV; Consultant, General Electric Company

LEARNING OBJECTIVES

1) Describe the kinetics of thymidine relevant to FLT PET imaging. 2) Discuss approaches to FLT image interpretation. 3) Describe studies that have tested FLT PET as a marker cancer response to treatment.

Honored Educators

Presenters or authors on this event have been recognized as RSNA Honored Educators for participating in multiple qualifying educational activities. Honored Educators are invested in furthering the profession of radiology by delivering high-quality educational content in their field of study. Learn how you can become an honored educator by visiting the website at: https://www.rsna.org/Honored-Educator-Award/

David A. Mankoff, MD, PhD - 2013 Honored Educator

RC511-02 Positron Emission Tomography (PET) Imaging of Chemokine Receptor CXCR4 in Patients with Solid Cancers: Initial Results

Wednesday, Dec. 2 9:00AM - 9:10AM Location: S505AB

Participants

Tibor Vag, MD, PhD, Munich, Germany (*Presenter*) Nothing to Disclose Carlos Gerngross, Munich, Germany (*Abstract Co-Author*) Nothing to Disclose Hans-Jurgen Wester, Munchen, Germany (*Abstract Co-Author*) CEO, SCINTOMICS GmbH Markus Schwaiger, MD, Munich, Germany (*Abstract Co-Author*) Nothing to Disclose

PURPOSE

CXCR4 is a chemokine receptor that is overexpressed in various human cancers and is involved in tumor metastasis. In this feasibility study we performed Positron Emission Tomography (PET) imaging of CXCR4 expression in patients suffering from various solid cancers.

METHOD AND MATERIALS

21 patients with histologically proven solid tumors underwent PET imaging using the novel CXCR4 nuclear probe [68Ga]Pentixafor. Maximum standardized uptake values (SUVmax) of the liver, spleen and bone marrow were measured for determination of physiological tracer distribution. For evaluation of in vivo CXCR4 expression on tumors, SUVmax and tumor-to-background ratios (T/B ratio) were determined in a total of 43 malignant lesions including 8 primary tumors, 3 local recurrent tumors and 32 metastases. When available, SUVmax of malignant lesions was compared to corresponding SUVmax measured in standard routine [18F]FDG PET.

RESULTS

Moderate tracer uptake was detectable in the liver, bone marrow and spleen with a mean SUVmax of 3.1, 3.7 and 5.6, respectively. By visual interpretation criteria, 9 of 11 primary and local recurrent tumors were detectable, exhibiting a mean SUVmax of 4.7 (range 2.1 to 10.9) and a mean T/B ratio of 2.9. 20 of 32 evaluated metastases were visually detectable (mean SUVmax of 4.5, range 3.2 to 13.8; mean T/B ratio of 2.8). Spearman's correlation revealed a low correlation between SUVmax and number of lesions per patient (r=0.3). Compared to [18F]FDG PET obtained in 10 patients, tracer uptake in [68Ga]Pentixafor PET revealed a lower SUVmax in all measured lesions.

CONCLUSION

PET Imaging of CXCR4 in patients with solid cancers is feasible. Based on the experience gained within this small number of patients, SUVmax of malignant solid tumors seems to be lower in [68Ga]Pentixafor PET compared to [18F]FDG PET. Moreover, CXCR4 expression in solid malignancies seems to be highly heterogeneous depending on factors, that have to be elucidated in further studies.

CLINICAL RELEVANCE/APPLICATION

Once the areas of Pentixafor imaging are more clearly defined, PET imaging of CXCR4 might prove as a valuable modality, either as a

stand alone diagnostic tool, or in combination with [18F]FDG PET, i.e. when considering [68Ga]Pentixafor for monitoring CXCR4 directed pharmacological or endoradiotherapeutic treatment.

RC511-03 Dual-tracer (11C-acetate and 18F-FDG) PET/CT in Evaluating Gastrointestinal Stromal Tumors and Predicting the Mitotic Rate

Wednesday, Dec. 2 9:10AM - 9:20AM Location: S505AB

Participants Thomas K. Cheng, MBBS, Hong Kong, Hong Kong (*Abstract Co-Author*) Nothing to Disclose Sirong Chen, Hong Kong, Hong Kong (*Presenter*) Nothing to Disclose Yim Lung Leung, Hong Kong, Hong Kong (*Abstract Co-Author*) Nothing to Disclose Ka Nin Wong, Hong Kong, Hong Kong (*Abstract Co-Author*) Nothing to Disclose William Cheung, Hong Kong, Hong Kong (*Abstract Co-Author*) Nothing to Disclose Chi Lai Ho, Hong Kong, Hong Kong (*Abstract Co-Author*) Nothing to Disclose

PURPOSE

18F-FDG (FDG) PET/CT is useful in risk stratification of Gastrointestinal stromal tumors (GIST) because it provides information for 3 predictors of tumor aggressiveness: mitotic rate (MiR), tumor size and primary site of involvement. GIST typically demonstrates high FDG avidity but false negative (FN) reports are not uncommon in those with low MiR. This study explores the detection sensitivity of 11C-acetate (ACT) and FDG PET/CT in GIST, and their relationship to cellular mitotic behavior.

METHOD AND MATERIALS

From 2013-14, 10 patients (M;7, F:3; mean age= $63\pm17y$) with primary GIST and 6 patients (M:5, F:1; mean age= $66\pm13y$) with metastatic GIST (primary excised previously) underwent preoperative ACT and FDG PET/CT. Postoperative pathology confirmed all primary/secondary GIST. The MiR was categorized as low ($\leq5/50$) or high (>5/50 mitoses/50 high-power fields) according to the mitotic index recommended by NCCN guidelines. ROC curve analysis was performed to explore the relationship of lesion SUVmax to MiR for ACT and FDG, respectively.

RESULTS

10 lesions were found in 10 patients with primary GIST (stomach:5, small bowel:4, omentum:1): 3 with high and 7 with low MiR (size:14.2±11.2 vs 3.7±0.7cm). FDG PET/CT was positive in 7/10 (70%) but FN in 3/7 lesions with low MiR. ACT PET/CT was positive in 9/10 (90%) including all 3 FDG-negative lesions. 6 metastatic GIST patients presented with 11 lesions (liver:2, adrenal:1, retroperitoneal lymph node:1, peritoneum:7): 6 with high and 5 with low MiR. FDG PET/CT was positive in 8/11 (73%) but FN in 1/6 with high and 2/5 with low MiR. ACT PET/CT was positive in all metastatic lesions (11/11:100%). The incremental value of ACT over FDG is significant for primary and metastatic GIST with low MiR (both P<0.05). By ROC curve analysis, a FDG SUVmax cut-off value>=4.4 and 3.1 could differentiate lesions of high from low MiR for primary and metastatic GIST, respectively (AUC=0.905 vs 0.875, both P<0.05).

CONCLUSION

Metabolic avidity of GIST for FDG has a predictive value for cellular mitotic behavior, but with the disadvantage of FN for lesions having low MiR. ACT PET/CT has a distinct incremental value over FDG for detecting primary/metastatic GIST, but appears to be independent of mitotic behavior.

CLINICAL RELEVANCE/APPLICATION

ACT PET/CT has a high sensitivity for both primary and metastatic GIST, particularly for lesions with low mitotic rate and non-avid for FDG. FDG avidity, however, predicts mitotic behavior of GIST.

RC511-04 Monitoring Response to Antiangiogenic Therapy of Non-Small Cell Lung Cancer using 150-water PET: The Relationship between Tumor Blood Flow and the Prognosis

Wednesday, Dec. 2 9:20AM - 9:30AM Location: S505AB

Participants

Masahiro Yanagawa, MD, PhD, Suita, Japan (*Presenter*) Nothing to Disclose Keiko Matsunaga, Suita, Japan (*Abstract Co-Author*) Nothing to Disclose Hiroki Kato, Suita, Japan (*Abstract Co-Author*) Nothing to Disclose Eku Shimosegawa, Suita, Japan (*Abstract Co-Author*) Nothing to Disclose Jun Hatazawa, MD, PhD, Osaka, Japan (*Abstract Co-Author*) Nothing to Disclose Noriyuki Tomiyama, MD, PhD, Suita, Japan (*Abstract Co-Author*) Nothing to Disclose Osamu Honda, MD, PhD, Suita, Japan (*Abstract Co-Author*) Nothing to Disclose Takashi Kijima, Suita, Japan (*Abstract Co-Author*) Nothing to Disclose Haruhiko Hirata, Suita, Japan (*Abstract Co-Author*) Nothing to Disclose Tomoyuki Otsuka, Suita, Japan (*Abstract Co-Author*) Nothing to Disclose Atsushi Kumanogoh, Suita, Japan (*Abstract Co-Author*) Nothing to Disclose

PURPOSE

Bevacizumab (BEV) is a humanized monoclonal antibody that targets circulating vascular endothelial growth factor. The purposes of this study were to evaluate tumor blood flow in patients with non small cell lung cancer (NSCLC) before and after treatment of BEV using 150-water PET and to examine the tumor blood flow change and time to tumor progression.

RESULTS

In 5 patients without BEV, median of tumor blood flow before and after treatment was 0.3506 and 0.3351, respectively. There was no significant difference (Wilcoxon test, p=0.81). Mean time to tumor progression after treatment was 80.4 days (range, 21 to 203). In 6 patients with BEV, median of tumor blood flow before and after treatment was 0.2785 and 0.1777, respectively. There was a significant difference (p=0.03). Mean time to tumor progression after treatment was 242.5 days (range, 86 to 413). The mean ratio (Fa/b) of tumor blood flow after BEV to that before BEV was 0.665 ml/cm³/min (range, 0.231 to 0.899). There was significant correlation between Fa/b and time to tumor progression (Correlation coefficient r=0.86, p=0.03): large decrease in blood flow early after treatment of BEV was associated with short time to tumor progression.

CONCLUSION

Mean tumor blood flow decreased within 1-2 days after administration of BEV. Large decrease in blood flow early after treatment of BEV correlated with short time to tumor progression.

CLINICAL RELEVANCE/APPLICATION

The antiangiogenic therapy might not have a benefit for patients with large decrease in blood flow early after treatment of BEV.

RC511-05 68Ga-PSMA-PET/CT in Patients with Renal Cell Cancer: Initial Results

Wednesday, Dec. 2 9:30AM - 9:40AM Location: S505AB

Participants

Lino Sawicki, MD, Dusseldorf, Germany (*Presenter*) Nothing to Disclose Philipp Heusch, MD, Duesseldorf, Germany (*Abstract Co-Author*) Nothing to Disclose Christian Buchbender, Duesseldorf, Germany (*Abstract Co-Author*) Nothing to Disclose Markus Giessing, MD, Berlin, Germany (*Abstract Co-Author*) Nothing to Disclose Hubertus Hautzel, MD, Juelich, Germany (*Abstract Co-Author*) Nothing to Disclose Gerald Antoch, MD, Duesseldorf, Germany (*Abstract Co-Author*) Nothing to Disclose

PURPOSE

68Gallium (68Ga) labelled prostate specific membrane antigen (PSMA) positron emission tomography / computed tomography (PET/CT) has been shown to be a reliable imaging method for the detection of prostate cancer and its metastases. Immunohistochemic studies revealed that PSMA is also expressed in the neovasculature of other solid tumors, especially renal cell cancer (RCC), making these cancers a potential target for 68Ga-PSMA-PET imaging. The aim of this study was to explore the feasibility of 68Ga-PSMA-PET/CT for detection of RCC in patients.

METHOD AND MATERIALS

Three male patients (mean age 66 years; range 52 - 74) with primary or metastatic RCC (n=2 clearcell RCC; n=1 papillary RCC) prospectively underwent whole body 68Ga-PSMA-PET/CT (mean Mbq: 179,3; Scanner: Siemens Biograph mCT, Siemens Healthcare, Erlangen, Germany). Quantitative assessement of tracer uptake was performed 1 hour after injection (p.i.) by measuring maximum standard uptake values (SUVmax) using isocontour VOIs in histopathologically proven tumor lesions. Additionaly, for each lesion tumor-to-background ratios were claculated.

RESULTS

All primary RCCs and known metastastic sites were detected by 68Ga-PSMA-PET/CT. Average SUVmax in clear cell and papillary RCC tumour lesions was 16.7 and 4.1, respectively. Mean tumor-to-background ratio was 18.6 for clear cell RCC lesions and was 4.1 for papillary RCC lesions.

CONCLUSION

Detection of primary tumors and metastases in RCC patients using 68Ga-PSMA-PET/CT is feasible. 68Ga-PSMA uptake is high in clear cell RCC but rather weak in papillary RCC. Thus the promising diagnostic potential of 68Ga-PSMA-PET/CT rather has to be investigated in clear cell RCC patients.

CLINICAL RELEVANCE/APPLICATION

Since RCCs have high metastatic potential exact staging is crucial. Imaging with CT, MRI but also 18F-FDG-PET/CT offers limited sensitivity. PET/CT using 68Ga-PSMA seems to be a promising alternative.

RC511-06 Hypoxia Imaging: FMISO PET Imaging in Oncology

Wednesday, Dec. 2 9:40AM - 10:10AM Location: S505AB

Participants

Kenneth A. Krohn, PhD, Seattle, WA (Presenter) Nothing to Disclose

LEARNING OBJECTIVES

1) Understand the evolution of tumor hypoxia and its biological implications. 2) Identify the mechanistic changes in tumor biology that will result in tumor resistance and poor patient outcome. 3) Learn novel ways to image tumor hypoxia with focus on FMISO PET imaging. 4) Understand the potential approaches to overcoming the negative impact of hypoxia.

ABSTRACT

The physiological microenvironment for a tumor is largely dictated by abnormal vasculature and metabolism. Many solid tumors develop areas of hypoxia during their evolution caused by unregulated cellular growth, resulting in greater demand on oxygen for energy metabolism. Hypoxia induces a cascade of changes that reflects the homeostatic attempts (highly conserved evolutionally) to maintain adequate oxygenation that may result in tumor cells to adapt by developing more aggressive survival traits; mediated by Hypoxia Inducible Factor (HIF1a) part of the cellular oxygen sensing mechanism. Hypoxic tumors are not effectively eradicated with conventional doses of radiation and show resistance to several chemotherapy drugs. Hypoxia may also result in angiogenesis (itself a marker of tumor aggressiveness) mediated by Vascular endothelial growth factor (VEGF). While angiogenesis is a frequent consequence of hypoxia, some tumors develop extensive angiogenesis without the presence of hypoxia and vice versa. Advances in PET imaging instrumentation, coupled with the development of an increasing array of novel molecular probes, provide opportunities for imaging and selection of appropriate therapies to overcome the cure limiting effects of these two fundamental aspects of tumor microenvironment. The biology of tumor microenvironment related to hypoxia and its effect on patient outcome and developments in imaging technology and novel radiotracers for hypoxia imaging with a focus on F-18 FMISO would be reviewed.Challernges and novel treatments to overcome the cure limiting ability of hypoxia will be discussed.

RC511-07 Prostate Cancer Choline PET Imaging and Other PET Tracers

Participants

Hossein Jadvar, MD, PhD, Los Angeles, CA, (jadvar@med.usc.edu) (Presenter) Nothing to Disclose

LEARNING OBJECTIVES

1) Review the major biological targets that may be useful for imaging in prostate cancer. 2) Understand the need for tailoring the imaging technique to the particular clinical phase of disease. 3) Analyze the current evidence with the potential utility of PET with various radiotracers in the imaging evaluation of prostate cancer.

ABSTRACT

ABSTRACT

Recent advances in the fundamental understanding of the complex biology of prostate cancer have provided increasing number of potential targets for imaging and treatment. In this presentation, I review the experience with a number of major PET radiotracers for potential use in the imaging evaluation of men with prostate cancer.

RC511-08 Primary Tumor Detection in CUP of Neuroendocrine Origin: Additional Value of 68Ga-DOTATATE-PET/CT Compared to Contrast-enhanced CT

Wednesday, Dec. 2 11:00AM - 11:10AM Location: S505AB

Participants

Philipp M. Kazmierczak, MD, Munich, Germany (*Presenter*) Nothing to Disclose
Axel Rominger, Munich, Germany (*Abstract Co-Author*) Nothing to Disclose
Christine Spitzweg, Munich, Germany (*Abstract Co-Author*) Advisory Board, Novartis AG; Advisory Board, Pfizer Inc; Advisory Board, Ipsen SA; Speaker, Novartis AG; Speaker, Pfizer Inc; Speaker, Ipsen SA
Christoph Auernhammer, MD, PhD, Munich, Germany (*Abstract Co-Author*) Research Grant, Novartis AG; Speaker, Novartis AG; Research Grant, Ipsen SA; Speaker, Ipsen SA; Advisory Board, Novartis AG
Maximilian F. Reiser, MD, Munich, Germany (*Abstract Co-Author*) Nothing to Disclose
Clemens C. Cyran, MD, Munich, Germany (*Abstract Co-Author*) Research Grant, Bayer AG Research Grant, Novartis AG Speakers
Bureau, Bayer AG
Carsten Rist, MD, Munich, Germany (*Abstract Co-Author*) Nothing to Disclose

PURPOSE

To evaluate the additional value of 68Ga-DOTATATE-PET/CT compared to contrast-enhanced CT for primary tumor detection in cancer of unknown primary (CUP) of neuroendocrine origin.

METHOD AND MATERIALS

Patients (n=38, 27 male, 11 female, mean age 62 years) with histologically proven metastatic disease of neuroendocrine origin undergoing contrast-enhanced 68Ga-DOTATATE-PET/CT (Biograph 64, Siemens Healthcare, Erlangen, Germany) for primary tumor detection and staging were consecutively included in this retrospective study. Two blinded readers independently evaluated the separated contrast-enhanced CT and 68Ga-DOTATATE-PET data sets and noted from which of the two imaging modalities they suspected a primary tumor. In case of divergent blinded reading results, a consensus was reached. The final diagnosis, confirmed by either histopathology (n=24) or clinical follow-up (n=14), served as standard of reference.

RESULTS

Primary tumors were suspected in n=33 patients, localized in the small bowel (n=19), the pancreas (n=12), the lung (n=1), and the thyroid gland (n=1) (mean tumor-to-spleen ratio 1.10 \pm 0.69; PET/CT: true positive n=30, true negative n=3; CT: true positive n=20, true negative n=5). In n=4 patients, no primary tumor was identified (true negative n=3). N=10 primary tumors were correctly detected by PET but not contrast-enhanced CT, resulting in a diagnostic accuracy of 87 % for the fused 68Ga-DOTATATE-PET/CT, compared to 66 % for the contrast-enhanced CT alone. High interobserver agreement was noted regarding the localization of the primary tumor (Cohen's k 0.90, p<0.001).

CONCLUSION

68Ga-DOTATATE-PET/CT provides a significantly higher diagnostic accuracy for primary tumor detection in CUP of neuroendocrine origin as compared to contrast-enhanced CT alone.

CLINICAL RELEVANCE/APPLICATION

The present study provides evidence for the routine use of 68Ga-DOTATATE-PET/CT in neuroendocrine CUP, allowing for a comprehensive tumor staging at improved diagnostic accuracy as compared to standard whole-body imaging.

RC511-09 Do we Need High-Dose Contrast-enhanced CT in the Detection of Extra-hepatic Metastasesusing Gallium-68-DOTATATE-PET/CT in Patients with Neuroendocrine Tumors (NET)?

Wednesday, Dec. 2 11:10AM - 11:20AM Location: S505AB

Participants

Jonas C. Apitzsch, MD, Marburg, Germany (*Presenter*) Nothing to Disclose Dirk R. Albanus, Aachen, Germany (*Abstract Co-Author*) Nothing to Disclose Z. Erdem, Zonguldak, Turkey (*Abstract Co-Author*) Nothing to Disclose Oktay Erdem, MD, Zonguldak, Turkey (*Abstract Co-Author*) Nothing to Disclose Anton F. Verburg, Aachen, Germany (*Abstract Co-Author*) Nothing to Disclose Florian F. Behrendt, MD, Aachen, Germany (*Abstract Co-Author*) Nothing to Disclose Felix Mottaghy, MD, PhD, Ulm, Germany (*Abstract Co-Author*) Nothing to Disclose Andreas H. Mahnken, MD, Aachen, Germany (*Abstract Co-Author*) Nothing to Disclose Alexander Heinzel, Aachen, Germany (*Abstract Co-Author*) Nothing to Disclose Previous studies have shown that PET/CT with 68Ga-labeled somatostatin analogues is useful in the assessment of metastatic disease in in patients with neuroendocrine tumors especially with regard to extra-hepatic lesions. It has to be noted that PET in combination with full-dose contrast-enhanced CT (ceCT) exposes the patients to a high dose of radiation whereas the non-contrast-enhanced low-dose CT (ldCT) might reduce the radiation and may in addition avoid side effects such as allergic reactions. Thus, we aimed to determine whether ceCT can be omitted from assessment for extra-hepatic metastases in patients with NET.

METHOD AND MATERIALS

We retrospectively compared the performance of PET/IdCT and PET/ceCT in 54 patients (26 male, 28 female) who underwent a Gallium-68-DOTATATE-PET/CT in our clinic. Selection criteria were as follows: available IdCT and ceCT; histologically confirmed NET; available follow-up of at least 6 months (median 12.6 months; range 6.1-23.2). PET/IdCT and PET/ceCT images were analyzed separately by four experienced physicians. The review process focused on metastases to lungs, bones and lymph nodes. Afterwards, the PET/IdCT and PET/ceCT results were compared to the reference standard consisting of clinical follow-up data to evaluate the diagnostic accuracy.

RESULTS

In PET/ceCT 139 true positive bone-lesions were detected compared to 140 in PET/ldCT, 106 true positive lymph node metastases (PET/ceCT) vs. 90 (PET/ldCT) and 26 true positive lung lesions (PET/ceCT) whereas PET/ldCT found ?? true positive lung lesions. On a per patient basis ld and ce PET-CT achieved similar sensitivity (both 100%) however, specificity was lower for PET/ldCT (89% vs. 77%). For lymph nodes PET/ceCT showed superior sensitivity and specificity (sensitivity 92% vs. 80% and specificity 83% vs. 65%). For the detection of pulmonary lesions the sensitivity of PET/ldCT was also clearly inferior (23 vs 100%) while specificity was similar (94% vs. 93%).

CONCLUSION

These results represent first evidence that ceCT should not be omitted for extra-hepatic staging using Gallium-68-DOTATATE-PET/CT in patients with neuroendocrine tumors. However, the results need to be confirmed in a prospective trial.

CLINICAL RELEVANCE/APPLICATION

PET/IdCT is sufficient in the detection of extrahepatic metastatic desease in NET. There is no further need for high-dose CeCT.

RC511-10 PSA and PSA Kinetics in Predicting 18F-NaF PET Positivity for First Bone Metastases in Patients with Biochemical Recurrence after Radical Prostatectomy

Wednesday, Dec. 2 11:20AM - 11:30AM Location: S505AB

Participants James Yoon, BA, Los Angeles, CA (*Presenter*) Nothing to Disclose Leslie Ballas, MD, Los Angeles, CA (*Abstract Co-Author*) Nothing to Disclose Bhushan Desai, MBBS, MS, Los Angeles, CA (*Abstract Co-Author*) Nothing to Disclose Lingyun Ji, MS, Los Angeles, CA (*Abstract Co-Author*) Nothing to Disclose Susan Groshen, PhD, Los Angeles, CA (*Abstract Co-Author*) Nothing to Disclose Hossein Jadvar, MD, PhD, Los Angeles, CA (*Abstract Co-Author*) Nothing to Disclose

PURPOSE

To evaluate PSA and PSA kinetics in addition to other pathologic factors to determine their predictive value for 18F-NaF PET positivity for first bone metastases in patients with biochemical recurrence after radical prostatectomy.

METHOD AND MATERIALS

All 18F-NaF PET scans that were performed at USC between 2010 and 2014 were queried to find patients who demonstrate biochemical recurrence after radical prostatectomy. Patients with known metastatic disease at the time of 18F-NaF PET were excluded. Records were reviewed to obtain data on PSA at the time of 18F-NaF PET, PSA kinetics, and pathologic features of the prostatectomy specimen, which were then used for receiver operating characteristic (ROC) analysis to determine predictability for 18F-NaF PET positivity.

RESULTS

36 patients met our inclusion criteria. Of these, 8 (22.2%) had positive 18F-NaF PET scans. Mean values for PSA, PSA doubling time, and PSA velocity were 2.02 ng/mL (range 0.06-11.7 ng/mL), 13.2 months, and 1.28 ng/mL/yr for 18F-NaF PET negative patients and 4.11 ng/mL (range 0.04-14.38 ng/mL), 8.9 months, and 9.06 ng/mL/yr for 18F-NaF PET positive patients (p=0.07, 0.47, and 0.02 respectively). ROC analysis for 18F-NaF positivity gave AUC values of 0.634 for PSA, 0.598 for PSA doubling time, and 0.688 for PSA velocity. ROC analysis with combined models gave AUC values of 0.723 for PSA and PSA doubling time, 0.689 for PSA and PSA velocity, and 0.718 for PSA, PSA doubling time, and PSA velocity. There was no significant association found between 18F-NaF PET positivity and Gleason score, TN staging, and status of surgical margins.

CONCLUSION

18F-NaF PET detected first time osseous metastases in 22.2% of patients with PSA relapse. PSA velocity was the best single variable for predicting 18F-NaF PET positivity. Combining PSA with PSA doubling time or PSA with PSA doubling time and PSA velocity resulted in higher predictability than any variable independently.

CLINICAL RELEVANCE/APPLICATION

18F-NaF PET can detect early prostate cancer bone metastases in the post-prostatectomy setting.

RC511-11 Bone PET Imaging: NaF PET in Oncology

Wednesday, Dec. 2 11:30AM - 12:00PM Location: S505AB

LEARNING OBJECTIVES

1) To identify the advantages of F-18 NaF PET/CT in oncology 2) To understand the importance of a standardized imaging protocol and reporting for F18-NaF PET/CT 3) To become comfortable in differentiating benign lesions from malignant ones on F18-NaF PET/CT

ABSTRACT

F-18 NaF PET/CT has been shown to have higher sensitivity than planar 99m-Tc MDP bone scanning in several studies. The concomitant acquisition of anatomic images permits immediate correlation of any abnormal findings. Additionally, F-18 NaF PET/CT bone imaging can be quantitated, allowing bone disease to be 'measureable', increasing its utility therapy monitoring. When a consistent F-18 NaF uptake period is used, the SUV values are highly reproducible, and due to the high extraction fraction, high quality images can be obtained with a radiation dose exposure similar to that of Tc-99m MDP (including the low dose CT scan). This presentation will discuss the benefits and challenges of F-18 NaF PET/CT in oncology.

ABSTRACT

F-18 NaF PET/CT has been shown to have higher sensitivity and specificity than planar 99m-Tc MDP bone scanning in several small studies. The concomitant acquisition of anatomic images permits immediate correlation of any abnormal findings. Additionally, F-18 NaF PET/CT bone imaging can be quantitated, allowing bone disease to be "measureable", increasing its utility therapy monitoring. When a consistent F-18 NaF uptake period is used, the SUV values are highly reproducible, and due to the high extraction fraction, high quality images can be obtained with a radiation dose exposure similar to that of Tc-99m MDP (including the low dose CT scan). This presentation will discuss the benefits and challenges of F-18 NaF PET/CT in oncology.

Fallopian Tube Catheterization (Hands-on)

Wednesday, Dec. 2 8:30AM - 10:00AM Location: E260



AMA PRA Category 1 Credits ™: 1.50 ARRT Category A+ Credits: 1.50

Participants

Amy S. Thurmond, MD, Portland, OR (*Moderator*) Nothing to Disclose Ronald J. Zagoria, MD, San Francisco, CA, (ron.zagoria@ucsf.edu) (*Presenter*) Nothing to Disclose Lindsay S. Machan, MD, Vancouver, BC (*Presenter*) Nothing to Disclose A. Van Moore JR, MD, Charlotte, NC (*Presenter*) Nothing to Disclose Anne C. Roberts, MD, La Jolla, CA (*Presenter*) Nothing to Disclose David M. Hovsepian, MD, Stanford, CA (*Presenter*) Nothing to Disclose

LEARNING OBJECTIVES

1) Obtain hands-on experience with fallopian tube catheterization using uterine models and commercially available catheters and guidewires. 2) Review the evolution of interventions in the fallopian tubes. 3) Learn safe techniques for fallopian tube recanalization for promoting fertility, and fallopian tube occlusion for preventing pregnancy. 4) Discuss the outcomes regarding pregnancy rate and complications. 5) Appreciate ways to improve referrals from the fertility specialists and expand your practice.

ABSTRACT

Fallopian tube catheterization using fluoroscopic guidance is a relatively easy, inexpensive technique within the capabilities of residency trained radiologists. Fallopian tube cathterization can be used to dislodge debris from the tube in women with infertility, or to place FDA-approved tubal occlusion devices in women who do not desire fertility. The fallopian tube is the 1 mm gateway between the egg and the sperm. Noninvasive access to this structure for promoting, and preventing, pregnancy has been sought for over 160 years. This hands-on course allows participants use commercially available catheters and devices in plastic models for fallopian tube catheterization, and to speak directly to world experts about this exciting procedure.

Dynamic Musculoskeletal US: Clicks and Clunks of the Lower Extremity (Hands-on)

Wednesday, Dec. 2 8:30AM - 10:00AM Location: E264

MK US

AMA PRA Category 1 Credits ™: 1.50 ARRT Category A+ Credits: 1.50

Participants

Viviane Khoury, MD, Philadelphia, PA, (viviane.khoury@uphs.upenn.edu) (Presenter) Nothing to Disclose Thomas Moser, MD, Montreal, QC, (thomas.moser@umontreal.ca) (Presenter) Nothing to Disclose Mark Cresswell, MBBCh, Vancouver, BC (Presenter) Nothing to Disclose Jon A. Jacobson, MD, Ann Arbor, MI, (jjacobsn@umich.edu) (Presenter) Consultant, BioClinica, Inc; Royalties, Reed Elsevier; ; ; J. Antonio Bouffard, MD, Detroit, MI (Presenter) Nothing to Disclose Joseph G. Craig, MD, Detroit, MI (Presenter) Nothing to Disclose David P. Fessell, MD, Ann Arbor, MI (Presenter) Nothing to Disclose Ghiyath Habra, MD, Royal oak, MI (Presenter) Nothing to Disclose Joseph H. Introcaso, MD, Neenah, WI (Presenter) Nothing to Disclose Marnix T. van Holsbeeck, MD, Detroit, MI (Presenter) Consultant, General Electric Company Consultant, Koninklijke Philips NV Stockholder, Koninklijke Philips NV Stockholder, General Electric Company Grant, Siemens AG Grant, General Electric Company Kenneth S. Lee, MD, Madison, WI (Presenter) Research Consultant, SuperSonic Imagine; Consultant, Echometrix, LLC; Royalties, Reed Elsevier Humberto G. Rosas, MD, Madison, WI (Presenter) Nothing to Disclose Catherine J. Brandon, MD, Ann Arbor, MI (Presenter) Stock options, VuCOMP, Inc Kambiz Motamedi, MD, Los Angeles, CA (Presenter) Nothing to Disclose Mary M. Chiavaras, MD, PhD, Ancaster, ON (Presenter) Nothing to Disclose Andrea Klauser, MD, Innsbruck, Austria (Presenter) Nothing to Disclose Robert R. Lopez, MD, Charlotte, NC (Presenter) Nothing to Disclose Carlo Martinoli, MD, Genova, Italy (Presenter) Nothing to Disclose Georgina M. Allen, MBBCh, FRCR, Oxford, United Kingdom (Presenter) Nothing to Disclose Girish Gandikota, MBBS, Ann Arbor, MI (Presenter) Nothing to Disclose

LEARNING OBJECTIVES

1) Identify anatomic structures which can impinge or move abnormally in the hip and ankle causing pain during normal range of motion. 2) Describe the ultrasound anatomy and scanning technique for a dynamic examination of these lesions. 3) Position patients optimally for the dynamic evaluation of the hip and ankle respecting ergonomics.

ABSTRACT

This course will demonstrate standardized techniques of performing the dynamic examination of hip and ankle lesions that are only or best demonstrated dynamically. These include the snapping hip, peroneal tendon subluxation/dislocation, flexor hallucis longus impingement, and ankle ligament instability. In the first portion of the course, probe positioning will be demonstrated on a model patient with overhead projection during live scanning. In the second portion of the course, an international group of expert radiologists will assist participants in learning positioning and scanning of hip and ankle joint lesions described. An emphasis on dynamic maneuvers and ergonomic documentation of tissue dynamics will be taught. Participants will be encouraged to directly scan model patients.

Honored Educators

Presenters or authors on this event have been recognized as RSNA Honored Educators for participating in multiple qualifying educational activities. Honored Educators are invested in furthering the profession of radiology by delivering high-quality educational content in their field of study. Learn how you can become an honored educator by visiting the website at: https://www.rsna.org/Honored-Educator-Award/

Jon A. Jacobson, MD - 2012 Honored Educator

Techniques of Musculoskeletal Interventional Ultrasound (Hands-on)

Wednesday, Dec. 2 8:30AM - 10:00AM Location: E263



AMA PRA Category 1 Credits ™: 1.50 ARRT Category A+ Credits: 1.50

Participants

Veronica J. Rooks, MD, Honolulu, HI (Moderator) Nothing to Disclose Peter L. Cooperberg, MD, Vancouver, BC (Presenter) Nothing to Disclose Alda F. Cossi, MD, Boston, MA (Presenter) Nothing to Disclose Nathalie J. Bureau, MD, MSc, Montreal, QC, (nathalie.bureau@umontreal.ca) (Presenter) Equipment support, Siemens AG James W. Murakami, MD, Columbus, OH (Presenter) Nothing to Disclose Michael A. Mahlon, DO, Tacoma, WA (Presenter) Nothing to Disclose Paolo Minafra, MD, Pavia, Italy, (paolominafra@gmail.com) (Presenter) Nothing to Disclose Paula B. Gordon, MD, Vancouver, BC (Presenter) Stockholder, OncoGenex Pharmaceuticals, Inc ; Scientific Advisory Board, Hologic, Inc; Scientific Advisory Board, RealImaging Hollins P. Clark, MD, MS, Winston Salem, NC (Presenter) Nothing to Disclose Carmen Gallego, MD, Madrid, Spain, (cgallego@salud.madrid.org) (Presenter) Nothing to Disclose Mabel Garcia-Hidalgo Alonso, MD, Madrid, Spain (Presenter) Nothing to Disclose Michael A. Dipietro, MD, Ann Arbor, MI (Presenter) Nothing to Disclose Horacio M. Padua JR, MD, Boston, MA (Presenter) Nothing to Disclose Patrick Warren, MD, Columbus, OH (Presenter) Nothing to Disclose Stephen C. O'Connor, MD, Boston, MA (Presenter) Nothing to Disclose Sara E. Smolinski, MD, Springfield, MA (Presenter) Nothing to Disclose

LEARNING OBJECTIVES

Identify basic skills, techniques, and pitfalls of freehand invasive sonography, with specific focus on musculoskeletal applications.
 Define and discuss technical aspects, rationale, and pitfalls involved in musculoskeletal interventional sonographic care procedures.
 Successfully perform basic portions of hands-on US-guided MSK procedures in a tissue simulation learning module, to include core biopsy, small abscess coaxial catheter drainage, cyst and ganglion aspiration, soft tissue foreign body removal, and intraarticular steriod injection.
 Incorporate these component skill sets into further life-long learning for expansion of competency and prepartaion for more advanced interventional MSK sonographic learning opportunities.

ABSTRACT

Ultrasound Guided Foreign Body Removal: Simulation Training and Clinical implementation Outcomes Purpose: USFBR can be taught to radiologists to generate competency, and radiologists can apply the technique in the patient setting to remove foreign bodies. Materials and Methods: Proof of concept was performed by a radiologist and surgeon removing nine 1-cm foreign bodies using the USFBR method (P) and traditional surgery (S) with and without wire guidance (W) on the cadaver model. Next, USFBR was taught to 48 radiologists at 4 hospitals. Training included didactic and hands-on instruction covering 7 components: instrument alignment, hand/transducer position, forceps use, foreign body definition, forceps grasp, recognition of volume averaging, and oblique cross cut artifact. Pre-training testing assessed single toothpick removal from turkey breast in 15 minutes. Post-training evaluation consisted of 5 toothpick removals. Ongoing clinical implementation data of USFBR by trained radiologists are being collected. Parameters including age of patient, which radiologist, removal success, type and size of foreign body, incision size, foreign body retention time, reason for removal, symptoms, modalities used in detection, wound closure, and sedation are recorded. Data analyzed using chi-squared and Fisher's exact tests for categorical outcomes and analysis of variance for continuous outcomes. Results: USFBR technique shows a higher success rate and smaller incision size in comparison to surgical technique alone in the cadaver. Removal success: P 100%, S 78%, and W 89%. With USFBR training, radiologists' scores improved from 21-52% pretraining to 90-100% post-training (p<0.001 for each component). In the clinical setting to date, USFBR has been 100% successful in 7 (of 25 expected) patients, ages 9-73 years, by four radiologists. Parameters included; length 4 to 30 mm, retention 2 to 864 days, incision, 2 to 8 mm. 1 suture closure. 1 sedation. Conclusion: USFBR is superior to non-guided surgical technique. The USFBR approach taught in simulation improves radiologist technique and removal outcomes. A radiologist who completes simulation training can remove a variety of imbedded foreign bodies.

Personalized Medicine: Head and Neck

Wednesday, Dec. 2 8:30AM - 10:00AM Location: S102D

HN NR RO PH

AMA PRA Category 1 Credits ™: 1.50 ARRT Category A+ Credits: 1.50

Participants

Kristy K. Brock, PhD, Ann Arbor, MI (Moderator) License agreement, RaySearch Laboratories AB;

ABSTRACT

Sub-Events

RC522A IGRT and Anatomical Adaptation

Participants Emilie Soisson, PhD, Montreal, QC (*Presenter*) Nothing to Disclose

LEARNING OBJECTIVES

1) Describe the evolution of adaptive radiotherapy and relevant technological advances as they pertain to head and neck radiotherapy. 2) Understand the clinical rational for of plan adaptation in the head and neck patient population. 3) Describe possible routes to clinical implementation. 4) Discuss risks associated with adaptive planning workflows and appropriate quality assurance.

ABSTRACT

This session will focus on the practical implementation of adaptive radiotherapy for head and neck cancer. Although the concept of adaptive radiation therapy (ART) has been around for more than two decades, routine plan adaptation has not become standard practice in the management of head and neck cancer despite huge technological advances in imaging, image registration software, and dose calculation speed. The remaining challenges in implementing ART for head and neck cancer in 2015 as well as an update of the demonstrated clinical need will be discussed. Features of successful adaptive radiotherapy implementations will be highlighted as well as a summary of useful clinical tools and required quality assurance.

RC522B Functional Targeting and Adaptation

Participants

Robert Jeraj, Madison, WI (Presenter) Founder, AIQ Services

LEARNING OBJECTIVES

1) To learn about appropriate anatomical and imaging modalities for selection and delineation of target volumes in HN. 2) To learn about biologically conformal approaches (dose painting) in HN. 3) To learn about quantitative imaging requirements for RT in HN.

ABSTRACT

Anatomical and molecular imaging is used to tailor radiation treatment by enabling proper selection and delineation of target volumes and organs, which in turn lead to dose prescriptions that take into account the underlying tumor biology. Dose modulation to different parts of target volume may also be used to match variable tumor radiosensitivity (so-called biologically conformal radiotherapy or dose-painting). For accurate implementation of targeted and adaptive IMRT, tools and procedures, such as accurate image acquisition and reconstruction, automatic segmentation of target volumes and organs at risk, non-rigid image and dose registration, and dose summation methods, need to be developed and properly validated.

Essentials of Genitourinary Imaging

Wednesday, Dec. 2 8:30AM - 10:00AM Location: S100AB

GU MR US

AMA PRA Category 1 Credits ™: 1.50 ARRT Category A+ Credits: 1.50

Participants Sub-Events

MSES41A Catching Ovarian Cancer

Participants

Elizabeth A. Sadowski, MD, Madison, WI (Presenter) Nothing to Disclose

LEARNING OBJECTIVES

1) Review the types of ovarian epithelial neoplasm seen on imaging. 2) Assess the risk of ovarian cancer based on imaging appearance of an adnexal lesion and clinical information. 3) Emphasize the role of MRI in further evaluation of adnexal lesions.

ABSTRACT

There is a spectrum of ovarian epithelial neoplasms ranging from benign to malignant. Current theories regarding the precursor lesions are debated; however, the pathway from benign epithelial neoplasm to low grade carcinoma follows an indolent course and is distinctly different from the aggressive evolution of high grade carcinoma. An understanding of the pathogenesis of low grade versus high grade ovarian epithelial neoplasms can be helpful to radiologists, when they are faced with an adnexal lesion. Identifying the imaging features suggestive of benign, intermediate and worrisome lesions can triage adnexal lesions into follow up versus treatment. The purpose of this presentation is to review the imaging features of benign, indeterminate and worrisome adnexal lesions and to discuss the appropriate follow up in each case.

MSES41B US and MRI: Imaging of Chronic Pelvic Pain in Women

Participants

Mostafa Atri, MD, Toronto, ON (Presenter) Nothing to Disclose

LEARNING OBJECTIVES

1) To review MRI and US features of adenomyosis and their correlation with pathology. 2) To discuss staging and US and MRI features of endometriosis and their role in the management of this condition. 3) To familiarize imagers with US features of diverticulosis/diverticulitis and how to differentiate it from colitis.

ABSTRACT

Chronic pelvic pain constitutes 10-40% of gynecology visits at a total cost of 39 billion dollars/year in USA. The most common etiologies are gynecological with GI, urology and MSK conditions being the other causes. During this presentation, imaging features of adenomyosis, endometriosis, pelvic congestion, and US features of diverticulosis/diverticulitis are reviewed. Both adenomyosis and endometriosis are common conditions affecting women. They are frequently seen as an incidental finding that can be accurately evaluated by MRI and US in symptomatic patients. There is close correlation between pathology and imaging features of adenomyosis. The main role of imaging in the evaluation of endometriosis is in the staging of the disease to plan for surgery. US features of uncomplicated diverticulitis are discussed. Transvaginal US can accurately diagnose diverticulosis/diverticulitis that should be sought for in women undergoing US to evaluate for chronic pelvic pain.

Handout:Mostafa Atri

http://abstract.rsna.org/uploads/2015/15001868/IMAGING CHRONIC PELVIC PAIN FINAL RSNA 2015 FINAL.pdf

MSES41C Imaging of the Bladder and Ureters

Participants

Manjiri K. Dighe, MD, Seattle, WA (Presenter) Research Grant, General Electric Company

LEARNING OBJECTIVES

1) Review embryology and discuss congenital anomalies of the bladder and ureter. 2) Classify and discuss imaging appearance of ureteric and bladder disease. 3) To discuss the protocols and imaging appearance of bladder and ureteric pathology on various modalities. 4) Review the staging of bladder and ureteric malignancies. 5) Discuss the imaging appearance of various stages of bladder and ureteric cancer. 6) Illustrate the newer techniques for imaging of bladder and ureter.

ABSTRACT

The ureter is an extra-peritoneal structure surrounded by fat.; The ureter is divided into three portions: the proximal ureter (upper) is the segment that extends from the ureteropelvic junction to the area where the ureter crosses the sacroiliac joint, the middle ureter courses over the bony pelvis and iliac vessels, and the pelvic or distal ureter (lower) extends from the iliac vessels to the bladder. It is a dynamic organ and not a simple conduit through which urine flows. Benign and malignant lesions can affect the ureter and these maybe due to contiguous involvement from the kidney or bladder. The ureter can be imaged by a variety of modalities including computed tomography (CT), magnetic resonance imaging (MR), direct pyelography (DP) both antegrade (AP) and retrograde (RP), nuclear medicine diuretic scan and voiding cystourethrography (VCUG). Benign lesions like endometriosis,

Ureteritis, Ureteritis cystica can affect the ureter as well. Transitional cell carcinoma in the ureter is usually diagnosed on imaging. Bladder carcinoma is the fourth most common cancer in men and women. Knowledge of imaging options and appearance is necessary for both radiologists and urologists. Transitional cell carcinoma (TCC) is the most common bladder neoplasm with squamous cell and adenocarcinoma found in less than 10% of cases.; Benign lesions are uncommon but some can be suggested by their imaging appearance. Cystoscopy allows tissue diagnosis and treatment of superficial lesions. Although magnetic resonance imaging (MRI) and computed tomography (CT) both have limitations in detailing depth of muscle invasion, both have a prominent role helping to define the lesion and in staging. This presentation illustrates the role of MR and CT in evaluating bladder and ureter with a discussion of the newer techniques of MR Diffusion Weighted Imaging (DWI) and virtual cystoscopy by CT or MR.

What's New from the American Board of Radiology

Wednesday, Dec. 2 8:30AM - 10:00AM Location: S104A

ED

AMA PRA Category 1 Credits ™: 1.50 ARRT Category A+ Credit: 0

Participants

Milton J. Guiberteau, MD, Houston, TX (Moderator) Nothing to Disclose

LEARNING OBJECTIVES

1) Describe ABR MOC requirements. 2) Describe methods to implement MOC into one's practice. 3) Assess the implications of "Board Eligible" status. 4) Assess the logistics and results of ABR certifying examinations. 5) Analyze the logistics of the new IR/DR pathway.

Sub-Events

RC502A Making MOC Work

Participants

Milton J. Guiberteau, MD, Houston, TX (Presenter) Nothing to Disclose

LEARNING OBJECTIVES

View learning objectives under main course title.

RC502B The Board Eligible Radiologist: Hiring Perspectives and Concerns

Participants Valerie P. Jackson, MD, Tucson, AZ (*Presenter*) Nothing to Disclose

LEARNING OBJECTIVES

View learning objectives under main course title.

Honored Educators

Presenters or authors on this event have been recognized as RSNA Honored Educators for participating in multiple qualifying educational activities. Honored Educators are invested in furthering the profession of radiology by delivering high-quality educational content in their field of study. Learn how you can become an honored educator by visiting the website at: https://www.rsna.org/Honored-Educator-Award/

Valerie P. Jackson, MD - 2014 Honored Educator

RC502C ABR Certifying Exams in Diagnostic Radiology

Participants Dennis M. Balfe, MD, Saint Louis, MO (*Presenter*) Nothing to Disclose

LEARNING OBJECTIVES

View learning objectives under main course title.

RC502D The Alphabet Soup of MOC, CC, and SA-CME

Participants Vincent P. Mathews, MD, Milwaukee, WI (*Presenter*) Nothing to Disclose

LEARNING OBJECTIVES

View learning objectives under main course title.

RC502E IR/DR Certificate and the IR Residency

Participants

Matthew A. Mauro, MD, Chapel Hill, NC (*Presenter*) Data Safety Monitoring Board, BTG International Ltd; Data Safety Monitoring Board, B. Braun Melsungen AG

LEARNING OBJECTIVES

View learning objectives under main course title.

Pediatric Series: Pediatric Oncology and Nuclear Medicine

Wednesday, Dec. 2 8:30AM - 12:00PM Location: S102AB

MRNMROPDAMA PRA Category 1 CreditsTM: 3.25

ARRT Category A+ Credits: 3.50

FDA Discussions may include off-label uses.

Participants

Sue C. Kaste, DO, Memphis, TN (*Moderator*) Nothing to Disclose Heike E. Daldrup-Link, MD, Palo Alto, CA (*Moderator*) Nothing to Disclose Stephan D. Voss, MD, PhD, Boston, MA (*Moderator*) Nothing to Disclose Robert Orth, MD, PhD, Houston, TX (*Moderator*) Research support, General Electric Company; Whal Lee, MD, PhD, Seoul, Korea, Republic Of (*Moderator*) Nothing to Disclose

Sub-Events

RC513-01 Bone Mineral Density Changes in Survivors of Childhood Cancer

Wednesday, Dec. 2 8:30AM - 8:50AM Location: S102AB

Participants Sue C. Kaste, DO, Memphis, TN (*Presenter*) Nothing to Disclose

LEARNING OBJECTIVES

1) Participants will learn risk factors for bone mineral density deficits in patients having been treated for childhood malignancies.

RC513-02 Bone Marrow Edema on MRI as an Indicator of Impending Bone Collapse in Pediatric Cancer Patients on High Dose Corticosteroid Therapy

Wednesday, Dec. 2 8:50AM - 9:00AM Location: S102AB

Participants

Preeti Sukerkar, MD, PhD, Palo Alto, CA (*Presenter*) Nothing to Disclose Shanshan Bao, MD, Winston Salem, NC (*Abstract Co-Author*) Nothing to Disclose Sandhya Kharbanda, Palo Alto, CA (*Abstract Co-Author*) Nothing to Disclose Stuart Goodman, Stanford, CA (*Abstract Co-Author*) Nothing to Disclose Heike E. Daldrup-Link, MD, Palo Alto, CA (*Abstract Co-Author*) Nothing to Disclose

PURPOSE

Osteonecrosis (ON) is a devastating complication of pediatric cancer therapy with high dose corticosteroids, with 20 % of cases progressing to bone collapse, at which point joint conservation therapy may no longer be possible. It was recently shown in adult ON patients that the presence of bone marrow edema (BME) adjacent to epiphyseal ON is correlated with the presence of micro- or macro-fractures on histopathology, and the puprose of out study is to determine whether BME correlates with eventual bone collapse in pediatric cancer patients to help identify high risk patients who would benefit from early interventions.

METHOD AND MATERIALS

We retrospectively reviewed imaging studies of 18 pediatric leukemia patients who underwent high dose corticosteroid therapy and had findings of epiphyseal ON on magnetic resonance imaging (MRI). Two radiologists evaluated the presence of BME. Follow up imaging was reviewed to determine lesion progression. Using Fisher's exact test, the presence of BME was compared to the patient's outcome.

RESULTS

Of the 18 patients, 12 were found to have pre-collapse ON lesions with sufficient follow up imaging. A total of 36 weight-bearing and 2 non-weight-bearing lesions were identified, of which 13 progressed to collapse and 22 remained stable or improved. The presence of BME was found to be significantly correlated with eventual bone collapse, with 100% of patients who progressed to collapse demonstrating BME on initial imaging (p < 0.0001). The absence of BME initially was associated with lesion stability or even improvement (p < 0.0001). 3 lesions were identified that progressed slightly but did not collapse, of which none had BME on initial scans.

CONCLUSION

The absence of BME early on is an indicator of future stability or even improvement of an ON lesion, while the presence of BME appears to precede bone collapse. These results suggest that the presence or absence of BME can be used to help identify high-risk patients earlier so they may receive joint preserving therapies. This study is ongoing to evaluate out findings in a larger patient cohort.

CLINICAL RELEVANCE/APPLICATION

Presence or absence of edema on MRI predicts osteonecrosis progression in pediatric cancer patients and is recommended for stratifying high-risk patients for joint preservation therapy.

RC513-03 To Assess the Added Value of Intravenous Gadolinium for Pre-Surgical Evaluation of Osteosarcoma in Long Bones in Pediatric Patients and Young Adults

Participants Theodore T. Pierce, MD, Boston, MA (*Presenter*) Nothing to Disclose Randheer Shailam, MD, Boston, MA (*Abstract Co-Author*) Nothing to Disclose Santiago Lozano Calderon, MD, PhD, Boston, MA (*Abstract Co-Author*) Nothing to Disclose Pallavi Sagar, MBBS, Boston, MA (*Abstract Co-Author*) Nothing to Disclose

PURPOSE

Osteosarcoma, a malignant bone tumor, is routinely evaluated using magnetic resonance imaging (MRI) with and without intravenous (IV) gadolinium prior to surgical intervention, typically both at initial staging and following neoadjuvant chemotherapy to determine tumor extent for operative planning. A paucity of data exists showing the utility of preoperative contrast enhanced MRI for operative planning and, so far, gadolinium does not reliably help in differentiating post treatment changes from residual disease. Preoperative parameters such as intramedullary tumor length and transphyseal tumor extension are best evaluated on non-contrast T1 or STIR sequences. Uncertainty remains as to the benefit of IV contrast for evaluating neurovascular bundle involvement (NBI) and intra-articular extension (IAE), key parameters for pre-surgical evaluation.

METHOD AND MATERIALS

At 2 time points, 2 pediatric radiologist independently analyzed MRI examinations of patients between the ages of 0-25 years with pathology proven extremity osteosarcoma for two parameters, NBI and IAE. Initial evaluation analyzed these parameters using noncontrast MRI images only (PRE) and, after 1 week, subsequent evaluation included both the pre and post contrast images (POST). Inter-rater discrepancies were resolved by consensus. Cohen's Kappa and McNemar's test were calculated to assess agreement between PRE and POST image interpretations of NBI and IAE.

RESULTS

56 patients with 90 preoperative MRI examinations were analyzed. PRE and POST interpretations agreed on 47 cases of NBI, 39 cases without NBI, and had 4 discordant cases. There were 63 cases with IAE, 25 without IAE, and 2 were discordant. Kappa was 0.91 for NBI and 0.95 for IAE. McNemar's test did not show a difference between PRE and POST imaging (p=0.61 NBI; p=0.48 IAE).

CONCLUSION

No statistical difference between PRE and POST image interpretation was found. A high level of agreement between PRE and POST image interpretation suggests that non-contrast enhanced MRI may be sufficient for pre-surgical planning for long bone osteosarcoma in pediatric patients.

CLINICAL RELEVANCE/APPLICATION

Avoiding unnecessary gadolinium use limits adverse reaction risk, obviates the need for intravenous access and shortens image acquisition, all of which are of particular benefit in pediatric patients.

RC513-04 Whole Body MRI including Diffusion-weighted Imaging as the Sole Staging and Follow-up Imaging Procedure in Pediatric Tumors - Comparison with Established Imaging Modalities

Wednesday, Dec. 2 9:10AM - 9:20AM Location: S102AB

Participants

Guenther K. Schneider, MD, PhD, Homburg, Germany (*Presenter*) Research Grant, Siemens AG; Speakers Bureau, Siemens AG; Speakers Bureau, Bracco Group; Research Grant, Bracco Group; Stefan R. Rick, Homburg, Germany (*Abstract Co-Author*) Nothing to Disclose Peter Fries, MD, Homburg, Germany (*Abstract Co-Author*) Nothing to Disclose Alexander Massmann, MD, Homburg/Saar, Germany (*Abstract Co-Author*) Nothing to Disclose Arno Buecker, MD, Homburg, Germany (*Abstract Co-Author*) Consultant, Medtronic, Inc Speaker, Medtronic, Inc Co-founder,

Aachen Resonance GmbH Research Grant, Siemens AG

PURPOSE

In 58 pediatric pts. with malignant tumors whole body MRI was evaluated as the sole staging procedure in comparison to established methods such as FDG-PET, MIBG or bone scintigraphy, CT and ultrasound. Findings in follow-up whole body MRI were used for evaluation of tumor response and tumor recurrence, again compared against other established imaging methods. Of particular interest was the detection of late recurrence (> 18 month post initial diagnosis) at time points, at which FDG-PET or MIBG scintigraphy are routinely not available based on actual imaging recommendations.

CONCLUSION

Whole body MRI performed with the described technique can correctly stage and diagnose a variety of malignant tumors in pediatric patients and late recurrence of disease is detected with a high accuracy at time points, at which PET or scintigraphy is routinely not performed.

CLINICAL RELEVANCE/APPLICATION

Inferior accuracy of whole body MRI using only STIR sequences or just DWI was recently published, this study demonstrates the potential of whole body MRI using more advanced techniques. Detection of late recurrence only in MRI highlights the need for advanced MRI in follow-up of pediatric malignancies.

RC513-05 Is the Whole Body MR Imaging Necessary in the Management of Children with Acute Myeloid Leukemia?

Wednesday, Dec. 2 9:20AM - 9:30AM Location: S102AB

Participants

Hee Mang Yoon, MD, Seoul, Korea, Republic Of (*Presenter*) Nothing to Disclose Jin Seong Lee, MD, Seoul, Korea, Republic Of (*Abstract Co-Author*) Nothing to Disclose Ah Young Jung, Seoul, Korea, Republic Of (*Abstract Co-Author*) Nothing to Disclose Young Ah Cho, Seoul, Korea, Republic Of (*Abstract Co-Author*) Nothing to Disclose Chong Hyun Yoon, Seoul, Korea, Republic Of (Abstract Co-Author) Nothing to Disclose

PURPOSE

Whole body MR imaging has been frequently used for the management of children with acute myeloid leukemia (AML) because it can provide additional information besides bone marrow evaluation. In this regard, we assess the use of the whole body magnetic resonance (MR) imaging in the management of the children with AML to validate its usefulness.

METHOD AND MATERIALS

Sixty nine whole body MR scans of 40 consecutive pediatric patients with AML were evaluated by two radiologists in consensus. Whole body MR imaging was acquired for the following purposes: work-up for initial diagnosis, work-up for relapsed AML, work-up for stem cell transplant, work-up for a new sign or symptom, or follow-up of pre-existing abnormality. We estimated the presence of abnormal findings including extramedullary granulocytic sarcoma (EGS), clinically occult lesions, and lesions explaining the patient's clinical symptoms, except the bone marrow involvement by AML.

RESULTS

Total 76 EGSs were identified in eleven of 40 patients (27.5 %). Nine of eleven patients (81.8%) had multiple EGSs. Thirty eight EGSs were incidentally detected on 9 whole body MR scans in seven patients (17.5 %). Positive findings were most commonly observed on whole body MR scans performed as work-up for a new sign or symptom (14 of 15 MR scans, 93.3%). Six clinically occult non-EGS lesions found on whole body MR scans were small intracranial hemorrhage (n=1), bilateral otomastoiditis (n=1), pneumonia (n=1), knee joint inflammation with effusion (n=1) and disseminated infection/inflammation (n=2). Multiple lesions at anatomically distant regions were successfully evaluated with 18 whole body MR scans (26.1%) in a single session head-to-toe imaging.

CONCLUSION

Whole body MR imaging could be helpful to detect multiple EGSs or clinically occult lesions and be used as a problem solving tool in children with a new sign or symptom by AML in a single session study.

CLINICAL RELEVANCE/APPLICATION

Whole body MR imaging is a useful imaging modality in management of the pediatric AML patients considering tendency for multiplicity of EGSs and prevalent occult lesions as well as the intrinsic advantages of whole body MR imaging.

RC513-06 Defining Optimal Dose Regimes for Pediatric Whole-body 18F-FDG-PET/MRI

Wednesday, Dec. 2 9:30AM - 9:40AM Location: S102AB

Participants

Sergios Gatidis, MD, Tubingen, Germany (Presenter) Nothing to Disclose

Holger Schmidt, PhD, Tuebingen, Germany (Abstract Co-Author) Nothing to Disclose

Christian la Fougere, Munich, Germany (*Abstract Co-Author*) Nothing to Disclose

Konstantin Nikolaou, MD, Tuebingen, Germany (Abstract Co-Author) Speakers Bureau, Siemens AG Speakers Bureau, Bracco Group Speakers Bureau, Bayer AG

Nina Schwenzer, MD, Tuebingen, Germany (Abstract Co-Author) Nothing to Disclose

Juergen F. Schaefer, MD, Tuebingen, Germany (Abstract Co-Author) Nothing to Disclose

PURPOSE

To find optimal tracer dose regimes for pediatric whole-body 18F-FDG PET/MRI with minimal radiation exposure and sufficient diagnostic quality.

METHOD AND MATERIALS

Whole-body PET data sets of 30 pediatric patients (14 female, mean age 12±6 [1-18] years) were retrospectively analyzed. PET data were acquired in list mode on a combined PET/MR scanner (Biograph mMR, Siemens) 65±14 min after injection of 3.1±0.5 MBq 18F-FDG per kg bw for 4 min per bed position.Based on the acquired list mode data, PET images of lower tracer doses (0.25 to 2.5 MBq/kg bw 18F-FDG) were simulated by retrospective undersampling of PET list mode data.Resulting data sets were analyzed quantitatively by measurement of standardized uptake values (SUVs) in healthy organs (liver, lungs, blood pool) and pathologic lesions by volume-of-interest (VOI) analysis.Qualitative analyzed beginning with the lowest simulated tracer dose (0.25 MBq/kg bw) and gradually increasing tracer doses up to the original acquired PET image. Conspicuity of organ structures (such as brain, thymus, muscle, heart etc.) and detectability of focal PET lesions were recorded and finally compared to the original full-dose data set.

RESULTS

Image quality steadily improved with increasing simulated tracer doses. SUVs showed higher relative deviations of about 10 % at tracer doses below 1 MBq/kg bw. Conspicuity of physiologic organ structures improved steadily with increasing simulated tracer doses and was equivalent with the original acquired PET data set at simulated doses of 1-1.5 MBq/kg bw. Detectability of focal PET lesions increased continuously with increasing simulated tracer doses; all focal lesion that were detectable in the original full-dose PET were already detectable at 1.5 MBq/kg bw.

CONCLUSION

Tracer doses can be significantly reduced in pediatric PET/MRI compared to existing standard regimes. Our results suggest that doses of 1.5 MBq/kg bw FDG are sufficient for accurate diagnostic quality of PET. These results have to be validated in larger clinical studies.

CLINICAL RELEVANCE/APPLICATION

Reduced tracer doses will result in lower diagnostic radiation exposure in pediatric patients. Variation of PET acquisition times may enable further reduction of tracer doses.

Participants

Andrew Sher, MD, Houston, TX (*Abstract Co-Author*) Nothing to Disclose Danial S. Bokhari, MD, Houston, TX (*Presenter*) Nothing to Disclose Matthew Goette, PhD, Houston, TX (*Abstract Co-Author*) Support, Koninklijke Philips NV Rajesh Krishnamurthy, MD, Houston, TX (*Abstract Co-Author*) Research support, Koninklijke Philips NV; Research support, Toshiba Corporation Victor J. Seghers, MD, PhD, Houston, TX (*Abstract Co-Author*) Nothing to Disclose

PURPOSE

Compare lesion based analysis of 18F-FDG PET/MR to 18F-FDG PET/CT in pediatric Langerhans Cell Histiocytosis (LCH) and Rosai Dorfman Disease (RD).

METHOD AND MATERIALS

This prospective, HIPAA compliant study had IRB approval. Following written informed consent 18 18F-FDG PET/CT and PET/MR examinations were performed on 9 patients (6 male, 3 female, mean age 6; range: 7 months to 16 years) following a single-injection dual-imaging protocol. The indication was LCH in 11 exams and RD in 7 exams. Two readers blinded to clinical history assessed the anonymized data for metabolically active disease by consensus read. PET/CT and PET/MR were viewed simultaneously and volumes of interest were drawn over lesions, with lesions defined as non-physiologic uptake above background. SUV maximum values were recorded. Lesion detection rates and classification agreement between modalities were analyzed and compared to the reference standard (all available examinations and clinical history).

RESULTS

94 metabolically active lesions were identified on PET/MR versus 100 on PET/CT. Of the 94 lesions identified on both exams there was concordant classification in 93 (99%), representing excellent agreement, $\kappa = .97$ (p <. 001), 95% CI (0.94-1.0). 6 lesions were identified on PET/CT but not PET/MR, 3 were foci of active disease, 1 was an inflammatory lymph node, and 2 were artifactual or physiologic. Per the standard of reference, 101 metabolically active lesions were available for analysis (80 were active disease while 21 were benign). Compared to the reference standard, the overall sensitivity (93% vs. 96%, p>.05) and specificity (100% vs. 95%, p > .05) of PET/MR vs. PET/CT, respectively, demonstrated no significant difference. The accuracies of PET/MR and PET/CT measured 94% and 96%, respectively. SUV analysis demonstrated lesions on PET/MR measuring 11% lower on average than PET/CT (p<.001). There was a strong correlation ($\rho = .76$) between the SUVs of the two modalities.

CONCLUSION

PET/MR demonstrates no statistical difference to PET/CT for lesion detection and classification in patients with LCH or RD. PET/MR imaging is a promising lower-radiation alternative to PET/CT for this patient population.

CLINICAL RELEVANCE/APPLICATION

PET/MR evaluation for pediatric histiocytoses demonstrates no statistical difference in sensitivity, specificity, or accuracy of lesion detection compared to PET/CT and can contribute to patient management with lower radiation dose.

RC513-08 Whole Body Imaging in Pediatric Oncology

Wednesday, Dec. 2 9:50AM - 10:10AM Location: S102AB

Participants Stephan D. Voss, MD, PhD, Boston, MA (*Presenter*) Nothing to Disclose

LEARNING OBJECTIVES

1) The participant should understand the various whole body multi-modality imaging techniques used in Pediatric Oncology2) The participant should be able to discuss strategies and opportunities for radiation dose reduction when performing multi-modality whole body examinations3) The audience should understand the appropriate indications for whole body imaging in pediatric oncology, including the role of whole body imaging in tumor surveillance and evaluation of patients with cancer predisposition syndromes.

ABSTRACT

RC513-09 Neuroblastoma - Imaging and Therapy Update

Wednesday, Dec. 2 10:30AM - 10:50AM Location: S102AB

Participants Adina L. Alazraki, MD, Atlanta, GA (*Presenter*) Nothing to Disclose

LEARNING OBJECTIVES

1) Identify the common indications for I-131 MIBG in pediatric patients. 2) Describe the necessary considerations for pediatric patients prior to I-131 MIBG therapy. 3) Discuss imaging protocols and typical pre and post therapy imaging appearance as part of monitoring of response to therapy.

RC513-10 PET/MR Imaging in Pediatric Sarcomas and Malignant Soft Tissue Tumors: Is There a Clinical Impact?

Wednesday, Dec. 2 10:50AM - 11:00AM Location: S102AB

Participants

Juergen F. Schaefer, MD, Tuebingen, Germany (*Presenter*) Nothing to Disclose Sergios Gatidis, MD, Tubingen, Germany (*Abstract Co-Author*) Nothing to Disclose Ilias Tsiflikas, MD, Tuebingen, Germany (*Abstract Co-Author*) Nothing to Disclose Guido Seitz, Tuebingen, Germany (*Abstract Co-Author*) Nothing to Disclose Martin Ebinger, Tuebingen, Germany (*Abstract Co-Author*) Nothing to Disclose Christian la Fougere, Munich, Germany (*Abstract Co-Author*) Nothing to Disclose Matthias Reimold, MD, Tuebingen, Germany (*Abstract Co-Author*) Nothing to Disclose Nina Schwenzer, MD, Tuebingen, Germany (*Abstract Co-Author*) Nothing to Disclose Konstantin Nikolaou, MD, Tuebingen, Germany (*Abstract Co-Author*) Speakers Bureau, Siemens AG Speakers Bureau, Bracco Group Speakers Bureau, Bayer AG

PURPOSE

To evaluate the clinical impact of PET/MRI in pediatric sarcomas and malignant soft tissue tumors.

METHOD AND MATERIALS

43 examinations in 30 patients (11 female, mean age 11.1 y \pm 5.4 y) with diagnoses of Ewing sarcoma (n=6), osteosarcoma (n=4), rhabdomyosarcoma (n=6), NF 1 suspected for MPNST (n=9), others (n=5) were included. Written informed consent was obtained. Two protocols were performed: In group A, 11 examinations were carried out using PET/CT (Biograph mCT, Siemens) and PET/MRI (Biograph mMR, Siemens). Data were acquired on the same day after administration of 161±88 MBq 18F-FDG. In group B, 32 examinations were performed using PET/MRI only, after administration of 114±67 MBq 18F-FDG. Additionally, if indicated an additional low dose chest CT was carried out. In Group A, image analysis was performed by two experienced rater teams blinded for the respective different modality. In group B, image analysis was performed by an experienced rater team: first MRI followed by PET-MRI. Histopathology and follow-up served as reference standard. Findings of PET/MRI were reevaluated by the institutional pediatric tumorboard regarding further clinical management (e.g. change of diagnostic or therapeutic regime).

RESULTS

Group A: The rate of focal uptake on PET/MRI was equivalent to PET/CT (52 vs. 53). Local staging (4/11), anatomic allocation (2/11) and relevant additional findings were improved by MRI. Group B: Findings of PET/MRI affecting clinical management were found in 8 /32 examinations (e.g. change of surgical approach or no additional radiation). Compared to chest CT, PET/MRI detected equal numbers of metastases in 5 patients and lower numbers in 5 patients. MRI was negative in 4 patients with nodules smaller than 4 mm who had no evidence of metastases in follow-up. There was no evidence of pulmonary metastasis in 16 patients.

CONCLUSION

Simultaneous PET/MRI in pediatric sarcomas allows a comprehensive diagnostic for both, local and systemic tumor spread. PET/MR substantially affected the clinical management. The lower detection rate of small pulmonary nodules by MRI needs to be discussed with respect to clinical importance.

CLINICAL RELEVANCE/APPLICATION

PET/MRI improves the clinical management in pediatric soft tissue tumors and both, local and systemic staging is possible in a single approach.

RC513-11 Brain Exams in Pediatric Epilepsy: PET/MRI Compared to PET/CT

Wednesday, Dec. 2 11:00AM - 11:10AM Location: S102AB

Participants

Matthew Goette, PhD, Houston, TX (*Presenter*) Support, Koninklijke Philips NV Erica Yang, MD, Houston, TX (*Abstract Co-Author*) Nothing to Disclose Nadia F. Mahmood, MD, Sugar Land, TX (*Abstract Co-Author*) Nothing to Disclose Jeremy Y. Jones, MD, Bellaire, TX (*Abstract Co-Author*) Nothing to Disclose Wei Zhang, PhD, Houston, TX (*Abstract Co-Author*) Nothing to Disclose Victor J. Seghers, MD, PhD, Houston, TX (*Abstract Co-Author*) Nothing to Disclose Andrew Sher, MD, Houston, TX (*Abstract Co-Author*) Nothing to Disclose Michael J. Paldino, MD, Houston, TX (*Abstract Co-Author*) Nothing to Disclose

PURPOSE

PET/MR offers the potential for diverse image contrasts in a single examination. To reach its full potential, this technology will require robust attenuation correction (AC) algorithms. The goal of this study was to compare the diagnostic accuracy of FDG-PET images of the brain processed according to MR-based AC (MRAC) with that of images obtained using traditional CT-based AC (CTAC).

METHOD AND MATERIALS

IRB approval and informed consent were obtained for this study. All patients referred for clinical FDG-PET/CT exams of the brain were prospectively recruited to undergo an additional FDG-PET acquisition on a Philips Ingenuity PET/MR system. A bootstrap power calculation was used to determine the number of patients required to detect a 10% difference in diagnostic accuracy (power: 0.8). Raw FDG-PET images were processed according to vendor-provided MRAC or CTAC algorithms. Five expert readers were blinded to the method of AC and all other clinical/imaging data. Consensus between readers at unblinded re-review of all data was considered the gold standard. Any potential difference in the accuracy of PET/MR compared to PET/CT was assessed using McNemar's test. Cohen's kappa was calculated to measure agreement between each reader's interpretation of MRAC and CTAC.

RESULTS

The study population comprised 35 patients referred for a diagnosis of epilepsy (mean age: 11y; range: 2-18y), with a paired PET/CT and PET/MR exam. Compared to the reference gold standard, the overall sensitivity (71.6% and 70.2%, p>0.05) and specificity (74.7% and 85.1%, p>0.05) of the blinded interpretation of the PET/MR and PET/CT images, respectively, demonstrated no significant difference. The accuracy of MRAC-processed images did not differ significantly from those obtained using CTAC (74.7% and 76.6%, respectively, p>0.3). Overall, there was good intra-reader agreement between the interpretation of PET/MR and PET/CT (κ range: 0.55-0.78).

CONCLUSION

The accuracy of FDG-PET images generated by an MRAC algorithm was comparable to that of FDG-PET images processed by traditional CTAC. These results further support the use of integrated PET/MR systems in clinical practice.

CLINICAL RELEVANCE/APPLICATION

The evaluation of pediatric brain exams for the diagnosis of epilepsy using PET/MR demonstrated no statistical difference in sensitivity, specificity, or accuracy compared to PET/CT, and support the use of PET/MR in patient management with lower radiation dose.

RC513-12 What is the Optimal Way to Measure Neuroblastoma Response to Chemotherapy?

Wednesday, Dec. 2 11:10AM - 11:20AM Location: S102AB

Participants

Lindsey R. Klingbeil, MD, Cincinnati, OH (*Presenter*) Nothing to Disclose Andrew T. Trout, MD, Cincinnati, OH (*Abstract Co-Author*) Advisory Board, Koninklijke Philips NV Alex Towbin, MD, Cincinnati, OH (*Abstract Co-Author*) Author, Reed Elsevier; Consultant, Reed Elsevier; Shareholder, Merge Healthcare Incorporated; Consultant, Guerbet SA; Grant, Guerbet SA Daniel von Allmen, MD, Cincinnati, OH (*Abstract Co-Author*) Nothing to Disclose

PURPOSE

The current recommendation for determining primary neuroblastoma tumor size and response to chemotherapy is to use 3D (anteroposterior, transverse, craniocaudal) measurements. This is in contrast to the 1D measurements recommended in RECIST 1.1 and the 2D measurements recommended for Hodgkin lymphoma. There is little evidence specific to neuroblastoma to show superiority of one measurement technique. The purpose of this study was to assess the correlation between the various measurement methods and actual tumor volume in terms of response assessment.

METHOD AND MATERIALS

We retrospectively analyzed the radiographic data of intermediate and high-risk neuroblastoma patients with either Stage 3 or 4 disease who were diagnosed between 2003 and 2012. Primary tumors were measured in 1D, 2D and 3D at the time of diagnosis and following chemotherapy with 2D and 3D measurements expressed as a product. True tumor volume at each time point was also measured by manual segmentation of the tumor. Tumor response for each measurement method was expressed in terms of a fraction of tumor size at diagnosis. Comparisons were based on Bland-Altman analyses with agreement expressed in terms of correlation coefficients.

RESULTS

Imaging from 34 patients was included in the study with comparison of tumor response to true volumes for 50 1D, 50 2D, and 39 3D measurements. A statistically significant correlation was seen between both the 2D (p<0.05) and the 3D (p<0.01) measurements and the volumetric method of tumor response assessments with the best correlation (r=0.47 versus 0.31) for the 3D measurements. 1D measurements had poor correlation with the volumetric response assessment (r=0.04). The mean difference in tumor response relative to volumetric assessment was higher for 2D measurements than 3D measurements (19% ±16% versus 10%±15%).

CONCLUSION

Correlation between single and multiplanar measurements and true tumor volume for assessment of neuroblastoma response to therapy is moderate at best likely reflecting the irregular shape and infiltrative character of these tumors. 3D measurements had the highest correlation with volumetric assessments but may over- or underestimate tumor response by 40%.

CLINICAL RELEVANCE/APPLICATION

Accurately determining the primary tumor response to chemotherapy using imaging is critical for making therapeutic decisions and surgical planning for neuroblastoma patients.

Honored Educators

Presenters or authors on this event have been recognized as RSNA Honored Educators for participating in multiple qualifying educational activities. Honored Educators are invested in furthering the profession of radiology by delivering high-quality educational content in their field of study. Learn how you can become an honored educator by visiting the website at: https://www.rsna.org/Honored-Educator-Award/

Alex Towbin, MD - 2014 Honored Educator

RC513-13 Evaluation of the Predictive Value of Doppler Ultrasonography in Children with Clinically Suspicious Hepatic Veno-occlusive Disease after Hematopoietic Stem Cell Transplantation

Wednesday, Dec. 2 11:20AM - 11:30AM Location: S102AB

Participants

Ji-Eun Park, Seoul, Korea, Republic Of (*Presenter*) Nothing to Disclose Young Hun Choi, MD, Seoul, Korea, Republic Of (*Abstract Co-Author*) Nothing to Disclose Hyun Suk Cho, Seoul, Korea, Republic Of (*Abstract Co-Author*) Nothing to Disclose Yu Jin Kim, MD, Seoul, Korea, Republic Of (*Abstract Co-Author*) Nothing to Disclose Jung-Eun Cheon, MD, Seoul, Korea, Republic Of (*Abstract Co-Author*) Nothing to Disclose Woo Sun Kim, MD, Seoul, Korea, Republic Of (*Abstract Co-Author*) Nothing to Disclose In-One Kim, MD, Seoul, Korea, Republic Of (*Abstract Co-Author*) Nothing to Disclose

PURPOSE

To evaluate the predictive value of Doppler ultrasonography in children with clinically suspicious hepatic veno-occlusive disease (VOD) after hematopoietic stem cell transplantation (HSCT).

METHOD AND MATERIALS

From January 2012 to January 2015, among 216 children who underwent HSCT, 56 children underwent Doppler ultrasonography for clinical suspicion of hepatic VOD (M:F = 22:34; mean age, 8.3years; age range 8months-20years). Among 56 patients, fifteen patients were confirmed as having VOD later (VOD group), while 41 patients turned out to have other conditions (acute graft-

versus-host disease, n=10; cytomegalovirus hepatitis, n=4; other virus hepatitis, n=6; aspergilosis, n=3; unrevealed cause, n=18; non-VOD group). Doppler ultrasonography was retrospectively reviewed for the following findings: hepatomegaly, splenomegaly, gall bladder(GB) wall edema, ascites, Doppler spectral parameters of the left portal vein (peak velocity, trough velocity, pulsatile index, flow inversion), Doppler spectral parameters of the left hepatic artery (peak systolic velocity, end systolic velocity, resistance index) and phasicity of the middle hepatic vein. The Doppler US findings were compared between two groups using Student t-test, Chi square test. Multivariate logistic regression was performed to reveal the significant predictor of VOD.

RESULTS

The VOD group showed significantly higher incidences of hepatomegaly (9/15, 60% vs. 10/41, 24%, p=0.016), GB wall edema (9/12, 80% vs. 9/41, 22%, p < 0.001) and ascites (12/15, 80% vs. 9/41, 22%, p < 0.001), relative to the non-VOD group. The peak systolic velocity of the left hepatic artery was significantly higher in VOD patients compared with non-VOD patients (73±33cm/sec vs. 49±21cm/sec, p=0.002). Other findings showed no statistically significant difference between the two groups. Multivariate analysis revealed that only ascites was significantly associated with VOD (β =0.345).

CONCLUSION

The presence of hepatomegaly, GB wall edema, ascites and increased peak systolic velocity of the hepatic artery were significantly associated with progression to definite VOD in pediatric HSCT patients with clinically suspicious VOD.

CLINICAL RELEVANCE/APPLICATION

Hepatic VOD is one of the most feared complications of HSCT. Our study identified Doppler ultrasonographic findings that could be helpful in predicting progression to definite VOD.

RC513-14 Correlation between Diffusion-weighted Imaging Combined with Conventional Magnetic Resonance Imaging Parameters and Histopathologic Findings in Eyes Primarily Enucleated for Advanced Retinoblastoma: A Retrospective Study

Wednesday, Dec. 2 11:30AM - 11:40AM Location: S102AB

Awards

Trainee Research Prize - Medical Student

Participants

Yanfen Cui, Shanghai, China (*Presenter*) Nothing to Disclose Dengbin Wang, Shanghai, China (*Abstract Co-Author*) Nothing to Disclose Huanhuan Liu, Shanghai, China (*Abstract Co-Author*) Nothing to Disclose Caiyuan Zhang, MD, Shanghai, China (*Abstract Co-Author*) Nothing to Disclose

PURPOSE

to evaluate the diagnostic accuracy of conventional MR imaging in detecting tumor invasion of intraocular retinoblastoma and to correlate ADC values with high-risk pathological prognostic parameters of retinoblastoma.

METHOD AND MATERIALS

The accuracy of MR imaging in detecting invasion extent of 63 tumors were determined. Furthermore, ADC value with b factors of 0 and 1000 seconds/mm2 were calculated and correlated with high risk pathological prognostic parameters. Additionally, the correlation of Ki-67 expression with ADC value were analysed.

RESULTS

The accuracy of conventional MRI in detecting prelaminar and postlaminar optic nerve invasion was 85.7%, focal and massive choroidal invasion 61.9%, scleral invasion 98.4% and ciliary body invasion was 95.2%. The ADC value of well-differentiated retinoblastoma were significantly different from poorly or undifferentiated tumors (p < 0.002). There was no significant difference in the ADC value between bilateral and unilateral retinoblastomas (P=0.09) and different growth pattern (P=0.74). The ADC value of postlaminar optic nerve invasion has significantly different with no optic nerve invasion (P=0.04). There was significant difference in the ADC of retinoblastoma with or without scleral invasion (P=0.007), but has no difference in chorodial invasion (P=0.629) or ciliary body invasion (P=0.532). Additionally, the ki-67 index was inversely correlated with the ADC value (p < 0.002).

CONCLUSION

Routine MRI has limitations in reliably predicting microscopic infiltration of the retinoblastoma, where ADC correlated well with highrisk pathological prognostic parameters and Ki-67 index for retinoblastoma and may serve as a noninvasive prognostic parameter for assessment of newly diagnosed retinoblastoma.

CLINICAL RELEVANCE/APPLICATION

Routine MRI has limitations in reliably predicting microscopic infiltration of the retinoblastoma, whereas ADC correlated well with high-risk pathological prognostic parameters and Ki-67 index for retinoblastoma and may serve as a noninvasive prognostic parameter for assessment of newly diagnosed retinoblastoma.

RC513-15 Imaging of Tumor Syndromes

Wednesday, Dec. 2 11:40AM - 12:00PM Location: S102AB

Participants

Andrew T. Trout, MD, Cincinnati, OH, (andrew.trout@cchmc.org) (Presenter) Advisory Board, Koninklijke Philips NV

LEARNING OBJECTIVES

1) Recognize some of the tumor predisposition syndromes that present in children/young adults. 2) Name the relevant tumors for the discussed syndromes. 3) Implement currently accepted imaging protocols for the discussed syndromes.

Adult Structural and Congenital Heart Disease (An Interactive Session)

Wednesday, Dec. 2 8:30AM - 10:00AM Location: S103AB

CA CT MR

AMA PRA Category 1 Credits ™: 1.50 ARRT Category A+ Credits: 1.50

FDA Discussions may include off-label uses.

Participants

ABSTRACT

Sub-Events

RC503A Systematic Approach to CT Interpretation in Congenital Heart Disease

Participants

Suhny Abbara, MD, Dallas, TX (*Presenter*) Author, Reed Elsevier; Editor, Reed Elsevier; Institutional research agreement, Koninklijke Philips NV; Institutional research agreement, Siemens AG

LEARNING OBJECTIVES

1) To understand the systematic segmental approach to congenital heart disease. 2) To recognize the CT specific imaging findings that relate to each step in the segmental approach to congenital heart disease.

ABSTRACT

Honored Educators

Presenters or authors on this event have been recognized as RSNA Honored Educators for participating in multiple qualifying educational activities. Honored Educators are invested in furthering the profession of radiology by delivering high-quality educational content in their field of study. Learn how you can become an honored educator by visiting the website at: https://www.rsna.org/Honored-Educator-Award/

Suhny Abbara, MD - 2014 Honored Educator

RC503B Tailoring CT Scan Acquisitions to Specific Indications

Participants

Brian B. Ghoshhajra, MD, Boston, MA (Presenter) Nothing to Disclose

LEARNING OBJECTIVES

1) To understand the different indications for cardiac CT, including calcium scoring, coronary CT angiography, electrophysiology procedural planning, structural heart disease interventions (including TAVR), congenital heart disease, myocardial evaluation, and mass workup. 2) To review the differences between various available equipment, and how available equipment might affect a given protocol. 3) To review basic protocols for each of the above exam types, and review specific features of each exam type. 4) To review the advantages and disadvantages of individualized settings within each of the above protocols.

Active Handout:Brian Burns Ghoshhajra

http://abstract.rsna.org/uploads/2015/14000914/RC503B Tailoring CT Scan Acquisitions to Specific Indications - Ghoshhajra Handout.pdf

RC503C Imaging of Cardiac Shunts

Participants

Harold I. Litt, MD, PhD, Philadelphia, PA (Presenter) Research Grant, Siemens AG; Research Grant, Heartflow, Inc;

LEARNING OBJECTIVES

1) Describe MR imaging methods for detection and quantification of intra and extracardiac shunts. 2) Describe CT imaging methods for detection and quantification of intra and extracardiac shunts. 3) Plan an optimized protocol for CT or MR imaging of shunts.

RC503D Role of MRI in Adult CHD Management

Participants

Mini V. Pakkal, MBBS, FRCR, Toronto, ON, (mini.pakkal@uhn.ca) (Presenter) Nothing to Disclose

Active Handout: Mini Vithal Pakkal

http://abstract.rsna.org/uploads/2015/14000924/RC503D RSNA final2015.pdf



BOOST: Genitourinary-Oncology Anatomy (An Interactive Session)

Wednesday, Dec. 2 8:30AM - 10:00AM Location: S103CD

GU RO AMA PRA Category 1 Credits ™: 1.50 ARRT Category A+ Credits: 1.50

FDA Discussions may include off-label uses.

Participants

Jelle O. Barentsz, MD, PhD, Nijmegen, Netherlands (*Presenter*) Nothing to Disclose Albert J. Chang, MD, PhD, San Francisco, CA (*Presenter*) Nothing to Disclose

LEARNING OBJECTIVES

1) Introduce imaging anatomy relevant to prostate cancer and review imaging issues for contouring primary tumors, nodal regions, and adjacent critical structures. 2) Review how the integration of different imaging modalities can affect tumor delineation. 3) How to choose appropriate imaging methods for specific purposes and to discuss the significance of certain imaging findings.

Molecular and Functional Imaging/Surrogate Markers in Radiation Oncology

Wednesday, Dec. 2 8:30AM - 10:00AM Location: S102C



AMA PRA Category 1 Credits ™: 1.50 ARRT Category A+ Credits: 1.50

Participants

Anca L. Grosu, MD, Freiburg, Germany (Moderator) Nothing to Disclose

LEARNING OBJECTIVES

1) To understand challenges of morphological radiological investigations for the detection and characterization of tumor biology and the timely assessment of tumor response in clinical cancer therapy and in clinical trials testing new therapy regimens. 2) To understand the role and the potential of functional and molecular imaging modalities and techniques used a. prior to therapy for tumor delineation and targeting, b. during cytotoxic therapy, such as radiation and chemotherapy for intra-treatment tumor response monitoring, and .) after cytotoxic therapy for response assessment. 3) To apply and integrate imaging modalities into the therapeutic management of cancer. 4) To review the role of imaging as predictors of tumor control and survival and their emerging role as short-term surrogate markers for long-term therapeutic outcome of cancer treatment regimens and its potential for adaptive therapy.

Sub-Events

RC520A Imaging Surrogate Markers in CNS Tumors

Participants

Anca L. Grosu, MD, Freiburg, Germany (Presenter) Nothing to Disclose

LEARNING OBJECTIVES

1) Clinical problem: Limitations of the morphological/radiological investigations (CT and MRI) for the detection of the gross tumor mass and visualization of tumor biology. 2) Gross Tumor Volume (GTV) Delineation: Amino- Acids PET (AA-PET) and SPECT: a. Sensitivity and specificity of MET-PET, FET-PET and IMT-SPECT b. Comparison MET-PET, FET-PET and IMT-SPECT c. AA-PET for GTV delineation in gliomas d. Future trials. 3) Tumor Biologys: a. Glucose metabolism: FDG-PET b. Tumor proliferation: FLT-PET c. Tumor hypoxia: F-MISO-PET d. Tumor angiogenesis: RGD-PET, MRI e. Visualization of tumor stemm cells in vivo: animal-PET f. Tumor heterogeneity: MRI.

ABSTRACT

1) Clinical problem: Limitations of the morphological/radiological investigations (CT and MRI) for the detection of the gross tumor mass and visualization of tumor biology. 2) Gross Tumor Volume (GTV) Delineation: Amino- Acids PET (AA-PET) and SPECT: a. Sensitivity and specificity of MET-PET, FET-PET and IMT-SPECT b. Comparison MET-PET, FET-PET and IMT-SPECT c. AA-PET for GTV delineation in gliomas d. Future trials. 3) Tumor Biologys: a. Glucose metabolism: FDG-PET b. Tumor proliferation: FLT-PET c. Tumor hypoxia: F-MISO-PET d. Tumor angiogenesis: RGD-PET, MRI e. Visualization of tumor stemm cells in vivo: animal-PET f. Tumor heterogeneity: MRI.

RC520B Imaging Surrogate Markers in Pelvic Tumors

Participants

Nina A. Mayr, MD, Seattle, WA (Presenter) Nothing to Disclose

LEARNING OBJECTIVES

View learning objectives under main course title.

RC520C Imaging Surrogate Markers in Lung Tumors

Participants Meng X. Welliver, MD, Columbus, OH (*Presenter*) Nothing to Disclose

LEARNING OBJECTIVES

View learning objectives under main course title.

RC520D Imaging Surrogate Markers in Head and Neck Cancer

Participants

Min Yao, MD, PhD, Cleveland, OH (Presenter) Nothing to Disclose

LEARNING OBJECTIVES

1) Prognostic indications of FDG PET in head and neck cancer. 2) How to use FDG PET in radiation treatment planning in head and neck cancer. 3) Further treatment decision based on PET. 4) Future prospectives including potential new tracers.

Novel Applications of Dual Energy CT

Wednesday, Dec. 2 8:30AM - 10:00AM Location: S504CD

СТ

AMA PRA Category 1 Credits [™]: 1.50 ARRT Category A+ Credits: 1.50

Participants

Myrna C. Godoy, MD, PhD, Houston, TX (Moderator) Nothing to Disclose

Sub-Events

RC517A Dual-Energy CT: Thoracic Applications

Participants Myrna C. Godoy, MD, PhD, Houston, TX (*Presenter*) Nothing to Disclose

LEARNING OBJECTIVES

1) To comprehend the basic physical principles of dual-energy CT (DECT). 2) To review the current clinical potential applications of DECT in thoracic imaging.

ABSTRACT

There are different methods by which dual-energy CT images can be generated. The advantages of DECT technique are twofold: 1) Low kilovoltage imaging with increased iodine conspicuity (based on increased photoelectric interactions) is especially useful for evaluation of vascular structures. 2) Material specific post-processing allows material differentiation (based on the differential CT attenuation of selected substances at two different energies), which can be tailored for each particular clinical indication, for example to evaluate for contrast enhancement in pulmonary nodules. The current potential clinical applications of DECT in thoracic imaging include evaluation of pulmonary arteries, aorta, pulmonary nodules, pleural masses and airways disease.

RC517B New Insights on Dual Energy CT in Oncology

Participants

Carlo N. De Cecco, MD, PhD, Charleston, SC, (dececco@musc.edu) (Presenter) Nothing to Disclose

LEARNING OBJECTIVES

1) To describe the basic principles of DECT imaging. 2) To explain how post-processing is practised. 3) To discuss radiation exposure issues. 4) To critically appraise the strengths and weaknesses of the technique in oncologic imaging. 5) To comment on the contribution of DECT imaging in oncologic patients management.

ABSTRACT

Dual Energy CT (DECT) is an innovative imaging technique, whose basic principle is the application of two distinct energy settings making able to distinguish materials with different molecular composition on the basis of their attenuation profiles and thus operating a transition from density based image to spectral imaging. DECT applications are based on two distinct capabilities: 1) material differentiation, which means achieving material-specific imaging with separation of distinct materials, for example iodine, calcium, and uric acid, within an image obtained during a single examination and 2) material identification and quantification, which means accurate assessment of the presence and amount of iodine within a target lesion. In particular, with DECT acquisition multiple data-sets such as elemental decomposition analysis, iodinated density map, monochromatic images or virtual unenhanced images can be obtained simultaneously making the Radiologist able to address different diagnostic problems and improving lesion detection and characterization. These technical characteristics make DECT an innovative imaging modality particularly useful in oncologic imaging, having clear advantages in tumor detection, lesion characterization, evaluation of response to therapy, and detection of oncologic-related disease.In conclusion, DECT represents an innovative imaging technique, which can significantly impact on the management of oncologic patients.

RC517C Musculoskeletal Imaging with DECT

Participants

Savvas Nicolaou, MD, Vancouver, BC (Presenter) Institutional research agreement, Siemens AG

LEARNING OBJECTIVES

1) Review the technique and principles of DECT and spectral imaging as it pertains to the musculoskeletal applications. 2) Demonstrate the musculoskeletal applications of DECT/spectral imaging in musculoskeletal imaging with an emphasis on the ability to diagnose and monitor progression of gout. 3) Display additional abilities and demonstrate imaging examples of DECT/spectral imaging for identification of bone marrow edema, soft tissue (tendon and ligamentous) injuries, reduction of metal artifacts and novel applications in the assessment of soft tissues. 4) Review the advantages and limitations of DECT compared to other imaging modalities for musculoskeletal imaging.

ABSTRACT

Dual energy CT and Spectral imaging are useful tools for musculoskeletal imaging. We will focus on the utility of this in the setting of musculoskeletal imaging of gout by demonstrating its ability to aid in diagnosis in challenging cases, delineate anatomy of crystal deposition disease, and monitor disease progression and treatment of the monosodium urate crystals. The audience will learn the utility of DECT/Spectral imaging for additional musculoskeletal applications such as characterization of acute bone marrow edema, identification of tendon and ligamentous injuries and reduction of metal artifacts using monoenergetic imaging.

What Is Driving Health Care Reform and How It Is Changing Your Radiology Practice

Wednesday, Dec. 2 8:30AM - 10:00AM Location: S105AB

HP LM

AMA PRA Category 1 Credits ™: 1.50 ARRT Category A+ Credits: 1.50

Participants

Sub-Events

RC532A Impact of Health Care Reform on Radiology: Intended and Unintended

Participants

Lawrence R. Muroff, MD, Tampa, FL, (LRMuroff@hotmail.com) (Presenter) Nothing to Disclose

LEARNING OBJECTIVES

1) Discuss the key elements of health reform as they impact radiology. 2) Develop strategies to deal with the intended and unintended consequences of health care reform. 3) Describe some of the alternative payment mechanisms that will be competing with fee-for-service, and discuss how radiologists will fit into these new compensation dynamics. (This course is part of the Leadership Track)

ABSTRACT

This presentation will review the trends impacting our specialty. Declining reimbursement, non-traditional competition, and more aggressive turf incursion will be examined, and strategies will be offered to enable radiologists the opportunity to survive and thrive in a time of change. The talk will cover alternative payment proposals and possible new practice models. Future opportunites will be discussed. Attendees of this session should have a better understanding of how our specialty will look in the new health care dynamic and what their role will be in this changed environment.

RC532B How has Health Care Reform Affected Funds Flow and Compensation?

Participants

Ronald L. Arenson, MD, San Francisco, CA (Presenter) Nothing to Disclose

LEARNING OBJECTIVES

1) Recognize the contributory elements promoting the implementation of significant healthcare reform in Massachusetts. 2) Review both the systemic shortfalls and benefits delivered to the citizens of Massachusetts during that state's implementation of universal health care. 3) Understand broad similarities and differences between the Massachusetts and National models of their respective Affordable Care Acts. (This course is part of the Leadership Track)

ASRT@RSNA 2015: Working with Obese Patients in Radiography

Wednesday, Dec. 2 9:20AM - 10:20AM Location: N230

ОТ

AMA PRA Category 1 Credit [™]: 1.00 ARRT Category A+ Credit: 1.00

Participants

Barbara J. Smith, BS, Portland, OR (Presenter) Nothing to Disclose

LEARNING OBJECTIVES

1) Explain obesity statistics and issues related to radiography. 2) Discuss sensitivity training and communication. 3) Identify transportation and transfer of obese patients for safety of patient and personnel. 4) Describe imaging challenges and how to locate anatomical landmarks. 5) Examine exposure related issues.

ABSTRACT

Obesity is affecting an increasing number of people throughout the world and is a growing global health problem. This presentation will define various degrees of obesity, review the statistics and discuss some of the health impacts. Included is a discussion of equipment specifically designed for transportation and the transfer of obese patients. Radiographic equipment designed to image obese patients will be included. The dignity of the patient should be kept in mind so patient care issues such as sensitivity training and communication require us to be more aware of the issues of obesity. There are many imaging challenges associated with obese patients and it is important to understand that the bony skeleton and organ locations have not changed, but it is difficult to locate common positioning landmarks. A new technique for locating anatomical landmarks will be presented to assist with positioning accuracy. Exposure factor use for images and how it affects the radiographic tube will be covered. Additional considerations will be discussed relating to image receptor size, collimation, focal spot size, grid use, AEC and dose.

Active Handout:Barbara Joeine Smith

http://abstract.rsna.org/uploads/2015/15001464/MSRT42.pdf

RSNA/ESR Emergency Symposium: Chest Emergencies (An Interactive Session)

Wednesday, Dec. 2 10:30AM - 12:00PM Location: S402AB

CH ER

AMA PRA Category 1 Credits ™: 1.50 ARRT Category A+ Credits: 1.50

Participants

Ronald J. Zagoria, MD, San Francisco, CA, (ron.zagoria@ucsf.edu) (*Moderator*) Nothing to Disclose Andras Palko, MD, PhD, Szeged, Hungary (*Moderator*) Medical Advisory Board, Affidea Group;

Sub-Events

MSSR42A Thoracic Injuries

Participants

Jorge A. Soto, MD, Boston, MA (Presenter) Nothing to Disclose

LEARNING OBJECTIVES

1) To recognize the most common vascular injuries seen in the setting of blunt thoracic trauma. 2) To understand the importance of differentiating traumatic aortic injuries from mimics, especially congenital variants. 3) To present a classification scheme that distinguishes between minor and major aortic injuries and how this classification influences patient management management. 4) Illustrate with examples other important injuries resulting from chest trauma: major airways, heart, lung parenchyma, pleura and diaphragm.

ABSTRACT

Vascular injuries caused by blunt or penetrating trauma are common and highly lethal. In patients who survive the initial event, rapid evaluation with CT may be life saving. This presentation will focus on the importance of recognizing the CT signs used to diagnose major and minor aortic injuries and will introduce a classification method that helps direct patient management. Other important injuries that the radiologist needs to be aware of will also be reviewed, such as those affecting the major airways, heart and diaphragm. The emerging role of CT in the management of penetrating thoracic trauma will also be discussed. Finally, examples illustrating potential pitfalls leading to false-negative or false-positive interpretations will be highlighted.

Honored Educators

Presenters or authors on this event have been recognized as RSNA Honored Educators for participating in multiple qualifying educational activities. Honored Educators are invested in furthering the profession of radiology by delivering high-quality educational content in their field of study. Learn how you can become an honored educator by visiting the website at: https://www.rsna.org/Honored-Educator-Award/

Jorge A. Soto, MD - 2013 Honored Educator Jorge A. Soto, MD - 2014 Honored Educator Jorge A. Soto, MD - 2015 Honored Educator

MSSR42B Non-Traumatic Thoracic Emergencies

Participants

Cornelia M. Schaefer-Prokop, MD, Nijmegen, Netherlands (Presenter) Advisory Board, Riverain Technologies, LLC

LEARNING OBJECTIVES

1) To get familiar with protocols and diagnostic performance of comprehensive cardiothoracic CT examinations to determine the presence of vascular life threatening events such as aortic dissection, acute coronary disease and pulmonary embolism. 2) To illustrate typical but also less classic CXR and CT findings of patients with pulmonary or mediastinal diseases causing acute dyspnoea and / or requiring immediate treatment and to learn about key imaging findings in these patients allowing for a fast differential diagnosis. 3) To learn how to adapt CT protocols to CXR findings and to integrate imaging findings with lab findings, patient history and clinical information for making the diagnosis.

ABSTRACT

Pulmonary symptoms such as chest pain, shortness of breath or wheezing are common non-traumatic symptoms prompting ER visits. Because clinical symptoms are very non-specific, imaging plays a major role in differentiating life threatening from less severe diseases and forming a diagnosis. The chest radiograph remains the first imaging despite its limited sensitivity for certain diseases and being prone to inter-observer variability. Comprehensive cardiothoracic CT examinations using most modern CT equipment are well evaluated in their diagnostic accuracy to determine the presence of vascular life threatening events such aortic dissection, acute coronary disease and pulmonary embolism. Protocols, literature evidence and appropriate examples will be discussed. In addition the course will highlight nonvascular emergencies such as mediastinal diseases (e.g., esophageal perforation, mediastinitis or pericarditis) and pulmonary emergencies (e.g., pneumonia, edema, pneumothorax, exacerbation of diffuse lung diseases) for which a more comprehensive consideration of imaging findings, lab findings, patient history and clinical information is needed for making the diagnosis.

MSSR42C Interactive Case Discussion

Cornelia M. Schaefer-Prokop, MD, Nijmegen, Netherlands (Presenter) Advisory Board, Riverain Technologies, LLC

Honored Educators

Presenters or authors on this event have been recognized as RSNA Honored Educators for participating in multiple qualifying educational activities. Honored Educators are invested in furthering the profession of radiology by delivering high-quality educational content in their field of study. Learn how you can become an honored educator by visiting the website at: https://www.rsna.org/Honored-Educator-Award/

Jorge A. Soto, MD - 2013 Honored Educator Jorge A. Soto, MD - 2014 Honored Educator Jorge A. Soto, MD - 2015 Honored Educator

Neuroradiology (Cognitive and Psychiatric Disorders)

Wednesday, Dec. 2 10:30AM - 12:00PM Location: N226

NR MR

AMA PRA Category 1 Credits ™: 1.50 ARRT Category A+ Credits: 1.50

FDA Discussions may include off-label uses.

Participants

Jody L. Tanabe, MD, Aurora, CO (*Moderator*) Nothing to Disclose John D. Port, MD, PhD, Rochester, MN (*Moderator*) Nothing to Disclose

Sub-Events

SSK13-01 Brain Microstructural Abnormalities in Medication-free Patients with Major Depressive Disorder: A Systematic Review and Meta-analysis of Diffusion Tensor Imaging

Wednesday, Dec. 2 10:30AM - 10:40AM Location: N226

Participants

Jing Jiang, Chengdu, China (*Presenter*) Nothing to Disclose Youjin Zhao, Chengdu, China (*Abstract Co-Author*) Nothing to Disclose Xinyu Hu, Chengdu, China (*Abstract Co-Author*) Nothing to Disclose Ming Y. Du, Chengdu, China (*Abstract Co-Author*) Nothing to Disclose Min Wu, Chengdu, China (*Abstract Co-Author*) Nothing to Disclose Kai M. Li, Chengdu, China (*Abstract Co-Author*) Nothing to Disclose Qiyong Gong, Chengdu, China (*Abstract Co-Author*) Nothing to Disclose

PURPOSE

Numerous neuroimaging studies have reported impaired white matter (WM) integrity in patients with major depressive disorder (MDD). However, due to inclusion of medicated patients, it is difficult to conclude whether the alterations observed in previous meta-analyses of diffusion tensor imaging studies were related to the disease itself. The present study was to provide a quantitative voxel-wise meta-analysis of WM alterations in medication-free MDD patients excluding interference from medication effects.

METHOD AND MATERIALS

A systematic search was conducted for the relevant studies. Anisotropic Effect Size version of Signed Differential Mapping (AES-SDM) was applied to analyse the WM alterations between medication-free MDD patients and healthy controls. Two subgroup analyses were separately conducted in medication wash-out patients and medication-naive patients. DTIquery software was used for fibre tracking.

RESULTS

15 primary studies comprising 434 MDD subjects (251 female; mean age 34 years) matched with 429 healthy controls (233 female; mean age 33 years) were included. Both the pooled meta-analysis and the subgroup meta-analysis in medication wash-out patients showed robustly fractional anisotropy (FA) reductions in the WM of the right cerebellum hemispheric lobule (CHL), the body of the corpus callosum (CC), and the bilateral superior longitudinal fasciculus III (SLF III), while FA reductions in the genu of the CC and the right anterior thalamic projections were only seen in medication-naive patients. Fibre tracking showed that the main tracts involved the right cerebellar tracts (CT), the body of the CC and the bilateral SLF III and arcuate network.

CONCLUSION

By excluding the confounding influences of medication status, the present study revealed the WM abnormalities in brain regions of MDD involved in cognition, memory function and emotional processing. These findings may contribute to a better understanding of the underlying neuropathology of MDD and be conducive to target selection for the non-drug therapy that the current era of psychosurgery utilizes as therapies for depression, such as electroconvulsive therapy, deep brain stimulation, and transcranial magnetic stimulation.

CLINICAL RELEVANCE/APPLICATION

By excluding the confounding influences of medication status, the disease-related brain regions of white matter abnormalities of MDD can be conducive to target selection for the non-drug therapy.

SSK13-02 Multimodal Voxel-Wise Meta-Analysis of White Matter Abnormalities in Autism Spectrum Disorder

Wednesday, Dec. 2 10:40AM - 10:50AM Location: N226

Participants

Xinyu Hu, Chengdu, China (*Presenter*) Nothing to Disclose Lizhou Chen, Chengdu, China (*Abstract Co-Author*) Nothing to Disclose Lei Li, Chengdu, China (*Abstract Co-Author*) Nothing to Disclose Ming Y. Du, Chengdu, China (*Abstract Co-Author*) Nothing to Disclose Yi Liao, Chengdu, China (*Abstract Co-Author*) Nothing to Disclose Ming Zhou, Chengdu, China (*Abstract Co-Author*) Nothing to Disclose Qi Liu, Chengdu, China (*Abstract Co-Author*) Nothing to Disclose Qiyong Gong, Chengdu, China (*Abstract Co-Author*) Nothing to Disclose Xiaoqi Huang, MD, Chengdu, China (*Abstract Co-Author*) Nothing to Disclose

PURPOSE

Autism spectrum disorder (ASD) is a neurodevelopmental disorder characterized by deficits in social interaction, communication, and stereotyped or repetitive behaviors. White matter (WM) abnormalities have long been suspected in ASD, but the available evidences have been inconsistent. We conducted the first multimodal meta-analysis of WM volume (WMV) and fractional anisotropy (FA) studies to elucidate the most robust WM abnormalities in ASD.

METHOD AND MATERIALS

PubMed, ISI Web of Science, PsycINFO, Cochrane Library, and EMBASE databases were searched between 1994 and 2014 for all voxel-wise studies comparing WMV or FA between patients with ASD and healthy control subjects (HCS). Manual searches were also conducted and authors were contacted soliciting additional data. Coordinates were extracted from clusters of significant WMV and FA difference between ASD patients and HCS. Anisotropic effect size signed differential mapping (AES-SDM) was used to examine regions of WMV and FA alterations in ASD patients compared to HCS separately. Furthermore, peak WMV and FA data were combined using novel multimodal meta-analytic methods implemented in AES-SDM. Meta regression methods were also used to explore potential effects of clinical profiles.

RESULTS

27 studies (providing 29 datasets: 20 WMV and 9 FA) were included comprising 544 adult and pediatric patients with ASD and 544 matched HCS). Patients with ASD showed widespread WM abnormalities including cerebellum, external capsule, cingulum and prefrontal WM, but findings were particularly robust in the crossing between the genu and anterior body of corpus callosum (CC), which showed both decreased WMV and decreased FA (Fig A-C). Meta-regression showed the age was negatively correlated with WMV in the left cerebellum while the percentage of male patients was negatively correlated with FA in the body of CC (Fig DandE).

CONCLUSION

This study gave a thorough profile for the WM abnormalities in ASD and provided evidence that inter-hemisphere was the most convergent circuitry affected in ASD. Meta-regression results perhaps revealed the structural underpinning of age and gender differences in epidemiological and clinical aspects of ASD.

CLINICAL RELEVANCE/APPLICATION

This study confirmed inter-hemisphere was the most convergent circuitry affected in ASD and suggested that structural underpinning of age and gender differences in epidemiological and clinical aspects of ASD.

SSK13-03 Disorganization of White Matter Microstructure in Attention-Deficit/Hyperactivity Disorder: A Tract-Based Spatial Meta-analysis

Wednesday, Dec. 2 10:50AM - 11:00AM Location: N226

Participants

Lizhou Chen, Chengdu, China (*Presenter*) Nothing to Disclose Xinyu Hu, Chengdu, China (*Abstract Co-Author*) Nothing to Disclose Qi Liu, Chengdu, China (*Abstract Co-Author*) Nothing to Disclose Ming Zhou, Chengdu, China (*Abstract Co-Author*) Nothing to Disclose Yi Liao, Chengdu, China (*Abstract Co-Author*) Nothing to Disclose Qiyong Gong, Chengdu, China (*Abstract Co-Author*) Nothing to Disclose Xiaoqi Huang, MD, Chengdu, China (*Abstract Co-Author*) Nothing to Disclose

PURPOSE

White matter (WM) abnormalities have been conceived as important substrates of Attention-deficit/hyperactivity disorder (ADHD), but the available studies involving diffusion tensor imaging (DTI) with tract-based spatial statistics (TBSS) analysis yielded variable findings. We conducted the first tract-based spatial meta-analysis contrasting ADHD patients with healthy control subjects (HCS) to clarify the consistent changes of regional fractional anisotropy (FA) underpinning this disorder.

METHOD AND MATERIALS

Systematic and comprehensive searches of the PubMed, ISI Web of Science, PsycINFO, Medline, Cochrane Library, and EMBASE databases were performed for TBSS studies published between 1994 and 2014 together with 'in press' articles. The reference lists of identified articles and review articles were also manually scrutinized to obtain additional papers. Coordinates were extracted from clusters of significant FA difference between ADHD and HCS. Anisotropic effect size signed differential mapping (AES-SDM) was used to examine regions of FA alterations in ADHD patients relative to HCS. DTIquery software was applied to help locate the fascicles involved in each region. Besides, meta-regression methods were used to explore potential effects of clinical profiles.

RESULTS

A total of 9 TBSS studies (including 11 datasets) were enrolled, comprising 363 ADHD patients and 293 HCS. ADHD patients showed significant FA reductions in the right sagittal stratum and splenium of corpus callosum (CC) compared with HCS (Fig. A and C). Fibers passed through these clusters included the inferior fronto-occipital fasciculus, the inferior longitudinal fasciculus, and the splenium of CC (Fig. D). Sensitivity analysis and subgroups analyses further confirmed these findings. Meta-regression showed that the age was positively correlated with the FA in the splenium of CC (Fig. B).

CONCLUSION

Our findings confirmed the most convergent WM abnormalities in ADHD and suggested that the posterior brain networks of WM tracts may be affected in ADHD, with the potential of disconnection of the gray matter regions they connect. Furthermore, the disruption in splenium of CC may be a key target in the neurodevelopment of ADHD.

CLINICAL RELEVANCE/APPLICATION

Through meta-analysis using signed differential mapping (SDM), our study suggested that the disorganized white matter microstructure of posterior brain network may be a target underpinning ADHD pathophysiology.

SSK13-04 Altered Intranetwork and Internetwork Functional Connectivities in Type 2 Diabetes Mellitus with and

without Cognitive Impairment

Wednesday, Dec. 2 11:00AM - 11:10AM Location: N226

Participants Shiqi Yang, Wuhan, China (*Presenter*) Nothing to Disclose Ying Xiong, Wuhan, China (*Abstract Co-Author*) Nothing to Disclose Yihao Yao, MD, PhD, Wuhan, China (*Abstract Co-Author*) Nothing to Disclose Yan Zhang, Wuhan, China (*Abstract Co-Author*) Nothing to Disclose Wenzhen Zhu, MD, PhD, Wuhan, China (*Abstract Co-Author*) Nothing to Disclose Yong Liu, Beijing, China (*Abstract Co-Author*) Nothing to Disclose

PURPOSE

To analyze the alteration of intranetwork and internetwork functional connectivities using resting-state functional MRI (rsfMRI) with type 2 diabetes mellitus (T2DM) progression.

METHOD AND MATERIALS

Nineteen T2DM patients with normal cognition (DMCN), 19 T2DM patients with cognitive impairment (DMCI), 19 heathy controls (HC) were evaluated by 3 T MR scanner. Altered functional connectivities derived from 36 prior well defined brain regions of interest (ROIs) of 5 important resting-state network (RSN) systems[default mode network (DMN), dorsal attention network (DAN), control network (CON), salience network (SAL), sensorimotor network (SMN)] were investigated at 3 levels (integrity, network, connectivity pairs) by one-way ANOVA.

RESULTS

At integrity level, decreased connectivity strength of bilateral posterior cerebellum (pCBLM) were found across DMCN and DMCI (P < 0.05), right insula (rIns) only in DMCI. At network level, impaired intranetwork in DMN and CON were found in DMCI while not in DMCN (P < 0.05), and no impaired internetwork in the 5 RSNs was found among the 3 groups. At connectivity level, significant differences of fifty connectivity pairs were found among HC, DMCN, DMCI (P < 0.05), the top three altered connectivity pairs were left anterior prefrontal cortex versus left superior parietal (laPFC-ISP), right anterior cingulate cortex versus right ventral anterior cingulate cortex (rACC-rvACC), right insula versus right primary visual (rIns-rV1) (P < 0.005). Fuctional connectivity strength of specific brain architectures in T2DM at 3 levels were found associated with HbA1c, duration, MMSE and MoCA (P < 0.05).

CONCLUSION

These altered profiles of intranetwork and internetwork indicated intergroup differences and cognitive impairment of DMCI, might be the potential biomarkers applied to predict the progression, evaluate the impairment of cognition, understand the pathophysiology further for T2DM.

CLINICAL RELEVANCE/APPLICATION

These findings might be the potential biomarkers applied to predict T2DM progression, evaluate recognition impairment, and understand T2DM pathophysiology further.

SSK13-05 Prequit Right NAcc-VTA Functional Connectivity as a Marker of Smoking Cessation Outcomes

Wednesday, Dec. 2 11:10AM - 11:20AM Location: N226

Participants

Zhujing Shen, Hangzhou, China (*Presenter*) Nothing to Disclose Wei Qian, Hangzhou, China (*Abstract Co-Author*) Nothing to Disclose Chao Wang SR, MD, Hangzhou, China (*Abstract Co-Author*) Nothing to Disclose Peiyu Huang, Hangzhou, China (*Abstract Co-Author*) Nothing to Disclose Yong Zhang, Hangzhou, China (*Abstract Co-Author*) Nothing to Disclose Minming Zhang, MD, PhD, Hangzhou, China (*Abstract Co-Author*) Nothing to Disclose

PURPOSE

Chronic smoking hijacks nicotine-dependent individuals' reward circuit, causing structural and functional alteration. However, the relationship between reward circuit and smoking cessation outcomes remains unclear. In the present study, we analyze the association between resting-state functional connectivity (rsFC) in reward circuit and subsequent smoking cessation outcomes(point prevalence abstinence at 4weeks).

METHOD AND MATERIALS

Functional magnetic resonance images from 53 smokers and 41 healthy controls were acquired using a 3.0T MRI scanner prior to quitting. After 12-week treatment, smokers were divided into relapsers (n=30) and abstainers (n=23). We then analyzed ROI-wise rsFC within reward circuit by setting 11 seeds (including VTA, bilateral NAcc, amygdala, hippocampus, mediodorsal thalamus and rostral anterior cingulate cortex).

RESULTS

The rsFC between right NAcc and VTA, right NAcc and right amygdala were significantly different in the three groups(p=0.014; p=0.002). While only right NAcc-VTA coupling differentiated relapsers from abstainers (higher in relapsers than abstainers, p=0.026). In addition, the strength of interhemispheric connectivity between NAcc ($r^2=0.255$, p=0.004) and hippocampus ($r^2=0.256$, p=0.004) were positively correlated with nicotine dependence severity(FTND) in relapsers.

CONCLUSION

These results suggest that right NAcc-amygdala coupling reflects smoking status, while enhanced right NAcc-VTA coupling, core projection implicated in rewarding, is a promising marker of relapse vulnerability. The findings also show that relapse-vulnerable smokers can be detected before quit attempts, which may optimize clinical intervention and improve smoking cessation outcomes.

Our study brings light to the neural mechanisms underlying smoking cessation. Prequit neuroimage data can help to identify relapse risk, which leads to personalized clinical strategies.

SSK13-06 Describing of Obsessive-compulsive Disorder in Seven Dimensions Using Multivariate Pattern Analysis Based on Gray Matter Anatomy

Wednesday, Dec. 2 11:20AM - 11:30AM Location: N226

Participants

Xinyu Hu, Chengdu, China (*Presenter*) Nothing to Disclose Xi Yang, Chengdu, China (*Abstract Co-Author*) Nothing to Disclose Qi Liu, Chengdu, China (*Abstract Co-Author*) Nothing to Disclose Ming Zhou, Chengdu, China (*Abstract Co-Author*) Nothing to Disclose Lizhou Chen, Chengdu, China (*Abstract Co-Author*) Nothing to Disclose Fei Li, MD, Chengdu, China (*Abstract Co-Author*) Nothing to Disclose Yanchun Yang, Chengdu, China (*Abstract Co-Author*) Nothing to Disclose Qiyong Gong, Chengdu, China (*Abstract Co-Author*) Nothing to Disclose Xiaoqi Huang, MD, Chengdu, China (*Abstract Co-Author*) Nothing to Disclose

PURPOSE

Obsessive-compulsive disorder (OCD) is one of the most common disabling psychiatric disorders. Although previous magnetic resonance imaging (MRI) studies have already revealed abnormalities of cortical folding patterns (ie. cortical thickness, surface area) in OCD patients, how these abnormalities can be translated to clinical application is still a challenging task. Multivariate pattern analysis (MVPA) approach is a promising analytical technique which allows the classification of individual observations into distinct groups and bears the advantage of individualized judgement in the future. Thus, in current study, we aimed to apply one of the MVPA approach known as Support Vector Machine (SVM) to distinguish OCD patients from healthy control subjects (HCS) based on multidimensional surface features of gray matter anatomy.

METHOD AND MATERIALS

High-resolution T1-weighted volumetric 3D MR images were acquired for 33 drug-naïve OCD patients and 33 matched HCS using a 3.0 T MRI system. Structural images were preprocessed with the FreeSurfer software to accurately and rapidly generate a set of seven morphometric parameters including volumetric and geometric features at each spatial location on the entire cortical surface (Fig A). Then all these parametric maps were used to discriminate OCD patients from HCS based on leave-one-out cross-validation approach with SVM using Probid software. We also drew a receiver operating characteristic (ROC) curve to help evaluate the performance of each parameter.

RESULTS

Classification accuracies, sensitivity and specificity for SVM classifier of combined left and right morphometric parameters are shown in Fig A. Among all parameters, the cortical thickness provided highest and above chance prediction accuracies for OCD patients (accuracy=75.76%, P<0.001) (Fig A and Fig B).

CONCLUSION

The current study illustrated that among all cortical features, cortical thickness showed the highest accuracy in classifying OCD patients from HCS, which indicated its potential diagnostic value in helping detecting OCD.

CLINICAL RELEVANCE/APPLICATION

The present study provides preliminary support for the suggestion that application of SVM to cortical thickness maps could be used to aid the identification of individuals with OCD in clinical practice.

SSK13-07 Phase II Clinical Trial: Efficacy of Methylene Blue in Human Cognitive and fMRI Measures

Wednesday, Dec. 2 11:30AM - 11:40AM Location: N226

Participants

Pavel Rodriguez, MD, San Antonio, TX (*Presenter*) Nothing to Disclose Wei Zhou, BS, San Antonio, TX (*Abstract Co-Author*) Nothing to Disclose Amar P. Singh, MD, San Antonio, TX (*Abstract Co-Author*) Nothing to Disclose Douglas W. Barrett, PhD, Austin, TX (*Abstract Co-Author*) Nothing to Disclose Wilson Altmeyer, MD, San Antonio, TX (*Abstract Co-Author*) Nothing to Disclose Juan E. Gutierrez, MD, San Antonio, TX (*Abstract Co-Author*) Speakers Bureau, Bayer AG Betty Heyl, San Antonio, TX (*Abstract Co-Author*) Speakers Bureau, Bayer AG Jinqi Li, MD, San Antonio, TX (*Abstract Co-Author*) Nothing to Disclose Jack L. Lancaster, PhD, San Antonio, TX (*Abstract Co-Author*) Nothing to Disclose Francisco Gonzalez-Lima, PhD, Austin, TX (*Abstract Co-Author*) Nothing to Disclose Timothy Duong, San Antonio, TX (*Abstract Co-Author*) Nothing to Disclose

PURPOSE

Methylene blue (MB) is a FDA grandfathered drug used in clinics for more than 100 years. MB acts in the mitochondria to sustain or enhance ATP energy production. MB has been shown efficacious in animal models of ischemic stroke, traumatic brain injury, and Alzheimer's disease (AD). A phase II clinical trial showed that daily oral MB (RemberTM) slowed the progression of AD compared to placebo. We have also found that low-dose MB increases brain glucose uptake, oxygen consumption, and evoked responses in the rat brain. Our goal was to use functional MRI (fMRI) to assess the efficacy of MB on cognitive and physiologic measures in the human brain.

METHOD AND MATERIALS

Double-blind, placebo-controlled, randomized clinical trial (NCT01836094) of 28 healthy young volunteers using delayed matching to sample (DMTS), psychomotor vigilance task (PVT), and visual-motor tasks (VMT) modeled using e-PRIME 2.0. *Interventions:* USP grade methylene blue (n=15) and placebo (n=13) administered orally at 280 mg once. All subject data were acquired in the same

scanner (Siemens TIM Trio 3.0 Tesla; 32 channel head coil). fMRI and regression analysis were conducted using SPM 8.0 (UCL) and FSL (FMRIB). Correlation analysis was performed using MarsBar and SPSS 22 (IBM), and CBF analysis was conducted using the ASLtbx (UPenn).

RESULTS

Mean age was 29-30 years, 65% of subjects were female, and mean education was 17.5 years for both groups. No difference in cerebrovascular reactivity in both groups using CO_2 challenge. Paired t-test analysis demonstrated that MB increased fMRI BOLD activity in midbrain, cerebellum, medial pallidum, prefrontal, parietal and occipital cortex (cluster-wise pFWE<0.05) during the encoding and maintenance phases of the DMTS memory task. MB subjects had a 7% increase in the number of correct responses during the DMTS task (p<0.01). MB subjects also had a significant decrease in mean CBF in the posterior cingulate and inferior parietal cortex during the VMT (cluster-wise pFWE <0.05).

CONCLUSION

MB has a robust effect enhancing visuospatial working memory and its underlying encoding and maintenance neural networks. MB is also associated with greater suppression of the default mode network during the VMT.

CLINICAL RELEVANCE/APPLICATION

As the first fMRI neuroimaging study of MB in healthy humans, our objective was to understand the effect of MB on working memory, vigilance and task-evoked BOLD and cerebral blood flow (CBF).

SSK13-08 Bayesian Analysis of fMRI Data: Application in Autism

Wednesday, Dec. 2 11:40AM - 11:50AM Location: N226

Participants

Parisa Mazaheri, MD, Baltimore, MD (*Presenter*) Nothing to Disclose Rong Chen, PhD, Baltimore, MD (*Abstract Co-Author*) Nothing to Disclose Edward H. Herskovits, MD, PhD, Baltimore, MD (*Abstract Co-Author*) Consultant, BioClinica, Inc; Shareholder, RadDx, Inc;

PURPOSE

The goal of this study was to establish an automated and reliable platform for whole-brain analysis of resting state fMR (rsfMR) images using Bayesian data mining. We further investigated the software's feasibility in differentiating the subjects with autism spectrum disorder (ASD) from typically developing controls (TC), based on individual fMRIs.

METHOD AND MATERIALS

An in house developed resting state functional connectivity (rsFC) analysis environment is used to analyze rsfMR images. The analysis environment performs four tasks: image preprocessing, variable selection, Bayesian analysis, and model aggregation. After standard preprocessing and eliminating motion artifacts, the algorithm generates voxel-based rsFC maps for each atlas-based seed region. Investigators can use any structural or functional atlases of their choice. Next, by employing a Bayesian Network data-mining approach the rsFC maps and group membership variable C (e.g., TC vs. ASD) are used as inputs for pattern extraction. The outputs are group of voxels strongly predictive of group membership, presented as potential neuroimaging biomarkers of the clinical condition under analysis. In the last step, the algorithm aggregates all significant connectivity patterns across all seeds and performs the final classification. The algorithm was tested on 116 subjects (ASD=54; mean age 11.29 \pm 2.66 years, 6 females) and (TC=62, mean age 12.16 \pm 3.02 years, 14 females) from NYU publically available data set.

RESULTS

We used 90 AAL atlas structures as seed regions. 26 connectivity models, from 14 seeds, were found to be highly predictive of ASD with accuracies ranging from 78% to 71%. Six out of those 14 seeds were in frontal lobe. When used all connectivity models, we could classify subjects with 90.5% accuracy. Detected circuits were strongly associated with various indices of clinical severity and accurately reflected the known anatomic distribution of affected regions described in ASD.

CONCLUSION

Compared with conventional methods that focus on group differences, we identified differences in brain connectivity patterns at an individual level and accurately classified subjects in a highly heterogeneous condition such as ASD.

CLINICAL RELEVANCE/APPLICATION

Provides physicians with an automated connectivity analysis environment, and facilitates understanding and subsequently management of highly complex and socially important conditions such as ASD.

SSK13-09 Voxelwise Meta-Analysis of Resting-state Brain Activity Abnormalities in Patients with Major Depressive Disorder

Wednesday, Dec. 2 11:50AM - 12:00PM Location: N226

Participants

Youjin Zhao, Chengdu, China (*Presenter*) Nothing to Disclose Ming Y. Du, Chengdu, China (*Abstract Co-Author*) Nothing to Disclose Xinyu Hu, Chengdu, China (*Abstract Co-Author*) Nothing to Disclose Jing Jiang, Chengdu, China (*Abstract Co-Author*) Nothing to Disclose Xiaoqi Huang, MD, Chengdu, China (*Abstract Co-Author*) Nothing to Disclose Graham J. Kemp, Liverpool, United Kingdom (*Abstract Co-Author*) Nothing to Disclose Qiyong Gong, Chengdu, China (*Abstract Co-Author*) Nothing to Disclose

PURPOSE

Resting-state brain activity abnormalities have long been suspected in major depressive disorder (MDD) but the available evidence has been inconsistent. Moreover, to our knowledge, there has been no meta-analysis utilized existent human neuroimaging literature to provide insights into the functional abnormalities in MDD at resting-state. To address this lack we conducted the first

meta-analysis of low-frequency fluctuation (ALFF) and fractional ALFF (fALFF) studies in MDD to help clarify the resting-state functional abnormalities underpinning this condition.

METHOD AND MATERIALS

A systematic search was conducted for ALFF and fALFF studies in MDD. A voxel-wise meta-analysis using the anisotropic effectsize Signed Differential Mapping (AES-SDM) method was conducted on ALFF/fALFF studies. Meta-regression was used to explore the effects of demographics and clinical characteristics.

RESULTS

A total of 8 ALFF and 4 fALFF studies comprising 345 MDD subjects (142/203 male/female; mean age 34 years) matched with 329 healthy controls (149/180 male/female; mean age 33 years) met the inclusion criteria. The pooled meta-analysis of the ALFF and fALFF studies on MDD patients showed significantly increased brain activities in the bilateral anterior cingulate cortex (ACC) extending to medial frontal gyrus and the left insula, and decreased brain activities in the right superior temporal gyrus, the left middle occipital gyrus, the left cerebellum and the right lingual gyrus relative to healthy controls (see Fig.1A). Meta-regression analyses indicated that the illness duration and the symptom severity of MDD patients were positively associated with brain activity in the left anterior cingulated cortex (LACC) and right medial superior frontal gyrus, respectively (RMSFG) (see Fig. 1B).

CONCLUSION

Meta-analysis revealed a pattern of neural abnormalities in MDD, characterized by functional brain abnormalities in brain regions involved in cognition, emotional processing and self-referential processes. These findings may contribute to a better understanding of the underlying pathophysiology as well as better characterization of the functional neural correlates of depressive symptoms.

CLINICAL RELEVANCE/APPLICATION

This study revealed resting-state brain activity abnormalities in major depressive disorder patients and could provide biomarkers for diagnosis and treatment evaluation.

Genitourinary (Prostate Imaging and Staging)

Wednesday, Dec. 2 10:30AM - 12:00PM Location: N228



AMA PRA Category 1 Credits ™: 1.50 ARRT Category A+ Credits: 1.50

Participants

Andrew B. Rosenkrantz, MD, New York, NY (*Moderator*) Nothing to Disclose Antonio C. Westphalen, MD, Mill Valley, CA (*Moderator*) Nothing to Disclose Ronaldo H. Baroni, MD, Sao Paulo, Brazil (*Moderator*) Nothing to Disclose

Sub-Events

SSK09-01 Computed Very High B-Value Diffusion-Weighted Imaging of the Prostate: How High Should We Go?

Wednesday, Dec. 2 10:30AM - 10:40AM Location: N228

Participants

Nainesh Parikh, MD, New York, NY (*Presenter*) Nothing to Disclose Justin M. Ream, MD, Ann Arbor, MI (*Abstract Co-Author*) Nothing to Disclose Andrea S. Kierans, MD, New York, NY (*Abstract Co-Author*) Nothing to Disclose Max X. Kong, MD, New York, NY (*Abstract Co-Author*) Nothing to Disclose Samir S. Taneja, MD, New York, NY (*Abstract Co-Author*) Consultant, Eigen Consultant, GTx, Inc Consultant, Bayer AG Consultant, Healthtronics, Inc Speaker, Johnson & Johnson Investigator, STEBA Biotech NV Royalties, Reed Elsevier Andrew B. Rosenkrantz, MD, New York, NY (*Abstract Co-Author*) Nothing to Disclose

PURPOSE

To assess the impact of a broad range of computed b-values (1,500-5,000 s/mm2) on prostate cancer detection.

METHOD AND MATERIALS

49 patients undergoing 3T prostate MRI before radical prostatectomy were included. Exams included DWI with a maximal acquired b-value of 1,000 s/mm2, from which six computed DWI image sets (b-values ranging from 1,500-5,000 s/mm2) were generated. Two radiologists [R1 (attending), R2 (fellow)] independently evaluated the ADC map as well as each DW image set, blinded to the b-value, to assess dominant lesion location. Pathologic findings from radical prostatectomy served as the reference standard.

RESULTS

Sensitivity for tumor: R1-82% (ADC), 80% (b1000), 86% (b1500), 88% (b2000), 86% (b2500), 84% (b3000), 76% (b4000), 65% (b5000); R2-71% (ADC), 63% (b1000), 76% (b1500), 71% (b2000), 70% (b2500), 65% (b3000), 57% (b4000), 37% (b5000). Sensitivity for Gleason score \geq 7 tumor: R1-83% (ADC), 80% (b1000), 93% (b1500), 93% (b2000), 90% (b2500), 90% (b2500), 90% (b3000), 80% (b4000), 65% (b5000); R2-75% (ADC), 68% (b1000), 80% (b1500), 78% (b2000), 78% (b2500), 70% (b3000), 60% (b4000), 38% (b5000). PPV for tumor: R1-95% (ADC), 95% (b1000), 93% (b1500), 96% (b2000), 98% (b2500), 93% (b3000), 95% (b4000), 87% (b5000); R2-85% (ADC), 82% (b1000), 93% (b1500), 96% (b2000), 94% (b3000), 93% (b3000), 95% (b4000), 87% (b5000); R2-85% (ADC), 82% (b1000), 93% (b1500), 88% (b2000), 92% (b2500), 94% (b3000), 93% (b4000), 75% (b5000). Dominant lesion visual conspicuity (1-5 scale): R1-3.4±1.5 (ADC), 2.5±1.2 (b1000), 3.3±1.4 (b1500), 3.2±1.3 (b2000), 3.2±1.4 (b2500), 3.1±1.4 (b3000), 2.8±1.4 (b4000), 2.7±1.5 (b5000); R2-3.2±1.6 (ADC), 2.1±1.1 (b1000), 3.2±1.5 (b1500), 3.1±1.6 (b2000), 3.0±1.6 (b2500), 2.5±1.5 (b3000), 1.8±1.0 (b4000), 1.3±0.6 (b5000). Reader confidence (1-5 scale): R1-3.2±1.5 (ADC), 2.6±1.3 (b1000), 3.1±1.4 (b1500), 3.1±1.4 (b2000), 3.1±1.5 (b2500), 3.1±1.5 (b2500), 3.1±1.6 (b4000), 2.8±1.7 (b2000), 3.1±1.8 (b3000), 2.6±1.6 (b4000), 1.9±1.3 (b5000).

CONCLUSION

Computed b-values in the range of 1,500-2,500 s/mm2 were optimal for prostate cancer detection, comparing favorably with the ADC map. b-values of 1,000 or 3,000-5,000 exhibited lower performance.

CLINICAL RELEVANCE/APPLICATION

Computed b-values of 1,500-2,500 s/mm2 (but not higher) help optimize prostate DWI, thereby facilitating targeted prostate biopsy and tailored treatments based on imaging guidance.

SSK09-02 Utility of Apparent Diffusion Coefficient (ADC) in Intermediate Grade (Gleason score 3+4=7) Prostate Cancer Diagnosed at Non-targeted TRUS-guided Needle Biopsy

Wednesday, Dec. 2 10:40AM - 10:50AM Location: N228

Participants

Radu Rozenberg, MD, Ottawa, ON (*Abstract Co-Author*) Nothing to Disclose Nicola Schieda, MD, Ottawa, ON (*Abstract Co-Author*) Nothing to Disclose Shaheed Hakim, Ottawa, ON (*Abstract Co-Author*) Nothing to Disclose Trevor A. Flood, MD, FRCPC, Ottawa, ON (*Abstract Co-Author*) Nothing to Disclose Rebecca Thornhill, PhD, Ottawa, ON (*Abstract Co-Author*) Nothing to Disclose Christopher Lim, MD, Ottawa, ON (*Presenter*) Nothing to Disclose

PURPOSE

To determine the ability of ADC analysis to predict Gleason score (GS) upgrading of tumor and extra-prostatic extension (EPE) after radical prostatectomy (RP) in 3+4=7 prostate cancer (PCa).

METHOD AND MATERIALS

With REB approval, 54 men with GS 3+4=7 PCa at non-targeted TRUS-guided biopsy underwent 3-Tesla MRI and RP between 2012-2013. Outcomes at RP included: A) upgrading to GS 4+3=7 and B) organ confined disease (OCD). >0.5 mL tumors were contoured by a blinded GU radiologist by correlating ADC to RP histopathology map. Mean ADC, ADC ratio (normalized to peripheral zone), histogram analysis (10th, 25th and 50th centile ADC) and texture analysis features were compared between groups using multi-variate analysis, regression modeling and ROC analysis.

RESULTS

25.9% (14/54) patients were upgraded to GS 4+3=7 and 51.9% (28/54) patients had EPE after RP. There was no difference in age (p=0.38, 0.85), PSA (p=0.96, 0.95) or % of core biopsies with Gleason pattern 4 (p=0.56, 0.89) between groups. Mean ADC (mm2/sec), ADC ratio, 10th, 25th and 50th centile ADC were similar between GS 3+4=7 (0.94 ± 0.24 , 0.58 ± 0.15 , 0.77 ± 0.31 , 0.94 ± 0.28 and 1.15 ± 0.24) and GS 4+3=7 tumors (0.96 ± 0.20 , 0.55 ± 0.11 , 0.71 ± 0.26 , 0.89 ± 0.19 and 1.11 ± 0.16), p>0.05. 10th centile ADC was lower in tumors with EPE (0.69 ± 0.31 versus 0.82 ± 0.28), p=0.02; with no difference comparing all other conventional ADC parameters, p>0.05. Regression models combining texture features improved prediction of GS upgrade: A) Kurtosis+Entropy+Skewness (AUC 0.76 [SE=0.07], p<0.001; sensitivity 71%, specificity 73%) and B) Kurtosis+Heterogeneity+Entropy+Skewness (AUC 0.77 [SE=0.07], p<0.001); sensitivity 71%, specificity 78%).

CONCLUSION

Amongst Gleason score 3+4=7 prostate cancers diagnosed at TRUS-guided biopsy, mean ADC and ADC histogram analysis is not predictive of upgrading after RP, while ADC texture-analysis improves accuracy. 10th centile ADC is predictive of EPE.

CLINICAL RELEVANCE/APPLICATION

Conventional ADC analysis cannot predict upgrading of Gleason score 3+4=7 prostate cancer diagnosed at TRUS-guided biopsy; however, ADC texture-analysis improves accuracy and 10th centile ADC can predict organ confined disease.

SSK09-03 High Resolution 3-Tesla Endorectal Prostate MR Imaging: A Multireader Study of Radiologist Preference and Perceived Interpretive Quality of 2D and 3D T2-weighted FSE MR Images

Wednesday, Dec. 2 10:50AM - 11:00AM Location: N228

Participants

Antonio C. Westphalen, MD, Mill Valley, CA (*Presenter*) Nothing to Disclose Susan M. Noworolski, PhD, San Francisco, CA (*Abstract Co-Author*) Nothing to Disclose Saunak Sen, San Francisco, CA (*Abstract Co-Author*) Nothing to Disclose Mukesh G. Harisinghani, MD, Boston, MA (*Abstract Co-Author*) Nothing to Disclose Kartik S. Jhaveri, MD, Toronto, ON (*Abstract Co-Author*) Speaker, Bayer AG Steven S. Raman, MD, Santa Monica, CA (*Abstract Co-Author*) Nothing to Disclose Andrew B. Rosenkrantz, MD, New York, NY (*Abstract Co-Author*) Nothing to Disclose Zhen J. Wang, MD, Hillsborough, CA (*Abstract Co-Author*) Nothing to Disclose Ronald J. Zagoria, MD, San Francisco, CA (*Abstract Co-Author*) Nothing to Disclose

PURPOSE

The goal of this study was to compare the perceived quality of 3-Tesla axial T2-weighted high-resolution 2D and high-resolution 3D FSE endorectal MR images of the prostate.

METHOD AND MATERIALS

We studied 85 men (median age=65 years, 46 to 83) with proven or suspected prostate cancer who had endorectal MR imaging with 2D and 3D T2-weighted FSE MR images. Six radiologists from various institutions independently reviewed axial T2 weighted MR images shown individually and paired. Readers identified their preferred images and scored using a 5-point scale their confidence in identifying tumor. They also scored the delineation of the zonal anatomy and capsule, tumor conspicuity, and image quality (artifacts, distortion, and sharpness) using a 3-point scale. We used a meta-analysis routine to calculate pooled estimates based on a random-effects model. A formal analysis of heterogeneity was also done. The presence of heterogeneity is consistent with differences in the readers' scores. We used a mixed effect logistic regression, taking into account the clustering effect, to determine if prior treatment and number of years of reader's experience were predictors of the option for 2D or 3D images.

RESULTS

Each reader had a strong preference for a given T2-weighted MR sequence, favoring one of the two techniques in at least approximately 70% of cases; but the choices were evenly distributed between the two sequence options. The pooled estimate shows that the 3D image is preferred in about 47% of the times (95% CI=20% to 74%). The choice for one or other techniques was not associated with prior treatment or readers' years of experience. There was no significant difference in confidence in tumor identification (p=0.16 to 1.00). There was no difference in delineation of the zonal anatomy (p=0.19), prostatic capsule (p=0.14), and tumor conspicuity (p=0.89). Similarly, no difference was found when assessing motion artifact (p=0.48) and distortion (p=0.41). 2D FSE images were significantly sharper than 3D FSE (p<0.001), but also more likely to exhibit artifacts not related to motion (p=0.002).

CONCLUSION

There are strong individual preferences for the 2D or 3D FSE MR images, but a wide variability among radiologists. There were differences in image quality, but not in the sequences' ability to delineate the glandular anatomy and depict cancer.

CLINICAL RELEVANCE/APPLICATION

2D and 3D FSE techniques appear to be equally adequate fro clinical use.

SSK09-04 Multi-Parametric MRI Performance in Prostate Cancer Detection: Stratified by Gleason Scores and Tumor Size on Whole Mount Histopathology

Participants Pooria Khoshnoodi, MD, Los Angeles, CA (*Presenter*) Nothing to Disclose Daniel J. Margolis, MD, Los Angeles, CA (*Abstract Co-Author*) Research Grant, Siemens AG Hector E. Alcala, MPH, Los Angeles, CA (*Abstract Co-Author*) Nothing to Disclose Nelly Tan, MD, Los Angeles, CA (*Abstract Co-Author*) Nothing to Disclose Wei-Chan Lin, MD, Taipei, Taiwan (*Abstract Co-Author*) Nothing to Disclose David Y. Lu, MD, Los Angeles, CA (*Abstract Co-Author*) Nothing to Disclose Jiaoti Huang, Los Angeles, CA (*Abstract Co-Author*) Nothing to Disclose Robert E. Reiter, MD, Los Angeles, CA (*Abstract Co-Author*) Nothing to Disclose David S. Lu, MD, Los Angeles, CA (*Abstract Co-Author*) Nothing to Disclose David S. Lu, MD, Los Angeles, CA (*Abstract Co-Author*) Nothing to Disclose David S. Lu, MD, Los Angeles, CA (*Abstract Co-Author*) Nothing to Disclose David S. Lu, MD, Los Angeles, CA (*Abstract Co-Author*) Nothing to Disclose David S. Lu, MD, Los Angeles, CA (*Abstract Co-Author*) Nothing to Disclose David S. Lu, MD, Los Angeles, CA (*Abstract Co-Author*) Nothing to Disclose David S. Lu, MD, Los Angeles, CA (*Abstract Co-Author*) Nothing to Disclose David S. Lu, MD, Los Angeles, CA (*Abstract Co-Author*) Nothing to Disclose David S. Lu, MD, Los Angeles, CA (*Abstract Co-Author*) Nothing to Disclose David S. Lu, MD, Los Angeles, CA (*Abstract Co-Author*) Nothing to Disclose David S. Lu, MD, Los Angeles, CA (*Abstract Co-Author*) Nothing to Disclose David S. Lu, MD, Los Angeles, CA (*Abstract Co-Author*) Nothing to Disclose

PURPOSE

To evaluate the prostate cancer (CaP) detection rate by multi-parametric MR imaging (MP-MRI) confirmed by whole mount histopathology (WMHP) stratified by Gleason Scores (GS) and tumor size.

METHOD AND MATERIALS

A HIPPA-compliant, IRB-approved study of 290 consecutive men who underwent prostate MP-MRI before radical prostatectomy (RP) from October 2010 to January 2015 was performed. Clinical, MP-MRI (T2W, DWI and DCE) and pathologic features (WMHP slides, GS, maximal diameter) were obtained. The index tumor was defined as the pathological lesion with the highest GS or largest tumor when multiple foci had identical GS. A genitourinary (GU) radiologist and a GU pathologist reviewed each case. Each tumor focus on WMHP which matched with concordant target on MP-MRI was considered detected tumor. Chi-squared tests were used to test difference in MRI tumor detection rates by tumor grade (GS=3+3 defined as low grade vs. GS>6 as high grade) and tumor size (<1 cm defined as small vs. \geq 1cm as large tumor). Logistic regression was used to test a tumor grade by tumor size in MRI detection. Statistical analyses were conducted using Stata 12.1. P-values below .05 were considered significant.

RESULTS

290 patients had 639 unique CaP foci on WMHP. Of 639 total tumors foci on pathology, 310 (48.5%) and of 290 total index lesions, 224 (77.2%) were detected on MP-MRI. MRI detected 86/326 (26.4%) of low grade tumors vs. 223/313 (71.2%) of high grade tumors, and 56/257 (21.8%) of small vs. 253/382 (66.2%) large tumors. MRI detected 44/212 (20.8%) of low grade small tumors vs. 12/45 (26.7%) of high grade small tumors, and 42/114 (36.8%) low grade large tumors vs. 211/268 (78.7%) of high grade large tumors. (p<.05)

CONCLUSION

We found that MP-MRI missed 51.6% of all CaP. However, when CaP stratified by size and GS, larger tumors were associated with increased detection rate for both high and low grade tumors. There was also a significant size by grade interaction, such that the difference in detection rates by grade was much larger among tumors 1cm or larger. These findings suggest that the MP-MRI tends to detect larger with higher grade CaP lesions. In our study, MP-MRI detected 78.7% of all high grade large CaP foci.

CLINICAL RELEVANCE/APPLICATION

MP-MRI which combines anatomic with functional and physiologic assessment of prostate cancer has substantially improved diagnostic capabilities of detecting clinically significant prostate tumors.

SSK09-05 Distortion in Diffusion-Weighted Prostate MRI: Readout-Segmented EPI DWI vs. Single-Shot EPI DWI

Wednesday, Dec. 2 11:10AM - 11:20AM Location: N228

Participants

Ivan Platzek, MD, Dresden, Germany (*Presenter*) Nothing to Disclose Angelika Borkowetz, MD, Dresden, Germany (*Abstract Co-Author*) Nothing to Disclose Marieta Toma, MD, Dresden, Germany (*Abstract Co-Author*) Nothing to Disclose Thomas Brauer, MD, Dresden, Germany (*Abstract Co-Author*) Nothing to Disclose Hagen H. Kitzler, Dresden, Germany (*Abstract Co-Author*) Nothing to Disclose Verena Plodeck, MD, Dresden, Germany (*Abstract Co-Author*) Nothing to Disclose Manfred Wirth, Dresden, Germany (*Abstract Co-Author*) Nothing to Disclose Michael Laniado, MD, Dresden, Germany (*Abstract Co-Author*) Nothing to Disclose

PURPOSE

The aim of this study was to evaluate the utility of segmented-readout echo planar diffusion-weighted imaging (SR EPI DWI) for prostate imaging in comparison to conventional single shot EPI DWI (SS EPI DWI), with an emphasis on distortion artifacts.

METHOD AND MATERIALS

Sixty-eight patients with suspected prostate cancer were included in this prospective study. Patient age varied between 46 and 77 y (65 y on average). All patients underwent multiparametric prostate MRI (mpMRI) at 3T, which included T2-weighted images, dynamic contrast-enhanced (DCE) images, and both SR EPI DWI and SS EPI DWI. Apparent diffusion coefficient maps (ADC) maps were generated for both SR EPI DWI and SS EPI DWI. Overall lesion classification was based on the PI-RADS scoring system proposed by the European society of Urogenital Radiology (ESUR). Distortion on ADC maps was classified on a five point scale. Furthermore, the maximum distortion in the anteroposterior direction was measured in each patient for both SR EPI DWI and SS EPI DWI.

RESULTS

ADC maps based on SR EPI DWI showed no evidence of distortion in 58/68 patients (85%), while ADC maps based on SS EPI DWI showed no distortion in 42/68 patients (61.7%). Distortion scores were higher (indicating stronger distortion) for SS EPI DWI as compared to SR EPI DWI in 19/68 patients (27.9%) and lower in only one patient (1.5%). Visual evaluation showed significantly less distortion for SR EPI DWI in comparison to EPI DWI (p = 0.0001). Average maximum distortion (1.5 ± 2.6 mm) was significantly lower

in SR EPI DWI in comparison to SS EPI DWI (4.9 ± 9.7 mm) (p < 0.0001). Ninety-six prostate lesions were detected with mpMRI in total. PI-RADS scores did not differ significantly between mpMRI including SR EPI DWI and mpMRI including SS EPI DWI (p = 0.464). Mean ADC values based on SS EPI DWI (0.93 ± 0.21) were slightly lower than those based on SR EPI DWI (0.96 ± 0.22)(p = 0.047).

CONCLUSION

SR EPI DWI of the prostate has significantly less pronounced distortion artifacts compared to SS EPI DWI. As prostate lesion detection and lesion classification based on PI-RADS scores do not change significantly when SR EPI DWI is used instead of SS EPI DWI, SR EPI DWI is a promising alternative to conventional diffusion-weighted sequences.

CLINICAL RELEVANCE/APPLICATION

The use of SR EPI DWI instead of conventional SS EPI DWI in prostate MRI reduces distortion and can help improve correlation between DWI and T2-weighted images.

SSK09-06 Accuracy and Inter-Observer Variability of Prostate Imaging-Report and Data System (PI-RADS) Version 2.0 for Characterization of Lesions Identified on Multiparametric Magnetic Resonance Imaging of the Prostate

Wednesday, Dec. 2 11:20AM - 11:30AM Location: N228

Participants

Andrei S. Purysko, MD, Cleveland, OH (*Presenter*) Nothing to Disclose Leonardo K. Bittencourt, MD, PhD, Rio De Janeiro, Brazil (*Abstract Co-Author*) Nothing to Disclose Brian R. Herts, MD, Cleveland, OH (*Abstract Co-Author*) Research Grant, Siemens AG Antonio C. Westphalen, MD, Mill Valley, CA (*Abstract Co-Author*) Nothing to Disclose Erick M. Remer, MD, Cleveland, OH (*Abstract Co-Author*) Nothing to Disclose Andrew J. Stephenson, MD, Cleveland, OH (*Abstract Co-Author*) Nothing to Disclose Jennifer Bullen, MSc, Cleveland, OH (*Abstract Co-Author*) Nothing to Disclose Cristina Magi-Galluzzi, MD, PhD, Cleveland, OH (*Abstract Co-Author*) Nothing to Disclose Eric Klein, Cleveland, OH (*Abstract Co-Author*) Nothing to Disclose

PURPOSE

To measure the accuracy and inter-observe variability of PI-RADS version 2.0 for the characterization of prostate lesions identified on mpMRI.

METHOD AND MATERIALS

IRB-approved, HIPAA compliant retrospective study including 171 men (mean age: 61.5 yrs.) either being investigated for prostate cancer (n = 128) or enrolled in active surveillance (n = 43), who were examined on a 3.0 T magnet without endorectal coil, and were found to have potential targets for biopsy. Two readers with 8 yrs. of experience in abdominal imaging independently reviewed and assigned a PI-RADS V.2 assessment category to the dominant MRI targets. The reference standard was the combined results from the MR/US fusion biopsy and transrectal ultrasound guided 12-core systematic biopsy (SB) performed in all the patients and in the same procedure. Clinically significant (CS) PCa was defined as tumors with Gleason score >= 3 + 4. Receiver operating characteristic (ROC) analysis was performed.

RESULTS

PCa was detected in 49.1% (84/171) and CS PCa was detected in 32.3% (55/171) of the men. Using PI-RADS category > 3 to discriminate any PCa from non-cancerous lesions, the sensitivity (Sen), specificity (Sp) and area under the ROC curve (AUC) were 77.4%, 84.9% and 85.7% for reader 1 and 69.1%, 87.2%, and 77.9% for reader 2. Using PI-RADS category > 3 to discriminate only clinically significant PCa from clinically insignificant prostate cancer and benign lesions, the Sen, Sp, and AUC were 98.2%, 79.1%, and 91.1% for reader 1 and 92.7%, 84.4%, and 90.4% for reader 2. The inter-observer agreement coefficient was 0.68 (95% CI: 0.61- 0.75).

CONCLUSION

PI-RADS V.2 had high sensitivity, specificity and accuracy for the discrimination of clinically significant PCa from other pathology, with good inter-observer agreement.

CLINICAL RELEVANCE/APPLICATION

Lesions with a PI-RADS V.2 assessment category > 3 should be considered for targeted biopsy, while avoiding the biopsy of lesions with a category < 3 reduces the number of negative biopsies and/or detection of clinically insignificant lesions.

SSK09-07 Predicting Organ-confined Prostate Cancer in the Era of Multiparametric MRI: Comparing the Accuracy of the Partin Tables and mpMRI

Wednesday, Dec. 2 11:30AM - 11:40AM Location: N228

Participants

Alison F. Brown, BA, Durham, NC (*Presenter*) Nothing to Disclose Thomas J. Polascik, MD, Durham, NC (*Abstract Co-Author*) Nothing to Disclose Rachel K. Silverman, MS, Chapel Hill, NC (*Abstract Co-Author*) Nothing to Disclose Kae Jack Tay, MBBS,MMed, Durham, NC (*Abstract Co-Author*) Nothing to Disclose Rajan T. Gupta, MD, Durham, NC (*Abstract Co-Author*) Consultant, Bayer AG; Speakers Bureau, Bayer AG; Consultant, Invivo Corporation

PURPOSE

To investigate the accuracy of the Partin tables and multiparametric magnetic resonance imaging (mpMRI) in predicting organconfined (OC) prostate cancer (PCa) after radical prostatectomy (RP), and to determine if radiologic staging information from mpMRI versus digital rectal exam (DRE) to augment the Partin tables increases the predictive accuracy of this widely used nomogram.

METHOD AND MATERIALS

In this retrospective, HIPAA-compliant, IRB-approved study, 157 patients underwent 3T mpMRI with endorectal coil before RP. MpMRI was used to assess clinical stage and an updated version of the Partin tables was used to calculate the probability of each patient to harbor OC disease. Logistic regression models predicting OC disease were created using mpMRI staging alone and with PSA as a covariate. Two sets of probabilities were obtained from the Partin tables, using clinical staging from either DRE or mpMRI. The area under curve (AUC) was used to calculate the predictive accuracy of each of these four predictive methods.

RESULTS

The predictive accuracy of mpMRI alone in predicting OC disease on pathological analysis is greater (AUC=0.86) than the Partin tables (AUC=0.70), and is further improved when combined with PSA values (AUC=0.88). The accuracy of the Partin nomogram in predicting OC disease decreases (AUC=0.59) when clinical stage is based on mpMRI versus DRE.

CONCLUSION

The superior predictive accuracy of mpMRI compared to Partin tables in predicting OC disease on pathological analysis validates results of smaller previously published studies, including one from our group. Partin table probabilities are calculated using clinical stage based on DRE result, a less sensitive test than mpMRI; therefore, this frequently leads to disease understaging. Consequently, although mpMRI has been shown to more accurately predict clinical stage than DRE, using mpMRI stage in the Partin nomogram does not improve its accuracy. In conclusion, mpMRI staging information is valuable as a stand-alone test when available based on its AUC value, but should not be applied to the Partin nomogram in its existing form.

CLINICAL RELEVANCE/APPLICATION

As more accurate clinical staging information is becoming available due to mpMRI, nomograms that incorporate mpMRI stage are needed to better predict OC PCa and assist in surgical planning prior to RP.

SSK09-08 Diagnostic Differentiation of Prostate Cancer from Prostatic Hyperplasia: What Diffusion Kurtosis Imaging Can Help Us?

Wednesday, Dec. 2 11:40AM - 11:50AM Location: N228

Participants

Chen Lihua, Dalian, China (*Presenter*) Nothing to Disclose Ailian Liu, MD, Dalian, China (*Abstract Co-Author*) Nothing to Disclose Qingwei Song, MD, Dalian, China (*Abstract Co-Author*) Nothing to Disclose Ma Chunmei, MD, Dalian, China (*Abstract Co-Author*) Nothing to Disclose Meiyu Sun, Dalian, China (*Abstract Co-Author*) Nothing to Disclose Zibin Tong, Dalian, China (*Abstract Co-Author*) Nothing to Disclose Ye Li, Dalian, China (*Abstract Co-Author*) Nothing to Disclose

PURPOSE

To evaluate the feasibility of the typical parameters of DKI in diagnositic differentiation of prostate carcinoma from prostatic hyperplasia.

METHOD AND MATERIALS

One hundred and thirteen patients with the suspicion of prostate disease were recruited in the study. All the patients, with written informed consent obtained, were performed MRI exams on a 3.0T scanner in a protocol containing the routine T1WI, T2WI, contrast-enhanced MRI, DWI and DKI. From the following histopathological examination, it was confirmed that prostate carcinoma was in 30 and prostatic hyperplasia in 29. MR images were reviewed and analyzed by author and one experienced radiologist who has five years experience in prostate diagnosis, using a dedicated software in Functool on GE ADW4.4 workstation. For each focus, the mean value of the parameters of DKI (MK, Ka, Kr, FA, MD, Da, Dr) and DWI(ADC) was measured: in PCa group, the area where shows low signal on T2WI image, high signal on MK image and histopathological positive was the focus, regions of interest (ROIs) drew three times in the tumor, the size of the ROI was chosen to cover the 2/3 of the tumor(fig 1), then the average value was used in statistics. In BPH group, three identical ROIs (70mm2)were drew in the central zone, the average value was used in statistics. The type of time-signal intensity curve(TIC) was observed by two observers collectively. ICC test was used to examine the consistency of the measurements, Pearson test was used to examine the relevance between MD and ADC value, and student's t-test was executed to compare the obtained parametric values with p> 0.05 concerned statistical significant. The ROC curve of all the parameters were drew and analyzed.

RESULTS

The ICC value of the DKI parameters and DWI parameter in the PCa group and BPH group were respectively, 0.963, 0.935, 0.959, 0.905, 0.970, 0.909, 0.967, 0.977 and 0.804, 0.899, 0.913, 0.901, 0.923, 0.902, 0.911, 0.931, exhibiting an amenable consistency. The mean MK, Ka, Kr of PCa were significantly higher (p < 0.01) than the BPH, while the mean MD, Da, Dr of cancerous tissue was found to be significantly lower (p < 0.01) than the hyperplasia tissue. No statistically significant difference was observed between FA values of two groups (p >0.05). The area under the ROC curve of all parameters were higher than 0.9.

CONCLUSION

DKI demonstrated can supply many meritorious parameters, with most useful in diagnostic differentiation of prostate cancer from prostatic hyperplasia. Combining with the routine prostate MRI, DKI may help in increasing the sensitivity and specificity of cancer detection.

CLINICAL RELEVANCE/APPLICATION

Combining with the routine prostate MRI, DKI may help in increasing the sensitivity and specificity of cancer detection.

SSK09-09 Incidental Bone Lesions on Staging MRI for Prostate Cancer: Prevalence and Clinical Importance

Wednesday, Dec. 2 11:50AM - 12:00PM Location: N228

Rachel Schor-Bardach, MD, New York, NY (*Presenter*) Nothing to Disclose Niamh M. Long, MD, New York, NY (*Abstract Co-Author*) Nothing to Disclose Jane D. Cunningham, FFRRCSI, New York, NY (*Abstract Co-Author*) Nothing to Disclose Anna Kirzner, MD, Brooklyn, NY (*Abstract Co-Author*) Nothing to Disclose Ramon E. Sosa, BA, New York, NY (*Abstract Co-Author*) Nothing to Disclose Debra A. Goldman, MS, New York, NY (*Abstract Co-Author*) Nothing to Disclose Chaya Moskowitz, New York, NY (*Abstract Co-Author*) Nothing to Disclose Hedvig Hricak, MD, PhD, New York, NY (*Abstract Co-Author*) Nothing to Disclose David M. Panicek, MD, New York, NY (*Abstract Co-Author*) Nothing to Disclose Hebert Alberto Vargas, MD, New York, NY (*Abstract Co-Author*) Nothing to Disclose

PURPOSE

To evaluate the prevalence of bone lesions identified on prostate MRI and determine the associations between their imaging features, clinical/pathologic characteristics and the presence of prostate cancer (PCa) bone metastases.

METHOD AND MATERIALS

In this IRB approved, retrospective study, the medical records of 3765 patients undergoing staging prostate MRI for newlydiagnosed (PCa) between 2000-2014 were reviewed. Amongst these, the MRI exams of all patients with bone metastases and a random selection of patients without bone metastases (matched with a 3:1 ratio to patients with bone metastases) were reviewed by 2 independent readers (R1 and R2) for presence, size and signal characteristics of bone lesions on T1-weighted sequences along with their subjective level of suspicion (1-5 Likert scale) for the likelihood of bone metastases on MRI. Prostate-specific antigen levels, biopsy Gleason Score, clinical stage and National Comprehensive Cancer Network (NCCN) risk categories were recorded. The reference standard was bone biopsy and/or at least 1-year follow-up after MRI. Associations between MRI and clinical/pathologic findings were tested using Fisher's exact and Wilcoxon Rank Sum tests. Inter-reader agreement and diagnostic accuracy for bone metastases detection were assessed using Cohen's simple Kappa statistic and areas under the receiving operating characteristics curve (AUC).

RESULTS

57 out of 3765 patients (1.5%) had bone metastases. None of the patients with low-risk PCa according to the NCCN criteria had bone metastases. Inter-reader agreement on MRI was fair to substantial (k=0.26-0.70). There was at least 1 bone lesion present on MRI in 72% (95% CI: 0.66-0.78) and 70% (95% CI: 0.64-0.76) of patients according to R1 and R2. The AUC for detecting bone metastases on MRI was 0.97 (95% CI: 0.94-1.00) and 0.90 (95% CI: 0.84-0.95) for R1 and R2. Larger lesion diameter (p<0.0001 for both) and absence of intratumoral fat (p=0.0013-0.0020) were significantly associated with bone metastases for both readers.

CONCLUSION

Bone lesions in prostate MRI are present in the majority of patients undergoing initial staging for PCa, and infrequently represent metastatic disease.

CLINICAL RELEVANCE/APPLICATION

MRI findings should be interpreted in the context of clinical features which increase the likelihood of metastatic disease.

Neuroradiology/Head and Neck (Head and Neck Tumors)

Wednesday, Dec. 2 10:30AM - 12:00PM Location: N229

HN NR MR AMA PRA Category 1 Credits ™: 1.50 ARRT Category A+ Credits: 1.50

FDA Discussions may include off-label uses.

Participants

Suresh K. Mukherji, MD, Northville, MI (*Moderator*) Nothing to Disclose Yoshimi Anzai, MD, Salt Lake Cty, UT (*Moderator*) Nothing to Disclose

Sub-Events

SSK14-01 Application of Diffusion-weighted Imaging and Dynamic Contrast-enhanced MRI in Differentiating Nasopharyngeal Carcinoma and Nasopharyngeal Lymphoma

Wednesday, Dec. 2 10:30AM - 10:40AM Location: N229

Participants

Chengru Song, Zhengzhou, China (*Presenter*) Nothing to Disclose Jingliang Cheng, MD, Zhengzhou, China (*Abstract Co-Author*) Nothing to Disclose Yong Zhang, DO, Zhengzhou, China (*Abstract Co-Author*) Nothing to Disclose Shanshan Xie, BMedSc, MMed, Zhengzhou, China (*Abstract Co-Author*) Nothing to Disclose Mengtian Ssun, Zheng-Zhou, China (*Abstract Co-Author*) Nothing to Disclose

PURPOSE

To evaluate the utility of dynamic contrast-enhanced MRI and diffusion weighted imaging (DWI) in the differentiation of nasopharyngeal carcinoma (NPC) and nasopharyngeal lymphoma (NPL).

METHOD AND MATERIALS

Forty-two patients with pathologically confirmed NPC and 27 patients with NPL were recruited and underwent conventional MRI and dynamic contrast-enhanced MRI. The MR signals, time signal-intensity curves (TIC) types, time to peak (TTP), enhancement peak (EP), maximum contrast enhancement ratio (MCER), mean apparent diffusion coefficient (ADC) value, and relative apparent diffusion coefficient (rADC) value of all the subjects were calculated and analyzed, thereafter, inter-group comparison was performed. The threshold values of ADC and rADC for differentiating NPC from NPL were determined using a receiver operating characteristic curve (ROC) analysis.

RESULTS

For NPC group, 32 cases (76.19%) demonstrated obvious heterogeneous enhancement. The mean TTP, EP, MCER and WR were (48.29 ± 12.20)s, 1475.38 ± 77.76 , (136.89 ± 24.41)% and 16.81 ± 8.36 , respectively. For NPL group, 24 cases (88.89%) demonstrated obvious homogeneous enhancement. The mean TTP, EP, MCER and WR were (63.21 ± 14.29)s, 1161.82 ± 64.04 , (113.47 ± 28.52)% and 7.39 ± 6.21 , respectively. The ADC value and rADC value were (842.34 ± 94.66)×10-6 mm2·s-1 and 0.74 ± 0.08 in NPC, whereas (652.15 ± 83.47)×10-6 mm2·s-1 and 0.56 ± 0.08 in NPL. The differences of TTP, EP, MCER, WR, ADC, rADC between NPC and NPL were statistically significant (P<0.05). The TTP of NPC was lower than that of NPL, whereas the opposite for the remaining parameters. The best differentiate threshold value of ADC and rADC were $736.5\times10-6$ mm2·s-1, $634.0\times10-6$ mm2·s-1, respectively. While the areas under the ROC curve (AUC), sensitivity, specificity and Youden index of ADC and rADC were 0.943, 0.909, 0.852, 0.761, and 0.951, 0.955, 0.852, 0.77, respectively. rADC value was slightly superior to ADC value in differentiating NPC from NPL.

CONCLUSION

DWI and Dynamic contrast-enhanced MRI are effective in differentiating NPC from NPL.

CLINICAL RELEVANCE/APPLICATION

Dynamic contrast-enhanced MRI and DWI can be applied in the differential diagnosis of NPC from NPI.

SSK14-02 Finding the Primary: Detection of Cervical CUP Based on Integrated PET/MRI versus MRI Alone

Wednesday, Dec. 2 10:40AM - 10:50AM Location: N229

Participants

Lale Umutlu, MD, Essen, Germany (*Presenter*) Consultant, Bayer AG Markus Ruhlmann, Essen, Germany (*Abstract Co-Author*) Nothing to Disclose Thomas C. Lauenstein, MD, Essen, Germany (*Abstract Co-Author*) Nothing to Disclose Wolfgang Sauerwein, Essen, Germany (*Abstract Co-Author*) Nothing to Disclose Benedikt M. Schaarschmidt, MD, Dusseldorf, Germany (*Abstract Co-Author*) Nothing to Disclose Michael Forsting, MD, Essen, Germany (*Abstract Co-Author*) Nothing to Disclose Marc U. Schlamann, Essen, Germany (*Abstract Co-Author*) Nothing to Disclose Verena Ruhlmann, Essen, Germany (*Abstract Co-Author*) Nothing to Disclose

PURPOSE

To evaluate and compare the diagnostic potential of 18F-FDG PET/MRI to MRI alone for detection of a potential primary cancer in patients suspect for cervical CUP (cancer of unknown primary).

A total of 21 patients with suspected cervical CUP underwent a simultaneous 18F-FDG PET/MRI examination (Biograph mMR, Siemens). The scan protocol comprised: 1) T1 TSE, 2) T2 TSE, 3) DWI, 4) T1 fs post-contrast VIBE and 5) T1 fs TSE imaging after the application of 0.05 mmol kg/bw Gadoteric acid (Dotarem, Guerbet). The corresponding datasets (PET/MRI and MRI alone) were read separately by two radiologists for detection and identification of potential primary cancer lesions (2 point ordinal scale), lesion conspicuity as well as diagnostic confidence (3 point ordinal scale). All available data (histology, prior examinations, PET/MRI, follow-up examinations) served as standard of reference. Mean values were compared using Wilcoxon rank sum test.

RESULTS

Cervical primary cancer was present in 13 of 21 patients. 18F-FDG PET/MRI enabled correct identification of all 13 (100%), while MRI alone allowed for detection of 9/13 malignancies (69.4%). Lesion conspicuity and diagnostic confidence were rated significantly higher for 18F-FDG PET/MRI compared to MRI alone datasets (e.g. diagnostic confidence: PET/MRI:2.7 \pm 0.3; MRI alone 1.8 \pm 0.5; p<0.05).

CONCLUSION

PET/MRI was shown to be superior towards MRI alone for detection of cervical CUP, offering a significantly higher diagnostic confidence in the discrimination of malignant lesions.

CLINICAL RELEVANCE/APPLICATION

Based on the significantly improved detection of malignant lesions while maintaining equal acquisitions times to MRI alone, integrated PET/MRI can be considered a highly valuable tool for assessment of cervical CUP.

SSK14-03 Post-treatment Change versus Recurrence of Squamous Cell Carcinoma in the Head and Neck: Histogram Analysis of the Area under the Curves Ratio from Dynamic Contrast-enhanced T1weighted Perfusion MRI

Wednesday, Dec. 2 10:50AM - 11:00AM Location: N229

Participants

Se Jin Cho, MD, Seoul, Korea, Republic Of (*Presenter*) Nothing to Disclose Jeong Hyun Lee, MD, PhD, Seoul, Korea, Republic Of (*Abstract Co-Author*) Nothing to Disclose Sang Hyun Choi, Seoul, Korea, Republic Of (*Abstract Co-Author*) Nothing to Disclose Ji Eun Park, Seoul, Korea, Republic Of (*Abstract Co-Author*) Nothing to Disclose Darlene Park, MD, Seoul, Korea, Republic Of (*Abstract Co-Author*) Nothing to Disclose Mi Sun Chung, MD, Seoul, Korea, Republic Of (*Abstract Co-Author*) Nothing to Disclose Hyo Weon Kim, Seoul, Korea, Republic Of (*Abstract Co-Author*) Nothing to Disclose Young Jun Choi, MD, Seoul, Korea, Republic Of (*Abstract Co-Author*) Nothing to Disclose Jung Hwan Baek, Seoul, Korea, Republic Of (*Abstract Co-Author*) Nothing to Disclose

PURPOSE

To evaluate the predictive value of the histogram parameters of AUCR (initial and final area under the time signal-intensity curves ratio) derived from dynamic contrast-enhanced perfusion MR imaging (DCE MRI) for differentiation of tumor recurrence from post-treatment change of in patients with squamous cell carcinoma in the head and neck (HNSCC).

METHOD AND MATERIALS

Forty-six patients after definitive treatment for HNSCC with contrast-enhancing lesions at the primary sites on follow-up MRI were assessed using conventional and DCE MRI. We calculated and correlated the time signal-intensity curve parameters (initial and final area under the time signal-intensity curves, the maximum signal-intensity from time of arrival to time to peak (Emax), the time at Emax (Tmax), initial slope of signal-intensity increase) and the cumulative histogram parameters of AUCR (AUCR50, AUCR75, AUCR90 and AUCR95) with the final pathologic or clinical diagnosis. The best predictor for differentiation of tumor recurrence from post-treatment change was determined by receiver operating characteristic curve analyses. We assessed the added value of AUCR histogram parameters to inconclusive results of conventional MRI alone after blinded review of conventional MR images by a neuroradiologist.

RESULTS

46 patients were subsequently classified as having tumor recurrence (n=17) or post-treatment change (n=29). Tumor recurrence group showed significantly shorter Tmax and significantly higher AUCR50, AUCR75 and AUCR90 compared to those of post-treatment change group (P < 0.05). AUCR90 was the best predictor for tumor recurrence (Az = 0.77; 95% CI, 0.64-0.91) with the estimated cut-off of 1.02. When AUCR90 was added on inconclusive results of conventional MRI alone, 17.6 % of recurrent tumors were more detected without significant difference in the diagnostic specificity.

CONCLUSION

Tumor recurrence of HNSCC can be differentiated from post-treatment change by using the histogram parameters of AUCR. The added value of AUCR histogram analysis is 17.6 % of more detection of recurrent tumors without compromise of diagnostic specificity.

CLINICAL RELEVANCE/APPLICATION

Our study signifies that recurrent HNSCC can be differentiated from post-treatment change by using the histogram parameters of AUCR. The added value of AUCR90 on inconclusive results of conventional MRI alone is 17 % more detection of tumor recurrence without compromise of diagnostic specificity

SSK14-04 Gaussian and non-Gaussian Diffusion MRI of the Head and Neck: The Effect of the Choice of B Values

Wednesday, Dec. 2 11:00AM - 11:10AM Location: N229

Shigeru Hirano, MD, PhD, Kyoto, Japan (Abstract Co-Author) Nothing to Disclose

Ichiro Tateya, MD, PhD, Kyoto, Japan (Abstract Co-Author) Nothing to Disclose

Morimasa Kitamura, MD,PhD, Kyoto, Japan (*Abstract Co-Author*) Nothing to Disclose Kaori Togashi, MD, PhD, Kyoto, Japan (*Abstract Co-Author*) Research Grant, Bayer AG Research Grant, DAIICHI SANKYO Group Research Grant, Eisai Co, Ltd Research Grant, FUJIFILM Holdings Corporation Research Grant, Nihon Medi-Physics Co, Ltd Research

Grant, Shimadzu Corporation Research Grant, Toshiba Corporation Research Grant, Covidien AG

PURPOSE

Diffusion MRI has been widely used for the diagnosis and monitoring of head and neck lesions. Non-Gaussian diffusion parameters (e.g. mean diffusion, ADCo, and kurtosis, K) have the potential to provide important information on tissue microstructure beyond ADC. The aim of this study was to investigate the value of quantitative diffusion assessment in the diagnosis of head and neck lesions.

METHOD AND MATERIALS

This IRB approved prospective study included 46 (27 malignant/19 benign) patients suspected of head and neck tumors between June 2014 and February 2015. Head and neck MRI was performed using a 3-T system equipped with a dedicated 16-channel head and neck coil. A read-out segmented EPI (RS-EPI) sequence combined with GRAPPA parallel acquisition and 2D-navigator-based reacquisition was used with 9 b values of 0, 75, 150, 300, 600, 1000, 1400, 1800, 2200 sec/mm2. Parametric maps of Gaussian and non-Gaussian diffusion parameters (K, ADCo and ADC) were generated by fitting the diffusion MRI signal using variable combinations of b values.

RESULTS

The performance (AUC) of ADC0-1400 (ADC derived from b values of 0 and 1400) (0.802) was higher than ADC0-600 or ADC0-1000 (0.753, 0.748) and ADC150-1400 (0.768). AUC of ADC0-1400 was significantly higher than that of ADC150-1000 (0.727, P<0.05). K or ADCo (0.71, 0.685, using all b values) didn't significantly change depending on the choice of b values, and gave the different information than ADC on their parametric maps.

CONCLUSION

The choice of b values could significantly affect the diagnostic performance of ADCs in head and neck lesions. Non-Gaussian diffusion parameters showed stable results regardless of the choice of b values, and their parametric maps have the potential to provide new information on tumor characteristics in addition to ADC.

CLINICAL RELEVANCE/APPLICATION

Non-Gaussian diffusion parameters beyond ADC give the stable results regardless of the choice of b values in head and neck lesions, easier to make comparison between facilities.

SSK14-05 Differentiation of Malignant and Benign Solid Nodules of the Thyroid Gland on Unenhanced Computed Tomography

Wednesday, Dec. 2 11:10AM - 11:20AM Location: N229

Participants

Ahmed-Emad Mahfouz, MD, Doha, Qatar (*Presenter*) Nothing to Disclose Hanan Sherif, MD, Doha, Qatar (*Abstract Co-Author*) Nothing to Disclose Ahmed Sayedin, MBBCh, Doha, Qatar (*Abstract Co-Author*) Nothing to Disclose

PURPOSE

The natural iodine content of benign thyroid nodules may be higher than that of malignant nodules. The purpose of this study is to assess the value of unenhanced computed tomography (CT) in differentiation of malignant and benign solid nodules of the thyroid gland based on this hypothesis.

METHOD AND MATERIALS

80 patients with solid thyroid nodules, initially seen on ultrasonography have been examined by an identical protocol of unenhanced and contrast-enhanced CT, including 48 patients with pathologically-proven thyroid carcinoma and 32 patients with pathologicallyproven nodular goiter. The attenuation value of the lesions on unenhanced CT has been measured. Statistical analysis has been done by the Student's t- test and the Chi-square test.

RESULTS

The attenuation value of malignant nodules on unenhanced CT has been 34 ± 11 HU, while the attenuation value of benign nodules has been 56 ± 21 HU. The difference has been statistically significant (p< 0.001). When the cut-off value for diagnosis of malignancy is \leq 50 HU, the sensitivity, specificity, positive predictive value, negative predictive value, and accuracy for the diagnosis of malignancy have been 89.6%, 68.8%, 81.1%, 81.5%, and 81.3% respectively compared to 72.9%, 71.9%, 79.5%, 63.9%, and 72.5% at a cut-off value of \leq 40 HU and 93.8%, 53.1%, 75.0%, 85.0%, and 77.5% at a cut-off value of \leq 55 HU respectively.

CONCLUSION

Malignant thyroid nodules have a statistically-significant lower attenuation value than benign nodules on unenhanced CT. Attenuation value \leq 50 HU has an accuracy of 81.5% for diagnosis of thyroid carcinoma.

CLINICAL RELEVANCE/APPLICATION

Unenhanced CT of the thyroid gland may be useful in differentiation of benign and malignant nodules of the thyroid and needs therefore to be included as part of the protocol of CT of the thyroid gland.

SSK14-06 Prospective Assessment of the Accuracy of Radiologic CT Staging of Extrinsic Tongue Muscle Involvement in Oral Cavity Cancer

Wednesday, Dec. 2 11:20AM - 11:30AM Location: N229

Participants Jacqueline Junn, MD, Atlanta, GA (*Presenter*) Nothing to Disclose Kristen L. Baugnon, MD, Atlanta, GA (*Abstract Co-Author*) Nothing to Disclose Eduardo Lacayo, MD, Atlanta, GA (*Abstract Co-Author*) Nothing to Disclose Patricia A. Hudgins, MD, Atlanta, GA (*Abstract Co-Author*) Nothing to Disclose Kelly Magliocca, Atlanta, GA (*Abstract Co-Author*) Nothing to Disclose Mark El-Deiry, Atlanta, GA (*Abstract Co-Author*) Nothing to Disclose J T. Wadsworth, Atlanta, GA (*Abstract Co-Author*) Nothing to Disclose Mihir Patel, R., Atlanta, GA (*Abstract Co-Author*) Nothing to Disclose Jonathan J. Beitler, MD, MBA, Atlanta, GA (*Abstract Co-Author*) Nothing to Disclose

PURPOSE

Pre-operative imaging plays an important role in staging advanced oral cavity cancer (OCC) treated with surgical resection followed by chemoradiation. Extrinsic tongue muscle invasion (ETMI) was added as a T4a classification in the 3rd edition of AJCC. The purpose of this prospective study was to examine the accuracy of preoperative contrast enhanced CT (CECT) and surgical assessment of ETMI using pathologic evaluation as the gold standard.

METHOD AND MATERIALS

This IRB approved prospective study recruited 34 consecutive patients with primary OCC between August 2014 and February 2015. Inclusion criteria were untreated primary OCC, available pre-operative CECT and surgical resection with pathological gross examination. Two neuroradiologists blindly reviewed the images for ETMI using the following scale: yes (Y), probably yes (PY), no (N), and probably no (PN). Three Head and Neck surgeons assessed for ETMI intra-operatively using the scale: Y, N or indeterminate. A single pathologist reviewed all gross examination notes for ETMI.

RESULTS

Twenty-five of the 34 patients met inclusion criteria. Six patients had pathologically proven ETMI. For statistical analysis, a radiologic score of yes/probably yes was scored as a yes and no/probably no as a no. Sensitivity (SN), specificity (SP), positive predictive value (PPV) and negative predictive value (NPV) for Radiologist 1 and 2 were: 83%, 84%, 62.5%, and 94%, and 100%, 84%, 67%, and 100%, respectively. Two intra-operative cases rated indeterminate by the surgeons were considered a no, leading to an overall intraoperative assessment SN, SP, PPV, and NPV of: 80%, 100%, 100%, 95%.

CONCLUSION

Although this preliminary study suggests that imaging findings on CECT may have a higher SN but lower SP than surgical observation, both radiographic and surgical determination of ETMI had equivocal cases. This highlights the importance of systematic assessment of the gross specimen to facilitate accurate pathologic ETMI to minimize unnecessary upstaging. Ongoing investigation with specific pathologic focus on ETMI would be needed to confirm the reproducibility of pathologic staging and follow up of clinical outcomes to determine the clinical significance.

CLINICAL RELEVANCE/APPLICATION

Radiographic ETMI should be verified with pathological findings and interdisciplinary communication between pathologists, surgeons, and radiologists to minimize unnecessary upstaging.

SSK14-07 Short-Term Effects of Concurrent Radiochemotherapy on Hypopharyngeal and Laryngeal Squamous Cell Carcinoma: Evaluated with Dual-Energy CT Quantitative Parameters

Wednesday, Dec. 2 11:30AM - 11:40AM Location: N229

Participants

Liang Yang, Beijing, China (*Presenter*) Nothing to Disclose Dehong Luo, MD, Beijing, China (*Abstract Co-Author*) Nothing to Disclose Yanfeng Zhao, MD, Beijing, China (*Abstract Co-Author*) Nothing to Disclose Li Lin, Beijing, China (*Abstract Co-Author*) Nothing to Disclose Meng Lin, Beijing, China (*Abstract Co-Author*) Nothing to Disclose

PURPOSE

To evaluate the value of dual-energy spectral computed tomography(CT) quantitative parameters in predicting short-term effects of concurrent radiochemotherapy on hypopharyngeal and laryngeal squamous cell carcinoma(SCC), and provide valuable evidence for early judging the response of the tumor to therapy in clinical pratice.

METHOD AND MATERIALS

This study was approved by the ethics committee and all patients provided written informed consent. Spectral parameters of 34 patients with laryngeal and hypopharyngeal SCC who underwent dual-energy spectral CT(GE Discovery CT 750 HD) scan with spectral mode before therapy were analyzed retrospectively, all cases were proven by pathological findings. Specral parameters contained IC-L (iodine concentration of lesion), WC-L (water concentration of lesion) and λ HU (slope of spectral HU curve), which were obtained by analyzing pretherapy CT scan datas with GSI Volume Viewer software in AW4.6 workstation. The following scans were taken at the 4th week after concurrent radiochemotherapy ended. By therapeutic effects, all patients were divided into treatment-sensitivity group (28 cases) and reatment-resistant group (6 cases). Parameters between two groups were compared, and the diagnosis experiment was evaluated.

RESULTS

Mean IC-L and λ HU in treatment-sensitivity group were 16.80±4.61 mg/cm3, 2.28±0.63 respectively, while the two parameters were 23.84±5.04 mg/cm3, 3.23±0.68 in the other group. IC-L and λ HU were significantly different between two groups (P<0.05).

However, WC-L was showing no significant difference(P>0.05). Receiver operating characteristic (ROC) analysis of IC-L, and λ HU in prediction of treatment-sensitivity showed: AUC (the area under curve) of IC-L was 0.81, larger than the AUC of λ HU(AUC=0.79). With IC-L≤18.43 mg/cm3 as diagnosis threshold in prediction of treatment-sensitivity, the sensitivity, specificity, positive predictive value, negative predictive and Youden's index value were 72.73%, 83.33%, 88.89%, 62.50%, 0.56 respectively.

CONCLUSION

IC-L could be helpful in the prediction short-term effects of concurrent radiochemotherapy on hypopharyngeal and laryngeal squamous cell carcinoma.

CLINICAL RELEVANCE/APPLICATION

Dual-energy spectral CT has a potentian value in clinical treatment options of hypopharyngeal and laryngeal SCC.

SSK14-08 Role of Magnetic Resonance Imaging in Thyroid Nodules ; Evaluation of the Magnetic Resonance Spectroscopy and Diffiusion Weighted in Differentiating Benign from Malignant Thyroid Nodules

Wednesday, Dec. 2 11:40AM - 11:50AM Location: N229

Participants

Pratiksha Yadav, Pune, India (Presenter) Nothing to Disclose

PURPOSE

To evaluate the diagnostic benefits of MRI in evaluation of thyroid lesionTo evaluate the role of DWI WITH ADC mappingTo evaluate the characteristic pattern of MR spectroscopy in various benign and malignant pathologies of thyroid

METHOD AND MATERIALS

This is prospective study carried out in 39 patients with already known thyroid nodules diagnosed on ultrasonography.All studies were done on 1.5 T Siemens Magnetom machine.Precontrast T1WI saggital .axial,STIR,T2WI coronal and axial,post contrast fat saturated axial T1WI were taken. DWI with ADC mapping ,single voxel MR spectroscopy were also done. Findings of MRI correlate with the final diagnosis on histopathological examination

RESULTS

Study was done on 39 cases. There were 19 cases of multinodular goiter, 5 cases of adenomas, 6 cases of thyroiditis and 9 cases of malignant lesion. The mean ADC value of the thyroid malignant lesion was significantly lower than the mean ADC value of thyroid benign lesions. The mean ADC value of the malignant lesions. Sensitivity of combined DW, ADC mapping and MRS show sensitivity of 98.9 % sensitivity to detect the malignant lesion with specificity of 93.4%

CONCLUSION

Thyroid lesions routine imaging could not differentiate malignant lesion from benign lesion. Diffusion weighted imaging with ADC mapping and Magnetic resonance Spectroscopy are good noninvasive investigation to diagnose malignancy.

CLINICAL RELEVANCE/APPLICATION

MRI evaluation of thyroid lesions combined with DWI & MRS are a good noninvasive test to diagnose the malignant lesion. It is useful to see the extent of the tumor, involvement of the surrounding structures, retrosternal extension and lymph nodal involvement.

SSK14-09 Prediction Study on Energy Spectrum Parameters in Larynx and Hypopharyngeal Squamous Cell Carcinoma with Different Pathological Grades

Wednesday, Dec. 2 11:50AM - 12:00PM Location: N229

Participants

Liang Yang, Beijing, China (*Presenter*) Nothing to Disclose Dehong Luo, MD, Beijing, China (*Abstract Co-Author*) Nothing to Disclose Yanfeng Zhao, MD, Beijing, China (*Abstract Co-Author*) Nothing to Disclose Lin Li, MD, Beijing, China (*Abstract Co-Author*) Nothing to Disclose Meng Lin, Beijing, China (*Abstract Co-Author*) Nothing to Disclose

PURPOSE

To discuss the effect of energy spectrum parameters in sDECT (single-source dual-energy spectral CT) on evaluating larynx and hypopharyngeal squamous cell carcinoma(SCC) with different pathological grades.

METHOD AND MATERIALS

Retrospective analysis was carried out in 60 patients with confirmed pathological diagnosis of larynx and hypopharyngeal SCC from January to August in 2014. They were all scanned by sDECT (Discovery CT 750 HD) before treatment. After scanning, all data was analyzed with GSI Volume Viewer software of GE AW4.6 workstation. IC-L (iodine concentration of lesion), WC-L (water concentration of lesion), s-SHC (slope of spectral Hu curve), CT value in 70Kev monoergic image, IC-C (iodine concentration of carotid sinus), WC-C (water concentration of carotid sinus), sIC(standardized IC) and sWC (standardized WC). According to cell differentiation, all the patients were divided into low differentiated group and mid-high differentiated group. Parameters between two groups were compared, and the diagnosis experiment was evaluated.

RESULTS

Mean IC-L, s-SHC and sIC in low differentiated group were 15.61 mg/cm3±5.06mg/cm3, 2.07±0.77 and 15.61mg/cm3±5.06mg/cm3 respectively, while the three parameters were 20.29±7.40mg/cm3,2.68±1.04 and 20.29±7.40mg/cm3 in the other group. All three parameters were significantly different between two groups (P<0.05). However, WC-L, CT value and sWC were showing no significant difference(P>0.05). ROC (receiver operating characteristic) analysis of IC-L, s-SHC, and sIC in prediction of low differentiated larynx and hypopharyngeal SCC showed: AUC (the area under curve) of sIC was 0.79, larger than the AUC of IC-L and s-SHC. AUC difference between s-SHC and sIC was significant (P<0.05), while it was not significant between IC-L and sIC (P>0.05). With sIC>5 as diagnosis threshold in prediction of low differentiated SCC, the sensitivity, specificity, positive predictive

value and negative predictive value were 84.21%, 75.61%, 61.5% and 91.2% respectively.

CONCLUSION

sIC could be helpful in the prediction of larynx and hypopharyngeal SCC with different pathological grades.

CLINICAL RELEVANCE/APPLICATION

sDECT maybe a potential method for judgeing the differentiation of pathological grade of Larynx and Hypopharyngeal SCC

Vascular/Interventional (Advances in Hepatic Tumor Ablation)

Wednesday, Dec. 2 10:30AM - 12:00PM Location: N227

GI IR MR

AMA PRA Category 1 Credits ™: 1.50 ARRT Category A+ Credits: 1.50

FDA Discussions may include off-label uses.

Participants

Nael E. Saad, MBBCh, Saint Louis, MO (Moderator) Research Consultant, Veran Medical Technologies, Inc; Proctor, Sirtex Medical Ltd

Charles Y. Kim, MD, Durham, NC (*Moderator*) Research Grant, Galil Medical Ltd; Consultant, Kimberly-Clark Corporation; Consultant, Cryolife, Inc

Sub-Events

SSK18-01 Long-Term Therapeutic Outcomes of Radiofrequency Ablation For Subcapsular versus Non-Subcapsular Hepatocellular Carcinoma

Wednesday, Dec. 2 10:30AM - 10:40AM Location: N227

Participants

Tae Wook Kang, MD, Seoul, Korea, Republic Of (*Abstract Co-Author*) Nothing to Disclose Hyo Keun Lim, MD, Seoul, Korea, Republic Of (*Abstract Co-Author*) Nothing to Disclose Mimi Kim, MD, Seoul, Korea, Republic Of (*Presenter*) Nothing to Disclose

PURPOSE

Recent clinical guidelines for management of hepatocellular carcinoma (HCC) have not recommended the radiofrequency (RF) ablation for subcapsular tumor due to a higher risk of incomplete ablation or major complications. However, these guidelines were mainly based on retrospective studies with insufficient sample size and follow-up. We retrospectively compared the long-term therapeutic outcomes of RF ablation for HCC in a subcapsular versus non-subcapsular location using propensity score matching

METHOD AND MATERIALS

508 patients (396 men, 112 women; age range, 30-80 years) with a single HCC (<5 cm) were treated with ultrasonography-guided percutaneous RF ablation as a first-line treatment. We divided the patients into two groups, subcapsular (n = 227) or non-subcapsular group (n = 281). We evaluated the association of subcapsular location and the long-term therapeutic outcomes of RF ablation including local tumor progression (LTP) and overall survival (OS) using the matched data and assessed the major complication rate in overall data.

RESULTS

After matching, there were 163 matched pairs of patients in both groups. In the matched groups, the 3- and 5-years cumulative LTP rates were estimated as 18.8% and 20.9%, respectively, for the subcapsular group, and 13.2% and 16.0% for the non-subcapsular group. The corresponding OS rates were 90.7% and 83.2% in the subcapsular group, and 91.4% and 79.1% in the non-subcapsular group, respectively. The hazard rates for LTP (HR [hazard ratio] = 1.37, P = 0.244) and OS (HR = 0.86, P = 0.604) were not significantly different between two matched groups. In addition, there was no significant difference in both groups in terms of major complications rates (P > 0.05).

CONCLUSION

The difference in long-term therapeutic outcomes of RF ablation for HCC was not significant between the subcapsular and nonsubcapsular groups.

CLINICAL RELEVANCE/APPLICATION

The consideration of overall technical difficulty of RF ablation for HCC under various clinical settings is more reasonable than the dichotomous view of recommendation for RF ablation judged by anatomical location including subcapsular HCCs.

SSK18-02 Ablation Margin Size and Not Modality Predicts Local Tumor Progression after Ablation of Colorectal Liver Metastases: A Case-control Study of RF and Microwave Ablation

Wednesday, Dec. 2 10:40AM - 10:50AM Location: N227

Participants

Waleed Shady, MBBCh, New York, NY (*Presenter*) Nothing to Disclose Joseph P. Erinjeri, MD, PhD, New York, NY (*Abstract Co-Author*) Nothing to Disclose Karen T. Brown, MD, New York, NY (*Abstract Co-Author*) Nothing to Disclose Anne M. Covey, MD, New York, NY (*Abstract Co-Author*) Nothing to Disclose Stephen B. Solomon, MD, New York, NY (*Abstract Co-Author*) Research Grant, General Electric Company Constantinos T. Sofocleous, MD, PhD, New York, NY (*Abstract Co-Author*) Consultant, Sirtex Medical Ltd Christina L. Zenobi, New York, NY (*Abstract Co-Author*) Nothing to Disclose Mithat Gonen, PhD, New York, NY (*Abstract Co-Author*) Nothing to Disclose Nancy Kemeny, MD, New York, NY (*Abstract Co-Author*) Nothing to Disclose

PURPOSE

To compare the local tumor progression rates of colorectal liver metastases ablated percutaneously using either microwave (MW) or radiofrequency (RF).

METHOD AND MATERIALS

We preformed an IRB-approved retrospective review of a prospectively created HIPAA-complaint ablation database. We included patients with CLM ablated using RF between November 2009 and December 2012. These were matched to a group of patients with CLM ablated using MW between November 2009 and July 2014. Patients were excluded if the percutaneous ablation was used to treat a local recurrence of a previous ablation. The ablation margin was measured on the 1st portal venous phase CT obtained post-ablation (4-8 weeks), and classified as either ≤ 5 mm or >5 mm. Patients/tumors were excluded if the ablation margin could not be measured due to either: (a) lack of a CT scan at baseline or at 4-8 weeks post-ablation, or (b) fused ablation defects. Clinical characteristics were compared between both groups. Kaplan-Meier methodology was used to calculate LTP-free survival. Stratified log-rank tests were used to analyze predictors of LTP.

RESULTS

The study enrolled 53 patients with 77 tumors ablated with RF in 64 sessions, and 36 patients with 43 tumors ablated with MW in 39 sessions. No differences existed between both groups in baseline clinical characteristics or mean tumor size (1.9 cm MW versus 1.9 cm RF) (P=0.9). The LTP-free survival rate at 2 years was 67% in the RF group and 71% in the MW group (P=0.9). The percentage of ablation margins >5 mm achieved with RF was 58% (45/77) and 42% with MW (18/43) (P=0.08). An ablation margin \leq 5 mm was a predictor of LTP in both the RF group (P<0.001) and the MW group (P=0.005). The median LTP-free survival in tumors with a margin \leq 5 mm was longer in the MW group than in the RF group (21 months versus 8 months), approaching statistical significance (P=0.09). The LTP-rate for tumor with an ablation margin >5mm was 4% in the RF group (2/45) and 6% (1/18) in the MW group (P=0.3). Minor complications rate for MW and RF were 26% (10/39) versus 13% (8/64) (P=0.09), and major complications rates were 15% (6/39) versus 13% (8/64) (P=0.7).

CONCLUSION

Local control after ablation of CLM is dependent on an adequate ablation margin and not the modality used.

CLINICAL RELEVANCE/APPLICATION

Sufficient ablation margins remain the most important factor to achieve prolonged LPFS regardless of thermal energy.

SSK18-03 Role of Microwave Ablation (MWA) Therapy of Liver Metastases from Colorectal Carcinoma Post systemic Chemotherapy: Tumor Control and Survival Rates

Wednesday, Dec. 2 10:50AM - 11:00AM Location: N227

Participants

Nour-Eldin A. Nour-Eldin, MD,PhD, Frankfurt Am Main, Germany (*Presenter*) Nothing to Disclose Mohammed A. Alsubhi, BMBS, Frankfurt Am Main, Germany (*Abstract Co-Author*) Nothing to Disclose Nagy N. Naguib, MD, MSc, Frankfurt Am Main, Germany (*Abstract Co-Author*) Nothing to Disclose Martin Beeres, MD, Frankfurt Am Main, Germany (*Abstract Co-Author*) Nothing to Disclose Thomas Lehnert, MD, Frankfurt Am Main, Germany (*Abstract Co-Author*) Nothing to Disclose Thomas J. Vogl, MD, PhD, Frankfurt, Germany (*Abstract Co-Author*) Nothing to Disclose

PURPOSE

to evaluate the safety, efficiency, effectiveness, and overall outcome in patients treated with microwave thermal ablation of colorectal metastases post systemic chemotherapy.

METHOD AND MATERIALS

An institutional review board-approval was obtained with informed consent of all patients. Retrospective analysis of prospective intention to treat study was performed from January 2008 to January 2013, and included 92 patients (mean age 56 years SD: 2.6) with 132 liver metastases measuring 0.7-5.0cm, who were treated with microwave ablation (MWA). Local tumor control, complications, and long-term survival were analyzed.

RESULTS

The mean follow-up period was 32.5 months. Complete ablation was achieved in 117 of 132 (88.6%) nodules. Seventeen of the 117 (14.5%) successfully treated nodules developed local recurrence. Univariate analysis showed that tumor size of < 3 cm is a significant risk factor (P = 0.04). Multivariate analysis showed that number of cycles of chemotherapy (FOLFOX) was a significant prognostic factor for overall recurrence (P=0.03), whereas disease-free interval was the significant prognostic factor for distant recurrence (P=0.03). Major complications occurred in 1.1% of patients. No procedure-related mortalities were observed. The 1, 2, 3, and 5-year overall survival rates after the initial ablation were 82, 61.2, 51.2, and 38.3%, respectively. The main cause of death was systemic tumor progression in 65.3% of the patients.

CONCLUSION

MWA is a safe and effective treatment therapeutic option for patients with liver metastases from Colorectal Carcinoma post systemic chemotherapy.

CLINICAL RELEVANCE/APPLICATION

MWA could be safely used as a part of the therapeutic armamentarium in the management of patients with hepatic colorectal metastasis post systemic chemotherapy.

SSK18-04 Local Response Assessment after Percutaneous CT-guided IRE of Hepatic Malignancies: How Useful is Diffusion-weighted MRI (DWI)?

Wednesday, Dec. 2 11:00AM - 11:10AM Location: N227

Participants

Alexandra Barabasch, MD, Aachen, Germany (*Presenter*) Nothing to Disclose Philipp Heil, Aachen, Germany (*Abstract Co-Author*) Nothing to Disclose Martina Distelmaier, Aachen, Germany (*Abstract Co-Author*) Nothing to Disclose Nils A. Kraemer, Aachen, Germany (*Abstract Co-Author*) Nothing to Disclose Christiane K. Kuhl, MD, Bonn, Germany (*Abstract Co-Author*) Nothing to Disclose Philipp Bruners, MD, Aachen, Germany (*Abstract Co-Author*) Nothing to Disclose

PURPOSE

Assessment of response to hepatic IRE using standard MR-sequences is difficult due to complex signal intensity (SI) changes of the ablation zones that occur during follow-up. DWI offers a high sensitivity for detection of liver metastases. Therefore, aim of this study was to evaluate if DWI is useful to help distinguish normal post-therapeutic SI changes after IRE from local recurrence.

METHOD AND MATERIALS

27 Patient (mean age 62y) with 37 malignant liver tumors (4 HCC, 33 metastases) underwent CT-guided percutaneous IRE. Preand post-interventional hepatic MRI (T2w TSE, dynamic CE T1w GE, T1w GE in late phase) with DWI (b=800) was performed before treatment, within 2 hours after IRE, at 24 hours after IRE, and at 1, 2, 4, 6, 8, 12 weeks after IRE, and every 3 months thereafter. MR-images were systematically analyzed by two readers in consent. The ablation volume was carefully manually rendered on each b=800 DW image of the ablation zone to create a volume of interest. Minimal ADC-values (ADCmin) were measured in the target lesion before treatment and in the ablation zone volume after treatment.

RESULTS

Within the first two days after IRE, ADCmin-values decreased significantly compared to pre-treatment ADCmin in 26 of 37 patients. Thereafter, ADCmin values increased continuously in all of these patients and, within 1-3 months after IRE, were back to normal, i.e. reached the level of the ADCmin values of normal liver parenchyma. In 8/37 patients, this normalization of ADCmin-values was not observed, but instead, exhibited a further decrease of ADCmin at follow up (6 weeks - 12 months) that were then lower than the baseline ADCmin of the tumor before IRE treatment. At the time when the ADC-min decrease was found, remaining hepatic MRI pulse sequences, including visual analysis of DWI, were not suspicious of local recurrence. Only at later follow-up MRI, presence of local tumor recurrence was confirmed in 7 out of these 8 cases.

CONCLUSION

These initial results suggest that quantitation of ADCmin is useful to identify local recurrencies after hepatic IRE, because changes of ADCmin (specifically, a new decrease of ADCmin after post-treatment ADC normalization) precede visually perceptible SI changes.

CLINICAL RELEVANCE/APPLICATION

DWI, with ADC-min quantitation, may allow early diagnosis of local tumor recurrence after IRE.

SSK18-05 MR Imaging Findings after Hepatic Irreversible Electroporation (IRE) - How to Depict Local Recurrence

Wednesday, Dec. 2 11:10AM - 11:20AM Location: N227

Participants

Alexandra Barabasch, MD, Aachen, Germany (*Presenter*) Nothing to Disclose Martina Distelmaier, Aachen, Germany (*Abstract Co-Author*) Nothing to Disclose Philipp Heil, Aachen, Germany (*Abstract Co-Author*) Nothing to Disclose Nils A. Kraemer, Aachen, Germany (*Abstract Co-Author*) Nothing to Disclose Philipp Bruners, MD, Aachen, Germany (*Abstract Co-Author*) Nothing to Disclose Christiane K. Kuhl, MD, Bonn, Germany (*Abstract Co-Author*) Nothing to Disclose

PURPOSE

We systematically followed patients after percutaneous IRE for primary or secondary liver malignancies according to a standardized follow-up MRI protocol. Our aim was to describe the normal changes of MR signal pattern over time that can be expected after IRE; this knowledge is important in order to allow the sensitive detection of signal intensity (SI) changes that are not within normal limits, i.e. likely represent local recurrence.

METHOD AND MATERIALS

27 patients (13 male, mean age 62y) with 37 malignant liver tumors (33 secondary, 4 HCC) underwent percutaneous CT-guided IRE. Patients underwent pre- and post-interventional hepatic MRI with Gd-EOB-DTPA according to a standardized protocol (including T2 TSE sequences, dynamic contast-enhanced T1w GE sequence, T1w GE in late phase) before treatment, within 2 hours after IRE, at 24 hours after IRE, and then at 1, 2, 4, 6, 8, 12 weeks after IRE, and every 3 months thereafter. MR images were systematically evaluated by two readers in consent.

RESULTS

Even after successful IRE, in 23/37 (62%) cases, the ablated tumor was still visible, with unchanged SI and internal architecture as before IRE, for 1-8 weeks after IRE in 8/23 cases, for 3-9 months in 12/23 cases, and for more than 12 months in 3/23 cases. The ablation zone itself appeared as an intermediately hyperintense area on T2w images until 1 week after IRE in all cases. Thereafter, the ablation zone inverted its SI and appeared on T2w images intermediately hypointense in the center, with a hyperintense rim, the latter exhibited strong contrast enhancement in 34/37 cases. This appearance persisted for 1-4 weeks in 17/34 cases, for 6-8 weeks in 10/34 and for 3-6 months in 7/34 cases. The ablation zones showed a steady decrease in size and disappeared completely in 21/37 cases (within 3 months in 16 cases). Local recurrences were observed in 7/37 (19%) cases and were visible as intermediately hyperintense masses on the edge of the intermediately low SI ablation zone on T2w images.

CONCLUSION

IRE induces complex signal intensity changes that vary over time. In the majority of cases, the treated target lesions were visible within the ablation zone over a longer period of time. This makes diagnoses of local recurrence difficult.

CLINICAL RELEVANCE/APPLICATION

Knowledge of the typical MR-imaging appearance of the IRE ablation zone and its changes over time is important to avoid diagnostic errors in the follow up of patients after IRE.

SSK18-06 Procedural Sedation and Analgesia versus General Anesthesia for Respiratory-gated MR-HIFU Ablation in the Liver

Wednesday, Dec. 2 11:20AM - 11:30AM Location: N227

Participants

Johanna M. van Breugel, MSc, Utrecht, Netherlands (*Presenter*) Nothing to Disclose Joost W Wijlemans, MD,PhD, Utrecht, Netherlands (*Abstract Co-Author*) Nothing to Disclose HHB Vaessen, MSc, Utrecht, Netherlands (*Abstract Co-Author*) Nothing to Disclose Martijn de Greef, PhD, Utrecht, Netherlands (*Abstract Co-Author*) Nothing to Disclose Chrit T. Moonen, PhD, Utrecht, Netherlands (*Abstract Co-Author*) Nothing to Disclose Maurice V. Bosch, MD, PhD, Utrecht, Netherlands (*Abstract Co-Author*) Nothing to Disclose Mario G Ries, PhD, Utrecht, Netherlands (*Abstract Co-Author*) Nothing to Disclose

PURPOSE

Investigate the feasibility of respiratory-gated MRHIFU ablation in the liver under PSA with spontaneous breathing in an animal experiment Validate the introduced respiratory depression by PSA in sedated human patients

METHOD AND MATERIALS

Five pigs were placed on a Philips Sonalleve MR-HIFU system (1.5T, Philips Healthcare). PSA was induced using propofol (4.5-6mg/kg/h) and remifentanil (4.8-5.8 μ g/kg/h). Volumetric sonications were performed under PSA (4x4x10mm3, 450W acoustic power, 15-25s). MRI and acoustic energy delivery were respiratory gated with a pencil beam navigator. Then, GA was induced using midazolam (1mg/kg/h), nimbex (0.09mg/kg/h), and sufentanil (11.3 μ g/kg/h). Mechanical ventilation was set to 13/min and the ablation protocol was repeated. For both protocols the nonperfused volumes (NPVs) were measured and the duty cycles (DC) of the therapeutic sonications were compared. PSA was induced in two patients prior to HIFU treatment using propofol (1.4 and 1.6 mg/kg/h) and remifentanil (2.5 and 0.3 μ g/kg/h). Vital functions were monitored.

RESULTS

Under GA a median DC of 64.0% (IQR 62-67, n=42) was achieved and of 79.5% (IQR 73-85, n=42) under PSA. The mean NPV per sonication was 0.09ml during GA and 0.16ml during PSA. Breathing frequency (BF) under PSA varied between 9-15 breaths/min. Vital functions remained stable. During both patient treatments under PSA the BF could be depressed to values as low as 5/min while the ETCO2 level stayed <6.5%, and blood pressure and heart rate values remained normal.

CONCLUSION

The animal experiments confirmed the feasibility of volumetric HIFU ablations using respiratory gating under PSA. The results were comparable or superior to those achieved under GA. The subsequent PSA procedures on human patients evidenced the similarity in respiratory depression of the PSA protocol while vital functions and patient safety were not impaired. Future work anticipates translation of these findings in a clinical liver ablation study.

CLINICAL RELEVANCE/APPLICATION

Magnetic Resonance-guided High Intensity Focused Ultrasound (MR-HIFU) ablation in the liver is complicated by the continuous target movement due to respiration. Respiratory gating represents a simple and robust solution, which usually requires general anesthesia (GA) to obtain a long resting phase. From a patient's perspective however, procedural sedation and analgesia (PSA) has advantages over GA: a lower risk of complications and shorter recovery.

SSK18-08 Preclinical Evaluation of an MR - Compatible Microwave Ablation System and Comparison with a Standard Microwave Ablation System in an ex Vivo Bovine Liver Model

Wednesday, Dec. 2 11:40AM - 11:50AM Location: N227

Participants

Rudiger Hoffmann, Tubingen, Germany (Presenter) Nothing to Disclose

David-Emanuel Kessler, Tubingen, Germany (Abstract Co-Author) Nothing to Disclose

Frank Eibofner, Tubingen, Germany (Abstract Co-Author) Nothing to Disclose

Jakob Weiss, Tubingen, Germany (Abstract Co-Author) Nothing to Disclose

Konstantin Nikolaou, MD, Tuebingen, Germany (Abstract Co-Author) Speakers Bureau, Siemens AG Speakers Bureau, Bracco Group Speakers Bureau, Bayer AG

Stephan Clasen, MD, Tuebingen, Germany (Abstract Co-Author) Nothing to Disclose

Philippe L. Pereira, MD, Heilbronn, Germany (*Abstract Co-Author*) Research Consultant, Terumo Corporation; Speaker, AngioDynamics, Inc; Speaker, BSD Medical Corporation; Speaker, Terumo Corporation; Speaker, CeloNova BioSciences, Inc; Speaker, Medtronic, Inc; Speaker, BTG International Ltd; Speaker, Biocompatibles International plc; Advisory Board, Siemens AG; Advisory Board, Terumo Corporation; Advisory Board, Bayer AG; Advisory Board, BTG International Ltd; Advisory Board, Medtronic, Inc; Support, Bracco Group; Support, PharmaCept GmbH; Support, Terumo Corporation; Support, Siemens AG; Support, Novartis AG; Support, GlaxoSmithKline plc; Consultant, CeloNova BioSciences, Inc; Research Grant, Biocompatibles International plc; Research Grant, Siemens AG; Research Grant, Terumo Corporation; Research Grant, BTG International Ltd Hans-Jorg Rempp, Tubingen, Germany (*Abstract Co-Author*) Nothing to Disclose

PURPOSE

To evaluate a newly developed MR-compatible microwave ablation system with focus on ablation performance and compare it with a corresponding standard microwave ablation system in an ex-vivo setting.

METHOD AND MATERIALS

Overall, 52 ablation procedures were performed in an ex vivo bovine liver phantom, with various non-perfusion cooled microwave ablation devices and varying ablation durations, using the following settings: [A] 16G standard antenna, 2cm active tip, 2.4m cable; [B] MR-compatible 16G-antenna, 2cm active tip, 2.4m cable; [C] MR-compatible 16G-antenna, 2cm active tip, extended 6m cable; [D] MR-compatible 16G-antenna, 4cm active tip, extended 6m cable. Ablation durations were 3min, 5min and 10min for settings [A]-[C], performing an additional 15min ablation for setting [D]. Settings [A]-[C] were compared regarding the size of the ablation, i.e., short axis diameter (SA), Volume (V), as well as the generator energy output (E), with analysis of variance and Tukey post

hoc test. Ablation performance of the MR-compatible settings [C] and [D] were compared regarding SA, V, E and sphericity index (SA/LA) with unpaired t-test.

RESULTS

No statistically significant differences were found between [A], [B] and [C] regarding SA and V (10min; [A]: SA=25.8±2.4mm, V=17.8±4.4cm³. [B]: SA=25.3±1.9mm, V=16.6 ± 3.0 cm³. [C]: SA=25.0±2.0mm, V=17.8 ± 2.7 cm³); however, the highest generator energy output was measured for setting [C] ([A]: $9.9\pm0.5kJ$, [B]: $10.1\pm0.5kJ$, [C]: $13.1\pm0.3kJ$, p<0.001). SA, V and E were significantly larger with setting [D] than [C] with 10min ablations ([D]: SA=34.0±2.9mm, V=39.4±7.5 cm³, E=16.7±0.8kJ) without significant difference in sphericity index ([C]: SA/LA=0.46±0.02, [D]: SA/LA=0.52±0.04, p=0.08). Largest ablation zone was achieved with setting [D] after 15 min ablation time (SA=41±1.4mm, V=60.9±5.2cm³, SA/LA=0.59±0.01).

CONCLUSION

The MR-compatible microwave antenna and a standard, comparable, non-MR-compatible microwave ablation device create similar ablation zones. Use of an extension cable for generator positioning outside the MR scanner room is possible without loss of ablation performance.

CLINICAL RELEVANCE/APPLICATION

The tested MR-compatible system can be used without loss of ablation performance compared to the standard system.

SSK18-09 Percutaneous of Microwave Ablation of Hepatic Dome: Assessment of Efficacy and Safety

Wednesday, Dec. 2 11:50AM - 12:00PM Location: N227

Participants

Nazanin H. Asvadi, MD, Boston, MA (*Presenter*) Nothing to Disclose Arash Anvari, MD, Boston, MA (*Abstract Co-Author*) Nothing to Disclose Raul N. Uppot, MD, Boston, MA (*Abstract Co-Author*) Nothing to Disclose Ashraf Thabet, MD, Boston, MA (*Abstract Co-Author*) Nothing to Disclose Ronald S. Arellano, MD, Boston, MA (*Abstract Co-Author*) Nothing to Disclose

PURPOSE

To evaluate the efficacy and safety of computed tomography (CT) guided microwave ablation of tumors in hepatic dome.

METHOD AND MATERIALS

An Interventional Radiology database was used to retrospectively identify patients who underwent CT-guided percutaneous microwave ablation for liver tumors located in the hepatic dome between June 2011 and December 2014. Creation of artificial ascites was attempted as an adjunctive maneuver to displace the liver away from the right hemidiaphragm to minimize the potential risks of phrenic nerve injury, pneumothorax or peritoneal burn.Treatment response was assessed by either contrast material enhanced CT or magnetic resonance imaging (MRI) at 1, 3, 6, 9, 12 months and every 3 months therafter. Primary clinical success was defined as absence residual tumor on one month post-ablation CT or magnetic resonance imaging. Secondary clinical success defined as no residual lesion after repeat microwave ablation.

RESULTS

Between June 2011 and December 2014, 46 patients (M: F = 31:15, mean age = 64.4 years, (range = 25-89 years) underwent CTguided percutaneous microwave ablation for 48 tumors in the hepatic dome. Creation of artificial ascites with 0.9% normal saline solution (0.9% NS) as an adjunctive maneuver to displace the dome from the right hemidiaphragm was performed in 34/48 (70%) of ablations with mean volume of 1237.5 ml of fluid (range=300-3000 ml). Primary success was achieved in 41/48 (85%). Four tumors required retreatment to achieve complete necrosis for a secondary success rate of 94%. There were no major complications. Two patients experienced small, asymptomatic pneumothoraces that were aspirated at the time of the procedure and did not result in thoracostomy or unexpected hospitalization.

CONCLUSION

Computed tomography guided microwave ablation of hepatic dome lesions is associated with high success rate and low complication rate. Creation of artificial ascites may have a protective effect on minimizing the risk of thermal injury to the diaphragm and/or risk of significant pneumothorax.

CLINICAL RELEVANCE/APPLICATION

Computed tomography guided microwave ablation of hepatic dome lesions is associated with high success and low complication rates.

Physics (Radiation Dose Measurement)

Wednesday, Dec. 2 10:30AM - 12:00PM Location: S404AB



Participants

Mitchell M. Goodsitt, PhD, Ann Arbor, MI (Moderator) Research collaboration, General Electric Company

Sub-Events

SSK16-01 A Computer Program to Assess Organ Doses for Pediatric and Adult Patients Undergoing CT Scans

Wednesday, Dec. 2 10:30AM - 10:40AM Location: S404AB

Participants

Choonsik Lee, PhD, Rockville, MD (*Presenter*) Nothing to Disclose Kwang Pyo Kim, Suwon, Korea, Republic Of (*Abstract Co-Author*) Nothing to Disclose Wesley E. Bolch, PhD, Gainesville, FL (*Abstract Co-Author*) Nothing to Disclose Les R. Folio, DO, MPH, Bethesda, MD (*Abstract Co-Author*) Research agreement, Carestream Health, Inc

PURPOSE

To develop a computer program to assess organ doses for pediatric and adult patients undergoing computed tomography (CT) scans using a series of reference pediatric and adult computational human phantoms coupled with the Monte Carlo transport simulation of x-ray in CT scans.

METHOD AND MATERIALS

A comprehensive set of organ dose conversion coefficients, organ dose normalized to CTDIvol, were calculated using 10 pediatric phantoms, recently adopted by International Commission on Radiological Protection (ICRP) as international reference, and the ICRP reference adult phantoms (ICRP Publication 110). The simulated organ doses were experimentally validated by physical anthropomorphic phantoms. A graphical user interface was designed to obtain the user input of patient and scan parameters. The routines for Size Specific Dose Estimates (SSDE) and organ doses under tube current modulation scans (based on mAs data abstracted from DICOM headers) were also programmed. To evaluate the performance of the computer program, organ doses were calculated for 10 pediatric and adult sample patients, and compared with existing CT dosimetry tools.

RESULTS

A computer program with GUI was developed for users to input CT scan parameters and assess organ doses and other dose descriptors as output. The calculated organ doses matched the measured values within 15%. The organ doses calculated for the 10 sample patients using our program showed up to 200% discrepancies compared to the existing CT dose calculators (CTDosimetry and CT-Expo). Detailed analysis of the anatomy of phantoms revealed that realistic human phantoms are crucial to improving accuracy in CT organ dosimetry.

CONCLUSION

A user-friendly computer program for CT dose calculations was developed and validated. The program is based on the realistic ICRP reference phantoms and up-to-date red bone marrow dosimetry methods, and provides several convenient features compared to the existing tools.

CLINICAL RELEVANCE/APPLICATION

The computer program developed in this study is a convenient tool providing organ doses for CT patients based on the ICRP reference phantoms. The program will be useful for epidemiological studies of CT risk and patient dose monitoring.

SSK16-02 Can Gaming Consoles Be Used to Improve X-Ray Imaging? A Feasibility Study

Wednesday, Dec. 2 10:40AM - 10:50AM Location: S404AB

Participants

Steven Don, MD, Saint Louis, MO (*Presenter*) Research Grant, Carestream Health, Inc; ; Robert MacDougall, MSc, Cambridge, MA (*Abstract Co-Author*) Nothing to Disclose William Clayton, St. Louis, MO (*Abstract Co-Author*) Nothing to Disclose

PURPOSE

To test the feasibility of using gaming console technology to improve the quality of X-ray projection imaging by automatically measuring body part thickness and mitigating the causes of repeat examinations.

METHOD AND MATERIALS

Proprietary software was developed for the Microsoft Kinect 1.0 for Windows using C#. Both the optical camera and infrared sensor outputs were recorded and tested with a mock-up wall stand. The software was designed to control radiation dose variation by measuring body-part thickness. It also was designed to reduce common reasons for repeating images including wrong body part, motion, positioning, and clipped anatomy.

RESULTS

The system recognized hady next and left wisht side of the hady to reduce taking the urrang hady next. This has a measurements

The system recognized body part and left/right side of the body to reduce taking the wrong body part. Thickness measurements were automatically displayed with a precision of 1 mm at the central ray, defined body part, or at a user-specified point. The system identified the relationship of the patient's ordered anatomy with respect to the location of automatic exposure chambers (AECs) and image receptor. The software was designed to highlight the body part in red when it was not overlying the AECs, yellow when partially on a specified AEC, and green when completely covering that AEC. Motion was tracked graphically over time displayed with red indicating gross motion, yellow as slight motion, and green as no motion. Clipped anatomy was displayed with an overlay of the collimated light field. Positioning was confirmed with the optical camera. The display output included a stylized body with highlighted body part, optical visualization of the patient, thickness measurement, and motion over time displayed graphically as shown in the figure (shown: left hand centered over the center AEC, recent but no current motion, and 19 mm thick in the AP projection at the central ray).

CONCLUSION

This feasibility study shows that body-part thickness can be measured automatically and can aid in setting technique based on patient thickness without physical contact measurement (e.g. calipers). The system can reduce repeat rates by confirmation of the correct body part, and checking for motion, positioning, and collimation immediately before the radiograph.

CLINICAL RELEVANCE/APPLICATION

This feasibility study indicates that technology can be adapted from mass-produced gaming consoles to control radiation dose and reduce repeat rates. This device can help the radiology community adhere to the ALARA principle.

SSK16-03 Making Proper Use of the ICRU/AAPM CT Dose Phantom: Recommendations and Limitations

Wednesday, Dec. 2 10:50AM - 11:00AM Location: S404AB

Participants

Donovan M. Bakalyar, PhD, Detroit, MI (Presenter) Nothing to Disclose Erin Angel, PhD, Tustin, CA (Abstract Co-Author) Employee, Toshiba Corporation

John M. Boone, PhD, Sacramento, CA (Abstract Co-Author) Research Grant, Siemens AG Research Grant, Hologic, Inc Consultant, Varian Medical Systems, Inc

Robert G. Dixon, MD, Chapel Hill, NC (Abstract Co-Author) Nothing to Disclose

Sarah E. McKenney, PhD, Washington, DC (Abstract Co-Author) Consultant, RadCal Corporation

Michael F. McNitt-Gray, PhD, Los Angeles, CA (Abstract Co-Author) Institutional research agreement, Siemens AG; Research support, Siemens AG; ; ; ; ; ; Wenzheng Feng, New York, NY (*Abstract Co-Author*) Nothing to Disclose

Paul B. Sunde, Monrovia, CA (Abstract Co-Author) Shareholder, Radcal Corporation; Employee, Radcal Corporation

Keith J. Strauss, FAAPM, FACR, Cincinnati, OH (Abstract Co-Author) Research Consultant, Koninklijke Philips NV; Speakers Bureau, Koninklijke Philips NV

Heather Chen-Mayer, PhD, Gaithersburg, MD (Abstract Co-Author) Nothing to Disclose

Sue Edyvean, London, United Kingdom (Abstract Co-Author) Nothing to Disclose

Richard L. Morin, PhD, Jacksonville, FL (Abstract Co-Author) Nothing to Disclose

Shuai Leng, PhD, Rochester, MN (Abstract Co-Author) Nothing to Disclose

Jeffrey H. Siewerdsen, PhD, Baltimore, MD (Abstract Co-Author) Research Grant, Siemens AG; Consultant, Siemens AG; Research Grant, Carestream Health, Inc; License agreement, Carestream Health, Inc; License agreement, Elekta AB; ; ;

Background

The ICRU/AAPM CT phantom was designed by AAPM Task Group 200 to implement the recommendations of TG111 for testing the radiation output of CT machines over all irradiation lengths L ; it is not limited to the single point at 100 mm determined using current CTDI methodology. It can also be employed over several types of CT platforms; however, there are situations where the results have to be carefully interpreted in order to avoid improper cross-platform comparisons.

Evaluation

For determining the rise to equilibrium function h (L) up to its limiting value, a small radiation detector is placed at the radial distance of interest in the central plane of the phantom. Two methods can be used: 1) integrated exposure is recorded for scans of varying length L for multi-detector CT (MDCT) or for collimations of varying width L for fixed-table platforms, symmetric about the longitudinal center of the phantom; 2) a single scan through the entire phantom while recording the exposure rate, dX / dt . Monte Carlo calculations have shown good agreement with measurement. Modifications to both methods have been used for measurements on interventional C-arms with CT reconstruction capability, including machines limited to sub 360° rotations.

Discussion

Helical scans using a narrow collimation and low pitch provide the high sampling frequency essential for the implementation of method 2 on multi-detector CT (MDCT) machines. Method 1 with L as the collimation width is often a better choice for C-arm CT. Also, with C-arm CT, the beam angle will often not intercept the entire diameter of the 30 cm phantom. Dose measurements are still meaningful since irradiation still occurs beyond the beam angle but the radial dose distribution will differ substantially near the edge of the phantom. A long phantom with smaller diameter would foster a more direct comparison between C-arm and MDCT.

Conclusion

The ICRU/AAPM phantom is a robust and flexible tool in determining h (L) with alternate measurement methods which show consistent results. For alternate platforms, there may be constraints not normally experienced in MDCT than need to be considered.

SSK16-04 Improving Staff Radiation Protection during Computed Tomography Using a Simple Traffic Light System

Wednesday, Dec. 2 11:00AM - 11:10AM Location: S404AB

Participants Christina Heilmaier, MD, Zurich, Switzerland (Presenter) Nothing to Disclose Niklaus Zuber, Zurich, Switzerland (Abstract Co-Author) Nothing to Disclose Andre Liebing, Zurich, Switzerland (Abstract Co-Author) Nothing to Disclose Dominik Weishaupt, MD, Zurich, Switzerland (Abstract Co-Author) Nothing to Disclose

PURPOSE

When scanning emergency and intensive-care patients medical staff frequently needs to remain in the scanner room to supervise patients during computed tomography (CT) scans. Often there is high uncertainty concerning staff's best position from a radiation protection perspective. The purpose was to establish a simple system, which helps medical staff to find the optimal position with regard to their own radiation protection.

METHOD AND MATERIALS

To provide guidance for staff we performed dose measurements (μ Gy/s) on different positions near the CT table using a portable dose detector. Based on these dose values we placed stickers with a diameter of 30 cm on different positions of the floor according to the traffic light system (red = worst position; orange = intermediate position; green = best position). Thereafter, we asked staff to provide evaluation of the new system using a 5-point-scale (1 = not true, 3 = undetermined, 5 = true).

RESULTS

Dose measurements yielded lowest radiation exposure of staff on the lateral part of the CT chassis (mean dose rate, 0.2 μ Gy/s) and highest values near the CT table close to the gantry (mean dose rate, 20.2 μ Gy/s). Intermediate dose rates were measured at the opposite end of the gantry and approximately 1.5 meters away from the table (mean rate, 1.9 μ Gy/s). Survey of 36 staff members revealed that overall judgment of the traffic light system was very positive (mean rating, 4.8). The majority of respondents tried to follow the stickers during the CT scan (mean rating, 4.6) and felt safer since the sticker were placed on the floor (mean rating, 4.5). However, some mentioned that it sometimes was impossible to stand in the green sticker as patient monitoring was limited. Evaluation of knowledge concerning best own position showed that many staff members had considerably misjudged their previous radiation exposure (mean rating of 'I already knew before where best position was', 3.4), which was especially evident in those with only few work experience (1-2 years; mean rating, 1.8).

CONCLUSION

From a radiation protection perspective best position of staff members is on the lateral part of CT chassis, while it is worst to stand near the table close to the gantry. By implementing a traffic light system staff protection and reassurance can be improved.

CLINICAL RELEVANCE/APPLICATION

A traffic light system helps staff members to find the best position during a CT scan to receive lowest possible radiation dose.

SSK16-05 Dose-splitting to Obtain Repeat Datasets of Varying Radiation Dose Levels without Repeat Acquisition: Methodology and Verification

Wednesday, Dec. 2 11:10AM - 11:20AM Location: S404AB

Participants

Daniele Marin, MD, Cary, NC (*Presenter*) Nothing to Disclose Juan Carlos Ramirez-Giraldo, PhD, Malvern, PA (*Abstract Co-Author*) Employee, Siemens AG Yakun Zhang, MS, Durham, NC (*Abstract Co-Author*) Nothing to Disclose Katharine Grant, PhD, Rochester, MN (*Abstract Co-Author*) Employee, Siemens AG Rendon C. Nelson, MD, Durham, NC (*Abstract Co-Author*) Consultant, General Electric Company Consultant, Nemoto Kyorindo Co, Ltd Consultant, VoxelMetrix, LLC Research support, Bracco Group Research support, Becton, Dickinson and Company Speakers Bureau, Siemens AG Royalties, Wolters Kluwer nv Ehsan Samei, PhD, Durham, NC (*Abstract Co-Author*) Nothing to Disclose Achille Mileto, MD, Durham, NC (*Abstract Co-Author*) Nothing to Disclose Alex Bibbey, MD, Durham, NC (*Abstract Co-Author*) Nothing to Disclose

PURPOSE

To develop and validate a methodology for precise and accurate comparison of three distinct radiation dose levels from a single MDCT acquisition

METHOD AND MATERIALS

The ACR CT accreditation phantom (Gammex 464) was scanned using a third-generation dual-source MDCT platform (Somatom Definition FORCE). The scanner was equipped with a prototype research scan mode that allows user-defined partitioning of the radiation dose between the two x-ray tubes (A and B) by independently selecting the milliamperage value of each tube when operating in the dual-source (DS) mode. All scans were performed using both single-source (SS) and DS acquisitions, at constant 120 kVp. For each DS acquisition, three radiation dose levels were reconstructed using the projection data of each radiation tube alone (A or B) or the two tubes combined (A + B). Six different dose levels were obtained for each acquisition mode, including (a) 200, 150, 100, 75, 50, and 25 mAs for SS and (b) 200 mAs (A = 150; B = 50 mAs) and 100 mAs (A = 75; B = 25 mAs) for DS acquisitions. Objective assessment of image quality was performed and compared between the SS and DS acquisitions. Analysis included evaluation of first order image quality metrics (noise, contrast, and CNR) as well as a more comprehensive detectability index, which accounts for the impact of noise, noise power spectrum (NPS), contrast, contrast-dependent task transfer function (TTF), task definition, and eye filter. Radiation dose data were also collected (CTDIvol, DLP).

RESULTS

For equal radiation dose levels, there was no significant difference between SS and DS acquisitions for measured image quality metrics, including noise (average difference, 1.4%; range, 0.2-3.2%), contrast (7.3%; 0.8-12.4%), and CNR (7.4%; 2.0-12.6). Differences between SS and DS were even smaller for the detectability index (0.7%; 0.1-2.3%). NPS and TTF curves for SS and DS acquisitions showed nearly perfect overlap for all radiation dose levels.

CONCLUSION

DS single-energy MDCT platform can precisely and accurately reconstruct datasets at different radiation dose levels from the projection data acquired of each radiation tube by itself or in combination with the second radiation tube.

CLINICAL RELEVANCE/APPLICATION

A reliable strategy to simultaneously obtain three dose levels from a single, dose-neutral, MDCT acquisition can overcome the

practical and ethical challenge of obtaining multiple dose levels from the same patient.

SSK16-06 RIS-integrated Dose Monitoring System: First Optimization Results for a Breast Screening Program on a Large Dataset of FFDM and DBT Exams

Wednesday, Dec. 2 11:20AM - 11:30AM Location: S404AB

Participants

Andrea Nitrosi, PhD, Reggio Emilia, Italy (*Presenter*) Nothing to Disclose Marco Bertolini, Reggio Emilia, Italy (*Abstract Co-Author*) Nothing to Disclose Cinzia Campari, Reggio Emilia, Italy (*Abstract Co-Author*) Nothing to Disclose Roberto Sghedoni, PhD, Reggio Emilia, Italy (*Abstract Co-Author*) Nothing to Disclose Pierpaolo Pattacini, Reggio Emilia, Italy (*Abstract Co-Author*) Nothing to Disclose Vladimiro Ginocchi, Reggio Emilia, Italy (*Abstract Co-Author*) Nothing to Disclose Lorenzo Ghiddi, Reggio Emilia, Italy (*Abstract Co-Author*) Nothing to Disclose Giulio Tondelli, Correggio, Italy (*Abstract Co-Author*) Nothing to Disclose Valentina Iotti, MD, Reggio Emilia, Italy (*Abstract Co-Author*) Nothing to Disclose Rita Vacondio, Reggio Emilia, Italy (*Abstract Co-Author*) Nothing to Disclose Mauro Iori, Reggio Emilia, Italy (*Abstract Co-Author*) Nothing to Disclose

PURPOSE

To show how a RIS-integrated dose monitoring systems can reduce variability of acquisition settings optimizing dose-image quality ratio in a population based breast screening program (BSP).

METHOD AND MATERIALS

Our Diagnostic Imaging Department (DID) adopted a RIS-PACS integrateddose monitoring system. For mammography, the average glandular dose (AGD), compression level, breast thickness and glandularity, as well as the selected automatic exposure control (AOP) mode (for FFDM one among three with increasing dose levels labelled as "dose", "standard" and "contrast", for DBT a single dose level called "tomo" are available) are registered for each projection. The DID BSP monitors about 55,000 examinations/year from eleven mammography units equally configured. To date we collected data from more than 500,000 mammographic exposures and more than 15,000 DBT ones.. AGD dependency on the compression force and the selected AOP has been verified. The compression force (at least 100N) and the FFDM AOP selection ("dose" mode) were standardized among the radiographers.

RESULTS

After standardization FFDM AGD variability decreased from 60% to 28% and the overall median AGD decreased from 1.38 to 1.22 mGy. For FFDM AOP dose, standard and contrast the median AGD (mGy) [25th percentile, 75th percentile] were respectively 1.18 [1.06, 1.37], 1.51 [1.35, 1.77], 1.85 [1.72, 2.05] while for DBT AOP tomo were 1.61 [1.44, 1.85]. The breast compressed thickness median both for FFDM and DBT was 53 mm, while the median glandularity calculated by the mammographic unit were respectively 40% and 20%.

CONCLUSION

It has been verified that AGD is highly dependent on the AOP mode selectd for FFDM and on the compression force both for FFDM and DBT. The glandularity evaluation is quite different between FFDM and DBT. This element probably impacts on AGD calculations.

CLINICAL RELEVANCE/APPLICATION

The iterative application of monitoring processes and integration with information systems like RIS for the qualification of image quality-dose ratio, may improve clinical quality performance in diagnostic imaging.

SSK16-07 Effects on Radiation Exposure and Image Quality of Abdominal CT with Attenuation-based Automatic Kilovoltage Selection

Wednesday, Dec. 2 11:30AM - 11:40AM Location: S404AB

Participants ShuTing Wang, Shenyang, China (*Abstract Co-Author*) Nothing to Disclose Ke Ren, MD, ShenYang, China (*Abstract Co-Author*) Nothing to Disclose Long Cui, MD, PhD, Shenyang, China (*Presenter*) Nothing to Disclose

PURPOSE

To compare the radiation dose and image quality between standard-dose CT and a low-dose CT obtained with the combined use of an attenuation-based automatic kilovoltage (kV) selection tool (kV Assist) and adaptive statistical iterative reconstruction (ASiR) for abdominal CT examination of adults with small or medium body size.

METHOD AND MATERIALS

Sixty consecutive patients with body mass index (BMI) below 26kg/m2 underwent abdominal contrast-enhanced CT(GE Discovery CT750 HD). Patients were divided into two groups, Automated adaption of both tube potential and tube current in group A (n=30) and with fixed 120 kV in group B(n=30).Data of two groups were reprocessed with 50% and 30%ASiR,respectively. CTDIvol and DLP were recorded and the effective dose(ED)was calculated. The objective image quality was assessed in both arterial phase and portal venous phase. Signal-to-noise ratio(SNR), contrast-to-noise ratio (CNR) of various tissues were calculated. The subjective image quality was assessed by two blinded and independent observers with a 5-point scale (1=non diagnostic; 5=excellent).

RESULTS

KV Assist protocol in group A resulted in a kV-decline from 120 to 100 kV in 20patients (66.67%) and to 80 kV in 10patients(33.33%). Overall CTDIvol (mGy), DLP(mGy·cm) and ED (mSv) of group A were significantly lower than in group B (21.85 \pm 7.19 vs. 36.91 \pm 8.43 mGy; 1099.48 \pm 379.72vs.1854.38 \pm 455.28 mGy·cm; 16.49 \pm 5.70vs. 27.82 \pm 6.83 mSv ;p<0.001), with a dose reduction of 40.80% (15.06/36.91), 40.71%(754.90/1854.38) and 40.73%(11.33/27.82), respectively. Although the noise was slightly higher in group A (13.60 \pm 1.74 vs. 12.27 \pm 1.73 HU in arterial phase while 13.92 \pm 2.11vs. 12.66 \pm 2.35 HU in portal venous phase; p<0.05), the SNRs and CNRs were similar to or even higher than that of standard 120-kV protocol. No significant differences

in subjective image quality (4.42 ± 0.64 vs. 4.67 ± 0.48 , p=0.127) were observed. The inter-observer consistency for subjective image quality was good(k=0.71).

CONCLUSION

The kV Assist protocol was demonstrated to be applicable in clinical routine of abdominal CT examinations for adults of small or medium body size which can reduced radiation dose while preserving image quality.

CLINICAL RELEVANCE/APPLICATION

Combined use of kV Assist and ASiR allowed a significant reduction in radiation exposure while maintaining image quality in abdominal CT.

SSK16-08 Does Body Mass Index (BMI) Outperform Body Weight as a Surrogate Parameter for Size Specific Dose Estimates (SSDE) in Adult Patients?

Wednesday, Dec. 2 11:40AM - 11:50AM Location: S404AB

Participants

Johannes Boos, MD, Boston, MA (*Abstract Co-Author*) Nothing to Disclose Rotem S. Lanzman, MD, Duesseldorf, Germany (*Abstract Co-Author*) Nothing to Disclose Christoph Schleich, Dusseldorf, Germany (*Abstract Co-Author*) Nothing to Disclose Patric Kroepil, MD, Duesseldorf, Germany (*Abstract Co-Author*) Nothing to Disclose Gerald Antoch, MD, Duesseldorf, Germany (*Abstract Co-Author*) Nothing to Disclose Christoph K. Thomas, MD, Dusseldorf, Germany (*Presenter*) Speaker, Siemens AG

PURPOSE

Body weight has been proposed as a comprehensive alternative to surrogate size specific dose estimates (SSDE). The aim of this study was to assess the value of the body mass index (BMI) in comparison to body weight as a surrogate parameter for SSDE in abdominal and chest CT of adult patients.

METHOD AND MATERIALS

211 patients (83 female, 128 male, mean age 61.6 ± 14.0 years) undergoing CT examinations of the chest (n=105) or abdomen (n=106) were included in this retrospective study. Weight and size of the patient at the time of the examinations were used to calculate the BMI (weight/size²). Effective diameter (Deff) was assessed performing diameter measurements in the axial midvolume CT-slice. Correlation between BMI, weight and effective diameter was calculated. SSDE were calculated based on Deff, weight and BMI.

RESULTS

Mean size, weight and BMI were 172.7 \pm 10.0cm, 80.2 \pm 19.9kg and 26.8 \pm 5.6kg/cm2, respectively. Mean lateral diameter, a.p. diameter and Deff were 35.9 \pm 4.9, 28.9 \pm 4.4 and 30.4 \pm 4.4, respectively. There was a significant correlation between BMI and Deff (r=0.82) as well as weight and Deff (r=0.82) (p<0.05 respectively). SSDE calculation based on BMI matched SSDE based on Deff (7.3 \pm 2.7mGy vs 7.3 \pm 2.7mGy), while SSDE calculation based on body weight led to a difference of 7% (7.8 \pm 4.4mGy, p>0.05). BMI showed a better correlation with Deff than body weight for abdominal CT (r=0.87 vs 0.84) while correlation was inferior for chest CT (r=0.76 vs 0.82).

CONCLUSION

SSDE based on BMI do not differ significantly from SSDE based on diameter measurements in thoracoabdominal CT and can be used to simplify the SSDE method. Furthermore, BMI is superior to body weight as a surrogate parameter for SSDE in abdominal CT of adult patients.

CLINICAL RELEVANCE/APPLICATION

BMI can be used as a surrogate for SSDE. Thereby, BMI can lead to relevant simplification of the SSDE method, especially in large scale register analysis.

SSK16-09 Body Mass Index Based GSI Assist in Abdominal CT: Investigation of Radiation Dose and Image Noise

Wednesday, Dec. 2 11:50AM - 12:00PM Location: S404AB

Participants

Chai Y. Ru III, MD, Zhengzhou, China (*Presenter*) Nothing to Disclose Jianbo Gao, MD, Zhengzhou, China (*Abstract Co-Author*) Nothing to Disclose Peijie Lv, MMed, Zhengzhou, China (*Abstract Co-Author*) Nothing to Disclose

PURPOSE

To investigate the radiation dose and image noise of spectral CT imaging with gemstone spectral imaging(GSI) assist in abdominal CT based on the body mass index(BMI) compared with conventional CT scan

METHOD AND MATERIALS

This study received institutional review board approval, and all participants provided written informed consent. 68 patients underwent CT plain scan with the conventional mode of 120 kVp and enhanced CT with spectral imaging mode in arterial phase (AP) and venous phase(VP). The optimal spectral imaging parameters were automatically selected with GSI assist on. 65 keV monochromatic images in venous phase were reconstructed and compared with plain CT images. All patients were divided into four groups according to BMI(group A,n=12:BMI <18.5 kg/m2; group B,n=28:BMI 18.5~23.9 kg/m2; group C,n=19:BMI 24~28.9 kg/m2; group D,n=9:BMI \geq 29 kg/m2). Image noise of liver, muscle and abdominal subcutaneous fat was measured, and volume CT dose index(CTDIvol) and effective dose(ED) were recorded among the four groups. Difference of radiation dose and image noise between the two scanning modes in each group were compared using paired t-test.

Between the conventional mode and spectral CT with GSI assist mode for all patients, the CTDIvol and ED showed no significant differences(P=0.071,0.059), while the image noise of liver, muscle and fat had significant differences(all P<0.001). In group A, the CTDIvol, ED and image noise of liver, muscle and fat for GSI assist mode were lower than conventional mode (all P<0.001). The CTDIvol and ED had no significant difference between the two scanning mode in group B(P=0.058,0.077) and group C(P=0.073,0.059), but higher for the GSI assist mode in group D(both P<0.001). Image noise of liver, muscle and fat in group B, C and D for GSI assist mode were all lower than conventional CT mode(all P<0.001) except for the image noise of fat in group D(P=0.055).

CONCLUSION

GSI assist scanning mode can reduce radiation dose in patients with BMI under 18.5 kg/m2 without sacrificing image quality and can reduce image noise in patients with BMI range between 24kg/m2 and 28.9 kg/m2 in equivalent radiation dose.

CLINICAL RELEVANCE/APPLICATION

Within a certain BMI range, GSI assist scan mode can reduce radiation dose or image noise, and is recommended clinical application for its easy operation.

Chest (Emphysema)

Wednesday, Dec. 2 10:30AM - 12:00PM Location: S404CD



AMA PRA Category 1 Credits ™: 1.50 ARRT Category A+ Credits: 1.50

FDA Discussions may include off-label uses.

Participants

Brett M. Elicker, MD, San Francisco, CA (*Moderator*) Nothing to Disclose Santiago E. Rossi, MD, Capital Federal, Argentina (*Moderator*) Advisory Board, Koninklijke Philips NV Speaker, Pfizer Inc Royalties, Springer Science+Business Media Deutschland GmbH

Sub-Events

SSK05-01 A New Subtype of COPD in Cigarette Smokers

Wednesday, Dec. 2 10:30AM - 10:40AM Location: S404CD

Participants

David A. Lynch, MBBCh, Denver, CO (*Presenter*) Research support, Siemens AG; Scientific Advisor, PAREXEL International Corporation; Consultant, Boehringer Ingelheim GmbH; Consultant, Gilead Sciences, Inc; Consultant, F. Hoffmann-La Roche Ltd; Consultant, Veracyte, Inc;

Carla G. Wilson, Denver, CO (*Abstract Co-Author*) Nothing to Disclose Mustafa Al Qaisi, MD, Denver, CO (*Abstract Co-Author*) Nothing to Disclose Teresa Gray, Denver, CO (*Abstract Co-Author*) Nothing to Disclose Stephen Humphries, Denver, CO (*Abstract Co-Author*) Nothing to Disclose James D. Crapo, MD, Denver, CO (*Abstract Co-Author*) Nothing to Disclose

PURPOSE

Although quantitative CT measurement of % low attenuation areas less than -950 HU (%LAA-950) is commonly used as a surrogate for emphysema, there is a subgroup of patients who meet quantitative criteria for emphysema, but who do not have visual evidence of emphysema. The purpose of this study was to determine the demographic and physiologic features of this discordant group, compared with a control group that did not have either visual or quantitative evidence of emphysema.

METHOD AND MATERIALS

2099 cigarette smokers enrolled in the COPDGene study underwent visual analysis by two trained research analysts, according to the Fleischner Society categorization of emphysema. From this group, we selected all subjects who had quantitative evidence of emphysema (%LAA-950>5%) but did not have visual evidence of emphysema (n=165). The control group comprised subjects with no visual or quantitative CT evidence of emphysema (n=677). All subjects underwent inspiratory and expiratory CT evaluation, with quantitative CT metrics. Expiratory air trapping was assessed quantitatively by measuring the % LAA <856 HU on expiration. Followup spirometry was obtained 5 years after the initial CT in 128 discordant subjects and in 448 controls. Differences between groups were evaluated using Chi-Square and Student t test as appropriate.

RESULTS

Kappa value for presence or absence of emphysema was 0.84. Compared with the control group, the discordant group were older (mean \pm s.d. 62 \pm 9 vs 59 \pm 9 years, p=0.0001), more likely to be male (63% vs 38%, p<0.0001), and less likely to be African American (5% vs 21% p<0.0001). Although the FEV1 % at baseline was similar in the two groups, the FEV1/FVC ratio was significantly lower in the discordant group (0.71 \pm .10 vs 0.77 \pm .07 p<0.0001). On quantitative expiratory CT, the %LAA-856 was 23 \pm 12 % in the discordant group compared with 11 \pm 9% in the controls (p<0.0001). On 5 year followup, the mean decrease in FEV1 in the discordant group was 241 \pm 271 ml, compared with 178 \pm 259 ml in the control group (p=0.018).

CONCLUSION

Even in the absence of visual emphysema, quantitative CT densitometry identifies a subgroup of smokers with evidence of airway obstruction, who demonstrate progression in airway obstruction over time.

CLINICAL RELEVANCE/APPLICATION

The high proportion of LAA-950 in the discordant group may be due to sub-resolution emphysema (perhaps panlobular), or to lobular overinflation related to small airways abnormality.

SSK05-02 Optimal Threshold for Quantification of Air-trapping Using Non-Rigid Image Registration of Inspiration/Expiration CT Scans in COPD

Wednesday, Dec. 2 10:40AM - 10:50AM Location: S404CD

Participants

Sang Min Lee, Seoul, Korea, Republic Of (*Presenter*) Nothing to Disclose Joon Beom Seo, MD, PhD, Seoul, Korea, Republic Of (*Abstract Co-Author*) Nothing to Disclose Sang Min Lee, MD, Seoul, Korea, Republic Of (*Abstract Co-Author*) Nothing to Disclose Namkug Kim, PhD, Seoul, Korea, Republic Of (*Abstract Co-Author*) Stockholder, Coreline Soft, Inc Sang Young Oh, MD, Seoul, Korea, Republic Of (*Abstract Co-Author*) Nothing to Disclose Yeon-Mok Oh, MD, PhD, Seoul, Korea, Republic Of (*Abstract Co-Author*) Nothing to Disclose

PURPOSE

I o restrospectively investigate the optimal threshold for quantification of air-trapping using non-rigid registration of inspiration and expiration CT scans in COPD patients in correlation with FEF25-75% and RV/TLC

METHOD AND MATERIALS

Institutional review board approval was obtained. From June 2005 to October 2010, 195 patients (166 COPD patients, 29 nonsmoker control) were included in our study. Inspiration and expiration CT scans were performed in the same CT scanner followed by non-rigid registration using an in-house software. Subtraction value per voxel between inspiration and registered expiration CT was obtained and volume fraction of air-trapping (air-trapping index, ATI), using variable thresholds (from 30 to 120 HU), was calculated. Calculated ATI using variable thresholds, expiration/inspiration ratio of mean lung density (E/I MLD), and the percent of lung voxels below -856HU on expiration CT (gas-trapping index, Exp -856) were correlated with pulmonary function parameters for small airway disease or air-trapping (FEF25-75% and RV/TLC).

RESULTS

All of ATI with variable thresholds were significantly correlated with both FEF25-75% and RV/TLC (all P<0.001). When correlated with FEF25-75%, the highest correlation coefficient was -0.656, using the threshold of 80HU. As for RV/TLC, as threshold increased, the correlation coefficient decreased. The highest correlation coefficient was 0.664, using the threshold of 30HU. When plotting the relation between subtraction thresholds and FEF25-75% and RV/TLC, threshold of 60 HU was suitable (r= -0.649 and 0.651, respectively). Those correlation coefficients were comparable to the results with E/I MLD (r= -0.670 and 0.657 for FEF25-75% and RV/TLC, respectively) and Exp -856 (r= -0.604 and 0.565 for FEF25-75% and RV/TLC, respectively). When the optimal threshold of 60HU was applied, the measured ATI of 23 nonsmoker normal controls and COPD patients were 24.2% \pm 16.8 and 65.7% \pm 17.7 (P<0.001).

CONCLUSION

Optimal threshold for quantification of air-trapping using non-rigid registration of inspiration and expiration CT scans in COPD patients is 60 HU with significant correlation with FEF25-75% and RV/TLC, and is comparable to E/I MLD and Exp -856.

CLINICAL RELEVANCE/APPLICATION

Quantification of air-trapping using optimal subtraction threshold of 60 HU using non-rigid image registration of inspiration and expiration CT scans may be useful in assessing small airway dysfunction in COPD patients.

SSK05-03 Impact of Endobronchial Coiling on Segmental Bronchial Lumen in Treated and Untreated Lung Lobes: Correlation with Changes in Lung Volume, Clinical and Pulmonary Functional Tests

Wednesday, Dec. 2 10:50AM - 11:00AM Location: S404CD

Participants

Christopher Kloth, Tuebingen, Germany (*Abstract Co-Author*) Nothing to Disclose Wolfgang M. Thaiss, MD, Tuebingen, Germany (*Abstract Co-Author*) Nothing to Disclose Hendrik Ditt, Forchheim, Germany (*Abstract Co-Author*) Employee, Siemens AG Juergen Hetzel, Tuebingen, Germany (*Abstract Co-Author*) Nothing to Disclose Konstantin Nikolaou, MD, Tuebingen, Germany (*Abstract Co-Author*) Nothing to Disclose Speakers Bureau, Bayer AG Marius Horger, MD, Tuebingen, Germany (*Presenter*) Nothing to Disclose

PURPOSE

To assess the impact of endobronchial coiling on crossectional area of segment bronchi and corresponding lobe volumes both at end-inspiration and end-expiration in patients with chronic obstructive lung disease (COLD) grade IV (GOLD) by using quantitative chest-CT.

METHOD AND MATERIALS

From January 2010 to December 2014 30 patients (female=15, median age=65.36y; range 48-76y) underwent chest-CT both before and after endobronchial coiling for lung volume reduction (LVR). Two thin-slice (0.6mm) non-enhanced image data sets were acquired both at end-inspiration and end-expiration. Clinical response was defined as an increase in the walking distance (6MWT) after LVR-therapy. Additionally, we used also PFT measurements with forced expiratory volume in 1 second (FEV1), ratio of residual volume over total lung capacity (RV/TLC) and single-breath diffusion capacity for carbon monoxide (DLCOSB) for correlation

RESULTS

In the treated segment bronchi, the cross-sectional area of the lumen showed a significant reduction (p<0.05) in inspiration and a tendency to an increased lumen in expiration (p>0.05). In the other ipsilateral lobe, the segment bronchial lumens showed no significant changes. In the contralateral lung, we found at inspiration a strong tendency towards an increased lumen (p=0.06). The lung volumes of the treated lobes directly correlated with the treated segment bronchial lumen in expiration (r = 0.80, p < 0.001). Clinical correlation with 6 minutes walking test (6MWT) and pulmonary function test (PFT) showed only in responders a statistically significant decrease of volume in the treated lobe. Responders showed a increase of the 6 MWT (p < 0.0001) and non-responders a significant decrease of the 6MWT (p < 0.0078). The responder subgroup showed an increase of FEV1, TLC and VC however not statistically significant

CONCLUSION

Endobronchial coiling causes a significant decrease in the crossectional area of treated segmental bronchi in inspiration and also a slight increase in expiration accompanied by a volume reduction whereas in the non-treated lung lobes a slightly opposite tendency was observed. 6MWT and PFT minimally, but statistically significant improved after LVR.

CLINICAL RELEVANCE/APPLICATION

Our data support the current understanding of coiling effects which claim that they stabilize and stiffen the lung parenchyma thus compensating for the loss of elasticity in the interstitium and reducing bronchial motility/collapsing.

SSK05-04 Lung Morphology Assessment of Cystic Fibrosis Using Non Contrast Proton MRI with Submillimeter Details at 1.5 Tesla

Awards

Trainee Research Prize - Medical Student

Participants

Gael Dournes, MD, PhD, Pessac, France (*Presenter*) Nothing to Disclose Julie Macey, Bordeaux, France (*Abstract Co-Author*) Nothing to Disclose Fanny Menut, Bordeaux, France (*Abstract Co-Author*) Nothing to Disclose Marjorie Salel, Bordeaux, France (*Abstract Co-Author*) Nothing to Disclose Michel Montaudon, MD, Pessac, France (*Abstract Co-Author*) Nothing to Disclose Olivier Corneloup, MD, Bordeaux, France (*Abstract Co-Author*) Nothing to Disclose Valerie Latrabe, MD, Pessac, France (*Abstract Co-Author*) Nothing to Disclose Hubert Cochet, MD, Pessac, France (*Abstract Co-Author*) Nothing to Disclose Jean Francois Chateil, MD, Bourdeaux, France (*Abstract Co-Author*) Nothing to Disclose Michael Fayon, Bordeaux, France (*Abstract Co-Author*) Nothing to Disclose Patrick Berger, MD, PhD, Bordeaux, France (*Abstract Co-Author*) Nothing to Disclose Francois H. Laurent, MD, Pessac, France (*Abstract Co-Author*) Nothing to Disclose

PURPOSE

The aim of the study was to assess the concordance between CT and non-contrast proton MRI for evaluation of structural cystic fibrosis (CF) changes using a respiratory-gated PETRA, a T1-VIBE and a T2-HASTE sequences.

METHOD AND MATERIALS

All consecutive CF patients under stable condition were enrolled from July 2014 to January 2015 in a single institution. All patients or their parents gave written informed consent. Patients had to complete both CT and MRI the same day. The Helbich-Bhalla score was used to assess CF severity. Concordance between CT and MRI was assessed using intraclass correlation coefficient (ICC) and Bland-Altman analysis. Intra and inter-observer reproducibility were assessed.

RESULTS

24 CF patients were enrolled (mean age=22.6 \pm 9.6, ranging from 9 to 48-year-old). Mean Helbich-Bhalla score at CT was 13.6 \pm 5.5. The concordance in overall Helbich-Bhalla score was very good using PETRA (ICC=0.99) while it was found good using VIBE and HASTE sequences (ICC=0.69 and 0.62, respectively). Bland-Altman plots showed that agreement between CT and PETRA was independent from the magnitude of score (mean difference (MD =-0.3 [-1.7; 1.3]), whereas there was systematic underestimation using VIBE (MD=-4.9 [-0.5; -9.3] and HASTE (MD=-5.6 [-0.4; -10.9]). Intra and interobserver reproducibility were very good for the whole imaging modalities (ICC=0.86-0.98).

CONCLUSION

In this pilot study, the Helbich-Bhalla score using PETRA matched closely with that of CT and showed higher level of concordance than either conventional T1-weighted or T2-weighted sequences. Further improvement in respiratory synchronization and acquisition time are expected, whereas future combination with functional information is warranted.

CLINICAL RELEVANCE/APPLICATION

Implication for patient care - PETRA is a clinically available sequence which provides assessment of lung structural-CF alterations with submillimeter details - Using lung MRI, non-invasive structural assessment of CF may no longer be restricted due to radiation concern for routine follow-up or under treatment.

SSK05-05 Different Progression of CT Defined Emphysema Depending of Trends in Smoking Habit in the ITALUNG Screening Trial

Wednesday, Dec. 2 11:10AM - 11:20AM Location: S404CD

Participants

Chiara Romei, Pisa, Italy (*Presenter*) Nothing to Disclose Barbara Conti, Pisa, Italy (*Abstract Co-Author*) Nothing to Disclose Laura Carrozzi, Pisa, Italy (*Abstract Co-Author*) Nothing to Disclose Franscesca Carozzi, Firenze, Italy (*Abstract Co-Author*) Nothing to Disclose Antonio Palla, Pisa, Italy (*Abstract Co-Author*) Nothing to Disclose Fabio Falaschi, MD, Pisa, Italy (*Abstract Co-Author*) Nothing to Disclose

PURPOSE

To evaluate with low dose computed tomography (LDCT) densitometric analysis, changes in pulmonary emphysema over 2 years, in subjects with different trends in smoking habit enrolled in the ITALUNG trial of lung cancer screening.

METHOD AND MATERIALS

284 subjects (male 69.7%; mean age 60.2±4.2) enrolled in the active arm of ITALUNG trial of lung cancer screening underwent to LDCT esamination at first (T1) and third (T3) annual screening round.LDCT evaluated parameters were: total lung volume (ml); % of Relative Areas (RA) at -910, -950, -960 Hounsfield Units (HU); 15th percentile density (PD15, g/L). Lung function tests (VC, FVC, FEV1, FEV1/VC, FEV1/FVC, FRC, RV, TLC, RV/TLC and DLCO) were performed.Four subgroups were identified based on the trends in smoking habit during the 2 years of follow-up: persistent current smokers, former smokers, quitters and re-starter. A predictive model for longitudinal variation of CT parameters during the study was applied, considering as independent variables: age, sex, smoking variation, lung function tests and total lung volume.

RESULTS

Longitudinally, an increase of the median value of %RA was observed: %RA-960 = 9.8 at T1 and 10.2 at T3, (p<.0001); %RA-950=13 at T1 and 13.5 at T3 (p<.0001); %RA-910=29.2 at T1 and 29.5 at T3 (p<.0003).On the contrary, PD15 g/l decreased (33.4 at T1 and 30 at T3, p<.0001). No functional tests and diffusion capacity demonstrated significant evolution in the 2 years of follow-up except FEV1/FVC (p=0.031).In the 142 current smokers, in the 93 former smokers and in the 42 quitters PD15 g/l

decreased respectively from 38.2 ± 20 at T1 to 39.21 ± 17.4 at T3 (p<.00504), from 24.2 ± 21.5 at T1 to 20 ± 18.6 at T3 (p=0.0063), from 36.6 ± 12.4 at T1 to 26.8 ± 16.2 al T3 (p<.0001). On the contrary in the 7 re-starter PD15 g/l increased without statistical relevance (38.6 ± 23.4 at T1 and 48.4 ± 18.6 at T3, p=0.1897).

CONCLUSION

LDCT densitometric analysis allows a short-term evaluation of progression of pulmonary emphysema in screened subjects. The different trends in smoking habit during the follow-up seems to independently determine the lung density change with the major decrease in quitters and former smokers, possibly dependent to the absence of inflammatory smoking induced effects.

CLINICAL RELEVANCE/APPLICATION

The short-term progression of emphysema can be evaluated by LDCT analysis in asymptomatic subjects and differ depending of trends in smoking habit in the period of follow-up.

SSK05-06 Assessment of Healthy Volunteers with COPD High Risk Factors by Quantitative CT: Correlation with Pulmonary Functional Tests

Wednesday, Dec. 2 11:20AM - 11:30AM Location: S404CD

Participants

Yi Xia, MD, Shanghai, China (*Presenter*) Nothing to Disclose Yu Guan, MD, Shanghai, China (*Abstract Co-Author*) Nothing to Disclose Li Fan, Shanghai, China (*Abstract Co-Author*) Nothing to Disclose Shiyuan Liu, PhD, Shanghai, China (*Abstract Co-Author*) Nothing to Disclose

PURPOSE

To investigate the association of quantitative CT (QCT) with spirometric measurements in healthy volunteers with COPD high risk factors between non-smoking group and smoking group.

METHOD AND MATERIALS

Seventy-four healthy volunteers were examined by PFT, inspiratory and expiratory CT. Inclusion criteria: 1. age>45y; 2. cigarette>10 pack*year; or chronic cough,sputum or dyspnea symptom; or emphysema on CT; 3. spirometry: FEV1%pred<95% and FEV1/FVC>70%; 4. informed consent acquired. The subjects were classified into 2 groups: non-smoking group(n=40) and smoking group(n=34). QCT parameters contained trachea volume, total lung volume (TLV) and emphysema index of threshold of lung area with attenuation lower than -950 HU (EI-950) on inspiratory CT; air trapping, defined as the percentage of attenuation area lower than -856 HU (LAA-856) on expiratory CT. To evaluate the correlation between QCT parameters and PFT values, Spearman correlation analysis was used. Compare the difference between non-smoking group and smoking group, t-test was used.

RESULTS

The TLV showed good correlation with FEV1, FVC and TLC(r=0.575, P<0.001;r=0.590, P<0.001;r=0.714, P<0.001)for all subjects. For non-smoking group, there were strong correlation between TLV and FEV1, FVC, TLC(r=0.498, P=0.001;r=0.580, P<0.001;r=0.757, P<0.001). However, there was no correlation between TLV and FEV1, FVC for smoking group. In addition, there was a correlation between total lung capacity (TLC) and EI-950 (r=0.236, P=0.043), between TLC and LAA-856 (r=0.265, P=0.026), respectively. For non-smoking group, the TLC had strong correlation with LAA-856(r=0.526, P=0.001); But, there was no statistical difference between TLC and EI-950 or LAA-856 for smoking group. Compared with smoking group, TLV (4.79±0.98 L vs. 3.75±1.06 L) and trachea volume(62.3±13 cm3 vs.43.3±18 cm3) were reduced significantly in non-smoking group. Smoking group [(2.69±0.33) L and (3.51±0.45) L] showed higher FEV1 and FVC vs. non-smoking group[(2.28±0.52)L and 2.95±0.69](P<0.001).

CONCLUSION

There were different correlations and features between PFT and CT volume in non-smoking group and smoking group for subjects with COPD high risk factors.

CLINICAL RELEVANCE/APPLICATION

Assessment of healthy volunteers with COPD high risk factors by QCT indicate that non-smoking group and smoking group have different features, which could guide clinical management.

SSK05-07 The Airway Remodelling and Emphysema Alteration as Determined by Quantitative CT Measurement: Correlations with the Frequency of COPD Exacerbation

Wednesday, Dec. 2 11:30AM - 11:40AM Location: S404CD

Participants

Yu Guan, MD, Shanghai, China (*Presenter*) Nothing to Disclose Li Fan, Shanghai, China (*Abstract Co-Author*) Nothing to Disclose Yi Xia, MD, Shanghai, China (*Abstract Co-Author*) Nothing to Disclose Shiyuan Liu, PhD, Shanghai, China (*Abstract Co-Author*) Nothing to Disclose

PURPOSE

We aimed to evaluate the change of airway remodelling and emphysema in COPD exacerbations as determined by quantitative CT measurement. We aslo study the relationship between COPD exacerbation frequency and quantitative CT measures of airway remodelling and emphysema.

METHOD AND MATERIALS

Volumetric CT was acquired for 80 patients who visited the emerency department for AECOPD. All images were reconstructed with 1mm slice and retrospectively analyzed using a software program with fully-automated 3D airway extraction and emphysema analysis. Total lung emphysema index were calculated automatically at the threshold of -950HU. Airway parameters including wall thickness(WT), luminal diameter(LD) and wall area percentage(WA%) were measured in the six segmetal bronchus as follows, RB1, RB4, RB10, LB1 and LB10. The frequency of COPD exacerbation in the prior year was determined by using a questionnaire.Statistical analysis was performed to examine evaluate the change of airway remodelling and emphysema in COPD exacerbations and the relationship of exacerbation frequency with quantitative CT measurements.

RESULTS

Emphysema index alteration was not influenced by the frequency of COPD exacerbation in the same patient. There was no significant correlations between emphysema index alteration and COPD exacerbation frequency(r=0.46, P=0.06). However, the wall area percentage(WA%) and wall thickness(WT) were measured in the six segmetal bronchus were associated with COPD exacerbation frequency(r=0.74, P=0.02; r=0.65, p=0.03, respectively). No significant correlations was found between luminal diameter(LD) and COPD exacerbation frequency(r=0.53, P=0.08).

CONCLUSION

Quantitative CT can identify the change of airway remodelling and emphysema index in COPD exacerbations. The small airway alterlation was associated with COPD exacerbations frequency.

CLINICAL RELEVANCE/APPLICATION

Quantitative CT can identify the change of small airway and emphysema of COPD exacerbations which may contributed to individual treatment.

SSK05-08 Meta-analysis of Repeatability of CT Lung Density Measures

Wednesday, Dec. 2 11:40AM - 11:50AM Location: S404CD

Participants

Sean B. Fain, PhD, Madison, WI (*Presenter*) Research Grant, General Electric Company Research Consultant, Marvel Medtech, LLC Heather Chen-Mayer, PhD, Gaithersburg, MD (*Abstract Co-Author*) Nothing to Disclose
Alfonso Rodriguez JR, MS, Madison, WI (*Abstract Co-Author*) Nothing to Disclose
Jered Sieren, Coralville, IA (*Abstract Co-Author*) Consultant, Vida Diagnostics, Inc
Matthew K. Fuld, PhD, Iowa City, IA (*Abstract Co-Author*) Researcher, Siemens AG
Bernice E. Hoppel, PhD, Vernon Hills, IL (*Abstract Co-Author*) Research support, Siemens AG; Scientific Advisor, PAREXEL International
Corporation; Consultant, Boehringer Ingelheim GmbH; Consultant, Gilead Sciences, Inc; Consultant, F. Hoffmann-La Roche Ltd;
Consultant, Veracyte, Inc;
Frank N. Ranallo, PhD, Madison, WI (*Abstract Co-Author*) Nothing to Disclose

PURPOSE

To determine the clinically relevant change of lung density CT metrics.

METHOD AND MATERIALS

The most established measures of lung parenchymal density are "RA950" and "Perc15". The RA950 is defined here as the relative lung area (or lung voxels) at total lung capacity (TLC) with CT attenuation below -950 Hounsfield units (HU). The Perc15 is defined as the HU value at which 15 percent of all voxels have a lower density. These measures are the most common, based on studies comparing to tissue histology in resected lung and established in longitudinal studies of emphysema progression. Literature review was conducted on recent clinical studies involving repeat scans of non-diseased or stable subjects to determining bias and repeatability. A meta-analysis was performed on the repeatability coefficient (RC) inclusive of recent studies that met three major criteria: 1) The study was performed using 16 or 64 slice architectures with 3D volumetric scanning similar to the specifications. 2) The study performed CT in subjects for at least two time points in identical CT scanners with \leq 4 months separating the two time points to mitigate the degree of possible disease progression. 3) The Perc15 and/or RA950 metrics were used to assess lung parenchymal density.

RESULTS

Most studies show that performing volume adjustment (VA) to compensate for the state of the lung inflation will improve the RC. Mean RCs were determined from the meta-analysis using the random effects model, shown in a summary Forest plot (Fig. 1), for before and after VA. Each study reported limits of agreement (LOA), defined as 1.96SDbias, from which the RC can be calculated. The RC is deemed the Smallest Real Difference (SRD), a reference for making clinical decisions.

CONCLUSION

Result of the meta-analysis suggests that without lung VA, a decrease in Perc 15 of at least 18 HU, is required for detection of an increase in the extent of emphysema, with 95% confidence. With lung VA, this SRD value is narrowed down to 11 HU. For RA 950 without VA, an increase of at least 3.7% constitutes a real change. There are insufficient studies to support a meta-analysis of RA950 with VA.

CLINICAL RELEVANCE/APPLICATION

Volume adjustment should be considered to improve repeatability and increase precision for longitudinal studies of emphysema progression in COPD using lung density CT.

SSK05-09 Quantitative Analysis of Pulmonary Peripheral Vessels Using CT in Healthy Subject and COPD Patients

Wednesday, Dec. 2 11:50AM - 12:00PM Location: S404CD

Participants

Sang Min Lee, MD, Seoul, Korea, Republic Of (*Abstract Co-Author*) Nothing to Disclose Joon Beom Seo, MD, PhD, Seoul, Korea, Republic Of (*Abstract Co-Author*) Nothing to Disclose Hyun Jung Koo, MD, Seoul, Korea, Republic Of (*Presenter*) Nothing to Disclose Namkug Kim, PhD, Seoul, Korea, Republic Of (*Abstract Co-Author*) Stockholder, Coreline Soft, Inc Jangpyo Bae, MS, Seoul, Korea, Republic Of (*Abstract Co-Author*) Nothing to Disclose Yeon-Mok Oh, MD, PhD, Seoul, Korea, Republic Of (*Abstract Co-Author*) Nothing to Disclose

PURPOSE

To analyze peripheral vascular changes at CT of COPD with new method and correlate them with emphysema index (EI) and pulmonary function tests.

METHOD AND MATERIALS

Non-contrast, inspiration volumetric CT of 30 healthy subjects (M:F = 25:5; 50.6 ± 7.6 yrs) and 73 COPD patients (M:F = 71:2; 64.3 ± 6.6 yrs) were included. Using in-house software, all pulmonary vessels were extracted automatically. Three imaging planes, which are 1cm, 2cm and 3cm distant from lung surface, respectively, were generated. The numbers of all vessels in each plane and per cm2 (No, No_rel, respectively) were counted. The mean area of each vessel and the percentage of vessel area at image plane (Ar, Ar%, respectively) were measured. The results were compared between two groups and correlated with emphysema index (EI) and PFT.

RESULTS

At imaging plane 1cm apart from the surface, the No, No_rel and Ar% in COPD patients were significantly smaller than healthy subjects (No: 2265 ± 650 vs. 2597 ± 741 ; No_rel: 1.08 ± 0.35 /cm² vs. 1.27 ± 0.40 /cm²; Ar%: 4.84 ± 1.61 vs. 5.75 ± 1.88). In addition, No_rel and Ar% at all planes showed significant negative correlation with EI (1cm: r = -0.344, -0.353; 2cm: r = -0.438, -0.414; 3cm: r = -0.423, -0.412, respectively), FEV1 (1cm: r = 0.224, 0.211; 2cm: r = 0.222, 0.231; 3cm: r = 0.226, 0.208, respectively), FEV1/FVC (1cm: r = 0.287, 0.276; 2cm: r = 0.260, 0.274; 3cm: r = 0.270, 0.281, respectively) and DLco (1cm: r = 0.351, 0.347; 2cm: r = 0.306, 0.325; 3cm: r = 0.282, 0.325, respectively).

CONCLUSION

In COPD patients, number of pulmonary vessels and vessel area percent are significant smaller than those in healthy subjects. Quantified number per cm2 and area percent of vessels significantly correlated with FEV1, FEV1/FVC and DLco.

CLINICAL RELEVANCE/APPLICATION

Detailed analysis of analysis of peripheral vascular changes is possible using volumetric CT and dedicated software. It may be helpful in the understanding of vascular changes in COPD.

The Electronic Physician Annotation Device (ePAD): An Introduction and Tutorial (Hands-on)

Wednesday, Dec. 2 10:30AM - 12:00PM Location: S401CD

IN

AMA PRA Category 1 Credits ™: 1.50 ARRT Category A+ Credit: 0

Participants

Daniel L. Rubin, MD, MS, Palo Alto, CA (*Presenter*) Nothing to Disclose Debra Willrett, Stanford, CA (*Presenter*) Nothing to Disclose

LEARNING OBJECTIVES

1) Evaluate current approaches to collecting image data results (semantic and quantitative image features), and identify gaps in current tools and methods. 2) Identify specific ways the ePAD tool meets current gaps in approaches to collecting semantic and quantitative image features. 3) Describe concrete use cases for ePAD and how its use will improve care thorugh capturing semantic and quantitative image features. 4) Reduce the barrier to adoption and encourage research synergies by demonstrating the use of ePAD in actual patient data and use cases.

ABSTRACT

As biomedical informatics efforts are undertaken to build the learning health system, there is a need to include the information provided by medical imaging in these efforts, since imaging provides detailed information about the disease phenotype for diagnosis and its response to treatment. However, at present, radiology images are not leveraged in many healthcare applications (other than viewing the raw images) because the disease phenotype information they contain is unstructured and not directly machine-accessible. We developed the electronic Physician Annotation Device (ePAD), a freely-available Web-based platform for capturing and storing the phenotypic information contained in radiological images (quantitative and semantic image features) in an explicit, standardized, and machine-accessible format that is interoperable with medical standards such as DICOM and HL7. The ePAD platform is extensible, permitting the community to extend its capabilities with respect to extracting and computing image features, as well as enabling developers to build applications that leverage the information in images in combination with other clinical data. ePAD is being used to at several institutions internationally as well as in national resources such as The Cancer Genome Atlas (TCGA) project of the NIH to enable a coordinated national collection of minable radiological image data. We anticipate the radiology community will find ePAD useful not only in research use cases, but in future clinical applications that optimally leverage the wealth of semantic and quantiative data in images.URL: http://epad.stanford.edu/

Honored Educators

Presenters or authors on this event have been recognized as RSNA Honored Educators for participating in multiple qualifying educational activities. Honored Educators are invested in furthering the profession of radiology by delivering high-quality educational content in their field of study. Learn how you can become an honored educator by visiting the website at: https://www.rsna.org/Honored-Educator-Award/

Daniel L. Rubin, MD, MS - 2012 Honored Educator Daniel L. Rubin, MD, MS - 2013 Honored Educator

Creating, Storing, and Sharing Teaching Files Using RSNA's MIRC® (Hands-on)

Wednesday, Dec. 2 10:30AM - 12:00PM Location: S401AB

ED IN

AMA PRA Category 1 Credits ™: 1.50 ARRT Category A+ Credits: 1.50

Participants

Krishna Juluru, MD, New York, NY (Presenter) Nothing to Disclose

LEARNING OBJECTIVES

1) Learn how to install the RSNA MIRC teaching file. 2) Demonstrate the ability to add new studies and create teaching files. 3) Share teaching file cases with other MIRC servers and other users.

ABSTRACT

Physics (CT VI-Cone Beam CT)

Wednesday, Dec. 2 10:30AM - 12:00PM Location: S403B

СТ РН

AMA PRA Category 1 Credits ™: 1.50 ARRT Category A+ Credits: 1.50

Participants

Stephen J. Glick, PhD, Silver Spring, MD (*Moderator*) Nothing to Disclose Bruce R. Whiting, PhD, Pittsburgh, PA (*Moderator*) Nothing to Disclose

Sub-Events

SSK15-01 Accurate Perfusion Maps from C-arm Cone Beam CT Perfusion Acquisition: A Canine Study

Wednesday, Dec. 2 10:30AM - 10:40AM Location: S403B

Participants

Kai Niu, MS, Madison, WI (*Presenter*) Nothing to Disclose Pengfei Yang, Shanghai, China (*Abstract Co-Author*) Nothing to Disclose Beverly A. Kienitz, MD, DDS, Madison, WI (*Abstract Co-Author*) Nothing to Disclose Ke Li, PhD, Madison, WI (*Abstract Co-Author*) Nothing to Disclose Sebastian Schafer, Madison, WI (*Abstract Co-Author*) Consultant, Siemens AG Kevin Royalty, PhD,MBA, Hoffman Estates, IL (*Abstract Co-Author*) Employee, Siemens AG Charles M. Strother, MD, Madison, WI (*Abstract Co-Author*) Research Consultant, Siemens AG Research support, Siemens AG License agreement, Siemens AG Guang-Hong Chen, PhD, Madison, WI (*Abstract Co-Author*) Research funded, General Electric Company; Research funded, Siemens AG

PURPOSE

C-arm cone beam CT perfusion (CBCTP) has shown promise to generate relatively accurate perfusion parameters. However, high noise, inadequate temporal resolution and temporal sampling due to the inferior detector dynamic range and slow gantry rotation can limit this accuracy. In this study we address these problems using newly developed techniques.

METHOD AND MATERIALS

Seven canines underwent endovascular surgery with IACUC approval. Acute ischemic stroke was introduced in five of the subjects through large vessel occlusion, with the remaining two subjects serving as controls with no stroke imparted. CTP was performed 3.5 hours post-induction and immediately followed by a CBCTP acquisition with a biplane system. CTP images were reconstructed using vendor's software, CBCTP images were reconstructed and post processed to reduce noise (using Prior Image Constrained Compressed Sensing (PICCS)) and to enhance temporal resolution and sampling (using the TEmporal REsolution and SAmpling Recovery (TERESAR)). The CTP and CBCTP images were coregistered, reformatted into 5mm slices and processed with the same software to compute perfusion maps. Arterial input functions (AIF) were selected at the same region (basilar artery) for both datasets. The maps were then randomized and reviewed by two experienced interventional neuroradiologists. Image quality scores as well as the confidence of diagnostic decision were recorded.

RESULTS

The noise in the post-processed CBCTP images was greatly reduced and 0.5s temporal resolution and sampling was achieved. The AIF was well recovered compared to the CTP dataset. Image quality scores show no statistical difference between CTP and CBCTP maps, and the confidence evaluations indicate strong agreement between the two imaging modalities for making stroke diagnoses.

CONCLUSION

By improving contrast to noise ratio and enhancing both temporal resolution and sampling density for CBCTP scans, perfusion maps were generated that correlate well with conventional CTP acquisitions. With the ability to produce accurate perfusion maps with C-arm systems in interventional suites, we now have the possibility to perform CBCTP scans pre- and post-interventional treatment for rapid patient diagnosis without transferring the patient.

CLINICAL RELEVANCE/APPLICATION

The workflow of endovascular treatment for acute ischemic stroke patient can be further optimized using this technique, potentially delivering improved patient outcomes.

SSK15-02 Time-resolved Contrast-enhanced Cone Beam CT Imaging of Livers in Rabbits

Wednesday, Dec. 2 10:40AM - 10:50AM Location: S403B

Participants

Yuncheng Zhong, PhD, Houston, TX (*Abstract Co-Author*) Nothing to Disclose Sanjay Gupta, MD, Houston, TX (*Abstract Co-Author*) Nothing to Disclose Chao-Jen Lai, PhD, Houston, TX (*Abstract Co-Author*) Nothing to Disclose Tianpeng Wang, Houston, TX (*Abstract Co-Author*) Nothing to Disclose Chris C. Shaw, PhD, Houston, TX (*Presenter*) Nothing to Disclose

PURPOSE

Currently available cone beam CT (CBCT) imaging methods do not allow temporal information with a single scan. We investigated the use of a time-resolved CBCT method to generate multiple phase imaging with a single post-injection scan and measured the contrast time-density curves in rabbit livers. Such information may help guide and transcatheter arterial interventional procedures.

METHOD AND MATERIALS

Contrast agents were injected into hepatic artery of rabbits with implanted VX-2 hepatic tumors with a rate of 0.5 ml/second and 8 ml in total. Two CBCT scans were made before and after the injection. Two flat panel (Varian 4030CB and Perkin Elmer 1621) x-ray imaging systems oriented at right angle to each other were used to simultaneously acquire two sets of projection images over 360° at a rate of 7.5 frames/second during each scan. Following the scans, regular CBCT image sets were reconstructed from the projections and the pre-injection image set was subtracted from the post-injection image set to form a 3D contrast map. Each of the two orthogonal post-injection projection sets was then divided into 12 subsets, thus creating 12 orthogonal pairs of 30° limited angle projection sets which were then reconstructed to form 12 3D image sets corresponding to 12 consecutive phases over the scanning time. A maximum likelihood estimation iterative algorithm was applied for image reconstruction with the contrast map used as the constraint.

RESULTS

We have successfully reconstructed 4D images of contrast flow and used them to obtain time-density curves over various regionsof-interest (ROIs). We have demonstrated differences of flow patterns between implanted tumors and normal tissues with the timedensity curves measured from the reconstructed 4D image data.

CONCLUSION

Dual-gantry image acquisition and constrained iterative reconstruction algorithm may help obtain multi-phasic CT images with a single post-injection scan allowing contrast flow to be dynamically imaged and quantified, which may help guide transcatheter arterial interventional procedures for liver tumors. This work was supported in part by research grants: CA104759 and CA124585, EB000117 from NIBIB, CA138502A1, and a subcontract from NIST-ATPs.

CLINICAL RELEVANCE/APPLICATION

Our method provides the capability of imaging contrast injection process in organs and the measured time-density curves may be of interest to differentiate malignant and benign tumors.

SSK15-03 Evaluation of H(L)ctr on CBCT with a Stationary Source

Wednesday, Dec. 2 10:50AM - 11:00AM Location: S403B

Participants

Sarah E. McKenney, PhD, Washington, DC (*Presenter*) Consultant, RadCal Corporation Donovan M. Bakalyar, PhD, Detroit, MI (*Abstract Co-Author*) Nothing to Disclose Vivek Singh, PhD, Detroit, MI (*Abstract Co-Author*) Nothing to Disclose

Background

The equilibrium dose Deq and rise to equilibrium H(L) are recognized as dose metrics that more fully capture the contributions of scattered radiation in multi-detector CT (MDCT). Deq and H(L) are not limited to MDCT, these metrics can be used to characterize cone beam CT (CBCT) systems as well.

Evaluation

Five sections from two TG200/ICRU polyethylene phantoms, with a total length of 1 m, were used as the scattering material. The phantom was centered at isocenter of an interventional system (Axiom Artis dTA, Siemens). A 0.6 cc thimble chamber with a real-time digitizer was centered within the middle section of the phantom. Because of symmetry at isocenter, rotation of the source was unnecessary. Serial integrated dose measurements were made with a series of 10 s exposures at collimation widths of 25-250 mm at 81 kV and 0 mm of Cu. A real-time dose profile, using the same technique factors, was obtained by translating the patient gantry at a constant speed of 14.7 cm/s. H(L)ctr was calculated from the dose profile. Additional acquisitions of the dose profile were performed at tube potentials of 50 kV; the maximum and minimum collimation; and 0.9 mm Cu beam filtration.

Discussion

Significant cone-angle effects at the wide collimation lengths require an offset, dependent on collimation width, for equivalence to the H(L)ctr determined using the real-time dose measurements. Because of the limited fan angle, the beam does not intercept the entire diameter of the phantom and so the radial dose behavior differs substantially in form from that typical of MDCT, particularly near the edge.

Conclusion

Though the radial dose distribution is altered near the edge due to the small beam angle, CBCT can still be characterized along the longitudinal axis. A series of measurements with known collimation widths can be used to determine H(L)ctr. While measurements performed with the real-time dosimeter can be obtained with a single exposure, a correction must be applied.

SSK15-04 Development of a Dedicated Cone-beam CT System for Imaging of Intracranial Hemorrhage

Wednesday, Dec. 2 11:00AM - 11:10AM Location: S403B

Participants

Jennifer Xu, Baltimore, MD (*Presenter*) Research Grant, Carestream Health, Inc Alejandro Sisniega, PhD, Baltimore, MD (*Abstract Co-Author*) Research Grant, Carestream Health, Inc Wojciech Zbijewski, PhD, Baltimore, MD (*Abstract Co-Author*) Research Grant, Carestream Health, Inc Hao Dang, Baltimore, MD (*Abstract Co-Author*) Research Grant, Carestream Health, Inc Joseph W. Stayman, PhD, Baltimore, MD (*Abstract Co-Author*) Research Grant, Elekta AB; Research Grant, Varian Medical Systems, Inc Xiaohui Wang, PhD, Rochester, NY (*Abstract Co-Author*) Employee, Carestream Health, Inc David Foos, MS, Rochester, NY (*Abstract Co-Author*) Employee, Carestream Health, Inc Nafi Aygun, MD, Baltimore, MD (*Abstract Co-Author*) Nothing to Disclose Vassiliss Koliatsos, MD, Baltimore, MD (*Abstract Co-Author*) Nothing to Disclose Jeffrey H. Siewerdsen, PhD, Baltimore, MD (*Abstract Co-Author*) Research Grant, Siemens AG; Consultant, Siemens AG; Research Grant, Carestream Health,Inc; License agreement, Carestream Health,Inc; License agreement, Elekta AB; ; ;

PURPOSE

Prompt detection of intracranial hemorrhage (ICH) is essential to accurate diagnosis of traumatic brain injury (TBI) and stroke. This work reports development of a dedicated cone-beam CT (CBCT) system that overcomes conventional limitations to low-contrast imaging performance to provide reliable detection of acute ICH at the point of care.

METHOD AND MATERIALS

An imaging performance model for task-based detectability index provided the foundation for system design and optimization, including system geometry, imaging technique, and detector choice. Experimentation on a CBCT bench investigated the influence of three important factors on image quality and dose: (1) bowtie filters formed from Al and Ti with various degrees of beam flattening; (2) optional incorporation of an antiscatter grid with grid ratio ranging from 6:1 to 12:1; and (3) selection of detector readout mode (low-gain (LG), high-gain (HG), and dynamic gain (DG) readout). Performance was quantified in CBCT images of an anthropomorphic head phantom with simulated ICH inserts in terms of image uniformity, noise magnitude and correlation, CNR, and spatial resolution, and dose was measured using a Farmer chamber throughout a 16 cm CTDI phantom.

RESULTS

CBCT images of the head acquired using optimal system geometry (source-axis and source-detector distance 75 and 110 cm, respectively) and technique (90 kV, 0.625 mAs / projection) exhibited good visualization of low-contrast ICH inserts: LG readout yielded CNR = 5.5; HG readout provided a 15% increase in CNR (6.3) but suffered skin line artifacts and HU inaccuracy due to barebeam saturation; DG readout yielded a 12% increase in CNR (6.2) and avoided saturation artifacts. Use of an Al bowtie filter in HG mode improved CNR by 23.4% (6.8), permitting lighter grids (or no grid) and reducing CTDIW by ~47% (10.1 mGy).

CONCLUSION

A CBCT head scanner designed according to task-based performance optimization and physical experimentation exhibited image quality suitable to ICH detection. Further improvement will be gained by integration with model-based image reconstruction and artifact correction. The work supports development of a scanner prototype now underway for clinical studies.

CLINICAL RELEVANCE/APPLICATION

A dedicated CBCT system will permit detection of acute ICH and improve diagnosis and treatment of patients with brain injuries at the point of care in the ICU, urgent care, and mobile environments.

SSK15-05 Respiratory and Cardiac Motion-Compensated 5D Cone-Beam CT (CBCT) of the Thorax Region

```
Wednesday, Dec. 2 11:10AM - 11:20AM Location: S403B
```

Participants

Sebastian Sauppe, Heidelberg, Germany (*Presenter*) Nothing to Disclose Marcus Brehm, Baden-Dattwil, Switzerland (*Abstract Co-Author*) Employee, Varian Medical Systems, Inc Pascal Paysan, PhD, Baden-Dattwil, Switzerland (*Abstract Co-Author*) Employee, Varian Medical Systems, Inc Marc Kachelriess, PhD, Heidelberg, Germany (*Abstract Co-Author*) Nothing to Disclose

PURPOSE

To provide motion artifact-free 5D CBCT images from a conventional flat detector-based CBCT scan.

METHOD AND MATERIALS

Image quality of retrospectively respiratory- and cardiac-gated volumes from flat detector cone-beam CT scans is deteriorated by severe sparse projection artifacts. These artifacts further complicate motion estimation, as it is required for motion compensated (MoCo) image reconstruction. For high quality 5D CBCT images at the same x-ray dose and the same number of projections as today's 3D CBCT we developed a double motion compensation approach based on the motion vector fields (MVFs) of respiratory as well as cardiac motion. In a first step our previously published artifact-specific cyclic motion-compensation (acMoCo) approach is applied to compensate for the respiratory patient motion, thus leading to high fidelity 4D CBCT images. With this information a cyclic phase-gated deformable heart registration algorithm is applied to the respiratory motion-compensated 4D CBCT data, thus resulting in cardiac MVFs and thereby in respiratory and cardiac motion-compensated 5D CBCT images. Our new 5D MoCo approach is validated using simulated rawdata obtained by deforming a clinical patient dataset by realistic deformation fields, and by processing patient data acquired with the TrueBeam 4D CBCT system (Varian Medical Systems), as it is used in radiation therapy.

RESULTS

The typical streak artifacts in gated, but non motion-compensated 4D CBCT reconstruction become even more severe when cardiac gating is additionally applied: In scenarios with a 10% respiratory and a 10% cardiac window only 1% of the initial data are available for reconstruction. Our double MoCo approach turned out to be very efficient and removed nearly all streak artifacts due to making use of 100% of the projection data for each reconstructed frame. The simulations show that the 5D MVFs represent the ground truth very well. The 5D MoCo patient data show fine details and no motion blurring, even in regions close to the heart where motion is fastest.

CONCLUSION

Our preliminary results indicate that the proposed double motion-compensated 5D CBCT results in high quality 5D images with full dose usage. This is guaranteed because now all data contribute to each time frame.

CLINICAL RELEVANCE/APPLICATION

High quality 5D images are a prerequisite for precise adaptive radiation treatment. Our approach may also be useful for interventional imaging with C-arm systems.

SSK15-06 Polyenergetic Known Component Reconstruction (KCR) for Flat-panel CBCT with Unknown Material Compositions and Unknown X-ray Spectra

Wednesday, Dec. 2 11:20AM - 11:30AM Location: S403B

Shiyu Xu, Carbondale, IL (Presenter) Nothing to Disclose

Wojciech Zbijewski, PhD, Baltimore, MD (Abstract Co-Author) Research Grant, Carestream Health, Inc

Ali Uneri, Baltimore, MD (Abstract Co-Author) Nothing to Disclose

Jeffrey H. Siewerdsen, PhD, Baltimore, MD (*Abstract Co-Author*) Research Grant, Siemens AG; Consultant, Siemens AG; Research Grant, Carestream Health, Inc; License agreement, Carestream Health, Inc; License agreement, Elekta AB; ; ;

A. Jay Khanna, MD, Bethesda, MD (Abstract Co-Author) Nothing to Disclose

Joseph W. Stayman, PhD, Baltimore, MD (Abstract Co-Author) Research Grant, Elekta AB; Research Grant, Varian Medical Systems, Inc

PURPOSE

Many imaging scenarios involve known devices in the field-of-view (e.g., intraoperative imaging of metal implants). Known component reconstruction (KCR), which integrates device shape and material information into the reconstruction, has demonstrated great potential to reduce metal artifacts and required x-ray exposures. However, accurate KCR requires spectral characterization of system and components (e.g., through pre-scans of devices in air - greatly reducing the practicality of KCR). In this work, we develop a calibration-free KCR that jointly estimates the patient volume and a spectral transfer function (STF) for homogeneous components from a single diagnostic scan.

METHOD AND MATERIALS

Because KCR decouples patient anatomy and known components, we may target high-fidelity models where they are needed most. Specifically, we adopt a polyenergetic component model while maintaining a simple monoenergetic model for the patient anatomy. We modify KCR to jointly estimate a STF with the reconstruction and component registration using alternating optimizations. We evaluate this new calibration-free KCR in cone-beam CT (CBCT) scans of objects containing metal pedicle screws with unknown material composition. The proposed methodology is compared with filtered-backprojection (FBP) and KCR using calibration scans.

RESULTS

STFs estimated using precalibration and the modified KCR were very similar and provided a good fit to air-scan data. In CBCT studies, FBP exhibited substantial metal artifacts due to beam hardening and photon starvation while KCR methods showed a strong capability for artifact reduction. The calibration-free KCR showed better performance, likely due to its ability to adapt to additional physical effects in the diagnostic scans (e.g. increased beam hardening due to surrounding tissues).

CONCLUSION

Calibration-free KCR has the capability to reduce artifacts through high-fidelity device models, outperforming FBP and a more cumbersome KCR method with precalibration. Improved image quality facilitates assessment of pedicle screw placement (including visualizations of possible complications near the device) as well as potential dose reductions.

CLINICAL RELEVANCE/APPLICATION

Metal artifacts are common in interventional imaging where implant knowledge is available. The proposed approach has potential widespread application in situations where visualization near implant boundaries is critical.

SSK15-07 High Quality Time-resolved C-arm Cone Beam CT Angiography Images for Large Vessel Occlusion Diagnosis

Wednesday, Dec. 2 11:30AM - 11:40AM Location: S403B

Participants

Kai Niu, MS, Madison, WI (*Presenter*) Nothing to Disclose Pengfei Yang, Shanghai, China (*Abstract Co-Author*) Nothing to Disclose Yijing Wu, Madison, WI (*Abstract Co-Author*) Nothing to Disclose Tobias Struffert JR, MD, Erlangen, Germany (*Abstract Co-Author*) Nothing to Disclose Arnd Dorfler, Erlangen, Germany (*Abstract Co-Author*) Nothing to Disclose Sebastian Schafer, Madison, WI (*Abstract Co-Author*) Nothing to Disclose Sebastian Schafer, Madison, WI (*Abstract Co-Author*) Consultant, Siemens AG Kevin Royalty, PhD,MBA, Hoffman Estates, IL (*Abstract Co-Author*) Employee, Siemens AG Yu Deuerling-Zheng, MD, Forchheim, Germany (*Abstract Co-Author*) Employee, Siemens AG Charles M. Strother, MD, Madison, WI (*Abstract Co-Author*) Research Consultant, Siemens AG Research support, Siemens AG License agreement, Siemens AG Guang-Hong Chen, PhD, Madison, WI (*Abstract Co-Author*) Research funded, General Electric Company; Research funded, Siemens AG

PURPOSE

With the demonstrated feasibility of measuring perfusion parameters, C-arm cone beam CT perfusion (CBCTP) scans performed directly in the interventional suite potentially enable faster patient triaging and improved patient outcomes. In this work, a method for creating time-resolved cone beam CT angiography (4D-CBCTA) images from the CBCTP acquisition and its potential benefits are discussed.

METHOD AND MATERIALS

Under IRB approval, 21 C-arm cone beam CT dynamic perfusion scans of 17 patients with acute ischemic strokes were acquired. For each multi-sweep CBCTP dataset, a 3D isotropic filtered back projection (FBP) image volume of each rotation was reconstructed and co-registered. All image volumes were post processed using Prior Image Constrained Compressed Sensing (PICCS) to reduce noise and TEmporal REsolution and SAmpling Recovery (TERESAR) to enhance temporal resolution and improve the temporal sampling density. The final image volumes were then imported into a research workstation enabling display of time-resolved volumetric renderings of a patient's cerebral vasculature. Two experienced interventional radiologists independently evaluated the image quality and diagnosed each case. Cronbach's alpha coefficients and ROC analysis were used to evaluate the inter-observer agreement and diagnostic value of this novel image presentation.

RESULTS

Post processing greatly reduced the noise contained in each volume and a half-second temporal resolution was achieved. Observers agreed that image quality for large cerebral arteries was very good and ROC curves demonstrated excellent diagnostic value for detecting large vessel occlusions (AUC=0.987 and 1).

CONCLUSION

4D-CBCTA derived from CBCTP datasets provides high quality images that allow accurate diagnosis of large vessel occlusions. With the ability to acquire both CBCTP images and high quality 4D-CBCTA images from a single C-arm acquisition, it may greatly reduce the time needed to transfer acute ischemic stroke patient between CT/MR room and interventional room.

CLINICAL RELEVANCE/APPLICATION

This technique can reduce the time from arrival to endovascular treatment for stroke patients, achieving better patient outcomes.

SSK15-08 Should Dental CBCT Devices be Equipped with Cu-filters? A Monte Carlo Organ Dose Comparison Study

Wednesday, Dec. 2 11:40AM - 11:50AM Location: S403B

Participants

Andreas Stratis, Leuven, Belgium (*Presenter*) Nothing to Disclose Guozhi Zhang, Leuven, Belgium (*Abstract Co-Author*) Nothing to Disclose Reinhilde Jacobs, Leuven, Belgium (*Abstract Co-Author*) Nothing to Disclose Ria Bogaerts, Herestraat 49, Belgium (*Abstract Co-Author*) Nothing to Disclose Hilde Bosmans, PhD, Leuven, Belgium (*Abstract Co-Author*) Co-founder, Qaelum NV Research Grant, Siemens AG

PURPOSE

To investigate the influence of different x-ray tube filter combinations on organ doses in a dental CBCT exam.

METHOD AND MATERIALS

Promax 3D Max x-ray tube (Planmeca, Finland) is equipped with 0.5mmCu and 2.5mmAl. Its equivalent source model (energy spectrum and filter description) was specified via half value layer (HVL) and air kerma measurements across the detector and by applying the Matlab Spektr tool (Mathworks,Inc). The tube housing (TH) equivalent Al filtration was also determined. Equivalent sources for different filter combinations were designed, employed to the x-ray tube and simulated: from (0 mmCu, 2.5mmAl) to (0.5mmCu, 2.5mmAl) in 0.1mmCu steps and from (0mmCu,2.5mmAl) to (0mmCu,10mmAl) in 2.5mmAl steps. Each spectrum was ray-traced through a 10 cm thick water phantom to determine the attenuation each spectrum undergoes. A spectrum specific scaling factor was calculated as the quotient of the total number of photons in the spectrum to the total number of photons of the lowest HVL spectrum (0 mmCu, 2.5mmAl) which yields the same amount of energy to the detector. Each source model was then used in an EGSnrc based Monte Carlo framework to simulate the jaw protocol (FOV: 130x90 mm2, 96kV, 85.2mAs) for the Zubal head voxel model. Organ doses were calculated for each different filtration such that the detector always receives the same amount of energy.

RESULTS

Increasing the HVL from 6.09mmAl (0mmCu,2.5mmAl,TH) to 9.05mmAl (0.5mmCu, 2.5mmAl,TH) results in dose decrease of 21.3% in skin, 9.4% decrease in cranial bone, 16.3% decrease in muscle, 6.5% decrease in ET and 16.6% decrease in blood doses. On the other hand, there is a 9.7% increase in the dose to brain, 4.5% increase in spinal bone marrow dose, 5.6% increase in eye lens dose and a 3.6% dose increase to the thyroid. In absolute values these doses remain very low.

CONCLUSION

The beam hardening impact of Cu filtration results in reducing the dose to the skin. On the other hand, the higher mean photon energy results in higher doses outside the primary beam due to more scatter radiation. For the jaw protocol, this is the case for the thyroid and the eye lenses.

CLINICAL RELEVANCE/APPLICATION

To determine whether or not the implementation of Cu filtration has a benefit on organ dose reduction.

SSK15-09 Ultra-High Resolution Quantitative Cone Beam CT of the Extremities with a CMOS X-ray Detector

Wednesday, Dec. 2 11:50AM - 12:00PM Location: S403B

Participants

Wojciech Zbijewski, PhD, Baltimore, MD (Presenter) Research Grant, Carestream Health, Inc

Qian Cao, Baltimore, MD (Abstract Co-Author) Nothing to Disclose

Joseph W. Stayman, PhD, Baltimore, MD (Abstract Co-Author) Research Grant, Elekta AB; Research Grant, Varian Medical Systems, Inc

John Yorkston, PhD, Rochester, NY (Abstract Co-Author) Employee, Carestream Health, Inc

Shadpour Demehri, MD, Baltimore, MD (*Abstract Co-Author*) Research support, General Electric Company; Researcher, Carestream Health, Inc; Consultant, Toshiba Corporation

Jeffrey H. Siewerdsen, PhD, Baltimore, MD (*Abstract Co-Author*) Research Grant, Siemens AG; Consultant, Siemens AG; Research Grant, Carestream Health, Inc; License agreement, Carestream Health, Inc; License agreement, Elekta AB; ; ;

PURPOSE

Early detection of pathological alterations in trabecular bone could accelerate treatment and improve prognosis in osteoporosis and osteoarthritis, but is currently challenged by a lack of high resolution imaging modality capable of resolving the trabecular structure (\sim 100 µm) while simultaneously providing diagnostic soft-tissue contrast. We investigate the feasibility of ultra-high resolution invivo imaging of trabecular bone by implementation of a CMOS x-ray detector on a previously developed extremities cone-beam CT (CBCT).

METHOD AND MATERIALS

CMOS detectors offer lower electronic noise (\sim 500 electrons/pixel), faster read-out (up to 30 frames/second for 30x30 cm field of view) and higher resolution than aSi flat panel detectors (FPDs) typically used in CBCT. Initial evaluation of CMOS-based extremities CBCT employed a Dalsa Xineos 1515 detector (99 µm pixels, 600 µm CsI scinitillator) and a rotating anode x-ray source (0.3 mm focal spot). Magnification was 1.25 (matching that of extremities CBCT prototype). A contrast phantom, a resolution phantom with

a 127 µm Tungsten wire for measurement of Point Spread Function (PSF), and a hand phantom (real skeleton in soft tissueequivalent plastic) were imaged at 90 kVp, 0.1 - 0.5 mAs/frame and 720 projections (0.5° steps).

RESULTS

Reconstructions of the contrast phantom show satisfactory soft tissue discrimination with adipose-to-water contrast-to-noise ratio ranging from 2.6 at 0.1 mAs/frame to 5.1 at 0.5 mAs/frame. Full-width half maximum of the PSF was 0.26 mm, indicating high spatial resolution. Further improvement of resolution via optimization of CsI thickness is being investigated. Images of the hand phantom show excellent visualization of the cancellous bone, with clearly delineated trabecular architecture down to ~0.2 mm.

CONCLUSION

CMOS-based extremities CBCT provides high spatial resolution and diagnostic soft tissue contrast, establishing a novel platform for in-vivo imaging of bone microarchitecture. When combined with model-based reconstruction with advanced models of detector blur, the system is anticipated to reach ~100 μ m detail size, opening applications in quantitative bone morphometrics for early detection of osteoporosis and osteoarthritis.

CLINICAL RELEVANCE/APPLICATION

Major improvement in spatial resolution of extremities CBCT is achieved with a CMOS detector, enabling in-vivo quantitative trabecular morphometry for early detection of osteoporosis and osteoarthritis.

Breast Imaging (Ultrasound Diagnostics)

Wednesday, Dec. 2 10:30AM - 12:00PM Location: E450A

BR US

AMA PRA Category 1 Credits ™: 1.50 ARRT Category A+ Credits: 1.50

FDA Discussions may include off-label uses.

Participants

Susan Weinstein, MD, Philadelphia, PA (*Moderator*) Consultant, Siemens AG Regina J. Hooley, MD, New Haven, CT (*Moderator*) Nothing to Disclose

Sub-Events

SSK02-01 Incremental Cancer Detection Utilizing Breast Ultrasound versus Breast MRI in the Evaluation of Newly Diagnosed Breast Cancer Patients

Wednesday, Dec. 2 10:30AM - 10:40AM Location: E450A

Participants

Jeri Sue Plaxo, Houston, TX (*Abstract Co-Author*) Nothing to Disclose Hongying He, MD, PhD, Houston, TX (*Presenter*) Nothing to Disclose Lei Huo, MD, Houston, TX (*Abstract Co-Author*) Nothing to Disclose Wei Wei, Houston, TX (*Abstract Co-Author*) Nothing to Disclose Rosalind P. Candelaria, MD, Houston, TX (*Abstract Co-Author*) Nothing to Disclose Wei T. Yang, MD, Houston, TX (*Abstract Co-Author*) Researcher, Hologic, Inc Henry M. Kuerer, MD, Houston, TX (*Abstract Co-Author*) Nothing to Disclose

PURPOSE

To determine the incremental detection of breast cancer utilizing bilateral whole breast ultrasound (BWBUS) versus dynamic contrast enhanced MRI in patients with biopsy proven primary breast cancer.

METHOD AND MATERIALS

A retrospective database search in a single institution identified 259 patients with newly diagnosed breast cancer from 1/ 2011 to 8/2014, who underwent mammography, BWBUS and MRI before surgery. Patient demographics, tumor characteristics, lesions seen on mammography, BWBUS, and MRI were recorded. Histopathology of each lesion was used to determine the incremental cancer detection rate by BWBUS and MRI and to calculate the sensitivity, specificity, positive predictive value (PPV), and negative predictive value (NPV) of mammography, BWBUS, and MRI. Multifocal, multicentric and contralateral disease were recorded and compared among the three imaging modalities. Effect on surgical planning was obtained from the medical records.

RESULTS

A total of 539 lesions were seen on at least one modality (mammography, BWBUS, or MRI) with histopathology, of which 393 (73%) were malignant and 146 (27%) benign. The sensitivity and specificity of mammography, BWBUS, and MRI were 77%, 89%, and 93%, and 75%, 67%, and 39%, respectively. PPV and NPV of mammography, BWBUS, and MRI were 89%, 88%, and 80%, and 55%, 69%, and 69%, respectively. MRI was significantly more sensitive than BWBUS (p=0.02). However, there was no significant difference in sensitivity between mammography plus BWBUS and MRI. In addition, mammography and BWBUS had significantly higher specificity than MRI (p<0.0001). Mammography plus BWBUS and mammography plus MRI significantly improved the detection of additional malignant foci (multifocal, multicentric or contralateral) (p<0.0001) compared to mammography alone. All three modalities combined further significantly improved the detection of additional malignant foci. However, surgical planning was not changed in the majority of the patients with multicentric disease found on MRI.

CONCLUSION

Breast MRI is more sensitive than BWBUS beyond mammography in breast cancer detection. Mammography and BWBUS are more specific than MRI. Addition of MRI improved the detection of multifocal, multicentric and contralateral disease, without altering surgical planning in the majority of patients with multicentric disease.

CLINICAL RELEVANCE/APPLICATION

The exact role of breast MRI in breast cancer detection and management needs to be further defined.

SSK02-02 The Breast Tumor Strain Ratio Is a Predictive Parameter for Axillary Lymph Node Metastasis in Patients with Invasive Breast Cancer

Wednesday, Dec. 2 10:40AM - 10:50AM Location: E450A

Participants

Jin You Kim, MD, Busan, Korea, Republic Of (*Abstract Co-Author*) Nothing to Disclose Shinyoung Park, MD, Busan, Korea, Republic Of (*Presenter*) Nothing to Disclose Jin Il Moon, MD, Busan, Korea, Republic Of (*Abstract Co-Author*) Nothing to Disclose Ji Won Lee, MD, Busan, Korea, Republic Of (*Abstract Co-Author*) Nothing to Disclose Suk Kim, MD, Pusan, Korea, Republic Of (*Abstract Co-Author*) Nothing to Disclose

PURPOSE

To evaluate the association between the breast tumor strain ratio and axillary lymph node metastasis in patients with invasive breast cancer.

METHOD AND MATERIALS

Between 2013 and 2014, 284 consecutive patients (mean age, 52.2 years; range, 24-78 years) diagnosed with invasive breast cancer (mean size, 2.3 ± 1.5 cm; range, 0.2-9.0 cm) underwent ultrasound (US) elastography before surgery. The strain ratio, defined as the fat-to-lesion ratio and indicative of the relative stiffness of the breast lesion, was calculated using dedicated software within the US equipment. The associations of axillary node metastasis with the tumor strain ratio and clinicobiological variables were evaluated using univariate and multivariate logistic regression analyses.

RESULTS

Among 284 tumors, 85 (29.9%) showed axillary lymph node metastasis by surgical histopathology. The strain ratio was significantly higher in tumors with a node-positive status than in those with a node-negative status ($5.19 \pm 1.28 \text{ vs. } 4.17 \pm 1.30$, respectively; P < 0.001). A receiver operating characteristic curve demonstrated that a tumor strain ratio of 3.89 was the optimal cutoff for predicting axillary nodal involvement in breast cancer (sensitivity, 91.8%; specificity, 45.7%; area under the curve, 0.701; SE, 0.032; P < 0.001). On univariate analysis, a higher strain ratio (> 3.89), larger tumor size (>2 cm), higher histologic grade (grade 3), presence of lymphovascular invasion, palpability, and higher expression of Ki-67 (≥ 14%) were associated with a higher probability of axillary node metastasis. On multivariate analysis, a higher strain ratio (> 3.89) (odds ratio (OR): 14.208; P < 0.001), presence of lymphovascular invasion (OR: 17.437; P < 0.001), and higher expression of Ki-67 (≥ 14%) (OR: 3.744; P = 0.002) maintained independent significance for predicting axillary lymph node metastasis.

CONCLUSION

The breast tumor strain ratio on US elastography is associated independently with axillary lymph node metastasis in patients with invasive breast cancer.

CLINICAL RELEVANCE/APPLICATION

Preoperative prediction of axillary nodal status is valuable. Implementation of US elastography during preoperative US evaluation could help predict axillary node metastasis in breast cancer patients.

SSK02-03 Differentiating Benign and Malignant Breast Tissue Using a Handheld Terahertz Probe

Wednesday, Dec. 2 10:50AM - 11:00AM Location: E450A

Participants

Maarten Grootendorst, MSc, London, United Kingdom (*Presenter*) Nothing to Disclose Susan Brouwer de Koning, BSC, London, United Kingdom (*Abstract Co-Author*) Nothing to Disclose Anthony J. Fitzgerald, Cambridge, United Kingdom (*Abstract Co-Author*) Nothing to Disclose Alessia Portieri, PhD, Cambridge, United Kingdom (*Abstract Co-Author*) Senior Scientist, Teraview Ltd Aida Santa Olalla, MSc, London, United Kingdom (*Abstract Co-Author*) Nothing to Disclose Massi Cariati, MBChB,PhD, London, United Kingdom (*Abstract Co-Author*) Nothing to Disclose Michael Pepper, PhD, London, United Kingdom (*Abstract Co-Author*) Nothing to Disclose Michael Pepper, PhD, London, United Kingdom (*Abstract Co-Author*) Nothing to Disclose Sarah Pinder, London, United Kingdom (*Abstract Co-Author*) Nothing to Disclose Arnie Purushotham, MD,PhD, London, United Kingdom (*Abstract Co-Author*) Nothing to Disclose

PURPOSE

To develop histopathological methods to analyse breast tissue samples scanned with a handheld TeraHertz (THz) probe, and evaluate the ability of THz time and frequency domain pulses and parameters to discriminate between benign and malignant tissue, with the aim of developing a technique to assess tumour resection margins in breast-conserving surgery.

METHOD AND MATERIALS

In all, 15 breast tissue samples (13 patients) from freshly excised wide local excision and mastectomy specimens were scanned using a handheld THz probe with a bandwidth of 0-2.0 THz (Teraview Ltd., UK). For each sample detailed pathology, including type of predominant tissue (tumour and tumour type, fibrous or adipose), type of background tissue, and cell density were obtained at 1.0mm-intervals, and correlated with THz data. Samples with a predominant tissue cell density of >= 60% were included. The full THz time and frequency domain pulses, as well as individual parameters, were evaluated. An area under the receiver operating characteristic curve (AUROC) analysis was performed to quantify the performance of each parameter in discriminating between tumour and fibrous tissue. Parameters with an AUROC value >0.75 were included. A Mann-Whitney U test was performed to determine whether the differences in parameter values were statistically significantly different.

RESULTS

In all, 6 invasive ductal carcinomas, 1 invasive lobular carcinoma, 4 fibrous and 4 adipose samples were used. Adipose tissue could be readily discriminated from tumour/fibrous tissue using the full time-domain pulse (Fig. 1). Tumour could be discriminated from fibrous tissue using a total of 35 parameters; all these parameters had parameter values that were statistically significantly different between tumour and fibrous (p<0.001). Especially, the power at frequency 0.18-0.29THz proved to be a strong discriminator (AUROC >= 0.97).

CONCLUSION

Time-domain pulses and parameters from handheld THz probe measurements can accurately discriminate between benign breast and malignant tissue in an ex vivo setting. More high-dense tumour samples from different tumour types and low-dense samples are needed to further evaluate this technique prior to in vivo patient studies.

CLINICAL RELEVANCE/APPLICATION

THz pulsed imaging distinguishes malignant from benign breast tissue and can potentially assess tumour margins intraoperatively in breast-conserving surgery, aiming to achieve lower re-excision rates

SSK02-04 Association of US Features and the 21-gene Recurrence Score Assays in Estrogen Receptor-Positive Invasive Breast Cancers

Participants Eun Young Chae, Seoul, Korea, Republic Of (*Presenter*) Nothing to Disclose Hak Hee Kim, MD, Seoul, Korea, Republic Of (*Abstract Co-Author*) Nothing to Disclose Woo Kyung Moon, Seoul, Korea, Republic Of (*Abstract Co-Author*) Nothing to Disclose Won Hwa Kim, MD, PhD, Seoul, Korea, Republic Of (*Abstract Co-Author*) Nothing to Disclose Joo Hee Cha, MD, Seoul, Korea, Republic Of (*Abstract Co-Author*) Nothing to Disclose Hee Jung Shin, MD, Seoul, Korea, Republic Of (*Abstract Co-Author*) Nothing to Disclose Woo Jung Choi, MD, Seoul, Korea, Republic Of (*Abstract Co-Author*) Nothing to Disclose Sei Hyun Ahn, Seoul, Korea, Republic Of (*Abstract Co-Author*) Nothing to Disclose

PURPOSE

To identify the relation of imaging features on ultrasound (US) and the recurrence score (RS) of the 21-gene expression assay in patients with estrogen receptor (ER) positive breast cancer.

METHOD AND MATERIALS

Institutional review board approved this study, and the requirement for informed consent was waived. 267 patients with ER-positive invasive breast cancer who underwent US and Oncotype Dx assay were included in this study. US images were independently reviewed by dedicated breast radiologists who were blind to the RS, according to BI-RADS lexicon. In addition, tumor roundness was measured by a laboratory-developed software program. The pathological data were also reviewed including immunohistochemistry results. Univariate analysis was done to assess the associations between the RS and each variables. Multiple logistic regression analysis was used to identify independent predictors of high RS (\geq 31).

RESULTS

Of 267 patients, 147 (55%) had low, 96 (36%) intermediate, and 24 (9%) had high RS. In univariate analysis, the parallel orientation, circumscribed margin, posterior acoustic enhancement, presence of calcification in the mass and tumor roundness was positively associated with high RS. Multiple logistic regression analysis showed that parallel orientation (OR=5.525) and tumor roundness (OR=1.699 per 10 increase) remained independent variables associated with high RS. The area under the ROC curve from the model was 0.78 in distinguishing high RS from low or intermediate RS and increased to 0.88 when combined with pathological data.

CONCLUSION

The tumor roundness and parallel orientation were independent variables that may predict a high RS in patients with ER-positive breast cancer.

CLINICAL RELEVANCE/APPLICATION

ER-positive breast cancers have distinguishing US features according to recurrence score. US can help to differentiate candidates for adjuvant chemotherapy in ER-positive cancer.

SSK02-05 Tumor Growth Rate during Wait Times for Surgery in Women with Breast Cancers Assessed by Ultrasonography

Wednesday, Dec. 2 11:10AM - 11:20AM Location: E450A

Participants

Su Hyun Lee, MD,PhD, Seoul, Korea, Republic Of (*Presenter*) Nothing to Disclose Sung Ui Shin, MD, Seoul, Korea, Republic Of (*Abstract Co-Author*) Nothing to Disclose Jung Min Chang, MD, Seoul, Korea, Republic Of (*Abstract Co-Author*) Nothing to Disclose Nariya Cho, MD, Seoul, Korea, Republic Of (*Abstract Co-Author*) Nothing to Disclose Woo Kyung Moon, Seoul, Korea, Republic Of (*Abstract Co-Author*) Nothing to Disclose

PURPOSE

To evaluate tumor growth rate (TGR) during the wait times for surgery in women with invasive breast cancers and to identify clinicopathologic factors associated with TGR.

METHOD AND MATERIALS

This study was approved by our institutional review board and the requirement for written informed consent was waived. A retrospective chart review in a tertiary care center identified 1,580 women who had breast surgery for invasive carcinoma between August 1, 2013 and August 31, 2014. Among them, a total of 307 consecutive women (mean age, 53 yrs; range, 27-81 yrs) with T1-2 breast cancers eligible for TGR assessment by using ultrasonography (US) were included. All women underwent serial breast US at the time of initial diagnosis and one day before surgery as a routine protocol in our hospital. The three perpendicular diameters of tumors were measured on US images at each time point and the maximum diameter and volume of tumors were compared using paired samples t-test. TGR was quantified using the parameter of specific growth rate (SGR; %/day) and was compared with clinicopathologic variables using univariate and multivariate analyses.

RESULTS

The median time from diagnosis to surgery was 31 days (range, 8-78 days). The maximum diameter and volume of tumors at surgery (mean, 15.8 ± 6.8 mm and 1.73 ± 2.6 cc) were significantly larger than those at diagnosis (15.0 ± 6.5 mm and 1.47 ± 2.3 cc) (P<0.001, both). Tumor subtype (ER-positive [n=206], HER2-positive [n=35], and triple negative cancers [n=66]) was the only independent clinicopathologic factor associated with SGR on multivariate analysis (P=0.006). Triple negative cancers showed the highest SGR (0.980 ± 1.071) followed by HER2-positive (0.550 ± 1.219) and ER-positive cancers (0.192 ± 0.995) (P < 0.001). Clinical T stage was not significantly changed between diagnosis and surgery in ER- and HER2-positive cancers, however, higher T stage at surgery was more frequent in triple negative cancers (P=0.027).

CONCLUSION

Triple negative cancers showed the highest TGR during the wait times for surgery and clinical T stage can be upgraded between diagnosis and surgery in triple negative cancers.

CLINICAL RELEVANCE/APPLICATION

It is desirable to minimize wait times for surgery in patients with triple negative breast cancers.

SSK02-06 Diagnostic Yield of Axillary Ultrasound and Fine-Needle Aspiration during Screening Breast Ultrasound

Wednesday, Dec. 2 11:20AM - 11:30AM Location: E450A

Participants

Inyoung Youn, MD, Seoul, Korea, Republic Of (*Abstract Co-Author*) Nothing to Disclose Min Jung Kim, MD, Seoul, Korea, Republic Of (*Abstract Co-Author*) Nothing to Disclose Eun-Kyung Kim, Seoul, Korea, Republic Of (*Abstract Co-Author*) Nothing to Disclose Hee Jung Moon, MD, Seoul, Korea, Republic Of (*Abstract Co-Author*) Nothing to Disclose Jung Hyun Yoon, MD, Seongnam, Korea, Republic Of (*Abstract Co-Author*) Nothing to Disclose Jieun Koh, MD, Seoul, Korea, Republic Of (*Presenter*) Nothing to Disclose

PURPOSE

The purpose of our study was to assess the positive predictive value (PPV), as a measure of the diagnostic yield, of ultrasound (US)-guided fine-needle aspiration (US-FNA) and cancer detection rate for incidentally detected abnormal axillary lymph node (LN) in patients who underwent screening US.

METHOD AND MATERIALS

We retrospectively reviewed 72 LNs of 69 patients (mean age, 44.9 years) who underwent US-FNA for incidentally detected abnormal axillary LNs on 50,488 screening US during January 2005 to December 2011. The PPV of US-FNA and cancer detection rate were calculated. We evaluated US images for LN size, abnormal findings (hilum loss, eccentric cortical thickening, round shape, extranodal extension or marked hypoechoic cortex), and mammography for the identification of abnormal LNs. The PPV of each finding were also calculated.

RESULTS

The PPV of US-FNA and cancer detection rate was 2.8% (2/72) and 0.004% (2/50,488). The mean measurements for long axis, short axis, and cortical thickening of the LNs were 14.9 ± 5.9 mm, 8.5 ± 3.5 mm, and 5.8 ± 2.8 mm. Of the positive LNs, US findings of hilum loss, eccentric cortical thickening, and extranodal extension were found, and each corresponding PPV was 6.3% (1/16), 1.8% (1/56), and 14.3% (1/7), respectively. The PPV of mammography was 14.3% (1/7).

CONCLUSION

Our results suggest that the PPV of US-FNA and the cancer detection rate for incidentally detected abnormal axillary LNs during screening US are too low to recommend axillary US during breast US screening and that follow-up is acceptable for abnormal LNs detected during screening breast US that do not have extranodal extension or are negative on mammography.

CLINICAL RELEVANCE/APPLICATION

Follow-up US would be acceptable for abnormal LNs detected during screening breast US that did not have extranodal extension or were negative in mammography.

SSK02-07 Microcalcifications in Breast Cancers Affect Ultrasound Dtrain Elastography

Wednesday, Dec. 2 11:30AM - 11:40AM Location: E450A

Participants

Yumi Kashikura, MD,PhD, Tsukuba, Japan (*Presenter*) Nothing to Disclose Ei Ueno, MD, PhD, Tsukuba, Japan (*Abstract Co-Author*) Nothing to Disclose Eriko Tohno, MD, Tsukuba, Japan (*Abstract Co-Author*) Nothing to Disclose Takeshi Umemoto, MD, Tsukuba, Japan (*Abstract Co-Author*) Nothing to Disclose Isamu Morishima, Tsukuba, Japan (*Abstract Co-Author*) Nothing to Disclose

PURPOSE

Some non-palpable breast cancer lesions may exhibit false-negative findings on ultrasound strain elastography. This study aims to investigate the causes of such false-negative findings.

METHOD AND MATERIALS

Between January 2012 and December 2014, 196 patients with pTis to pT1b breast cancer underwent surgery at our hospital. We retrospectively divided the patients into 2 groups by the presence or absence of microcalcifications and compared their elastography data. The presence or absence of calcifications was confirmed by mammography (MMG), and negative lesions were reconfirmed by microscopy. Elastography was performed by several experienced physicians and sonographers, and each physician classified the images according to the 1 to 5 scale of the Tsukuba Elasticity Score. Considering the effect of previous interventions, patients with a history of core needle biopsy and vacuum-assisted biopsy were excluded from the study. Accordingly, 79 patients were excluded and 117 cases were included.

RESULTS

Microcalcifications were absent in 51 (43.6 %) lesions and present in 66 (56.4 %) lesions. The presence of calcifications was microscopically confirmed in 14 patients. Of the lesions without calcifications, 1 (2.0%), 15 (29.4%), 15 (29.4%), and 23 (45.1%) showed elasticity scores of 2, 3, 4, and 5, respectively, while of those with calcifications, 3 (4.5%), 14 (21.2%), 16 (24.2%), 16 (24.2%), and 17 (25.8%) showed elasticity scores of 1, 2, 3, 4, and 5, respectively. Assuming that scores of 3, 4, and 5 indicate positive findings, the overall sensitivity was 84.6 %, while sensitivity for the lesions with and without calcifications was 74.2% and 98.0%, respectively (P = 0.003). When the presence of microcalcifications was judged only by MMG, the sensitivity for the lesions with and without calcifications was 73.1% and 96.9%, respectively. As strain elastography is based on combined autocorrelation, microcalcifications seem to cause an apparent strain even though the tissue is harder than normal.

Although breast ultrasound elastography shows high sensitivity, our study revealed an obvious difference in sensitivity between the lesions with and without microcalcifications.

CLINICAL RELEVANCE/APPLICATION

Clinicians should be careful while evaluating breast ultrasound strain elastography findings for lesions with microcalcifications on mammography.

SSK02-08 Mass-like Focal Breast Fibrosis - A Benign Entity Mimicking Malignancy on Ultrasonography

Wednesday, Dec. 2 11:40AM - 11:50AM Location: E450A

Participants

Eleonora Horvath, MD, Santiago, Chile (*Abstract Co-Author*) Nothing to Disclose Aleen V. Altamirano, MD, Masaya, Nicaragua (*Presenter*) Nothing to Disclose Eduardo Soto, Santiago, Chile (*Abstract Co-Author*) Nothing to Disclose Marcela Uchida, Santiago, Chile (*Abstract Co-Author*) Nothing to Disclose Miguel A. Pinochet, MD, Santiago, Chile (*Abstract Co-Author*) Nothing to Disclose Claudio S. Silva Fuente-Alba, MD, MSc, Santiago, Chile (*Abstract Co-Author*) Nothing to Disclose Marcela Gallegos, Santiago, Chile (*Abstract Co-Author*) Nothing to Disclose Jocelyn Galvez, Vitacura, Chile (*Abstract Co-Author*) Nothing to Disclose Maria Flavia Pizzolon, MD, Vitacura, Chile (*Abstract Co-Author*) Nothing to Disclose

PURPOSE

To determine the sonographic characteristics of core biopsy-proven Mass-like Focal Breast Fibrosis (MFBF).

METHOD AND MATERIALS

IRB approved, retrospective study. Between April 2007 and January 2015, 3051 US-guided breast biopsies with 14G core needle, were performed, 251 of them with a diagnosis of stromal breast fibrosis. We excluded 128 cases where fibrosis was not the primary histologic diagnosis. Only MFBF cases were included, histopathologically defined as a localized area of dense fibrous tissue associated with hypoplastic mammary ducts and lobules, without vascular structures and inflammatory changes. Imaging features were tabulated and analyzed. Follow-up imaging was reviewed to document lesion stability.

RESULTS

In 121 women (median age: 50 years, range: 25-83) we found 123 cases of MFBF (incidence: 4%). Lesion size ranged from 4 to 35 mm (median: 10 mm), non-palpable in 94% of the cases. Eighty-seven (71%) of them developed in highly or heterogeneously dense breast (ACR 4 and 3). Only 7 (6%) were evident on mammography. We identified two distinct sonographic patterns of MFBF. Pattern A (28%): well-circumscribed, hypoechoic, avascular mass. Pattern B (72%): ill defined, irregular, avascular, markedly hypoechogenic or spiculated lesion with or without a definable mass and markedly shadowing, located intraparenchymatous or under Cooper ligament. Sixty-seven (54%) lesions were reported as BI-RADS 5, 4C or 4B. MRI study was performed in 7 patients with negative outcome. One lesion was surgically removed and in 4 patients a new large (8G) core biopsy was performed due to radio-histological discordance, obtaining the same results. Patients remain in follow-up (median: 30 months, range: 2 to 94 months), without malignancy.

CONCLUSION

The mass-like focal breast fibrosis is a benign entity with the potential to mimic malignancy. Is important that radiologists know the specific US patterns and if proven on core needle biopsy, it may be taken as a concordant diagnosis.

CLINICAL RELEVANCE/APPLICATION

We report a large series of MFBF, detailing its US-pattern. Should these US patterns be identified, it is reasonable to accept this benign histopathological diagnosis postbiopsy as concordant.

SSK02-09 Hypoechoic Non-mass Lesion on Screening Breast Ultrasound

Wednesday, Dec. 2 11:50AM - 12:00PM Location: E450A

Participants

Jin Hwa Lee, MD, Busan, Korea, Republic Of (*Presenter*) Nothing to Disclose Cherie M. Kuzmiak, DO, Chapel Hill, NC (*Abstract Co-Author*) Research Grant, FUJIFILM Holdings Corporation; Ji Hyun Lee, Busan, Korea, Republic Of (*Abstract Co-Author*) Nothing to Disclose Jong-Young Oh, Busan, Korea, Republic Of (*Abstract Co-Author*) Nothing to Disclose Hee-Jin Kwon, MD, Busan, Korea, Republic Of (*Abstract Co-Author*) Nothing to Disclose

PURPOSE

The current ACR BI-RADS lexicon only covers mass lesions. The purpose of this study is to determine the significance of hypoechoic non-mass lesion (HNML) which is recognized during screening breast ultrasound (SBUS).

METHOD AND MATERIALS

An IRB approved retrospective database review was performed from March 2008 to June 2012 of patients who had SBUS. The indications of SBUS at our institution were asymptomatic patients with dense breast tissue on mammography, routine follow-up of a BI-RADS category 3 lesion with 2 years of stability or a biopsy-proven benign lesion on prior examination, and postoperative screening after surgery for breast cancer. We included patients with HNML on ultrasound and with no suspicious finding on mammography. Excluded from the study were lesions related to the past history of biopsy or operation at the area of HNML. A HNML was defined as a hypoechoic area that does not conform to the definition of a mass and has different character from that of surrounding glands or the same area in the contralateral breast. The final diagnoses were based on pathology results and clinical or sonographic follow-up more than 12 months. We calculated the incidence and likelihood of malignancy of the HNML on SBUS.

A total of 17868 SBUS were performed on 8856 asymptomatic patients. Ninety-six HNMLs were detected in 89 patients (1.0%). On final pathology or follow-up of HMLs, three (3.1%) lesions were malignant, 78 (81.3%) lesions were benign, and two (2.1%) lesions were high risk. In addition, there were 13 (13.5%) lesions that were lost to follow-up or without final surgical pathology. The likelihood of malignancy of a HNML on SBUS was 3.1%.

CONCLUSION

The likelihood of malignancy for a hypoechoic non-mass lesion on SBUS was greater than 2%. Therefore, it should be classified as a BI-RADS category 4 lesion and tissue diagnosis is warranted.

CLINICAL RELEVANCE/APPLICATION

Large prospective studies are needed to further validate which management recommendation is most appropriate for the HNML on SBUS.

ISP: Gastrointestinal (Pancreas Benign Diseases)

Wednesday, Dec. 2 10:30AM - 12:00PM Location: E353B

GI CT MR US

AMA PRA Category 1 Credits ™: 1.50 ARRT Category A+ Credits: 1.50

Participants

Elizabeth M. Hecht, MD, New York, NY (*Moderator*) Nothing to Disclose Koenraad J. Mortele, MD, Boston, MA (*Moderator*) Nothing to Disclose Atif Zaheer, MD, Baltimore, MD (*Moderator*) Nothing to Disclose

Sub-Events

SSK07-01 Gastrointestinal Keynote Speaker: Update on Imaging Benign Pancreatic Diseases

Wednesday, Dec. 2 10:30AM - 10:40AM Location: E353B

Participants

Koenraad J. Mortele, MD, Boston, MA (Presenter) Nothing to Disclose

SSK07-02 Using T1 Mapping for the Diagnosis of Mild Chronic Pancreatitis

Wednesday, Dec. 2 10:40AM - 10:50AM Location: E353B

Participants

Temel Tirkes, MD, Indianapolis, IN (*Abstract Co-Author*) Nothing to Disclose Jordan K. Swensson, MD, Indianapolis, IN (*Presenter*) Nothing to Disclose Chen Lin, PhD, Indianapolis, IN (*Abstract Co-Author*) Nothing to Disclose Qun Zhong, MD, PhD, Fuzhou, China (*Abstract Co-Author*) Nothing to Disclose Qiushi Wang, MD, Indianapolis, IN (*Abstract Co-Author*) Nothing to Disclose Evan Fogel, MD, Indianapolis, IN (*Abstract Co-Author*) Nothing to Disclose Fatih Akisik, MD, Indianapolis, IN (*Abstract Co-Author*) Nothing to Disclose Kumaresan Sandrasegaran, MD, Carmel, IN (*Abstract Co-Author*) Nothing to Disclose

PURPOSE

To determine if the pancreatic signal intensity on T1 mapping can be used to diagnose mild chronic pancreatitis.

METHOD AND MATERIALS

This retrospective study analyzed patients with suspected chronic pancreatitis who underwent MRI between March 2014 and December 2014. All MRI studies were performed on 3.0 T Magnetom Verio (Siemens Medical Solutions, Malvern, PA) scanner. T1 mapping was acquired with gradient echo sequence using TR 3.87 ms, TE 1.32, flip angles of 2° and 13°, NEX of 1 and matrix of 320x168. Of 127 patients scanned, patients < 18 years age, and those with acute pancreatitis, pancreatic neoplasm, iron overload, or cystic fibrosis were excluded from the analysis. Patients were grouped as normal or mild chronic pancreatitis based on secretinenhanced MR pancreatography using the Cambridge classification. There were 55 normal and 21 patients with mild chronic pancreatitis. Region of interest (ROI) measurements (~1cm2) were drawn in the homogenous regions of the head, body and tail of the pancreas by two independent and blinded reviewers. The two-tailed t-test was used to determine differences of T1 relaxation times between the normal and mild CP patients. Receiver operating characteristic (ROC) curve analysis was performed to determine the accuracy of the T1 relaxation time as a differentiating criterion.

RESULTS

There was a significant difference (p< 0.0001) in the T1 relaxation times of the pancreas between the normal (mean 819 ms, 95%CI: 739-898) and mild chronic pancreatitis (mean: 1141 ms, 95%CI: 1027-1255) groups. T1 relaxation time cut off value of 1000 ms was 72% sensitive (95%CI: 48-89) and 75% specific (95%CI: 61-85) for the diagnosis of mild chronic pancreatitis (AUC=0.80, p<0.0001). There was substantial inter-observer agreement (kappa=0.74) of measured T1 relaxation times.

CONCLUSION

There is significant difference in the T1 relaxation times of the pancreas between the normal and mild chronic pancreatitis patients.

CLINICAL RELEVANCE/APPLICATION

T1-mapping may be a practical imaging technique for diagnosis of mild chronic pancreatitis.

Honored Educators

Presenters or authors on this event have been recognized as RSNA Honored Educators for participating in multiple qualifying educational activities. Honored Educators are invested in furthering the profession of radiology by delivering high-quality educational content in their field of study. Learn how you can become an honored educator by visiting the website at: https://www.rsna.org/Honored-Educator-Award/

Temel Tirkes, MD - 2013 Honored Educator Temel Tirkes, MD - 2014 Honored Educator Kumaresan Sandrasegaran, MD - 2013 Honored Educator Kumaresan Sandrasegaran, MD - 2014 Honored Educator Fatih Akisik, MD - 2014 Honored Educator

SSK07-03 Quantitative MRI Evaluation of the Pancreatic Parenchyma in Diabetes Mellitus

Participants

Fabio A. Uyeno, MD, Sao Carlos, Brazil (*Presenter*) Nothing to Disclose Jorge Elias JR, MD, PhD, Ribeirao Preto, Brazil (*Abstract Co-Author*) Nothing to Disclose Natalia P. Ito, MD, Ribeirao Preto, Brazil (*Abstract Co-Author*) Nothing to Disclose Iana M. Araujo, Ribeirao Preto, Brazil (*Abstract Co-Author*) Nothing to Disclose Adriana L. Carvalho, Ribeirao Preto, Brazil (*Abstract Co-Author*) Nothing to Disclose Francisco A. Paula, Ribeirao Preto, Brazil (*Abstract Co-Author*) Nothing to Disclose Valdair F. Muglia, MD, PhD, Ribeirao Preto, Brazil (*Abstract Co-Author*) Nothing to Disclose

PURPOSE

To assess the pancreatic fat fraction and ADC in healthy, obese and diabetic (type 1 and 2) subjects

METHOD AND MATERIALS

A retrospective study of abdominal MR images of 89 subjects (56 controls incluing obese subgroup; 33 diabetics) was carried out. Two radiologists reviewed all images independently and proceed the calculation of pancreatic fat fraction through in and out-ofphase GRE T1-weighted sequences, and the ADC through diffusion with maximum b=1000. Pancreatic fat fractions and average values of ADC were obtained and compared.

RESULTS

We observed significant differences between pancreatic fat fractions of diabetics type 2 (DM2) and healthy and diabetic type 1 (DM1) individuals, with p values of 0.01 and 0.02 for men and 0.02 and 0.01 for women, with good interobserver reliability (intraclass correlation coefficients > 0.8). Obese non-diabetic sujects showed high pancreatic fat fraction similar to DM2. There was also a significant difference in ADC values between DM2 and DM1 and healthy individuals (p: 0.02 and 0.03 in males; p: 0.002 and 0.001 in females), lower in DM2.

CONCLUSION

We observed significantly higher pancreatic fat fractions in DM2, when compared to healthy and DM1 subjects. This finding favors the hypothesis of fatty infiltration of the organ as a possible associated causal factor to the pancreatic beta cells failure, although obese subjects had pancreatic fat fractions similar to DM2.

CLINICAL RELEVANCE/APPLICATION

Pancreatic fatty infiltration ocurring can be evaluated by MRI and its role in Diabetes Mellitus need further assessment.

SSK07-04 Co-existing Liver and Pancreas Steatosis Related to Chronic Non-alcoholic Liver Diseases (NALD) but not to Viral Infection

Wednesday, Dec. 2 11:00AM - 11:10AM Location: E353B

Participants

Manuela Franca, MD, Porto, Portugal (*Presenter*) Nothing to Disclose Angel Alberich-Bayarri, MD, Valencia, Spain (*Abstract Co-Author*) Nothing to Disclose Luis Marti-Bonmati, MD, PhD, Godella, Spain (*Abstract Co-Author*) Nothing to Disclose Joao A. Oliveira, Porto, Portugal (*Abstract Co-Author*) Nothing to Disclose Francisca E. Costa, MD, Porto, Portugal (*Abstract Co-Author*) Nothing to Disclose Jose Ramon Vizcaino Vazquez, Porto, Portugal (*Abstract Co-Author*) Nothing to Disclose Helena Pessegueiro Miranda, Porto, Portugal (*Abstract Co-Author*) Nothing to Disclose

PURPOSE

Liver steatosis is related to metabolic syndrome but is also present in other diffuse liver diseases. Pancreas steatosis may be also present in association with steatohepatitis and metabolic syndrome. However, little is known about pancreas fat deposition in other diffuse liver diseases such as viral hepatitis. Our purpose was to assess the Proton Density Fat Fraction (PDFF) of the liver and pancreas, with a multiecho GRE MR sequence, in patients with diffuse liver diseases, and to evaluate the relationship between fat infiltration of both organs and the influence of the underlying liver disease.

METHOD AND MATERIALS

The study population included consecutive patients with diffuse liver disorders and clinically indicated liver biopsy, who underwent a 3T MR examination using a single breath-hold multiecho chemical shift GRE sequence with 12 echoes. PDFF quantification was performed with magnitude and phase reconstruction, T1 and T2* biases corrected, selecting a ROI in the biopsied liver segment and also in 3 pancreatic regions (head, body, tail). Differences of liver and pancreas PDFF between histologic grades were assessed by ANOVA tests. The relationship between liver and pancreas PDFF values and histologic grading was assessed with Spearman correlation analysis. Furthermore, the study population was categorized by clinical diagnosis (chronic viral hepatitis vs. chronic NALD).

CONCLUSION

We found a significant correlation between liver and pancreas PDFF quantification, in patients with NALD but not in patients with viral hepatitis.

CLINICAL RELEVANCE/APPLICATION

Fat deposition in liver and pancreas appears to be related in patients with chronic non-alcoholic disease but not in chronic viral hepatitis.

SSK07-05 Intravoxel Incoherent Motion Diffusion-weighted MR Imaging in Characterizing Tumorous and Inflammatory Pancreatic Diseases

Participants

Bohyun Kim, MD, Suwon, Korea, Republic Of (*Presenter*) Nothing to Disclose Seung Soo Lee, MD, Seoul, Korea, Republic Of (*Abstract Co-Author*) Nothing to Disclose Yu Sub Sung, Seoul, Korea, Republic Of (*Abstract Co-Author*) Nothing to Disclose Jin Hee Kim, MD, Seoul, Korea, Republic Of (*Abstract Co-Author*) Nothing to Disclose Hyoung Jung Kim, MD, Seoul, Korea, Republic Of (*Abstract Co-Author*) Nothing to Disclose Jae Ho Byun, MD, Seoul, Korea, Republic Of (*Abstract Co-Author*) Nothing to Disclose

PURPOSE

To evaluate the feasibility of intravoxel incoherent motion (IVIM) parameters in differentiating acute pancreatitis, autoimmune pancreatitis (AIP), neuroendocrine tumor (NET), solid pseudopapillary tumor (SPT), pancreatic ductal adenocarcinoma (PAC), and normal pancreas.

METHOD AND MATERIALS

The institutional board approved this retrospective study, and informed consent was waived. We evaluated IVIM diffusion-weighted images (10 b values for 0 to 900 sec/mm^2) of 104 consecutive patients (mean age, 53.7 years; M:F=58:46) with pathologically confirmed pancreatic neoplasms (n = 54; 15 NETs, 9 SPTs, and 30 PACs) > 2cm, acute pancreatitis (n = 13), AIP (n = 7), and normal pancreas (n = 30). The slow diffusion coefficient (Dslow), fast diffusion coefficient (Dfast), and perfusion fraction (f) were measured on two consecutive sections covering the largest part of the lesions. The differences in IVIM parameters among the diagnoses of pancreatic lesions were compared using the ANOVA test and the post-hoc Bonferroni multiple comparisons test.

RESULTS

PAC had significantly lower f values (0.13 ± 0.06) than normal pancreas (0.24 ± 0.05) , NET (0.21 ± 0.06) , and acute pancreatitis (0.25 ± 0.01) and significantly lower Dfast values $(20.0 \pm 12.6 \times 10^{-3}\text{mm}^{2}\text{/sec})$ than normal pancreas $(48.2 \pm 23.9 \times 10^{-3}\text{mm}^{2}\text{/sec})$ (P<.05). For AIP, f value (0.14 ± 0.06) was significantly lower than that of normal pancreas (P<.05). Dfast values of acute pancreatitis $(25.4 \pm 14.6 \times 10^{-3}\text{mm}^{2}\text{/sec})$, NET $(26.5 \pm 19.9 \times 10^{-3}\text{mm}^{2}\text{/sec})$, and SPT $(17.8 \pm 9.5 \times 10^{-3}\text{mm}^{2}\text{/sec})$ were lower than that of normal pancreas. Although the Dslow of AIP $(1.06 \pm 0.19 \times 10^{-3}\text{mm}^{2}\text{/sec})$ were lower than normal pancreas $(1.14 \pm 0.15 \times 10^{-3}\text{mm}^{2}\text{/sec})$ and the other pancreatic diseases, the difference was not statistically significant.

CONCLUSION

Perfusion related parameters (f and Dfast) are more helpful in characterizing pancreatic diseases than Dslow . PAC and AIP are characterized by decreased perfusion fraction (f) compared with normal pancreas.

CLINICAL RELEVANCE/APPLICATION

IVIM is feasible for assessing the different perfusion and diffusion characteristics of pancreatic diseases.

SSK07-06 Evaluation of Pancreatic Exocrine Insufficiency by Cine-Dynamic MRCP Using Spatially Selective IR Pulse: Correlation with Severity of Chronic Pancreatitis based on Morphological Changes of Pancreatic Duct

Wednesday, Dec. 2 11:20AM - 11:30AM Location: E353B

Participants

Kazuya Yasokawa, Kurashiki, Japan (*Presenter*) Nothing to Disclose Katsuyoshi Ito, MD, Okayama, Japan (*Abstract Co-Author*) Nothing to Disclose Tsutomu Tamada, MD, PhD, Kurashiki, Japan (*Abstract Co-Author*) Nothing to Disclose Akira Yamamoto, MD, Kurashiki, Japan (*Abstract Co-Author*) Nothing to Disclose Akihiko Kanki, MD, Kurashiki, Japan (*Abstract Co-Author*) Nothing to Disclose Daigo Tanimoto, MD, Kurashiki, Japan (*Abstract Co-Author*) Nothing to Disclose Yasufumi Noda, Kurashiki, Japan (*Abstract Co-Author*) Nothing to Disclose Ayumu Kido, Kurashiki, Japan (*Abstract Co-Author*) Nothing to Disclose Teruyuki Torigoe, Kurashiki, Japan (*Abstract Co-Author*) Nothing to Disclose

PURPOSE

Recent study showed a significantly positive correlation between secretion grades of pancreatic juice at cine dynamic MRCP with a selective inversion recovery (IR) pulse and pancreatic exocrine function test. This study evaluated pancreatic exocrine insufficiency by cine-dynamic MRCP using spatially selective IR pulse in patients with chronic pancreatitis in correlation with the severity of morphological changes of pancreatic duct.

METHOD AND MATERIALS

41 patients with suspected chronic pancreatitis underwent cine-dynamic MRCP with a spatially selective IR pulse. Mean secretion grading score (5-point scale) based on the moving distance of pancreatic juice inflow on cine-dynamic MRCP was assessed. Based on the previous report, cutoff value of secretion grade less than 0.70 in cine-dynamic MRCP was used for the criterion of pancreatic exocrine insufficiency. Mean secretion grades were compared with Cambridge grade which defined the severity of chronic pancreatitis based on morphological changes of pancreatic duct.

RESULTS

In comparisons among patient groups with Cambridge grade1 (normal; n=6), 2 (equivocal; n=3), 3 (mild; n=6), 4 (moderate; n=9) and 5 (severe; n=17), median secretion grading score of Cambridge5 (score=0) was significantly lower than Cambridge1-4 (1.13, 0.55, 0.50, 0.15; P<0.001, P<0.015, P<0.002, P<0.028, respectively). In all 17 patients in Cambridge5, secretion grading score was less than 0.70. Median secretion grading score of Cambride1 was significantly higher than Cambridge3-5 (P<0.030, P<0.011, P<0.001, respectively). In Cambridge2-4, there were no significant differences in secretion grading score between any groups. In Cambridge2, secretion grading score was less than 0.70 in 2 (67%) of 3 patients showing pancreatic exocrine insufficiency. Conversely, in Cambridge3 and 4, secretion grading score was more than 0.70 in 3 (20%) of 15 patients showing normal pancreatic exocrine function.

CONCLUSION

It should be noted that the degree of morphological changes of pancreatic duct does not necessarily reflect the severity of pancreatic exocrine insufficiency at cine-dynamic MRCP in Cambridge grade 2-4 (equivocal to moderate) chronic pancreatitis.

CLINICAL RELEVANCE/APPLICATION

Cine-dynamic MRCP with selective IR pulse may have a potential to evaluate pancreatic exocrine insufficiency in patients with Cambridge grade 2-4 (equivocal to moderate) chronic pancreatitis.

SSK07-07 Imaging Evaluation of Ablative Margin and Index Tumor Immediately after Combined Treatment of TACE and RF Ablation for Hepatocellular Carcinoma: Comparison between Multi-detector CT and MR Imaging

Wednesday, Dec. 2 11:30AM - 11:40AM Location: E353B

Participants

Jin Woong Kim, MD, Jeollanamdo, Korea, Republic Of (*Abstract Co-Author*) Nothing to Disclose Sang Soo Shin, MD, Gwangju, Korea, Republic Of (*Presenter*) Nothing to Disclose Suk Hee Heo, MD, Hwasun-Gun, Korea, Republic Of (*Abstract Co-Author*) Nothing to Disclose Hyo Soon Lim, MD, Jeollanam-Do, Korea, Republic Of (*Abstract Co-Author*) Nothing to Disclose Jun Hyung Hong, Gwang-Ju, Korea, Republic Of (*Abstract Co-Author*) Nothing to Disclose Young Hoe Hur, Jeollanam-Do, Korea, Republic Of (*Abstract Co-Author*) Nothing to Disclose Yong-Yeon Jeong, MD, Chonnam, Korea, Republic Of (*Abstract Co-Author*) Nothing to Disclose

PURPOSE

To prospectively compare multi-detector CT and MR imaging in assessment of ablative margin (AM) and index tumor within ablation zones immediately after combined treatment of transcatheter arterial chemoembolization (TACE) and radiofrequency (RF) ablation for hepatocellular carcinoma (HCC)

METHOD AND MATERIALS

Based on our preliminary data, necessary number of patients was estimated to be at least 30 when an a error of 0.05 and a β error of 0.2 were applied. A total of 33 consecutive patients with 45 HCCs, who had successfully undergone contrast-enhanced CT and MR imaging after RF ablation combined with TACE, was enrolled in this study. CT and MR imaging were performed within 3 and 7 hours after completion of combined therapy of TACE and RF ablation, respectively. Both CT and MR images were reviewed in consensus by two radiologists in two separate sessions regarding visual discrimination between AM and index tumor and status of AM within ablation zones. The status of AM was classified as AM plus (AM completely surrounded tumor), AM zero (AM was partly discontinuous, without protrusion of tumor beyond postulated border of ablated area) and AM minus (AM was partly discontinuous, with protrusion of tumor). Any ablation zone with AM plus or AM zero was considered as imaging evidence to predict technical effectiveness, which was based on one-month follow-up CT, as well as to represent technical success.

RESULTS

With CT and MR imaging, visual discrimination between AM and index tumor was possible in 34 (75.6%) and 40 (88.9%) of 45 ablation zones, respectively (P = .1094). Among 34 and 40 ablation zones in which status of AM could be evaluated on CT and MR imaging, AM status was categorized into AM plus (n=25 and 31, respectively), AM zero (n=9 and 8, respectively) and AM minus (n=0 and 1, respectively). The technical effectiveness was noted in all of ablation zones on one-month follow-up CT. Based on CT and MR imaging, technical success and effectiveness were determined to be achieved in 34 (75.6%) and 39 (86.7%), respectively (P = .1797).

CONCLUSION

There was no significant difference in assessment of ablative margin and index tumor within ablation zones immediately after combined treatment of TACE and RF ablation between CT and MR imaging.

CLINICAL RELEVANCE/APPLICATION

CT and MR imaging have equivalent ability to evaluate technical success immediately after combined treatment of TACE and RFA. Thus, MR imaging may not be necessary.

SSK07-08 Methodology for True Dynamic Contrast-Enhanced MRI of Pancreatic Lesions

Wednesday, Dec. 2 11:40AM - 11:50AM Location: E353B

Participants Eric Paulson

Eric Paulson, Milwaukee, WI (*Presenter*) Nothing to Disclose Paul M. Knechtges, MD, Milwaukee, WI (*Abstract Co-Author*) Nothing to Disclose Beth A. Erickson, MD, Milwaukee, WI (*Abstract Co-Author*) Nothing to Disclose

PURPOSE

Dynamic contrast-enhanced (DCE) MR imaging offers promise to improve the diagnosis, therapy planning, and response assessment of pancreatic lesions. However, organ motion arising from respiration and peristalsis can challenge voxel-wise estimation of pharmacokinetic (PK) parameters in abdominal DCE-MRI. We introduce here a novel methodology to correct DCE-MRI datasets for inter-scan motion, facilitating true voxel-wise DCE-MRI in the abdomen.

METHOD AND MATERIALS

Five patients with pancreatic cancer were imaged at 3T. An anti-peristaltic agent (glucagon, 1mg IV) was administered to suppress bowel motion. Multi-flip angle breath hold images (2/5/15/25 deg) were acquired using a 3D Dixon VIBE sequence. A time series of 16 breath hold 3D Dixon VIBE images was then acquired before (3), during (1), and after (12) bolus administration of contrast (0.1 mmol/kg, Multihance). Deformable image registration (DIR) software was used to construct deformation vector fields (DVFs) required to align the fat-only Dixon (FD) images at each time point to one pre-contrast FD reference image. The DVFs were then applied to the corresponding water-only Dixon (WD) images at each time point to motion-correct the DCE-MRI time series. Baseline T1 maps were estimated using a linearized Ernst model fit to the multi-flip angle WD images. PK parameters (Ktrans, kep, ve, vp) were estimated on a voxel-wise basis by fitting of the linearized Extended Tofts model to concentration-time curves constructed using the motion-corrected WD images.

RESULTS

FD images were robust against spatial and temporal variations in signal intensity arising from wash-in and wash-out of contrast, facilitating construction of DVFs. Applying the FD-derived DVFs to WD successfully corrected the WD images for inter-scan motion arising from inconsistent breath holds, facilitating voxel-wise PK parameter estimation for all patients studied. The methodology facilitated extraction of late-arterial phase images for conventional radiologic interrogation.

CONCLUSION

The novel use of Dixon and DIR facilitates voxel-wise estimation of PK parameters from abdominal DCE-MRI datasets. Future work will incorporate Dixon with radial k-space sampling to improve intra-scan motion robustness during breath hold acquisitions.

CLINICAL RELEVANCE/APPLICATION

Potential to improve disease diagnosis, therapy selection and planning, and response assessment of abdominal organs (e.g., pancreas, liver, kidneys, etc).

SSK07-09 Test-retest Reliability of 3D-EPI MR Elastography in Pancreas

Wednesday, Dec. 2 11:50AM - 12:00PM Location: E353B

Participants

He An, Shenyang, China (*Presenter*) Nothing to Disclose Yu Shi, PhD, Shengyang, China (*Abstract Co-Author*) Nothing to Disclose Qiyong Guo, MD, Shenyang, China (*Abstract Co-Author*) Nothing to Disclose

PURPOSE

The aim of the study is to conduct a rigorous evaluation of the repeatability of pancreas stiffness assessed by 3D echo-planarimaging magnetic resonance elastography (3D-EPI MRE) in healthy volunteers, patients with chronic pancreatitis and pancreatic ductal adenocarcinoma (PDAC).

METHOD AND MATERIALS

A repeatability study using 3D-EPI MRE was conducted in 5 healthy volunteers and 8 patients confirmed by histopathologic examinations (5 with PDAC and 3 with chronic pancreatitis). Subjects were scanned by using a GE 3.0 T MR scanner to assess the mean stiffness of the tumors in PDAC cases, the parenchyma of pancreas in chronic pancreatitis cases and healthy volunteers with a multi-slice EPI pulse sequence(timepoint 1). Direct inversion algrithm with 3D post-processing was used to estimate shear stiffness and generate stiffness maps. Subjects were re-evaluated one day later (timepoint 2).Stiffness was measured by 2 independent analysts (one with three and another with one year experience of MRE measurement).

RESULTS

For the 2 analysts, the mean stiffness in all subjects was highly reproducible with intraclass correlation coefficient (ICC) of 0.975(95% confidence interval [CI]: 0.944-0.989) across timepoints (r=0.973,P<0.001). Bland-Altman analysis showed mean stiffness difference was 0.01kPa(95% agreement limits:-0.54-0.55kPa). For the 2 timepoints, the ICC was 0.973(95% CI: 0.940-0.988) across the 2 analysts (r=0.975,P<0.001). Bland-Altman analysis showed the stiffness difference was 0.05kPa(95% agreement limits:-0.51-0.62kPa). The averaging stiffness value was $1.46\pm0.21kPa$ for chronic pancreatitis and $3.28\pm1.09kPa$ for PDAC, in contrast with $1.11\pm0.08kPa$ for normal pancreas.

CONCLUSION

3D MRE is a highly reproducible modality for assessing stiffness of pancreas.

CLINICAL RELEVANCE/APPLICATION

It is suggested to incorporate MRE into a standard MRI study, which offers stable and accurate stiffness of pancreas and pancreatic masses relatively.

BR

DM

Breast Imaging (Density and Risk Assessment)

Wednesday, Dec. 2 10:30AM - 12:00PM Location: Arie Crown Theater

AMA PRA Category 1 Credits ™: 1.50 ARRT Category A+ Credits: 1.50

FDA Discussions may include off-label uses.

Participants

Jennifer A. Harvey, MD, Charlottesville, VA (*Moderator*) Researcher, Hologic, Inc; Researcher, VuCOMP, Inc; Researcher, Matakina Technology Limited; Shareholder, Hologic, Inc

Emily F. Conant, MD, Philadelphia, PA (*Moderator*) Speaker, Hologic, Inc; Scientific Advisory Board, Hologic, Inc; Consultant, Siemens AG

Martin J. Yaffe, PhD, Toronto, ON (*Moderator*) Research collaboration, General Electric Company Founder, Matakina International Ltd Shareholder, Matakina International Ltd Co-founder, Mammographic Physics Inc

Sub-Events

SSK01-01 Breast Density: Who is Informing the Patients?

Wednesday, Dec. 2 10:30AM - 10:40AM Location: Arie Crown Theater

Participants

Shadi Aminololama-Shakeri, MD, Sacramento, CA (*Presenter*) Nothing to Disclose Machelle D. Wilson, Sacramento, CA (*Abstract Co-Author*) Nothing to Disclose Kathleen A. Khong, MD, Sacramento, CA (*Abstract Co-Author*) Nothing to Disclose Jonathan B. Hargreaves, MD, Boston, MA (*Abstract Co-Author*) Nothing to Disclose Karen K. Lindfors, MD, Sacramento, CA (*Abstract Co-Author*) Research Grant, Hologic, Inc

PURPOSE

To assess the impact of California's Breast Density law on radiology technologists.

METHOD AND MATERIALS

Attendees of an educational conference targeted to radiology technologists in California were surveyed anonymously and voluntarily. Fisher's Exact Test was used to test for association between practice responses and technologist characteristics. Data were analyzed using SAS® software version 9.3 (SAS Institute, Cary, NC). A p-value of <=0.05 was considered significant.

RESULTS

110 of 133 attendees (83% response rate) completed the survey. 67% of respondents have noticed a change in patients' level of concern about breast density with 53% answering breast density related questions daily. The majority of respondents reported being asked what breast density means and what dense breasted patients should do subsequently (82%); specifically, 59% reported the topic of supplemental screening tests due to dense breasts as a common patient concern. More than half refer the patient to her doctor (63%) and explain that the patient may need additional imaging (55%). While 71% reported being completely/mostly comfortable, 22% were only somewhat comfortable and 5% were not comfortable in answering patient questions about breast density (2% reported not receiving any density questions). As expected, technologist level of comfort answering these questions was higher for those with >20 years of experience (79%) in comparison to those with <=20 years of work experience (57%, p=0.02) and was independent of dedicated mammography work time (p=0.304). 88% of technologists expressed an interest in further education regarding breast density.

CONCLUSION

Although the California breast density law recommends that patients discuss their breast density and supplementary screening tests with their primary care physicians, women are seeking information from radiology technologists about breast density daily. While technologists with more than 20 years of experience are more comfortable answering these questions, the majority of technologists regardless of years of experience are interested in further education about breast density and its impact on breast cancer screening.

CLINICAL RELEVANCE/APPLICATION

Breast density is of great concern to patients and providers. Radiology technologists are often the first provider the patient encounters for breast cancer screening. There is a need for additional technologist education.

SSK01-02 National Trends in Reporting of Breast Density in Response to Breast Density Notification Legislation

Wednesday, Dec. 2 10:40AM - 10:50AM Location: Arie Crown Theater

Awards

Trainee Research Prize - Fellow

Participants

Manisha Bahl, MD, MPH, Durham, NC (*Presenter*) Nothing to Disclose Jay A. Baker, MD, Durham, NC (*Abstract Co-Author*) Research Consultant, Siemens AG Mythreyi Bhargavan-Chatfield, PhD, Reston, VA (*Abstract Co-Author*) Nothing to Disclose Eugenia K. Brandt, Washington, DC (*Abstract Co-Author*) Nothing to Disclose Sujata V. Ghate, MD, Durham, NC (*Abstract Co-Author*) Nothing to Disclose Since 2009, a total of 21 states have enacted laws that mandate notification of patients and their referring physicians if the patient's breast density is interpreted as heterogeneously dense or extremely dense on mammography. The purpose of this study is to evaluate trends in the reporting of breast density in response to breast density notification legislation.

METHOD AND MATERIALS

Using the American College of Radiology's National Mammography Database (NMD), we collected state-level data, month-by-month over a 20-month period, on the percentage of mammograms reported as heterogeneously dense or extremely dense and the breast cancer detection rate. Z -tests were used to calculate differences in proportions, and p -values less than 0.05 were considered statistically significant.

RESULTS

Thirteen of 17 states that had breast density notification legislation in place as of 2014 had submitted data to the NMD before and after law enactment and were thus included in the analysis. 959,648 mammograms were performed over a 20-month period, ten months before and after law enactment. There was a statistically significant decrease in the percentage of mammograms reported as dense in the month after law enactment compared to the month before (40.0% vs 43.0%, p <0.001). The percentage of mammograms reported as dense reached its nadir two months after law enactment (39.3%) but increased to 42.8% by ten months after law enactment. There was no statistically significant difference in the percentage of mammograms reported as dense in the month before law enactment compared to ten months after law enactment (43.0% vs 42.8%, p =0.65). There were no statistically significant differences in the breast cancer detection rate in the month before and after law enactment (3.9/1000 vs 3.8/1000, p =0.79) or in the month before law enactment compared to ten months after law enactment (3.9/1000 vs 4.2/1000, p =0.55).

CONCLUSION

The percentage of mammograms reported as dense decreased immediately after enactment of breast density notification legislation but then returned to pre-legislation percentages during the study period.

CLINICAL RELEVANCE/APPLICATION

Enactment of breast density notification legislation has an immediate but not long term impact on the reporting of dense breasts on mammography.

SSK01-03 Body Mass Index, Breast Density and the Risk of Breast Cancer Development

Wednesday, Dec. 2 10:50AM - 11:00AM Location: Arie Crown Theater

Participants Rasha M. Kamal, MD, Cairo, Egypt (*Presenter*) Nothing to Disclose Dorria S. Salem, MD, Cairo, Egypt (*Abstract Co-Author*) Nothing to Disclose Sarah A. Maksoud, MBBCh, Cairo, Egypt (*Abstract Co-Author*) Nothing to Disclose Rasha Wessam, MD, PhD, Cairo, Egypt (*Abstract Co-Author*) Nothing to Disclose Soha T. Hamed, MD, Cairo, Egypt (*Abstract Co-Author*) Nothing to Disclose Ahmed M. Hatw, Cairo, Egypt (*Abstract Co-Author*) Nothing to Disclose

PURPOSE

The relationship between body mass index (BMI), mammographic breast density and breast cancer is complex.BMI is negatively correlated with mammographic density and in the same time they are both accused of increasing the risk of breast cancer.Therefore, the aim of this study is to assess the relationship between BMI, mammographic density and breast cancer in a screened population.

METHOD AND MATERIALS

The study included 117,636 women, above the age of 45 years, who joined a National Breast Cancer Screening Program in the period from October 2007 to April 2014. All patients performed a mammography examination and the breast density was reported by 3 independent readers. The breast density was classified according to the ACR BI-RADS lexicon breast density classification from a completely fatty breast (a) to an extremely dense breast (d). The weight and height were measured and the BMI was calculated. Individuals with a BMI> 25 are considered overweight and above 30 as obese. Categorical data was expressed as frequencies and relative frequencies, measures of association were verified by calculating the relative risk (RR), Odds Ratio (OR) and confidence interval (CI). The p value was calculated using the chi square test..

RESULTS

The study included 117,636 women out of which 1048 (0.89%) cases had breast cancer. Increased BMI was associated with statisticaly significant increased risk of breast cancer development than normal weight individuals (p value: 0.02). The calculated RR is 1.4 (95% CI: 1.0355 - 1.896) and odds ratio is 1.4 (95% CI: 1.036 - 1.905). The mammographic breast density was not associated with an increased risk of breast cancer development were the RR is 0.959 (95%CI: 0.59 - 1.57) and OR is 0.95 (95% CI: 0.58 - 1.57). High BMI was associated with a fatty breast parenchyma (p value: 0.0001) and the calculated RR was 13.9 (95% CI: 6.4 - 30.1)

CONCLUSION

A strong negative correlation exists between BMI and breast density where as the BMI increases the breast density decreases. In the current study increased BMI was associated with an indreased risk of breast camcer development while an increased breast density was not.

CLINICAL RELEVANCE/APPLICATION

Obesity is a strong risk factor for breast cancer development. Breast cancer preventive strategies should be applied with higher concern for obese women and strict weight control strategies should be implemented especially for women at higher age risks of developing breast cancer.

SSK01-04 Quantifying the Potential Masking Risk of Breast Density in Mammographic Screening

Wednesday, Dec. 2 11:00AM - 11:10AM Location: Arie Crown Theater

Participants

Stamatia V. Destounis, MD, Scottsville, NY (*Presenter*) Research Grant, FUJIFILM Holdings Corporation; Research Grant, Hologic, Inc; Research Grant, QT Ultrasound LLC

Ariane Chan, PhD, Wellington, New Zealand (Abstract Co-Author) Employee, Matakina Technology Limited;

Andrea L. Arieno, BS, Rochester, NY (Abstract Co-Author) Nothing to Disclose

Renee Morgan, RT, Rochester, NY (Abstract Co-Author) Nothing to Disclose

Lisa R. Johnston, PhD, Wellington, New Zealand (Abstract Co-Author) Consultant, Matakina Technology Limited

Ralph P. Highnam, PhD, Wellington, New Zealand (*Abstract Co-Author*) CEO, Matakina Technology Limited; CEO, Volpara Solutions Limited

PURPOSE

To compare the current method of reporting on reduced mammographic sensitivity, using the American College of Radiology (ACR) BI-RADS density categories, with quantitatively assessed volumetric breast density (VBD).

METHOD AND MATERIALS

This IRB-approved, retrospective study included histologically confirmed DCIS, invasive ductal or invasive lobular breast cancers detected at screening (SC; n = 654) or in the interval between screens (IC; n = 120), in women (aged > 40 y) diagnosed at a community based breast center between Jan 2009 and Dec 2012. Women with bilateral cancer, prior breast surgery or missing raw digital images were excluded from the analysis. Density was determined according to the ACR BI-RADS 4th edition density categories 1-4, and an automated equivalent, Volpara Density Grade (VDG), which uses preset thresholds of VBD to assign each category (i.e. <4.5, 4.5-7.5, 7.5-15.5, >15.5%). Sensitivity (SC/[SC + IC]) was compared between the two density measures and within each VDG category, by dividing each category into high and low using the mid-point of each VDG thresholds (i.e. 3.75, 6, 11 and 25.5%, for VDG 1, 2, 3 and 4, respectively).

RESULTS

The decreasing sensitivity of double-reading mammographic screening across increasing ACR density categories 1 to 4 was clear for automated BI-RADS (95/89/83/66%) but less so for visual BI-RADS, apart from 1 versus 4 (82/90/84/67%). Further dichotomization of each VDG category showed a striking linear relationship between VBD and sensitivity (R2=0.97). Sensitivity was similar between low versus high VDG1 (100% and 94%, respectively) and low versus high VDG2 cases (89% and 89%, respectively), but decreased more dramatically between low versus high VDG3 and low versus high VDG4 cases (87% to 75% and 68% to 53%, respectively).

CONCLUSION

Quantitative VBD captures the potential masking risk of breast density more precisely compared to the widely used BI-RADS density classification system. In the US, women with dense breasts (BI-RADS 3 and 4 density categories) comprise \sim 50% of all women, and our results indicate that within these categories there is a large range in sensitivity that is not being captured using the BI-RADS system.

CLINICAL RELEVANCE/APPLICATION

Volumetric breast density shows a linear relationship with mammographic sensitivity and can be used to more accurately determine the effect of density on masking compared to BI-RADS density categories.

SSK01-05 Assessing Breast Cancer Masking Risk with Automated Texture Analysis in Full Field Digital Mammography

Wednesday, Dec. 2 11:10AM - 11:20AM Location: Arie Crown Theater

Participants

Michiel Kallenberg, Copenhagen, Denmark (*Presenter*) Former Employee, Matakina Technology Limited; Employee, Biomediq A/S; Employee, Screenpoint Medical BV

Martin Lillholm, PhD, Copenhagen, Denmark (Abstract Co-Author) Employee, Biomedia A/S Shareholder, Biomedia A/S

Pengfei Diao, Copenhagen, Denmark (Abstract Co-Author) Nothing to Disclose

Kersten Petersen, Copenhagen O, Denmark (Abstract Co-Author) Employee, Biomediq A/S

Katharina Holland, Nijmegen, Netherlands (Abstract Co-Author) Nothing to Disclose

Nico Karssemeijer, PhD, Nijmegen, Netherlands (*Abstract Co-Author*) Shareholder, Matakina Technology Limited; Consultant, QView Medical, Inc; Shareholder, QView Medical, Inc; Director, ScreenPoint Medical BV; Shareholder, ScreenPoint Medical BV;

Christian Igel, Copenhagen, Denmark (*Abstract Co-Author*) Research funded, Biomediq A/S

Mads Nielsen, PhD, Copenhagen, Denmark (*Abstract Co-Author*) Stockholder, Biomediq A/S Research Grant, Nordic Bioscience A/S Research Grant, SYNARC Inc Research Grant, AstraZeneca PLC

PURPOSE

The goal of this work is to develop a method to assess the risk of breast cancer masking, based on image characteristics beyond breast density.

METHOD AND MATERIALS

From the Dutch breast cancer screening program we collected 285 screen detected cancers, and 109 cancers that were screen negative and subsequently appeared as interval cancers. To obtain mammograms without cancerous tissue, we took the contralateral mammograms. We developed a novel machine learning based method called convolutional sparse autoencoder to characterize mammographic texture. The reason for focusing on mammographic texture rather than the amount of breast density is that a developing cancer may not only be masked because it is obscured; it may also be masked because its mammographic signs resemble the texture of normal tissue. The method was trained and tested on raw mammograms to determine cancer detection status in a five-fold cross validation. To assess the interaction of the texture scores with breast density, Volpara Density Grade (VDG) was determined for each image using Volpara, Matakina Technology, New Zealand.

RESULTS

We grouped women into low (VDG 1/2) versus high (VDG 3/4) dense, and low (Quartile 1/2) versus high (Quartile 3/4) texture risk score. We computed odds ratios (OR) for breast cancer masking risk (i.e. interval versus screen detected cancer) for each of the

subgroups. The OR was 1.63 (1.04-2.53 95%CI) for the high dense group (as compared to the low dense group), whereas for the high texture score group (as compared to the low texture score group) this OR was 2.19 (1.37-3.49). Women who were classified as low dense but had a high texture score had a higher masking risk (OR 1.66 (0.53-5.20)) than women with dense breasts but a low texture score.

CONCLUSION

Mammographic texture is associated with breast cancer masking risk. We were able to identify a subgroup of women who are at an increased risk of having a cancer that is not detected due to textural masking, even though their breasts are non-dense.

CLINICAL RELEVANCE/APPLICATION

Automatic texture analysis enables assessing the risk that a breast cancer is masked in regular mammography, independently of breast density. As such it offers opportunities to further enhance personalized breast cancer screening, beyond breast density.

Agreement between Breast Density Estimates from Standard versus Synthetic Digital Mammograms SSK01-06

Wednesday, Dec. 2 11:20AM - 11:30AM Location: Arie Crown Theater

Participants

Brad M. Keller, PhD, Philadelphia, PA (Presenter) Nothing to Disclose Jinbo Chen, PhD, Philadelphia, PA (Abstract Co-Author) Nothing to Disclose Lauren Pantalone, BS, Philadelphia, PA (Abstract Co-Author) Nothing to Disclose Shonket Ray, PhD, Philadelphia, PA (Abstract Co-Author) Nothing to Disclose Marie Synnestvedt, Philadelphia, PA (Abstract Co-Author) Nothing to Disclose Emily F. Conant, MD, Philadelphia, PA (Abstract Co-Author) Speaker, Hologic, Inc; Scientific Advisory Board, Hologic, Inc; Consultant, Siemens AG

Despina Kontos, PhD, Philadelphia, PA (Abstract Co-Author) Nothing to Disclose

PURPOSE

Mammographic density is an established risk factor for breast cancer, with legislation now mandating the reporting of a woman's breast density in many states. However, as synthetic 2D mammograms are being used to reduce dose when screening is performed with digital breast tomosynthesis (DBT), standard-dose mammograms that have commonly been used to evaluate breast density may no longer be acquired. As such, the purpose of this study is to evaluate the agreement between breast density estimates from standard dose versus synthetic mammograms.

METHOD AND MATERIALS

We retrospectively analyzed 755 negative (BIRADS 1 or 2) DBT screening exams consecutively acquired over a four week period at our institution for which both standard dose and synthetic mammograms were available. All mammograms were acquired on a Hologic Selenia Dimensions system, and synthetic mammograms were generated using the FDA-approved Hologic "C-View" software. The "For Presentation" standard-dose and synthetic mammograms were analyzed using a publically available algorithm developed at our institution that provides validated, reproducible breast percent density (PD%) estimates from digital mammograms. Agreement between PD% estimates from the two modalities was assessed via Pearson's correlation and linear regression, and Student's paired t-test was used to evaluate the presence of a systematic difference in density estimates between the two mammogram types.

RESULTS

Breast PD% estimates made on the synthetic and standard dose mammograms were highly correlated (r=0.92, p<0.001). However, a significant difference was observed between the two mammogram types, with synthetic mammograms yielding larger PD% estimates by an average of 2.0% higher than standard dose mammograms (p<0.001), with larger disagreement in highly dense women.

CONCLUSION

Breast density estimates made from synthetic mammograms are comparable to those made from standard dose mammograms. Furthermore, fully-automated analysis of breast density from synthetic mammograms is feasible, which may become important as standard dose images are increasingly no longer required when screening with DBT.

CLINICAL RELEVANCE/APPLICATION

Synthetic mammograms may allow for accurate estimation of a woman's breast density if standard dose mammograms are not obtained in DBT screening, particularly if automated software is utilized.

SSK01-07 Associations of Dense and Fatty Breast-Tissue Heterogeneity with Breast Cancer Risk: Preliminary **Evaluation Using Parenchymal Texture Measurements Driven by Breast Anatomy**

Wednesday, Dec. 2 11:30AM - 11:40AM Location: Arie Crown Theater

Participants

Aimilia Gastounioti, Philadelphia, PA (Presenter) Nothing to Disclose Brad M. Keller, PhD, Philadelphia, PA (Abstract Co-Author) Nothing to Disclose Lauren Pantalone, BS, Philadelphia, PA (Abstract Co-Author) Nothing to Disclose Meng-Kang Hsieh, Philadelphia, PA (Abstract Co-Author) Nothing to Disclose Andrew Oustimov, Philadelphia, PA (Abstract Co-Author) Nothing to Disclose Emily F. Conant, MD, Philadelphia, PA (Abstract Co-Author) Speaker, Hologic, Inc; Scientific Advisory Board, Hologic, Inc; Consultant, Siemens AG Despina Kontos, PhD, Philadelphia, PA (Abstract Co-Author) Nothing to Disclose

PURPOSE

We investigate the potential different contributions of dense versus fatty breast tissue in breast cancer risk assessment, using quantitative descriptors of parenchymal heterogeneity driven by breast anatomy.

Contralateral, raw mediolateral-oblique (MLO) view digital mammograms (DMs) from 106 women with unilateral invasive breast cancer and 318 age- and side-matched controls were retrospectively analyzed. DMs were acquired with either a GE Healthcare 2000D or DS FFDM system and the "For Processing" images were used. A previously validated algorithm was used to automatically segment the dense and fatty tissue areas within the breast and estimate percent density (%PD). Parenchymal heterogeneity analysis was performed using a breast-anatomy-driven framework, in which a polar grid following the anatomy of the breast parenchyma was overlaid on the DM. Established tissue-heterogeneity descriptors were extracted (i.e., a total of 15 gray-level, non-uniformity, contrast, correlation, etc. texture features), aligned with the structure of the polar grid. The mean values of these texture descriptors over the dense and fatty breast sub-regions were estimated. Associations between heterogeneity features and breast cancer were evaluated using logistic regression and the area under the receiver operating characteristic (ROC) curve (AUC) was used to assess discriminatory capacity, where model performance was compared using the DeLong's test.

RESULTS

Individual tissue heterogeneity features had different discriminatory capacity in dense versus fatty parenchyma. Multivariable models were equally associated with breast cancer for both dense and fatty tissue (AUC: 0.82, p<0.001), though different texture features were deemed significant for each tissue type. There was no performance improvement by adding %PD, while the strongest association was achieved when dense and fatty tissue heterogeneity features were combined (AUC: 0.87, p<0.001).

CONCLUSION

Heterogeneity features for dense and fatty parenchymal patterns, as measured using a breast-anatomy-driven framework, may hold a promising role in breast cancer risk prediction.

CLINICAL RELEVANCE/APPLICATION

Inherent biological factors, which are associated with the risk of breast cancer, might be expressed in parenchymal tissue as an interplay between dense and fatty tissue heterogeneity.

SSK01-08 Background Parenchymal Uptake (BPU) at Molecular Breast Imaging as a Novel Breast Cancer Risk Factor

Wednesday, Dec. 2 11:40AM - 11:50AM Location: Arie Crown Theater

Participants

Carrie B. Hruska, PhD, Rochester, MN (*Presenter*) Institutional license agreement, Gamma Medica, Inc Christopher G. Scott, MS, Rochester, MN (*Abstract Co-Author*) Nothing to Disclose Deborah J. Rhodes, MD, Rochester, MN (*Abstract Co-Author*) Nothing to Disclose Amy L. Conners, MD, Rochester, MN (*Abstract Co-Author*) Nothing to Disclose Dana H. Whaley, MD, Rochester, MN (*Abstract Co-Author*) Nothing to Disclose Michael K. O'Connor, PhD, Rochester, MN (*Abstract Co-Author*) Royalties, Gamma Medica, Inc Celine M. Vachon, Rochester, MN (*Abstract Co-Author*) Consultant, Pfizer Inc

PURPOSE

In prior evaluations of molecular breast imaging (MBI) for supplemental screening in dense breasts, we observed wide variability in background parenchymal uptake (BPU), which refers to the relative uptake of Tc-99m sestamibi within normal fibroglandular tissue compared to fat. In women with similar mammographic density, BPU varied from photopenic (fibroglandular uptake less intense than fat uptake) to marked (fibroglandular uptake >2 times as intense as fat uptake). Here, we investigated whether BPU is associated with subsequent breast cancer development.

METHOD AND MATERIALS

We conducted a nested case-control study among women with MBI examinations performed between the years 2005-2014. Women with breast cancer history or diagnosis within 60 days after MBI were excluded. A total of 77 incident breast cancer cases were identified through linkage our institution's tumor registry; 225 controls were matched to cases on age, MBI date, menopausal status, and follow-up. While blinded to case-control status, BPU was assessed by an expert reader according to a validated MBI lexicon into one of 4 categories: photopenic, minimal-mild, moderate, or marked. Conditional logistic analysis was performed.

RESULTS

Women with high BPU at MBI (moderate or marked) had a greater risk of breast cancer compared to women with low BPU (photopenic or minimal-mild); odds ratio (OR (95% CI) = 5.5 (2.6,11.6)). Results were unchanged with adjustment for BI-RADS density (OR = 5.5 (2.6, 11.6)) and BMI (OR = 5.4 (2.6, 11.4)). The association of BPU and breast cancer was stronger for cases diagnosed <3 years (OR=10.6) compared to cases diagnosed \geq 3 years (OR=4.2), although power was limited.

CONCLUSION

BPU at MBI is associated with breast cancer risk. The odds of developing breast cancer was 5.5 times greater for women with high BPU compared to women with low BPU.

CLINICAL RELEVANCE/APPLICATION

Over 40% of the screening-eligible population have mammographically dense breasts. BPU is a breast cancer risk factor, based on functional behavior of fibroglandular tissue, that may help identify the subset of women with dense breasts who are most likely to benefit from supplemental screening and risk-reduction options.

SSK01-09 Volumetric Breast Density a Strong Independent Predictor of Interval Cancer Risk

Wednesday, Dec. 2 11:50AM - 12:00PM Location: Arie Crown Theater

Participants

Stamatia V. Destounis, MD, Scottsville, NY (*Presenter*) Research Grant, FUJIFILM Holdings Corporation; Research Grant, Hologic, Inc; Research Grant, QT Ultrasound LLC

Ariane Chan, PhD, Wellington, New Zealand (*Abstract Co-Author*) Employee, Matakina Technology Limited; Andrea L. Arieno, BS, Rochester, NY (*Abstract Co-Author*) Nothing to Disclose Renee Morgan, RT, Rochester, NY (*Abstract Co-Author*) Nothing to Disclose Ralph P. Highnam, PhD, Wellington, New Zealand (*Abstract Co-Author*) CEO, Matakina Technology Limited; CEO, Volpara Solutions Limited

Lisa R. Johnston, PhD, Wellington, New Zealand (Abstract Co-Author) Consultant, Matakina Technology Limited

PURPOSE

Breast density (BD) is a key factor limiting the sensitivity of mammographic screening. We sought to evaluate which patient factors might best predict the risk of being diagnosed with an interval cancer.

METHOD AND MATERIALS

This IRB-approved, retrospective analysis included histologically confirmed DCIS, invasive ductal or invasive lobular breast cancers detected at screening (SC; n = 514) or in the interval between screens (IC; n = 82). Patient histories were reviewed for women aged over 40 y, diagnosed between January 2009 and December 2012, and with raw mammographic images available. In addition to BD categories assessed visually (BI-RADS 1-4) and automatically (Volpara Density Grade; VDG 1-4), BD was assessed using a continuous measure of volumetric breast density (VBD). Univariate analyses and multivariate logistic regression (adjusting for age and menopausal status) were used to identify predictors of IC risk.

RESULTS

BD was the only independent predictor of IC risk in the multivariate analyses. Women with BI-RADS4 and VDG4 breasts were at 3.6fold [CI 1.7 - 7.7] and 3.9-fold [CI 2.0 - 7.6] more likely to be diagnosed with an IC versus a SC, compared to women with nondense breasts (BI-RADS/VDG 1 and 2), or 4.0-fold [CI 1.8 - 8.8] for women in the highest quartile of VBD versus the lowest. Restricted to invasive cancers only (n = 456), VDG, VBD and BI-RADS were all independent risk factors for IC versus SC (i.e. 4.7fold [CI 2.3 - 9.7] for VDG4 versus VDG1/2; 4.5-fold [CI 1.9 - 10.6] for the highest quartile of VBD versus the lowest quartile; and 3.5-fold [CI 1.6 - 8.1] for BI-RADS4 versus BI-RADS1/2).

CONCLUSION

Although VBD, and visual and automated assessments of BI-RADS density categories are all strongly associated with being diagnosed with an IC versus a SC, volumetric methods were stronger predictors of invasive IC risk and could be used to accurately identify which women may benefit the most from supplementary imaging.

CLINICAL RELEVANCE/APPLICATION

Volumetric breast density is a strong independent predictor of interval cancer risk and, due to its continuous nature, can be used to better identify women who might benefit from adjunctive screening.

ISP: Gastrointestinal (Colon Cancer Screening and Staging)

Wednesday, Dec. 2 10:30AM - 12:00PM Location: E351

GI CT MR OI

AMA PRA Category 1 Credits ™: 1.50 ARRT Category A+ Credits: 1.50

FDA Discussions may include off-label uses.

Participants

David H. Kim, MD, Madison, WI (*Moderator*) Consultant, Viatronix, Inc; Co-founder, VirtuoCTC, LLC; Medical Advisory Board, Digital ArtForms, Inc; Stockholder, Cellectar Biosciences, Inc

Christine O. Menias, MD, Scottsdale, AZ (Moderator) Nothing to Disclose

Sub-Events

SSK06-01 Gastrointestinal Keynote Speaker: Update on Colon Cancer Screening and CTC

Wednesday, Dec. 2 10:30AM - 10:40AM Location: E351

Participants

David H. Kim, MD, Madison, WI (*Presenter*) Consultant, Viatronix, Inc; Co-founder, VirtuoCTC, LLC; Medical Advisory Board, Digital ArtForms, Inc; Stockholder, Cellectar Biosciences, Inc

SSK06-02 CT Colonography versus Flexible Sigmoidoscopy for Colorectal Cancer Screening. Outcomes of a Randomized Controlled Trial (RCT)

Wednesday, Dec. 2 10:40AM - 10:50AM Location: E351

Participants

Daniele Regge, MD, Candiolo, Italy (*Presenter*) Speakers Bureau, General Electric Company Loredana Correale, PhD, Turin, Italy (*Abstract Co-Author*) Researcher, im3D SpA Carlo Senore, MD, Torino, Italy (*Abstract Co-Author*) Nothing to Disclose Cesare Hassan, Rome, Italy (*Abstract Co-Author*) Nothing to Disclose Gabriella Iussich, MD, Locarno, Switzerland (*Abstract Co-Author*) Consultant, im3D SpA Nereo Segnan, Torino, Italy (*Abstract Co-Author*) Nothing to Disclose Stefania Montemezzi, MD, Verona, Italy (*Abstract Co-Author*) Nothing to Disclose

PURPOSE

To compare detection rate (DR) of CT colonography (CTC) and flexible sigmoidoscopy (FS) for CRC screening.

METHOD AND MATERIALS

An invitation letter to participate in a multicenter randomized screening trial was mailed to people aged 58-60 years, living in the Piedmont Region, Italy and in Verona, Italy. Individuals with a history of CRC/adenomas, inflammatory bowel disease, recent colonoscopy, or two first-degree relatives with CRC were excluded from invitation by their general practitioners. Responders to the invitation were randomized to either CTC or FS and scheduled for screening procedure. CTC interpretations were remotely performed via telediagnosis, and were assisted by a Computer-aided detection software. Participants with polyps≥6-mm at CTC and those with "high-risk" distal lesions (i.e., adenomas>10-mm, or high-grade dysplasia, or villous component >20%, or >2 adenomas of any type) at FS were referred for colonoscopy (CC). The primary outcome was DR of advanced neoplasia (AN), namely, the number of participants with CRC or advanced adenomas relative to the total number of participants. Differences were expressed as relative risk (RR) with 95% CIs.

RESULTS

5412 people agreed to take part in the trial: 2738 randomly assigned to FS and 2674 to CTC. After excluding participants with inadequate bowel preparation, analysis included 2673 (1298 females) adequate FS examinations and 2595 (1266 females) diagnostic CTC exams. Of FS participants, 271 (10.1%) were referred to CC; compliance to CC was 86.7% (235). Of CTC participants. 264 (10.2%) were offered CC, of whom 260 (98.5%) performed the exam. DR of AN was 4.7% (127 including 9 CRCs) for FS vs. 5.1% (133 including 10 CRCs) for CTC [RR: 1.1; 95% CI: 0.9-1.4; P=0.524]. DR of distal AN was 4.1% (109) for FS and 2.9% (76) for CTC [RR: 0.72; 95% CI: 0.54-0.96; P=0.025]. DR of proximal AN was 1.3% (34) for FS and 2.7% (69) for CTC [RR: 2.06; 95% CI: 1.37-3.10; P<0.001]. Isolated proximal AN were present in 2.3% and 0.67% of CTC and FS participants, respectively.

CONCLUSION

No significant differences were seen in AN detection for the two screening groups. However, DR of distal AN was 30% lower in CTC than in FS screening, while DR of proximal AN was two times higher following screening with CTC than with FS.

CLINICAL RELEVANCE/APPLICATION

Our study supports the hypothesis that CTC screening may have a larger impact on reduction of proximal CRC incidence than FS.

SSK06-03 Natural Course of Medium-sized Polyps during a 3-year Surveillance Interval: Linear and Volumetric Assessment with CT Colonography in Correlation with Histology

Wednesday, Dec. 2 10:50AM - 11:00AM Location: E351

Participants Charlotte J. Tutein Nolthenius, Amsterdam, Netherlands (*Presenter*) Nothing to Disclose Thierry N. Boellaard, MD, PhD, Amsterdam, Netherlands (*Abstract Co-Author*) Nothing to Disclose Yung Nio, MD, Amsterdam, Netherlands (*Abstract Co-Author*) Nothing to Disclose Maarten G. Thomeer, MD, Rotterdam, Belgium (*Abstract Co-Author*) Nothing to Disclose Shandra Bipat, MS, Amsterdam, Netherlands (*Abstract Co-Author*) Nothing to Disclose Margriet de Haan, MD, Utrecht, Netherlands (*Abstract Co-Author*) Nothing to Disclose A D. Montauban van Swijndregt, MD, PhD, Amsterdam, Netherlands (*Abstract Co-Author*) Nothing to Disclose Katharina Biermann, PhD, Rotterdam, Netherlands (*Abstract Co-Author*) Nothing to Disclose Marc van de Vijver, Amsterdam, Netherlands (*Abstract Co-Author*) Nothing to Disclose Ernst Kuipers, MD, Rotterdam, Netherlands (*Abstract Co-Author*) Nothing to Disclose Evelien Dekker, MD, PhD, Amsterdam, Netherlands (*Abstract Co-Author*) Nothing to Disclose Jaap Stoker, MD, PhD, Amsterdam, Netherlands (*Abstract Co-Author*) Research Consultant, Robarts Clinical Trials

PURPOSE

Volumetric growth assessment in medium-sized polyps has shown to be more reliable than linear measurements and it seems a promising biomarker for determination of clinical importance. This is however not standard practice in reporting on polyps with CT colonography (CTC) and more experience and research is needed.

METHOD AND MATERIALS

Ethics approval and written informed consent were obtained. After participating in an invitational population-based CTC screening trial 101 participants harbored one or two 6-9 mm polyps as the largest lesion(s) for which surveillance CTC was advised after 3 years. Participants with lesion(s) of \geq 6 mm at surveillance CTC were offered colonoscopy and polypectomy. Volumetric and linear measurements were performed on index and surveillance CTC and polyps were classified into baseline growth categories according to \pm 30% volumetric change over the entire surveillance interval (>30% growth as progression, 30% growth to -30% decrease as stable and >-30% decrease as regression). Polyp growth was correlated to histopathological findings and other polyp characteristics.

RESULTS

Between July 2012 and May 2014, 78 of 101 patients underwent surveillance CTC (mean age 65.6 (SD 6.7); 51% male). After a mean surveillance interval of 3.3 years (SD 0.3; range 3.0-4.6 years) of 95 polyps 33 (35%) progressed, 36 (38%) remained stable and 26 (27%) regressed, including an apparent resolution in 13 (14%) polyps. Of 20 proven advanced adenomas, 14 (70%) progressed and 6 (30%) remained stable, compared to 13 (37%) and 16 (46%) of 35 non-advanced adenomas. No associations were found between growth categories and polyp morphology, location and size at index CTC. Other linear or volumetric thresholds used did not identify more advanced adenomas.

CONCLUSION

Volumetric assessment showed one-third of medium-sized polyps to progress over time emphasizing the importance of these polyps. However, growth assessment was not able to identify all advanced adenomas as one-third remained stable in size over a 3-year surveillance interval. These findings must be taken into account when deciding on proper colonoscopy referral guidelines.

CLINICAL RELEVANCE/APPLICATION

Volumetric assessment showed one-third of medium-sized polyps to progress over time emphasizing the importance of these polyps.

SSK06-04 Five Years of CT Colonography in One Institution - How Many Cancers Have We Missed?

Wednesday, Dec. 2 11:00AM - 11:10AM Location: E351

Participants

David Little, MBChB, FRCR, Bristol, United Kingdom (*Presenter*) Nothing to Disclose Will Loughborough, MBChB,BSC, Bristol, United Kingdom (*Abstract Co-Author*) Nothing to Disclose Adam Youssef, BMedSc, BMBS, Bristol, United Kingdom (*Abstract Co-Author*) Nothing to Disclose Thomas Mendes da Costa, Bristol, United Kingdom (*Abstract Co-Author*) Nothing to Disclose Paul McCoubrie, MBBS, FRCR, Bristol, United Kingdom (*Abstract Co-Author*) Nothing to Disclose

PURPOSE

CT colonography is used in our institution in the diagnosis of colorectal carcinoma in both screening and symptomatic populations. The primary purpose of this study was to determine the sensitivity of CT colonography in our institution and compare with published evidence to ensure we are meeting quality standards.

METHOD AND MATERIALS

Our sample includes all patients with a diagnosis of colorectal carcinoma entered onto the cancer registry (the gold standard in UK cancer monitoring) between January 2010 and January 2015 who had previously had a CT colonography investigation. Each of these patients were reviewed on our radiological information system (RIS) to confirm whether CT colonography was used as part of the primary diagnosis. Demographic data and details about the tumour (such as location within the colon) were recorded. Any patients in which there was a suggestion that a carcinoma had been missed were reviewed in detail.

RESULTS

5058 CT colonography studies were performed in 4921 patients between January 2010 and January 2015 at our institution. 261 (5.1%) of these patients were identified as having a diagnosis of colorectal carcinoma on the cancer registry. 63 patients that underwent CT colonography following diagnosis (i.e. to look for synchronous tumour or as follow-up) were excluded. 198 (3.9%) of patients were diagnosed with colorectal carcinoma following a CT colonography investigation. In 3 (1.5%) of these patients the colorectal carcinoma was missed on CT colonography.

CONCLUSION

The sensitivity of CT Colonography for colorectal carcinoma in our institution is 98.5% which compares favourably with other published studies on CT colonography and colonoscopy. This confirms CT colonography as an important and valid tool in the diagnosis of colorectal carcinoma.

CLINICAL RELEVANCE/APPLICATION

Our study confirms that CT colongraphy is an important tool in the diagnosis of colorectal malignancy and is an example to other institutions in monitoring CT colonography outcomes and maintaining quality standards. During this presentation we will explore the common reasons for missed malignancy on CT colonography.

SSK06-05 CT Findings of Postpolypectomy Coagulation Syndrome in Patients Who Underwent Colonoscopic Polypectomy: Comparison with Those of Perforation

Wednesday, Dec. 2 11:10AM - 11:20AM Location: E351

Participants

Yoon Joo Shin, MD, Seongnam, Korea, Republic Of (*Presenter*) Nothing to Disclose Young Hoon Kim, MD, PhD, Seongnam-Si, Korea, Republic Of (*Abstract Co-Author*) Nothing to Disclose Yoon Jin Lee, MD, Seongnam-si, Korea, Republic Of (*Abstract Co-Author*) Nothing to Disclose Ji Hoon Park, MD, Seongnam-Si, Korea, Republic Of (*Abstract Co-Author*) Research Grant, Bracco Group Kyoung Ho Lee, MD, Seongnam-Si, Korea, Republic Of (*Abstract Co-Author*) Nothing to Disclose Ji Ye Sim, MD, MS, Seongnam-Si, Korea, Republic Of (*Abstract Co-Author*) Nothing to Disclose

PURPOSE

To describe CT findings of postpolypectomy coagulation syndrome (PPCS) and to identify the features that can distinguish it from colonic perforation after colonoscopic polypectomy.

METHOD AND MATERIALS

From January 2011 to November 2014, a total of 5542 adult (age>40yr) patient who underwent colonoscopic polypectomy were found according to search through hospital database. After reviewing the patient's medical and imaging records, eight patients (0.14%) with PPCS and six patients (0.11%) with perforation were identified. Because five patients were excluded due to absence of CT examination, four (1 male; age range, 52-75 years with mean age, 69 years) with PPCS and five patients (5 male; age range, 46-67 years with mean age, 54 years) with perforation were finally included. Two abdominal radiologists reviewed the abdominal CT images in a consensus manner. The following CT findings were assessed: presence of pneumoperitoneum or pneumoretroperitoneum, presence of fluid collection, presence of colonic wall thickening, if present, patterns, thickness and length of an involved segment, enhancement pattern of an involved segment, presence of mural defect in an involved segment, and presence of surrounding infiltration around an involved segment. Clinical findings including patient's symptom and sign were also assessed.

RESULTS

Although three patients with perforation eventually underwent surgery, all patients with PPCS were completely recovered only with conservative management. The clinical presentation including presence of abdominal pain or leukocytosis was not different between two groups. On CT, an involved colonic wall was more longer and thicker in PPCS group (mean length and width: 124 ± 81.3 mm, 16 ± 4.9 mm) than perforation group (41.4 ± 11.8 mm, 7.4 ± 1.5 mm). In all four patients with PPCS, CT images showed a marked low attenuation wall thickening with severe pericolic infiltration around an involved segment. None of the patients with PPCS showed free air on CT.

CONCLUSION

PPCS, a very rare complication after colonoscopic polypectomy (prevalence of 0.14%), shows severe low attenuating mural thickening. In comparison with perforation, PPCS does not demonstrate free air in peritoneal or retroperitoneal space

CLINICAL RELEVANCE/APPLICATION

The imaging features on CT can be useful to promptly distinguish PPCS from colonic perforation.

SSK06-06 Extracolonic Findings at Screening CT Colonography: Analysis of Incompletely Characterized and Likely Insignificant (C-RADS E3) Findings

Wednesday, Dec. 2 11:20AM - 11:30AM Location: E351

Participants

Bryan D. Pooler, MD, Madison, WI (Presenter) Nothing to Disclose

David H. Kim, MD, Madison, WI (*Abstract Co-Author*) Consultant, Viatronix, Inc; Co-founder, VirtuoCTC, LLC; Medical Advisory Board, Digital ArtForms, Inc; Stockholder, Cellectar Biosciences, Inc

Perry J. Pickhardt, MD, Madison, WI (*Abstract Co-Author*) Co-founder, VirtuoCTC, LLC; Stockholder, Cellectar Biosciences, Inc; Research Consultant, Bracco Group; Research Consultant, KIT; Research Grant, Koninklijke Philips NV

PURPOSE

To assess the incidence and outcomes of unexpected extracolonic findings at screening CTC which are likely insignificant and/or incompletely characterized (C-RADS E3), but may require further evaluation.

METHOD AND MATERIALS

7,952 consecutive patients (mean age 56.7±7.3 years, M:F 3,675:4,277) underwent first-time CTC screening over a 98-month interval. Persons with unsuspected C-RADS E3 findings were extracted and outcomes determined.

RESULTS

Previously unknown C-RADS E3 findings were identified in 9.2% (731/7,952; mean age 57.2±7.7 years; M:F 268:463) of the screening CTC population; 25 patients had multiple findings for a total of 757 E3 findings. Consideration for further imaging, if clinically appropriate, was suggested for 84% (634/757) of these findings, with clinical correlation suggested in the remainder. Dedicated follow-up imaging was obtained in 4.4% (353/7,952) of patients. Conditions requiring treatment or ongoing surveillance were diagnosed in 0.9% (72/7,952) of patients. Common extracolonic finding categories included: adnexal/uterine (24%, 185/757), lung (20%, 155/757), kidney/GU (20%, 149/757), and liver (11%, 85/757). Malignant or potentially malignant lesions were found in 0.2% (18/7,952) of patients, including renal cell carcinoma, lymphoma, breast cancer, and malignant/borderline ovarian cancer.

CONCLUSION

Likely insignificant/incompletely characterized (C-RADS E3) findings were found in 9.2% of patients undergoing screening CTC with consideration for additional imaging suggested in the majority. Follow-up imaging was actually obtained in 4.4%, with conditions ultimately requiring treatment or ongoing surveillance diagnosed in 0.9%. Malignant or potentially malignant lesions were found in 0.2% of the total cohort.

CLINICAL RELEVANCE/APPLICATION

Incompletely characterized and likely insignificant extracolonic (C-RADS E3) findings are uncommon, occurring in less than 10% of patients. Fewer than 1% of patients were diagnosed with conditions requiring treatment or continued surveillance. Extracolonic malignancies are rare in this group.

Honored Educators

Presenters or authors on this event have been recognized as RSNA Honored Educators for participating in multiple qualifying educational activities. Honored Educators are invested in furthering the profession of radiology by delivering high-quality educational content in their field of study. Learn how you can become an honored educator by visiting the website at: https://www.rsna.org/Honored-Educator-Award/

Perry J. Pickhardt, MD - 2014 Honored Educator

SSK06-07 Effect of Reducing Abdominal Compression during Prone CT Colonography on Ascending Colonic Rotation Occurring with Supine-to-prone Positional Change

Wednesday, Dec. 2 11:30AM - 11:40AM Location: E351

Participants

Jong Keon Jang, MD, Seoul, Korea, Republic Of (*Presenter*) Nothing to Disclose Seong Ho Park, MD, Seoul, Korea, Republic Of (*Abstract Co-Author*) Nothing to Disclose Jong Seok Lee, Seoul, Korea, Republic Of (*Abstract Co-Author*) Nothing to Disclose Hyun Jin Kim, MD, Seoul, Korea, Republic Of (*Abstract Co-Author*) Nothing to Disclose Ah Young Kim, MD, Seoul, Korea, Republic Of (*Abstract Co-Author*) Nothing to Disclose Hyun Kwon Ha, MD, Seoul, Korea, Republic Of (*Abstract Co-Author*) Nothing to Disclose

PURPOSE

Colonic rotation that mimics lesion mobility on CT colonography (CTC) can be particularly deceptive when it happens in unexpected locations such as the ascending colon. This study was to evaluate the effect of reducing abdominal compression during prone CTC on ascending colonic rotation that occurs with supine-to-prone positional change.

METHOD AND MATERIALS

Consecutive patients fulfilling following criteria were found from 1218 CTC cases (January 2013 to July 2014): a) prone CTC obtained with cushion blocks placed under the chest and pelvis to reduce abdominal compression, b) air-distended ascending colon on both supine and prone CTC, and c) colonoscopy-proven sessile polyps >=6mm in straight mid-ascending colon. Radial locations along the luminal circumference (°) of 24 polyps and 54 colonic teniae (3 teniae in each patient) in mid-ascending colon of 18 patients (M:F, 16:2; 65 ± 12 years) were measured on supine and prone CTC images and supine-to-prone difference was determined. A coordinate system designed to offset effects of torso rotation was used. The supine-to-prone difference was given a value between -180° (- for internal rotation) and $+180^{\circ}$ (+ for external rotation). Degrees of abdominal compression (Abd comp) and posterior displacement of mid-ascending colon (Asc disp) in prone position were quantitatively measured and were correlated with the radial location change of ascending colonic polyps and teniae.

RESULTS

The radial location change was -22° to 61° (median, 10.4°) for the polyps and was similar for colonic teniae, which was considerably smaller than the reported ascending colonic rotation. However, 50-56% of the polyps and teniae still showed external rotation >10°. The radial location change was not significantly correlated with Abd comp (P =.131 to .287) but was correlated with Asc disp (r =.562 to .702; P =.001 to .015). Posterior displacement of the ascending colon still occurred in prone position due to gravitational anterior displacement of other mobile abdominal contents despite the lack of abdominal compression.

CONCLUSION

Ascending colonic rotation on CTC ocurring with supine-to-prone positional change was incompletely prevented by reducing abdominal compression during prone CTC.

CLINICAL RELEVANCE/APPLICATION

Careful confirmation of lesion mobility or lack of it is fundamental for accurate CTC interpretation although reducing abdominal compression during prone CTC may decrease the related pitfall in the ascending colon.

SSK06-08 Computer-aided Supine-only Reading in Full-cathartic CT Colonography: Observer Performance Study

Wednesday, Dec. 2 11:40AM - 11:50AM Location: E351

Participants

Yasuji Ryu, MD, Boston, MA (*Presenter*) Nothing to Disclose Janne J. Nappi, PhD, Boston, MA (*Abstract Co-Author*) Royalties, Hologic, Inc; Royalties, MEDIAN Technologies; Hiroyuki Yoshida, PhD, Boston, MA (*Abstract Co-Author*) Patent holder, Hologic, Inc; Patent holder, MEDIAN Technologies;

PURPOSE

To assess the performance of an advanced computer-aided "supine-only reading" of full-cathartic CTC in the detection of polyps in patients with average or high risk of colorectal cancer.

A total of 266 CTC cases were sampled from a multi-center CTC trial for patients with average or high risk of colorectal cancer, in which patients underwent cathartic bowel preparation with 2L polyethylene glycol solution and 20mL sodium diatrizoate for tagging of residual fluid, followed by automated CO2 insufflation. A computer-aided detection (CADe) system that had been trained with cases independent from this study was used to review the CTC cases. One expert reader (\geq 600 cases reading experience) reviewed the cases in "supine-only reading" mode, in which only the supine scans of these cases were interpreted using CADe as a second reader, and recorded all detected lesions \geq 6 mm. The per-patient sensitivities and the areas under the receiver operating curve (AUC) in the detection of adenomas and carcinomas were compared between unaided and CADe-aided readings, as well as between the supine-only reading and "conventional reading" result from the trial, in which both supine and prone scans were used for interpretation of the CTC cases.

RESULTS

There were 53 and 28 patients with adenomas and/or carcinomas ≥ 6 mm and ≥ 10 mm, respectively. Corresponding per-patient sensitivities (AUCs) for CADe-aided supine-only reading were 91% (.92) and 93% (0.96), respectively, whereas those of conventional reading were 90% (.91) and 93% (.96), respectively. The differences in sensitives and AUCs were not statistically significant (Fisher's exact test, P>.5). For 6-9 mm lesions, the per-patient sensitivity (AUCs) of CADe-aided supine-only reading was 83% (.88), which was higher (McNemar's test, P<.05) than those of unaided, supine-only reading of 69% (.81).

CONCLUSION

In full-cathartic CTC, CADe-aided supine-only reading may yield an equally high performance in the detection of adenomas and carcinomas as that of the conventional, supine-prone reading. CADe may also significantly improves the detection performance of polyps 6-9 mm in size in size in the supine-only reading

CLINICAL RELEVANCE/APPLICATION

Computer-aided supine-only reading has the potential to allow one-position scanning in CTC, thereby effectively reducing the radiation dose and reading time into a half of those of conventional reading.

SSK06-09 Observer Study for Detection of Lesions in Viewing CT Colonography Using a New Eye Gaze Tracking System

Wednesday, Dec. 2 11:50AM - 12:00PM Location: E351

Participants

Mitsuru Sato, Maebashi, Japan (*Presenter*) Nothing to Disclose Toshihiro Ogura, PhD, Maebashi, Japan (*Abstract Co-Author*) Nothing to Disclose

Mika Okajima, Gunma, Japan (*Abstract Co-Author*) Nothing to Disclose

Yushi Hirano, Otaru, Japan (*Abstract Co-Author*) Nothing to Disclose

Mikio Hasegawa, Tokyo, Japan (Abstract Co-Author) Nothing to Disclose

Kunio Doi, PhD, Chicago, IL (*Abstract Co-Author*) Shareholder, Hologic, Inc; License agreement, Hologic, Inc; License agreement, Riverain Technologies, LLC; License agreement, Mitsubishi Corporation; License agreement, MEDIAN Technologies; License agreement, General Electric Company; License agreement, Toshiba Corporation; Research support, Deus Technologies, LLC; Research support, E. I. du Pont de Nemours & Company; Research support, Elcint Medical Imaging Ltd; Research support, FUJIFILM Holdings Corporation; Research support, General Electric Company; Research support, Hitachi, Ltd; Research support, Eastman Kodak Company; Research support, Konica Minolta Group; Research support, Mitaya Manufacturing Co, Ltd; Research support, Mitsubishi Corporation; Research support, Seiko Corporation; Research support, Siemens AG; Research support, 3M Company; Research support, Toshiba Corporation Shoko Tsutsumi, Maebashi, Japan (*Abstract Co-Author*) Nothing to Disclose

Kiyoshi Isobe, Tokyo, Japan (*Abstract Co-Author*) Nothing to Disclose

Atsuko Torimoto, Otaru, Japan (Abstract Co-Author) Nothing to Disclose

PURPOSE

Monitoring the eye tracking of the observer in the detection of lesions is important in order to understand image interpretation process for CT colonography. Head-mount eye tracker system has been used to track observers' viewing points on radiological images. However, it is difficult to use this system casually due to a problem of an obtrusive device for observation. We investigated gaze points for image interpretation of CTC images by experts and non-experienced observers, and analyze the time and the gaze point for detection of lesions using a new eye gaze tracking system, which was designed to detect the pupil point and corneal reflection point in the dark pupil eye tracking by using two infrared cameras.

METHOD AND MATERIALS

Observers for CTC image reading commonly use virtual gross pathology (VGP) images which were obtained as a stretched views of the inner colonic surface. We used an eye gaze point sensing system (JVCKenwood Co.,Yokohama,Japan) which consisted of an eye tracking sensor with two infrared light emitting diode (LED) laser emitters combined with two infrared cameras. Observer studies were performed by two expert observers (over 13 years experience) and two non-experienced observers on nineteen VGP images including tumors, polyps and other abnormalities.

RESULTS

Eye gaze tracking data of the observers can be obtained without a device put on the head such as a headgear, with proper training of about 20 minutes. The average reading time (32.6sec) by expert observers was significantly shorter (p<0.001) than that (46.2sec) by non-experienced observers. The detection rates of target areas such as tumors by expert observers (84.18%) was higher than that of non-experienced observers (68.35%). Non-experienced observers in CTC reading were prolonged with low detection rates. On other hand, experienced observers provided shortened viewer's gaze dwells time on the target areas.

CONCLUSION

A new eye gaze tracking system for CTC images can be performed without a head-mount eye tracker. Although the reading time of expert observers was short, the target areas on VGP images were observed with a high detection rate.

CLINICAL RELEVANCE/APPLICATION

 An eye gaze tracking analysis using infrared cameras can be set-up easily. Gaze points on CTC images by experts and nonexperienced observers can be determined for understanding of image readings for detection of lesions.

ISP: Musculoskeletal (Spine)

Wednesday, Dec. 2 10:30AM - 12:00PM Location: E353C

MK MR

AMA PRA Category 1 Credits ™: 1.50 ARRT Category A+ Credits: 1.50

FDA Discussions may include off-label uses.

Participants

Christian W. Pfirrmann, MD, MBA, Forch, Switzerland (*Moderator*) Advisory Board, Siemens AG; Consultant, Medtronic, Inc Jung-Ah Choi, MD, Hwaseong, Korea, Republic Of (*Moderator*) Nothing to Disclose

Sub-Events

SSK12-01 Musculoskeletal Keynote Speaker: Spine MRI-From Technique to Clinical Application

Wednesday, Dec. 2 10:30AM - 10:50AM Location: E353C

Participants

Lawrence N. Tanenbaum, MD, New York, NY (*Presenter*) Speaker, General Electric Compnny; Speaker, Bracco Group; Speaker, Bayer AG; Speaker, Siemens AG; Speaker, Guerbet SA

SSK12-04 Imaging of Cervical Disc Degeneration in 3D Ultrashort Echo Time MR Imaging Comparing with Conventional T2 Weighted Spin Echo Sequences; An in Vivo Preliminary Study

Wednesday, Dec. 2 11:00AM - 11:10AM Location: E353C

Participants

Yeo Ju Kim, Incheon, Korea, Republic Of (*Presenter*) Nothing to Disclose Jang Gyu Cha, MD, Bucheon, Korea, Republic Of (*Abstract Co-Author*) Nothing to Disclose Sangwoo Lee, Seoul, Korea, Republic Of (*Abstract Co-Author*) Researcher, General Electric Company Michael Carl, Menlo Park, CA (*Abstract Co-Author*) Researcher, General Electric Company Mi Young Kim, MD, Incheon, Korea, Republic Of (*Abstract Co-Author*) Nothing to Disclose Youn Jeong Kim, MD, Incheon, Korea, Republic Of (*Abstract Co-Author*) Nothing to Disclose Ha-Young Lee, MD, Incheon, Korea, Republic Of (*Abstract Co-Author*) Nothing to Disclose Soon Gu Cho, MD, Incheon, Korea, Republic Of (*Abstract Co-Author*) Nothing to Disclose

PURPOSE

To evaluate the image findings of cervical disc degeneration in 3 dimensional ultrashort echo time MR imaging (3D UTE) according to disc degeneration in conventional T2 weighted spin echo sequences (T2 SE).

METHOD AND MATERIALS

A total of 315 discs of 63 patients (36 men and 27 women; mean age 53.62 years, age range - 19-85) were imaged with sagittal T2 SE (repetition time msec/time to echo msec, 2800/90) and sagittal 3D UTE (16.1/0.028, 4.4, echo-subtraction). In T2 SE, disc degenerations were evaluated from C2-3 to C6-7 using a grading system proposed by Pfirrmann et al. In 3D UTE, discs were classified as follows, according to the morphology of the cartilaginous endplate (CEP), and the signal intensity of the nucleus purposes (NP): type I (smooth thin CEP; low signal intensity of the NP), type III (mild irregular CEP; low signal intensity of the NP), type III (irregular and thickened CEP with or without high signal intensities in some portion of the NP), and type IV (an irregular and thickened CEP with high signal intensities in nearly all of the NP). Each type of disc in the UTE was compared with grades of disc degeneration in T2 SE and analyzed by a linear- by-linear association.

RESULTS

In mild degeneration (grade 2, n=127), type I discs (107/127, 84.3%) were most frequently seen but none of the type IV discs were found in 3D UTE. In cases of severe degenerations (grade 4, n= 11), type IV discs (6/11, 54.5%) were most frequently found but none of the type I discs were seen in 3D UTE. There was a statistically significant tendency between the types of disc in UTE and grades of disc degeneration in T2 weighted SE sequences (P<0.05).

CONCLUSION

The degenerative cervical discs showed thick irregular CEPs and increased prevalence of high signal intensity at the NP in 3D UTE.

CLINICAL RELEVANCE/APPLICATION

The change of cartilaginous endplates and increased amount of short T2 components in a nucleus pulposus according to degeneration in 3D UTE may help to understand and diagnosedisc degeneration.

SSK12-05 T1rho and T2 Mapping of Lumbar Intervertebral Disc: Correlation with Degeneration and Morphologic Changes

Wednesday, Dec. 2 11:10AM - 11:20AM Location: E353C

Participants

Min A Yoon, MD, Seoul, Korea, Republic Of (*Presenter*) Nothing to Disclose Suk-Joo Hong, MD, Rochester, MN (*Abstract Co-Author*) Nothing to Disclose In Seong Kim, PhD, Seoul, Korea, Republic Of (*Abstract Co-Author*) Nothing to Disclose Baek Hyun Kim, MD, Ansan, Korea, Republic Of (*Abstract Co-Author*) Nothing to Disclose Seun Ah Lee, MD, Seoul, Korea, Republic Of (*Abstract Co-Author*) Nothing to Disclose

PURPOSE

To evaluate correlation between T1rho (T1 ρ), T2 values and disc degeneration and morphologic changes in the lumbar intervertebral discs.

METHOD AND MATERIALS

Twenty-two subjects (M:F=8:14; mean age 55.5 years; range 26-84 years) with 109 lumbar intervertebral discs (from L1-2 to L5-S1) were examined at 3.0T MRI. Disc degeneration was evaluated using the 5-level Pfirrmann grading system and the disc morphology was categorized into five groups: normal, bulging, annular tear, protrusion, extrusion. For T1p and T2 quantification, regions of interest (ROIs) were drawn on the three mid-sagittal images at nucleus pulposus (NP), posterior annulus fibrosus (AF), and junction of the NP and posterior AF for each disc on T1p and T2 maps. Quantitative measurements for herniated discs were made within the protruded or extruded portion. Statistical analysis was performed using Spearman rank correlation and partial correlation.

RESULTS

The Pfirrmann grades showed strong correlations with the T1p values at the NP (r=.800, p<.001), T2 values at the NP (r=.-792, p<.001), and T2 values at the junction (r=-784, p<.001). Disc morphology was moderately correlated with T2 values at the junction (r=-.603, p<.001), T2 values at the NP (r=-.578, p<.001), and T1p values at the NP (r=.509, p<.001). After correction for effects of patient age and disc level, there was strong to moderate correlation between the Pfirrmann grades and T1 p values at the NP (r=.750, p<.001 after correction of age effect and r=.697, p<.001 after correction of disc level effect).

CONCLUSION

T1p and T2 mapping, especially T1p values at the NP and T2 values at NP and junction, provided quantitative measurements of the progression of the intervertebral disc degeneration with strong correlations. T2 values at the junction proved good relationship in the assessment of the disc morphologic changes.

CLINICAL RELEVANCE/APPLICATION

T1p and T2 mapping provide quantitative measurements for disc degeneration and morphologic changes, which can be used as a synergistic modality for evaluation of lumbar degenerative disc disease.

SSK12-06 Spin Echo Based T2-weighted Modified Dixon (mDixon) Images for Detection of Vertebral Metastasis: Can T1-weighted MR Images Be Replaced by Fat Images of T2 mDixon?

Wednesday, Dec. 2 11:20AM - 11:30AM Location: E353C

Participants

Seok Hahn, MD, Seoul, Korea, Republic Of (*Abstract Co-Author*) Nothing to Disclose Young Han Lee, MD, Seoul, Korea, Republic Of (*Presenter*) Nothing to Disclose Seung Hyun Lee, MD, Seoul, Korea, Republic Of (*Abstract Co-Author*) Nothing to Disclose Jaemoon Yang, Seoul, Korea, Republic Of (*Abstract Co-Author*) Nothing to Disclose Jin-Suck Suh, MD, Seoul, Korea, Republic Of (*Abstract Co-Author*) Nothing to Disclose

PURPOSE

To evaluate diagnostic performance of spin echo based T2-weighted mDixon MR images and to compare with T1-weighted MR images for detection of vertebral metastasis

METHOD AND MATERIALS

From April to September 2014, we found 124 patients who underwent whole spine MRIs with spin echo mDixon for the evaluation of vertebral metastasis. We obtained conventional T1-weighted images, mDixon images including water and fat images of T2 mDixon, and contrast-enhanced water images of T1 mDixon. We found 23 bone metastases of 12 patients by inclusion criteria: 1) patients with a record of a bone metastasis diagnosis as the primary or secondary diagnosis and 2) Positron emission tomography-computed tomography (PET-CT) scan within one month. The lesion at same level on PET-CT scan was utilized as a reference. Two radiologists reviewed fat and water images of T2 mDixon and contrast enhanced water image of T1 mDixon in random order separately. We calculated sensitivities, specificities, accuracies, positive and negative predictive values, inter-observer agreements.

RESULTS

Of 23 metastatic lesions, the reviewer 1 detected 16 on T1-weighted images, 16 on water images, 15 on fat images of T2 mDixon, 20 on contrast enhanced water images of T1 mDixon. And the reviewer 2 detected 19, 18, 18 and 22, respectively. Contrastenhanced water images of T1 mDixon showed higher sensitivity than other images (76.1% vs. 73.9% vs. 71.7% vs. 91.3%). Specificities, accuracies, positive and negative predictive values of three spin echo based mDixon images were similar values to conventional T1-weighted images (98.9% vs. 98.0% vs. 98.8% vs. 98.1%; 97.2% vs. 96.2% vs. 96.7% vs. 97.7%; 85.4% vs. 75.6% vs. 82.5% vs. 80.8%; 98.0% vs. 97.7% vs. 99.3%). The kappa values of inter-observer agreement were moderate degree (0.712, 0.679, 0.679 and 0.790, respectively).

CONCLUSION

The spin echo based T2-weighted mDixon MR images show good diagnostic performances in sensitivity, specificity, accuracy, positive and negative predictive values compared with T1-weighted MR images for detection of vertebral metastasis.

CLINICAL RELEVANCE/APPLICATION

Using spin echo based T2-weighted mDixon technique, we can obtain water and fat images with single scan, which have similar diagnostic performances to conventional T1-weighted images for the detection of vertebral metastases. And fat images of T2 mDixon can be used for detection of vertebral metastasis instead of T1-weighted images.

SSK12-07 Vertebral Involvement in SAPHO Syndrome: A Follow-up Study of 13 Cases Using MR Imaging

Wednesday, Dec. 2 11:30AM - 11:40AM Location: E353C

Participants Emilie A. Dodre, MD, Lille, France (*Presenter*) Nothing to Disclose Caroline Parlier, MD, Paris, France (*Abstract Co-Author*) Nothing to Disclose Gilles Hayem, Paris, France (*Abstract Co-Author*) Nothing to Disclose Jean-Denis Laredo, MD, Paris, France (*Abstract Co-Author*) Research Consultant, Cardinal Health, Inc; Research Consultant, Laurane Medical; Research Consultant, F. Hoffman-La Roche Ltd; Research Grant, SERVIER

PURPOSE

To retrospectively describe the course of magnetic resonance (MR) imaging findings of vertebral involvement in patients with synovitis, acne, pustulosis, hyperostosis and osteitis (SAPHO) syndrome and to seek for clues in the pathophysiology of spondylitis in SAPHO syndrome.

METHOD AND MATERIALS

Between October 1992 and January 2012, 13 patients (10 women, 3 men; median age at first MR imaging: 33 years) with SAPHO syndrome involving the spine underwent 2 MR examinations of the spine after an interval of at least 3 months. Three musculoskeletal radiologists reviewed MR spinal images in consensus. Erosions of vertebral bodies defined lesional foci. Lesional foci separated by one or more normal vertebral corner were analyzed as distinct lesions. Cortical bone erosions, vertebral signal intensity (SI) alterations compared with normal vertebral body SI, soft-tissue involvement, intervertebral disk SI and disk height compared with the other disks and osseous bridges were evaluated.

RESULTS

27 lesional foci were identified in the 13 patients on initial MR images. Extension of the erosions was seen in 20 foci (74%) and 3 new lesional foci appeared. During follow-up, 31 of the 75 (41%) initial erosions spread by degrees within a single vertebra to the adjacent vertebral parts and to the vertebral corner of the adjacent vertebrae. Changes in SI of the vertebral body were seen in 21 of the 27 (78%) initial foci. In 8 (30%) of the 27 initial lesional foci, a soft tissue involvement at the anterior or lateral paraspinal region was noted. Thickness of this involvement progressed compared to initial examinations in 3 of the 27 foci (11%). A decrease in disk space height was observed on follow-up MRI in 10 of the 27 initial foci (37%) and was associated with high SI on T2-weighted images or gadolinium enhancement of the disk space in 3 (11%), further mimicking disk space infection. Bony bridges over the disk space increased in 3 lesional foci (11%) and appeared in 2 (7%) during follow-up.

CONCLUSION

During the course of the SAPHO syndrome, vertebral involvement spread by degrees within a single vertebra to the adjacent cortices as well as to the vertebral corner of the adjacent vertebrae.

CLINICAL RELEVANCE/APPLICATION

The gradual local spread of the vertebral disease process strongly suggests SAPHO syndrome in the appropriate clinical context.

SSK12-08 CT Manifestations of Spinal Lesions in SAPHO Syndrome

Wednesday, Dec. 2 11:40AM - 11:50AM Location: E353C

Awards

Trainee Research Prize - Medical Student

Participants Wenrui Xu, MD, Beijing, China (*Presenter*) Nothing to Disclose Chen Li, Beijing, China (*Abstract Co-Author*) Nothing to Disclose Xue Zhao, Beijing, China (*Abstract Co-Author*) Nothing to Disclose Wen Zhang, Beijing, China (*Abstract Co-Author*) Nothing to Disclose Wei-hong Zhang, MD, Baltimore, MD (*Abstract Co-Author*) Nothing to Disclose

PURPOSE

In this study, we retrospectively evaluated the CT manifestations of spinal lesions in 54 patients with SAPHO (synovitis, acne, pustulosis, hyperostosis and osteitis) syndrome to increase the diagnostic ability of this disease.

METHOD AND MATERIALS

Our study included 54 SAPHO patients (female:male,36:18; mean±SD age, 42.2±10.0 years; age range,16-62 years) with spinal involvement, among whom 50 patients had characteristic cutaneous disorders. The mean±SD values for hs-C-reactive protein and erythrocyte sedimentation rate were 19.7 ±16.8 mg/L and 6.5±10.5 mmHg/h ,respectively (normal range:0-3 mg/L and 0-20 mmHg/h).CT images of the whole spinal column obtained in the subjects using Toshiba Aquilion ONE 640 (thickness: 2mm,window width: 2000HU,window level: 400HU) were analyzed. A total of 1350 vertebrae were evaluated (25 vertebrae for each individual, from the first cervical vertebra to sacrum).

RESULTS

Spinal involvement in SAPHO syndrome is mainly characterized by enthesitis, endplate inflammation and ossification of paravertebral ligaments. On CT images, enthesitis and endplate inflammation manifested as focal cortical erosion of the vertebral corner and endplate, respectively, with reactive osteosclerosis in surrounding cancellous bone or in some cases the entire vertebral body, and progressed to the formation of syndesmophyte, bony bridge and flattening of vertebral body. Enthesitis and endplate inflammation were observed in 17.5%(236/1350) and 5.4%(73/1350) vertebrae, respectively. Ossifications of paravertebral ligaments were observed in 43 out of the 54 patients, 81.4 % (35/43) on the supraspinous ligament, 20.9 % (9/43) on interspinous ligament, 27.9% (12/43) on anterior longtitudinal ligament and 18.6 % (8/43) on posterior longtitudinal ligament.

CONCLUSION

In conclusion, a better understanding of the CT manifestations of spinal lesions in SAPHO patients may support clinical diagnosis in

the absence of characteristic signs.

CLINICAL RELEVANCE/APPLICATION

A deep understanding of the CT manifestations of spinal lesions in SAPHO patients may support clinical diagnosis in the absence of cutaneous disorders and typical anterior chest wall involvement.

SSK12-09 Evaluation of T2-weighted WARP Sequences in Patients with Spinal Prosthesis

Wednesday, Dec. 2 11:50AM - 12:00PM Location: E353C

Participants

Shun Qi, Xi'an, China (*Presenter*) Nothing to Disclose Ying Liu, MD, PhD, Xian, China (*Abstract Co-Author*) Nothing to Disclose Panli Zuo, Beijing, China (*Abstract Co-Author*) Nothing to Disclose Hong Yin, MD, PhD, Xi'an, China (*Abstract Co-Author*) Nothing to Disclose

PURPOSE

MRI is an important modality for imaging the spine as it allows assessment of the spinal cord, adjacent soft tissues and osseous structures. In this study, we compared images quality and diagnostic sensitivity between WARP with standard TSE sequences in interbody fixation patients with titanium screws.

METHOD AND MATERIALS

30 patients (11 males and 19 females; age range, 35-72 years) who were clinically examined discomfort after interbody fixation surgery with titanium screws were scanned at a 1.5T MR scanner (MAGNETOM Aera, Siemens). The T2-weighted sagittal and axial images were acquired using a standard TSE sequence and a WARP TSE sequence implemented the SEMAC and VAT techniques as well as increased bandwidth for radiofrequency and readout pulses. SEMAC factor was 6 for all WARP imaging. The cumulative area of signal void was measured on the axial image, which was defined as the area without discernible anatomic information for both low and high-signal-intensity artifacts induced by the prosthesis (Fig. 1A). Length of spinal canal obscuration on the sagittal image was also measured (Fig. 1B).

RESULTS

On axial T2-weighted images, the area of signal void at the level of the prosthesis (mean \pm standard deviation) was 10.4 cm2 \pm 4.5 for WARP and 26.6 cm2 \pm 10.2 for standard TSE images (Fig. 1C). On sagittal T2-weighted images, the length of spinal canal obscuration at the level of the prosthesis was 1.8 cm \pm 0.3 for WARP and 5.4 cm \pm 1.2 for standard TSE images (Fig. 1D). Visualizations of all periprosthetic anatomic structures were significantly better for WARP compared with standard imaging. Interobserver agreement for visualizations of anatomic structures was good for both WARP (k = 0.73) and standard (k = 0.71) imaging. The number of abnormal findings noted on WARP images (28 findings) was significantly higher than the number of findings detected on standard images were also noted on WARP images.

CONCLUSION

MR images with WARP sequences significantly reduced metal-related artifacts and improved delineation of the prosthesis and periprosthetic region therefore increased the diagnostic sensitivity in patients with clinical abnormities.

CLINICAL RELEVANCE/APPLICATION

WARP sequences significantly reduced metal-related artifacts

Genitourinary (Functional Imaging of the Kidneys)

Wednesday, Dec. 2 10:30AM - 12:00PM Location: E450B

GU MR US

AMA PRA Category 1 Credits ™: 1.50 ARRT Category A+ Credits: 1.50

Participants

Harriet C. Thoeny, MD, Bern, Switzerland (*Moderator*) Nothing to Disclose Zhen J. Wang, MD, Hillsborough, CA (*Moderator*) Nothing to Disclose

Sub-Events

SSK08-01 Assessing the Role of Quantification of Shear Wave Velocity and Tissue Elasticity in the Detection of Interstitial Fibrosis within the Transplant Kidney

Wednesday, Dec. 2 10:30AM - 10:40AM Location: E450B

Participants

David Ferguson, MBBCh, Vancouver, BC (*Presenter*) Nothing to Disclose Amdad M. Ahmed, MBChB, FRCR, Birmingham, United Kingdom (*Abstract Co-Author*) Nothing to Disclose Mohammed F. Mohammed, MBBS, Vancouver, BC (*Abstract Co-Author*) Nothing to Disclose Caitlin Schneider, Vancouver, BC (*Abstract Co-Author*) Nothing to Disclose Christopher Nguan, Vancouver, BC (*Abstract Co-Author*) Nothing to Disclose Alison C. Harris, MBChB, Vancouver, BC (*Abstract Co-Author*) Nothing to Disclose

PURPOSE

Novel ultrasound techniques allow for the assessment of tissue fibrosis. One such technique ('Virtual Touch IQ') allows for both qualitative and quantitative measurement of shear wave velocity to assess tissue strain and detect underlying fibrosis. Using this technique, in the setting of renal allograft failure, we aim to compare the gold standard of renal biopsy and histological grade with that of shear wave velocity measurement to evaluate for potential underlying interstitial fibrosis.

METHOD AND MATERIALS

Patients undergoing renal biopsy for renal graft dysfunction within the ultrasound department were enrolled prospectively over an eight-month period. In addition to routine routine renal ultrasound with Doppler imaging, shear wave velocity measurements using 'Virtual Touch IQ' were obtained from the target area for renal cortical biopsy. Sufficient magnitude of the shear wave was confirmed on quality display. Biopsies were performed and reviewed by a nephropathologist, blinded to the imaging results, with histological categorization according to the Banff classification.Shear wave velocities and histological grade were compared to determine significance. Statistical analysis was performed using the Mann Whitney test and Spearman-correlation-coefficient (rho).

RESULTS

Fourteen patients were identified and subcategorized according to the Banff category with respect to interstitial fibrosis as normal (n=4), grade 1(n=4), grade 2 (n=3) and grade 3(n=3). Median shear wave velocity was demonstrated to be significantly higher in renal transplants with biopsy proven interstitial fibrosis (median=2.512m/s) than those without interstitial fibrosis (median=1.925m/s) (Mann Whitney U=4, n1=4, n2=10, p<0.05). Positive correlation was also identified between the mean shear wave velocity and Banff categories (rho= 0.731, p=0.003).

CONCLUSION

Preliminary data indicates that shear wave velocity within cortex of the transplant kidney correlates significantly with interstitial fibrosis in the context of renal allograft failure.

CLINICAL RELEVANCE/APPLICATION

Shear wave velocity analysis is a potentially valuable non-invasive tool to assess for renal allograft interstitial fibrosis.

SSK08-02 Improved Temporal Resolution and Image Contrast for Kidney DCE-MRI by 3D Spoiled Gradientrecalled Echo Sequence with Compressed Sensing

Wednesday, Dec. 2 10:40AM - 10:50AM Location: E450B

Participants

Kai Zhao, PhD, Beijing, China (*Presenter*) Nothing to Disclose Bin Chen, Beijing, China (*Abstract Co-Author*) Nothing to Disclose Jue Zhang, Beijing, China (*Abstract Co-Author*) Nothing to Disclose Xiaoying Wang, MD, Beijing, China (*Abstract Co-Author*) Nothing to Disclose

PURPOSE

To verify the feasibility of combine Compressed Sensing (CS) technique in dynamic contrast-enhanced magnetic resonance imaging (DCE-MRI) of kidney

METHOD AND MATERIALS

Nine healthy New Zealand rabbits underwent kidney DCE-MRI studies on a clinical 3.0T MR scanner. 3D spoiled gradient-recalled echo sequence modified with CS scheme was scanned before and after the administration of 0.05 mmol/kg of Gd-DTPA with the following parameters: TR = 3.3ms, TE = 1.3ms, FA = 15°, slice thickness = 3 mm, matrix = 128×128 , FOV = 180mm and 16 slices were acquired. Four accelerations (2-x, 3-x, 4-x, 8-x) were scanned as well as the fully sampling every other day for each animal in

DCE MR imaging. The contrast-to-noise ratio (CNR) and signal-to-noise ratio (SNR) of the reconstructed images of the kidney were analyzed and compared to that of the fully sampled images separately.

RESULTS

The images with 2-X, 3-X, 4-X, 8-X CS acceleration and fully sampled results were shown from row 1 to row 5. The 8-X accelerated images appeared blurring which may due to the loss of a mass of high frequency information (Figure 1).Signal intensity curves of cortex and medulla were represented in Figure 2. The reconstructions of 8-X were also blurring.Superior CNR performance between cortex and tissue CNR_ct, and medulla and tissue CNR_mt were found for all the time points after contrast administration. CNR_ct of CS reconstructed images were significantly larger than that of the conventional fully sampled images at all accelerations throughout the enhancement (p<.01 for 2-X; p<.001 for 3-X and 4-X). CNR_mt of CS reconstructed images were also significantly larger than that of the fully sampled images (p<.01 for 2-X; p<.001 for 3-X and 4-X). CNR_cm measured from cortical and medullary regions were larger in CS reconstructed images, especially at the initial time of enhancement: 44.00 10.0 for 2-X, 43.30 8.0 for 3-X and 49.78 14.9 for 4-X vs. 15.28 6.7 for 1-X (p<.001 for all) (Table 1).In SNR analysis, SNR-cortex (SNR_c) and SNR-medulla (SNR_m) of CS reconstructed images were all found statistically different from conventional fully sampled images (p<.001) (Table 2).

CONCLUSION

Compressed sensing is a feasible and promising acceleration method to improve temporal resolution and image contrast in renal DCE-MRI.

CLINICAL RELEVANCE/APPLICATION

CS is a promising imaging method with both improved temporal resolution and image contrast, which will be widely used in the future.

SSK08-03 Noninvasive Evaluation of Stable Renal Allograft Function Using Shear-Wave Elastography

Wednesday, Dec. 2 10:50AM - 11:00AM Location: E450B

Participants

Jung Jae Park, MD, Seoul, Korea, Republic Of (*Presenter*) Nothing to Disclose Chan Kyo Kim, MD, PhD, Seoul, Korea, Republic Of (*Abstract Co-Author*) Nothing to Disclose Beom Jun Kim, Seoul, Korea, Republic Of (*Abstract Co-Author*) Nothing to Disclose Byung Kwan Park, MD, Seoul, Korea, Republic Of (*Abstract Co-Author*) Nothing to Disclose

PURPOSE

Protocol renal allograft biopsies improve outcomes via early detection and treatment of subclinical rejection (SCR). Shear-wave elastography (SWE) assesses quantitatively the tissue elasticity. The aim of our study was to investigate the feasibility of SWE in evaluating patients with stable renal allograft function who underwent protocol biopsies.

METHOD AND MATERIALS

95 patients (mean age, 48.3 years; range, 21-73 years) with stable renal allograft function who underwent ultrasound (US)-guided protocol biopsies at 10 days or 1 year after transplantation were enrolled in this retrospective study. All US and elasticity examinations of renal allograft were performed by a commercial scanner using a convex transducer (C5-1 ElastoPQ, Philips iU 22). SWE was performed immediately before protocol biopsies. Tissue elasticity (kPa) in the cortex was measured for all renal allografts. Clinical and US variables were compared between patients with SCR and without SCR using the Student t -test. The correlation between estimated glomerular filtration rate (eGFR) and tissue elasticity was evaluated in all patients by Pearson correlation. Diagnostic performance of tissue elasticity to distinguish between patients with SCR and without SCR was analyzed using a receiver operating characteristics (ROC) curve analysis.

RESULTS

Acute rejection (AR) was pathologically confirmed in 34 patients. The mean tissue elasticity of ARs (31.0 ± 12.8 kPa) was statistically greater than that no ARs (24.5 ± 12.2 kPa) (P < 0.001), while the resistive index values did not show statistical difference between ARs and no ARs (P = 0.112). Clinical variables including age, kidney size, creatinine and eGFR revealed statistical differences between ARs and no ARs (P < 0.05). Tissue elasticity demonstrated a moderate negative correlation with eGFR (correlation coefficient= -0.604, P < 0.001). At ROC curve analysis, the area under the curve (AUC) of tissue elasticity was 0.651 and followed eGFR (AUC= 0.728).

CONCLUSION

SWE, as a noninvasive tool, may be feasible in distinguishing between allograft with SCR and without SCR in patients with stable renal function. Moreover, it may demonstrate functional state of renal allografts.

CLINICAL RELEVANCE/APPLICATION

As a feasible technique, shear-wave elastography may help to noninvasively assess functional state of patients with stable renal allograft function.

SSK08-04 Assessment of Renal Allograft Function Early after Transplantation Using Renal IVIM with Healthy as Control

Wednesday, Dec. 2 11:00AM - 11:10AM Location: E450B

Participants

Lihua Chen, Tianjin, China (*Presenter*) Nothing to Disclose Tao Ren, Tianjin, China (*Abstract Co-Author*) Nothing to Disclose Wen Shen, Tianjin, China (*Abstract Co-Author*) Nothing to Disclose Panli Zuo, Beijing, China (*Abstract Co-Author*) Nothing to Disclose

PURPOSE

Graft dvsfunction is a common complication following transplantation. which is associated with allograft survial. Intravoxel incoherent

motion (IVIM) has potential to assess renal function in patients with renal and allograft dysfunction. The purpose of the current study in renal allografts early after transplantation was to investigate relationship between estimated glomerular filtration rate (eGFR) and diffusion and perfusion parameters calculated using IVIM imaging, compared with healthy kidney, and to gain the sensitive IVIM parameters for monitoring allograft function.

METHOD AND MATERIALS

A total of 71 subjects were performed on a 3.0T MRI scanner (MAGNETOM Trio, a Tim system, Siemens AG, Erlangen, Germany) using IVIM sequence with 11 b values(0, 10, 20, 40, 60, 100, 150, 200, 300, 500, and 700 s/mm2). Subjects were divided into 3 groups: group 1, healthy volunteers (n=19); group 2, allografts with good allograft function(eGFR≥60mL/min/1.73m2, n=33); group 3, allografts with impaired allograft function(eGFR<60mL/min/1.73m2, n=19).To separate the perfusion and diffusion, a biexponential fit was used to calculate the diffusion coefficient of slow (ADCslow); the diffusion coefficient of fast (ADCfast) and perfusion fraction (FP). Differences in IVIM parameters between the cortex and medulla in each group were compared using paired samples t test. Differences of IVIM parameters between three groups were compared using LSD test.Relationships between eGFR and IVIM parameters were assessed using spearman correlation coefficient.

RESULTS

The ADC, ADCslow, Fp values of renal cortex were significantly higher in group 1 and group 2 compared to group 3(all p<0.01). The ADC, ADCslow values of renal medulla were significantly higher in group 1 and group 2 compared to group 3(all p<0.01). For allografts, significant differences in ADC, ADCslow, FP values of renal cortex and ADC, ADCslow values of renal medulla were observed between group 2 and group 3. In renal allografts, there was a significant positive correlation between eGFR and ADC, ADCslow value of medulla(all p<0.05).

CONCLUSION

The ADC, ADCslow, FP values of renal cortex and ADC, ADCslow values of renal medulla may be useful for detect renal allograft dysfunction. IVIM technique is a reliable imaging for evaluating and monitoring allograft function.

CLINICAL RELEVANCE/APPLICATION

IVIM technique can be used to evaluate and monitor allograft function

SSK08-05 Renal Hemodynamics and Oxygenation Evaluated by ASL, BOLD and Oxygen Extraction Fraction (OEF) Imaging in Animal Model of Diabetic Nephropathy

Wednesday, Dec. 2 11:10AM - 11:20AM Location: E450B

Awards

Trainee Research Prize - Medical Student

Participants

Rui Wang, PhD, Beijing, China (*Presenter*) Nothing to Disclose Xiaoying Wang, MD, Beijing, China (*Abstract Co-Author*) Nothing to Disclose Xuedong Yang, Beijing, China (*Abstract Co-Author*) Nothing to Disclose Kai Zhao, PhD, Beijing, China (*Abstract Co-Author*) Nothing to Disclose Xueqing Sui, Beijing, China (*Abstract Co-Author*) Nothing to Disclose Zhiyong Lin, Beijing, China (*Abstract Co-Author*) Nothing to Disclose

PURPOSE

To investigate the feasibility of evaluating renal hemodynamics and oxygenation changes by arterial spin labeling (ASL), blood oxygen level dependent (BOLD) and oxygen extraction fraction (OEF) imaging in diabetic nephropathy (DN) rabbits.

METHOD AND MATERIALS

Seventeen New Zealand rabbits were divided into 2 groups: DN group, 12 rabbits with intravenously injection of alloxan at 100 mg/kg; and control group, 5 rabbits with injection of same dosage of 0.9% saline. At 72hr after the injection, blood glucose level was tested for all. Rabbits with blood glucose level higher than 16.0 mmol/L were considered as successfully established of diabetes mellitus (DM) model. MR examination was performed at 3T MR scanner (GE) with an 8-channel knee coil. For each rabbit, 2 times of MR exam were performed: baseline (before injection) and 72hr after model established successfully. ASL imaging was conducted with the labeling strategy of flow-sensitive alternating inversion recovery (FAIR) and BOLD was conducted with multiple gradient echo (mGRE) sequence. The measurement of renal OEF was derived from Yoblonsky's model with multi-echo gradient and spin echo (MEGSE) sequence. Then the rabbits were sacrificed for pathological study of the kidney. Quantitative RBF, R2* and OEF values were obtained within manually drawn ROIs, including cortex (CO) and outer medulla (OM). One-way ANOVA and paired-sample T test was performed to test the differences of RBF, R2* and OEF for inter- and inner-group.

RESULTS

Ten of 12 rabbits in DN group were successfully established DM model and renal pathological damages can be observed in these rabbits. There was no statistically significant difference of RBF, $R2^*$ or OEF between two groups at baseline (p>0.05). Compared with baseline, $R2^*$ and OEF in OM at 72 hr was significantly increased in DN group (p=0.018 and 0.048, respectively), while the control group was not (p>0.05). In CO, R2* also elevated significantly at 72 hr compared with baseline (p=0.04). For control group, there was no significant difference in CO or OM between baseline and 72 hr (p>0.05).

CONCLUSION

The combination of ASL, BOLD and OEF MRI may enable a comprehensive assessment of the functional status of early DN pathophysiological changes.

CLINICAL RELEVANCE/APPLICATION

It would be valuable for clinicians to early detect renal pathophysiological changes for diabetes without symptoms.

SSK08-06 Diffusion Weighted Imaging and Diffusion Tensor Imaging for Detection of Acute Kidney Injury in Patients Following Lung Transplantation

Participants

Susanne Tewes, MD, Hannover, Germany (*Presenter*) Nothing to Disclose Gregor Warnecke, Hannover, Germany (*Abstract Co-Author*) Nothing to Disclose Mi-Sun Jang, Hannover, Germany (*Abstract Co-Author*) Nothing to Disclose Dagmar Hartung, MD, Hannover, Germany (*Abstract Co-Author*) Nothing to Disclose Matti Peperhove, MD, Hannover, Germany (*Abstract Co-Author*) Nothing to Disclose Marcel Gutberlet, Dipl Phys, Hannover, Germany (*Abstract Co-Author*) Nothing to Disclose Christine Fegbeutel, Hannover, Germany (*Abstract Co-Author*) Nothing to Disclose Bjoern Juettner, Hannover, Germany (*Abstract Co-Author*) Nothing to Disclose Axel Haverich, Hannover, Germany (*Abstract Co-Author*) Nothing to Disclose Frank K. Wacker, MD, Hannover, Germany (*Abstract Co-Author*) Nothing to Disclose Frank K. Wacker, MD, Hannover, Germany (*Abstract Co-Author*) Nothing to Disclose Frank K. Wacker, MD, Hannover, Germany (*Abstract Co-Author*) Nothing to Disclose Frank K. Wacker, MD, Hannover, Germany (*Abstract Co-Author*) Nothing to Disclose Katja Hueper, Hannover, Germany (*Abstract Co-Author*) Nothing to Disclose

PURPOSE

Loss of renal function is a frequent complication after lung transplantation (lutx) and is associated with higher morbidity. Thus, imaging biomarkers to noninvasively monitor renal damage and to guide treatment strategies to preserve renal function are of clinical relevance. The purpose was to evaluate diffusion weighted imaging (DWI) and diffusion tensor imaging (DTI) for detection of renal impairment in lutx-patients.

METHOD AND MATERIALS

54 patients 14±2 days after lutx and 12 healthy volunteers underwent MRI on a 1.5T scanner. Respiratory-triggered DWI (10 bvalues, 0-1000 s/mm²) and DTI sequences (20 diffusion direction, b=0,600 s/mm²) were acquired. Maps of apparent diffusion coefficient (ADC) and fractional anisotropy (FA) were calculated. Renal function was monitored daily and acute kidney injury (AKI) was defined according to AKIN-criteria within 48h after surgery. Factors contributing to AKI such as duration of surgery, immunosuppressive drugs and blood product infusion were documented. Statistical analysis comprised ANOVA and correlation analysis. Values are given as mean±SEM.

RESULTS

59% (32/54) of lutx-patients developed AKI. ADC of renal medulla was significantly lower in patients with AKI compared to patients without AKI ($2.07\pm0.03 \text{ vs } 2.17\pm0.04*10^{-3} \text{ mm}^2/\text{s}$, p<0.05) and to healthy volunteers ($2.07\pm0.03 \text{ vs } 2.21\pm0.03*10^{-3} \text{ mm}^2/\text{s}$, p<0.01). FA-values of renal medulla were significantly reduced compared to healthy volunteers in both groups (AKI: 0.27 ± 0.01 , no AKI: 0.28 ± 0.01 , healthy: 0.33 ± 0.02 , p<0.001), and did not differ between patients with and without AKI. ADC and FA negatively correlated with the amount of blood product infusion (r=-0.41 and r=-0.42, p<0.01) and ADC was correlated with eGFR at the day of MRI (r=-0.52, p<0.001). No correlations with duration of surgery and tacrolimus levels at the day of the MRI were observed.

CONCLUSION

Diffusion imaging showed significant renal changes in lutx-patients compared to healthy volunteers irrespective of whether AKI was diagnosed according to standard criteria. ADC reduction was stronger in patients with AKI. Amount of blood product infusion correlated with MRI parameters and may be a contributing factor to renal damage following major surgery.

CLINICAL RELEVANCE/APPLICATION

Diffusion imaging detects renal damage following major surgery and may help to improve patient management to prevent further renal damage.

SSK08-07 Evaluation of Ultra-fast, Single Breath-Hold Renal ASL Perfusion-Preliminary Results of Healthy Volunteers

Wednesday, Dec. 2 11:30AM - 11:40AM Location: E450B

Participants

Melissa Ong, MD, Mannheim, Germany (*Presenter*) Nothing to Disclose Thorsten Honroth, Bremen, Germany (*Abstract Co-Author*) Research funded, Siemens AG Guenther Matthias, Bremen, Germany (*Abstract Co-Author*) Research funded, Siemens AG Bernd Kuehn, PhD, Erlangen, Germany (*Abstract Co-Author*) Nothing to Disclose Stefan O. Schoenberg, MD, PhD, Mannheim, Germany (*Abstract Co-Author*) Institutional research agreement, Siemens AG Daniel Hausmann, MD, Mannheim, Germany (*Abstract Co-Author*) Nothing to Disclose

PURPOSE

Evaluation of 3D ultra-fast, single breath-hold arterial spin labeling magnetic resonance imaging (ASL MRI) for the measurement of renal perfusion.

METHOD AND MATERIALS

We included 7 (5 male, mean age 29) healthy volunteers who did not suffer from any medical condition. A single-shot pulsed ASL (PASL) prototype sequence with a 3D GRASE readout using background suppression was implemented on a 3.0 Tesla Magnetom Skyra MRI scanner (Siemens Healthcare, Erlangen, Germany). 24 slices with a resolution of 4.7mm x 4.7mm x 4mm were acquired for 4 different inflow times (TI = 750ms, 1000ms, 1250ms, 1500ms) within a single breath-hold of 23s, including an integrated calibration scan (M0). The prototype sequence allowed a multi-slice measurement of the whole kidney in one exam. The exam was performed using a standard 18-channel body matrix coil. No contrast agent was applied. Subjective image quality was rated by two radiologists according to a 5-point Likert-scale (5=excellent; 1=non-diagnostic). Mean renal cortical and medullary blood flow was measured in the upper and lower pole of the kidney.

RESULTS

All images were rated as diagnostic. Overall image quality was rated as good (4; 25-75% quartile 3-4). Mean cortical perfusion values were 224 ± 28 mL/100mL/min for the upper and 224 ± 37 mL/100mL/min for the lower pole, mean medullary perfusion value

ranged between 107±16 mL/100mL/min and 101±14 mL/100mL/min for the upper and lower pole, respectively.

CONCLUSION

Ultra-fast, single breath-hold renal ASL perfusion in healthy volunteers shows promising results regarding image quality and feasibility.

CLINICAL RELEVANCE/APPLICATION

Ultra-fast, single breath-hold ASL perfusion facilitates contrast-free creation of parametric perfusion maps, which can be repeated arbitrarily and hence potentially serve to monitor therapy.

SSK08-08 Diffusion-weighted Magnetic Resonance Imaging of Kidneys in Patients with Chronic Kidney Disease

Wednesday, Dec. 2 11:40AM - 11:50AM Location: E450B

Participants

Katarzyna M. Sukowska, MD, Warsaw, Poland (*Presenter*) Nothing to Disclose Piotr Palczewski, MD, Warsaw, Poland (*Abstract Co-Author*) Nothing to Disclose Agnieszka Furmanczyk-Zawiska, Warsaw, Poland (*Abstract Co-Author*) Nothing to Disclose Wojciech Szeszkowski, Warsaw, Poland (*Abstract Co-Author*) Nothing to Disclose Dorota Piotrowska-Kownacka, Warsaw, Poland (*Abstract Co-Author*) Nothing to Disclose Magdalena Durlik, Warsaw, Poland (*Abstract Co-Author*) Nothing to Disclose Marek Golebiowski, Warsaw, Poland (*Abstract Co-Author*) Nothing to Disclose

PURPOSE

To assess the apparent diffusion coefficient (ADC) values of renal parenchyma in patients in different stages of chronic kidney disease (CKD). To correlate ADC measurements with creatinine blood level, estimated glomerular filtration rate (eGFR), and ADC values obtained from healthy subjects.

METHOD AND MATERIALS

20 healthy volunteers and 34 patients in different stages of CKD were examined on a 1.5 unit (Ingenia, Philips, The Netherlands). The inclusion criteria for patients with CKD were: biopsy proven CKD and no hydronephrosis or renal artery stenosis. Blood samples to assess the serum creatinine level were taken immediately before examination. The MR examination included two diffusion weighted sequences: one with 16 b values uniformly distributed from 0 to 750; the other one with 10 b values including 6 low (0-150) and 4 high (300-900) b values. ADC values were measured with whole-kidney manually placed region of interest. Statistical analysis was performed using the Statistica software (version 10.0; Statsoft, Inc., US). Unpaired Student's t-test were used to evaluate the differences in ADC. ROC curves were drawn to find out area under the curve for differentiation of CKD groups and cut-off ADC values were calculated so as to achieve the highest average sensitivity and specificity. To investigate the relationship between ADC values and serum creatinine / eGFR, Pearson's correlation coefficient was calculated by bivariate correlation. All P values <0.05 were taken as statistically significant.

RESULTS

A significant positive correlation between ADC and eGFR and a negative correlation between ADC and creatinine blood level was observed. There were statistical differences between ADC values in healthy individuals and patients in moderate and severe stage of CKD. Based on ADC measurements cut-off values were established allowing for identification of patients with eGFR higher than 60 ml/min/1.73m2 and lower then 30ml/min/1.73m2.

CONCLUSION

The DWI has a potential role in assessing renal function as ADC values correlate with eGFR and the level of renal damage in severe stages of CKD.

CLINICAL RELEVANCE/APPLICATION

The ability of DWI to noninvasively assess eGFR may provide an additional tool for monitoring the course of disease and for stratifying the risk of contrast medium administration in patients with CKD.

SSK08-09 Intravoxel Incoherent Motion MRI for Differentiating Renal Hypoperfusion from Increased Cellularity after Ischemia-Reperfusion

Wednesday, Dec. 2 11:50AM - 12:00PM Location: E450B

Participants

Mike Notohamiprodjo, Munich, Germany (*Presenter*) Nothing to Disclose Katharina Stella Winter, Munich, Germany (*Abstract Co-Author*) Nothing to Disclose Michael Staehler, MD, Munich, Germany (*Abstract Co-Author*) Nothing to Disclose Andreas D. Helck, MD, Munich, Germany (*Abstract Co-Author*) Nothing to Disclose Olaf Dietrich, PhD, Munich, Germany (*Abstract Co-Author*) Nothing to Disclose Moritz Schneider, Munich, Germany (*Abstract Co-Author*) Nothing to Disclose

PURPOSE

To differentiate hypoperfusion from inflammatory hypercellularity after renal ischemia-reperfusion due to partial nephrectomy using Intravoxel Incoherent Motion MRI.

METHOD AND MATERIALS

This IRB approved prospective study was performed according to the declaration Helsinki. 15 patients with renal tumors underwent MR at 3T (Magnetom Verio, Siemens Healthcare) directly before and one week after partial nephrectomy. Diffusion weighted imaging was acquired with an EPI-sequence (10 b-values 0-800 s/mm2, 3 averages, 6 directions). IVIM-analysis was performed with homebuilt software (PMI 0.4, IDL) by biexponential fitting of the tissue Dslow (mm2/s*10-3) and the pseudo-diffusion Dfast (mm2/s*10-3) as well as the perfusion component f (%). Apparent diffusion coefficient (ADC; mm2/s*10-3) was derived from monoexponential analysis. To compare parameters between baseline and follow-up the paired Wilcoxon signed-rank test and to compare nonnephrectomized and partially nephrectomized kidneys the non-paired Mann-Whitney U test was used.

RESULTS

In the baseline examination prior to partial nephrectomy there were no significant differences between tumor bearing and contralateral kidney, whereas the follow-up measurement showed significant differences for ADC (p<0.001), Dfast (p=0.02) and most pronounced for f (p<0.001). Partially nephrectomized kidneys showed a significant decrease of ADC ($2.5\pm0.3 \text{ vs. } 2.3\pm0.2$, p<0.01), Dfast ($8.6\pm1.8 \text{ vs. } 7.3\pm1.7$, p = 0.02) and again most pronounced for f ($19.2\pm3.0 \text{ vs. } 13.7\pm4.4 \text{ p} < 0.01$). There were no significant differences for Dslow (operated kidney $2.0\pm0.2 \text{ vs. } 2.0\pm0.2$; contralateral kidney $2.1\pm0.2 \text{ vs. } 2.0\pm0.1$) Non-nephrectomized contralateral kidneys expressed a significant increase of ADC ($2.5\pm0.2 \text{ vs. } 2.7\pm0.3$, p < 0.01), and f ($19.3\pm2.6 \text{ vs. } 21.5\pm4.0$, p = 0.03). There was no significant correlation of the alteration of each parameter to clamping time.

CONCLUSION

IVIM detects significant changes, particularly of the perfusion fraction in the operated and contralateral kidney after partial nephrectomy suggesting that ischemia-reperfusion associated diffusion restriction is correlated to hypoperfusion rather than increasing inflammatory cellularity.

CLINICAL RELEVANCE/APPLICATION

IVIM MRI suggest that renal ischemia-reperfusion associated diffusion restriction is correlated to hypoperfusion rather than increasing inflammatory cellularity.

Molecular Imaging (Staging and Therapy Control)

Wednesday, Dec. 2 10:30AM - 12:00PM Location: S504CD



AMA PRA Category 1 Credits ™: 1.50 ARRT Category A+ Credits: 1.50

FDA Discussions may include off-label uses.

Participants

Umar Mahmood, MD, PhD, Charlestown, MA (*Moderator*) Research Grant, Sabik Medical Inc; Advisory Board, Blue Earth Diagnostics Limited;

Suzanne E. Lapi, PhD, Saint Louis, MO (Moderator) Research Grant, ImaginAB, Inc

Sub-Events

SSK11-01 Noninvasive Monitoring of Early Antiangiogenic Therapy Response using RGD-conjugated Ultrasmall Superparamagnetic Iron Oxide Nanoparticles in an Orthotopic Human Nasopharyngeal Carcinoma Model

Wednesday, Dec. 2 10:30AM - 10:40AM Location: S504CD

Participants

Yanfen Cui, Shanghai, China (*Presenter*) Nothing to Disclose Caiyuan Zhang, MD, Shanghai, China (*Abstract Co-Author*) Nothing to Disclose Huanhuan Liu, Shanghai, China (*Abstract Co-Author*) Nothing to Disclose Dengbin Wang, Shanghai, China (*Abstract Co-Author*) Nothing to Disclose

PURPOSE

Molecular imaging is merging as a powerful tool for the noninvasive imaging of the biological processes. The purpose of this study was to validate a novel integrin $\alpha\nu\beta$ 3-targeted ultrasmall superparamagnetic iron oxide (USPIO) nanoparticles, Fe3O4@PAA-RGD, for its ability to detect tumor angiogenesis and assess the early response of an antiangiogenesis agent Avastin® in an orthotopic human nasopharyngeal carcinoma (NPC) model.

METHOD AND MATERIALS

The specific uptake of Fe3O4@PAA-RGD in HUVECs and CNE-2 Cells was evaluated using Prussian blue staining, transmission electron microscopy (TEM). The ability of Fe3O4@PAA-RGD to noninvasively assess $\alpha\nu\beta3$ integrin positive vessels in NPC tumor xenografts was evaluated with a 3.0T MR scanner. For the assessment of antiangiogenesis therapy, the mice bearing human NPC tumor xenografts were intraperitoneally injected with Avastin® (n=12) or normal saline (n=12) three times in a week at a dose of 200 µg/mouse .T2* mapping was performed baseline and after 2 and 7 days of treatment.

RESULTS

The specific uptake of the particles was mainly dependent on the interaction between RGD and integrin $\alpha\nu\beta3$ of HUVEC, which could be competitively inhibited by addition of unbound RGD. The tumor targeting of Fe3O4@PAA-RGD was observed in the orthotopic NPC model, which demonstrates accumulation of nanoparticles exclusively at the neovasculature but not within tumor cells. The vascular accumulation of Fe3O4@PAA-RGD caused significantly higher changes of the R2* value of tumors than observed for unlabelled USPIO. Bevacizumab treatment resulted in a significant reduction of the R2* values compared with the control group both at day2 and day7, confirmed by the immunohistochemistry of MVD after treatment.

CONCLUSION

This study demonstrates that RGD-coupled, PAA-coated USPIOs efficiently label integrin $\alpha\nu\beta$ 3expressed on endothelial cells. Furthermore, these molecular MR imaging probes are capable of noninvasive monitoring of the tumor response to bevacizumab therapy at early stages of treatment.

CLINICAL RELEVANCE/APPLICATION

RGD-coupled, PAA-coated USPIOs efficiently label integrin αvβ3expressed on endothelial cells. Furthermore, these molecular MR imaging probes are capable of noninvasive monitoring of the tumor response to bevacizumab therapy at early stages of treatment.

SSK11-02 Point of Care Assessment of Melanoma Tumor Signaling and Metastatic Burden from µNMR Analysis of Tumor Fine Needle Aspirates and Peripheral Blood

Wednesday, Dec. 2 10:40AM - 10:50AM Location: S504CD

Participants

Michael S. Gee, MD, PhD, Jamaica Plain, MA (*Presenter*) Nothing to Disclose Arezou Ghazani, PhD, Boston, MA (*Abstract Co-Author*) Nothing to Disclose Hakho Lee, PhD, Boston, MA (*Abstract Co-Author*) Nothing to Disclose Ralph Weissleder, MD, PhD, Boston, MA (*Abstract Co-Author*) Investor, T2 Biosystems, Inc

PURPOSE

To use μ NMR technology for molecular profiling of tumor fine needle aspirates and peripheral blood of melanoma patients, in order to assess BRAF signaling compared with genetic reference and metastatic burden compared with imaging reference.

METHOD AND MATERIALS

uNMR in vitro assessment of expression of melanocyte (MelanA, HMB45) and MAP kinase signaling (pERK, pS6K) molecules was

performed in human cell lines on a miniaturized μ NMR device as described (JB Haun, Sci Transl Med 2011) using nanoparticleconjugated antibodies. Clinical μ NMR validation was performed in an IRB-approved study of melanoma patients scheduled for biopsy of suspected metastasis, who also underwent tumor FNA and peripheral blood sampling for μ NMR. Tumor FNA specimens were assessed for pERK and pS6K, while peripheral blood was evaluated for circulating tumor cells (CTC) as described (AA Ghazani, Neoplasia 2012). Reference standards for μ NMR results included Western blot, BRAF genetic analysis, and metastatic burden on clinical imaging obtained near the time of biopsy. Student's t-test was used to assess for statistical significance.

RESULTS

 μ NMR in vitro analysis showed increased expression of melanocyte markers MART1 and HMB45 in human melanoma cell lines compared with nonmelanoma cells (P<0.0001). Expression of MAP kinase targets pERK and pS6K was significantly increased in BRAF mutant compared with BRAF WT melanoma cells (P < 0.01), with levels confirmed by Western blot. Ten patients in the clinical study included 5 BRAF wild-type and 5 BRAF V600E mutant melanoma patients. μ NMR analysis of tumor FNA samples showed increased pERK (41.0 +/- 8.6) and pS6K (34.4 +/- 15.5) levels in BRAF mutant compared with BRAF WT (24.8 +/- 15.0 and 23.5 +/- 9.0; P= 0.009 and 0.13 respectively) melanomas. μ NMR blood CTC level was significantly increased in patients with multiple metastases on imaging (90.3 +/- 57.9) compared with those with 0-1 lesions (39.3 +/- 31.5; P = 0.045). CTC threshold >60 was associated with significantly higher RECIST metastatic score on imaging and had 80% acc/83% sens/75% spec for multiple metastases.

CONCLUSION

 μ NMR technology provides point of care evaluation of tumor signaling in patients with cancer in a minimally invasive manner. μ NMR-based blood CTC level is significantly associated with metastatic burden on imaging.

CLINICAL RELEVANCE/APPLICATION

Molecular tracking of metastatic disease is possible by serial sampling of tumor cells and peripheral blood.

SSK11-03 Optical Molecular Imaging of Mesenchymal-Epithelial Transition Factor (c-Met) for Enhanced Detection and Characterization of Primary and Metastatic Hepatic Tumors

Wednesday, Dec. 2 10:50AM - 11:00AM Location: S504CD

Awards

Trainee Research Prize - Resident

Participants Shadi A. Esfahani, MD, MPH, Boston, MA (*Presenter*) Nothing to Disclose Pedram Heidari, MD, Boston, MA (*Abstract Co-Author*) Nothing to Disclose Umar Mahmood, MD, PhD, Charlestown, MA (*Abstract Co-Author*) Research Grant, Sabik Medical Inc; Advisory Board, Blue Earth Diagnostics Limited;

PURPOSE

Primary liver cancer as well as metastatic liver disease, predominantly from colorectal cancer (CRC) are major causes of cancer death. The success of liver cancer therapy depends on accurate diagnosis at the time of biopsy and efficiency of cytoreductive surgery. c-Met is a proto-oncogene overexpressed in 74-90 % of hepatocellular carcinoma (HCC) and CRC. We assessed whether optical imaging of c-Met using a targeted fluorescence probe, can be used to delineate and characterize the liver tumors and be effectively employed for intraoperative interventions and personalized therapy.

METHOD AND MATERIALS

A modified cyanine 5-tagged peptide with high affinity to c-Met was used. Cell binding assay was performed by incubation of human HCC cells (HepG2,Huh-7), CRC cells (HT-29), and cMET-negative cells (LNCaP) with probe ± HGF. Fluorescence signal was correlated to c-Met expression level. Focal models of primary and metastatic liver cancer were generated by injection of HepG2, Huh-7, and HT-29 in hepatic subcapsular space of nude mice (n=24). Near infrared fluorescence (NIRF) imaging was performed over 8 h after probe injection. Uptake in liver and tumor, and tumor to background ratio (TBR) were calculated. Probe biodistribution was assessed by measuring NIRF signal in multiple organs. IHC evaluation of c-Met expression in human CRCs and HCCs was performed using tissue arrays.

RESULTS

Incubation of cells with probe showed enhanced fluorescence signal in c-Met expressing cells compared to LNCaP, and strong correlation between signal and c-MET expression level (R2=0.99, p<0.0001). NIRF imaging showed high uptake in subcapsularly grown tumors and greater signal compared to the liver over 8 h; TBR reached a peak of 5.46±0.46 in Huh-7, 3.55±0.38 in HepG2 and 15.93±0.61 in HT-29, 4 h post-injection. IHC of tissue arrays confirmed c-Met overexpression in 86% of CRC and 84.9% of HCC cores.

CONCLUSION

High TBR achieved in our tumor models and overexpression of c-Met in a majority of human HCC and metastatic CRC tumors suggest that optical imaging of c-Met is a promising approach for accurate delineation and characterization of liver tumors. This is a translatable advancement for intraoperative image-guided interventions and personalized treatment.

CLINICAL RELEVANCE/APPLICATION

c-MET receptor imaging helps in precise delineation and in-situ characterization of primary hepatic tumors and metastases of other cancers to the liver.

SSK11-04 Volumetric Molecular Ultrasound Imaging of Tumor Angiogenesis: Intra-Animal Comparison with Volumetric Dynamic Contrast-Enhanced Imaging

Wednesday, Dec. 2 11:00AM - 11:10AM Location: S504CD

Participants

Huaijun Wang, MD, PhD, Stanford, CA (*Presenter*) Nothing to Disclose Dimitre Hristov, PhD, Stanford, CA (*Abstract Co-Author*) Research Grant, Koninklijke Philips NV; Partner, SoniTrack Systems, Inc

Lu Tian, Stanford, CA (Abstract Co-Author) Nothing to Disclose

Juergen K. Willmann, MD, Stanford, CA (*Abstract Co-Author*) Research Consultant, Bracco Group; Research Consultant, Triple Ring Technologies, Inc; Research Grant, Siemens AG; Research Grant, Bracco Group; Research Grant, Koninklijke Philips NV; Research Grant, General Electric Company

PURPOSE

To perform an intra-animal comparison between 3D ultrasound molecular imaging (USMI) using clinical grade vascular endothelial growth factor receptor 2 (VEGFR2)-targeted contrast microbubble (MBVEGFR2) and 3D dynamic contrast-enhanced (DCE)-US for assessing tumor angiogenesis and anti-angiogenic treatment effects in a murine model of human colon cancer.

METHOD AND MATERIALS

Subcutaneous human colon cancers were induced in 19 mice and randomized to either anti-angiogenic treatment (n=11; i.v. single dose of anti-angiogenic agent, bevacizumab at 10mg/kg) or vehicle treatment (n=8; saline). 3D US imaging was performed with a clinical system (IU22 xMATRIX; Philips) and a matrix array transducer (X6-1; 3.2MHz) using 2 techniques: 1) USMI was performed 4min after i.v. injection of 5×107 MBVEGFR2; and 2) DCE-US was performed with destruction-replenishment approach by constantly infusing non-targeted microbubbles at 40µL/min. VEGFR2-targeted signal intensity (SI) was quantified from USMI and 2 perfusion parameters, relative blood volume (rBV) and flow (rBF) were calculated from DCE-US. VEGFR2 expression levels and the percent area of blood vessels (PABV) were assessed ex vivo using immunofluorescence (IF) and correlated with correponding in vivo US parameters.

RESULTS

Both 3D US imaging techniques showed strong anti-angiogenic treatment effects. All 3 parameters including VEGFR2-targeted SI (58%, P=0.002), rBV (52%, P=0.002) and rBF (38%, P=0.02) significantly decreased following anti-angiogenic treatment compared to controls. IF showed significantly diminished VEGFR2 expression (P=0.03) and PABV (P=0.03) in treated tumors, while no significant change was observed in control tumors. SI was highly correlated with VEGFR2 expression (r=0.95, P=0.001), and rBV (r=0.71, P=0.08) and rBF (r=0.82, P=0.02) showed good correlation with PABV.

CONCLUSION

Both 3D USMI and 3D DCE-US provide complementary in vivo information on anti-angiogenic treatment effects and allow accurate quantification of tumor angiogenesis in human colon cancer xenografts compared to ex vivo reference gold standard techniques.

CLINICAL RELEVANCE/APPLICATION

3D imaging capabilities may further expand the future clinical role of both USMI and DCE-US in cancer imaging.

SSK11-05 Accurate Prediction of Nodal Status in Preoperative Patients with Thyroid Carcinoma Using Next-Gen Nanoparticle

Wednesday, Dec. 2 11:10AM - 11:20AM Location: S504CD

Participants

Aoife Kilcoyne, MBBCh, Boston, MA (*Presenter*) Nothing to Disclose Roy Phitayakorn, Boston, MA (*Abstract Co-Author*) Nothing to Disclose Gilbert H. Daniels, MD, Boston, MA (*Abstract Co-Author*) Nothing to Disclose Sareh Parangi, Boston, MA (*Abstract Co-Author*) Nothing to Disclose Gregory Randolph, Bosotn, MA (*Abstract Co-Author*) Nothing to Disclose Mukesh G. Harisinghani, MD, Boston, MA (*Abstract Co-Author*) Nothing to Disclose

PURPOSE

The goal of the study is to test the ability to image lymph node metastases in thyroid cancer by a novel MRI imaging agent the ferromagnetic nanoparticle Ferumoxytol (Feraheme; AMAG Pharmaceuticals, Lexington, MA), which has residual magnetic properties that are detectable by MRI. These carboxymethyl dextran-coated iron oxide ((FeO)1 - n(Fe2O3)n) nanoparticles slowly extravasate and travel through the lymphatic system to lymph nodes. The particles are subsequently internalized into macrophages, presumably through macropinocytosis. Prior studies using this approach with other malignancies (such as prostate cancer) demonstrated abnormal nanoparticle accumulation patterns which are detectable by MRI. We prospectively enrolled 12 patients with confirmed metastatic thryoid carcinoma (3 medullary, 9 papillary) undergoing surgery and compared preoperative MRI appearance of lymph nodes to post-operative histopathologic analysis. The study group consisted of 5 male and 7 female patients, with an mean of 34 nodes resected (range from 1 - 135).

METHOD AND MATERIALS

This exploratory study was performed as a prospective, single-dose pilot study and was approved by the Institutional Review Board. All patients with known thyroid cancer who were scheduled for surgical resection were eligible for enrollment in this study. Exclusion criteria included: age < 18, history of iron overload or known allergy to parenteral iron.

RESULTS

)We demonstrated 76.92% sensitivity and 95.74% specificity, 90.91% PPV (CI 70.84% to 98.88%) NPV 88.24% (76.13% to 95.56%) for the detection of central nodes. There was 82.76% sensitivity and 91.78% specificity, PPV 61.54% (CI 49.83% to 72.34%) NPV 97.1% (CI 94.73% to 98.6%) for the detection of peripheral nodes.

CONCLUSION

Lymph node metastases correlate with recurrent disease in patients with thyroid carcinoma. We currently have limited ability to image central lymph nodes prior to thyroidectomy in patients with thyroid carcinoma. This preliminary study suggests that MRI imaging following nanoparticle injection is a potentially worthwhile imaging modality. Additional studies are necessary comparing this with other established methods.

CLINICAL RELEVANCE/APPLICATION

Our study has demonstrated that nanoparticle-enhanced MRI is an accurate and safe method for pre-operatively detecting nodal metastases in patients with thyroid carcinoma.

SSK11-06 Chemical Exchange Saturation Transfer (CEST) Imaging: Comparison of Capability for Differentiation of Malignant from Benign Pulmonary Nodules and/ or Masses with FDG-PET/CT

Wednesday, Dec. 2 11:20AM - 11:30AM Location: S504CD

Participants

Yoshiharu Ohno, MD, PhD, Kobe, Japan (*Presenter*) Research Grant, Toshiba Corporation; Research Grant, Koninklijke Philips NV; Research Grant, Bayer AG; Research Grant, DAIICHI SANKYO Group; Research Grant, Eisai Co, Ltd; Research Grant, Terumo Corporation; Research Grant, Fuji Yakuhin Co, Ltd; Research Grant, FUJIFILM Holdings Corporation; Research Grant, Guerbet SA; Masao Yui, Otawara, Japan (*Abstract Co-Author*) Employee, Toshiba Corporation Cheng Ouyang, Vernon Hills, IL (*Abstract Co-Author*) Employee, Toshiba Corporation Mitsue Miyazaki, PhD, Vernon Hills, IL (*Abstract Co-Author*) Employee, Toshiba Corporation Shinichiro Seki, Kobe, Japan (*Abstract Co-Author*) Nothing to Disclose Hisanobu Koyama, MD, PhD, Kobe, Japan (*Abstract Co-Author*) Nothing to Disclose Takeshi Yoshikawa, MD, Kobe, Japan (*Abstract Co-Author*) Research Grant, Toshiba Corporation Sumiaki Matsumoto, MD, PhD, Kobe, Japan (*Abstract Co-Author*) Research Grant, Toshiba Corporation Kazuro Sugimura, MD, PhD, Kobe, Japan (*Abstract Co-Author*) Research Grant, Toshiba Corporation; Kazuro Sugimura, MD, PhD, Kobe, Japan (*Abstract Co-Author*) Research Grant, Toshiba Corporation; Kazuro Sugimura, MD, PhD, Kobe, Japan (*Abstract Co-Author*) Research Grant, Toshiba Corporation; Kazuro Sugimura, MD, PhD, Kobe, Japan (*Abstract Co-Author*) Research Grant, Toshiba Corporation; Kazuro Sugimura, MD, PhD, Kobe, Japan (*Abstract Co-Author*) Research Grant, Toshiba Corporation; Kazuro Sugimura, MD, PhD, Kobe, Japan (*Abstract Co-Author*) Research Grant, Toshiba Corporation Research Grant, Koninklijke Philips NV Research Grant, Bayer AG Research Grant, Eisai Co, Ltd Research Grant, DAIICHI SANKYO Group

PURPOSE

To directly and prospectively compare the capability of chemical exchange saturation transfer (CEST) imaging targeted to amide groups (-NH) for differentiation of malignant from benign pulmonary nodules and/ or masses with FDG-PET/CT.

METHOD AND MATERIALS

Thirty-six consecutive patients (26 men and 10 women; mean age 67 years) with pulmonary nodules and/ or masses underwent CEST imaging, FDG-PET/CT and pathological and/or follow-up examinations. According to final diagnoses, all lesions were divided into malignant (n=26) and benign (n=10) groups. To obtain CEST imaging data in each subject, respiratory-synchronized fast advanced spin-echo images were conducted following a series of magnetization transfer (MT) pulses. Then, magnetization transfer ratio asymmetry (MTRasym) was calculated from z-spectra at 3.5ppm in each pixel, and MTRasym map was computationally generated. To evaluate the capability for differentiation between two groups at each lesion, MTRasym and SUVmax were assessed by ROI measurements. Then, MTRasym was statistically correlated with SUVmax. To compare each index between two groups, Student's t-test was performed. Then, ROC-based positive test was performed to determine each feasible threshold value for differentiation of two groups. Finally, sensitivity, specificity and accuracy were compared each other by McNemar's test.

RESULTS

MTRasym had no significant correlation with SUVmax (p=0.10). Mean MTRasym ($0.1\pm5.5\%$) and SUVmax (3.0 ± 0.8) of malignant group were significantly higher than those of benign group (MTRasym: $-4.2\pm4.4\%$, p=0.03; SUVmax: 2.5 ± 0.5 , p=0.04). When applied each feasible threshold value, sensitivity (SE: 80.8 [21/26] %), specificity (SP: 70.0 [7/10] %) and accuracy (77.8 [28/36] %) of MTRasym had no significant difference with those of SUVmax (SE: 69.2 [18/26] %, p=0.25; SP: 60.0 [6/10] %, p=1.0; AC: 66.7 [24/36] %, p=0.13).

CONCLUSION

CEST imaging is considered at least as valuable as FDG-PET/CT for differentiation of malignant from benign pulmonary nodules and/ or masses.

CLINICAL RELEVANCE/APPLICATION

CEST imaging is considered at least as valuable as FDG-PET/CT for differentiation of malignant from benign pulmonary nodules and/ or masses.

SSK11-07 Radiofrequency Hyperthermia (RFH)-Enhanced Herpes Simplex Virus-Thymidine Kinase/Ganciclovir (HSV-TK/GCV) Gene Therapy of Hepatocellular Carcinoma: Monitored by Ultrasound and Optical Imaging

Wednesday, Dec. 2 11:30AM - 11:40AM Location: S504CD

Awards

Molecular Imaging Travel Award

Participants Jianfeng Wang, MD, Seattle, WA (*Presenter*) Nothing to Disclose Feng Zhang, MD, Seattle, WA (*Abstract Co-Author*) Nothing to Disclose Yaoping Shi, MD, Seattle, WA (*Abstract Co-Author*) Nothing to Disclose Zhibin Bai, Seattle, WA (*Abstract Co-Author*) Nothing to Disclose Long-Hua Qiu, Shanghai, China (*Abstract Co-Author*) Nothing to Disclose Renyou Zhai, MD, Beijing, China (*Abstract Co-Author*) Nothing to Disclose Xiaoming Yang, MD, PhD, Seattle, WA (*Abstract Co-Author*) Nothing to Disclose

PURPOSE

To determine the possibility of using radiofrequency hyperthermia (RFH) to enhance therapeutic effect of herpes simplex virus thymidine kinase/ganciclovir (HSV-TK/GCV) on hepatocellular carcinoma (HCC).

METHOD AND MATERIALS

Human HCC cells (HepG2) were first transfected with lentivirus/luciferase. For both in-vitro confirmation and in-vivo validation, Luciferase-labeled HCC cells and HCC tumor xenografts on mice received different treatments: (i) combination therapy of intratumoral HSV-TK/GCV-mediated gene therapy plus MR imaging-heating-guidewire (MRIHG)-mediated RFH; (ii) gene therapy only; (iii) RFH only; and (iv) phosphate-buffered saline (PBS) as control. Cell proliferation was quantified by MTS assay. Tumor size and signal changes were monitored by ultrasound imaging and optical imaging before and at days 7 and 14 after treatments, which were correlated with subsequent histology.

RESULTS

Of in vitro experiments, MTS assay demonstrated the lowest cell proliferation in combination therapy group compared with those in three control groups ($29\pm6\%$ VS 56 $\pm9\%$, $93\pm4\%$, and $100\pm5\%$, p<0.05). Of in vivo experiments, ultrasound imaging showed smaller relative tumor volume in combination therapy group than those in three control groups (0.74 ± 0.19 VS 1.79 ± 0.24 , 3.14 ± 0.49 and 3.22 ± 0.52 , p<0.05). Optical imaging demonstrated significant decrease of bioluminescence signals of tumors in the combination therapy group, compared to those in three control groups (1.2 ± 0.1 VS $1.9\pm0.2\%$ VS $3.3\pm0.6\%$ VS $3.5\pm0.4\%$, p<0.05)(Figure). These imaging findings were correlated well with histologic confirmation.

CONCLUSION

RF-hyperthermia can enhance HSV-TK/GCV-mediated gene therapy of hepatocellular cancer, which may open new avenues for efficient management of hepatocellular carcinoma using MR/RF hyperthermia-integrated interventional gene therapy.

CLINICAL RELEVANCE/APPLICATION

RF-hyperthermia can enhance HSV-TK/GCV-mediated gene therapy of hepatocellular cancer.

SSK11-08 Identification of a Prognostic PET-miRNA Radiogenomic Signature Associated with the mir-200 Family

Wednesday, Dec. 2 11:40AM - 11:50AM Location: S504CD

Awards

Molecular Imaging Travel Award

Participants

Shota Yamamoto, MD, Los Angeles, CA (*Presenter*) Nothing to Disclose Christopher W. Migdal, Petaluma, CA (*Abstract Co-Author*) Nothing to Disclose Ronald L. Korn, MD, PhD, Scottsdale, AZ (*Abstract Co-Author*) Chief Medical Officer, Imaging Endpoints; Founder, Imaging Endpoints; Shareholder, Imaging Endpoints Michael B. Gotway, MD, Scottsdale, AZ (*Abstract Co-Author*) Nothing to Disclose Neema Jamshidi, MD, PhD, Los Angeles, CA (*Abstract Co-Author*) Nothing to Disclose Michael D. Kuo, MD, Los Angeles, CA (*Abstract Co-Author*) Nothing to Disclose

PURPOSE

To use radiogenomic analysis to define and contextualize a prognostic microRNA signature in non-small-cell lung carcinoma (NSCLC).

METHOD AND MATERIALS

Using a known prognostic PET signature, differential expression analysis using linear models of microarray data (limma) was performed on 10 NSCLC (adenocarcinoma ad squamous cell carcinoma) patients with Positron Emission Tomography (PET) and microRNA (miRNA) expression data to identify potential prognostic PET associated radiogenomic signatures. The same signature candidate was selected and analyzed on a public dataset of 105 patients with clinical outcome and miRNA expression data to confirm its prognostic value. Furthermore, the PET phenotype was validated in an independent dataset with PET and outcomes data in 21 patients.

RESULTS

Significant correlations between high SUV max lesion normalized to the SUV mean liver and the downregulation of hsa-mir-200b and hsa-miR-149 were identified (p<0.05). Low expression of the mir-200 family is a well known marker for aggressive lung cancer behavior and chemoresistance. Testing of the miRNA surrogate for SUV signature in the PET-miRNA validation was validated in the public dataset as a predictor of survival (P=0.04). The PET trait also stratified patient outcome in an independent dataset (p=0.048).

CONCLUSION

Radiogenomic analysis allows integration of multiple independent datasets thereby providing not only molecular biological context behind a given biomarker, but also enabling robust validation of biomarkers that is often not feasible with existing approaches.

CLINICAL RELEVANCE/APPLICATION

This approach allows integration of independent datasets thereby providing biological context behind a given biomarker in a cost effective way.

SSK11-09 Differential Receptor Tyrosine Kinase PET Imaging in Response to Targeted Inhibition

Wednesday, Dec. 2 11:50AM - 12:00PM Location: S504CD

Awards

Trainee Research Prize - Resident

Participants

Eric Wehrenberg-Klee, MD, Boston, MA (*Presenter*) Nothing to Disclose Nafize S. Turker, PhD, Boston, MA (*Abstract Co-Author*) Nothing to Disclose Pedram Heidari, MD, Boston, MA (*Abstract Co-Author*) Nothing to Disclose Mauri Scaltriti, PhD, New York, NY (*Abstract Co-Author*) Nothing to Disclose Umar Mahmood, MD, PhD, Charlestown, MA (*Abstract Co-Author*) Research Grant, Sabik Medical Inc; Advisory Board, Blue Earth Diagnostics Limited;

PURPOSE

The targeted AKT inhibitor GDC-0068 shows promise for the treatment of triple-negative breast cancer (TNBC). Resistance to AKT inhibition is mediated through upregulation of the receptor tyrosine kinases (RTK) EGFR and HER3, however the profile of upregulation differs across cell lines, and may be predictive of treatment response. We sought to noninvasively image these

expression changes for the purpose of therapeutic guidance.

METHOD AND MATERIALS

64Cu-DOTA-cetuximab F(ab´)2 and 64Cu-DOTA-HER3 F(ab´)2 were prepared and probe affinity for their targets assessed. The TNBC cell lines MDMBA468 and HCC70 were treated with the AKT inhibitor GDC-0068 for one day at a range of concentrations. Following treatment, uptake of EGFR probe or HER3 probe was assessed, and results compared to protein expression changes of EGFR or HER3, respectively, as assessed by Western blot. MDAMB468 mice were then treated with GDC-0068 or control for 2 days. After treatment, mice were imaged with either 64Cu-DOTA-EGFR F(ab´)2 or 64Cu-DOTA-HER3 F(ab´)2 to assess changes in EGFR or HER3 expression, respectively.

RESULTS

Treatment of the TNBC cell lines MDAMB468 and HCC70 with GDC-0068 resulted in increased EGFR Probe uptake of 6% and 88% respectively. Interrogation of the same cell lines with HER3 Probe demonstrated uptake changes of 74% and 102%. These findings correlate closely to changes in protein expression as assessed by Western blot. MDAMB468 mouse xenografts treated with control or AKT inhibitor for two days and then imaged demonstrate no significant change in SUVmean of EGFR PET Probe (0.48 vs. 0.53, p=0.11), however demonstrate a significant change in SUVmean of HER3 PET Probe (0.35 vs 0.73, p<0.01).

CONCLUSION

TNBC resistance to AKT inhibition can be mediated through increased RTK expression in a pattern that differs across cell lines and patient tumors. We demonstrate that the differential change in RTK expression can be noninvasively assessed, demonstrating in a model of TNBC that while imaged EGFR expression does not change, imaged HER3 expression increases by 108%. These noninvasively assessed differential changes in RTK expression may inform subsequent therapeutic choices.

CLINICAL RELEVANCE/APPLICATION

The pattern of RTK expression change induced by AKT inhibition is not known prior to treatment. RTK PET imaging may allow for noninvasive assessment of these changes to optimize therapeutic regimens.

BOOST: Genitourinary-Integrated Science and Practice (ISP) Session

Wednesday, Dec. 2 10:30AM - 12:00PM Location: S103CD



AMA PRA Category 1 Credits ™: 1.50 ARRT Category A+ Credits: 1.50

FDA Discussions may include off-label uses.

Participants

Stanley L. Liauw, MD, Chicago, IL (*Moderator*) Nothing to Disclose George B. Rodrigues, MD, London, ON (*Moderator*) Nothing to Disclose

Sub-Events

MSR042-01 Invited Speaker:

Wednesday, Dec. 2 10:30AM - 10:40AM Location: S103CD

Participants

Rodney J. Ellis, MD, Pepper Pike, OH (Presenter) Nothing to Disclose

MSR042-02 A Phase I Dose Escalation Study of Hypofractionated Radiation Therapy for Favorable Risk Prostate Cancer: Acute Toxicity and Early Efficacy

Wednesday, Dec. 2 10:40AM - 10:50AM Location: S103CD

Participants

Nicholas J. Sanfilippo, MD, New York, NY (*Presenter*) Nothing to Disclose William C. Huang, MD, New York, NY (*Abstract Co-Author*) Nothing to Disclose Herbert Lepor, MD, New York, NY (*Abstract Co-Author*) Nothing to Disclose Silvia C. Formenti, MD, New York, NY (*Abstract Co-Author*) Nothing to Disclose Benjamin Cooper, New York, NY (*Abstract Co-Author*) Nothing to Disclose Smith Beverly, New York, NY (*Abstract Co-Author*) Nothing to Disclose Barry Rosenstein, New York, NY (*Abstract Co-Author*) Nothing to Disclose Samir S. Taneja, MD, New York, NY (*Abstract Co-Author*) Nothing to Disclose Samir S. Taneja, MD, New York, NY (*Abstract Co-Author*) Consultant, Eigen Consultant, GTx, Inc Consultant, Bayer AG Consultant, Healthtronics, Inc Speaker, Johnson & Johnson Investigator, STEBA Biotech NV Royalties, Reed Elsevier

ABSTRACT

Purpose/Objective(s): The optimal radiation schedule for the curative treatment of prostate cancer remains unknown. Prostate cancer patients receiving definitive external beam radiation therapy (EBRT) are typically treated 5 days per week for 7-9 weeks. This prolongation of treatment time increases healthcare costs and is less convenient for patients. There is data supporting the notion that the a/β ratio for prostate cancer cells is between 1 and 3, suggesting a clinical benefit to hypofractionation. We therefore conducted a Phase I dose escalation trial in men with low to low-intermediate risk prostate

adenocarcinoma.Materials/Methods: All men with clinical T1-2c, Gleason Score (GS) 6, prostate cancer with a prostatic specific antigen (PSA) less than 10 ng/dL were eligible for this trial. Men with clinical T1-2c, GS 7 prostate cancer and/or PSA 10 - 20 ng/dL were included provided the biopsy demonstrated low volume disease (Results: From June, 2012 to December, 2014, 9 patients were accrued to the three dose cohorts with a median follow-up of 11 months (range: 2 - 30). Patients had a median age of 63, pre-treatment PSA of 4.9 ng/dL, and pre-treatment AUA score of 10. Four patients had a GS of 7. The maximum tolerated dose (MTD) was 57.6 Gy with all patients completing treatment with less than or equal to grade 2 maximum gastrointestinal, genitourinary, dermatologic or fatigue related toxicity (Table 1). Six patients have at least 1 PSA post-treatment (3 months after completion) with a median PSA decrease of 65%. One patient of the six with > 11 month follow-up had grade 2 rectal telangiectasia requiring minor endoscopic cautery. The remaining 5 patients had no grade 2 toxicity thus far.Conclusion: All three dose levels were well tolerated with no MTD identified. Further follow-up is warranted for long term toxicity and efficacy.Table 1: Acute toxicity in patients undergoing hypofractionated radiation.Grade of ToxicityCTCAE v. 4.0Dose Level 154 Gy/ 18 Fxn = 3Dose Level 255.8 Gy/ 18 Fxn = 3Dose Level 357.6 Gy/ 18 Fxn =

3 Gastrointestinal 023011032000 Genitourinary 000212312100 Dermatitis 0333 Fatigue 03111022

MSR042-03 Robotic Stereotactic Body Radiation Therapy for Organ Confined Prostate Cancer

Wednesday, Dec. 2 10:50AM - 11:00AM Location: S103CD

Participants

Jonathan A. Haas, MD, Mineola, NY (*Presenter*) Speaker, Accuray Incorporated Aaron E. Katz, MD, Garden City, NY (*Abstract Co-Author*) Nothing to Disclose Seth Blacksburg, MD, MBA, New York, NY (*Abstract Co-Author*) Speakers Bureau, Bayer AG; Owen Clancey, PhD, Mineola, NY (*Abstract Co-Author*) Nothing to Disclose Michael Santoro, MD, East Meadow, NY (*Abstract Co-Author*) Nothing to Disclose Richard Ashley, MD, Garden City, NY (*Abstract Co-Author*) Nothing to Disclose Dimitri Kessaris, MD, Manhasset, NY (*Abstract Co-Author*) Nothing to Disclose Robert Mucciolo, MD, Massapequa, NY (*Abstract Co-Author*) Nothing to Disclose Diane Accordino, RN, Mineola, NY (*Abstract Co-Author*) Nothing to Disclose Diane Accordino, RN, Mineola, NY (*Abstract Co-Author*) Nothing to Disclose Susan Lowery, BA, Mineola, NY (*Abstract Co-Author*) Nothing to Disclose William Macmelville, Mineola, NY (*Abstract Co-Author*) Nothing to Disclose Christopher Mendez, BA, Mineola, NY (*Abstract Co-Author*) Nothing to Disclose

ABSTRACT

Purpose/Objective(s): The unique radiobiology of prostate cancer supports a hypofractionated as opposed to a conventionally fractionated dose regimen with a potential for improved outcomes and reduced toxicities. We report on our continued experience using a robotic linear accelerator to deliver stereotactic body radiation therapy for localized prostate cancer.Materials/Methods: From April 2006 through December 2014, a total of 1207 patients with localized carcinoma of the prostate were treated with robotic stereotactic body radiation therapy at a single institution. All patients had T1c to T2b disease. 493 patients had low risk disease. 548 patients had intermediate risk disease. 166 patients had high risk disease. Pretreatment PSAs ranged from .77 to 205. 126 patients received hormonal therapy prior to treatment at the discretion of their urologist. Treatment planning was done with CT scans fused with an MRI scan except in 31 cases where an MRI scan could not be done for medical reasons such as a pacemaker. Dose was prescribed to the 83% to 87% line, 5 mm beyond the capsule except posteriorly 3 mm. 1037 patients with low and intermediate risk disease received CyberKnife only to a dose of 3500 to 3625 cGy over 5 fractions. All patients received 1500 mg of amifostine intrarectally 50 minutes prior to each treatment fraction. Results: The median initial PSA was 6.2. The median follow-up was 33 months. The median post treatment PSA is 0.35. At the time of last follow-up, 12 patients have had a PSA failure by Phoenix biochemical definition. 1 patient with low risk disease failed. 7 patients with intermediate risk disease failed and 4 patients with high risk disease failed. There were 136 patients with a minimum follow up of at least 36 months and 56 patients with a minimum follow up of at least 48 months. There are 26 patients with a minimum follow up of 60 months. 272 patients achieved a PSA below 0.2 and 413 patients reached a PSA below 0.4. The median treatment PSA at 12 months is 0.90. The median PSA at 24 months is 0.45. The median PSA at 36 months is 0.40. the median PSA at 48 months is 0.25. The median treatment PSA at 60 months is 0.20. With a median follow up of 33 months, the biochemical disease free survival for low risk, intermediate risk, and high risk was 99.7%, 98.7%, and 97.5% respectively. 2 patients had symptomatic hematuria which resolved with hyperbaric oxygen. 2 patients required green light laser for urinary retention. 1 patient has required catheterization. 3 patients had rectal bleeding which resolved with rowasa enemas and hyperbaric oxygen. Conclusion: Stereotactic body radiation therapy using a robotic linear accelerator continues to be extremely well tolerated and efficacious in the management of localized prostate cancer. High rates of local control can be achieved while also achieving low rates of bladder and rectal toxicity. This study confirms prior reported series with a larger number of patients.

MSR042-04 The Effect of Radiation Timing on PSA Reduction in High Risk Prostate Cancer Patients Treated with Definitive Radiation Therapy

Wednesday, Dec. 2 11:00AM - 11:10AM Location: S103CD

Participants Apar Gupta, Boston, MA (*Presenter*) Nothing to Disclose Steven Vernali, Boston, MA (*Abstract Co-Author*) Nothing to Disclose Ankit Agarwal, BS, Boston, MA (*Abstract Co-Author*) Nothing to Disclose Muhammad M. Qureshi, MBBS,MPH, Boston, MA (*Abstract Co-Author*) Nothing to Disclose Alexander E. Rand, BA, Boston, MA (*Abstract Co-Author*) Nothing to Disclose

Ariel E. Hirsch, MD, Boston, MA (*Abstract Co-Author*) Nothing to Disclose

ABSTRACT

Purpose/Objective(s): We previously found that neither time to treatment (TTT) nor elapsed time of treatment (ETT) had any effect on PSA velocity in patients with low- and intermediate-risk prostate cancer. In this analysis, we sought to examine the effects of TTT and ETT on PSA change in patients with high-risk prostate cancer. Materials/Methods: We performed a retrospective review of 1,584 patients who were diagnosed with prostate cancer at our institution between January 2005 and December 2013, and found 412 patients with non-metastatic disease who completed treatment with definitive external beam radiation therapy (EBRT). A total of 146 patients who also received concurrent androgen-deprivation therapy (ADT) were included in the analysis. TTT was calculated as days between positive prostate biopsy and EBRT start date, and ETT was calculated as days between EBRT start and stop date. Demographic data on race/ethnicity, primary language spoken, insurance status, marital status, and age were also collected. Analysis of variance was performed to analyze the relationship of these factors with absolute and percentage change in pre- and post-EBRT PSA levels. Data were analyzed using a 0.05 level of significance.Results: Median age at diagnosis was 67 years (range 50-85 years); 11% had a Gleason score (GS) of 6, 49% GS 7, and 40% GS 8-10. Median TTT was 134 days and median ETT was 62 days. No demographic variable was found to be significantly related to absolute or percentage change in PSA. No optimal threshold of days from diagnosis to treatment (TTT) was identified to predict change in PSA level. ETT was significantly related to PSA change, after adjusting for demographic variables. Those who fell in the upper quartile of ETT (>64 days) were found to have a 94.2% decline in PSA, compared to 98.0% for those who fell in the lower three quartiles (p=0.03).Conclusion: A delay in treatment prior to starting EBRT did not have an effect on post-EBRT PSA level, relative to initial PSA level. However, a delay during EBRT was related to a lesser reduction in PSA decline. Further research is warranted in this area to elucidate the clinical significance of differences in PSA reduction.

MSR042-05 Patient Inversion Therapy for Bowel (PITB) to Achieve Maximum Displacement in Radiotherapy for Prostate Cancer

Wednesday, Dec. 2 11:10AM - 11:20AM Location: S103CD

Participants

Gordon L. Grado, MD,PhD, Scottsdale, AZ (*Abstract Co-Author*) Nothing to Disclose David Constantinescu, Charleston, IL (*Presenter*) Nothing to Disclose Scott Thompson, CMD, Scottsdale, AZ (*Abstract Co-Author*) Nothing to Disclose Carrie S. Petrone, RN, Scottsdale, AZ (*Abstract Co-Author*) Nothing to Disclose Mary M. Grado, BSN,MS, Scottsdale, AZ (*Abstract Co-Author*) Nothing to Disclose Michael C. Grado, BA, Scottsdale, AZ (*Abstract Co-Author*) Nothing to Disclose Thayne Larson, MD, Scottsdale, AZ (*Abstract Co-Author*) Nothing to Disclose

PURPOSE

The purpose of this study was to evaluate a new and novel approach to the valuation and reduction of small bowel volume from the irradiated fields in the treatment of prostate cancer. This technique utilizes inversion therapy to either completely displace small or large bowel from the irradiated field or to significantly reduce the volume of bowel irradiated in the PTV. This procedure has potential application in multiple areas of abdominal and pelvic radiation therapy.

METHOD AND MATERIALS

Between January 2014 and March 2015, 14 consecutive patients were identified where small or large bowel was directly within the irradiated PTV. Patients were evaluated with bladder distention, patient positioning, and inversion therapy to displace bowel from the irradiated PTV. Inversion therapy had the greatest effect in displacing and maintaining displacement of bowel from the irradiated volume. Several inversion tables were evaluated prior to the procedure and the two safest devices with the most clinical experience for inversion therapy were selected for this trial. Dose volume histograms were compared with and without inversion.

RESULTS

Patients were identified with loops of bowel directly within the radiated field due to previous surgery or anatomy. Standard techniques for bowel displacement (patient positioning, bladder distention, belly-board), were ineffective at displacing sufficient bowel from the irradiated volume to affect greater radiation dose delivery. Inversion therapy was selected for bowel displacement which when combined with bladder distention maintained the displacement during the course of radiation therapy. 13/14 patients were found to have sufficient bowel displacement to allow greater radiation dose delivery to the PTV without compromising field size or prescribed dose. 1/14 patients did not benefit from this technique.

CONCLUSION

Patient inversion therapy for bowel (PITB) achieved excellent bowel displacement for radiation therapy to the pelvis. In these patients, neither the radiation therapy field nor the prescribed dose had to be compromised. Patients also had fewer bowel and bladder symptoms during the pelvic radiation therapy. This technique is determined to be useful, easily applicable, and well tolerated by patients.

CLINICAL RELEVANCE/APPLICATION

This procedure permits higher radiation therapy dose delivery to the PTV with fewer side effects and morbidity due to less small/large bowel volume irradiated.

MSR042-06 Institutional Experience of Long-term (10-15 Years) Results with High Dose Rate (HDR) Salvage Therapy for Recurrent Prostate Cancer

Wednesday, Dec. 2 11:20AM - 11:30AM Location: S103CD

Participants

Nevine M. Hanna, MD, Sandy, UT (Presenter) Nothing to Disclose

ABSTRACT

Purpose/Objective(s): Limited treatments are available for recurrent prostate cancer patients. Modality selection can be challenging for both the patient and their physicians. HDR brachytherapy has been used extensively as a boost after external beam radiation therapy, but is increasingly being tested as salvage treated for locally recurrent prostate cancer. We report our long-term results for HDR salvage brachytherapy in patients with initially low, intermediate, and high risk prostate cancer.Materials/Methods: Patients (n=27) with a median age of 71 (57-84) years at recurrence with low- (n=10), intermediate- (n=8), and high-risk prostate cancer (n=9) treated at the California Endocurietherapy (CET now at UCLA) between 1991 and 2009 were analyzed. Median HDR brachytherapy dose prescription was 36 (22-46) Gy in 6 (3-8) fractions. Five patients did receive additional external beam radiation therapy (EBRT) after HDR brachytherapy to an EBRT dose of 36 (36-50) Gy. Presenting disease characteristics were median recurrent PSA 8.1 (1.4-86.7) ng/mL, Gleason Score 7 (5-10), median prostate volume 23.2 (0-80) cc. Androgen deprivation therapy (ADT) was administered in 68% for a median of 6 (3-96) months. Risk groups were defined according to the NCCN guidelines. Sustained PSA nadir+2 was used to define biochemical relapse. Statistical analyses being performed are to include Kaplan-Meier analyses and univariate and multivariate Cox proportional analyses. Results: Preliminary analysis shows that the median overall follow-up time was 6.90 (0.30-15.92) years. The 5, 10 and 15 year overall survival (OS) rates were 86%, 36% and 11%, respectively. The 5, 10 and 15 year distant metastases-free survival (DMFS) rates were 68%, 29% and 11%, respectively. Biochemical progression free survival (BPFS) for the initially presenting low, intermediate and high grade patients is 122, 59, and 41 months, respectively. On univariate analyses, BPFS after salvage HDR was most significantly impacted by PSA at recurrent diagnosis (p=0.007) but not significantly affected by risk group at initial diagnosis (P>0.05). Univariate Cox analyses and multivariate analyses are currently underway to determine the impact of ADT on these parameters. Conclusion: Our long-term data validates HDR salvage brachytherapy in recurrent prostate cancer patients as a standard treatment option which offers excellent rates of disease control.

MSR042-07 Designing and Implementing an Innovative Phantom-Based Simulator Training Program for Prostate Brachytherapy Using Advanced Magnetic Resonance Imaging

Wednesday, Dec. 2 11:30AM - 11:40AM Location: S103CD

Awards

Trainee Research Prize - Resident

Participants Nikhil G. Thaker, MD, Houston, TX (*Presenter*) Nothing to Disclose Tze Yee Lim, Houston, TX (*Abstract Co-Author*) Nothing to Disclose Rajat Kudchadker, Houston, TX (*Abstract Co-Author*) Nothing to Disclose Tharakeswara K. Bathala, MD, Houston, TX (*Abstract Co-Author*) Nothing to Disclose Thomas Pugh, Houston, TX (*Abstract Co-Author*) Nothing to Disclose Usama Mahmood, Houston, TX (*Abstract Co-Author*) Nothing to Disclose Deborah A. Kuban, MD, Houston, TX (*Abstract Co-Author*) Nothing to Disclose Teresa Bruno, Houston, TX (*Abstract Co-Author*) Nothing to Disclose Jihong Wang, PhD, Houston, TX (*Abstract Co-Author*) Nothing to Disclose R. Jason Stafford, PhD, Houston, TX (*Abstract Co-Author*) Nothing to Disclose Thomas A. Buchholz, MD, Houston, TX (*Abstract Co-Author*) Nothing to Disclose S J. Frank, MD, Houston, TX (*Abstract Co-Author*) Board Member, C4 Imaging LLC; Stockholder, C4 Imaging LLC; Advisory Board, Elekta AB

PURPOSE

Prostate brachytherapy (PB) is a well-established treatment for localized prostate cancer and has the potential to deliver excellent

outcomes at low cost. However, high-quality PB requires hands-on training and expertise in image-guidance, which is minimally emphasized in current radiation oncology training. Additionally, MRI holds promise of improving target delineation over CT imaging. Our objective was to design and implement a unique pilot training program that utilizes advanced MRI and a phantom simulator approach to improve the quality of PB education.

METHOD AND MATERIALS

Our existing PB phantom simulator program was adapted to introduce MRI treatment planning and post-implant evaluation. The simulator program emphasized six core areas: patient selection, simulation, treatment planning, implantation, treatment evaluation, and outcome assessment. Trainees in the simulator program were residents, fellows, or physicists. The program utilized the Iodine-125 pre-operative planning technique and a transrectal ultrasound device to implant prostate phantoms. MRI markers were substituted for spacers to allow for visualization.

RESULTS

Forty one trainees have completed the phantom simulator program to date. Ten implants were successfully conducted during the MRI-phantom simulator pilot program. MRI 3DT2 CUBE sequence could adequately delineate the prostate, seminal vesicles, rectum and bladder in the CIRS 053MM phantom. Dummy seeds could be well-visualized with post-implant CT scans. However, seed identification on MRI required a learning curve due to the need to identify MRI markers, which flanked each dummy seed (Figure). The MRI markers facilitated detection of up to 97% of seeds in implanted phantoms by identifying the signal voids between MRI markers.

CONCLUSION

This proof-of-principle educational curriculum successfully adapted a phantom simulator training program to implement advanced MRI simulation, treatment planning, and post-implant dosimetry. Analysis of implants showed that most organs could be adequately visualized with MRI and that most seeds could be identified with the aid of MRI markers. Phantom-based simulator training programs can provide a valuable educational opportunity to learn the PB process and to learn how to implement advanced image-guidance.

CLINICAL RELEVANCE/APPLICATION

Phantom-based simulator training can enhance practical expertise with advanced imaging technology and image-guide therapies.

MSR042-09 Stereotactic Body Radiation Therapy for Primary Lesion of Renal Cell Carcinoma

Wednesday, Dec. 2 11:50AM - 12:00PM Location: S103CD

Participants

Hotaka Nonaka, Chuo, Yamanashi, Japan (Presenter) Nothing to Disclose

ABSTRACT

Purpose/Objective(s): We assessed the efficacy and toxicity of stereotactic body radiation therapy (SBRT) for primary lesion of renal cell carcinoma (RCC).Materials/Methods: We retrospectively reviewed 9 patients (7 male and 2 female) with stage I RCC treated with SBRT between 2007 and 2014. The diagnosis of RCC was judged according to imaging. The median age was 73 years old (range, 59-79). Three patients had high serum creatinine level before SBRT. Four patients had history of prior contralateral nephrectomy. The median diameter of tumor was 18 mm (range, 9-26). A total dose of 60-70 Gy in 10 fractions was administered at the 95% of planning target volume or internal target volume. Median biologically effective dose was 119 Gy (range 96-119), using an a/ß value of 10 Gy. Overall survival (OS) and local progression-free survival (LPFS) were based on Kaplan Meier estimates. Toxicity was scored according to NCI-CTCAE, version 4.0. Renal disorder was graded by referring to pretreatment renal function. Results: The median follow-up duration after SBRT was 28 months (range, 11-89). Clinical response was partial response (PR) in 5 tumors, stable disease (SD) in 4 tumors. Five tumors with PR has decreased gradually in size for 11-56 months (median, 42) after SBRT. Three patients developed distant metastases. The 2- and 3- year OS rate were 85.7% and 64.3%, respectively (median survival time, 44 months). The 3- year LPFS rate was 100%. In a case of a patient with SD tumor, autopsy was performed at 29 months after SBRT, and it showed almost complete necrosis of tumor tissues with a small amount of viable renal carcinoma cells. Three patients developed Grade 3 chronic kidney disease (CKD), 1 had Grade 2 CKD. All patients with Grade 3 CKD had high serum creatinine level before SBRT, and 2 of these patients had prior contralateral nephrectomy before SBRT. Severe toxicity for other organs at risk was not observed. Conclusion: SBRT for primary lesion of RCC resulted in acceptable LPFS and toxicity. Because of slow tumor response, we need long-term follow up to observe the effect of SBRT for RCC. Multicenter prospective study is mandatory to evaluate true local effect and toxicity and to compare SBRT versus other local treatment modalities for RCC.

Essentials of Breast Imaging

Wednesday, Dec. 2 10:30AM - 12:00PM Location: S100AB

BR DM

AMA PRA Category 1 Credits ™: 1.50 ARRT Category A+ Credits: 1.50

Participants Sub-Events

Sub-Lvents

MSES42A Update on Breast US BI-RADS

Participants

Marcela Bohm-Velez, MD, Pittsburgh, PA (*Presenter*) Consultant, Koninklijke Philips NV; Researcher, Siemens AG; Researcher, Dilon Technologies, Inc;

LEARNING OBJECTIVES

1) Discuss the need to optimize the sonographic technique and understand breast anatomy for best use of the US lexicon. 2) Discuss the descriptors that are used in assessing a lesion and the need for consistent and standardized terminology. 3) Discuss integration of US findings with mammographic, MRI and MBI studies and the subsequent management options.

ABSTRACT

The ACR BI-RADS for US is designed to standardize reporting, providing an organized approach to image interpretation and management. Understanding breast anatomy and optimizing the sonographic image is crucial for using the lexicon, which enables better communication of results to other physicians and their patients. This will also facilitate data collection for audits to monitor results and determine accuracy of image interpretation. Use and examples of the descriptors will be discussed.

MSES42B Imaging the Post-Surgical Breast

Participants

Ellen B. Mendelson, MD, Chicago, IL, (emendels@nm.org) (*Presenter*) Medical Advisory Board, Delphinus Medical Technologies, Inc; Research support, Siemens AG; Consultant, Siemens AG; Speaker, Siemens AG; Medical Advisory Board, Quantason, LLC; Consultant, Quantason, LLC;

LEARNING OBJECTIVES

1) Recognize postsurgical changes on mammography, US, and MRI. 2) Define the time course of posttherapy changes, which slowly resolve after radiation therapy. 3) Describe surgical and reconstructive procedures used in treatment of breast cancer.

ABSTRACT

MSES42C Tomosynthesis - Is It Ready for Screening?

Participants

Fiona J. Gilbert, MD, Cambridge, United Kingdom (*Presenter*) Medical Advisory Board, General Electric Company; Research Grant, GlaxoSmithKline plc; Research Grant, General Electric Company

LEARNING OBJECTIVES

1) To learn about the evidence from retrospective studies for screening with Digital Breast Tomosynthesis. 2) To learn about the evidence from prospective studies for screening with Digital Breast Tomosynthesis. 3) To appreciate the information that is still required before adoption into routine screening.

ISP: Health Service, Policy and Research (Education)

Wednesday, Dec. 2 10:30AM - 12:00PM Location: S102D

ED HP

AMA PRA Category 1 Credits ™: 1.50 ARRT Category A+ Credits: 1.50

Participants

Paul P. Cronin, MD, MS, Ann Arbor, MI (*Moderator*) Nothing to Disclose Laura M. Fayad, MD, Baltimore, MD (*Moderator*) Nothing to Disclose

Sub-Events

SSK10-01 Health Service, Policy and Research Keynote Speaker: Innovative Teaching Methods in Radiology Education

Wednesday, Dec. 2 10:30AM - 10:40AM Location: S102D

Participants

Aine M. Kelly, MD, Ann Arbor, MI (Presenter) Nothing to Disclose

SSK10-02 Comparison of High-fidelity Hands-on Simulation Team Training to Lecture/computer-simulation Based Training for Both Contrast Reaction Management and Teamwork Skills

Wednesday, Dec. 2 10:40AM - 10:50AM Location: S102D

Participants

Carolyn L. Wang, MD, Seattle, WA (*Presenter*) Nothing to Disclose Sankar Chinnugounder, MD, Worcester, MA (*Abstract Co-Author*) Nothing to Disclose Daniel S. Hippe, MS, Seattle, WA (*Abstract Co-Author*) Research Grant, Koninklijke Philips NV; Research Grant, General Electric Company Ryan O'Malley, MD, Seattle, WA (*Abstract Co-Author*) Nothing to Disclose

Puneet Bhargava, MD, Shoreline, WA (*Abstract Co-Author*) Editor, Reed Elsevier Sadaf F. Zaidi, MD, Spokane, WA (*Abstract Co-Author*) Nothing to Disclose William H. Bush JR, MD, Seattle, WA (*Abstract Co-Author*) Nothing to Disclose

PURPOSE

To compare the performance of teams of radiologists, technologists and nurses trained with high-fidelity hands-on simulation versus lecture/computer-based simulation training for contrast reaction management and teamwork skills on a high-fidelity severe contrast reaction scenario.

METHOD AND MATERIALS

Eleven nurses, 11 technologists and 11 PGY2 radiology residents were prospectively recruited for this IRB and HIPAA compliant study. Participants were arranged into teams of 3 (1 resident, 1 nurse and 1 technologist). Six teams underwent hands-on training (HO) and 5 teams underwent lecture/computer-based training (CB) for contrast reaction management (CRM) and teamwork skills (TS). All similarly trained participants were tested in novel teams using a high-fidelity simulation scenario. Three CRM expert radiologists independently graded the CRM skills and three TS experts independently graded the TS skills tested. Objective scores were based on whether key actions were taken or not taken. Subjective scores were based on a 7-point Likert-like scale (strongly disagree to strongly agree). Objective and subjective scores were compared between training groups using the Mann-Whitney test. Spearman's correlation coefficient was used to compare objective and subjective scores.

RESULTS

The HO teams tended to score better than CB teams on the objective CRM ($95.3\pm3.1 \text{ vs. } 80.8\pm15.3 \text{ p}=0.17$) and subjective CRM scores ($6.3\pm0.5 \text{ vs. } 5.6\pm0.8 \text{ p}=0.33$). The HO and CB teams score more similarly on both objective TS ($51.0\pm6.1 \text{ vs. } 52.4\pm6.8 \text{ p}=0.66$) and subjective TS ($3.7\pm0.4 \text{ vs. } 4.1\pm0.9 \text{ p}=0.25$). There was good correlation between the objective and subjective TS scores (r=0.78, p=0.007). However, the overall objective score percentages were higher for CRM skills than TS skills for both the HO (p=0.03) and CB teams (p=0.06).

CONCLUSION

High-fidelity simulation based training may be better than lecture/computer-based training for teams of radiologists, technologists and nurses for contrast reaction management. However, a single session of high-fidelity simulation-based training or computer-based training appears to be similarly inadequate to master teamwork skills.

CLINICAL RELEVANCE/APPLICATION

High-fidelity simulation-based training may be better than computer-based training for teams of radiologists, technologist and nurses for contrast reaction management, but not for teamwork skills.

Honored Educators

Presenters or authors on this event have been recognized as RSNA Honored Educators for participating in multiple qualifying educational activities. Honored Educators are invested in furthering the profession of radiology by delivering high-quality educational content in their field of study. Learn how you can become an honored educator by visiting the website at: https://www.rsna.org/Honored-Educator-Award/

SSK10-03 Integrating Simulated Clinical Decision Support at the Point-of-Order into Medical Student Radiology Education via a Blended-Learning Environment

Wednesday, Dec. 2 10:50AM - 11:00AM Location: S102D

Participants

Marc H. Willis, DO, Houston, TX (*Presenter*) Nothing to Disclose L. Alexandre R. Frigini, MD, Houston, TX (*Abstract Co-Author*) Nothing to Disclose Jay Lin, MD, Bellaire, TX (*Abstract Co-Author*) Nothing to Disclose David M. Wynne, MD, Pearland, TX (*Abstract Co-Author*) Nothing to Disclose Karla A. Sepulveda, MD, Houston, TX (*Abstract Co-Author*) Nothing to Disclose

PURPOSE

Develop a case-based education portal simulating clinical decision support (CDS) at the point-of-order to highlight best practice in appropriate imaging utilization and patient safety. Pilot the portal with medical students transitioning from preclinical courses to clinical rotations, introducing these students to evidence-based decision making before they are exposed to unexplained variance in clinical ordering habits.

METHOD AND MATERIALS

An education portal was built on the American College of Radiology's Radiology Curriculum Management System (RCMS). RCMS and the CDS tool (ACR Select) were integrated via application programming interface. The cases simulate common clinical scenarios from a primary care practice setting, including questions regarding Choosing Wisely topics. Institutional review board approval was obtained for the pilot project. Learners navigated through the portal, receiving CDS feedback prior to and after selecting answers for the cases. Assessment was via a pre-test, post-test and survey questions.

RESULTS

On the survey, 85.29% of learners believe this portal with simulated CDS should be included in their medical school curriculum. The learners self-assessment of their level of preparatoin to appropriately order imaging studies for their patients increased. All learners percieved value in the virtual classroom simulated CDS experience. A statistically significant improvement in the number of correct answers from the pre-test to the post-test was achieved in four categories: Intermediate difficulty case scenarios (p-value <0.0001), advanced difficulty case scenarios (p-value 0.0013), Choosing Wisely questions (p-value 0.0207) and the overal total (p-value <0.0001).

CONCLUSION

This novel approach has potential to address many needs in medical education, delivers value, and make a meaningful contribution to medical education. Timing of this project coincides with calls for physicians to embrace decision support. Using a readily available decision support software program, there is an opportunity to develop and implement standard key components of medical education curricula and assessment on the national level.

CLINICAL RELEVANCE/APPLICATION

This web-based product is scalable and could be used for future education projects such as graduate medical education, allied health education, quality improvement projects, and continuing medical education for practicing medical providers.

SSK10-04 iPad Driven Small Group Radiology Sessions within Gross Anatomy Laboratory: Effectiveness at 12 months

Wednesday, Dec. 2 11:00AM - 11:10AM Location: S102D

Participants

Robert J. Ward, MD, Boston, MA (*Presenter*) Nothing to Disclose Gene M. Weinstein, MD, Boston, MA (*Abstract Co-Author*) Nothing to Disclose Daniel H. MacArthur, MD, Boston, MA (*Abstract Co-Author*) Nothing to Disclose Katherine Malcolm, Boston, MA (*Abstract Co-Author*) Nothing to Disclose Leah Ahn, MS, MA, Boston, MA (*Abstract Co-Author*) Nothing to Disclose Margaret K. Chung, MD, La Jolla, CA (*Abstract Co-Author*) Nothing to Disclose

PURPOSE

To evaluate the effectiveness of iPad driven radiologic anatomy small group sessions within the first year clinical anatomy laboratory.

METHOD AND MATERIALS

The faculty and residents of the radiology department of Tufts Medical Center participated in 23 of 27 gross anatomy sessions. Groups of 7-12 students of the Class of 2016 rotated through a 4-5 minute small group discussion in front of a 65- inch wall mounted flat screen LCD display hooked up to an Apple TV (Apple, Inc). An iPad 3 (Apple, Inc.) equipped with iOS 5.1 and running OsiriX 3.5 (Pixmeo SARL) was used to project dicom images on the display. Projectional as well as cross sectional images specific to the laboratory curriculum were utilized. Images shown during the laboratory sessions were later used on the 4 lab practical examinations. A 20 question multiple choice examination was administered to the class of 2015 approximately 12 months following their completion of clinical anatomy. The class of 2015 clinical anatomy lab did not include the iPad driven radiologic anatomy minicourse and thereby functioned as the control group. The test was then administered to the Class of 2016 at the same 12 month interval following completion of their clinical anatomy course. First order test questions focused on anatomic concepts were utilized. No imaging was utilized on the exam. The study is IRB approved.

RESULTS

108 of 208 Class of 2016 second year clinical anatomy students completed the 20 multiple choice anatomy examination 12 months following completion of their clinical anatomy course including the iPad driven anatomic radiology laboratory minicourse. The Class of 2016 scored an average 60.7% on the exam. 113 of 202 members of the control group, Class of 2015, scored an average of 55.6%. The experimental group performed statistically significantly better (P=0035) with a 9.1% improvement. Both the class of 15 and 16 had comparable MCAT scores average aggregates of 32.8 and 32.0 respectively.

CONCLUSION

An iPad driven radiologic anatomy laboratory minicourse led by radiologists proved effective in improving student's 12 month retention of clinical anatomy knowledge.

CLINICAL RELEVANCE/APPLICATION

Small group anatomy instruction is effective at teaching anatomic concepts through imaging.

SSK10-05 Coming Out of the Dark: A Curriculum for Teaching and Evaluating Radiology Residents' Communications Skills through Simulation

Wednesday, Dec. 2 11:10AM - 11:20AM Location: S102D

Participants

Carolynn M. Debenedectis, MD, Worcester, MA (*Presenter*) Nothing to Disclose Jean-Marc Gauguet, MD, PhD, Worcester, MA (*Abstract Co-Author*) Nothing to Disclose Joseph Makris, MD, Worcester, MA (*Abstract Co-Author*) Nothing to Disclose Stephen D. Brown, MD, Boston, MA (*Abstract Co-Author*) Nothing to Disclose Max P. Rosen, MD, MPH, Worcester, MA (*Abstract Co-Author*) Stockholder, Everest Scientific Inc; Consultant, PAREXEL International Corporation; Stockholder, Cynvenio Biosystems, Inc; Medical Advisory Board, Cynvenio Biosystems, Inc

PURPOSE

The purpose of this project is to develop a curriculum to teach radiology residents communication skills through simulation. Communication skills are a core competency for which radiology residents must be evaluated. As Radiology has moved from "film" to PACS, opportunities for direct communication between Radiologists and referring clinicians have decreased. Additionally, radiologists increasingly must communicate effectively with patients. Simulation has been shown an effective tool, and we believe it can be used to teach and evaluate communication skills for radiology residents.

METHOD AND MATERIALS

Current first (N=5) and fourth year (N=3) radiology residents (PGY 2 and PGY 5) participated in 6 baseline communication scenarios with trained professional patient "actors". Scenarios included error and apology, delivering bad news, canceling examination/procedure, radiation risk counseling, giving results in pediatric imaging, and angry referring physician. Resident performance in the scenarios was evaluated by attending radiologists with prior communication skills training and the patient actors, using the Gap-Kalamazoo Communication Skills (GKCS) Assessment Form. All activities were videotaped at our interprofessional Center for Experiential Learning and Simulation (iCELS). Immediately following completion of all 6 scenarios, residents were debriefed, and defined teaching points were identified. Following a 2 week washout period and additional training, residents participated in a second similar simulation.

RESULTS

The average GKCS score for all the residents improved to 79% (range 66-86%) in part 2 compared to 74% (range 65-82%) in part 1. Fourth year residents performed better on both part 1 and 2 of the simulation when compared to first year residents. Average fourth year's score for part 1 was 77% vs. 72% for first year residents. Average fourth year's score for part 2 was 81% vs. 76% for first year residents.

CONCLUSION

Simulation is a promising method for teaching and evaluating residents' communication skills.

CLINICAL RELEVANCE/APPLICATION

Simulation can be used to teach and evaluate radiology residents' communication skills in compliance with the core competency requirement.

SSK10-06 Use of in-situ High-fidelity Severe Contrast Reaction Simulation Radiology Team Performance Testing to Identify Gaps in Knowledge for Teamwork Skills Based on TeamSTEPPS®

Wednesday, Dec. 2 11:20AM - 11:30AM Location: S102D

Participants

Carolyn L. Wang, MD, Seattle, WA (*Presenter*) Nothing to Disclose Sankar Chinnugounder, MD, Worcester, MA (*Abstract Co-Author*) Nothing to Disclose Daniel S. Hippe, MS, Seattle, WA (*Abstract Co-Author*) Research Grant, Koninklijke Philips NV; Research Grant, General Electric Company Ryan O'Malley, MD, Seattle, WA (*Abstract Co-Author*) Nothing to Disclose Puneet Bhargava, MD, Shoreline, WA (*Abstract Co-Author*) Editor, Reed Elsevier Sadaf F. Zaidi, MD, Spokane, WA (*Abstract Co-Author*) Nothing to Disclose William H. Bush JR, MD, Seattle, WA (*Abstract Co-Author*) Nothing to Disclose

PURPOSE

To perform in-situ hands-on high-fidelity simulation testing of teams of radiology residents, nurses and technologists with a severe contrast reaction scenario to identify gaps in knowledge on teamwork skills.

METHOD AND MATERIALS

Eleven nurses, 11 technologists and 11 PGY2 radiology residents were recruited for this IRB and HIPAA compliant study. Participants were arranged into teams of 3 (1 resident, 1 nurse and 1 technologist). All participants underwent TeamSTEPPS® training with an interactive lecture. Eleven teams underwent in-situ high-fidelity simulation scenario testing with a severe contrast reaction scenario with built in medical mistakes. Three TeamSTEPPS® expert trainers independently graded the teamwork skills (TS) tested and their grades were averaged. Grades (out of 100%) for each skill were computed by adding up grades for each skill. The sub-item grades were examined to determine on which skill sub-items participants generally performed particularly poorly to help refine the training program.

RESULTS

The overall TS grades were low (52±6%). The grades for each major skill were also low (40-59%) including SBAR (Situation Background, Assessment, Recommendation), closed loop communication, CUS (Concerned, Uncomfortable, Safety issue), huddle and leadership. For SBAR, the low grades were due to participants rarely using the specific word from the acronym and not offering recommendations. For closed-loop communication, participants rarely named an individual for a call out and frequently failed to close the loop. Only 2 of the 11 groups had an identifiable team leader on whom all graders agreed. The majority of huddles were not being performed in a timely fashion and the teams rarely attempted to create a shared mental model.

CONCLUSION

In-situ high-fidelity severe contrast reaction simulation testing of teams of radiology residents, nurses and technologists can be used to identify knowledge gaps in teamwork skills. This allows focused training to include improving methods of relaying patient information, identifying a situational leader, and proper closed loop communication.

CLINICAL RELEVANCE/APPLICATION

Patient safety requires effective teamwork skills. Training radiology teams (nurses, technologists and radiologists) should focus on teamwork skills and in-situ high-fidelity simulation testing can identify specific gaps.

Honored Educators

Presenters or authors on this event have been recognized as RSNA Honored Educators for participating in multiple qualifying educational activities. Honored Educators are invested in furthering the profession of radiology by delivering high-quality educational content in their field of study. Learn how you can become an honored educator by visiting the website at: https://www.rsna.org/Honored-Educator-Award/

Puneet Bhargava, MD - 2015 Honored Educator

SSK10-07 Teaching from Every Angle: Integrating 3D Anatomy with Interactive Case-based Radiology Playlists

Wednesday, Dec. 2 11:30AM - 11:40AM Location: S102D

Participants

Derek A. Smith, MBChB, Edinburgh, United Kingdom (*Presenter*) Nothing to Disclose Jeremy B. Jones, MRCP, FRCR, Melbourne, Australia (*Abstract Co-Author*) Nothing to Disclose

PURPOSE

As clinical imaging becomes more accessible, radiologists have an ever-increasing opportunity to be actively engaged with medical student teaching. We sought to assess how this teaching can be aided by innovative approaches and new technologies.

METHOD AND MATERIALS

Case based tutorials were designed for medical students on their clinical orthopaedics placement. Normal anatomy was viewed and manipulated using a three-dimensional (3D) imaging 'Sectra Table'. Plain film and cross-sectional imaging was then displayed through the device to discuss common and important fractures and injuries. Groups of 6-10 students attended sessions run by a radiologist (consultant or clinical fellow).Post-session feedback was collected online with quantitative Likert scales and qualitative free-text comments.

RESULTS

Sessions were rated by 53 students (from January to March 2015) on a scale of 'poor' (1) to 'awesome' (5), for the following criteria: content (median score 4.6), relevance (4.6), style of presentation (4.8) and quality of display aids (4.9).Feedback praised the use of the imaging table relating 3D anatomy to clinical imaging ("brilliant aid, great technology"). The ability to view plain film and cross-sectional imaging and explore associated anatomical structures was highly valued.Having the opportunity to go through imaging on a case-by-case basis with a radiologist was appreciated and many requested more radiology teaching.

CONCLUSION

Using the interactive 3D surface is an exciting new model for student and teacher, and this was reflected by the high feedback scores and comments. It reinforces the importance of understanding underlying anatomy and highlights the value of the information gained from plain films. Interactive teaching with a radiologist proved popular and helps to introduce advanced imaging concepts at an appropriate level.

CLINICAL RELEVANCE/APPLICATION

Integrated anatomy and radiology teaching with an interactive case-based approach using novel 3D technology proved popular and engaged students while enhancing their clinical knowledge.

SSK10-08 Improving First-Year Resident Education in Musculoskeletal Imaging: Comparison of Workflow Using the Customary Chronologic Approach with the Novel Anatomy Based Approach

Wednesday, Dec. 2 11:40AM - 11:50AM Location: S102D

Participants

Leon Lenchik, MD, Winston-Salem, NC (*Presenter*) Nothing to Disclose Robert D. Boutin, MD, Sacramento, CA (*Abstract Co-Author*) Nothing to Disclose Jasjeet Bindra, MBBS, MD, Davis, CA (*Abstract Co-Author*) Nothing to Disclose Bahram Kiani, MD, Winston Salem, NC (*Abstract Co-Author*) Nothing to Disclose Cyrus Bateni, MD, Sacramento, CA (*Abstract Co-Author*) Nothing to Disclose Scott D. Wuertzer, MD, MS, Winston-Salem, NC (*Abstract Co-Author*) Nothing to Disclose

PURPOSE

Determine if organization of a PACS worklist by chronologic order versus anatomic order influences first-year radiology resident performance, resident satisfaction, or faculty satisfaction.

METHOD AND MATERIALS

In a prospective study conducted at two major academic institutions, first-year residents on their first musculoskeletal imaging rotation were randomly divided into two groups based on chronologic or anatomic sorting of their worklist. Residents in the chronologic group (CG) sorted their worklist based on the date of the study with the oldest studies interpreted first. Residents in the anatomy group (AG) sorted their worklist based on an anatomic region for the day (Day 1: Shoulder, humerus, elbow; Day 2: Forearm, wrist, hand; Day 3: Pelvis, hip; Day 4: Femur, knee, leg; Day 5: Ankle, foot). At the end of the 4-week rotation, residents took a 25-question, image-based examination and completed a satisfaction survey, which assessed experience, teaching, and workload on a scale of 1 to 5 (1=poor; 5=excellent). For each resident, the faculty completed a similar survey that assessed the experience, teaching, and workload. Resident and faculty surveys also included three open-ended questions to provide qualitative assessment of satisfaction. Data from the two institutions were pooled, and the CG and AG groups were compared.

RESULTS

There were 7 residents in the CG group and 9 in the AG group. The numbers of correct answers on the post-rotation examination were slightly higher in the AG group (14.8) than the CG group (14.1). Resident satisfaction scores of overall experience were higher in the AG group (4.7) than the CG group (4.0). Resident satisfaction scores relating to teaching were similar in the AG group (4.8) and CG group (4.9). Resident satisfaction scores relating to workload were similar in the AG group (3.9) and CG group (4.0). Faculty satisfaction scores were similar in the two groups. Qualitative assessment of resident and faculty satisfaction comments were overwhelmingly positive for both groups. The single negative comment was from one resident assigned to the CG group.

CONCLUSION

For first-year residents rotating on the musculoskeletal service, organizing the PACS worklist by anatomic region rather than by date improves learning and increases resident satisfaction.

CLINICAL RELEVANCE/APPLICATION

Novel approaches to managing resident workflow can improve their experience on the musculoskeletal service.

SSK10-09 Health Service, Policy and Research Keynote Speaker: Simulation in Medical Education: An Evolving Tool for Training in Radiology

Wednesday, Dec. 2 11:50AM - 12:00PM Location: S102D

Participants

Laura M. Fayad, MD, Baltimore, MD (Presenter) Nothing to Disclose

ISP: Radiation Oncology (Outcomes/Quality of Life I)

Wednesday, Dec. 2 10:30AM - 12:00PM Location: S104A

RO SQ

AMA PRA Category 1 Credits ™: 1.50 ARRT Category A+ Credits: 1.50

Participants

Martin Colman, MD, Houston, TX (*Moderator*) Nothing to Disclose James S. Welsh, MD, MS, Batavia, IL (*Moderator*) Nothing to Disclose

Sub-Events

SSK17-01 Radiation Oncology Keynote Speaker: Perspectives in Breast Cancer

Wednesday, Dec. 2 10:30AM - 10:40AM Location: S104A

Participants

Anna Shapiro, MD, Syracuse, NY (Presenter) Nothing to Disclose

SSK17-02 An Institutional Review of Radiation Doses from Radiological Imaging Procedures in Image-guided Radiotherapy of Cancers

Wednesday, Dec. 2 10:40AM - 10:50AM Location: S104A

Participants

Li Zhou, PhD, Chengdu, China (*Abstract Co-Author*) Nothing to Disclose Yibao Zhang, Beijing, China (*Abstract Co-Author*) Nothing to Disclose Jun Deng, PhD, New Haven, CT (*Presenter*) Nothing to Disclose

PURPOSE

To systematically compare radiation doses to organs-at-risk (OARs) between planning CTs and image-guided procedures during image-guided radiotherapy (IGRT) of cancers.

METHOD AND MATERIALS

With IRB approval, 4832 cancer patients who underwent IGRT at our institution between Sep. 2009 and Apr. 2014 were included in this retrospective study. Their gender, age, circumference were collected as well as all the radiological imaging procedures performed, including computed tomography (CT), kilo-voltage portal imaging (kVPI), megavoltage portal imaging (MVPI) and kilo-voltage cone-beam computed tomography (kVCBCT). Correlations between patient's size and organ dose were first established via Monte Carlo dose calculations in patient anatomy, and then used for patient-specific organ dose estimation. The imaging doses to brain, lungs and red bone marrow (RBM) were analyzed.

RESULTS

A total of 142017 imaging procedures were performed on 4832 patients, 5113 of which were CT scans. Regardless of age, average CT doses to brain, lungs and RBM were 0.5, 0.6, 0.6 cGy for males, and 0.5, 0.6, 0.6 cGy for females, accounting for 1.6%, 3.5%, 2.0%, 1.6%, 4.0% and 3.3% of combined dose, respectively. Peaking at 45 cGy, kVPI contributed largest doses to brain, about 47 times of CT doses. In lungs and RBM, average kVPI dose remained higher for most children but decreased below 14 cGy in adults. Unlike kVPI, average MVPI doses to OARs were less than 10 cGy, peaking at 16 cGy in RBM for eldest males. kVCBCT doses were generally 0-8 cGy except for males of 51 years and older who received largest number of scans in pelvis.

CONCLUSION

While CT scans deposited a small portion of radiation doses to cancer patients, image-guided procedures employed in IGRT can contribute up to 50 cGy of cumulative imaging doses to brain, 30 cGy to lungs and 40 cGy to RBM in pediatric patients. This study indicated a pressing need for personalized imaging protocol to maximize clinical benefits of imaging procedures while reducing imaging doses and associated cancer risks.

CLINICAL RELEVANCE/APPLICATION

(dose comparison among imaging procedures) This study reveals a strong need for personalized imaging protocol to maximize clinical benefits of imaging procedures while reducing imaging doses and associated cancer risks.

SSK17-03 Impact of Single Day Multidisciplinary Clinics on the Lead Time from Diagnosis to Initiation of Treatment in Head and Neck Cancers

Wednesday, Dec. 2 10:50AM - 11:00AM Location: S104A

Participants

Raju Vaddepally, Oak Brook, IL (Presenter) Nothing to Disclose

ABSTRACT

Purpose/Objective(s): We evaluated the impact of single day multidisciplinary clinics (MDC) on the lead time from diagnosis to treatment in head and neck cancers compared with matching patients prior to the implementation of MDC. We also wanted to investigate the relationship of demographic factors to the lead time.Materials/Methods: We retrospectively analyzed clinical and demographical variables of 310 patient's records collected from head and neck cancer tumor registry at St. Joseph Mercy Hospital, Ann Arbor, from 2007 to 2013. We had 170 cases with in the MDC period compared to 140 prior to the MDC.Results: We excluded 60 cases from our analysis because of missing data; no date of biopsy (N=5), no documentation of first treatment date (N=42)

and tumor resected on the same day of biopsy (N=22). This left 129 cases (76%) in the MDC period and 112 cases (80%) in the Pre-MDC period. Mean age was 63 in both the groups. Frequencies of other demographic factors include males (76% vs 79%), Caucasians (91% vs 88%), married (66% vs 62%) and insurance as Medicare (57% vs 50%), median distance from clinic (22 miles vs 17), in the MDC vs Pre-MDC groups respectively. Most of the cancers were squamous cell carcinomas (88% vs 83%), however, we had more stage 4 disease in MDC (56%) when compared to the Pre-MDC group (41%). To compare the two groups, after adjusting for demographic variables and an interaction between stage and site, we fit a generalized linear regression model. There was no difference in the median number of days from biopsy to definitive treatment between the two groups, (35 MDC vs 33.5 in pre-MDC, p = 0.14. The average number of days from biopsy to definitive treatment was 1.13 times longer, for the MDC group (95% CI: 0.96 to 1.32). Marital status was the only variable statistically significantly related to lead time (p = 0.04). Time to definitive treatment was 0.83 (95% CI: 0.70 to 0.99) times shorter, on average for married vs unmarried patients in both the groups. Post hoc analysis was also done to investigate the association between MDC and time to first radiation dose, where radiation was the first treatment. There were only 78 cases that met these criteria, Pre-MDC (N=37) and MDC (N=41). The negative binomial regression model showed no association of MDC with time to first radiation treatment (median time in days was, 40 in pre-MDC vs 38 in MDC). Time to radiation treatment was 0.91 (95% CI: 0.74 to 1.10) times shorter in the MDC when compared to the pre-MDC group. Conclusion: There was no significant difference in lead time with single day MDC compared to patients Pre-MDC in head & neck cancer patients. However, patients in the MDC group had more advanced cancer, which could reflect more complex work-up and management, resulting in longer lead time. Interestingly, marital status was associated with decrease in lead time in married compared to unmarried patients, in both the groups.

SSK17-05 A Review of Studies Using Self-reported Measures of Sexual Function among Female Cancer Patients Treated with Radiation Therapy, 2008-2014

Wednesday, Dec. 2 11:10AM - 11:20AM Location: S104A

Participants

Anuja Jhingran, MD, Houston, TX (Presenter) Nothing to Disclose

ABSTRACT

Purpose/Objective(s): A systematic review was conducted to identify and characterize self-reported sexual function (SF) measures administered to women who had received radiation therapy (RT) for cancer.Materials/Methods: Using 2009 PRISMA guidelines, we searched electronic bibliographic databases for quantitative studies published January 2008-September 2014 that used a selfreported measure of SF, or a quality of life (QOL) measure that contained at least one item pertaining to SF. Of these studies, we selected articles that reported the percentage of females who had received any form of RT.Results: Of 1,487 articles initially identified, 83 met inclusion criteria. The studies originated in 28 different countries with 23% from the U.S.A. Most studies focused on women treated for breast, gynecologic, or colorectal cancer, with the percent of women having received RT ranging from 7% to 100%. Only 19 articles (23%) provided information about radiation dose, number of fractions, field, or type of RT equipment SF was assessed with 27 unique self-reported measure, the most common being the EORTC QLQ modules (considered as one measure), the Female Sexual Function Inventory, and the Sexual Function Vaginal Changes Questionnaire. Of the 32 studies designed to compare SF by treatment modality, one-third found no statistically significant difference between RT and other modalities, and 28% found worse SF associated with RT. Only 4 studies reported on interventions to improve SF.Conclusion: The paucity of RT information in the reviewed articles, and the large number of measures used to assess SF limit comparative analysis. Needed are intervention studies with common metrics, preferably dedicated SF measures developed with cancer patients treated with RT. This systematic review will assist radiation oncologists select SF measures and encourage assessment of this quality of life domain in patient care.

SSK17-06 The Impact of Weight Loss on Set-up Accuracy with Patients Receiving Head and Neck Cancer Radiation Therapy

Wednesday, Dec. 2 11:20AM - 11:30AM Location: S104A

Participants

Sayyad Y. Zia, MA, MD, New York, NY (*Presenter*) Nothing to Disclose Awais Mirza, Mineola, NY (*Abstract Co-Author*) Nothing to Disclose Umut Ozbek, New York, NY (*Abstract Co-Author*) Nothing to Disclose Ren-Dih Sheu, PhD, New York, NY (*Abstract Co-Author*) Nothing to Disclose Vishal Gupta, MD, Sacramento, CA (*Abstract Co-Author*) Nothing to Disclose Richard L. Bakst, MD, New York, NY (*Abstract Co-Author*) Nothing to Disclose

ABSTRACT

Purpose/Objective(s): Patients receiving radiation therapy for head and neck cancers often experience severe weight loss and in some cases require re-planning. The purpose of this study was to evaluate whether we can determine at what point patients daily shifts vary greatly in relation to their specific weight loss to ensure the safe delivery of radiation therapy to our patients.Materials/Methods: 99 consecutive patients with head and neck cancers were treated with radiation therapy (+/chemotherapy) at our institution. Patient and disease characteristics: median age 59 (41-94), 14% female, 86% male, 3% Stage 0, 10% Stage I, 12% Stage II, 15% Stage III, 60% Stage IV. Weight loss was measured and recorded during weekly on treatment visits. KV imaging was performed daily to ensure setup accuracy. All shifts were recorded on a daily basis to include AP, LR, and SI shift. Spearman correlation coefficients were used in statistical analysis. Results: The mean weight loss during treatment in our cohort was 13.6kgs (+2.4kgs to - 24.9kgs). Stage of disease was found to correlate with percent weight loss (p=0.040). Mean weight loss was found to increase with advanced stage disease (Table 1).MEAN WEIGHT LOSSStageMean Weight Loss(kg)01.81I4.26II6.58III6.28IV7.75In regards to treatment, there was no statistical correlation between treatment being adjuvant or definitive with regards to percentage weight change (p=0.56). The largest PA (posterior-anterior) shift (p=.309), SI (superior-inferior) shift (p=.517), LR (left-right) shift (p=.303) compared to the largest shift (p=.247) were trended against weight loss and found not to be statistically significant. Conclusion: Our study demonstrates that despite weight loss of head and neck cancer patients, there was no significant correlation with setup inaccuracy. Increasing stage was found to be predictive of an increase in percent weight change. This study suggests that most patients undergoing head and neck radiation therapy will have a reliable set-up when properly immobilized despite weight loss. Further, this study highlights the importance of daily KV imaging and close monitoring of patients weight in head and neck cancer patients.

SSK17-07 Technology Meets Quality for Physician Collaboration in Oncology Peer Review

Participants Dawn Henrich, San Jose, CA (*Presenter*) Employee, iCAD, Inc; Stockholder, iCAD, Inc; Ajay Bhatnagar, MD, Pittsburgh, PA (*Abstract Co-Author*) Consultant, iCAD, Inc Bridget Krueger, San Jose, CA (*Abstract Co-Author*) Employee, iCAD, Inc Kamal Gogineni, San Jose, CA (*Abstract Co-Author*) Employee, iCAD, Inc

ABSTRACT

Purpose/Objective(s): Surface electronic brachytherapy is becoming recognized for treatment of non-melanoma skin cancer (NMSC). Radiation Oncologists providing these treatments may not have peer-to-peer collaboration available. This abstract will demonstrate feasibility in performing peer review within multiple non-affiliated organizations using a cloud-based platform to increase quality and safety. Materials/Methods: The oncology system stores patient specific clinical and dosimetric data for electronic brachytherapy and was utilized for multi-fraction treatment across several facilities. A total of 37,000 consecutive treatments were captured over a period of 2.5 years. The oncology platform is used to facilitate workflow management and documentation in a process structured environment. Mandatory fields throughout the care path allow consistent data to maximize comprehensive peer reviews. The cloud-based infrastructure permitted quick access to pertinent chart details across multiple nonaffiliated locations to streamline the peer review method. Evaluation elements specific to surface electronic brachytherapy were determined at onset. These included a variety of specifications regarding clinical presentation, diagnosis including pathology, informed consent, radiation prescription including dose fractionation scheme, treatment delivery parameters and presence of appropriate clinical documentation. An independent Radiation Oncologist was chosen to review 2 patient charts per month at each location during the validation process between July-December 2014. Results: Peer Review of 69 unique NMSC lesions was completed in 65 patients with a mean age of 78 years (Range 56-96). Pathologic histology presented with Basal Cell, Squamous Cell, Carcinoma in Situ, and Basosquamous in anatomic locations throughout the face, trunk, and scalp (63%, 31%, and 6%, respectively.) The peer reviewed patients were supervised by 22 Radiation Oncologists located across 11 unique locations. A dose prescription was present in 100% of patient charts which varied between 500cGy, 400cGy, and 450cGy per fraction (84%, 13%, and 3% respectively). These were prescribed at depths of 2, 3, and 4 mm with 55% most commonly prescribed at 2 mm. Additional data fields such as lesion size, cone size, and cutout type assisted in determining appropriateness of treatment parameters. Appropriateness of care was satisfactory in all patient charts evaluated.Conclusion: A cloud-based management platform enables a single Radiation Oncologist to remotely complete peer reviews effectively across multiple non-affiliated locations. The concept of utilizing data systems to complete peer review for surface electronic brachytherapy is feasible and should be introduced in the broader oncology community for data capture and predictive analytics to improve patient care.

SSK17-08 Proton Radiation Therapy for Incurable Head and Neck Disease by the Palliative QUAD Shot Regimen

Wednesday, Dec. 2 11:40AM - 11:50AM Location: S104A

Participants

Stanley Gutiontov, MD, Chicago, IL (Presenter) Nothing to Disclose

ABSTRACT

Purpose/Objective(s): To report our institutional experience of palliative proton radiotherapy (RT) for cancers in the head and neck with the QUAD SHOT regimen. Materials/Methods: Seventeen patients completed at least 1 cycle of palliative RT to the head and neck with proton therapy for incurable primary or metastatic disease based on the RTOG 85-02 QUAD SHOT regimen (370 CGE twice daily over 2 consecutive days at 2 to 3 week intervals up to a total dose of 4400 CGE) between July 2013 and January 2015 at our center; two were lost to follow-up. In the remaining fifteen patients, we defined palliation as relief of the presenting symptom(s) or tumor response by clinical exam or imaging. Overall survival (OS) was estimated by the Kaplan-Meier (KM) method. The Spearman rho test was used to examine the correlation between various clinical factors and palliative response. Toxicity was scored using the NCI CTCAE v4.0.Results: Median patient age was 70 years (range 54 to 89). 66% were male and 34% were female. The most common histology was squamous cell carcinoma (66%), followed by adenocarcinoma of the lung metastatic to the head and neck (13%), non-anaplastic thyroid carcinoma (7%), mucosal melanoma (7%), and adenocarcinoma (7%). Primary or recurrent AJCC stage was I (7%), II (13%), III (0%), IV (67%), and unknown (13%). The stage I patient also had metastatic SCLC. Five patients (33%) had a history of surgical resection at the primary disease site, eleven patients (73%) had previously received systemic chemotherapy, and ten patients (66%) had received significant prior RT at the palliative site (median dose 66 Gy; range, 21 to 75 Gy). Three patients had received two prior courses of RT to the site. KPS was =70 in all patients. The most common presenting symptoms were visual changes (16%), dysphagia/odynophagia (16%), pain (12%), and/or epistaxis (12%). Seven patients (47%) completed three QUAD SHOT cycles, and six patients (40%) received systemic therapy, typically targeted agents, concurrently. Palliative response was observed in 73% of patients. Median OS was 4.17 months (range, 0.57-17.0). No Grade 3 or higher acute toxicities were observed. One patient, who had received two prior courses of RT to the site, developed a Grade 2 dermatitis. The most common toxicity was Grade 1 fatigue (27%). By the log-rank test, palliative response (p=0.018) was associated with improved OS. Using bivariate analysis, palliative response was correlated with increasing number of QUAD SHOT cycles (p=0.017) but not with KPS, histology, or concurrent chemotherapy. Conclusion: Delivery of the QUAD SHOT regimen by proton radiotherapy for patients with loco-regionally advanced or metastatic disease in the head and neck provides excellent rates of palliative response with no Grade 3 or higher acute toxicity. The minimal toxicity profile in these heavily pre-irradiated patients is encouraging and warrants further study.

SSK17-09 Patterns of Local and Distant Recurrence Based on MAP Kinase Pathway Mutations in Patients with Stage III Melanoma Treated with Lymph Node Dissection and Adjuvant Radiation Therapy

Wednesday, Dec. 2 11:50AM - 12:00PM Location: S104A

Participants

Priyanka Chablani, BA,MS, Columbus, OH (*Presenter*) Nothing to Disclose Steve Walston, DO, Columbus, OH (*Abstract Co-Author*) Nothing to Disclose Erinn Hade, PhD, Columbus, OH (*Abstract Co-Author*) Nothing to Disclose Sara Peters, MD,PhD, Columbus, OH (*Abstract Co-Author*) Nothing to Disclose Terence M. Williams, MD, PhD, Columbus, OH (*Abstract Co-Author*) Nothing to Disclose Evan J. Wuthrick, MD, Columbus, OH (*Abstract Co-Author*) Nothing to Disclose

PURPOSE

The role of adjuvant radiation therapy (ART) after lymph node dissection (LND) in pts with Stage III melanoma is controversial.

Recently, different sub-groups of melanoma have emerged based on the presence of BRAF and NRAS driver mutations in the MAP Kinase pathway. We sought to determine clinical outcomes after LND and ART on the basis of BRAF, NRAS, and MAPK-wild-type (wt) status.

METHOD AND MATERIALS

We reviewed the records of patients (pts) treated with LND followed by ART at our institution from 2006 to mid-2014. 65 pts met our study criteria. We collected information on demographic, pathologic, and treatment-related variables from medical records. We tested melanoma tissue samples from all pts for BRAF/NRAS mutations using PCR-based genetic assays. Loco-regional and distant recurrences were assessed using follow-up imaging and exam findings. We examined the association of variables collected with clinical outcomes using Kaplan and Meier methods and Cox proportional hazards models.

RESULTS

Of the 65 pts, 42 (65%) were male and the median age was 57 yrs (range 22 - 87). 19 pts (29%) received LND and ART to the head and neck, 28 (43%) to the axilla, and 18 (28%) to the groin. Pts received external beam RT with the majority receiving 30 Gy/5 fractions (61%) or 48 Gy/20 fractions (26%). 32 pts (49%) were BRAF-positive, 33 pts (51%) were BRAF-negative. Of the 33 BRAF-negative pts, 15 pts (23%) had NRAS mutations, 18 pts (28%) were MAPK-wt. Median follow up time was 1.6 years (0.2-7.8). Presence of BRAF mutation was significantly associated with local-regional recurrence (HR: 4.3; 95% CI 0.9-20.0; p = 0.06). At 2-yr follow-up, 33% of BRAF+ pts failed loco-regionally, compared to 7% of BRAF- pts. There were a total of 11 loco-regional failures. Presence of BRAF mutation was not significantly associated with distant failure (aHR: 0.75; 95% CI 0.4-1.4; p = 0.34). At 2-yr follow-up, 54% of BRAF+ pts had distant failure, compared to 65% of BRAF- pts. There were a total of 37 distant failures.

CONCLUSION

BRAF-positive pts had significantly increased rates of loco-regional failure but similar rates of distant failure compared to BRAFnegative pts after LND and ART for Stage III Melanoma.

CLINICAL RELEVANCE/APPLICATION

BRAF-positive pts may derive less loco-regional control than BRAF-negative pts from ART after LND for Stage III melanoma; adjuvant immunotherapy or targeted therapy may be better options for these pts.

Cardiac (General Topics)

Wednesday, Dec. 2 10:30AM - 12:00PM Location: S504AB



AMA PRA Category 1 Credits ™: 1.50 ARRT Category A+ Credits: 1.50

Participants

Pamela K. Woodard, MD, Saint Louis, MO (*Moderator*) Research Consultant, Bristol-Myers Squibb Company; Research Grant, Astellas Group; Research Grant, F. Hoffmann-La Roche Ltd; Research Grant, Bayer AG; Research agreement, Siemens AG; Research Grant, Actelion Ltd; Research Grant, Guerbet SA; ; ; Robert J. Herfkens, MD, Stanford, CA (*Moderator*) Nothing to Disclose Istvan Battyani, MD, PhD, Pecs, Hungary (*Moderator*) Nothing to Disclose

Sub-Events

SSK04-01 Dynamic First Pass CT Perfusion Imaging of the Myocardium vs. Intracoronary Transluminal Attenuation Gradient in Coronary CT Angiography for the Assessment of Coronary Artery Stenosis

Wednesday, Dec. 2 10:30AM - 10:40AM Location: S504AB

Participants

Bettina M. Gramer, MD, Munich, Germany (*Presenter*) Nothing to Disclose Isabella Baur, Munich, Germany (*Abstract Co-Author*) Nothing to Disclose Michael Rasper, Munich, Germany (*Abstract Co-Author*) Nothing to Disclose Alexander W. Leber, MD, Munich, Germany (*Abstract Co-Author*) Nothing to Disclose Johannes Rieber, MD, Munich, Germany (*Abstract Co-Author*) Nothing to Disclose Ellen Hoffmann, Munich, Germany (*Abstract Co-Author*) Nothing to Disclose Mani Vembar, MS, Cleveland, OH (*Abstract Co-Author*) Nothing to Disclose First J. Rummeny, MD, Munich, Germany (*Abstract Co-Author*) Nothing to Disclose Armin M. Huber, MD, Munchen, Germany (*Abstract Co-Author*) Nothing to Disclose

PURPOSE

To compare the diagnostic accuracy of dynamic first pass CT perfusion (CTP) imaging and the transluminal attenuation gradient derived from coronary CT angiography in the assessment of coronary artery stenosis.

METHOD AND MATERIALS

34 patients with suspicion of coronary artery disease, who underwent invasive coronary angiography (CA) and assessment of intermediate coronary artery lesions (50-75% diameter reduction) by an invasive pressure wire examination (FFR) were included. All patients underwent a coronary CTA and a dynamic CTP examination under adenosine stress at a 256 slice CT scanner with an 8 cm wide detector. Myocardial blood flow was determined using the dynamic first pass CTP data. Transluminal attenuation gradient (TAG) was calculated as the linear regression coeffcient between luminal attenuation and the distance of the location in the coronary artery from its origin. MBF and TAG were compared with the results CA and FFR. ROC curves were calculated. Sensitivity and specificity were calculated using Youden's index.

RESULTS

The area under the ROC curve was 0.92 (0.80 to 0.95) for MBF and 0.64 (0.46 to 0.793) for TAG (p=0.002). The optimal threshold using Youden's index was 1.51 for TAG and 1.21 for MBF. Sensitivity and specificity for detection of hemodynamically relevant coronary artery lesions were 71.4 (41.9- 91.4) and 73.2 (57.1- 85.8) for TAG. Sensitivity and specificity were 90.9 (58.7- 98.5) and 84.6 (65.1- 95.5) for MBF.

CONCLUSION

MBF derived from dynamic CTP imaging of the myocardium is superior compared to the TAG derived from coronary CTA for the assessment of coronary artery stenosis.

CLINICAL RELEVANCE/APPLICATION

In spite of being inferior compared to the MBF the TAG can be used as additional functional parameter in the assessment of coronary artery stenosis derived from coronary CTA without additional contrast agent or radiation exposure and may contribute to improve diagnostic accuracy of CTA.

SSK04-02 Detection and Differentiation of Ischemic Myocardial Lesions with Quantitative Post-mortem Cardiac 1.5T MRI

Wednesday, Dec. 2 10:40AM - 10:50AM Location: S504AB

Participants

Wolf-Dieter Zech, MD, Bern, Switzerland (*Presenter*) Nothing to Disclose Nicole Schwendener, Bern, Switzerland (*Abstract Co-Author*) Nothing to Disclose Anders Persson, MD, PhD, Linkoping, Sweden (*Abstract Co-Author*) Nothing to Disclose Marcel Warntjes, Linkoping, Sweden (*Abstract Co-Author*) Employee, SyntheticMR AB Christian Jackowski, MD, Bern, Switzerland (*Abstract Co-Author*) Nothing to Disclose

PURPOSE

MR quantification of T1 and T2 relaxation times and proton density (PD) is feasible for characterizing tissue lesions. Since quantitative T1 and T2 values are dependent on magnetic field strength and temperature there is a need for evaluation of

quantitative values with regard to magnetic field strength and tissue temperatures. The purpose of this study was to assess the quantitative T1, T2 and PD values of ischemic myocardial lesions for a post-mortem 1.5T application and to relate quantitative values to tissue temperature.

METHOD AND MATERIALS

Eighty forensic postmortem short axis cardiac 1,5T MR examinations were quantified using a quantification sequence prior to autopsy. During the MR examination the temperature of corpses was assessed. Quantitative T1, T2 and PD values of myocardial lesions were assessed in synthetically calculated cardiac MR images. The quantitative values were related to temperature and correlated with autopsy and histology findings.

RESULTS

A total of 95 ischemic lesions were detected at histology and autopsy (early acute n=61, acute n=14, subacute n=10, chronic n=10). Of 61 histologically confirmed early acute lesions a total of 22 lesions (36.1 %) were not visible in conventional PMMR images. These lesions were targeted in MR images at the location of histologic specimens and presented with quantitative T1 and T2 values that differed significantly from the quantitative values of normal myocardium. ANOVA revealed that the quantitative values of all assessed ischemic lesions and normal myocardium differed significantly from each other. Temperature correction of quantitative values led to lower standard deviations and better differentiability of all lesions.

CONCLUSION

Postmortem 1,5T MR quantification is feasible for detection and diagnosis of different age stages of myocardial ischemia and enables to assess early acute myocardial ischemia not visible in conventional MR images. The quantification approach provides a base for computer aided detection and diagnosis of ischemic myocardial lesions.

CLINICAL RELEVANCE/APPLICATION

If quantitative values are extrapolated to 37°C diagnostic criteria validated in quantitative cardiac PMMR scans may be applied for the detection of myocardial ischemia in living patients.

SSK04-03 Imaging for Suspected Coronary Artery Disease: Recent Utilization Trends Point Downward

Wednesday, Dec. 2 10:50AM - 11:00AM Location: S504AB

Participants

David C. Levin, MD, Philadelphia, PA (*Presenter*) Consultant, HealthHelp, LLC; Board of Directors, Outpatient Imaging Affiliates, LLC Laurence Parker, PhD, Philadelphia, PA (*Abstract Co-Author*) Nothing to Disclose Vijay M. Rao, MD, Philadelphia, PA (*Abstract Co-Author*) Nothing to Disclose

PURPOSE

In recent years, appropriate use criteria have been developed for cardiac imaging by both the ACR and the American College of Cardiology. Our purpose was to attempt to determine if these criteria affected utilization of the 3 major imaging tests for suspected coronary artery disease (CAD) - nuclear myocardial perfusion imaging (MPI), stress echocardiography (SE), and coronary CT angiography (CCTA).

METHOD AND MATERIALS

The nationwide Medicare Part B databases from 2001 through 2013 were studied. The CPT codes for primary MPI, SE, and CCTA were selected. Procedure volumes were tabulated for all places of service, and utilization rates per 1000 Medicare fee-for-service beneficiaries were calculated. Medicare specialty codes were used to ascertain the relative roles of radiologists and cardiologists.

RESULTS

The utilization rate per 1000 of MPI increased from 63.4 in 2001 to a peak of 88.0 in 2006, then declined to 61.9 in 2013 (-30% vs 2006 peak). In 2013, cardiologists did 77% of the MPIs; radiologists did 17%; the rest were done by other physicians. The utilization rate of SE was 12.5 in 2001 and remained relatively stable through 2010, then declined to 10.8 by 2013 (-14% vs 2010). Radiologists had essentially no role in SE. CCTA utilization could only be tracked since 2006, the first complete year codes were available for that study. The rate per 1000 that year was 1.0. It went up to 2.1 the following year, but then declined every year thereafter to 1.1 in 2013 (-48% vs peak). In 2013, radiologists did 49% of CCTAs; cardiologists did 46%; other physicians did the rest. That year, 56 times as many MPIs as CCTAs were performed.

CONCLUSION

The utilization rate of noninvasive imaging in patients with suspected CAD is declining. The cause is likely multifactorial. The decline is more pronounced in MPI than in SE. The use of CCTA has also dropped, but its rate is far lower than that of MPI and SE. CCTA is probably underused in comparison to those 2 techniques. Radiologists have no role in SE, a relatively small role in MPI, but an important role in CCTA.

CLINICAL RELEVANCE/APPLICATION

n/a

SSK04-04 Automated 3D MRI Volumetry of the Pulmonary Arteries: Evaluation in Patients with Pulmonary Arterial Hypertension and Potential for Predicting Pulmonary Hypertension

Wednesday, Dec. 2 11:00AM - 11:10AM Location: S504AB

Awards

Trainee Research Prize - Resident

Participants Fabian Rengier, MD, Heidelberg, Germany (*Presenter*) Nothing to Disclose Stefan Woerz, Heidelberg, Germany (*Abstract Co-Author*) Nothing to Disclose Claudius Melzig, Heidelberg, Germany (*Abstract Co-Author*) Nothing to Disclose Sebastian Ley, MD, Heidelberg, Germany (*Abstract Co-Author*) Nothing to Disclose Christian Fink, MD, Mannheim, Germany (*Abstract Co-Author*) Nothing to Disclose Nicola Ehlken, Heidelberg, Germany (*Abstract Co-Author*) Nothing to Disclose Sasan Partovi, MD, Cleveland, OH (*Abstract Co-Author*) Nothing to Disclose Hendrik Von Tengg-Kobligk, MD, Bern, Switzerland (*Abstract Co-Author*) Research Grant, W. L. Gore & Associates, Inc Karl Rohr, Heidelberg, Germany (*Abstract Co-Author*) Nothing to Disclose Hans-Ulrich Kauczor, MD, Heidelberg, Germany (*Abstract Co-Author*) Research Grant, Siemens AG; Research Grant, Bayer AG; Speakers Bureau, Boehringer Ingelheim GmbH; Speakers Bureau, Siemens AG; Speakers Bureau, Novartis AG; Speakers Bureau, GlaxoSmithKline plc ; Speakers Bureau, Almirall SA

Ekkehard Gruenig, MD, Heidelberg, Germany (Abstract Co-Author) Nothing to Disclose

PURPOSE

Increased pulmonary artery diameters have been shown to indicate pulmonary hypertension, but 2D diameter measurements are only a limited representation of 3D geometry. Purpose of this study was to demonstrate feasibility of 3D volumetry of pulmonary arteries based on magnetic resonance angiography (MRA), to assess pulmonary artery volumes in patients with pulmonary arterial hypertension compared to healthy volunteers, and to investigate its potential for predicting pulmonary hypertension (PH).

METHOD AND MATERIALS

MRA of the pulmonary arteries was acquired at 1.5T in 37 subjects (mean age 42+/-14 years) with a slice thickness of 1.6mm and in-plane resolution of 1.3x1.3mm². 20 patients had pulmonary arterial hypertension (WHO classification Group 1) confirmed by right heart catheterization, 17 healthy volunteers had no history of cardiovascular disease. Using in-house developed 3D model-based image analysis software, main, right and left pulmonary arteries (mPA, rPA and IPA) were automatically segmented after placement of seed points. Volumes for mPA, rPA and IPA were computed and corrected for body surface area (BSA). For comparison purposes, diameter of mPA was manually measured on axial reconstructions by an experienced radiologist.

RESULTS

Volumes for patients/volunteers were (in mm³/m² BSA): mPA 25570/13927 (p=0.002), rPA 10484/3807 (p<0.001) and IPA 7533/3899 (p<0.001). ROC analysis of volumes showed: mPA AUC 0.874 (95% CI 0.748-0.999, p=0.001), rPA AUC 1.0 (95% CI 1.0-1.0, p<0.001) and IPA AUC 0.889 (95% CI 0.774-1.0, p=0.001). Sensitivity, specificity, positive predictive value and negative predictive value for predicting PH were highest for rPA volume with 100%, 100%, 100% and 100% using 6000mm³/m² BSA as sexindependent cut-off, compared to 95%, 78%, 82% and 93% for mPA diameter using 29/27mm as cut-off for males/females as suggested by the Framingham Heart Study.

CONCLUSION

MRA-based 3D volumetry of pulmonary arteries is feasible and demonstrated significantly increased volumes for main, right and left pulmonary arteries in patients with pulmonary arterial hypertension compared to healthy volunteers. Volume of right pulmonary artery might be an accurate predictor for PH but validation in a larger study population is warranted.

CLINICAL RELEVANCE/APPLICATION

3D pulmonary artery volumes might be more accurate than 2D diameter measurements in the prediction and evaluation of pulmonary hypertension.

SSK04-05 Pulmonary Arterial Hypertension is Associated with Increased T1 Relaxation Times and Decreased Left Ventricular Performance in Spite of Preserved Left Ventricular Function

Wednesday, Dec. 2 11:10AM - 11:20AM Location: S504AB

Participants

Rami Homsi, Bonn, Germany (*Presenter*) Nothing to Disclose Julian A. Luetkens, Bonn, Germany (*Abstract Co-Author*) Nothing to Disclose Dirk Skowasch, Bonn, Germany (*Abstract Co-Author*) Nothing to Disclose Julia Meyer zur Heide, Bonn, Germany (*Abstract Co-Author*) Nothing to Disclose Juergen Gieseke, DSc, Bonn, Germany (*Abstract Co-Author*) Nothing to Disclose Juergen Gieseke, DSc, Bonn, Germany (*Abstract Co-Author*) Employee, Koninklijke Philips NV Hans H. Schild, MD, Bonn, Germany (*Abstract Co-Author*) Nothing to Disclose Claas P. Naehle, MD, Bonn, Germany (*Abstract Co-Author*) Consultant, Medtronic, Inc

PURPOSE

Pulmonary arterial hypertension (PAH) mainly affects the right (RV), but also the left ventricle (LV). Strain analysis allows for detection of ventricular dysfunction even in patients with preserved ventricular function. Cardiac magnetic resonance (CMR) mapping techniques with determination of T1 and T2 relaxation times (T1 resp T2) may allow for discrimination between healthy myocardium and diffuse fibrosis in PAH patients. This study was performed to evaluate the association between myocardial changes assessed by strain analysis and by native T1 and T2 map in patients with PAH.

METHOD AND MATERIALS

16 Patients with PAH (8 men, 8 women, mean age $63.75y \pm 13.85$) and 17 healthy volunteers (8 men,9 women, mean age $57.56y \pm 12.45$) were examined on a 1.5 Tesla MR system (Ingenia, Philips). Native T1s were assessed using the modified Look-Locker inversion recovery sequence and T2s were assessed using a GraSE sequence. RV and LV longitudinal strain was assessed during postprocessing of standard SSFP Cine images by CMR feature tracking using a dedicated software (Diogenes, TomTec, Unterschleissheim, Germany). LV and RV function were assessed by volumetric analysis.

RESULTS

LV ejection fraction did not differ between PAH patients and healthy volunteers (61.26 ± 7.13 vs. 61.53 ± 6.48 ; p>0.05). Left ventricular T1 s however were significantly higher in patients with PAH (1050.17 ± 47.90 vs. 980.72 ± 45.5 ; p<0.01). LV longitudinal strain was significantly lower in patients with PAH (-17.01 ± 5.34 vs. -23.05 ± 3.57 , p<0.01). RV longitudinal strain and RV-Ejection fraction were both significantly lower in patients with PAH. There were no significant differences in T2 relaxation times, age, body mass index, or sex.

CONCLUSION

111 musecardial fibracia as indicated by increased T1 reduces 111 strain despite of normal 111 function in nationals with DAU

LV INVOCATUIALINDOSIS AS INDICALED DY INCLEASED IT TEQUCES LV STRAIN DESPICE OF NOTIFIAL LV TUNCTION IN PALIENCE WITH PAR.

CLINICAL RELEVANCE/APPLICATION

Increased T1 as an indicator for LV involvement in PAH may be useful to identify patients at risk and to determine the intensity of treatment even when myocardial function is preserved.

SSK04-06 Cardiac Effects of Prolonged Apnea in Elite Divers Investigated with Comprehensive Cardiac Magnetic Resonance

Wednesday, Dec. 2 11:20AM - 11:30AM Location: S504AB

Participants

Jonas Doerner, MD, Bonn, Germany (*Presenter*) Nothing to Disclose Lars Eichhorn, Bonn, Germany (*Abstract Co-Author*) Nothing to Disclose Jean-Marc Lunkenheimer, Bonn, Germany (*Abstract Co-Author*) Nothing to Disclose Julian A. Luetkens, Bonn, Germany (*Abstract Co-Author*) Nothing to Disclose Juergen Gieseke, DSc, Bonn, Germany (*Abstract Co-Author*) Nothing to Disclose Juergen Gieseke, DSc, Bonn, Germany (*Abstract Co-Author*) Employee, Koninklijke Philips NV Rainer Meyer, 53115, Germany (*Abstract Co-Author*) Nothing to Disclose Andreas Hoeft, 53105, Germany (*Abstract Co-Author*) Nothing to Disclose Hans H. Schild, MD, Bonn, Germany (*Abstract Co-Author*) Nothing to Disclose Claas P. Naehle, MD, Bonn, Germany (*Abstract Co-Author*) Consultant, Medtronic, Inc

PURPOSE

Apnea diving is getting more and more popular as a recreational sport activity and performance of apnea divers has been constantly rising in the recent years. Prolonged apnea leads to the so-called diving response (i.e. bradycardia, reduced cardiac output, peripheral vasoconstriction) which burdens the heart and leads to changes in circulation. This study investigated the effects of prolonged apnea to the heart and hemodynamic alterations using comprehensive cardiac magnetic resonance imaging (CMR).

METHOD AND MATERIALS

We investigated 17 (15 male, 2 women) elite divers using CMR at 1,5T before, during, and after apnea in air. Subjects performed two sessions: in the first cardiac function (left ventricular end-diastolic volume (LV-EDV), end-systolic volume (LV-ESV), ejection fraction (LV-EF), fractional shortening (FS)) was repeatedly measured using steady state free precision (SSFP) imaging in SAX and VLA; in the second blood flow was measured in both common carotid arteries (ACC) using phase contrast imaging. Apnea was performed in maximal inspiration.

RESULTS

Mean breath hold duration was 297s±52 in the cardiac session and 276s±78 in the flow session. Maximal apnea time reached was 8:03min. Over time, apnea (AP) resulted in a progressive increase of LV-EDV (baseline: $131ml\pm33$; AP: $190ml\pm35$; p<0.0001), slight decrease of LV-EF (baseline: $63\%\pm10$; AP: $58\%\pm8$; p=0.0112) and a consecutive increase of LV-ESV (baseline: $49ml\pm20$; AP: $80ml\pm18$; p<0.0001). FS as a parameter of regional function also decreased significantly during apnea (baseline: $35\%\pm5$; AP: $25\%\pm5$; p<0.0001). Flow measurement revealed an increase of blood-flow to the brain (left ACC; baseline: $5.0ml\pm2.0$; AP: $12.8ml\pm6.4$; p=0.0026; right ACC; baseline: $5.1ml\pm2.2$; AP: $12.4ml\pm6,3$; p=0.0009).

CONCLUSION

This work reveals that prolonged apnea results in massive hemodynamic changes to the heart and an increase of blood-flow to the brain as expected from the diving reflex. In particular, apnea leads to a transient cardiac dilation, decrease of LV-EF and fractional shortening, a similar pattern as seen in patients with systolic heart failure.

CLINICAL RELEVANCE/APPLICATION

This study shows that prolonged apnea has tremendous effects to the heart and the vascular system; therefore moderate trained subjects, especially with known medical conditions, should perform maximal apnea with caution.

SSK04-07 Is it Possible to Investigate Archeological Hearts Using CT and MRI? About Five Archeological Hearts

```
Wednesday, Dec. 2 11:30AM - 11:40AM Location: S504AB
```

Participants

Fatima-Zohra Mokrane, MD, Toulouse, France (*Presenter*) Nothing to Disclose Rozenn Colleter, Cesson-Sevigne, France (*Abstract Co-Author*) Nothing to Disclose Sylvie Duchesne, MSc, Saint Orens de Gameville, France (*Abstract Co-Author*) Nothing to Disclose Ramiro Moreno, MS, Toulouse, France (*Abstract Co-Author*) Nothing to Disclose Anou Sewonu, PhD, Toulouse, France (*Abstract Co-Author*) Nothing to Disclose Herve P. Rousseau, MD, Toulouse, France (*Abstract Co-Author*) Nothing to Disclose Eric Crubezy, MD,PhD, Toulouse, France (*Abstract Co-Author*) Nothing to Disclose Norbert Telmon, Toulouse, France (*Abstract Co-Author*) Nothing to Disclose Fabrice H. Dedouit, MD, PhD, Toulouse, France (*Abstract Co-Author*) Nothing to Disclose

PURPOSE

Five archeological hearts were found in an archeological site last year. Several graves were found in the basement of a church. In addition to different archeological bones found, five heart shaped lead polls were discovered. These findings were found in vaults from elite class families. At the opening of the polls, findings were very interesting: five well conserved hearts dating form the end on the 16th century, to the beginning of the 17th century.

METHOD AND MATERIALS

Thanks to the embalming process, archeological hearts were well conserved. Each archeological heart has been studied with CT scanner and with MRI, before and after balm extraction, and after rehydration.CT parameters were standard, using a 16 row CT scanner. MRI parameters were difficult to optimize. This was due to lack of hydration of these archeological pieces.

First images acquired were very impressive, but with poor information. This was due to important vegetal embalming process. Hearts were first scanned with their balms. Then, they were carefully "cleaned". Finally, they were rehydrated.CT and MR examinations where performed for each heart.Because of an intra tissue lead diffusion, especially in infra epicardial fat, there was an impressive natural contrast on CT images. This element permitted to identify different heart structures like chambers, valves and coronary arteries.MRI images were hard to obtain because of lake of hydration. Therefore, images after rehydration were relevant and allowed to better identify myocardial muscles

CONCLUSION

Study of archeological smooth tissues like heart is possible using CT and MRI, but it requires a good knowledge of the embalming process and MR technical parameters.

CLINICAL RELEVANCE/APPLICATION

Until now, no radiological examination of archeological hearts was described in the literature data.

SSK04-08 Atherosclerotic Plaque Burden Assessment: Coronary CT Angiography versus Invasive Coronary Angiography

Wednesday, Dec. 2 11:40AM - 11:50AM Location: S504AB

Participants

Pal Maurovich-Horvat, MD,PhD, Budapest, Hungary (*Presenter*) Nothing to Disclose Szilard Voros, Richmond, VT (*Abstract Co-Author*) Shareholder, Global Genomics Group; Employee, Global Genomics Group Balint Szilveszter, MD, Budapest, Hungary (*Abstract Co-Author*) Nothing to Disclose Marton Kolossvary, Budapest, Hungary (*Abstract Co-Author*) Nothing to Disclose Istvan Edes, Budapest, Hungary (*Abstract Co-Author*) Nothing to Disclose Zsolt Bagyura, Budapest, Hungary (*Abstract Co-Author*) Nothing to Disclose Bela Merkely, MD,PhD, Budapest, Hungary (*Abstract Co-Author*) Speakers Bureau, Medtronic, Inc

PURPOSE

Strong relationship exists between atherosclerotic disease burden and risk for adverse events as assessed by coronary computed tomography angiography (CTA) and conventional invasive coronary angiography (ICA). Despite widespread use of CTA and ICA for coronary plaque burden assessment, few studies have compared coronary CTA and ICA regarding semi-quantitative plaque burden measurements.

METHOD AND MATERIALS

We enrolled 71 consecutive patients (mean age 60.8±11.7 yrs, 36.6% women) who underwent both 256-slice coronary CTA and conventional ICA within no more than 120 days. A total of 1016 coronary segments were evaluated for the presence of plaque and stenosis severity. On average, 32 [IQR:15-62.5] days passed between the two examinations. A total of 16 segments were excluded due to presence of a stent. We calculated the segment stenosis score (SSS), which describes the amount and severity of the stenosis (0-normal, 1-minimal, 2-mild 3-moderate 4-severe 5-occluded). The presence of plaques has been described by the segment involvement score (SIS) (0-intact, 1-plaque). The SSS index (SSSi)=SSS/all assessed segments and SIS index (SISi)=SIS/all assessed segments were also calculated. CTA and ICA scores were compared using Wilcoxon rank sum test (SPSS 22).

RESULTS

CT detected coronary artery plaques in 48.7% of all assessed segments (487/1000), whereas ICA showed coronary plaques in only 23.5% (235/1000) of 1000 segments (p<0.001). Importantly, CTA detected atherosclerotic plaque in 34.8 % (266/765) of coronary segments where the ICA was negative. Conversely, ICA detected plaques only in 2.7% (14/513) segments where CTA was negative. We found significant differences between the two methods for segment involvement and luminal stenosis indices, CTA versus ICA; SISi: 0.49 ± 0.22 vs. 0.24 ± 0.14 (p<0.001); SSSi: 1.17 ± 0.64 vs. 0.67 ± 0.50 (p<0.001).

CONCLUSION

Coronary CTA detected approximately twice as many coronary segments with atherosclerotic plaques as ICA. Our findings are in line with previous histological studies, according to which a significant number of plaques do not cause luminal stenosis. Using coronary CTA for atherosclerotic plaque burden assessment may allow for better risk stratification and improved patient outcomes.

CLINICAL RELEVANCE/APPLICATION

Coronary CTA for atherosclerotic plaque burden assessment may allow for improved risk stratification as compared to invasive coronary angiography.

SSK04-09 Effect of Calcium Blooming in Coronary Arteries at Different Monoenergetic Levels of a Novel Spectral Detector CT and Comparison with Polyenergetic Conventional Image

Wednesday, Dec. 2 11:50AM - 12:00PM Location: S504AB

Participants

Majid Chalian, MD, Cleveland Heights, OH (*Presenter*) Nothing to Disclose Bahar Mansoori, MD, Cleveland, OH (*Abstract Co-Author*) Nothing to Disclose Hamid Chalian, MD, Cleveland, OH (*Abstract Co-Author*) Nothing to Disclose Prabhakar Rajiah, MD, FRCR, Cleveland, OH (*Abstract Co-Author*) Institutional Research Grant, Koninklijke Philips NV

PURPOSE

To evaluate the extent of calcium blooming in coronary arteries at different virtual monoenergetic levels of a novel spectral detector CT (SDCT) and compare with the conventional polychromatic image.

METHOD AND MATERIALS

This study included 59 patients who had coronary CTA using an SDCT prototype (Philips Healthcare, Cleveland, OH, USA). 17

patients were found to have coronary artery calcifications and recruited in the study. Two independent readers evaluated calcified plaques for plaque diameter, plaque area, luminal diameter, and percentage of stenosis. Measurements were performed at conventional polychromatic image as well as virtual monoenergetic images from 70 to 140 keV at 10 keV intervals. The images were also evaluated qualitatively for vascular enhancement, noise, and mage quality on a 5-point scale (1 -worst, 5-best). Repeated measure ANOVA test was used to compare differences at different energy levels. Intra-class correlation coefficient (ICC) was used to evaluate inter-observer reliability.

RESULTS

Diameter of calcification, area of calcification, and degree of stenosis demonstrated gradual statistically significant (p<0.001) decrease at different incrementally increasing monochromatic imaging keVs from 70 to 140 keV (3.41mm to 1.55mm, 9.96mm2 to 3.39 mm2, and 70% to 30% stenosis, respectively). Also, diameter and area of lumen demonstrated gradual ncrease at higher monochromatic energy levels (1.56mm to 2.74mm and 4.47mm2 to 8.61mm2, respectively, p<0.001). Comparison of monochromatic reconstructed images with conventional polychromatic imaging also demonstrated the same pattern of changes, with progressive improvement at higher energy levels. The monochromatic images at 80 keV provided the best image quality metrics. There was excellent inter-observer reliability between two readers (ICC> 0.970). Subjective analysis showed that the image quality progressively declined above 80 keV due to decreasing vascular enhancement, with the maximum image quality seen at 80 keV (4.8 at 80 keV to 2 at 140 keV).

CONCLUSION

Calcium blooming significantly decreases at higher monoenergy levels compared to polychromatic images with resultant increased luminal size and decreased stenotic grade. 80 keV is the best level due to declining image quailty at higher levels

CLINICAL RELEVANCE/APPLICATION

Use of monoenergetic images decreases the effect of calcium blooming in coronary arteries compared to polychromatic images.

Honored Educators

Presenters or authors on this event have been recognized as RSNA Honored Educators for participating in multiple qualifying educational activities. Honored Educators are invested in furthering the profession of radiology by delivering high-quality educational content in their field of study. Learn how you can become an honored educator by visiting the website at: https://www.rsna.org/Honored-Educator-Award/

Prabhakar Rajiah, MD, FRCR - 2014 Honored Educator

RCC42

Ergonomics

Wednesday, Dec. 2 10:30AM - 12:00PM Location: S501ABC

IN

AMA PRA Category 1 Credits ™: 1.50 ARRT Category A+ Credits: 1.50

Participants

LEARNING OBJECTIVES

1) The attendee will learn how the radiology reading room environment can physically affect the radiologist. 2) Learn about repetitive stress injuries and how they may affect radiologists and technologists. 3) Learn about how PACS workstations (including mice, keyboards, screens, etc.); room lighting, sounds and temperature; and room furniture may be optimized to help prevent repetitive stress injuries. 4) Learn how radiologic technologists can also be affected by repetitive stress injuries.

ABSTRACT

This presentation will review the features of a reading a study at a PACS, and the interactions of the radiologist with the various devices. This includes desktops/tables height, chairs, keyboard location, monitor position, mouse position (and cleanliness), microphone positioning, room temperature, sound volume, ambient light, and body positioning. Each of these components will be discussed, showing how to prevent future problems with repetitive stress disorders. The goal is to raise awareness of ergonomics for the radiologist.

Sub-Events

RCC42A Introduction to Ergonomics

Participants William J. Weadock, MD, Ann Arbor, MI (*Presenter*) Owner, Weadock Software, LLC

LEARNING OBJECTIVES

View learning objectives under main course title.

RCC42B Lessons Learned from Our Reading Room of the Future Lab

Participants

Eliot L. Siegel, MD, Severna Park, MD (*Presenter*) Research Grant, General Electric Company; Speakers Bureau, Siemens AG; Board of Directors, Carestream Health, Inc; Research Grant, XYBIX Systems, Inc; Research Grant, Steelcase, Inc; Research Grant, Anthro Corp; Research Grant, RedRick Technologies Inc; Research Grant, Evolved Technologies Corporation; Research Grant, Barco nv; Research Grant, Intel Corporation; Research Grant, Dell Inc; Research Grant, Herman Miller, Inc; Research Grant, Virtual Radiology; Research Grant, Anatomical Travelogue, Inc; Medical Advisory Board, Fovia, Inc; Medical Advisory Board, Toshiba Corporation; Medical Advisory Board, McKesson Corporation; Medical Advisory Board, Carestream Health, Inc; Medical Advisory Board, Bayer AG; Research, TeraRecon, Inc; Medical Advisory Board, Bracco Group; Researcher, Bracco Group; Medical Advisory Board, Merge Healthcare Incorporated; Medical Advisory Board, Microsoft Corporation; Researcher, Microsoft Corporation

LEARNING OBJECTIVES

View learning objectives under main course title.

RCC42C No Strain, No Pain: A Guide to Reducing Musculoskeletal Strain and Eye Fatigue Among Radiologists

Participants

Rebecca L. Seidel, MD, Atlanta, GA, (rseidel@emory.edu) (Presenter) Nothing to Disclose

LEARNING OBJECTIVES

View learning objectives under main course title.

ABSTRACT

Cardiac (Contrast Media)

Wednesday, Dec. 2 10:30AM - 12:00PM Location: S502AB



AMA PRA Category 1 Credits ™: 1.50 ARRT Category A+ Credits: 1.50

FDA Discussions may include off-label uses.

Participants

Ethan J. Halpern, MD, Philadelphia, PA (*Moderator*) Nothing to Disclose Hans-Christoph R. Becker, MD, PhD, Stanford, CA (*Moderator*) Nothing to Disclose Jean Jeudy JR, MD, Baltimore, MD (*Moderator*) Nothing to Disclose

Sub-Events

SSK03-01 Long-term Adverse Effects of Low-osmolar Compared with Iso-osmolar Contrast Media after Coronary Angiography: A Propensity Score Analysis

Wednesday, Dec. 2 10:30AM - 10:40AM Location: S502AB

Participants

Yuan-Cheng Wang, Nanjing, China (*Presenter*) Nothing to Disclose Adrian Tang, MRCP, FRCR, London, United Kingdom (*Abstract Co-Author*) Nothing to Disclose Shenghong Ju, MD, PhD, Nanjing, China (*Abstract Co-Author*) Nothing to Disclose

PURPOSE

The long-term adverse effects of low-osmolar contrast media (LOCM) versus iso-osmolar contrast media (IOCM) remain unclear. This study aims to compare the long-term mortality, renal injury and cardiovascular events between LOCM and IOCM after coronary angiography using propensity scoring in a large retrospective cohort.

METHOD AND MATERIALS

12611 Cardiology patients underwent coronary angiography between January 2006 to July 2013 using either LOCM (iohexol, iopromide) or IOCM (iodixanol). For each contrast medium Primary (all-cause mortality) and Secondary outcomes (renal injury and cardiovascular events beyond 90 days) was recorded. Propensity scoring with subsequent 1:1 matching (PSM) or re-weighting with inverse probability of treatment (IPW) was applied to minimize the selection bias between groups.

RESULTS

Unadjusted all-cause mortality was significantly lower with LOCM versus IOCM (hazard ratio [HR] = 0.28; 95% CI, 0.23-0.34). After propensity adjustment, all-cause mortality became comparable and lost statistical significance. LOCM subgroup analysis showed a trend to lower odds of kidney injury with iopromide vs iohexol after propensity adjustment. Chronic kidney disease (CKD) subgroups had higher mortality risk when receiving LOCM compared with IOCM (PSM: HR = 3.48, 95% CI: 1.24-9.78; IPW: HR = 4.34, 95% CI: 1.36-13.91).

CONCLUSION

After coronary angiography, patients receiving LOCM had comparable overall long-term mortality compared with IOCM after propensity adjustment. IOCM may have significantly lower long-term mortality in CKD cohort.

CLINICAL RELEVANCE/APPLICATION

LOCM had comparable long-term adverse effects to IOCM in overall population receiving coronary angiography. However, IOCM might be more advisable than LOCM for patients with CKD.

SSK03-02 Evaluation of Individually Body Weight Adapted Contrast Media Injection in Coronary CTangiography

Wednesday, Dec. 2 10:40AM - 10:50AM Location: S502AB

Participants

Casper Mihl, MD, Maastricht, Netherlands (*Presenter*) Nothing to Disclose Madeleine Kok, Maastricht, Netherlands (*Abstract Co-Author*) Nothing to Disclose Sibel Altintas, Maastricht, Netherlands (*Abstract Co-Author*) Nothing to Disclose Bastiaan Kietselaer, Maastricht, Netherlands (*Abstract Co-Author*) Nothing to Disclose Joachim E. Wildberger, MD, PhD, Maastricht, Netherlands (*Abstract Co-Author*) Nothing to Disclose Marco Das, MD, Maastricht, Netherlands (*Abstract Co-Author*) Research Consultant, Bayer AG; Research Grant, Siemens AG; Speakers Bureau, Siemens AG; Research Grant, Koninklijke Philips NV

PURPOSE

Ideally, contrast media (CM) injection protocols should be customized to the individual patient. The aim of this study was to determine if software tailored CM injections result in diagnostic vascular enhancement of the coronary arteries and if attenuation values were comparable between different weight categories.

METHOD AND MATERIALS

265 consecutive patients referred for routine coronary computed tomography angiography (CTA) were scanned on a 2nd generation dual-source CT at 100kV. Group 1 (n=141) received an individual CM bolus based on weight categories (39-59kg; 60-74kg; 75-

94kg; 95-109kg) and scan duration ('high-pitch: 1s; 'dual-step prospective triggering': 7s), as determined by contrast injection software (CertegraTM P3T, Bayer). Group 2 (n=124) received a standard fixed CM bolus; Iopromide 300mgI/ml; volume: 75ml; flow rate: 7.2ml/s. Contrast enhancement was measured in all proximal and distal coronary segments. Statistical analysis was performed using SPSS (IBM, version 20.0).

RESULTS

For group 1, mean attenuation values of all segments were diagnostic (>325HU) and without statistical significant differences between different weight categories (p>0.17), proximal-distal: 449±65-373±58HU (39-59kg); 443±69-367±81HU (60-74kg); 427±59-370±61HU (75-94kg); 427±73-347±61HU (95-109kg). Mean CM volumes were: 55±6ml (39-59kg); 61±7ml (60-74kg); 71±8ml (75-94kg); 84±9ml (95-109kg). For group 2, mean attenuation values were not all diagnostic with differences between weight categories (p<0.01), proximal-distal: 611±142-408±69HU (39-59kg); 562±135-389±98HU (60-74kg); 481±83-329±81HU (75-94kg); 420±73-305±35HU (95-109kg).

CONCLUSION

Individually tailored CM injection protocols yield diagnostic attenuation in all scans and a more homogeneous enhancement pattern between different weight groups compared to a fixed injection protocol. In addition, overall CM volumes could be reduced for the majority of patients utilizing P3T software.

CLINICAL RELEVANCE/APPLICATION

Individually tailored CM injection protocols in coronary CTA allow substantial reduction of CM volume for the majority of patients while keeping images diagnostically sufficient.

SSK03-03 Comparison of Three Iodine Concentrations in the Visualization of Coronary Arteries by CT Angiography: A Randomized European Multicenter Trial

Wednesday, Dec. 2 10:50AM - 11:00AM Location: S502AB

Participants

Hans-Christoph R. Becker, MD, PhD, Stanford, CA (Presenter) Nothing to Disclose

PURPOSE

To assess the diagnostic efficacy of iobitridol 350 compared to iopromide 370 and iomeprol 400in the visualization of coronary arteries by CT.

METHOD AND MATERIALS

Prospective, randomized, multi-center, double blind, non-inferiority phase IV trial including 468 patients with suspected coronary artery disease (CAD) and scheduled for clinically indicated coronary CT angiography. The primary endpoint was the CT scan evaluability for CAD diagnosis in terms of quality and interpretability of images. It was based on the full evaluation of 18 coronary segments for each patient assessed by 2 off-site independent readers. Secondary endpoints were related to the safety and efficacy of the 3 contrast media (mainly image quality, stenosis assessment, and signal quantification).

RESULTS

Out of the 452 patients completed for the primary analysis, 92.1% had their 18 segments fully evaluable in the iobitridol group, vs. 94.6 and 95.4% in the iomeprol and iopromide groups respectively. Non-inferiority for the primary outcome was statistically demonstrated (p<0.05). Mean image quality was good to excellent for all contrast media, and no relevant differences were observed for the other secondary endpoints between the 3 groups. The mass of iodine (in g) injected was significantly different between the 3 groups: 27.8±3.4 (iobitridol), 29.3±3.8 (iopromide) and 31.7±3.8 (iomeprol), p<0.001. The good general safety profile of products was confirmed.

CONCLUSION

Coronary CT angiography using iobitridol 350 is non-inferior to higher concentration contrast agents regarding image quality and evaluability while the amount of iodine required can be significantly reduced.

CLINICAL RELEVANCE/APPLICATION

The present study addresses the patient safety perspective based on the reduction of iodine loading while keeping adequate diagnostic capacity in coronary CTA.

SSK03-04 Impact of Contrast Media Iodine Dose on Radiation Induced DNA Damage after Cardiac CTA

Wednesday, Dec. 2 11:00AM - 11:10AM Location: S502AB

Participants

Toon Van Cauteren, MSc, Brussels, Belgium (*Presenter*) Nothing to Disclose Nico Buls, DSc, PhD, Jette, Belgium (*Abstract Co-Author*) Nothing to Disclose Gert Van Gompel, PhD, Brussel, Belgium (*Abstract Co-Author*) Speaker, General Electric Company Johan De Mey, Jette, Belgium (*Abstract Co-Author*) Nothing to Disclose

PURPOSE

To investigate the impact of the administered contrast media iodine dose on the radiation induced DNA double-strand breaks in peripheral blood lymphocytes after a diagnostic cardiac CTA in a porcine model.

METHOD AND MATERIALS

A Göttingen minipig (Ellegaard, Denmark) was scanned with a constant cardiac CTA protocol (100 kV, Auto mA, ECG gated, 0-300% phase, CTDIvol = 45 mGy) on a Revolution CT (GE Healthcare) with an inter-scan delay of one week. We asses a range of contrast media with different iodine concentrations (0-160-200-320 mg I/mL) while keeping the injection parameters constant (3 mL/s and 60 mL followed by a 12 mL saline flush). Before and 15 min after each CT scan, blood samples were collected and put on ice. The lymphocytes were isolated from these blood samples and immunofluoresce microscopy was performed to quantify the γ H2AX foci

representing the radiation induced DNA double strand breaks. At least 750 lymphocytes were analyzed for each condition. Statistical analysis was performed using an independent sample t-test.

RESULTS

We report preliminary results of the first experiments without contrast media (0 mg I/mL) and with 320 mg I/mL contrast media iodine concentration. The amount of DNA double strand breaks was significantly higher when contrast media was present (0.45 \pm 0.19 foci/cell) compared to the identical scan protocol without contrast media (0.17 \pm 0.15 foci/cell) (p-value < 0.001).

CONCLUSION

The presence of iodine contrast has an impact on the amount of radiation induced DNA double strand breaks. The iodine blood concentration results in a higher photoelectric effect which lead to an increase in the formation of secondary electrons responsible for the induction of DNA double strand breaks.

CLINICAL RELEVANCE/APPLICATION

Due to the iodine dose dependent side effect of contrast media, the administration should be continuously reassessed in function of the evolving CT technology.

SSK03-05 Comparison of Different Concentration Iodinated Contrast Medium in Coronary CT Angiography

Wednesday, Dec. 2 11:10AM - 11:20AM Location: S502AB

Participants Yanhua Duan, MD, Jinan, China (*Presenter*) Nothing to Disclose Ximing Wang, PhD, Jinan, China (*Abstract Co-Author*) Nothing to Disclose

PURPOSE

To compare the image quality of DSCT coronary angiography by different concentration iodinated contrast medium with same iodine volume.

METHOD AND MATERIALS

In this study, 180 consecutive patients underwent DSCT coronary angiography were enrolled between Jan. 2013 to Jan. 2015 in our institute. Prospective ECG-triggered high-pitch spiral scanning mode was performed in all patients. A tube-voltage of 100 kV was adopted in all patients. All patients were assigned to 4 groups randomly according to the different concentration of contrast medium: 270 mgI/ml iodinated contrast medium (n=45, group A), 320 mgI/ml iodinated CM (n=45, group B), 350 mgI/ml iodinated CM (n=45, group C), 370 mgI/ml iodinated CM (n=45, group D). All patients were administrated with same iodine volume (296 mgI/kg body weight). A volume of 1.1ml/kg, 0.93ml/kg, 0.85 ml/kg and 0.8 ml/kg body weight iodinated CM (296 mgI/kg body weight) was adopted in group A, B, C and D, respectively. The injection time of CM was fixed at 12 seconds. Injection rate was calculated at total injection volume of CM divided by 12 seconds.Subjective image quality was independently assessed by two radiologists by 4-grade scoring system. Objective image quality (enhancement value, image noise, signal-to-noise ratio and contrast-to-noise ratio of RCA and LAD) was compared among groups.

RESULTS

All prospective ECG-triggering high-pitch spiral DSCT coronary angiographic scans were successful. BMI, age and heart rate were not statistically different among groups. The image quality scores of groups A, B, C and D were 2.00 ± 0.93 , 2.13 ± 1.01 , 2.85 ± 1.23 , 2.93 ± 0.95 , respectively. The subjective image quality was significantly higher in group C and D than in the other groups. Mean attenuation in RCA and LAD of group D was significant higher than that in the other groups. The image noise in group A was significantly higher than the other groups. The SNR and CNR in group A were significantly lower than the other groups.

CONCLUSION

The different concentration of contrast medium has a significant impact on the image quality with a same dose of iodine. Considered the image quality and dose of iodine together, higher-concentration of contrast medium provides better image quality of coronary arteries.

CLINICAL RELEVANCE/APPLICATION

Higher-concentration of contrast medium provides better image quality of CT coronary arteries.

SSK03-07 Contrast Media Administration in Coronary Computed Tomography Angiography- A Systematic Review and Meta-analysis

Wednesday, Dec. 2 11:30AM - 11:40AM Location: S502AB

Participants

Casper Mihl, MD, Maastricht, Netherlands (*Presenter*) Nothing to Disclose Jakub Turek, Maastricht, Netherlands (*Abstract Co-Author*) Nothing to Disclose Madeleine Kok, Maastricht, Netherlands (*Abstract Co-Author*) Nothing to Disclose Joachim E. Wildberger, MD, PhD, Maastricht, Netherlands (*Abstract Co-Author*) Nothing to Disclose Marco Das, MD, Maastricht, Netherlands (*Abstract Co-Author*) Research Consultant, Bayer AG; Research Grant, Siemens AG; Speakers Bureau, Siemens AG; Research Grant, Koninklijke Philips NV

PURPOSE

Scanner related parameters, patient related factors and contrast media (CM) application parameters all significantly influence contrast enhancement of the coronary arteries. No consensus exists in the literature on the optimal CM injection protocol. Thus the aim of this review and meta-analysis is to provide an update on the effect of different CM injection parameters on the attenuation in coronary computed tomography angiography (CCTA).

METHOD AND MATERIALS

Relevant studies published between January 2001 and May 2014 identified by Pubmed, Embase and MEDLINE were evaluated. Using

predefined inclusion and exclusion criteria and a data extraction form, two reviewers independently assessed the content of each eligible study after primary selection. A possible relationship between the parameters iodine delivery rate (IDR), injection rate, CM concentration, total iodine dose (TID), CM volume and attenuation of the coronary arteries was assessed using multivariable random-effects meta-regression analysis.

RESULTS

In the primary literature search, 2552 potential studies were identified. After examination, a total of 36 studies were found to be eligible for this systematic review. Extracted data on CM-, patient-, and scan-related parameters proved to be heterogeneous and often inconsistent. In a multivariable analysis, IDR and CM injection rate proved to be significantly associated with arterial enhancement of the coronary arteries (p<0.05), while CM concentration, TID and CM volume did not.

CONCLUSION

Multivariable meta-regression analysis showed that both IDR and CM injection rate are decisive for attenuation of the coronary arteries. No evidence of any association between CM concentration and attenuation levels was found.

CLINICAL RELEVANCE/APPLICATION

A thorough understanding of the factors responsible for optimal attenuation of the coronary arteries is considered an absolute requirement for optimizing CM injection protocols in the near future. Multivariable meta-regression analysis showed that both IDR and CM injection rate are decisive for opacification of the coronary arteries.

SSK03-08 Preserving Kidney Function with Ultra-low Contrast Volume CT Angiography

Wednesday, Dec. 2 11:40AM - 11:50AM Location: S502AB

Participants

Alexander S. Misono, MD, MBA, Boston, MA (*Presenter*) Nothing to Disclose Elie R. Balesh, MD, Boston, MA (*Abstract Co-Author*) Nothing to Disclose George R. Oliveira, MD, Newton Center, MA (*Abstract Co-Author*) Nothing to Disclose Anand M. Prabhakar, MD, Somerville, MA (*Abstract Co-Author*) Nothing to Disclose Brian B. Ghoshhajra, MD, Boston, MA (*Abstract Co-Author*) Nothing to Disclose

PURPOSE

Ultra-low contrast volume (ULCV) technique for CT angiography (CTA) has been advocated for pre-operative workup for patients undergoing transcatheter aortic valve implantation (TAVI) as the majority of candidates have chronic kidney disease (CKD), a suspected risk factor for contrast-induced nephrotoxicity (CIN). While feasibility has been demonstrated, impact on kidney function in this vulnerable population is a topic of continued inquiry. This study aims to quantify changes in kidney function after ULCV scans.

METHOD AND MATERIALS

In this IRB-approved, HIPAA compliant study, adult ULCV CTA examinations performed from 2012-2015 at a tertiary care hospital were identified. Reports were reviewed for indication and total contrast administered. For each patient, laboratory values of creatinine (Cr) and GFR were identified pre- and post-exam. Patients were excluded if they did not have pre-exam labs within the preceding 3 months or if post-exam labs exceeded 30 days after examination. Paired t tests were performed to assess for change in kidney function between time points, with statistical significance set at p<0.05.

RESULTS

75 ULCV scans were identified, of which 56 (75%) had lab results within the prescribed timeframe. Of note, all of the exams were technically successful. The sample included patients with average age 79 +/- 12.9 (mean +/- SD) with a range of 27-95, including 52% male, 48% female. Indications for studies were primarily for poor renal function (98%) with the majority specifically for TAVI planning (73%); 2% of patients underwent this technique for prior anaphylactoid reaction. Contrast bolus ranged from 15 to 45 cc with an average of 22.3 +/- 6.3. Post-exam labs were obtained 10 +/- 6 days after contrast CT. For the study population, post-exam Cr of 2.1 +/- 1.5 was not significantly changed from pre-exam CF of 2.1 +/- 1.7 (p=0.248). Similarly, post-exam GFR of 32.3 +/- 10.7 was not significantly changed from pre-exam GFR of 32.1 +/- 10.8 (p=0.901).

CONCLUSION

ULCV CT angiography is likely a suitable technique in patients with poor baseline kidney function, with no detectable change in preversus post-exam creatinine or GFR in this cohort study.

CLINICAL RELEVANCE/APPLICATION

In patients with CKD, ULCV technique likely allows for diagnostic contrast-enhanced CT without detrimental effect on kidney function.

SSK03-09 Lower Volume of Lower Concentration Isotonic Contrast Medium for 320-Row Detector Coronary CT Angiography

Wednesday, Dec. 2 11:50AM - 12:00PM Location: S502AB

Participants

Yi Liang, Wuhan, China (*Presenter*) Nothing to Disclose Bolin Du, MD, Wuhan, China (*Abstract Co-Author*) Nothing to Disclose Zhen Li, Wuhan, China (*Abstract Co-Author*) Nothing to Disclose Hanlin Wang, wuhan, China (*Abstract Co-Author*) Nothing to Disclose Jingxiong Tao, wuhan, China (*Abstract Co-Author*) Nothing to Disclose Jia Wang, wuhan, China (*Abstract Co-Author*) Nothing to Disclose Jie Zhou, Wuhan, China (*Abstract Co-Author*) Nothing to Disclose Yang Gao, Wuhan, China (*Abstract Co-Author*) Nothing to Disclose To investigate the feasibility of 320 row coronary CT angiography by using lower volume of lower concentration isotonic contrast medium while maintaining image quality.

METHOD AND MATERIALS

64 patients whose heart beat rate are 70 bpm or less,normal cardiac rhythm,and BMI \leq 24 kg/m² were scanned by 320 row detector dynamic volume CT using 100 kVp (lower tube voltage) and a kind of contrast medium (270mgI/mL). Prospective ECG gating technique and adaptive iterative dose reduction algorithm reconstruction were used. In group A,22 patients in group A were injected 50ml fixed dose of contrast medium by a rate of 5.0ml/s;In group B, 21 patients were injected with the volume of contrast medium calculated by body weight(0.7 ml/kg),injection rate was 4.5 ml/s;In group C, 21 patients were injected with the dosage of contrast medium calculated by body weight (0.6 ml/kg) and the injection rate was 4.0 ml/s. The attenuation value,signal-to-noise(SNR),contrast-to-noise ratio(CNR),image quality and iodine intake between three groups were compared using One-Way ANOVA.

RESULTS

There was no significant statistic difference of age,sex ratio,BMI,heart rate between the three groups (P>0.05). However, the dosage of the contrast agent and different injection rate had statistical significance (P<0.05). The attenuation value from group A to group B and then to group C was on the decline,the CT value of group A was obviously higher than that of group B and group C,the differences were statistically significant (P < 0.05),and there was no statistically significant difference between the group B and group C (P >0.05). The image quality,SNR and CNR in three groups did not have significant difference (P >0.05). The total iodine and iodine injection rates were lowest in group C.

CONCLUSION

Using 320 row detector dynamic volume CT with 100kVp tube voltage and iterative reconstruction algorithm, the patients whose heart beat rates are 70 bpm or less, $BMI \le 24$ kg/m2 are injected with lower concentration of contrast medium by 0.6 ml/kg dose injection give a good image quality of coronary CT angiography which can meet the diagnostic requirement. Meanwhile, it can also reduce the iodine intake and the risk of contrast induced nephrology (CIN).

CLINICAL RELEVANCE/APPLICATION

320 row coronary CT angiography by using lower volume of lower concentration isotonic contrastmedium maintain image quality, meanwhile, it can also reduce the iodine intake and the risk of contrast induced nephrology (CIN).

Case-based Review of Pediatric Radiology (An Interactive Session)

Wednesday, Dec. 2 10:30AM - 12:00PM Location: S406A

NR NM ER PD

AMA PRA Category 1 Credits ™: 1.50 ARRT Category A+ Credits: 1.50

Participants

Sudha A. Anupindi, MD, Philadelphia, PA (Director) Nothing to Disclose

LEARNING OBJECTIVES

1)To apply a systematic approach in the evaluation of pediatric diseases. 2)To identify essential imaging features of various pediatric congenital, musculoskeletal, abdominal and neurological diseases using a multimodality approach. 3) To understand and develop best imaging practice for various pediatric diseases.

ABSTRACT

To apply a systematic approach in the evaluation of pediatric diseases To identify essential imaging features of various pediatric congenital, musculoskeletal, abdominal and neurological diseases using a multimodality approach To understand and develop best imaging practice for various pediatric diseases

Sub-Events

MSCP42A Pediatric Brain Abnormalities

Participants

Manohar M. Shroff, MD, Toronto, ON, (manohar.shroff@sickkids.ca) (*Presenter*) Consultant, Guerbet SA; Consultant, Magellan Health, Inc

LEARNING OBJECTIVES

View learning objectives under main course title.

MSCP42B Pediatric Sport Injuries

Participants Kirsten Ecklund, MD, Boston, MA, (kirsten.ecklund@childrens.harvard.edu) (*Presenter*) Nothing to Disclose

LEARNING OBJECTIVES

View learning objectives under main course title.

MSCP42C Pediatric Nuclear Medicine Cases

Participants

Ruth Lim, MD, Boston, MA (Presenter) Consultant, Alexion Pharmaceuticals, Inc; Officer, New England PET Imaging System

LEARNING OBJECTIVES

View learning objectives under main course title.

ASRT@RSNA 2015: Best Practices in Digital Radiography

Wednesday, Dec. 2 10:40AM - 11:40AM Location: N230

ОТ

AMA PRA Category 1 Credit $^{\text{TM}}$: 1.00 ARRT Category A+ Credit: 1.00

Participants

Donna L. Long, RT, Indianapolis, IN (Presenter) Nothing to Disclose

LEARNING OBJECTIVES

1) Discuss best practices in digital radiography. 2) Comprehend and analyze ASRT position statements and practice standards pertinent to best practices. 3) Analyze the effects of technical factor selection on the digital image. 4) Discuss and apply quality control issues in digital imaging. 5) Analyze and apply exposure indicator systems and values.

ABSTRACT

Digital Radiography has been in practice for quite some time. However we are still working to provide education and best practices for technologists and students regarding the use of digital imaging versus film/screen equipment. This presentation will cover best practices in digital radiography referencing the ASRT white paper, position statements and practice standards. Recommendations regarding future research will also be presented.

Active Handout:Donna L. Long

http://abstract.rsna.org/uploads/2015/15001465/MSRT43.pdf

Creating Radiology eBooks for the iPad (Hands-on)

Wednesday, Dec. 2 12:30PM - 2:00PM Location: S401CD



AMA PRA Category 1 Credits ™: 1.50 ARRT Category A+ Credits: 1.50

Participants

Henry J. Baskin JR, MD, Salt Lake Cty, UT (*Presenter*) Nothing to Disclose Justin Cramer, MD, Salt Lake City, UT (*Presenter*) Nothing to Disclose Justin La Plante, MD, Sayre, PA (*Presenter*) Nothing to Disclose

LEARNING OBJECTIVES

1) Become familiar with Apple's free ebook authoring tool, iBooks Author. 2) Create a sample radiology ebook during the course. 3) Learn how to freely share your ebook with others.

Correlating Imaging with Human Genomics (Hands-on)

Wednesday, Dec. 2 12:30PM - 2:00PM Location: S401AB

IN

AMA PRA Category 1 Credits ™: 1.50 ARRT Category A+ Credits: 1.50

Participants

Daniel L. Rubin, MD, MS, Palo Alto, CA (Presenter) Nothing to Disclose Sandy Napel, PhD, Stanford, CA (Presenter) Medical Advisory Board, Fovia, Inc; Consultant, Carestream Health, Inc; Scientific Advisor, EchoPixel, Inc

Olivier Gevaert, PhD, Stanford, CA (Presenter) Nothing to Disclose

LEARNING OBJECTIVES

1) Understand the methods for and the potential value of correlating radiological images with genomic data for research and clinical care. 2) Learn how to access genomic and imaging data from The Cancer Genome Atlas (TCGA) and The Cancer Imaging Archive (TCIA) databases, respectively. 3) Learn about methods and tools for annotating regions within images with semantic and computational features. 4) Learn about methods and tools for analyzing molecular data, generating molecular features and associating them with imaging features.

ABSTRACT

Radiogenomics is an emerging field that integrates medical images and genomic data for the purposes of improved clinical decision making and advancing discovery of critical disease processes. In cancer, both imaging and genomic data are becoming publicly available through The Cancer Imaging Archive (TCIA) and The Cancer Genome Atlas (TCGA) databases, respectively. The TCIA/TCGA provide examples of matched molecular and image data for five cancer types, namely breast, lung, brain, prostate and kidney. The data in TCGA includes various omics data such as gene expression, microRNA expression, DNA methylation and mutation data. The community is beginning to extract image features from the MRI, CT and/or PET images in TCIA, including tumor volume, shape, margin sharpness, voxel-value histogram statistics, image textures, and specialized features developed for particular acquisition modes. They are also annotating the images with semantic descriptors using controlled terminologies to record the visual characteristics of the diseases. The availability of these linked imaging-genomic data provides exciting new opportunities to recognize imaging phenotypes that emerge from molecular characteristics of disease and that can potentially serve as biomarkers of disease and its response to treatment. They also provide an opportunity to discover key molecular processes associated with distinct image features, within one cancer type and across different cancer types. This workshop will describe datasets and tools that enable research at the intersection of imaging and genomics, and that point to opportunities to develop future applications that leverage this knowledge for diagnostic decision support and treatment planning.

Honored Educators

Presenters or authors on this event have been recognized as RSNA Honored Educators for participating in multiple qualifying educational activities. Honored Educators are invested in furthering the profession of radiology by delivering high-guality educational content in their field of study. Learn how you can become an honored educator by visiting the website at: https://www.rsna.org/Honored-Educator-Award/

Daniel L. Rubin, MD, MS - 2012 Honored Educator Daniel L. Rubin, MD, MS - 2013 Honored Educator

Clinical Applications of 3D Printing (Part II)

Wednesday, Dec. 2 12:30PM - 2:00PM Location: S501ABC

IN

AMA PRA Category 1 Credits ™: 1.50 ARRT Category A+ Credits: 1.50

FDA Discussions may include off-label uses.

Participants

Jane S. Matsumoto, MD, Rochester, MN (*Moderator*) Nothing to Disclose Glenn E. Green, MD, Ann Arbor, MI (*Moderator*) Nothing to Disclose

Sub-Events

RCC43A 3D Printed Models for Interventional Cardiovascular Planning

Participants

Zhen Qian, PhD, Atlanta, GA (Presenter) Research Grant, TeraRecon, Inc

LEARNING OBJECTIVES

1) Learn the potential role of 3D printed models in the planning of transcatheter valve replacement. a. Will demonstrate how to produce patient-specific 3D printed models that are anatomically accurate and biomechanically comparable to human valves. b. Will give examples of in-vitro simulation using 3D printed models integrated with sensors and imaging techniques for the planning of transcatheter valve replacement.

RCC43B 3D Printing in Otolaryngology

Participants Glenn E. Green, MD, Ann Arbor, MI (*Presenter*) Nothing to Disclose Maryam Ghadimi Mahani, MD, Ann Arbor, MI (*Presenter*) Nothing to Disclose

LEARNING OBJECTIVES

1) Become familiar with role of imaging in 3D print in otolaryngology. 2) Become familiar with novel treatment of tracheobronchomalacia in children using 3D print technology.

ABSTRACT

RCC43C 3D Printing in Interventional Radiology and Vascular Surgery

Participants

Matthew D. Tam, FRCR, Westcliff on Sea, United Kingdom, (matthewtam2005@gmail.com) (Presenter) Nothing to Disclose

ABSTRACT

3D printing in medicine and radiology is an exciting and growing field. Vascular surgery and interventional radiology procedures can benefit from 3D printing. It can be incorporated into daily practice through procedure planning and procedure execution. It can potentially advance the field through aiding implant design and development.Learning objectives:1) Understand the potential roles of 3D printing in vascular surgery and interventional radiology2) Gain an overview of the production of solid and hollow luminal models3) See examples of use of 3D models in real cases in a vascular interventional service

RCC43D 3D Printing in Forensic Medicine

Participants

Jonathan M. Morris, MD, Rochester, MN (Presenter) Nothing to Disclose

RCC43E 3D Models in Orthopedic Reconstructive Surgery

Participants

Michael Yaszemski, MD, PhD, Rochester, MN, (yaszemski.michael@mayo.edu) (Presenter) Nothing to Disclose

RCC43F 3D Printing as an Educational Tool

Participants

Jane S. Matsumoto, MD, Rochester, MN (Presenter) Nothing to Disclose

LEARNING OBJECTIVES

1) Will demonstrate use of color coded segmentation tools for teacing important anatomic relationships for a range of medical learners. 2) Will provide examples of role of 3D anatomic models of complex disease in enhancing comprehension of complex anatomy and aid in surgical education. 3) Will highlight the value of 3D models in patient education and informed consent.

ASRT@RSNA 2015: Famous Feet: Weber, Lisfranc, and Jones. The Fractures. The Men.

Wednesday, Dec. 2 1:00PM - 2:00PM Location: N230

мк

AMA PRA Category 1 Credit ™: 1.00 ARRT Category A+ Credit: 1.00

Participants

Ken L. Schreibman, PhD, MD, Madison, WI (Presenter) Nothing to Disclose

LEARNING OBJECTIVES

1) To get a better understanding of 3 common fracture patterns in the foot/ankle: a. Ankle twisting injuries and the Weber staging system. b. Fracture/dislocations of the Lisfranc joint c. Fractures of the proximal 5th metatarsal, distinguishing between avulsion and Jones fractures.

Active Handout:Ken L. Schreibman

http://abstract.rsna.org/uploads/2015/15001466/MSRT44.pdf

RSNA/ESR Emergency Symposium: Abdominal Emergencies (An Interactive Session)

Wednesday, Dec. 2 1:30PM - 3:00PM Location: S402AB

GI CT ER

AMA PRA Category 1 Credits ™: 1.50 ARRT Category A+ Credits: 1.50

Participants

Ronald J. Zagoria, MD, San Francisco, CA, (ron.zagoria@ucsf.edu) (*Moderator*) Nothing to Disclose Andras Palko, MD, PhD, Szeged, Hungary (*Moderator*) Medical Advisory Board, Affidea Group;

Sub-Events

MSSR43A Abdominal Injuries

Participants

Andras Palko, MD, PhD, Szeged, Hungary, (palko.andras@med.u-szeged.hu) (Presenter) Medical Advisory Board, Affidea Group;

LEARNING OBJECTIVES

1) To explain the significance of injury mechanism and its role in the formation of consequent abdominal lesions and their complications. 2) To outline the role of proper imaging technique and diagnostic algorithm in the sufficiently fast diagnosis of abdominal injuries. 3) To learn more about the typical and unusual findings of various abdominal traumatic conditions.

ABSTRACT

Abdominal injuries require a timely and reliable diagnosis in order to prevent the potentially lethal outcome. The armory of clinical tools (physical examination, lab tests) does not fulfill these criteria, since they are either not fast, or not reliable. Imaging diagnostic modalities help the clinician to acquire the necessary amount of information to initiate focused and effective treatment. However, the selection of the appropriate imaging algorithm, modality and technique, as well as the precise detection and interpretation of essential imaging findings are frequently challenging, especially because the circumstances, under which these examinations are performed (open wounds, bandages, non-removable life-supporting equipment, lack of patient cooperation, etc.), are frequently less than optimal. Knowledge of critical imaging signs, symptoms and the role they play in the evaluation of the patient's condition, but also fast decision-making and ability to closely cooperate with the clinicians are skills of key importance for radiologist members of the trauma team.

MSSR43B The Enemy Within, Non-Traumatic Abdominal Emergencies

Participants

Ronald J. Zagoria, MD, San Francisco, CA, (ron.zagoria@ucsf.edu) (Presenter) Nothing to Disclose

LEARNING OBJECTIVES

1) Attendees will be able to better analyze CT scans for non-traumatic causes of abdominal pain. 2) Attendees will learn the CT signs and causes of bowel ischemia. 3) Attendees will learn the CT findings of common causes of an "acute" abdomen. 4) Attendees will learn the imaging findings of acute, nontraumatic urinary tract and GI tract emergencies.

ABSTRACT

This segment of the course will go over the optimal imaging approach for patients presenting with acute abdominal pain. CT findings will be emphasized. Key imaging findings of nontraumatic causes of acute abdominal pain including gastrointestinal tract and urinary tract pathology will be explained. A systematic approach for the imaging evaluation of patients wih abdominal emergencies will be illustrated and explained including proper scan protocols and analysis of imaging findings. Imaging diagnosis of urinary tract obstruction, infection, bowel obstruction, and ischemia will be emphasized.

MSSR43C Interactive Case Discussion

Participants

Andras Palko, MD, PhD, Szeged, Hungary (*Presenter*) Medical Advisory Board, Affidea Group; Ronald J. Zagoria, MD, San Francisco, CA, (ron.zagoria@ucsf.edu) (*Presenter*) Nothing to Disclose

LEARNING OBJECTIVES

1) Attendees will be able to better analyze CT scans for traumatic and non-traumatic causes of abdominal pain. 2) Attendees will learn the CT signs and causes of bowel ischemia and injuries. 3) Attendees will learn the CT findings of common causes of a traumatic and non-traumatic 'acute' abdomen. 4) Attendees will learn the imaging findings of acute, traumatic and nontraumatic urinary tract and GI tract emergencies.

ABSTRACT

Using cases and an audience response system, this segment of the course will go over the optimal imaging approach for patients presenting with acute abdominal pain and abdominalk injuries. CT findings will be emphasized. Key imaging findings of traumatic and nontraumatic causes of acute abdominal pain including gastrointestinal tract and urinary tract pathology will be explained. A systematic approach for the imaging evaluation of patients wih abdominal emergencies will be illustrated and explained including proper scan protocols and analysis of imaging findings. Imaging diagnosis of blunt an penetrating abdominal injuries, urinary tract obstruction, infection, bowel obstruction, and ischemia will be emphasized.

Wednesday Plenary Session

Wednesday, Dec. 2 1:30PM - 2:45PM Location: Arie Crown Theater

RO

AMA PRA Category 1 Credits ™: 1.25 ARRT Category A+ Credit: 1.00

Participants

Ronald L. Arenson, MD, San Francisco, CA (Presenter) Nothing to Disclose

Sub-Events

PS40A Announcement of Education Exhibit Awards

Participants

PS40B Annual Oration in Radiation Oncology: NRG Oncology and the National Cancer Institute's National Clinical Trials Network: A Case Study for Innovation in Multi-Disciplinary Cancer Research

Participants

Walter J. Curran JR, MD, Atlanta, GA (*Presenter*) Committee member, Bristol-Myers Squibb Company; Committee member, AstraZeneca PLC

Nina A. Mayr, MD, Seattle, WA (Presenter) Nothing to Disclose

Abstract

The National Cancer Institute (NCI) modified its publicly funded cancer research program from a system of ten groups with cooperative agreements, some of which dated back to the 1950's, to a network of five groups beginning in March 2014. The new network, known as the National Clinical Trials Network (NCTN), builds on the decades of practice-defining success of the cooperative groups and also seeks to be responsive to issues raised by the Institute of Medicine (IOM) in 2010. The IOM raised concerns that the cooperative groups were too slow to respond to new scientific discoveries, too cumbersome as an infrastructure, and too underfunded. The IOM also praised the groups for their remarkable accomplishments despite these obstacles. NRG Oncology is one of the five new NCTN groups and arose from the cooperation between three legacy cooperative groups: the National Surgical Adjuvant Breast and Bowel Project (NSABP), the Radiation Therapy Oncology Group (RTOG), and the Gynecologic Oncology Group (GOG). NRG Oncology focuses its clinical and translational research efforts on patients afflicted with malignancies in one of these seven cancer disease site categories: brain tumors, head and neck cancers, lung cancers, breast cancers, gastrointestinal cancers, and genitourinary cancers, and gynecologic cancers. The means by which NRG Oncology develops and executes practice-defining research for such patients on a global basis will be discussed.

Case-based Review of US (An Interactive Session)

Wednesday, Dec. 2 1:30PM - 3:00PM Location: S406A

VA IR US

AMA PRA Category 1 Credits ™: 1.50 ARRT Category A+ Credits: 1.50

Participants

Deborah J. Rubens, MD, Rochester, NY (Director) Nothing to Disclose

LEARNING OBJECTIVES

1) Recognize the diverse applications of ultrasound throughout the body and when it provides the optimal diagnostic imaging choice. 2) Understand the fundamental interpretive parameters of ultrasound contrast enhancement and its applications in the abdomen. 3) Know the important factors to consider when choosing ultrasound vs CT for image guided procedures and how to optimize ultrasound for technical success.

ABSTRACT

Ultrasound is a rapidly evolving imaging modality which has achieved widespread application throughout the body. In this course we will address the major anatomic areas of ultrasound use, including the abdominal and pelvic organs, superficial structures and the vascular system. Challenging imaging and clinical scenarios will be emphasized to include the participant in the decision-making process. Advanced cases and evolving technology will be highlighted, including the use of ultrasound contrast media as a problem solving tool, and the appropriate selection of procedures for US-guided intervention.

Sub-Events

MSCU41A Problem Solving with Contrast Enhanced Ultrasound

Participants

Stephanie R. Wilson, MD, Calgary, AB (*Presenter*) Research Grant, Lantheus Medical Imaging, Inc; Equipment support, Siemens AG; Equipment support, Koninklijke Philips NV

LEARNING OBJECTIVES

1) Attendees will appreciate the multiple varied applications for CEUS in the abdomen. 2) They will recognize the value of CEUS as a real time procedure with exquisite sensitivy to its contrast agent allowing for superior detection of arterial phase vascularity. 3) They will realize the safety of CEUS with no requirement for ionizing radiation, and no nephrotoxicity for evaluation of any problems requiring contrast enhancement in those with renal failure. 4) They will understand the fundamentals for interpretation of contrast enhancement patterns for the noninvasive diagnosis of focal liver masses and other pathology.

ABSTRACT

MSCU41B Image Guided Intervention: When Is Ultrasound Best?

Participants

Michael D. Beland, MD, Providence, RI (Presenter) Consultant, Hitachi, Ltd

LEARNING OBJECTIVES

1) Understand factors to consider when choosing ultrasound versus CT as a modality for image guidance. 2) Review the potential challenges and advantages of ultrasound for procedure guidance. 3) Demonstrate the variety of cases for which ultrasound can be used to perform image guided procedures and learn some techniques for maximizing success.

ABSTRACT

Image-guided procedures are commonly performed. There are several important considerations when selecting an appropriate imaging modality to guide the procedure. Ultrasound has several advantages over CT but there are also limitations. These advantages and disadvantages will be reviewed, including various factors to consider when evaluating a case for a potential procedure. When ultrasound is used, there are techniques which may offer increased likelihood of success or decreased procedural time. Through multiple case presentations, this session will review the considerations and techniques for successful ultrasound guided interventions.

MSCU41C Vascular Ultrasound Update

Participants Laurence Needleman, MD, Philadelphia, PA (*Presenter*) Nothing to Disclose

LEARNING OBJECTIVES

View learning objectives under main course title.

VSIO41

Interventional Oncology Series: Mechanisms Matter: Basic Science Every IO Should Know

Wednesday, Dec. 2 1:30PM - 6:00PM Location: S405AB

GI IR RO AMA PRA Category 1 Credits ™: 4.50 ARRT Category A+ Credits: 5.00

FDA Discussions may include off-label uses.

Participants

S. Nahum Goldberg, MD, Ein Kerem, Israel, (sgoldber@bidmc.harvard.edu) (*Moderator*) Consultant, AngioDynamics, Inc; Research support, AngioDynamics, Inc; Research support, Cosman Medical, Inc; Consultant, Cosman Medical, Inc;

LEARNING OBJECTIVES

1) Gain an appreciation of the basic scientific underpinnings of interventional oncology. 2) Understand how and why these mechanistic studies can have an impact on both daily clinical practice and future therapeutic paradigms. 3) Characterize the most important advances of tumor ablation over the last two decades. 4) Gain a better understanding of the cutting edge imaging techniques that facilitate successful state of the art interventional oncologic practice.

ABSTRACT

The first half of the session has been organized into a thematic unit entitled: "Mechanisms Matter: Basic science every IO should know" and will be dedicated to gaining an appreciation of the basic scientific underpinnings of interventional oncology and understand how and why such studies can have an impact on both daily clinical practice and future therapeutic paradigms. This will include an initial lecture outlining the many insights and lessons that can be directly applied from radiation therapy and hyperthermia, followed by lectures that center upon key mechanistic pathways that are being used to improve transcatheter embolization and tumor ablation. Two presentations will outline our current understanding of the potential systemic effects of postprocedure, cytokine-mediated inflammation - the negative effects leading to tumorigenesis and the potential beneficial immune (abscopic) effects of IO therapies. A highlight of the session will be a keynote address "20 years of thermal ablation: Progress, Challenges and Opportunities". Dr. Solomon, a noted thought leader in the field will not only characterize the most important advances of tumor ablation over the last two decades and place them in their proper historical and developmental context, but will also identify key areas of research in device and technique development that hold the potential to propel the field forward in the upcoming decade. The second half of the session "Advancing IO with cutting-edge imaging techniques" will be dedicated to the cutting edge imaging modalities that facilitate successful state of the art IO practice. Leading authorities will provide an in depth look at advances and adaptation of 5 of the main technologies as they relate to enhancing interventional oncology including: advanced ultrasound and fusion techniques; state-of-the-art angiographic imaging (including Cone beam CT and subtraction reconstruction); tailoring MR for IO; the the role of PET/CT; and molecular imaging.

Sub-Events

VSI041-01 Ischemia-The Prime Mover: Apoptosis, Hif-1a, and VEGF Pathways

Wednesday, Dec. 2 1:30PM - 1:45PM Location: S405AB

Participants

Jean-Francois H. Geschwind, MD, Westport, CT (*Presenter*) Researcher, BTG International Ltd; Consultant, BTG International Ltd; Researcher, Koninklijke Philips NV; Consultant, Koninklijke Philips NV; Researcher, Guerbet SA; Consultant, Guerbet SA; Consultant, Terumo Corporation; Consultant, Threshold Pharmaceuticals, Inc; Consultant, PreScience Labs, LLC; Researcher, Boston Scientific Corporation; Consultant, Boston Scientific Corporation

LEARNING OBJECTIVES

View learning objectives under main course title.

VSI041-02 Exploiting Tumor Hypoxia with Transarterial Chemoembolization to Treat Liver Cancer: Selective Hypoxia-Activated Intra-arterial Therapy in a Rabbit Model

Wednesday, Dec. 2 1:45PM - 1:55PM Location: S405AB

Awards

Trainee Research Prize - Fellow

Participants Rafael Duran, MD, Baltimore, MD (Presenter) Nothing to Disclose Sahar Mirpour, MD, Baltimore, MD (Abstract Co-Author) Nothing to Disclose Vasily Pekurovsky, Chicago, IL (Abstract Co-Author) Nothing to Disclose Shanmugasundaram Ganapathy-Kanniappan, PhD, Baltimore, MD (Abstract Co-Author) Nothing to Disclose Cory F. Brayton, Pharm D, Baltimore, MD (Abstract Co-Author) Nothing to Disclose Toby Charles Cornish, MD, PhD, Baltimore, MD (Abstract Co-Author) Research Consultant, DigiPath, Inc Stockholder, DigiPath, Inc Boris Gorodetski, Baltimore, MD (Abstract Co-Author) Nothing to Disclose Julius Chapiro, MD, Berlin, Germany (Abstract Co-Author) Nothing to Disclose Ruediger E. Schernthaner, MD, Vienna, Austria (Abstract Co-Author) Nothing to Disclose Ming De Lin, PhD, Cambridge, MA (Abstract Co-Author) Employee, Koninklijke Philips NV Constantine Frangakis, Baltimore, MD (Abstract Co-Author) Nothing to Disclose Jean-Francois H. Geschwind, MD, Westport, CT (Abstract Co-Author) Researcher, BTG International Ltd; Consultant, BTG International Ltd; Researcher, Koninklijke Philips NV; Consultant, Koninklijke Philips NV; Researcher, Guerbet SA; Consultant, Guerbet SA; Consultant, Terumo Corporation; Consultant, Threshold Pharmaceuticals, Inc; Consultant, PreScience Labs, LLC; Researcher, Boston Scientific Corporation; Consultant, Boston Scientific Corporation

PURPOSE

Hypoxia is a common physiological alteration of solid tumors and has been correlated with treatment failure. Hypoxia resulting from embolization also contributes to chemoresistance after TACE. Evofosfamide (Evo) [previoulsy called TH-302] is administered as a nontoxic prodrug which is selectively activated by hypoxia resulting in DNA damage and tumor cell death. The purpose of this study was to investigate the feasibility, safety and antitumor efficacy of hepatic hypoxia; activated intra-arterial therapy (HAIAT) in a rabbit model.

METHOD AND MATERIALS

Twenty-eight VX2 tumor; bearing rabbits were assigned to 4 intraarterial therapy (IAT) regimens: 1) saline (control group); 2) Evo; 3) doxorubicin; Lipiodol emulsion followed by embolization with 100; 300µm beads (conventional, cTACE); or 4) a combination of Evo and cTACE (Evo; cTACE). Blood samples were collected pre; IAT, 24/48h and 7/14days post; IAT. Efficacy was assessed quantitatively on MDCT (24h pre;, 7/14 days post; IAT). Necrotic fraction (NF) was quantified on HandE by slide; by; slide segmentation. Hypoxic fraction (HF) and compartment (HC) were determined by pimonidazole staining. Markers of tumor DNA damage, apoptosis, cell proliferation, endogenous hypoxia and metabolism were quantified (Y-H2AX, annexin V, caspase-3, Ki-67, HIF1a, MCT4, LDH).

RESULTS

Evo; cTACE showed similar profile in liver enzyme elevation compared to cTACE except at day 7 where ALT was higher. No hematologic/renal toxicity was observed. Animals treated with Evo-cTACE demonstrated smaller tumor volumes, lower tumor growth rate and higher NF compared to cTACE. Evo resulted in a marked reduction in the HF and HC. A significant negative correlation was found between the HF or HC and the magnitude of the NF. Evo or Evo; cTACE promoted antitumor effects as evidenced by increased expression of γ ; H2AX and apoptotic biomarkers, with decreased proliferation. Increased HIF1a expression and tumor glycolysis validated HAIAT.

CONCLUSION

HAIAT with Evo was feasible, had a favorable toxicity profile and demonstrated antitumor effects by selective targeting of tumor hypoxic areas.

CLINICAL RELEVANCE/APPLICATION

The embolic effect of TACE provides an attractive setting for selective activation of bioreductive prodrugs and HAIAT allows for the delivery of high drug doses that may reach tumor regions where hypoxic cells reside in pharmacological sanctuary.

VSI041-03 Lessons Learned from XRT/Hyperthermia

Wednesday, Dec. 2 1:55PM - 2:10PM Location: S405AB

Participants

Mark W. Dewhirst, DVM, PhD, Durham, NC (*Presenter*) Stockholder, Celsion Corporation; Research Grant, Biomimetix Corporation; Research Grant, Johnson & Johnson; Consultant, Nevro Corp; Consultant, Merck KGaA; Consultant, Siva Corporation

LEARNING OBJECTIVES

1) Understand the complimentary interactions between hyperthermia and radiotherapy that increase cell killing. 2) Understand importance of measuring temperature during heating and methods for how this is accomolished. 3) Be able to articulate how hyperthermia affects tumor physiology and how these effects influence treatment responses.

ABSTRACT

There are more than a dozen positive phase III trials showning that hyperthermia can increase local tumor control when it is combined with radiotherapy. Such trials include head and neck cancer, cervix cancer, GBM, esophageal al cancer and chest wall recurrences of breast cancer. It has been known for more than two decades that hyperthermia augments the cytotoxicity of radiotherapy. Basic tenants underlying this interaction include proof that hyperthermia inhibits DNA damage-repair. Hyperthermia has complimentary cytotoxicity with radiotherapy in different parts of the cell cycle. Further, hyperthermia can increase tumor perfusion, thereby increasing oxygen delivery; lack of oxygen is a source of relative resistance to radiotherapy. In recent years, however, new insights have been made into how these two treatment modalities interact. These insights come from: 1) innovative clinical trials involving functional imaging and genomics and 2) examination of how hyperthermia affects the process of DNA damage repair. These developments point the way toward new methods to further therapeutic gain by taking advantage of cellular responses to these therapies.

VSIO41-04 The Safety and Efficacy Profile of TACE for Treating Hepatocellular Carcinoma in Patients Co-infected with HIV and HCV: A Propensity Score Matching Study

Wednesday, Dec. 2 2:10PM - 2:20PM Location: S405AB

Participants

Jae Ho Sohn, MD,MS, New Haven, CT (*Presenter*) Nothing to Disclose Reham R. Haroun, Salt Lake City, UT (*Abstract Co-Author*) Nothing to Disclose Julius Chapiro, MD, Berlin, Germany (*Abstract Co-Author*) Nothing to Disclose Sonia P. Sahu, New Haven, CT (*Abstract Co-Author*) Nothing to Disclose Yan Zhao, MS, Baltimore, MD (*Abstract Co-Author*) Nothing to Disclose Rafael Duran, MD, Baltimore, MD (*Abstract Co-Author*) Nothing to Disclose Florian N. Fleckenstein, MS, New Haven, CT (*Abstract Co-Author*) Nothing to Disclose Ruediger E. Schernthaner, MD, Vienna, Austria (*Abstract Co-Author*) Nothing to Disclose Li Zhao, New Haven, CT (*Abstract Co-Author*) Nothing to Disclose Susanne Smolka, New Haven, CT (*Abstract Co-Author*) Nothing to Disclose Ming De Lin, PhD, Cambridge, MA (*Abstract Co-Author*) Nothing to Disclose International Ltd; Researcher, Koninklijke Philips NV; Consultant, Koninklijke Philips NV; Researcher, Guerbet SA; Consultant, Guerbet SA; Consultant, Terumo Corporation; Consultant, Threshold Pharmaceuticals, Inc; Consultant, PreScience Labs, LLC; Researcher, Boston Scientific Corporation; Consultant, Boston Scientific Corporation

PURPOSE

Hepatocellular carcinoma (HCC) is becoming an increasing cause of morbidity and mortality in patients co-infected with HIV and HCV. TACE is an important treatment option for unresectable HCC, but to date, there is paucity of data on the safety and efficacy profile of TACE in this specific cohort. The purpose of this study is to compare HCC patients with HIV/HCV co-infection treated with TACE against HCC patients with HCV mono-infection treated with TACE through survival analysis and recording of major complications.

METHOD AND MATERIALS

This single institution and retrospective study included 456 patients. 35 HIV/HCV co-infected HCC patients with CD4 > 100 (group EXP) and 421 HCV-only HCC patients (group CTRL) who received TACE from 2001 - 2014 were included. Propensity score matching (PSM) with the nearest-neighbor method was performed, adjusting for sex, ethnicity, and BCLC/HKLC, which take into account Child-Pugh Class, ECOG performance score, and tumor characteristics. Covariate balance was confirmed. Kaplan-Meier (KM) estimates with median overall survival (MOS) and log-rank statistic were calculated. Cox regression was performed on EXP group to identify infectious disease parameters of potential significance on survival, such as detectable HIV viral load, CD4 count, and anti-retroviral therapy (ART). Significant complications were recorded.

RESULTS

Of the 456 patients, 35 patients in EXP group were successfully matched to 75 patients in CTRL group. 15 (42.9%) patients had detectable HIV viral load. Median CD4 count was 406 x 106 cells/mm3 (range 121 to 1086). 31 (88.5%) patients were on ART. The cohort spanned all BCLC/HKLC stages. KM revealed MOS of 20.0 months for the EXP group and MOS of 21.3 months for the CTRL group (p = 0.907). Cox model on EXP group did not identify any infectious disease variables of significance on survival. No significant complication, such as death, ICU stay, or fulminant liver failure within 30 days of TACE, was observed in the EXP group.

CONCLUSION

In HCC patients with HIV/HCV co-infection and CD4 > 100, TACE demonstrated comparable safety and efficacy profile as in HCC patients with HCV only.

CLINICAL RELEVANCE/APPLICATION

Interventional oncologists should feel comfortable offering TACE as a treatment option to HCC patients with HIV/HCV co-infection.

VSI041-05 Tailoring Nanodrugs for IO: Free Radicals, Heat Shock Proteins, and beyond

Wednesday, Dec. 2 2:20PM - 2:35PM Location: S405AB

Participants

S. Nahum Goldberg, MD, Ein Kerem, Israel (*Presenter*) Consultant, AngioDynamics, Inc; Research support, AngioDynamics, Inc; Research support, Cosman Medical, Inc; Consultant, Cosman Medical, Inc;

LEARNING OBJECTIVES

View learning objectives under main course title.

VSI041-06 Circulating Tumor Cells Early Predict Prognosis of Hepatocellular Carcinoma Treated with Transarterial Chemoembolization: A Prospective Study

Wednesday, Dec. 2 2:35PM - 2:45PM Location: S405AB

Participants

Guowei Yang, MD, Shanghai, China (*Presenter*) Nothing to Disclose Bo Zhou, Shanghai, China (*Abstract Co-Author*) Nothing to Disclose Rong Liu, Shanghai, China (*Abstract Co-Author*) Nothing to Disclose Jian-Hua Wang, Shanghai, China (*Abstract Co-Author*) Nothing to Disclose

PURPOSE

To evaluate the potential utility of circulating tumor cells (CTCs) measurements in predicting prognosis of hepatocellular carcinoma (HCC) patients received transarterial chemoembolization (TACE) treatments, including their differences in different vein sites and the immediate and delayed impact of TACE on CTCs.

METHOD AND MATERIALS

CTCs from consecutive patients with HCC were quantified before and immediately and 6-8 weeks after TACE. CTCs were examined in both samples derived from the peripheral vein (PV) and the hepatic vein (HV).

RESULTS

A total of 46 consecutive patients with HCC were recruited into the prospective study and 38 were analysed at last. CTCs counts in HV were significantly higher than in PV (P<0.001). TACE led to a statistically significant immediate fall in CTCs numbers, especially in HV(P<0.001). Patients with CTCs levels ≥ 2 in PV or ≥ 8 in HV at baseline per 7.5 ml blood samples, compared with the group with fewer CTCs in PV or HV, had a shorter median progression-free survival (PFS, 5.2 months vs. 12.0 months, P=0.01; 5.2 months versus 9.5 months, P=0.003, respectively). At the 6-8 weeks after TACE, patients with CTCs ≥ 2 in PV or ≥ 3 in HV had a similarly shorter PFS (5.0 months vs. 12.0 months, P<0.001; 5.1 months versus 11.2 months, P<0.001, respectively). Further analysis showed that patients with higher CTC levels also had a higher intrahepatic metastasis rate. The multivariate Cox regression analyses and ROC curves showed that the levels of CTCs at baseline and 6-8 weeks after TACE were significant independent prognostic factors of PFS.

CONCLUSION

The number of CTCs in peripheral and hepatic vein before and 6-8 weeks after TACE are independent predictors of PFS in HCC patients received TACE treatments. TACE immediately reduces the number of CTCs get into the blood circulation.

CLINICAL RELEVANCE/APPLICATION

CTCs detection is a promising method to predict prognosis in HCC patients underwent TACE. TACE immediately reduce the number of CTCs get into the blood and may reduce the rate of metastasis.

VSIO41-07 Understanding Post-procedure Inflammation: AKT and c-met Pathways

Wednesday, Dec. 2 2:45PM - 3:00PM Location: S405AB

Participants

David A. Woodrum, MD, PhD, Rochester, MN (Presenter) Nothing to Disclose

LEARNING OBJECTIVES

View learning objectives under main course title.

VSIO41-08 Microwave Hepatic Ablation Induces Dose Dependent Local Inflammation and Distant Pro-oncogenic Effects

Wednesday, Dec. 2 3:00PM - 3:10PM Location: S405AB

Participants

Erik Velez, BS, San Francisco, CA (*Presenter*) Nothing to Disclose Nahum Goldberg, Jerusalem, Israel (*Abstract Co-Author*) Nothing to Disclose Gaurav Kumar, PhD, Boston, MA (*Abstract Co-Author*) Nothing to Disclose Yuanguo Wang, Boston, MA (*Abstract Co-Author*) Nothing to Disclose Christopher L. Brace, PhD, Madison, WI (*Abstract Co-Author*) Shareholder, NeuWave Medical Inc; Consultant, NeuWave Medical Inc; Shareholder, Symple Surgical Inc; Consultant, Symple Surgical Inc Muneeb Ahmed, MD, Wellesley, MA (*Abstract Co-Author*) Nothing to Disclose

PURPOSE

To determine how different doses of microwave ablation (MWA) induce local inflammation and distant pro-oncogenic effects compared to radiofrequency ablation (RFA) in a small animal model.

METHOD AND MATERIALS

F344 rats (n=24) were implanted with single subcutaneous R3230 tumors. Average tumor diameter and tumor growth rates were assessed daily. At mean tumor diameter of 10 mm, animals were divided into four groups (n=6/arm), and assigned to one of four treatments: sham (needle x 5 minutes), RFA (70°C x 5 minutes), rapid high-dose MWA (20W x 15 seconds), or slower low-dose MWA (5W x 2 minutes). Settings were selected to produce 11.4 ± 0.8 mm coagulation zones for all ablation settings. Tumors were measured daily for 7 days post-treatment to determine growth rates. Thickness of periablational liver inflammation (heat shock protein 70; Hsp70), local liver IL-6 levels, and distant tumor proliferative indices (Ki-67) were also compared.

RESULTS

Hepatic MWA-5W and RFA increased distant tumor growth rates compared to the MWA-20W and sham arms, such that the 7 day mean tumor diameter was greater (MWA-5W 16.3±1.1 mm, RFA 16.3±0.9 mm vs. sham 13.6±1.3 mm, p<0.01, and MWA-20W 14.6±0.9 mm, p<0.05). Although less than MWA-5 or RFA, MWA-20W also resulted in a significantly greater change in tumor diameter compared to the sham arm (p=0.04). Similarly, higher distant tumor proliferation was observed after hepatic MWA-5W and RFA, followed by MWA-20W compared to sham (proliferative indices: MWA-5W 0.82±0.05, RFA 0.79±0.05, MWA-20W 0.65±0.02 vs. sham 0.49±0.05, p<0.01). Finally, lower-energy hepatic MWA and RFA resulted in greater periablational inflammation (Hsp70: RFA 141.5 μ m (mean), MWA-5W 134.1 μ m, vs. MWA-20W (349±22 pg/mL, p<0.01) with a trend for elevation in IL-6 levels for RFA (542±61 pg/ml) and MWA-5W (486±101 pg/ml), vs. MWA-20W (349±22 pg/mL, p<0.08).

CONCLUSION

Hepatic MW ablation can incite periablational inflammation and increased distant tumor growth similar to what has been recently reported for RFA. Yet, such undesired effects may be dependent on heating paradigms, and less pronounced with more rapid, higher power heating.

CLINICAL RELEVANCE/APPLICATION

MWA and RFA can have 'off-target' tumor stimulatory effects, which may be decreased using higher MW energy to reduce secondary inflammation in the tissue surrounding the ablation zone.

VSI041-09 Systemic Implications of IO Therapies: Increased Tumorigenesis?

Wednesday, Dec. 2 3:10PM - 3:25PM Location: S405AB

Participants

Muneeb Ahmed, MD, Wellesley, MA, (mahmed@bidmc.harvard.edu) (Presenter) Nothing to Disclose

LEARNING OBJECTIVES

View learning objectives under main course title.

VSI041-10 Systemic Implications of IO Therapies: Beneficial Immune Effects?

Wednesday, Dec. 2 3:25PM - 3:40PM Location: S405AB

Participants

Joseph P. Erinjeri, MD, PhD, New York, NY, (erinjerj@mskcc.org) (Presenter) Nothing to Disclose

LEARNING OBJECTIVES

View learning objectives under main course title.

VSI041-11 Panel Discussion: So What Does This All Mean?

Wednesday, Dec. 2 3:40PM - 3:55PM Location: S405AB

Participants

LEARNING OBJECTIVES

View learning objectives under main course title.

VSI041-12 20 Years of Thermal Ablation: Progress, Challenges and Opportunities

Wednesday, Dec. 2 4:00PM - 4:25PM Location: S405AB

Participants

Stephen B. Solomon, MD, New York, NY (Presenter) Research Grant, General Electric Company

LEARNING OBJECTIVES

View learning objectives under main course title.

VSI041-13 Advancing IO with Cutting-edge Imaging Techniques

Participants

LEARNING OBJECTIVES

View learning objectives under main course title.

VSI041-14 Advanced Ultrasound and Fusion Techniques

Wednesday, Dec. 2 4:25PM - 4:40PM Location: S405AB

Participants

Luigi Solbiati, MD, Busto Arsizio, Italy, (lusolbia@tin.it) (Presenter) Nothing to Disclose

LEARNING OBJECTIVES

View learning objectives under main course title.

VSI041-15 State-of-the-Art Angiographic Imaging: Cone Beam CT and beyond

Wednesday, Dec. 2 4:40PM - 4:55PM Location: S405AB

Participants

Ming De Lin, PhD, Cambridge, MA (Presenter) Employee, Koninklijke Philips NV

LEARNING OBJECTIVES

1) Discuss the role of cone-beam computed tomography (CBCT) for intraprocedural imaging during transcatheter arterial chemoembolization (TACE). 2) Explain the advantages of CBCT over standard 2D angiography in the detection of hepatocellular carcinoma lesions and their feeding arteries. 3) Describe how CBCT during TACE can be used to assess the technical endpoint of embolization. 4) Demonstrate how to choose a CBCT technique using a decision-making algorithm to optimize the use of CBCT at each step of TACE for the identification of the lesion, guidance to reach the lesion, and assessment of embolization end points.

ABSTRACT

Cone-beam computed tomography (CBCT) is an imaging technique that provides 3D imaging intraprocedurally from a rotational scan acquired with a C-arm equipped with a flat panel detector. Utilizing CBCT images during interventional procedures bridges the gap between the world of diagnostic imaging, where the image acquisition is typically performed separately from the procedure, and that of interventional radiology, which traditionally has been 2-dimensional (fluoroscopy and angiography). In the scope of transcatheter arterial chemoembolization (TACE), CBCT is capable of providing more information than standard two-dimensional imaging alone in localizing and/or visualizing liver tumors ("seeing" the tumor) and targeting tumors though precise microcatheter placement in close proximity to the tumors ("reaching" the tumor). It can also be useful in evaluating treatment success at the time of procedure ("assessing" treatment success).

VSIO41-16 Contrast Patterns on Intra-procedural Cone-beam CT Can Predict Early Tumor Response to DEB-TACE in Patients with Hepatocellular Carcinoma

Wednesday, Dec. 2 4:55PM - 5:05PM Location: S405AB

Participants

Sonia P. Sahu, New Haven, CT (*Presenter*) Nothing to Disclose Ruediger E. Schernthaner, MD, Vienna, Austria (*Abstract Co-Author*) Nothing to Disclose Yan Zhao, MS, Baltimore, MD (*Abstract Co-Author*) Nothing to Disclose Jae Ho Sohn, MD,MS, New Haven, CT (*Abstract Co-Author*) Nothing to Disclose Florian N. Fleckenstein, MS, New Haven, CT (*Abstract Co-Author*) Nothing to Disclose Alessandro G. Radaelli, PHD, MS, Best, Netherlands (*Abstract Co-Author*) Employee, Koninklijke Philips NV Martijn Van Der Bom, MSC, Andover, MA (*Abstract Co-Author*) Employee, Koninklijke Philips NV Rafael Duran, MD, Baltimore, MD (*Abstract Co-Author*) Nothing to Disclose Ming De Lin, PhD, Cambridge, MA (*Abstract Co-Author*) Employee, Koninklijke Philips NV Jean-Francois H. Geschwind, MD, Westport, CT (*Abstract Co-Author*) Researcher, BTG International Ltd; Consultant, BTG International Ltd; Researcher, Koninklijke Philips NV; Consultant, Koninklijke Philips NV; Researcher, Guerbet SA; Consultant, Guerbet SA; Consultant, Terumo Corporation; Consultant, Threshold Pharmaceuticals, Inc; Consultant, PreScience Labs, LLC; Researcher, Boston Scientific Corporation; Consultant, Boston Scientific Corporation

PURPOSE

Cone-beam CT (CBCT) is routinely utilized to determine the optimal location for drug delivery and technical success of embolization during drug-eluting beads transarterial chemoembolization (DEB-TACE). As such, the relationship between intraprocedural CBCT findings and therapy response should be investigated. This study examined whether quantified contrast patterns on intraprocedural CBCT could predict tumor response on 1 month follow-up magnetic resonance (MR) imaging in hepatocellular carcinoma (HCC) patients treated with DEB-TACE.

METHOD AND MATERIALS

This retrospective study included 53 lesions in 49 patients (38 men, median age 62.7 years) who underwent DEB-TACE. All patients had a contrast-enhanced CBCT image taken immediately before and an unenhanced CBCT image taken immediately after drug delivery. However, enhancement was seen on the post-TACE CBCT due to retained contrast medium from drug delivery. MR imaging was performed at baseline and 1 month follow-up. On the CBCT images, enhancement of the target lesions was measured in 1 dimension (D), 2D, and 3D. On follow-up MR, patients were classified as responders or non-responders using mRECIST, EASL, and quantitative EASL (qEASL). qEASL defines response as $a \ge 65\%$ decrease in 3D enhancement. To assess whether contrast patterns on CBCT could predict 1 month MR response, uni- and multivariate logistic regressions. Baseline characteristics significant in univariate analysis were included in the multivariate model.

RESULTS

On pre- and post-TACE CBCT, median 1D, 2D, and 3D tumor enhancement was 3.4 vs 3.6 cm (p=0.5), 9.9 vs 10.4 cm2 (p=0.7), and 60.7 vs 73.0 % (p=0.4). Response was seen in 34% (mRECIST) and 38% (EASL and qEASL) of lesions. Neither 1D nor 2D enhancement on CBCT could predict mRECIST or EASL response, respectively. However, 3D enhancement was predictive of qEASL response in univariate (pre-TACE CBCT: OR 1.07, 95% CI 1.03-1.11; post-TACE CBCT: OR 1.10, 95% CI 1.5-1.16) and multivariate analysis adjusted for age, hepatitis C, and tumor size (pre-TACE CBCT: OR 1.06, 95% CI 1.02-1.10; post-TACE CBCT: OR 1.09, 95% CI 1.03-1.15).

CONCLUSION

3D enhancement on intraprocedural CBCT can predict 3D tumor response on MR in HCC patients treated with DEB-TACE.

CLINICAL RELEVANCE/APPLICATION

CBCT contrast patterns during DEB-TACE are associated with future tumor response and therefore should guide intraprocedural decisions.

VSIO41-17 Tailoring MR for IO

Wednesday, Dec. 2 5:05PM - 5:20PM Location: S405AB

Participants

Philippe L. Pereira, MD, Heilbronn, Germany (*Presenter*) Research Consultant, Terumo Corporation; Speaker, AngioDynamics, Inc; Speaker, BSD Medical Corporation; Speaker, Terumo Corporation; Speaker, CeloNova BioSciences, Inc; Speaker, Medtronic, Inc; Speaker, BTG International Ltd; Speaker, Biocompatibles International plc; Advisory Board, Siemens AG; Advisory Board, Terumo Corporation; Advisory Board, Bayer AG; Advisory Board, BTG International Ltd; Advisory Board, Medtronic, Inc; Support, Bracco Group; Support, PharmaCept GmbH; Support, Terumo Corporation; Support, Siemens AG; Support, Novartis AG; Support, GlaxoSmithKline plc; Consultant, CeloNova BioSciences, Inc; Research Grant, BTG International plc; Research Grant, Siemens AG; Research Grant, Terumo Corporation; Research Grant, BTG International Ltd

LEARNING OBJECTIVES

View learning objectives under main course title.

ABSTRACT

Image guided tumor ablation is a minimally invasive therapy option in the treatment of primary and secondary hepatic malignancies. Magnetic resonance (MR) imaging offers an accurate pre-interventional imaging having important impact on patient selection and planning of the ablation procedure. Peri-interventional imaging is used for targeting, monitoring, and controlling of the ablation procedure. Due to a high soft-tissue contrast offering delineation of tumor tissue and the surrounding anatomy, coupled with multiplanar capabilities, MR imaging is an advantageous targeting technique compared with ultrasonography (US) or computed tomography (CT). Furthermore, a near-online imaging is feasible at interventional MR units facilitating a fast and precise placement of the probe inside the target tissue. MR imaging is sensitive to thermal effects enabling a monitoring of ablation therapy. At low-field, MR scanner T2 weighted sequences are accurate to near-online monitor acute effects of thermally induced coagulation subsequently being supportive to control the ablation procedure. Therefore, MR imaging can fulfil the conditions for overlapping ablations by enabling a precise repositioning of the MR compatible thermal applicator if required. MR imaging can be utilized to define the end point of thermal ablation after complete coverage of the target tissue is verified. Thus, the probability of achieving complete coagulation in larger tumors within a single therapy session is supposedly increased. A monitoring of the target tissue. Subsequently, the possibility to monitor and control thermal ablation by MR imaging has an important impact on the safety and effectiveness of the ablation procedure. At least, first use of MR compatible microwave antennas will be presented in this refresher.

VSI041-18 3D Quantitative Tumor Burden Analysis in Patients with Hepatocellular Carcinoma before TACE: Comparing Multi-lesion vs. Single-lesion Imaging Biomarkers as Predictors of Patient Survival

Wednesday, Dec. 2 5:20PM - 5:30PM Location: S405AB

Participants

Florian N. Fleckenstein, MS, New Haven, CT (*Presenter*) Nothing to Disclose
Rafael Duran, MD, Baltimore, MD (*Abstract Co-Author*) Nothing to Disclose
Ruediger E. Schernthaner, MD, Vienna, Austria (*Abstract Co-Author*) Nothing to Disclose
Jae Ho Sohn, MD,MS, New Haven, CT (*Abstract Co-Author*) Nothing to Disclose
Sonia P. Sahu, New Haven, CT (*Abstract Co-Author*) Nothing to Disclose
Yan Zhao, MS, Baltimore, MD (*Abstract Co-Author*) Nothing to Disclose
Bernhard Gebauer, MD, Berlin, Germany (*Abstract Co-Author*) Research Consultant, C. R. Bard, Inc; Research Consultant, Sirtex

Medical Ltd; Research Grant, C. R. Bard, Inc; Research Consultant, PAREXEL International Corporation;

Bernd K. Hamm III, MD, Berlin, Germany (*Abstract Co-Author*) Research Consultant, Toshiba Corporation; Stockholder, Siemens AG; Stockholder, General Electric Company; Research Grant, Toshiba Corporation; Research Grant, Koninklijke Philips NV; Research Grant, Siemens AG; Research Grant, General Electric Company; Research Grant, Elbit Imaging Ltd; Research Grant, Bayer AG; Research Grant, Guerbet SA; Research Grant, Bracco Group; Research Grant, B. Braun Melsungen AG; Research Grant, KRAUTH medical KG; Research Grant, Boston Scientific Corporation; Equipment support, Elbit Imaging Ltd; Investigator, CMC Contrast AB Roberto Ardon, Suresnes Cedex, France (*Abstract Co-Author*) Employee, Koninklijke Philips NV

Ming De Lin, PhD, Cambridge, MA (*Abstract Co-Author*) Employee, Koninklijke Philips NV Julius Chapiro, MD, Berlin, Germany (*Abstract Co-Author*) Nothing to Disclose

Jean-Francois H. Geschwind, MD, Westport, CT (*Abstract Co-Author*) Researcher, BTG International Ltd; Consultant, BTG International Ltd; Researcher, Koninklijke Philips NV; Consultant, Koninklijke Philips NV; Researcher, Guerbet SA; Consultant, Guerbet SA; Consultant, Terumo Corporation; Consultant, Threshold Pharmaceuticals, Inc; Consultant, PreScience Labs, LLC; Researcher, Boston Scientific Corporation; Consultant, Boston Scientific Corporation

PURPOSE

This study compared the value of multi-lesion vs. single-lesion assessment for the prediction of overall survival (OS) in patients with hepatocellular carcinoma (HCC) before transarterial chemoembolization (TACE) using 3D quantitative and diameter-based tumor burden analysis.

METHOD AND MATERIALS

122 patients with HCC treated with TACE were retrospectively included. Baseline arterial-phase, contrast-enhanced MRI was used to measure overall and enhancing diameters in a total of 296 HCC lesions. A 3D segmentation analysis was performed to assess total liver volumes and to quantify enhancing tumor volume (ETV) for each lesion. Enhancing tumor burden (ETB) was defined as the ratio between total ETV and total liver volume. Patients were stratified into high and low tumor burden groups following the BCLC staging (5cm for unifocal HCC and 3cm for 3 lesions for multifocal HCC; accordingly 65cm3 and 45cm3 were used for 3D cutoffs). A threshold of 4%, based on the ROC curve, was used for ETB. Survival was assessed using Kaplan-Meier analysis as well as uni- and multivariate cox proportional hazard ratios (HR). Concordances of each assessment technique were calculated and the method with the highest correlation was further evaluated in order to identify the ideal number of lesions needed for an accurate prediction of OS.

RESULTS

A significant separation of the survival curves was achieved for all methods (log rank, p<0.05). Multivariate analysis, according to 3D methods showed the highest predictivity of OS as compared to 1D techniques (HR 5.2 [95%CI, 3.1-8.8, p<0.001] for ETV and HR 6.6 [95%CI, 3.7-11.5, p<0.001] for ETB vs. HR 2.6 [95%CI, 1.2-5.6, p=0.012] for overall diameter and HR 3.0 [95%CI, 1.5-6.3, p=0.003] for enhancing diameter). Concordances were found to be the highest for ETB. The difference between ETB concordances of all (0.782) and single largest lesion (0.759) was below two-times the standard error (0.038).

CONCLUSION

3D quantitative assessment of enhancing tumor burden as represented by the largest HCC lesion is a stronger predictor of OS as compared to diameter-based measurements. Assessing multiple lesions on baseline imaging provides no added accuracy in predicting patient OS.

CLINICAL RELEVANCE/APPLICATION

3D volumetric analysis of the largest lesion is a strong predictor of OS and superior to 1D diameter-based methods used in current staging systems. Hence, 3D methods should be considered for future staging systems.

VSI041-19 Interventional PET/CT

Wednesday, Dec. 2 5:30PM - 5:45PM Location: S405AB

Participants

Paul B. Shyn, MD, Boston, MA, (pshyn@bwh.harvard.edu) (Presenter) Nothing to Disclose

LEARNING OBJECTIVES

1) Compare advantages of PET/CT with other imaging modalities in guiding interventional radiology procedures. 2) Describe strategies to improve lesion targeting during PET/CT interventional procedures. 3) Apply various PET/CT imaging techniques for the intraprocedural assessment of tumor ablation margins.

ABSTRACT

Positron Emission Tomography/Computed Tomography (PET/CT) enhances our capabilities in image-guided interventions in multiple ways. PET/CT enables targeting of disease foci not visible using other imaging modalities, provides uninterrupted visibility of targets despite intraprocedural changes in surrounding tissues or thermal effects of ablation, and facilitates unique intraprocedural strategies for assessing tumor ablation results. Many case examples will be shown that highlight rationales, strategies and emerging techniques for successful PET/CT-guided interventions.

VSIO41-20 Molecular Imaging

Wednesday, Dec. 2 5:45PM - 6:00PM Location: S405AB

Participants

Bradford J. Wood, MD, Bethesda, MD (*Presenter*) Researcher, Koninklijke Philips NV Researcher, Celsion Corporation Researcher, BTG International Ltd Researcher, W. L. Gore & Associates, Inc Researcher, Delcath Systems, Inc Pending research funded, Perfint Healthcare Pvt Ltd Patent agreement, VitalDyne, Inc Intellectual property, Koninklijke Philips NV Intellectual property, BTG International Ltd

LEARNING OBJECTIVES

View learning objectives under main course title.

Hospital Administrator's Symposium

Wednesday, Dec. 2 1:30PM - 4:50PM Location: S103AB



AMA PRA Category 1 Credits ™: 3.25 ARRT Category A+ Credits: 4.00

Participants

Jonathan W. Berlin, MD, Evanston, IL (Moderator) Nothing to Disclose

LEARNING OBJECTIVES

1) Describe possible future health payment and delivery changes and their relationship to radiology. 2) Consider practical techniques for leading change in radiology. 3) Understand methods of radiology data analysis that may be helpful to a hospital. 4) Consider how the principles of high reliability can improve radiology quality. 5) Contemplate the benefits of radiology integration in the era of population health. 6) Familiarize themselves with the 2017 CMS mandate for decision support regarding advanced imaging.

ABSTRACT

This program is geared toward physicians, non-physician healthcare providers, and administrators. Vendors will also find it helpful. The session will be comprised of six speakers, each speaking for 30 minutes. There are two scheduled question and answer periods with ample opportunity for audience discussion if desired. Speakers are a mix of physicians and administrators, and topics are designed to address current strategic planning and economic issues pertinent to radiology, including leadership, the levaging of big data, radiology quality, future healthcare payment and delivery, radiology integration and population health management, and the 2017 CMS mandate for pre-order decision support.

URL

Sub-Events

SPHA41A Introduction

Participants Jonathan W. Berlin, MD, Evanston, IL (*Presenter*) Nothing to Disclose

LEARNING OBJECTIVES

View learning objectives under main course title.

SPHA41B How Your Radiology Group's Big Data can Leverage Your Hospital's Success

Participants

T. Scott Law, Carmel, IN (Presenter) Founder, Zotec Partners; CEO, Zotec Partners

LEARNING OBJECTIVES

View learning objectives under main course title.

SPHA41C Practical Techniques for Leading Change in Radiology

Participants Frank J. Lexa, MD, Philadelphia, PA (*Presenter*) Nothing to Disclose

LEARNING OBJECTIVES

View learning objectives under main course title.

SPHA41D Healthcare Economics: Market Trends and Transformation

Participants Tom E. Szostak, Tustin, CA (*Presenter*) Employee, Toshiba Corporation

LEARNING OBJECTIVES

View learning objectives under main course title.

ABSTRACT

URL

SPHA41E Question and Answer 1

Participants T. Scott Law, Carmel, IN (*Presenter*) Founder, Zotec Partners; CEO, Zotec Partners Frank J. Lexa, MD, Philadelphia, PA (*Presenter*) Nothing to Disclose

LEARNING OBJECTIVES

View learning objectives under main course title.

SPHA41F Radiology Integration: How and Why in the Era of Population Health Management

Participants John P. Anastos, DO, Park Ridge, IL (*Presenter*) Nothing to Disclose

LEARNING OBJECTIVES

View learning objectives under main course title.

SPHA41G The 2017 Mandate for Pre-order Decision Support: What Does It Mean and Why Is It Significant?

Participants

Mark D. Hiatt, MD, MBA, Salt Lake City, UT, (mark.hiatt@regence.com) (*Presenter*) Medical Director, Regence BlueCross BlueShield; Board Member, RadSite ; Former Officer, HealthHelp, LLC

LEARNING OBJECTIVES

View learning objectives under main course title.

ABSTRACT

View abstract under main course title.

SPHA41H Question and Answer 2

Participants

John P. Anastos, DO, Park Ridge, IL (*Presenter*) Nothing to Disclose Mark D. Hiatt, MD, MBA, Salt Lake City, UT, (mark.hiatt@regence.com) (*Presenter*) Medical Director, Regence BlueCross BlueShield; Board Member, RadSite ; Former Officer, HealthHelp, LLC

LEARNING OBJECTIVES

View learning objectives under main course title.

Essentials of Pediatric Imaging

Wednesday, Dec. 2 1:30PM - 3:00PM Location: S100AB

CH ER PD

AMA PRA Category 1 Credits ™: 1.50 ARRT Category A+ Credits: 1.50

Participants

Sub-Events

MSES43A Traumatic Hemorrhage within the Extra-axial Spaces: Accidental or Inflicted?

Participants

Gary L. Hedlund, DO, Salt Lake City, UT, (gary.hedlund@imail.org) (Presenter) Nothing to Disclose

LEARNING OBJECTIVES

1) Contrast the differences between pediatric and adult epidural intracranial hemorrhages. 2) Develop an expanded understanding of traumatic pediatric subdural hemorrhage. 3) Identify the clinical significance and imaging characteristics of subdural hygroma. 4) Describe the CT and MRI features of subdural hemorrhage arising from abusive and accidental trauma. 5) Identify pediatric subarachnoid hemorrhage, recognize its significance, and differentiate it from pseudo-subarachnoid hemorrhage.

ABSTRACT

The presence of post-traumatic hemorrhage within the pediatric intracranial extra-axial compartments should be viewed as a proxy for underlying brain injury. This live RSNA activity will review the coverings of the brain and the compartments that may be involved in accumulating post-traumatic hemorrhage. The session will address hemorrhage within the epidural space, subdural compartment, and subarachnoid space. The focus will be upon hemorrhages within the subdural compartment, their clinical significance in the pediatric population, origin, imaging characteristics, and the features of subdural hemorrhage more commonly observed with accidental and inflicted head trauma. The complimentary nature of non-enhanced CT (NECT) and MRI in characterizing and estimating age of the pediatric subdural hemorrhage will be emphasized. The value of serial imaging will be discussed.

MSES43B Imaging of Congenital Chest Abnormalities

Participants

Stephanie P. Ryan, MD, Dublin, Ireland (Presenter) Nothing to Disclose

LEARNING OBJECTIVES

1) Interpret chest radiographs in newborns with congenital pulmonary abnormality. 2) Plan further imaging assessment in the newborn with congenital pulmonary abnormality. 3) Recognise imaging findings and plan further imaging investigation in an older child with congenital pulmonary abnormality.

ABSTRACT

This session will address the radiographic findings and further imaging in congenital chest abnormalities including cystic adenomatoid malformation, congenital lobar emphysema and different forms of sequestration. The imaging findings of tracheo-esophageal fistula, of chylothorax and of different types of diaphragmatic hernia will also be addressed. There will be an emphasis on the imaging findings that affect management and some controversies around imaging and management will be reviewed.

MSES43C Ventral Wall Abnormalities in the Neonate

Participants

Henry J. Baskin JR, MD, Salt Lake Cty, UT (Presenter) Nothing to Disclose

LEARNING OBJECTIVES

1) Describe the most common ventral wall abnormalities in neonates, including omphalocele, gastroschisis, bladder exstrophy, and prune-belly syndrome. 2) Compare and contrast the clinical characteristics of these defects. 3) Identify the imaging features of each of these ventral wall abnormalities. 4) Understand the treatment of these defects, and be familiar with their imaging implications in older children.

ABSTRACT

Neonatal ventral wall abnormalities encompass a broad group of rare congenital defects such as omphalocele, gastroschisis, bladder exstrophy, and prune-belly syndrome. Although these congenital abnormalities are varied in terms of pathophysiology, clinical findings, and treatment, their similarities allow them to be easily confused by radiologists. This is especially problematic as children with ventral wall abnormalities have very high rates of associated gastrointestinal, musculoskeletal, urogenital, and cardiovascular problems, and so often require fairly extensive medical imaging expertise. This activity will compare and contrast the clinical characteristics of ventral wall abnormalities, illustrate the important imaging features of each, and familiarize the attendee with how these abnormalities are treated. ASRT@RSNA 2015: Interventional Cardiovascular MRI (iCMR): Clinical and Pre-Clinical Applications

Wednesday, Dec. 2 2:20PM - 3:20PM Location: N230



AMA PRA Category 1 Credit ™: 1.00 ARRT Category A+ Credit: 1.00

Participants

Jonathan Mazal, MS, RRA, Bethesda, MD (*Presenter*) Nothing to Disclose Toby Rogers, BA, MRCP, Bethesda, MD (*Presenter*) Nothing to Disclose

LEARNING OBJECTIVES

1) Define interventional cardiovascular magnetic resonance (iCMR). 2) Compare advantages and disadvantages of MRI versus other imaging modalities to guide cardiovascular interventions. 3) Describe personnel and infrastructure requirements to start an iCMR program. 4) Identify current clinical applications of iCMR. 5) Review pre-clinical applications of iCMR to inform future clinical directions.

RCA44

National Library of Medicine: PubMed Tools: Save Searches and Create Personalized Search Options (Handson)

Wednesday, Dec. 2 2:30PM - 4:00PM Location: S401AB

IN

AMA PRA Category 1 Credits ™: 1.50 ARRT Category A+ Credits: 1.50

Participants

Tina Griffin, Chicago, IL (*Presenter*) Nothing to Disclose Holly Ann Burt, MLIS, Chicago, IL (*Presenter*) Nothing to Disclose

LEARNING OBJECTIVES

1) Personalize PubMed by saving search strategies and creating email alerts. 2) Use My NCBI filters to link to library full-text articles and to focus PubMed searches. 3) Save collections of citations including a personal bibliography.

ABSTRACT

In this hands-on workshop session, explore the free My NCBI tool in PubMed. Discover how to develop and save search strategies, create email alerts on your research topics, and build permanent online bibliographies. With your My NCBI account, add permanent library filters and evidence-based filters to PubMed, use My Bibliography to create an online list of personal publications, limit searches to high impact journals, and utilize the link between the NIH Manuscript Submission System and PubMed. The National Library of Medicine (NLM) provides free web access to nearly 25 million citations for biomedical and clinical medical articles through PubMed.gov; MEDLINE is a subset of PubMed.

Handout:Holly Ann Burt

http://abstract.rsna.org/uploads/2015/15004107/2015myncbiRSNA.pdf

Monitoring Radiation Exposure: Standards, Tools and IHE REM

Wednesday, Dec. 2 2:30PM - 4:00PM Location: S501ABC



AMA PRA Category 1 Credits ™: 1.50 ARRT Category A+ Credits: 1.50

Participants

Kevin O'Donnell, Vernon Hills, IL (*Moderator*) Employee, Toshiba Corporation; Kevin O'Donnell, Vernon Hills, IL (*Presenter*) Employee, Toshiba Corporation;

Michael F. McNitt-Gray, PhD, Los Angeles, CA (Presenter) Institutional research agreement, Siemens AG; Research support, Siemens AG; ; ; ;

William W. Boonn, MD, Penn Valley, PA, (wboonn@gmail.com) (Presenter) Founder, Montage Healthcare Solutions, Inc; President, Montage Healthcare Solutions, Inc; Shareholder, Montage Healthcare Solutions, Inc; Shareholder, Nuance Communications, Inc; Shareholder, Merge Healthcare Incorporated

LEARNING OBJECTIVES

1) Learn about key radiation exposure metrics, such as CTDI, and how to interpret them. 2) Learn about radiation exposure monitoring methods and tools including 2a) Capturing dose information with the DICOM Radiation Dose SR (RDSR) standard. 2b) Managing RDSR objects with the IHE Radiation Exposure Monitoring (REM) Profile. 2c) Integrating 'CT dose screens' from legacy systems into RDSR. 2d) Pre-scan dose pop-ups on the CT console defined by the MITA Dose Check standard and AAPM guidance on their use. 3) Learn how to specify the above features when purchasing and integrating Radiology Systems. 9) Learn about components of a dose management program such as protocol optimization. 4) Participation in the ACR Dose Registry, and reporting requirements such as California SB-1237.

Active Handout: Michael F. McNitt-Gray

http://abstract.rsna.org/uploads/2015/11034700/RCC44 RSNA2015_RCC44_Monitoring_Radiation_Dose_mmg_handout.pdf

Honored Educators

Presenters or authors on this event have been recognized as RSNA Honored Educators for participating in multiple qualifying educational activities. Honored Educators are invested in furthering the profession of radiology by delivering high-quality educational content in their field of study. Learn how you can become an honored educator by visiting the website at: https://www.rsna.org/Honored-Educator-Award/

William W. Boonn, MD - 2012 Honored Educator

Nuclear Medicine (Cardiovascular Imaging)

Wednesday, Dec. 2 3:00PM - 4:00PM Location: S505AB

CA CT NM

AMA PRA Category 1 Credit ™: 1.00 ARRT Category A+ Credit: 1.00

FDA Discussions may include off-label uses.

Participants

Charles M. Intenzo, MD, Philadelphia, PA (*Moderator*) Nothing to Disclose Andrew C. Homb, MD, Louisville, KY (*Moderator*) Nothing to Disclose

Sub-Events

SSM16-01 Anthropometric-based Radiopharmaceutical Dosing to Reduce Radiation in SPECT MPI: Initial Experience

Wednesday, Dec. 2 3:00PM - 3:10PM Location: S505AB

Participants

Jie Zhang, PhD, Lexington, KY (*Presenter*) Nothing to Disclose Vince Sorrell, MD, Lexington, KY (*Abstract Co-Author*) Nothing to Disclose Paul Anaya, Lexington, KY (*Abstract Co-Author*) Nothing to Disclose M. Elizabeth Oates, MD, Lexington, KY (*Abstract Co-Author*) Nothing to Disclose

PURPOSE

Myocardial perfusion imaging (MPI) using gated single photon emission computed tomography (SPECT) is a well-established approach to detect coronary artery disease and risk-stratify patients. For a typical 1-day rest/stress SPECT protocol, standard administered activities of Tc-99m sestamibi are 10 mCi (rest)/30 mCi (stress), resulting in a patient radiation dose of ~12 mSv.. The American Society of Nuclear Cardiology recommended decreasing radiation exposure to < 9 mSv in 50% of patients by 2014. To comply with this recommendation, we employed a new anthropometric-based dosage regimen.

METHOD AND MATERIALS

We investigated the relationship between administered Tc-99msestamibi activity, patient size, and image quality. Patients undergoing SPECT MPI were recruited over two consecutive weeks; measures of weight (kg), height (m), and chest circumference (cm) [ITS1] were recorded. Body Mass Index (BMI) was calculated (kg/m2). Image quality was evaluated by a board-certified nuclear radiologist and a nuclear cardiologist.

RESULTS

Thirty-one patients underwent 1-day rest/stress SPECT MPI. A convenient BMI-based 1-day rest/stress dosing regimen was developed through analyses of administered activity, patient size, and image quality. Administered activities were 6 mCi/18 mCi for BMI < 25 kg/m2, 7 mCi/21 mCi for BMI 25-30 kg/m2, 8 mCi/24 mCi for BMI30-35 kg/m2, and 10 mCi/30 mCi for BMI > 35 kg/m2. The patient radiation doses were 7.26 mSv, 8.47 mSv, 9.68 mSv and 12.10 mSv, respectively. Image quality met clinical diagnostic requirements. Scan time remained the same. With the proposed dosing regimen, radiation exposures in ~ 60% of 31 patients were < 9 mSv.

CONCLUSION

Using "older" gamma camera technology anthropometric-based dosing of Tc-99m sestamibi significantly reduces radiation exposure while maintaining diagnostic image quality.

CLINICAL RELEVANCE/APPLICATION

BMI-adjusted dosing of Tc-99m sestamibi for rest/stress SPECT MPI can significantly reduce patient radiation dose while maintaining image quality.

SSM16-02 Effect of Inflammatory Cardiac Sarcoidosis on Myocardial Blood Flow Assessed by PET/CT

Wednesday, Dec. 2 3:10PM - 3:20PM Location: S505AB

Participants

Matthew J. Kruse, MD, Baltimore, MD (*Presenter*) Nothing to Disclose Thomas H. Schindler, MD, Geneva, Switzerland (*Abstract Co-Author*) Nothing to Disclose

PURPOSE

Inflammatory cardiac sarcoidosis, as evidenced by FDG PET/CT imaging, confers an increased risk for sudden cardiac death and onset of heart failure. Dysfunction of the coronary circulation may represent a mechanistic link between inflammatory sarcoidosis activity and adverse outcomes. In this respect, we aimed to investigate effects of inflammatory cardiac sarcoidosis on coronary circulatory function.

METHOD AND MATERIALS

Individuals were 13 patients with biopsy-proven or clinical/imaging evidence of cardiac sarcoidosis undergoing baseline and followup cardiac PET/CT studies (31 total studies). Quantitative myocardial blood flow (MBF) was determined at rest and during pharmacologic vasodilation with N-13 ammonia or Rb-82 PET/CT, with calculation of myocardial flow reserve (MFR). Following a sarcoid diet protocol, FDG PET/CT was additionally performed to determine the presence of abnormal FDG uptake in the heart. Myocardial segmentation was performed using the 17-segment model. Maximum SUV and metabolic volume above previously published SUV thresholds was calculated.

RESULTS

Myocardial segments with abnormal FDG activity (n=122) demonstrated decreased MBF during vasodilation (1.96 +/- 0.86 ml/g/min vs. 2.13 +/- 0.84 ml/g/min; p=0.045, Mann-Whitney Test) and decreased MFR (2.40 +/- 0.81 vs. 2.75 +/- 1.05; p=0.002). Resting MBF was not significantly different (0.82 ml/g/min vs. 0.79 ml/g/min; p=0.305). Myocardial segments that developed abnormal FDG activity on follow-up study (n=47) demonstrated a greater decrease in MFR compared with segments that remained FDG-negative (n=200) (p=0.003). Segments that normalized on follow-up study (n=31) demonstrated decreased resting MBF compared with segments that remained FDG-positive (n=28) (p=0.013). Global MFR was not significantly correlated with maximum SUV, metabolic volumes, or clinical factors. BMI was weakly inversely correlated with both resting (Pearson r=-0.364, p=0.044) and vasodilation (r=-0.485, p=0.007) global MBF.

CONCLUSION

Myocardial segments involved with active sarcoidosis as evidenced by abnormal FDG activity demonstrate decreased vasodilation MBF and MFR, indicative of regional microvascular dysfunction that may reflect a basis for increased cardiovascular risk.

CLINICAL RELEVANCE/APPLICATION

Further studies are needed to determine if microvascular dysfunction detected by PET/CT perfusion quantitation may predict the risk of poor outcomes in cardiac sarcoidosis.

SSM16-03 The Influence of Myocardial Scar as Assessed by Myocardial Perfusion SPECT on the Development of Electrical Reverse Remodeling after Cardiac Resynchronization Therapy

Wednesday, Dec. 2 3:20PM - 3:30PM Location: S505AB

Participants Guang-Uei Hung, MD, Lugang, Taiwan (*Presenter*) Nothing to Disclose Ji Chen, Atlanta, GA (*Abstract Co-Author*) Nothing to Disclose

PURPOSE

Cardiac resynchronization therapy (CRT) can provide cardiac reverse remodeling (RR), which may include electrical (ERR: QRS duration shortened \geq 10 ms) and/or mechanical (MRR: ESV reduced \geq 15%) reverse remodeling. However, the pathophysiological mechanism is not clear. Myocardial perfusion SPECT (MPS) provided a comprehensive evaluation of LV perfusion, function and mechanical activation. The purpose of this was to explore the mechanism of RR with MPS.

METHOD AND MATERIALS

Forty-one patients (26 men, mean age 66±10 yrs) with heart failure received CRT for at least 12 months underwent resting MPS under transient CRT-off. The patients were divided into three groups according to their RR levels: group I: MRR+ERR, group II: MRR only and group III: non-responder. Emory cardiac toolbox was used for analysis of MPS to assess myocardial scar, LV volume, EF, dyssynchrony, activation sequence and contraction delay.

RESULTS

Between the three groups of patients, there were significant differences for scar burden ($15.9\pm9.5\%$, $26.8\pm16.1\%$ and $45.6\pm15.1\%$, for group I, II and III, respectively, p < 0.001), EDV ($136.6\pm64.9ml$, $221.6\pm123.9ml$ and $351.8\pm216.3ml$, p = 0.002), ESV ($82.6\pm59.8ml$, $172.3\pm117.2ml$ and $293.3\pm209.6ml$, p = 0.001), LVEF ($44.9\pm15.0\%$, $25.6\pm10.9\%$ and $21.5\pm11.7\%$, p < 0.001), systolic phase SD ($23.4\pm10.3^{\circ}$, $36.0\pm16.2^{\circ}$ and $57.0\pm22.2^{\circ}$, p < 0.001) and diastolic phase SD ($32.1\pm12.4^{\circ}$, $48.4\pm18.3^{\circ}$ and $64.7\pm22.5^{\circ}$, p < 0.001). As shown on the polar map of phase analysis (see attached figures), myocardial scar interfered with the normal propagation of mechanical activation and resulted in heterogeneous activation sequences. Compared to group II, group I had significantly less initiation points ($1.9 \pm 1.0 vs$. 2.6 ± 0.7 , p< 0.05) and smaller maximal contraction delay ($46.9 \pm 12.9^{\circ}vs$. $58.8 \pm 18.5^{\circ}$, p < 0.05).

CONCLUSION

The perfusion, function and mechanical activation parameters as assessed by MPS were significantly associated with different levels of RR. The volume of myocardial scar may play a critical role in the development of electrical RR.

CLINICAL RELEVANCE/APPLICATION

The comprehensive evaluation of myocardial substrates by myocardial perfusion SPECT disclosed the pathophysiological mechanisms of different reverse remodeling patterns post CRT.

SSM16-04 Development of a Novel Software for Calculating Myocardial Flow Reserve from Dynamic Kinetic Analysis Using a Cadmium-zinc-telluride (CZT) SPECT

Wednesday, Dec. 2 3:30PM - 3:40PM Location: S505AB

Participants

Masao Miyagawa, MD, PhD, Toon, Japan (*Presenter*) Nothing to Disclose Yoshiko Nishiyama, MD, Toon, Japan (*Abstract Co-Author*) Nothing to Disclose Rami Yokoyama, Toon, Japan (*Abstract Co-Author*) Nothing to Disclose Kana S. Ide, Toon, Japan (*Abstract Co-Author*) Nothing to Disclose Ryo Ogawa, MD, Toon, Japan (*Abstract Co-Author*) Nothing to Disclose Tomoyuki Kido, Toon, Japan (*Abstract Co-Author*) Nothing to Disclose Akira Kurata, PhD, Toon, Japan (*Abstract Co-Author*) Nothing to Disclose Teruhito Mochizuki, MD, Toon, Japan (*Abstract Co-Author*) Nothing to Disclose

PURPOSE

CZT camera enables fast acquisition of serial dynamic images during the first pass of flow agents. The aims are to develop a novel

software for calculating myocardial flow reserve (MFR) and validate the utility for screening patients (pts) with multi-vessel coronary artery disease (CAD).

METHOD AND MATERIALS

Dynamic myocardial perfusion imaging (MPI) starting with 30-s bolus of Tc-99m perfusion agents was performed during adenosine stress and at-rest using a CZT camera (DNM 530c). The interval between two imaging was 3 hours and a 30-s pre-scan count was subtracted from the dynamic data at-rest. We generated 200 3-D volumes integrating 3-s time frames in the course of 600-s. Routine summed MPI were also acquired thereafter. The software allows the automatic edge detection of volume of interest for the blood pool in the left ventricle and the myocardium. Global time activity curves were fitted to a 2-compartment kinetic model (2-com), a Patlak plot analysis (PPA), and a dose uptake ratio of MPI (DUR) with input function. K1 and K2 were calculated for the stress and rest images. MFR index was calculated as follows: MFR index=K1 stress/K1 at-rest. The validation study included 45 consecutive pts who underwent CZT SPECT and coronary angiography within 2 weeks. (25 males, 68±11 y).

RESULTS

There were 17 pts with multi-vessel CAD while 28 had 0 or 1-vessel CAD. In the multi-vessel group, global MFR estimated by 2-com was 1.12 ± 0.16 (Figure), which was significantly lower than 1.35 ± 0.15 for pts with 0 or 1-vessel CAD (p<0.0001). The area under the curve (AUC) by receiver operating characteristic (ROC) analysis was 0.85, 0.73, and 0.65 for 2-com, PPA, and DUR, respectively. Using a cut-off value of 1.3, the sensitivity was 94% and specificity was 64% for diagnosing multi-vessel CAD. Moreover, multivariate analysis reveals that the global MFR by 2-com was an independent predictor of multi-vessel CAD among 11 clinical and MPI variables (chi-square: 5.46, p=0.02).

CONCLUSION

We developed and validated a novel software for calculating MFR from dynamic kinetic analysis using a CZT SPECT. It improves the detectability of multi-vessel CAD which causes globally decreased MFR and adds incremental diagnostic value to the standard MPI.

CLINICAL RELEVANCE/APPLICATION

Dynamic myocardial perfusion imaging with the 2-compartment analysis using the CZT SPECT enables us to estimate myocardial flow reserve and may improve the detectability of multi-vessel CAD.

SSM16-05 Physiologic Correlates of Rb-82 PET/CT Left Ventricular Mass: Volume Ratios

Wednesday, Dec. 2 3:40PM - 3:50PM Location: S505AB

Participants

Kenneth Nichols, PhD, New Hyde Park, NY (*Presenter*) Royalties, Syntermed, Inc; Andrew Van Tosh, MD, Roslyn, NY (*Abstract Co-Author*) Consultant, Pfizer Inc; Consultant, Bracco Group; Consultant, Cardinal Health, Inc; Consultant, Ion Beam Applications, SA Nathaniel Reichek, MD, Roslyn, NY (*Abstract Co-Author*) Nothing to Disclose Christopher J. Palestro, MD, New Hyde Park, NY (*Abstract Co-Author*) Nothing to Disclose

PURPOSE

MRI and echocardiography investigators have found that computing the ratio of left ventricular (LV) mass:volume, indexed to a pt's body size, is a useful means of characterizing ventricular remodeling, including aiding in predicting the likelihood of adverse cardiac events. We sought to identify the pathophysiologic mechanisms leading to abnormal M/Vi by examining whether LV myocardial blood flow (MBF) measured by Rb-82 PET/CT is also abnormal for pts with low Mi/Vi.

METHOD AND MATERIALS

We performed a retrospective investigation of data acquired for 194 pts who underwent rest/stress Rb-82 PET/CT imaging for suspected cardiac disease. LV mass indexed to body size (Mi) = $100 \cdot \text{resting mass}/(a \cdot \text{height}^{0.54} \cdot \text{weight}^{0.61})$, where a = 6.82 for women, 8.25 for men. LV end-diastolic volume indexed to body (Vi) = $100 \cdot \text{resting end-diastolic volume}/(b \cdot \text{height}^{1.25} \cdot \text{weight}^{0.43})$, where b = 10.0 for women, 10.5 for men. The normal range for Mi/Vi = 1.0-1.5. We compared ejection fraction (EF), myocardial blood flow (MBF), and coronary vascular resistance (CVR) against Mi/Vi. LV MBF and CVR were computed from the first pass transit of injected Rb-82 using a 2-compartment model, and volumes and EF values were computed from subsequent myocardial gated equilibrium data.

RESULTS

55 pts had Mi/Vi < 1.0 (mean 0.86±0.08) and 139 pts had Mi/Vi \geq 1.0 (mean 1.32±0.22). Compared to pts with Mi/Vi \geq 1.0, those with Mi/Vi < 1.0 had abnormally low rest values of EF (45±16% versus 60±15%, p<0.0001) and low MBF (0.58±0.25 versus 0.96±0.59 ml/g/min, p < 0.0001) and abnormally high CVR (182±71 versus 131±80 mm Hg/ml/g/min, p = 0.0001). Differences were even more pronounced at stress, with abnormally low values of EF (45±17% versus 65±14%, p<0.0001) and low MBF (1.06±0.61 versus 1.89 ± 0.96ml/g/min, p < 0.0001) and abnormally high CVR (107±49 versus 64±42 mm Hg/ml/g/min, p = 0.0001). For pts with Mi/Vi < 1.0, rest and stress MBF and EF were significantly lower, and CVR significantly higher, than published normal limits for these parameters.

CONCLUSION

Our results suggest that a finding of an abnormally low indexed mass-to-volume ratio in an individual is consistent with impaired myocardial blood flow, which hampers EF response to stress.

CLINICAL RELEVANCE/APPLICATION

A finding of low indexed mass-to-volume ratio should be followed up by more specific procedures such as coronary arteriography to assess more completely arterial status.

SSM16-06 F-18 FLT PET/CT Imaging for Diagnosis of Cardiac Sarcoidosis

Wednesday, Dec. 2 3:50PM - 4:00PM Location: S505AB

Takashi Norikane, Kita-gun, Japan (*Presenter*) Nothing to Disclose Yuka Yamamoto, MD, PhD, Kagawa, Japan (*Abstract Co-Author*) Nothing to Disclose Yukito Maeda, Kita-Gun, Japan (*Abstract Co-Author*) Nothing to Disclose Takahisa Noma, Kita-Gun, Japan (*Abstract Co-Author*) Nothing to Disclose Yoshihiro Nishiyama, MD, Kagawa, Japan (*Abstract Co-Author*) Nothing to Disclose

PURPOSE

2-deoxy-2-F-18 fluoro-D-glucose (FDG) positron emission tomography (PET) has been proposed to play a role in the diagnosis of cardiac sarcoidosis. However, assessing inflammatory lesions in cardiac sarcoidosis using FDG can be challenging because the FDG accumulates in normal myocardium. In contrast to FDG, 3'-deoxy-3'-F-18 fluorothymidine (FLT) uptake in normal myocardium is low. The purpose of this study was to investigate the feasibility of FLT PET/CT for the detection of cardiac sarcoidosis.

METHOD AND MATERIALS

Sixteen FLT PET/CT studies in 12 patients suspected of having cardiac sarcoidosis were performed. Six studies were performed before therapy and 10 studies were performed after immunosuppressive therapy. Fifty min after an intravenous injection of FLT, a 10-min emission scan of the heart was obtained. CT data for attenuation correction was obtained. Myocardial FLT uptake in cardiac sarcoidosis was defined as a "focal" or "focal on diffuse" pattern. In case of abnormal uptake, the maximal standardized uptake value (SUV) of lesions was measured. In case of no abnormal uptake, the mean SUV of myocardium was measured.

RESULTS

Five of 6 FLT studies before therapy showed a focal pattern of FLT uptake. Four of 10 FLT studies after therapy showed a focal pattern of FLT uptake. The mean (\pm SD) SUV after therapy (1.68 \pm 0.59) was significantly lower than that before therapy (3.02 \pm 0.90) (p<0.02).

CONCLUSION

These preliminary results indicate that FLT PET/CT might be a potentially useful tracer in the detection and therapy monitoring of cardiac sarcoidosis.

CLINICAL RELEVANCE/APPLICATION

FLT PET/CT might be a potentially useful tracer in the detection and therapy monitoring of cardiac sarcoidosis.

ISP: Health Service, Policy and Research (Medical/Practice Management)

Wednesday, Dec. 2 3:00PM - 4:00PM Location: S102D

MR HP SQ

AMA PRA Category 1 Credit [™]: 1.00 ARRT Category A+ Credit: 1.00

Participants

James V. Rawson, MD, Augusta, GA (*Moderator*) Nothing to Disclose Paul P. Cronin, MD, MS, Ann Arbor, MI (*Moderator*) Nothing to Disclose

Sub-Events

SSM12-01 Health Service, Policy and Research Keynote Speaker: Medical/Practice Management

Wednesday, Dec. 2 3:00PM - 3:10PM Location: S102D

Participants

James V. Rawson, MD, Augusta, GA (Presenter) Nothing to Disclose

SSM12-02 Using Modality Log Files to Guide MR Protocol Optimization and Improve Departmental Efficiency

Wednesday, Dec. 2 3:10PM - 3:20PM Location: S102D

Participants

Martin L. Gunn, MBChB, Seattle, WA (*Presenter*) Research support, Koninklijke Philips NV; Spouse, Consultant, Wolters Kluwer NV; Medical Advisor, TransformativeMed, Inc;

Bruce E. Lehnert, MD, Seattle, WA (Abstract Co-Author) Research support, Koninklijke Philips NV

Jeffrey H. Maki, MD, PhD, Seattle, WA (Abstract Co-Author) Research support, Bracco Group; Speakers Bureau, Lantheus Medical Imaging, Inc;

Christopher Hall, PhD, Briarcliff Manor, NY (Abstract Co-Author) Employee, Koninklijke Philips NV

Thomas Amthor, Hamburg, Germany (Abstract Co-Author) Employee, Koninklijke Philips NV

Julien Senegas, Hamburg, Germany (Abstract Co-Author) Employee, Koninklijke Philips NV

Norman J. Beauchamp JR, MD, Seattle, WA (Abstract Co-Author) Research Grant, Koninklijke Philips NV

PURPOSE

Imaging equipment log files contain detailed data about workflow and equipment utilization that is unavailable on RIS and PACS sources. The purpose of this study was to investigate the use of log files to identify areas of waste based on scanner time, variability and number of sequances, and measure the impact of a departmental MR efficiency process.

METHOD AND MATERIALS

Log files (MRLFs) were extracted from 4 MR scanners from 07/2013 to 02/2015 and were parsed to extract several parameters (e.g. protocol, sequences, exam duration, idle time, table movement). Using RIS data and MRLFs, we identified protocols with the greatest volume, duration and variation. Using MRLFs, we monitored system utilization of liver mass (MRLiv) and abdo/pelvis survey (MRAP) protocols pre and post protocol optimization. Optimization included assigning MRLiv patients with cirrhosis undergoing HCC screening to a new abbreviated protocol (MRLivCirr), and sequence reduction and optimization (MRAP). Statistical comparisons included a 2 tailed T-test and F-test.

RESULTS

Mean monthly MRLiv patient volume (+/- s.d.) was 55 ± 16 before and 20 ± 1 after optimization. The remaining 38 +/- 18 patients/month were for HCC screening and were assigned to the new MRLivCirr protocol. Mean monthly MRAP exams before was 20.6 ± 7.3 and after was 17.6 ± 2.3. Exam duration (table time ± s.d.) for MRLiv patients was 30.9 ± 9.3 min before and 31.4 ± 11.7 min after (p=0.7). However, for patients in the new MRLivCirr protocol group, mean time reduced by 7.2 min/exam to 23.7 ± 7.9 min(p<0.001). Duration for patients undergoing MRAP reduced from 52.9 ±16.6 min to 43.1± 15.6 min, saving 9.8 min/exam (p<0.001). At an estimated rate of \$650/hr, potential yearly savings could reach \$36k for cirrhosis screening, and \$22k for MRAP patients. The predictability of the exam length was improved with the s.d. of the MRLivCirr group (7.9 min) lower than the MRLiv group (11.7 min); F-Test, p<0.02.

CONCLUSION

MRLFs can be used to identify opportunities for equipment utilization improvement and measure the impact with accuracy. During our process we were able measure exact time savings and decreased variability per patient.

CLINICAL RELEVANCE/APPLICATION

Log files provide a way to measure modality utilization during image acquisition that are unavailable from RIS and PACS sources. They can be used to evaluate operational improvements in the department, potentially saving cost, and improving patient satisfaction.

SSM12-03 Comparison between Tumor Evaluation Using Free-text and RECIST 1.1 Criteria in Everyday Work

Wednesday, Dec. 2 3:20PM - 3:30PM Location: S102D

Participants Juliane Schelhorn, MD, Essen, Germany (*Abstract Co-Author*) Nothing to Disclose Julia Hoischen, Duesseldorf, Germany (*Abstract Co-Author*) Nothing to Disclose Haemi P. Schemuth, Essen, Germany (*Presenter*) Nothing to Disclose Elena Stenzel, Essen, Germany (*Abstract Co-Author*) Nothing to Disclose Felix Nensa, MD, Essen, Germany (*Abstract Co-Author*) Nothing to Disclose Kai Nassenstein, Essen, Germany (*Abstract Co-Author*) Nothing to Disclose

PURPOSE

Different criteria have been established to improve and standardize tumor response evaluation. Currently, these criteria are used in clinical trials, but are rarely employed in daily work. This retrospective study compared tumor response evaluation by free-text and RECIST 1.1 criteria in everyday tumor patients.

RESULTS

Main included tumor entities were lung (17%), colorectal (16%), and breast cancer (14%). Median time intervals between CT follow-ups were 9-12 weeks. At first follow-up, 51% of patients were rated with different response categories comparing free-text and RECIST 1.1. This was significant (p<0.001) with an obvious underrepresentation of SD and an overrepresentation of PR and PD in free-text evaluation. At second follow-up, 46% had categorical differences, which was significant (p<0.003). At the later follow-ups, categorical differences were obvious, but not significant (3. follow-up: 42% differences, p=0.570; 4. follow-up: 35%, p=0.824; 5. follow-up: 47%, p=0.209). The severity of categorical differences increased with increasing follow-up time (up to a difference of three response categories) due to different reference points used for image analysis.

CONCLUSION

Severe differences in tumor response evaluation were detected comparing evaluation by free-text and RECIST 1.1. Given this, tumor response criteria should be implemented in the daily routine.

CLINICAL RELEVANCE/APPLICATION

To improve routine tumor patient monitoring tumor response criteria should be used in everyday work.

SSM12-04 Implementing a Collaborative Approach to Imaging Utilization Managementat a Provider-Owned Managed Services Organization

Wednesday, Dec. 2 3:30PM - 3:40PM Location: S102D

Participants

Daniel Durand, MD, Baltimore, MD (*Presenter*) Stockholder, Evolent Health, LLC; Advisor, National Decision Support Company; Advisor, Radiology Response; Founder, am-I-ok.com

Criag Reich, MD, Oakland, CA (Abstract Co-Author) Nothing to Disclose

Jeffrey D. Robinson, MD, MBA, Seattle, WA (*Abstract Co-Author*) Consultant, HealthHelp, LLC; President, Clear Review, Inc; David B. Larson, MD, MBA, Los Altos, CA (*Abstract Co-Author*) Intellectual property license agreement, Bayer AG; Potential royalties, Bayer AG

Richard Sankary, MD, Oakland, CA (Abstract Co-Author) Nothing to Disclose

PURPOSE

While effective at controlling utilization, radiology benefit managers (RBMs) are disliked because they require ordering physicians to demonstrate medical necessity to an imaging gatekeeper who is not part of the community in which care occurs. Provider-owned health plans often utilize RBMs because their non-radiologist Medical Directors (MDs) are not imaging specialists. The purpose of our study was to demonstrate that radiologists can train local MDs to be effective stewards of imaging using collaborative techniques and produce results on par with RBMs but with fewer denials.

METHOD AND MATERIALS

A provider-owned Managed Services Organization (MSO) underwent an imaging utilization management (UM) process redesign. Prior to 2015, only PET/CTs and MRI exams ordered by primary care physicians were reviewed. After 1/1/15, all requests for CT, MRI, PET/CT, nuclear caradiology, and echocardiography were reviewed using Milliman Care Guidelines. The UM MD staff attended a daylong workshop led by two radiologists expert in collaborative imaging stewardship. The peer-to-peer process was rescripted to emphasize the risks of imaging (e.g. radiation) and suggesting alternative management plans (e.g. alternative imaging modalities) when appropriate. To assess the efficacy of the intervention, the MSO pre-authorization database was queried for the intervention period (Q1 2015) and a seasonally-matched baseline period (Q1 2014). The data elements extracted are shown in Figure 1. Impact rate was defined as the percentage of cases modified, withdrawn, or denied.

RESULTS

There was a significant increase in impact rate (0.4% vs. 4.6%, p=0.005) during the intervention period versus the control period. The number of requests modified or withdrawn by the ordering physician increased significantly (0.4% vs. 3.8%, p=0.01), while the number of requests denied by MDs was not significantly different (0.0% vs. 0.6%, p=0.51). Overall, the number of studies authorized per 1,000 patients declined significantly after the intervention (96.8 vs. 89.0, p=0.006).

CONCLUSION

Local MDs trained by radiologists can be effective stewards of imaging by using collaborative techniques that significantly reduce unnecessary imaging utilization without significantly increasing the use of denials.

CLINICAL RELEVANCE/APPLICATION

Radiologists can create significant value for health systems by training local MDs to be effective stewards of imaging UM using collaborative techniques.

Honored Educators

Presenters or authors on this event have been recognized as RSNA Honored Educators for participating in multiple qualifying educational activities. Honored Educators are invested in furthering the profession of radiology by delivering high-quality educational content in their field of study. Learn how you can become an honored educator by visiting the website at: https://www.rsna.org/Honored-Educator-Award/

SSM12-05 Has Use of Prostate Biopsy and Transrectal Ultrasound Declined as Concerns Mount about Overdiagnosis of Prostate Cancer?

Wednesday, Dec. 2 3:40PM - 3:50PM Location: S102D

Participants

David C. Levin, MD, Philadelphia, PA (*Presenter*) Consultant, HealthHelp, LLC; Board of Directors, Outpatient Imaging Affiliates, LLC Laurence Parker, PhD, Philadelphia, PA (*Abstract Co-Author*) Nothing to Disclose Ethan J. Halpern, MD, Philadelphia, PA (*Abstract Co-Author*) Nothing to Disclose Vijay M. Rao, MD, Philadelphia, PA (*Abstract Co-Author*) Nothing to Disclose

PURPOSE

In recent years there has been considerable debate about the issue of overdiagnosing prostate cancer (PCa). Since it is often an indolent disease and the potential harms from diagnosis and treatment are considerable, some have advocated a more conservative approach to conducting screening and diagnostic procedures. For example, the U.S. Preventive Services Task Force has issued a grade D recommendation against PSA-based screening. Our purpose was to study trends in the use of prostate biopsy (PB) and transrectal ultrasound (TRUS) over a recent 13-year period.

METHOD AND MATERIALS

The nationwide Medicare Part B Physician/Supplier Procedure Summary Master Files for 2001 through 2013 were used. They cover all Medicare fee-for-service beneficiaries (17.2 million males in 2013). CPT codes for PB and TRUS were selected and trends in procedure volume were evaluated. Utilization rates per 1000 males were calculated. Medicare specialty codes were used to identify the specialty of the physicians performing the procedures.

RESULTS

PB volume peaked in 2002, when a total of 292,045 were performed in Medicare patients. A generally downward trend then followed in subsequent years, reaching 165,382 in 2013 (-43%). The rate of PBs per 1000 male Medicare beneficiaries was 17.4 in 2002, decreasing to 9.6 in 2013. In that last year, urologists performed 87% of the biopsies, while radiologists performed 0.6%. Most of the rest were done in independent diagnostic testing facilities, in which the provider specialty could not be determined. TRUS volume peaked in 2006 at 318,518, then declined in subsequent years to 214,980 in 2013 (-33%). In that last year, urologists performed 4%. The remaining 6% were performed by physicians in various other specialties.

CONCLUSION

The use of both PB and TRUS has declined substantially in recent years. This appears to reflect a more conservative approach to screening for PCa, which in turn has resulted from the extensive debate about the risks, costs, and benefits of identifying and treating the disease.

CLINICAL RELEVANCE/APPLICATION

Physicians are now performing fewer procedures relating to prostate cancer diagnosis.

SSM12-06 Calmative Training of MR Imaging Support Staff Improving Study Completion Rates and Patient Show-Up Rates

Wednesday, Dec. 2 3:50PM - 4:00PM Location: S102D

Participants

Alexander M. Norbash, MD, Boston, MA (*Presenter*) Co-founder, Boston Imaging Core Laboratories, LLC;
William T. Yuh, MD, Seattle, WA (*Abstract Co-Author*) Nothing to Disclose
E. Kent Yucel, MD, Boston, MA (*Abstract Co-Author*) Nothing to Disclose
Elvira V. Lang, MD, Brookline, MA (*Abstract Co-Author*) Founder and President, Hypnalgesics, LLC;
Stephen Pauker, MD, Boston, MA (*Abstract Co-Author*) Nothing to Disclose
Amna A. Ajam, MBBS, Little Rock, AR (*Abstract Co-Author*) Nothing to Disclose
Gheorghe Doros, Boston, MA (*Abstract Co-Author*) Nothing to Disclose
Nina A. Mayr, MD, Seattle, WA (*Abstract Co-Author*) Nothing to Disclose

PURPOSE

The throughput efficiency of high cost imaging services such as Magnetic Resonance Imaging (MRI) has major impact to the financial status of the imaging service, particularly given decreasing overall diminishing healthcare margins. We evaluated whether a simple and inexpensive calmative training to the imaging staff team as a cost-effective way to improve the throughput and impact the financial bottom line.

METHOD AND MATERIALS

A total of 97,712 patient visits from 3 tertiary academic medical centers participated, including 49,733 visits during one-year period prior to the calmative training and 47,979 one-year after training. The center's MRI teams received calmative skill training with advanced communication and calmative techniques through onsite proctoring, and additional education using case-based simulations with scenarios requiring calmative interventions and utilizing electronic educational tools. The study's incompletion rate and patient no-show rate during-year intervals before and after training were compared using two-sided chi-square tests for proportions at a 0.05 significance level.

RESULTS

Despite variations in the patient population at the different sites with differing baseline no-show rates (ranged 5-19.4%) and study incompletion rates (ranged 0.8-6.9%) prior to training, the combined patients data showed significant (p<0.0001) improvement of patient throughput with calmative training. Based upon the one-year data intervals compared before and after training, no-show rates decreased from 11.2% to 8.7% and incompletion rates decreased from 2.3 to 1.4% for all show-up patients. Additonally, increasingly lengthy and complex studies such as cardiac, whole body, or combined imaging studies were performed without an increase in no-show or incompletion rates following calmative training.

CONCLUSION

The results suggest that calmative training of the imaging support staff can significantly improve the no-show and incompletion rates of the MRI service, thereby improving the throughput and utilization of high-value and expensive imaging modalities such as MRI which happens to have offputting physical features including noise and a constrained bore.

CLINICAL RELEVANCE/APPLICATION

Calmative training of supportive staff can significantly improve the no-show and incompletion rates of the MRI service, improving throughput and resource use without added capital budget investment.

ISP: Pediatrics (General and Neonatal Imaging)

Wednesday, Dec. 2 3:00PM - 4:00PM Location: S102AB

OB PD

AMA PRA Category 1 Credit ™: 1.00 ARRT Category A+ Credit: 1.00

Participants

Richard A. Barth, MD, Stanford, CA (*Moderator*) Nothing to Disclose Ellen M. Chung, MD, Bethesda, MD (*Moderator*) Nothing to Disclose

Sub-Events

SSM20-01 Biomodeling and 3D Printing for Simulation of Surgical Separation of Conjoint Twins

Wednesday, Dec. 2 3:00PM - 3:10PM Location: S102AB

Participants

Rajesh Krishnamurthy, MD, Houston, TX (*Presenter*) Research support, Koninklijke Philips NV; Research support, Toshiba Corporation Nicholas Dodd, Houston, TX (*Abstract Co-Author*) Nothing to Disclose Darrell Cass, Houston, TX (*Abstract Co-Author*) Nothing to Disclose Amrita Murali, Houston, TX (*Abstract Co-Author*) Nothing to Disclose Jayanthi Parthasarathy, Dallas, TX (*Abstract Co-Author*) Employee, VanDuzen, Inc

PURPOSE

We describe a unique use of biomodeling and 3D printing in the setting of surgical simulation of thoracoabdominal conjoint twin separation.

METHOD AND MATERIALS

Surgical planning on thoraco-omphalo-pyopagus female twins commenced at 7 months for planned separation at 10 months of life. The modeling process was initiated by a volumetric CT using a 320 detector scanner with target mode prospective EKG gating for the cardiovascular structures, and helical ungated acquisition for the chest, abdomen and pelvis. Intravenous contrast was separately administered into both twins, while oral contrast was administered only into 1 twin. Image segmentation yielded individual segments of the skin, skeleton, heart, lungs, airway, GI tract, abdominal vasculature, urinary tract, and gynecologic structures. In preparation for 3D printing, structures to support the models in a vertical position were created. In one operation, polyjet multi-material 3D printing was used to print skeletal structures, base and supports in hard plastic resin, and the organs in rubber like material. The livers were printed as separate pieces of the transparent resin, with the hepatic and portal vessels in white for better visibility. Pegs were designed so the liver could be attached or removed from the assembly. The models were designed such that they could be assembled together or separated during the surgical planning process. Findings on biomodels and 3-D print were compared to findings at surgical separation.

RESULTS

The twins underwent surgical separation by a multidisciplinary surgical team. No discrepancy was noted involving the cardiopulmonary, hepatic, intestinal, renal and skeletal anatomy. Preoperative simulation successfully predicted assignment of the pelvic viscera to each twin based on the vasculature. There was one hemorrhagic complication at surgery, unrelated to preoperative anatomical characterization.

CONCLUSION

We have demonstrated a unique use of 3D modeling and 3D printing for simulation and planning of conjoint twin separation, with representation of the surgically relevant viscera and vasculature in a single 3D printed model.

CLINICAL RELEVANCE/APPLICATION

Describe a novel application of 3D printing for simulating conjoint twin separation, which involves representation of all surgically relevant visceral and vascular anatomy in a single 3D print.

SSM20-02 Estimates of Diagnostic Reference Levels for Common Pediatric Fluoroscopic Procedures

```
Wednesday, Dec. 2 3:10PM - 3:20PM Location: S102AB
```

Participants

Keith J. Strauss, FAAPM, FACR, Cincinnati, OH (*Presenter*) Research Consultant, Koninklijke Philips NV; Speakers Bureau, Koninklijke Philips NV

Rami Nachabe, PhD, Best, Netherlands (*Abstract Co-Author*) Employee, Koninklijke Philips NV Steven J. Kraus, MD, Cincinnati, OH (*Abstract Co-Author*) Nothing to Disclose

PURPOSE

To survey radiation dose indices of four common general pediatric fluoroscopic procedures at a tertiary care pediatric hospital. These results allow estimates of diagnostic reference levels (DRLs) from dose indices.

METHOD AND MATERIALS

Radiation dose structured reports were retrospectively collected for > 2,000 pediatric general fluoroscopic cases. Kerma Area Product (KAP), air Kerma (Kair), fluoroscopy time (FT), thickness of body part irradiated, and patient age were collected for pediatric video swallow (VS), upper GI (UGI), lower GI (LGI) and voiding cystourethrogram (VCUG) studies. Each group of patients for a study was limited to a size variance of only 3 cm with targeted number of cases > 30 per group. 1st, 2nd, 3rd quartiles for

each group were calculated for each type of study. A fitted exponential curve of mean patient Kair vs thickness and 95% predictive bounds are presented with a scatter plot of data for each type of study. Nineteen of 20 additional patients should fall within the 95% predictive bounds.

RESULTS

Only data for the Kair for our 585 VCUG cases is presented here. For group sizes of 5-7, 8-10, 11-13, 14-16, 17-19, 20-22, 23-25 cm the number of cases and 3rd percentile estimate of DRL respectively were 16, 99, 229, 133, 67, 29,14 and 0.26, 0.55, 0.89, 1.46, 3.52, 6.39, 11.28 mGy. For an exponential fit of patient Kair vs thickness (ae-bx), a = 0.07 and b = 0.2. In addition to scatter plots of the data with fitted curves for each type of study, a data table is also provided for each study type that lists the 1st, 2nd, and 3rd quartile of AK, KAP, FT, AK/FT, KAP/FT as a function of the patient group thicknesses along with published average age, height, mass, and BMI corresponding to that measured thicknesses. Calculated DAP/AK ratios allow conversion between these two indices if one is known.

CONCLUSION

Estimates of 3rd quartile dose indices of four common pediatric fluoroscopic procedures as a function of patient thickness should assist departments in the development of DRL values using dose indices.

CLINICAL RELEVANCE/APPLICATION

Fluoroscopic DRL values based on a department's unique patients and imaging equipment foster better management of radiation dose and image quality to improve pediatric patient care.

SSM20-03 Optimizing the US Diagnosis of Biliary Atresia with a Modified Triangular Cord Thickness and More Objective Gallbladder Classification

Wednesday, Dec. 2 3:20PM - 3:30PM Location: S102AB

Participants

Zhou Lu-Yao, Guangzhou, China (*Presenter*) Nothing to Disclose Xiao-Yan Xie, Guangzhou, China (*Abstract Co-Author*) Nothing to Disclose

PURPOSE

To evaluate the diagnostic performance of US in identification and exclusion of biliary atresia by a modified triangular cord thickness metric together with agallbladder classification scheme, as well as hepatic artery(HA) diameter and liver and spleen size, in a large sample of jaundiced infants.

METHOD AND MATERIALS

Ethics Committee approved the study, and written informed parental consent was obtained.273 infants with conjugated hyperbilirubinemia(total bilirubin \ge 31.2µmol/L with direct bilirubin>indirect bilirubin)underwent detailed abdominal US examination to exclude biliary atresia and on this basis were classified as biliary atresia(n=129) or not-biliary atresia(n=144). A modified triangular cord thickness measured at the anterior branch of the right portal vein and a gallbladder classification scheme that incorporated the appearance of the gallbladder as well as length: width ratio \le 5.2 when the lumen was visualized, as well as HA diameter, liver and spleen size, were identified and measured. Reference standard diagnosis was based on one or more of the following: surgery, liver biopsy, cholangiography, and clinical follow-up. Area under the receiver operating characteristic curve (AUC), binary logistic regression analyses, Fisher's exact test and unpaired t test were performed.

RESULTS

Triangular cord thickness, HA diameter, the ratio of gallbladder length to gallbladder width, liver size and spleen size exhibited statistically significant differences (all P<.05) between the biliary atresia and not-biliary atresia groups. AUCs of triangular cord thickness, gallbladder ratio of length over width and HA diameter were 0.952, 0.844 and 0.838, respectively. Logistic regression analysis demonstrated that these three US parameters were significantly associated (all P<.05) with biliary atresia. The combination of triangular cord thickness and gallbladder classification could yield a comparable AUCs (0.915 vs 0.933, P=.400) and a higher sensitivity (96.9% vs 92.2%), compare to triangular cord thickness alone.

CONCLUSION

Using the combination of the modified triangular cord thickness and a gallbladder classification scheme, most infants with biliary atresia could be identified.

CLINICAL RELEVANCE/APPLICATION

Use of a modified triangular cord thickness measurement and a gallbladder classification, can potentially reduce the number of patients requiring nuclear scintigraphy and liver biopsy.

SSM20-04 Pediatrics Keynote Speaker: How Does Fetal Imaging Influence Neonatal Imaging?

Wednesday, Dec. 2 3:30PM - 3:40PM Location: S102AB

Participants

Richard A. Barth, MD, Stanford, CA (Presenter) Nothing to Disclose

SSM20-05 Virtual Rounds: Bringing Radiology Back to the ICU

Wednesday, Dec. 2 3:40PM - 3:50PM Location: S102AB

Participants

Janet R. Reid, MD, Philadelphia, PA (*Abstract Co-Author*) Nothing to Disclose David T. Saul, MD, Philadelphia, PA (*Presenter*) Nothing to Disclose Maria A. Bedoya, MD, Philadelphia, PA (*Abstract Co-Author*) Nothing to Disclose Hannah Stinson, MD, Philadelphia, PA (*Abstract Co-Author*) Nothing to Disclose Brian Hopely, BA, Philadelphia, PA (*Abstract Co-Author*) Nothing to Disclose Parvez Kazmi, MD, Philadelphia, PA (*Abstract Co-Author*) Nothing to Disclose Donald Boyer, MD, Philadelphia, PA (*Abstract Co-Author*) Nothing to Disclose

PURPOSE

Digital imaging has greatly improved clinician access to images and timely reports but may have eroded face-to-face communication between clinicians and radiologists, especially in the ICU.Increased radiology workload together with demands for on-site presence of ICU house staff have made it difficult to hold morning radiology rounds. Despite this, benefits of digital imaging have far outweighed the limitations, and the new hurdles require new thinking.This project leverages simple technology to create personalized point of care radiology consultation in the ICU.

METHOD AND MATERIALS

Using Lync 13, 20 minute interactive rounds were delivered by a radiologist from a workstation located in the radiology reading room to a clinical team in a 55 bed pediatric ICU. Images were shared from PACS (Philips iSite) to a large screen in a central meeting space in the ICU, with both stations equipped with panoramic web-cams with built-in audio. There were 12 sessions over 1 month, first and last session reserved for testing. Ten micro-didactic lectures were prepared covering top 10 items from the ABP Core Content for Critical Care; each session started with the lecture followed by review of daily inpatient imaging including all modalities and body systems. Assessment tools: Demographics (experience and background); Skills (image-based pre-and post-test); Confidence (self-reporting questionnaire); Format (learning effectiveness, strengths and weaknesses). The study was granted IRB exemption with consent.

RESULTS

8 residents participated (4 control/4 intervention). There was a more significant increase in test scores in the intervention group over the controls (p=0.031). Test time: 12.9 minutes(8-17). Confidence scores increased significantly for modalities and diagnoses, with pre to post-test scores of 55.6% (40.7-59.3) to 57.4%(44.4-77.8) p=0.031 and 66.7%(47.9-89.6) to 81.1%(62.5-100) p=0.016 respectively. Format scored 4-5/5, with positive comments about level of interactivity and time alottment. Weaknesses included intermittent video bandwidth loss and limited time to cover the curriculum.

CONCLUSION

Virtual conferencing contributes positively to radiology education, has potential for significant impact on patient care in the ICU and is a viable alternative to interdepartmental travel for radiology rounds.

CLINICAL RELEVANCE/APPLICATION

Interdisciplinary dialogue is essential in building knowledge and adds value to patient care through radiology consultation.

SSM20-06 Getting Published in Paediatric Radiology: What Does it Take?

Wednesday, Dec. 2 3:50PM - 4:00PM Location: S102AB

Participants

Susan C. Shelmerdine, MBBS,FRCR, London, United Kingdom (*Presenter*) Nothing to Disclose Jeremy Lynch I, BMBCh, London, United Kingdom (*Abstract Co-Author*) Nothing to Disclose Owen Arthurs, MBBChir, PhD, Cambridge, United Kingdom (*Abstract Co-Author*) Nothing to Disclose

PURPOSE

Presentation of new research and emerging techniques at scientific conferences allows dissemination of expertise and enables future development within the specialty. Studies that do not result in a subsequent publication limit the impact of the work undertaken. This study establishes the conversion rate and identifies predictive factors for journal publication of oral scientific presentations within paediatric radiology.

METHOD AND MATERIALS

Oral presentations from the European Society of Paediatric Radiology, International Society of Pediatric Radiology and Society of Pediatric Radiology conferences between 2010 and 2012 were identified from published conference proceedings. A literature search was performed to ascertain whether publication in a MEDLINE indexed journal was achieved by April 2015. Logistic regression was performed using R, version 3.1.3 to identify predictive factors.

RESULTS

300 out of 715 (41%) oral presentation abstracts were subsequently published, most commonly in the journals: Pediatric Radiology (74, 25%), AJR (34, 11%) and Radiology (22, 7%). The majority of presentations (169, 56%) were published within 24 months of the conference date (1 - 59 months). Countries with the highest abstract to publication conversion rates were USA (169, 56%), Canada (18, 6%), France (16, 5%) and United Kingdom (15, 5%). Factors that were predictive of publication included sample size (p=0.007), publication within the subspecialty subject areas of radiation protection (p=0.02), neurological imaging (p=0.03), and functional imaging (p=0.04). Factors that did not have any effect on subsequent publication included study type, prospective nature of the study or origin of study from an academic or paediatric tertiary centre.

CONCLUSION

In this retrospective study of pediatric radiology conference proceedings, fewer than half of all presented oral abstracts result in publication. Studies with a larger sample size and within certain subspecialty areas in paediatric radiology were associated with subsequent publication. Identification of predictive factors in journal publications may help future investigators plan and design successful research projects.

CLINICAL RELEVANCE/APPLICATION

Identification of predictive factors in journal publications may help future investigators plan and design successful research projects.

Radiation Oncology (Radiation Biology)

Wednesday, Dec. 2 3:00PM - 4:00PM Location: S104A

RO

AMA PRA Category 1 Credit ™: 1.00 ARRT Category A+ Credit: 1.00

FDA Discussions may include off-label uses.

Participants

Meng X. Welliver, MD, Columbus, OH (*Moderator*) Nothing to Disclose

Sunil Krishnan, MD, Houston, TX (Moderator) Research Grant, Shell Oil Company; Researcher, Celgene Corporation

Sub-Events

SSM22-01 Treatment of Primary Tumors through Immunogenic Cell Death, with Concurrent Treatment of Metastasized Tumors through the Abscopal Effect, Via Targeted anti-CD4 siRNA, HMGB1, and ATP Nanoparticles Combined with Radiotherapy

Wednesday, Dec. 2 3:00PM - 3:10PM Location: S104A

Participants

Satoshi G. Harada, MD, Morioka, Japan (*Presenter*) Nothing to Disclose Shigeru Ehara, MD, Morioka, Japan (*Abstract Co-Author*) Nothing to Disclose Keizo Ishii, PhD, Sendai, Japan (*Abstract Co-Author*) Nothing to Disclose Takahiro Satoh, DSc, Takasaki, Japan (*Abstract Co-Author*) Nothing to Disclose Koichiro Sera, Takizawa, Japan (*Abstract Co-Author*) Nothing to Disclose

PURPOSE

We aimed to image and treat primary tumors through immunogenic cell death (ICD) and metastasized tumors through the abscopal effect in LM17 cell xenografts in BALB/c mice using microcapsules that release liposome-protamine-hyaluronic acid nanoparticles (LPH-NPs) in response to three sessions of radiation.

METHOD AND MATERIALS

For session one, LPH-NPs containing 5% iopamiron were mixed with 1.0 mL of a solution containing 4.0% alginate, 3.0% hyaluronate, 1 mg ascorbate, and 1 μ g/mL P-selectin. LPH-NPs were then added to 0.5 mM FeCl2 supplemented with 1 μ g/mL ad β 1 antibody (Ab). Mice were injected intravenously (IV) with microcapsules. The primary tumor was exposed 9 h later to 10 or 20 Gy 60Co γ -rays. In session two, dendritic cell (DC)-associated cross-priming of CD8+ T cells was intensified for treatment of lung metastases by the abscopal effect. To this end, LPH-NPs containing 250 nmol anti-CD47 siRNA, 250 nmol anti-CD47 siRNA (modified with an scFv Ab against CD4), 40 ng HMGB1, and 10 μ mol ATP were mixed with the abovementioned cocktail and added to 0.5 mM FeCl2 supplemented with 1 μ g/mL anti-P-selectin Ab. Microcapsules (ten billion) were injected IV and they interacted with P-selectin. After 9 h, the second radiation session was conducted using the same protocol as for the first session. In session three, 4 cGy 60Co whole-body γ -rays were administered at 24-h intervals for 5 d to activate CD8+ T cells.

RESULTS

Anti-α4β1 microcapsules accumulated around the primary tumor and metastases, which was detected by computed tomography. The microcapsules in the primary tumor released P-selectin-Ag with LPH-NPs after the first irradiation. In session two, microcapsules accumulated around the primary tumor through P-selectin the Ag-Ab reaction and released LPH-NPs containing anti-CD47 siRNA, HMGB1, and ATP, which intensified ICD in the primary tumor and DC-associated cross-priming of CD8+ T cells. In session three, primed CD8+ T cells were activated and targeted metastases. These treatments reduced the sizes of the primary tumor and metastases by 91.7%.

CONCLUSION

Our microcapsules improved diagnoses and promoted the effects of radiotherapy on metastases.

CLINICAL RELEVANCE/APPLICATION

Imaging-targeted ICD and promotion of the abscopal effect by anti-CD47 siRNA, HMGB1, and ATP improved diagnoses and extended the effects of radiotherapy to metastases.

SSM22-04 Transient Hypoxia with Accelerated EPR pO2 Images using a Low-rank Tensor/navigator Projection Image Model

Wednesday, Dec. 2 3:30PM - 3:40PM Location: S104A

Participants

Howard J. Halpern, MD, PhD, Chicago, IL (*Presenter*) Nothing to Disclose Boris Epel, PhD, Chicago, IL (*Abstract Co-Author*) Nothing to Disclose Zhi-Pei Liang, PhD, Urbana, IL (*Abstract Co-Author*) Nothing to Disclose Anthony Christodoulou, Urbana, IL (*Abstract Co-Author*) Nothing to Disclose Victor Tormyshev, PhD, Novosibirsk, Russia (*Abstract Co-Author*) Nothing to Disclose

PURPOSE

The role of transient hypoxia is an outstanding question in tumor physiology. Electron paramagnetic resonance (EPR) imaging has been shown to define regions of mouse tumors that are hypoxic and correlated the extent of this hypoxic region with sensitivity to radiation. Changes in hypoxia can significantly affect the relevance of such measurements. Thus we need to accelerate the rate at

which molecular oxygen images can be obtained.

METHOD AND MATERIALS

We developed a low-rank tensor image model to acquire and analyze dynamic pO2 maps from highly undersampled (k,t)-space data. The model represents a set of dynamic images collected with different pulse sequence parameters in a low-dimensional, timevarying parameter subspace. Correlations between images across time, parameter space (pO2), and location are captured and extends our previous work on accelerated parameter mapping using low-rank models and dynamic imaging using low-rank models. The model dictates a data acquisition scheme allowing direct determination of the time-varying parameter subspace and a reconstruction algorithm to recover high-quality images from highly undersampled (k,t)-space data using the resulting subspace constraint.

RESULTS

To demonstrate the model utility for dynamic pO2 imaging, we performed simulations and in vivo experiments. We will show results from a simulation using a numerical phantom for which one region experiences an instantaneous change in pO2. In vivo results were obtained from a mouse tumor image, wherein pO2 fluctuations were induced by cycling the fraction of inspired oxygen (FiO2), toggling the FiO2 with variable timing. 3D pO2 images at one time point as well as a graph of the pO2 variation over time for one voxel at the center of the tumor showed resolution and image quality of the low-rank tensor method to be superior to previous methods.

CONCLUSION

Low-rank tensor method captures oxygen fluctuations with a temporal resolution of 31 seconds.

CLINICAL RELEVANCE/APPLICATION

The oxygen variation frequency captured by this technique are comparable to the highest frequencies in the literature. This will show the biologic and clinical relevance of transient hypoxia.

SSM22-06 DNA Double-strand Breaks in Blood Lymphocytes of Patients Undergoing Coronary CT: Comparison with the Physical CT Radiation Exposure Index

Wednesday, Dec. 2 3:50PM - 4:00PM Location: S104A

Participants

Wataru Fukumoto, Hiroshima, Japan (*Presenter*) Nothing to Disclose
Mari Ishida, Hiroshima, Japan (*Abstract Co-Author*) Nothing to Disclose
Satoshi Tashiro, Hiroshima, Japan (*Abstract Co-Author*) Nothing to Disclose
Kenji Kajiwara, Hiroshima, Japan (*Abstract Co-Author*) Nothing to Disclose
Makoto Iida, Hiroshima, Japan (*Abstract Co-Author*) Nothing to Disclose
Kazuo Awai, MD, Hiroshima, Japan (*Abstract Co-Author*) Research Grant, Toshiba Corporation; Research Grant, Hitachi, Ltd;
Research Grant, Bayer AG; Reseach Grant, DAIICHI SANKYO Group; Medical Advisor, DAIICHI SANKYO Group; Research Grant, Eisai
Co, Ltd; Research Grant, Nemoto-Kyourindo; ;; ;;
Chikako Fujioka, RT, Hiroshima, Japan (*Abstract Co-Author*) Nothing to Disclose

Masao Kiguchi, RT, Hiroshima, Japan (Abstract Co-Author) Nothing to Disclose

PURPOSE

DNA double-strand breaks (DSBs) are the most significant DNA damage inflicted by ionizing radiation (IR) and phosphorylated form of histon H2AX (γ -H2AX) has drawn attention as a DSB biomarker. However, it remains undetermined whether CT-induced DSBs are accurately estimated with γ -H2AX. The purpose of this study was to assess the DSBs induced by radiation exposure from coronary CT and to determine the relationship between γ -H2AX and the physical CT radiation exposure index, e.g. the CT dose index (CTDI), size-specific dose estimates (SSDE), and the dose length- and the SSDE length product (DLP, SSDE-LP).

METHOD AND MATERIALS

We obtained institutional review board approval and the written informed consent from 45 patients (40 men, 5 women, median age 63 years, range 30-76 years) with arrhythmia who underwent coronary CT before ablation therapy. Blood samples were obtained before- and 15 min- and a few days after CT performed before ablation therapy. We identified DSBs in lymphocytes as cytologically visible "foci" by using an antibody against γ -H2AX. For data analysis, we applied the Tukey-Kramer test. To assess the relationship between the physical CT radiation exposure index (CTDI, SSDE, DLP, and SSDE-LP) and increase rate of γ -H2AX ([15 minutes after CT - before CT]/before CT) and subjected the results to the Pearson correlation coefficient test.

RESULTS

The mean γ -H2AX foci number before CT, 15 min after CT, and a few days after CT were 1.21, 1.92, and 1.06 x10-3 foci/cell, respectively. The γ -H2AX foci number were significantly increased after CT and returned to baseline after a few days. The mean CTDI, SSDE, DLP, and SSDE-LP were 102.5 mGy, 138.2 mGy, 1560.5 mGy cm, and 1932.5 mGy cm, respectively. A statically significant correlation was observed between γ -H2AX foci number and CTDI, SSDE, DLP, and SSDE-LP (r=0.53, 0.54, 0.54, and 0.53).

CONCLUSION

DSBs were significantly increased after coronary CT and the radiation-induced γ -H2AX level correlated with the physical CT radiation exposure index.

CLINICAL RELEVANCE/APPLICATION

DSBs were induced by radiation exposure even after a single CT study. This finding alerts to the importance of reducing the radiation dose for CT.

Chest (Other/Nodule)

Wednesday, Dec. 2 3:00PM - 4:00PM Location: S406B

СН СТ

AMA PRA Category 1 Credit [™]: 1.00 ARRT Category A+ Credit: 1.00

Participants

Jonathan D. Dodd, MD, Dublin 4, Ireland (*Moderator*) Nothing to Disclose Kyung S. Lee, MD, PhD, Seoul, Korea, Republic Of (*Moderator*) Nothing to Disclose

Sub-Events

SSM06-01 Does FDG PET/CT Have Value in Detecting Recurrence of Esophageal Carcinoma?

Wednesday, Dec. 2 3:00PM - 3:10PM Location: S406B

Participants

Sonia L. Betancourt Cuellar, MD, Houston, TX (*Presenter*) Nothing to Disclose Patricia M. de Groot, MD, Houston, TX (*Abstract Co-Author*) Nothing to Disclose Marcelo K. Benveniste, MD, Houston, TX (*Abstract Co-Author*) Nothing to Disclose Carol C. Wu, MD, Houston, TX (*Abstract Co-Author*) Author, Reed Elsevier Diana M. Palacio, MD, Tucson, AZ (*Abstract Co-Author*) Nothing to Disclose Edith M. Marom, MD, Ramat Gan, Israel (*Abstract Co-Author*) Nothing to Disclose

PURPOSE

The purpose of this study was to determine the utility of FDG-PET/CT in detecting recurrent disease in patients with esophageal cancer after surgical resection.

METHOD AND MATERIALS

Subjects in this retrospective study were 125 consecutive esophageal cancer patients who were surgically treated between 3/31/2003 and 4/30/2012 and had routine follow up FDG PET/CT examinations. The number and sites of FDG avid lesions were retrospectively analyzed and were correlated with histological assessment and/or continued progression by imaging.

RESULTS

Of the 125 patients who met the inclusion criteria, 50 patients were confirmed to have recurrence in 62 sites, 53-1097 days postsurgery (median: 416 days). Recurrence was detected in 57% and 20% of patients within the first 12 and 24 months respectively after surgery. Forty-one patients (66%) had recurrence in distant organs (most commonly liver [20, 48 %]), 16 (26%) lymph node metastases and 5 (8%) had recurrence at the anastomotic site. The sensitivity, specificity, positive predictive value, negative predictive value and accuracy of FDG-PET/CT for diagnosing recurrence at the anastomosis is 83%, 32%, 16%, 98% and 75%, for lymph nodes metastasis was 100%, 90%, 61%, 100%, and 92%. For metastases to distant organs was 100%, 96%, 93%, 96%, and 97%.

CONCLUSION

FDG PET/CT is accurate in detecting recurrence in patients after resection of esophageal cancer when recurrence is to metastatic lymph nodes or distant organs but has very low specificity and positive predictive value in the evaluation of anastomotic recurrence.

CLINICAL RELEVANCE/APPLICATION

This study clarifies the role of FDG-PET/CT in detecting recurrence in patients with esophageal cancer.

Honored Educators

Presenters or authors on this event have been recognized as RSNA Honored Educators for participating in multiple qualifying educational activities. Honored Educators are invested in furthering the profession of radiology by delivering high-quality educational content in their field of study. Learn how you can become an honored educator by visiting the website at: https://www.rsna.org/Honored-Educator-Award/

Sonia L. Betancourt Cuellar, MD - 2014 Honored Educator Edith M. Marom, MD - 2015 Honored Educator

SSM06-02 Low Attenuation of the Thyroid Gland on Noncontrast Chest CT is Predictive of Hypothyroidism

Wednesday, Dec. 2 3:10PM - 3:20PM Location: S406B

Participants

Michael A. Kadoch, MD, Stanford, CA (*Presenter*) Nothing to Disclose Ann N. Leung, MD, Stanford, CA (*Abstract Co-Author*) Nothing to Disclose Gabriela Gayer, MD, Palo Alto, CA (*Abstract Co-Author*) Nothing to Disclose

PURPOSE

To determine whether the mean computed tomography (CT) attenuation value of the thyroid gland can be used to predict hypothyroidism.

METHOD AND MATERIALS

A search of the electronic medical record was performed to identify patients with a diagnosis of hypothyroidism who received a noncontrast chest CT scan. Consecutive patients without known thyroid gland dysfunction and with normal thyroid function tests who received a noncontrast chest CT scan were selected as a euthyroid control group. The mean CT attenuation value of the thyroid gland in Hounsfield units (HU) was determined for each patient using the standard workstation region-of-interest measurement tool.

RESULTS

210 patients (69% female; 31% male; mean age 66 years) with medically established hypothyroidism and 50 euthyroid patients (72% female; 28% male; mean age 65 years) were available for analysis. Mean CT attenuation values of \leq 50 HU and \leq 70 HU were highly predictive of hypothyroidism (specificity 100% [95% CI: 92-100%; P=0.01] and 98% [95% CI: 89-100%; P<0.001], respectively). The sensitivity of a mean CT attenuation value of \leq 100 HU for detecting hypothyroidism was 74% [95% CI: 71-77%; P=0.006]. Overall, lower mean CT attenuation values predicted a higher relative risk for hypothyroidism.

CONCLUSION

Low mean CT attenuation (≤70 HU) of the thyroid gland on noncontrast chest CT is highly predictive of hypothyroidism.

CLINICAL RELEVANCE/APPLICATION

Hypothyroidism is an established treatable risk factor for cardiovascular disease. Many cases of hypothyroidism are subclinical. Hypothyroidism can be detected with high specificity on screening and diagnostic noncontrast chest CT scans, which can be used to augment the comprehensive cardiovascular risk assessment afforded by this examination.

SSM06-03 Generalized Mucositis-related Bronchiolitis in the Setting of Allogeneic Stem Cell Transplantation: A Potential Mimic of Lower Respiratory Tract Infection

Wednesday, Dec. 2 3:20PM - 3:30PM Location: S406B

Participants

Christopher Kloth, Tuebingen, Germany (*Presenter*) Nothing to Disclose Ulrich Grosse, MD, Tuebingen, Germany (*Abstract Co-Author*) Nothing to Disclose Stefan Wirths, Tuebingen, Germany (*Abstract Co-Author*) Nothing to Disclose Sergios Gatidis, MD, Tubingen, Germany (*Abstract Co-Author*) Nothing to Disclose Wolfgang Bethge, Tuebingen, Germany (*Abstract Co-Author*) Nothing to Disclose Konstantin Nikolaou, MD, Tuebingen, Germany (*Abstract Co-Author*) Nothing to Disclose Speakers Bureau, Bayer AG

Marius Horger, MD, Tuebingen, Germany (Abstract Co-Author) Nothing to Disclose

PURPOSE

To describe a little known therapy-related small airway phenomenon presumably caused by mucosal irritation in patients undergoing allogeneic stem cell transplantation (allo-SCT).

METHOD AND MATERIALS

Retrospective database search at our institution identified 739 hematological patients who underwent chemotherapy+allo-SCT between September 2004 and March 2014. After excluding infectious pulmonary complications, 75 patients (female=24; male=51; median age=47y) with signs of generalized bronchiolitis (GB) on chest-HRCT were identified. CT was performed proximate to chemotherapy-onset; 92% had follow-up-CT (mean, 1.9weeks). The presence of centrilobular nodules/bronchial wall thickening(BWT)/tree-in-bud(distributed diffuse vs. focal)/ground-glass-opacity(GGO)/ airspace opacification/luminal impactions/air-trapping was correlated with occurrence and duration of oral mucositis and therapy characteristics. Intensity of tree-in-bud and centrilobular nodules was graded absent(grade=0), moderate(grade=1) and marked(grade=2).

RESULTS

Overall incidence of GB among allo-SCT-patients was 10.7%. GB was diagnosed at the time point of transplantation with a mean duration of CT-findings of 4 weeks(± 2.7). Tree-in-bud (17%[grade 2] and 83%[grade 1]) and BWT was present in 100%. Centrilobular nodules were found in 45.5% of patients (20% [grade 2], 24% [grade 1] and 56%[none]) being always diffusely distributed. Air-trapping/mosaic pattern were found in 13% and 16%, respectively. Resolution of GB was spontaneous. GB and its severity correlated with the temporal course and grade of oral mucositis; frequency and degree was not significantly influenced by the chemotherapy regimen. The incidence of GB in HRCT was statistically significant higher in patients with oral mucositis (p<0.035).

CONCLUSION

GB is frequent during chemotherapy for allo-SCT and is characterized by even distribution of tree-in-bud/ BWT/ centrilobular nodules, mild clinical symptoms and spontaneous resolution.

CLINICAL RELEVANCE/APPLICATION

Severe pulmonary complications occur in patients undergoing allo-SCT. Treatment strategy depends primarily on differentiation between infectious and non-infectious genesis. In the setting of respiratory symptoms lower respiratory tract infection must be suspected. However, knowledge of potential mimics is essential for accurate patient management. At this point, mucosal barrier injury (mucositis) represents a potential differential diagnosis.

SSM06-04 Dual-input Perfusion of Lung Lesions with 320-detector-row CT: Its Reproducibility, Value in differentiating Malignant from Benign Lesions and Correlation with Lesion Micro-vessel Density

Wednesday, Dec. 2 3:30PM - 3:40PM Location: S406B

Participants Hui Liu, Shanghai, China (*Presenter*) Nothing to Disclose Jiang Lin, MD, PhD, Shanghai, China (*Abstract Co-Author*) Nothing to Disclose Jiamei Yao, Shanghai, China (*Abstract Co-Author*) Nothing to Disclose Xiuliang Lu, Shanghai, China (*Abstract Co-Author*) Nothing to Disclose

PURPOSE

To investigate the reproducibility of dual-input CT perfusion (DI-CTP) of lung lesions with 320-detector-row CT, its value in differentiation of malignant and benign lesions and the correlation between CTP parameters and micro-vessel density (MVD).

METHOD AND MATERIALS

116 patients with various lung lesions confirmed by pathology underwent DI- CTP. There were 95 malignant and 21 benign lesions. The pulmonary trunk and the descending aorta were selected as input arteries for measuring contributions from pulmonary and bronchial circulation to the lesions . Pulmonary flow (PF), bronchial flow (BF), and perfusion index (PI) were calculated by two independent radiologists. Intraclass correlation coefficient (ICC) and Bland-Altman statistics were used to evaluate intra- and interobserver agreement. 94 lesions had immunohistochemical staining with CD34. DI-CTP parameters were compared between malignant and benign lesions. Correlation between DI-CTP and MVD was studied.

RESULTS

Both intra- and inter-observer agreements were good to excellent (ICC>0.90). PF and PI of benign lesions were higher than those of malignant lesions.BF of malignant lesions was higher than that of benign lesions.Statistically significant differences of BF, PF and PI were found between malignant and benign lesions (P<0.05) with the area under the PI ROC curve being 0.936, the largest of the three perfusion parameters. There was statistically significant difference in MVD between benign and malignant lesions (P<0.05). BF, PF and TPF values were positively correlated with MVD (P<0.05).

CONCLUSION

DI-CTP is reproducible and reflects the angiogenesis of lung lesions. It can provide additional information for differential diagnosis of malignant from benign lung lesions.

CLINICAL RELEVANCE/APPLICATION

DI-CTP is reproducible and reflects the angiogenesis of lung lesions. It can provide additional information for differential diagnosis of malignant from benign lung lesions.

SSM06-05 The Effectiveness of Digital Tomosynthesis for the Nodule Detection in Danger Zone vs Non-Danger Zone: Phantom Study

Wednesday, Dec. 2 3:40PM - 3:50PM Location: S406B

Participants

Eun Young Kim, MD, Seoul, Korea, Republic Of (*Presenter*) Nothing to Disclose Joo Sung Sun, MD, Suwon-Si, Korea, Republic Of (*Abstract Co-Author*) Nothing to Disclose Taehee Kim, MD, PhD, Suwon, Korea, Republic Of (*Abstract Co-Author*) Nothing to Disclose Seon Young Park, MD, Suwon-si, Korea, Republic Of (*Abstract Co-Author*) Nothing to Disclose Kyung Joo Park, MD, Suwon, Korea, Republic Of (*Abstract Co-Author*) Nothing to Disclose

PURPOSE

To compare the effectiveness of digital tomosynthesis (DT) with dual-energy subtraction radiography (DES) and chest radiography (CXR) for detecting simulated pulmonary nodules (SPN) according to the nodule size and location.

METHOD AND MATERIALS

Four different sizes (5, 8, 10 and 12mm in a diameter) of SPNs (1~4 nodules/1 exam) were inserted into 8 different area of lung phantom classified as danger or non-danger zone (Fig 1). Three modalities of DT, DES, and CXR were all performed at the same time for every 96 examinations. Additional 96 examinations 3 modalities without nodule (normal control) were performed. Finally, a total of 192 examinations were prepared for each set of modality. Three sets of image data were randomly arranged and three observers independently reviewed all images in a random order. Three observers were asked to identify nodule and score confidence with 4 scales. Also asked to measure largest diameter of each nodule and record interpretation time. The jackknife alternative free-response receiver operating characteristic (JAFROC) was used to analyze overall diagnostic performance for each modality.

RESULTS

FROC analyses revealed significantly better performance (P <0.05) of DT than CXR and DES for the detection of pulmonary nodules. The observer-averaged figure of merit (FOM) was 0.78, 0.77 and 0.95 for CXR, DES, and DT, respectively. The TPF increased with an increase in size of the nodules. Except the smallest nodules (5 mm), the TPF for DT was about 1.5 times higher than CXR and DES (0.99 vs 0.677 and 0.670) in danger zone but there was a little difference in non- danger zone (0.988, 0.889, and 0.905 for DT, CXR and DES) (Fig 2). The FPF was significantly lower in DT than CXR and DES (0.003, 0.133 and 0.126 for DT, CXR and DES). The mean interpretation time for DT (mean±SD, 53 ± 19 s) was higher (P<0.05; Wilcoxon test) than for CXR (28 ± 12 s) and DES (30 ± 11 s).

CONCLUSION

The DT significantly improved the diagnostic performance to detect pulmonary nodules than CXR and DES, especially nodules located in danger zone that easily obscured by superimposed vascular structure and bone structure.

CLINICAL RELEVANCE/APPLICATION

DT seems to be a superior modality for work up of pulmonary nodule with higher image quality and boosts its ability for nodule located in danger zone that easily obscured by superimposed bone and vascular structure on CXR and DES

SSM06-06 Lung Nodule Classification using Learnt Texture Features on a Single Patient Population

Wednesday, Dec. 2 3:50PM - 4:00PM Location: S406B

Participants

Lyndsey C. Pickup, MEng, DPhil, Oxford, United Kingdom (*Presenter*) Employee, Mirada Medical Ltd Aambika Talwar, MA, MBBCHIR, Oxford, United Kingdom (*Abstract Co-Author*) Nothing to Disclose Shameema Stalin, Oxford, United Kingdom (*Abstract Co-Author*) Nothing to Disclose Aymeric Larrue, PhD, Oxford, United Kingdom (*Abstract Co-Author*) Employee, Mirada Medical Ltd Djamal Boukerroui, PhD, Oxford, United Kingdom (*Abstract Co-Author*) Employee, Mirada Medical Ltd Mark J. Gooding, MENG, DPhil, Oxford, United Kingdom (*Abstract Co-Author*) Employee, Mirada Medical Ltd Fergus V. Gleeson, MBBS, Oxford, United Kingdom (*Abstract Co-Author*) Consultant, Alliance Medical Limited; Consultant, Blue Earth Diagnostics Limited; Consultant, Polarean, Inc; Timor Kadir, Oxford, United Kingdom (*Abstract Co-Author*) Employee, Mirada Medical Ltd

PURPOSE

To validate the use of texture features and a machine learning approach to generate a "probability-of-malignancy" score for lung nodules.

METHOD AND MATERIALS

A database with 705 distinct pulmonary nodules (PNs) was created with contrast CTs from 139 patients in a selected geographical region. All patients with reported PNs from Jan-Apr 2013 were included; those with unavailable scans or malignancy status (by histology or 2-year stable follow-up) were excluded. The dataset contained 328 benign nodules, 7 primary cancers, and 370 metastases. 522 image texture features in 2D/3D were extracted from each PN and its borders (contoured using Mirada XD, Mirada Medical Ltd). These included Haralick, Gabor and Laws features, fractal dimensions, plus combinations and difference features, with dimensionality reduction using principal component analysis. A greedy algorithm selected maximally discriminative features one by one, and mapped feature responses to malignancy probabilities using a Support Vector Regressor (LibSVM). For robust analysis, the dataset was partitioned into distinct thirds: one for training, one for cross-validation (setting SVR parameters, using a simplex method), and one for testing (reporting AUC). For each feature set, 100 different splits were evaluated, with the mean AUC on each split being compared. A leave-one-out validation result was also computed, for ease of comparison to other work. The work was repeated on a dataset excluding patients undergoing chemotherapy at the time of the scan, leaving 160 malignant and 230 benign nodules.

RESULTS

A mean AUC of 0.872 (std 0.020) was obtained by the feature set selected. The best single feature was the standard deviation of a Gabor filter response on the nodule boundary, and the peak mean AUC overall was obtained with 40 features. The leave-one-out AUC was 0.905, and this increase is to be expected because leave-one-out is less robust to overfitting than the three-fold approach. For the chemo-free population, the AUC was 0.942.

CONCLUSION

This texture feature model is successful at discriminating malignant and benign nodules over a large selection of nodules drawn from a single patient population. Future work should include more primary cancers.

CLINICAL RELEVANCE/APPLICATION

Differentiating malignant and benign pulmonary nodules is a common clinical problem in which software may help support clinical decisions and guide patient management.

Cardiac (Angiography)

Wednesday, Dec. 2 3:00PM - 4:00PM Location: S504AB

СА СТ

AMA PRA Category 1 Credit [™]: 1.00 ARRT Category A+ Credit: 1.00

Participants

Phillip M. Young, MD, Rochester, MN (*Moderator*) Nothing to Disclose Shawn D. Teague, MD, Indianapolis, IN (*Moderator*) Stockholder, Apple Inc Antoinette S. Gomes, MD, Culver City, CA (*Moderator*) Stockholder, St. Jude Medical, Inc; Research Consultant, Boston Scientific Corporation

Sub-Events

SSM04-01 Four-dimensional Noise Reduction Using the Time Series of CT Datasets in Short Interval Times; Initial Comparison in Clinical Cases

Wednesday, Dec. 2 3:00PM - 3:10PM Location: S504AB

Participants

Tatsuya Nishii, MD, PhD, Kobe, Japan (*Presenter*) Nothing to Disclose Atsushi K. Kono, MD, PhD, Kobe, Japan (*Abstract Co-Author*) Nothing to Disclose Wakiko Tani, RT, Kobe, Japan (*Abstract Co-Author*) Nothing to Disclose Erina Suehiro, RT, Kobe, Japan (*Abstract Co-Author*) Nothing to Disclose Noriyuki Negi, RT, Kobe, Japan (*Abstract Co-Author*) Nothing to Disclose Yoshiaki Watanabe, MD, Tokyo, Japan (*Abstract Co-Author*) Nothing to Disclose Satoru Takahashi, MD, Kobe, Japan (*Abstract Co-Author*) Nothing to Disclose Kazuro Sugimura, MD, PhD, Kobe, Japan (*Abstract Co-Author*) Nothing to Disclose Shumpei Mori, Kobe, Japan (*Abstract Co-Author*) Nothing to Disclose Tatsuro Ito, MD, PhD, Kobe, Japan (*Abstract Co-Author*) Nothing to Disclose Tatsuro Ito, MD, PhD, Kobe, Japan (*Abstract Co-Author*) Nothing to Disclose Tatsuro Ito, MD, PhD, Kobe, Japan (*Abstract Co-Author*) Nothing to Disclose

PURPOSE

A four-dimensional noise reduction (4DNR) method applied to datasets having short interval times (\leq 50 ms), referred to as legato, has been reported using phantom analysis to significantly reduce noise without changing the CT numbers or spatial resolution. Coronary CT angiography (CCTA) usually acquires datasets that include "padding" phases centered on the end-diastole. However, the additional information provided by additional phases has largely been ignored. Legato can be applied to such datasets to reduce image noise in CCTA. The present study conducts quantitative image quality analysis using retrospective clinical cases to examine the hypothesis that post-processing with legato reduces noise in CCTA images.

METHOD AND MATERIALS

The records of 25 consecutive patients (mean 63 [range 15-80] years old, 7 female) who had undergone routine CCTA using a retrospective ECG-gated helical scan (120 kVp, reference tube current-time product as 390 mAs) with a 128-detector row dualsource CT, were retrospectively reviewed. The three datasets for the end-diastolic phase were reconstructed with iterative reconstruction, and were post-processed including the implementation of legato. Image datasets for the center phase obtained from the collected and computed datasets are referred to as non-legato and legato images. Objective image quality was measured for various regions of interest, and subjective image quality was evaluated with a five-point Likert scale. The difference in image quality between non-legato and legato images was assessed by the Welch test and the Cochran-Armitage test.

RESULTS

Using legato, contrast-to-noise ratio and signal-to-noise ratio were significantly improved from 13.6 ± 2.8 to 22.9 ± 4.6 , and 19.6 ± 4.1 to 29.7 ± 7.1 for the aortic root, and 17.7 ± 3.6 to 29.6 ± 5.5 , and 14.2 ± 3.5 to 23.0 ± 6.6 for the mean of the proximal coronary arteries (P < 0.001 for each). Further, the subjective image score was also significantly improved using legato (median 4 to 5, P = 0.028).

CONCLUSION

Our proposed post-processing 4DNR method with short internal time reduced 40% of the image noise in clinical CCTA, and significantly improved image quality.

CLINICAL RELEVANCE/APPLICATION

Using the "padding" data, image quality of coronary CT angiography could be significantly improved using the post-processing 4DNR method.

SSM04-03 Intelligent Boundary Registration Technique (IBR) in Correcting Banding Artifact of Coronary CTA(CCTA) in 64-slice CT

Wednesday, Dec. 2 3:20PM - 3:30PM Location: S504AB

Participants Yan Feng, Shanghai, China (*Presenter*) Nothing to Disclose Qingguo Wang, Shanghai, China (*Abstract Co-Author*) Nothing to Disclose Zhiguo Zhou, Shanghai, China (*Abstract Co-Author*) Nothing to Disclose Na Gao, Shanghai, China (*Abstract Co-Author*) Nothing to Disclose Gui-Xiang Zhang, MD, Shanghai, China (Abstract Co-Author) Nothing to Disclose

PURPOSE

To assess the effect of IBR technique in correcting banding artifact of CCTA in 64-slice CT.

METHOD AND MATERIALS

Coronary CTA was performed on 70 patients with diagnosed or suspected coronary artery disease, using a 64-row CT scanner (GE Discovery CT750 HD). Image quality between standard reconstruction(group standard) and IBR reconstruction(group IBR) was compared by 2 experienced readers on GE AW4.6 workstation., using a 5-point scale, according to a standard 15-segment model by American Heart Association.

RESULTS

Mean heart rate range 43-132bpm, 71 \pm 13.29 bpm,There were 163 segments with 220 motion artifacts, IBR construction corrected 73.6%(162/220) of the artifacts. Stepladder as the most artifact, 97.27% of which were recovered after IBR reconstruction, and the majority artifacts of split-level, disconnection, density gradient were recovered well. Significant higher image quality was observed in IBR group than standard group (3.97 \pm 0.93VS4.11 \pm 0.92,P<0.001).The interpretability was increased after IBR reconstruction at level of segment and artery with no statistical difference between two groups.

CONCLUSION

IBR technique is helpful in correcting banding artifact in CCTA of 64-slice CT.

CLINICAL RELEVANCE/APPLICATION

IBR technique provides a convenient and effective method to correct banding artifact ,especially for ladder artifact,which is helpful in improving image quality and diagnostic accuracy of coronary CTA.

SSM04-04 High-pitch Single Heart Beat Coronary CT Angiography, The Effect of Heart Rate on Image Quality ? A 2nd and 3rd Generation Dual Source CT Study

Wednesday, Dec. 2 3:30PM - 3:40PM Location: S504AB

Participants

Adriaan Coenen, MD, Rotterdam, Netherlands (*Presenter*) Nothing to Disclose Philip V. Linsen, BSc, Rotterdam, Netherlands (*Abstract Co-Author*) Nothing to Disclose Raluca G. Saru, MD, Rotterdam, Netherlands (*Abstract Co-Author*) Nothing to Disclose Marcel L. Dijkshoorn, RT, Rotterdam, Netherlands (*Abstract Co-Author*) Consultant, Siemens AG Mohamed Ouhlous, MD, PhD, Rotterdam, Netherlands (*Abstract Co-Author*) Nothing to Disclose Koen Nieman, MD, PhD, Rotterdam, Netherlands (*Abstract Co-Author*) Speakers Bureau, Siemens AG Speakers Bureau, Toshiba Corporation Research Grant, Bayer AG Research Grant, General Electric Company

PURPOSE

Coronary CT angiography (CCTA) is a reliable examination with a strong ability to rule out coronary artery disease. However the radiation exposure from a CCTA examination was relatively high, in the last decade multiple technical improvements resulted in a decrease in radiation exposure. The high-pitch spiral scan mode allows for further reduction in radiation dose. However as the scan is made in a single heart beat a low heart rate has always been a necessity. With the introduction of the 3rd generation dual source CT (DSCT) the time needed for the acquisition has been reduced, allowing for acquisition in patients with higher heart rates. In this study we investigate the effect of heart rate on image quality when using the high-pitch spiral mode comparing the 2nd and 3rd generation DSCT.

METHOD AND MATERIALS

We retrospectively investigated the first 50 patients scanned with the 2nd and 3rd generation DSCT at our institution. The heart rate during acquisition was recorded. Tube voltage and current were selected semi-automatic. The table movement speed increased from 458mm/sec to 737mm/sec with the 3rd generation DSCT. Subjective image quality was measured by two independent observers using a five-point Likert score.

RESULTS

The mean heart rate was 56.4 \pm 6.0 for the 2nd and 59.0 \pm 7.4 for the 3rd generation DSCT (p= 0.045). Subjective image quality was better for the 3rd generation DSCT with a mean Likert score of 4.2 \pm 0.8 vs 3.0 \pm 0.7 (p=<0.0001). The decrease in image quality due to higher heart rates started at a later point for the 3rd generation compared to the 2nd generation DSCT (figure 1). The radiation dose for high-pitch spiral mode is already low, with a lower radiation dose of 0.6 \pm 0.3 mSv for the 3rd generation DSCT (p<0.0001).

CONCLUSION

Higher heart rates increase the change of a lower quality CCTA. When comparing the 3rd and 2nd generation DSCT the 3rd generation allows for a utilization of the high-pitch spiral mode at higher heart rates, increasing the population suitable for high-pitch spiral scan mode.

CLINICAL RELEVANCE/APPLICATION

With the applicability of the high-pitch spiral mode with higher heart rates the clinical usage can be further increased. Decreasing radiation exposure without concerns for image quality.

SSM04-06 Radiation Dose Levels of Retrospectively ECG-Gated Coronary CT Angiography Using 70 kVp Tube Voltage in Patients with High or Irregular Heart Rates

Wednesday, Dec. 2 3:50PM - 4:00PM Location: S504AB

Holger Haubenreisser, Mannheim, Germany (*Abstract Co-Author*) Speaker, Siemens AG; Speaker, Bayer AG
U. Joseph Schoepf, MD, Charleston, SC (*Abstract Co-Author*) Research Grant, Bracco Group; Research Grant, Bayer AG; Research Grant, General Electric Company; Research Grant, Siemens AG; Research support, Bayer AG; ; ;
Rozemarijn Vliegenthart, MD, PhD, Groningen, Netherlands (*Abstract Co-Author*) Nothing to Disclose
Melissa Ong, MD, Mannheim, Germany (*Abstract Co-Author*) Nothing to Disclose
Christina Doesch, Tubingen, Germany (*Abstract Co-Author*) Nothing to Disclose
Sonja Sudarski, MD, Mannheim, Germany (*Abstract Co-Author*) Nothing to Disclose
Martin Borggrefe, Mannheim, Germany (*Abstract Co-Author*) Nothing to Disclose
Stefan O. Schoenberg, MD, PhD, Mannheim, Germany (*Abstract Co-Author*) Nothing to Disclose
Stefan O. Schoenberg, MD, PhD, Mannheim, Germany (*Abstract Co-Author*) Nothing to Disclose
Stefan O. Schoenberg, MD, PhD, Mannheim, Germany (*Abstract Co-Author*) Nothing to Disclose

PURPOSE

To evaluate radiation dose and number of inconclusive coronary segments at coronary CT angiography (cCTA) using retrospective electrocardiographic (ECG) gating at 100/70kV.

METHOD AND MATERIALS

With IRB approval, 154 patients (median age 54 years; 98 men) with high or irregular heart rate prospectively underwent retrospectively ECG-gated cCTA on a third generation dual-source CT (DSCT) system at 70kV (n=103) or on a second generation DSCT system at 100kV (n=51). Images were reconstructed in best diastolic phase (BDP), best systolic phase (BSP), and in all phases (AP) at 10% intervals across the R-R cycle. Objective and subjective image quality were evaluated as well as the presence of motion artifacts with the three different reconstruction approaches. Comparisons between the groups were analyzed with two-way ANOVA or Wilcoxon-Rank-Sum Test depending on the distribution of the data.

RESULTS

Mean heart rate was 93 ± 16 beats per minute. The mean effective radiation dose was 4.5 mSv for 70kV compared to 8.4 for 100kV (p<0.05). At BDP reconstruction, 110 patients showed motion artifacts in one or more coronary segments (in total, 246 segments). At BSP reconstruction, the number of patients with motion artifacts decreased to 57 (147 segments). In contrast, if images were reconstructed with the AP approach, all vessels and coronary segments were evaluable with both cCTA protocols.

CONCLUSION

Retrospectively ECG-gated cCTA at 70kV results in 52% decreased radiation dose. This is especially important as the AP algorithm allows evaluating all coronary segments for stenosis, in contrast to best BDP or BSP phase alone. Furthermore, retrospectively ECG-gated cCTA allows for the evaluation of left ventricular function as a potentially useful diagnostic and prognostic adjunct.

CLINICAL RELEVANCE/APPLICATION

Retrospectively-ECG-gated coronary CTA at 70 kV without ECG-controlled tube current modulation strengthens the robustness of cCTA by significantly reducing the number of non-diagnostic coronary segments while radiation dose can be reduced.

Informatics (Clinical Workflow, Displays and Mobile Devices)

Wednesday, Dec. 2 3:00PM - 4:00PM Location: S403A

IN

AMA PRA Category 1 Credit [™]: 1.00 ARRT Category A+ Credit: 1.00

Participants

Vamsi R. Narra, MD, FRCR, Saint Louis, MO (*Moderator*) Consultant, Biomedical Systems; Rasu B. Shrestha, MD, MBA, Pittsburgh, PA (*Moderator*) Advisory Board, General Electric Company; Medical Advisory Board, Nuance Communications, Inc; Editorial Advisory Board, Anderson Publishing, Ltd; Advisory Board, KLAS Enterprises LLC; Advisory Board, Peer60; Board, Omnyx, LLC; Board, Health Fidelity, Inc

Sub-Events

SSM13-01 Novel Use of Redmine Issue Tracking Software as a Radiology Workflow Management Tool

Wednesday, Dec. 2 3:00PM - 3:10PM Location: S403A

Participants

Nathaniel Swinburne, MD, New York, NY (*Presenter*) Nothing to Disclose Bradley N. Delman, MD, New York, NY (*Abstract Co-Author*) Nothing to Disclose Luke C. Gerke, MD, New York, NY (*Abstract Co-Author*) Nothing to Disclose

Background

While the most basic radiology workflow entails a single viewing of a study by a radiologist and the rendering of a report, often a more complex process is required. A finding may need to be followed up or reviewed with a colleague; an improperly acquired study may necessitate a conversation with the technologist and patient recall for further imaging; a radiology resident may need to be alerted about a missed finding. We noted that these workflows are similar to those encountered in other industries and that a number of generic software packages exist to facilitate such tasks. We hypothesized that Redmine (http://redmine.org), a widely used free, open-source issue tracking application primarily used for software development, could be successfully adapted to handle these workflows within a large academic radiology department.

Evaluation

In 2014, we installed Redmine on a server running behind the department's firewall, ensuring data security and HIPAA compliance. Small modifications to the Redmine source code and PACS configuration files enable bidirectional communication between PACS and Redmine. The radiologist runs the browser-based client alongside PACS and creates an 'issue' in Redmine for a given study. With the installation of one of many existing Redmine plugins, key images may be attached from PACS. A user may be assigned to the issue, indicating responsibility for seeing it to completion. Multiple users may be added as 'watchers', receiving auto-generated emails when the record is updated (e.g., with pathology results or surgical findings). Existing records are viewed in a searchable database, allowing users to manage due dates and priorities and mark issues as resolved.

Discussion

Since launching, over 800 studies have been followed within our department using Redmine, enabling a broad range of issues to be tracked to completion. The application functions as an efficient, crowd-sourced teaching file and quality assurance system.

Conclusion

Workflows encountered in radiology are similar to those found in other industries. Our adaptation of Redmine demonstrates that tools designed for these other industries may be easily adapted for a clinical radiology practice.

SSM13-02 Hooking based Gesture-controlled Interface for Operating Rooms and Reading Rooms without Modification of Source Codes

Wednesday, Dec. 2 3:10PM - 3:20PM Location: S403A

Participants

Ben J. Park, BS, Seoul, Korea, Republic Of (*Presenter*) Nothing to Disclose Taekjin Jang, Seoul, Korea, Republic Of (*Abstract Co-Author*) Nothing to Disclose Namkug Kim, PhD, Seoul, Korea, Republic Of (*Abstract Co-Author*) Stockholder, Coreline Soft, Inc Sang Min Lee, MD, Seoul, Korea, Republic Of (*Abstract Co-Author*) Nothing to Disclose Sang Young Oh, MD, Seoul, Korea, Republic Of (*Abstract Co-Author*) Nothing to Disclose Jong-Woo Choi, Seoul, Korea, Republic Of (*Abstract Co-Author*) Nothing to Disclose

Background

Recent technological advances in gesture based user interface have brought in numerous innovative ideas in viewing medical images. However, despite new attempts constantly being made to replace keyboards and mice, it is hard to find applications used in clinical practice. Physicians required interfaces that maintain aseptic conditions and seamlessly control medical images. Therefore, we developed and applied a message hooking program that maps a gesture to specific functions without any modification of the source codes of frequently used programs.

Evaluation

The program was set up in two different settings with a Leap Motion[™] device for gesture detection. First, we installed this hooking program in the operating room. The aim was to accurately and safely browse images of a rhinoplasty and genioplasty patient from three different programs: CT images from a PACS viewer, volume rendered images from a 3D PACS viewer and patient photos from a basic image viewer. All three programs were seamlessly controlled by gestures and motions solely by the physician.Second, the

program was set up in the reading room to measure the performance compared to traditional input devices. Since contactless interfaces were not required in reading rooms, our goal was to use this program as a secondary device that provide several dominant features. We scanned through 96 images of a dynamic biliary CT study by gestures and compared the results with those of a mouse. Gesture based inputs significantly shortened time required to scan through images, 13.99±1.06 to $8.57\pm0.65sec(p<0.001)$.

Discussion

The most important feature of the program was providing a contactless interface to control medical images from multiple programs without modification of source codes The program can be used solely with the sensor device or together with other input devices. Either way the program provided unparalleled user experience and increased performance in clinical setting.

Conclusion

We developed a message hooking program that detect gestures to control programs and applied it to operating and reading rooms. This program provided surgeons a new way to safely browse images during surgery and increased reading performances for radiologists.

SSM13-03 Does Color Visualization Affect Medical Image Interpretation? Sizing a Clinical Study Using Laboratory Pilot Reader Data

Wednesday, Dec. 2 3:20PM - 3:30PM Location: S403A

Participants

Silvina Zabala Travers, MD, Silver Spring, MD (*Presenter*) Researcher, Barco nv Brandon D. Gallas, PhD, Rockville, MD (*Abstract Co-Author*) Nothing to Disclose Wei-Chung Chen, PHD, Silver Spring, MD (*Abstract Co-Author*) Nothing to Disclose Tom Kimpe, Kortrijk, Belgium (*Abstract Co-Author*) Employee, Barco nv Aldo Badano, PhD, Silver Spring, MD (*Abstract Co-Author*) Research Grant, Barco nv

PURPOSE

The gap between laboratory and clinical studies is a known issue in imaging research. We describe a laboratory study aimed at determining if the choice of color scale and display device hardware affects the visual assessment of functional medical images. In addition, we present methodology for sizing a follow-up clinical study to confirm laboratory findings.

METHOD AND MATERIALS

The experiments used perfusion magnetic resonance imaging (MRI) as the basis for designing and performing the study. Synthetic images resembling dynamic, contrast-enhanced MRI of the brain were used to assess the performance of a rainbow (jet), a heated black-body (hot), and a gray (gray) scale with various display devices on the detection of small changes in intensity. We used a two-alternative, forced-choice design with 17 readers and 600 image pairs on four display devices: a medical-grade three-million-pixel display, a consumer-grade monitor, a tablet device and a phone. We used a custom-made software package (iMRMC) to calculate the percent of correct answers and uncertainties accounting for reader and case variability. We used the software to estimate the number of readers and cases necessary for achieving acceptable levels of statistical power in a follow-up clinical study.

RESULTS

The estimates of percent correct show that jet outperformed hot and gray in the high and low range of the color scales for all devices with a maximum difference in performance of 18% (CI: 6%, 30%). Performance with hot was differently for high and low intensity, comparable with respect to jet for the high range, and worse than gray for lower intensity values. Similar performance was seen between devices using jet and hot while gray performance was better for handheld devices. Time of performance was shorter with jet. The iMRMC sizing estimates indicate that a smaller set of images with fewer readers could provide similar statistical power.

CONCLUSION

Our findings demonstrate that the choice of color scale and display hardware affects the visual comparative analysis of color images.

CLINICAL RELEVANCE/APPLICATION

Color visualization is gaining popularity among imaging techniques. However, little evidence has surfaced on the effect of color on the interpretation of images. Our study suggests that color visualization might affect clinical interpretation and proposes a method to bridge the gap between laboratory and clinical studies to corroborate findings.

SSM13-04 The First High-resolution Mobile Virtual-reality Devices Are Here, Could They Become the Next Step in Mobile Diagnostic Imaging and Enable a New Dimension in Radiology?

Wednesday, Dec. 2 3:30PM - 3:40PM Location: S403A

Participants

Vasileios Moustakas, MD, Athens, Greece (*Presenter*) Nothing to Disclose Demosthenes D. Cokkinos, MD, Athens, Greece (*Abstract Co-Author*) Nothing to Disclose Sofia Tsolaki, Athens, Greece (*Abstract Co-Author*) Nothing to Disclose Theodoros Kolios, MD, Athens, Greece (*Abstract Co-Author*) Nothing to Disclose Maria G. Skilakaki, MD, Athens, Greece (*Abstract Co-Author*) Nothing to Disclose Ploutarhos A Piperopoulos, MD, PhD, Athens, Greece (*Abstract Co-Author*) Nothing to Disclose

PURPOSE

The primary purpose of our research was to obtain one of the first high-resolution mobile virtual-reality (VR) prototypes and see if we could enable VR visualization of dicom images, without compromising stability or image quality, so that this mobile system could then be used for diagnostic imaging. Our secondary purpose was to verify that remote diagnosis of complete CT examinations performed elsewhere, using our mobile VR system, was feasible.

METHOD AND MATERIALS

The mobile VR system weighs only 0.3 kg, it is powered by a high-tech smartphone, with an ultra-high density 550ppi display. Using the system is like being in front of a 175 inch mega screen, while enabling visualization at 360 degrees. Once the dicom images are downloaded to the system via 4G/LTE, the user wears the device and can scroll through the images, viewing up to 56 at any time, while being on the move. Even if our VR system can visualize any dicom image, we chose to test the device using CT images, because it's a modality vastly used by emergency departments and requires the visualization of multiple images, taking advantage of the virtual 175 inch display. Once the VR system was ready, 271 exams were reviewed by a Consultant Radiologist in the hospital. The CT exams were reviewed remotely using VR by another Consultant Radiologist in another area, with no contact to the first examining doctor. The two doctors' independent double blinded reports were compared using standardized reporting systems to assess imaging quality of the VR system in comparison to the hospital's workstation.

RESULTS

In 1318/1355 (97.27%) results complete interobserver agreement was observed. The few 37/1355 (2.73%) contradicting results were limited to evaluations which also often present discrepancies between different examiners on the same monitor.

CONCLUSION

In most of the evaluated parameters, good interobserver agreement showed that the use of our VR system did not affect image quality and therefore did not alter the diagnosis. This technique can be used for remote diagnosis, avoiding the limitations of the relatively small displays of normal mobile devices. Therefore, remote diagnosis of complete CT examinations performed elsewhere using a mobile VR setting is feasible and useful.

CLINICAL RELEVANCE/APPLICATION

Remote diagnosis of CT examinations from a mobile VR device, that provides the equivalent of standing in front of a 175 inch display with a 360 degree view.

SSM13-06 Image Sharing Using Ubiquitous Patient Storage Services as an Alternative to Image Enabled PHR's

Wednesday, Dec. 2 3:50PM - 4:00PM Location: S403A

Participants

Eliot L. Siegel, MD, Severna Park, MD (*Abstract Co-Author*) Research Grant, General Electric Company; Speakers Bureau, Siemens AG; Board of Directors, Carestream Health, Inc; Research Grant, XYBIX Systems, Inc; Research Grant, Steelcase, Inc; Research Grant, Anthro Corp; Research Grant, RedRick Technologies Inc; Research Grant, Evolved Technologies Corporation; Research Grant, Barco nv; Research Grant, Intel Corporation; Research Grant, Dell Inc; Research Grant, Herman Miller, Inc; Research Grant, Virtual Radiology; Research Grant, Anatomical Travelogue, Inc; Medical Advisory Board, Fovia, Inc; Medical Advisory Board, Toshiba Corporation; Medical Advisory Board, McKesson Corporation; Medical Advisory Board, Carestream Health, Inc; Medical Advisory Board, Bayer AG; Research, TeraRecon, Inc; Medical Advisory Board, Bracco Group; Researcher, Bracco Group; Medical Advisory Board, Merge Healthcare Incorporated; Medical Advisory Board, Microsoft Corporation; Researcher, Microsoft Corporation Mohammed Shoura, PhD, Newton, MA (*Abstract Co-Author*) Employee, Paxeramed Corp Mohammed I. Quraishi, MD, Louisville, KY (*Presenter*) Nothing to Disclose

Background

Our initial experience with the RSNA's Image Sharing initiative has been positive with patients reporting a high level of satisfaction with ready access to their own images and reports in the cloud after selecting a commercial image enabled personal health record. However this has required a workflow in which patients who almost never already have an image enabled PHR are required to sign up for one of these PHR providers, create a password, and learn how to interact with the specific PHR system portal. Patients are or will eventually be required to sign up for a paid service for storage and access to these sites. The purpose of our pilot study is to investigate an alternative approach in which a patient's existing cloud storage service can be utilized to store patient images.

Evaluation

A pilot study was performed utilizing a commercial PACS with interfaces to ubiquitously utilized storage available from providers such as Google Drive®, One drive®, DropBox® and others that offer both free and paid storage options to users. Alternatively, users are given the option not to utilize the cloud but to have images "pushed" to the local storage in their smart phones. Images from these various patient directed storage options can be viewed on a single viewer which has interfaces to the commercial email and storage providers. Survey data will be collected to determine the relative efficacy of this alternative standards based approach with regard to patient satisfaction. Relative patient preference for local (smartphone) or cloud storage will also be assessed.

Discussion

Initial experience with the pilot study has been that the approach has the advantages of the current RSNA image sharing approach including elimination of CD's, ready access of images and reports to patients and clinicians without the relative challenges and costs associated with an image enabled PHR provider.

Conclusion

Initial experience with a system that empowers patients to utilize their own existing storage providers for archival and review of images including opting out of cloud storage to store images on their smart phones has been encouraging. Survey results from patients and providers are expected to provide additional insights.

ISP: Cardiac (Congenital Heart Disease/Cardiac Stents)

Wednesday, Dec. 2 3:00PM - 4:00PM Location: S502AB



AMA PRA Category 1 Credit ™: 1.00 ARRT Category A+ Credit: 1.00

Participants

Cynthia K. Rigsby, MD, Chicago, IL (*Moderator*) Nothing to Disclose U. Joseph Schoepf, MD, Charleston, SC (*Moderator*) Research Grant, Bracco Group; Research Grant, Bayer AG; Research Grant, General Electric Company; Research Grant, Siemens AG; Research support, Bayer AG; ; ;

Sub-Events

SSM03-01 Iterative Reconstructions for Imaging of Coronary-Artery Stents with Computed Tomography: First In-vitro Experience

Wednesday, Dec. 2 3:00PM - 3:10PM Location: S502AB

Participants

Tilman Hickethier, MD, Cologne, Germany (*Presenter*) Nothing to Disclose Jan Robert Kroger, MD, Cologne, Germany (*Abstract Co-Author*) Nothing to Disclose Jochen von Spiczak, Muenster, Germany (*Abstract Co-Author*) Nothing to Disclose Bettina Baessler, MD, Cologne, Germany (*Abstract Co-Author*) Nothing to Disclose Dirk K. Mueller, PhD, Hamburg, Germany (*Abstract Co-Author*) Nothing to Disclose Dirk K. Mueller, PhD, Hamburg, Germany (*Abstract Co-Author*) Employee, Koninklijke Philips NV Walter Giepmans, Best, Netherlands (*Abstract Co-Author*) Employee, Koninklijke Philips NV Guido Michels, Cologne, Germany (*Abstract Co-Author*) Nothing to Disclose David C. Maintz, MD, Koln, Germany (*Abstract Co-Author*) Nothing to Disclose Alexander C. Bunck, Koln, Germany (*Abstract Co-Author*) Nothing to Disclose

PURPOSE

In-stent restenosis is one of the most important limitations of coronary angioplasty (PCI). Accurate assessment of coronary stents after PCI using non-invasive CT imaging remains challenging despite new stent materials and improvements in CT technology. New model-based iterative reconstruction (IR) filters have been shown to significantly improve the assessment of native coronary vessels. In our study we systemically evaluated the influence of IR on visualization of coronary stent lumen.

METHOD AND MATERIALS

Ten coronary stents of various materials placed in plastic tubes filled with contrast agent (345 HU) were scanned with a 256-slice CT (iCT, Philips). Images were reconstructed (0.67mm slice thickness, 0.35mm increment) with standard filtered back projection, hybrid IR (iDose L4) and two different model-based IR settings (Cardiac Routine (CR) & Cardiac Sharp (CS)) at 3 strength levels (IMR, Philips). Each stent and reconstruction was assessed using established parameters: image noise (standard deviation (SD) in a standardized ROI), in-stent attenuation (mean attenuation difference between stented and non-stented lumen of the contrast agent-filled tube) and image sharpness (calculated maximum slope of signal intensity profiles across the stents).

RESULTS

Image noise was significantly lower in IMR data, being lowest at higher iteration levels (FBP 25.4/iDose 18.8/IMRCR1 9.6/IMRCR2 6.1/IMRCR3 3.4/IMRCS1 12.9/IMRCS2 8.6/IMRCS3 4.7 HU; p < .01). Differences in attenuation across the stents were significantly smaller in IMR data when applying the CR setting which showed the best depiction of the in-stent attenuation (FBP 372.8/iDose 353.9/IMRCR1 90.1/IMRCR2 110.8/IMRCR3 112.6 HU; p < .01). IMR CS however suppressed stent-blooming artifacts excessively with in parts severely reduced densities in stented tube lumina which might be explained by limitations of spatial resolution.Maximum image sharpness was significantly higher in IMR data (FBP 387.2/iDose 386.8/IMRCR1 656.2/IMRCR2 661.8/IMRCR3 647.0/IMRCS1 845.3/IMRCS2 862.8/IMRCS3 879.7 HU/pixel; p < .01).

CONCLUSION

Well-established objective CT image-quality assessment parameters of coronary stents are significantly improved by using modelbased IR when the adequate setting is applied.

CLINICAL RELEVANCE/APPLICATION

Non-invasive evaluation of coronary stents is an important and challenging task. Model-based IR has the potential of significantly improving coronary-stent assessment.

SSM03-02 Assessment of Iterative Metal Artifact Reduction (iMAR) in Cardiac CT for Patients with Pacemakers and Implantable Defibrillators

Wednesday, Dec. 2 3:10PM - 3:20PM Location: S502AB

Participants

Juan Montoya, Rochester, MN (*Presenter*) Nothing to Disclose Shuai Leng, PhD, Rochester, MN (*Abstract Co-Author*) Nothing to Disclose Ahmed Halaweish, PhD, Rochester, MN (*Abstract Co-Author*) Employee, Siemens AG Cynthia H. McCollough, PhD, Rochester, MN (*Abstract Co-Author*) Research Grant, Siemens AG Eric E. Williamson, MD, Rochester, MN (*Abstract Co-Author*) Research Grant, General Electric Company

PURPOSE

Metal artifacts from pacemaker leads and implantable cardioverter defibrillators (ICD) can significantly obscure relevant anatomy in

cardiac CT. This study aimed to apply iterative metal artifact reduction (iMAR) to Cardiac CT for improved visualization of lead tips and surrounding anatomy in patients with pacemakers and ICDs.

METHOD AND MATERIALS

CT raw data were retrospectively collected for patients that underwent clinically indicated gated CT of the heart using a dualsource CT scanner (Somatom Definition and Definition Flash, Siemens Healthcare) and had a pacemaker or ICD. Images were reconstructed using routine weighted-filtered back projection (WFBP) and a research prototype of cardiac iMAR using an offline reconstruction workstation. A cardiac radiologist evaluated WFBP and iMAR images side-by-side, blinded to the reconstruction method. Another investigator determined post hoc which image was WFBP and iMAR so that the following grading scale was applied to the iMAR images: 1= obviously worse, degrades diagnosis confidence, 2=slightly worse, does not affect diagnosis confidence, 3=equivalent, 4=slightly better, does not affect diagnosis confidence, 5=obviously better, improves diagnosis confidence. For objective metal artifact evaluation, the length of severe artifacts from each lead were measured in multiple axial images. Wilcoxon signed rank test was used to compare the radiologist evaluation as well as the difference in the length of metal artifacts.

RESULTS

16 patients (13 pacemakers, 3 ICDs) had a total of 31 leads. Mean reader grade was 4.5 for iMAR (P-value<0.001) indicating significant improvement of image quality and diagnostic confidence. The average reduction in the length of severe metal artifacts caused by the leads was 4.5 mm using iMAR compared to WFBP (p-value < 0.0001). Better metal artifact reduction was achieved in right ventricle leads, which we suspect is due to increased motion in the right atrium. Two iMAR cases created artifacts in anatomical regions different than lead tips.

CONCLUSION

The use of iMAR for cardiac CT in patients with pacemakers or ICDs can improve the visualization of anatomical structures close to the leads, resulting in improved diagnostic confidence.

CLINICAL RELEVANCE/APPLICATION

The use of iMAR in cardiac CT could improve the visualization of critical anatomy by significantly reducing artifacts from metal devices, leading to improved diagnostic confidence.

SSM03-03 Cardiac Keynote Speaker: Congenital Heart Disease

Wednesday, Dec. 2 3:20PM - 3:40PM Location: S502AB

Participants

Albert De Roos, MD, Leiden, Netherlands (Presenter) Nothing to Disclose

SSM03-05 Pulmonary Insufficiency Assessment by Cardiac Magnetic Resonance: Regurgitation Fraction or Absolute Value of Reverse Volume?

Wednesday, Dec. 2 3:40PM - 3:50PM Location: S502AB

Participants

Francesco Secchi, MD, Milano, Italy (*Presenter*) Nothing to Disclose Marcello Petrini, Milano, Italy (*Abstract Co-Author*) Nothing to Disclose Paola Maria Cannao, MD, San Donato Milanese, Italy (*Abstract Co-Author*) Nothing to Disclose Elda Chiara Resta, Milano, Italy (*Abstract Co-Author*) Nothing to Disclose Massimo Chessa, San Donato Milanese, Italy (*Abstract Co-Author*) Nothing to Disclose Francesco Sardanelli, MD, San Donato Milanese, Italy (*Abstract Co-Author*) Speakers Bureau, Bracco Group Research Grant, Bracco Group Speakers Bureau, Bayer AG Research Grant, Bayer AG Research Grant, IMS International Medical Scientific Mario Carminati, MD, San Donato Milanese, Italy (*Abstract Co-Author*) Nothing to Disclose

PURPOSE

To compare the use pulmonary regurgitation fraction (PRF) or absolute value of pulmonary reverse volume (PRV) in the evaluation of pulmonary insufficiency with cardiac magnetic resonance (CMR).

METHOD AND MATERIALS

We retrospectively studied 44 patients (mean age 23±11 mean value±standard deviation, 17 females and 27 males) with pulmonary/conduit insufficiency due to various congenital heart diseases who underwent CMR (1.5 T) before and after surgical valve implantation (14 patients) or percutaneous Melody valve implantation (30 patients). We performed short axis ECG triggered cine true-FISP (fast imaging with steady state precession) and phase contrast sequences. A reader with four-year of experience in CMR segmented endocardial contours of right ventricle (RV) to obtain end diastolic volume index (EDVi), stroke volume index (SVi) and analyzed the flow. We obtained both PRF (%, retrograde flow divided by anterograde) and PRV (ml/m2) and we correlated them with RVEDVI, SVi and differences (Δ) of RVEDVI before and after procedures. Spearman test was used.

RESULTS

Overall PRF (%), PRV (ml/m2), RVEDVi (ml/m2) and SVi (ml) were 23 \pm 25, 0.29 \pm 0.22, 99 \pm 43 and 45 \pm 16 respectively. RVEDVI was significantly correlated with PRF (r=0.480; P=.001) and PRV (r=0.549; P<.001). RVSVi was significantly correlated with PRF (r=0.605; P<.001) and PRV (r=0.701; P<.001). Δ RVEDVi was significantly correlated with PRF (r=0.427; P=.004) and PRV (r=0.489; P=.001).

CONCLUSION

PRV is stronger correlated with RVEDVi, RVSVi and Δ RVEDVi than PRF.

CLINICAL RELEVANCE/APPLICATION

Pulmonary reverse volume is a stronger indicator of RV dysfunction than regurgitant fraction.

SSM03-06 Assessment and Intervention Planning in Aortic Coarctation Based on Anatomic and 4D PC MRI

Participants

Anja Hennemuth, PhD, Bremen, Germany (*Presenter*) Nothing to Disclose Hanieh Mirzaee, Bremen, Germany (*Abstract Co-Author*) Nothing to Disclose Mathias Neugebauer, Bremen, Germany (*Abstract Co-Author*) Nothing to Disclose Johann Drexl, Bremen, Germany (*Abstract Co-Author*) Nothing to Disclose Christian Schumann, Bremen, Germany (*Abstract Co-Author*) Nothing to Disclose Marcus Kelm, MD, Berlin, Germany (*Abstract Co-Author*) Nothing to Disclose

PURPOSE

Aortic coarctation is a narrowing of the aorta in the region of the transition between the aortic arch and the descending aorta where the fetal ductus arteriosus had joined. The AHA Guidelines recommended therapy for patients with a systolic coarctation pressure gradient of more than 20 mmHg.We have implemented a solution for the non-invasive assessment of aortic diameters and pressure gradients based on an MRI protocol combining a whole heart or angiographic MRI with a 4D PC MRI.

METHOD AND MATERIALS

The EXTENTO software prototype works with a 3D whole heart covering the aortic arch or MR angiography of the aorta for the extraction of the anatomical information and geometrical measurements. This is fused with a 4D PCMRI sequence for the assessment of the corresponding hemodynamics. The workflow consists of an interactive segmentation followed by the exploration of diameters as well as the centerline pressure difference curve for an interactively selected vessel region. Furthermore, pressure maps are visualized in 3D.The provided application has been applied to 5 datasets of patients scheduled for stenting therapy of aortic coarctation (age 11-44). All data were acquired with a Philips Achieva 1.5T scanner. Whole heart volumes were acquired with a resolution of 1.42x1.42x2mm³, 4D PC MRI had a velocity encocing between 3 and 4 m/s, a spatial resolution of 1.41x1.41x2.3mm³, and a temporal resolution of 40ms.

RESULTS

Data processing was possible in all cases and took 10 to 15 minutes. Systolic pressure gradients along the selected centerline sections were between 15 and 22mmHg and clearly visible in the calculated parameter maps.

CONCLUSION

The presented results suggest that the proposed MR imaging protocol and image processing solution could be suitable for the noninvasive assessment of stenoses in clinical practice.

CLINICAL RELEVANCE/APPLICATION

Aortic coarctation occurs in about 7% of all congenital heart defects. The high afterload induced by the stenosis can lead to ventricular dysfunction and thus a major therapy goal is to remove the pressure gradient. Pressure catheters are the standard diagnostic tool for the assessment of intravascular pressures. The suggested imaging and analysis aims at enabling the non-invasive measurement of relevant anatomic and hemodynamic information.

BOOST: Genitourinary-Case-based Review (An Interactive Session)

Wednesday, Dec. 2 3:00PM - 4:15PM Location: S103CD



AMA PRA Category 1 Credits ™: 1.25 ARRT Category A+ Credits: 1.50

Participants

Spencer C. Behr, MD, Burlingame, CA (*Moderator*) Research Grant, General Electric Company; Consultant, General Electric Company Paul Nguyen, Boston, MA (*Moderator*) Consultant, Medivation, Inc; Consultant, GenomeDx Biosciences Inc Daniel J. Margolis, MD, Los Angeles, CA, (daniel.margolis@ucla.edu) (*Presenter*) Research Grant, Siemens AG George B. Rodrigues, MD, London, ON (*Presenter*) Nothing to Disclose Todd Morgan, MD, Ann Arbor, MI (*Presenter*) Research funded, Myriad Genetics, Inc; Research funded, MDxHealth SA Russell Szmulewitz, MD, Chicago, IL (*Presenter*) Advisory Board, Pfizer Inc; Advisory Board, Bayer AG

LEARNING OBJECTIVES

1) To apply oncologic decision making in prostate cancer. 2) To recognize critical clinical manifestations of prostate cancer. 3) To discern clinically significant from insignificant signs and findings in prostate cancer.

Molecular Imaging (Inflammation/Immunology)

Wednesday, Dec. 2 3:00PM - 4:00PM Location: S504CD



AMA PRA Category 1 Credit ™: 1.00 ARRT Category A+ Credit: 1.00

FDA Discussions may include off-label uses.

Participants

Michael S. Gee, MD, PhD, Jamaica Plain, MA (*Moderator*) Nothing to Disclose Tomio Inoue, MD, PhD, Yokohama, Japan (*Moderator*) Nothing to Disclose

Sub-Events

SSM14-01 Assessment of Renal Allograft Pathology by Arterial Spin Labelling and Diffusion Weighted Imaging

Wednesday, Dec. 2 3:00PM - 3:10PM Location: S504CD

Awards

RSNA Country Presents Travel Award

Participants

Katja Hueper, Hannover, Germany (*Presenter*) Nothing to Disclose
Marcel Gutberlet, Dipl Phys, Hannover, Germany (*Abstract Co-Author*) Nothing to Disclose
Dagmar Hartung, MD, Hannover, Germany (*Abstract Co-Author*) Nothing to Disclose
Song Rong, MD, Hannover, Germany (*Abstract Co-Author*) Nothing to Disclose
Frank K. Wacker, MD, Hannover, Germany (*Abstract Co-Author*) Research Grant, Siemens AG Research Grant, Pro Medicus Limited
Faikah Gueler, MD, Hannover, Germany (*Abstract Co-Author*) Nothing to Disclose
Jan Hinrich Braesen, Hannover, Germany (*Abstract Co-Author*) Nothing to Disclose
Bennet J. Hensen, Hanover, Germany (*Abstract Co-Author*) Nothing to Disclose
Martin Meier, PhD, Hannover, Germany (*Abstract Co-Author*) Nothing to Disclose
Rongjun Chen, Hannover, Germany (*Abstract Co-Author*) Nothing to Disclose
Michael Mengel, Edmonton, AB (*Abstract Co-Author*) Nothing to Disclose

PURPOSE

Renal allograft dysfunction early after kidney transplantation (ktx) is frequent, and may be caused by ischemia reperfusion injury or acute rejection. The purpose was to investigate renal allograft pathology in a mouse model of allogenic and isogenic ktx by perfusion imaging with arterial spin labelling (ASL) and diffusion weighted imaging (DWI) in correlation to histology.

METHOD AND MATERIALS

Allograft rejection was induced by allogenic ktx of C57BI/6 (B6)-kidneys to Balb/c-mice in n=14 animals, isogenic ktx (B6-kindeys to B6-mice) was performed in n=18 mice. Cold and warm ischemia times were 60 and 30 min, respectively, in both groups. Healthy B6-mice served as controls. MRI was performed 1 and 6 days after ktx using a 7T-scanner. Flow alternating inversion recovery (FAIR) ASL and DWI sequences (7 b-values) were acquired, and maps of renal perfusion and apparent diffusion coefficient (ADC) were calculated. Renal histology was assessed for rejection and the severity of tubular injury and cell infiltration.

RESULTS

Following allogenic ktx animals developed a T-cell-mediated rejection, whereas isogenic mice had mild tubular injury but no rejection. Renal perfusion at d1 was reduced after allogenic ($262\pm43 \text{ ml}/(\min*100g)$) and isogenic ktx ($335\pm41 \text{ ml}/(\min*100g)$) compared to normal B6-mice ($483\pm23 \text{ ml}/(\min*100g)$, p<0.001). After allogenic ktx, renal perfusion further decreased until d6 and was lower than in the isogenic group ($80\pm13 \text{ vs } 260\pm33 \text{ ml}/(\min*100\text{ml})$, p<0.001). In contrast, ADC was unchanged after isogenic ktx compared to normal B6-mice. In the allogenic group with acute rejection ADC was reduced compared to the isogenic group at d1 ($1.24\pm0.11 \text{ vs } 1.61\pm0.03*10^{-3}\text{mm}^2$ /s, p<0.001) and d6 ($1.09\pm0.04 \text{ vs } 1.55\pm0.07*10^{-3}\text{mm}^2$ /s, p<0.001). Higher tubular injury and inflammation scores and higher percentage of infiltrating T-cells significantly correlated with ADC reduction at d1and6 and perfusion impairment at d6.

CONCLUSION

Renal allograft rejection is associated with progressive perfusion impairment and ADC reduction representing inflammation and cell infiltration. Isogenic ktx with prolonged cold ischemia time leads to moderate perfusion impairment without ADC reduction. MRI parameters correlate with histology.

CLINICAL RELEVANCE/APPLICATION

Functional MRI with ASL and DWI allows differentiation of renal graft pathology after transplantation. Parameters correlate with histology and may improve non-invasive diagnosis in ktx patients.

SSM14-02 The Value of Whole Body Fully Integrated 18F-FDG-PET/MR in Idiopathic Retroperitoneal Fibrosis

Wednesday, Dec. 2 3:10PM - 3:20PM Location: S504CD

Awards Molecular Imaging Travel Award

Participants Ingo Einspieler, Munich, Germany (*Presenter*) Nothing to Disclose Klaus Thurmel, Munich, Germany (*Abstract Co-Author*) Nothing to Disclose Sabine Wolfram, Munich, Germany (*Abstract Co-Author*) Nothing to Disclose Martin Henninger, Munich, Germany (*Abstract Co-Author*) Nothing to Disclose Matthias J. Eiber, MD, Muenchen, Germany (*Abstract Co-Author*) Speakers Bureau, Johnson & Johnson Markus Schwaiger, MD, Munich, Germany (*Abstract Co-Author*) Nothing to Disclose Markus Essler, MD, Muenchen, Germany (*Abstract Co-Author*) Nothing to Disclose

PURPOSE

Idiopathic retroperitoneal fibrosis (IRF) is a rare inflammatory condition potentially leading to severe complications such as renal failure. Besides, there is evidence of associated large vessel vasculitis (LVV), potentially causing life-threatening consequences such as vessel stenosis and aneurysms. Therefore, early and precise assessment of both disease extent and activity is essential to guide therapy decision. Due to the lack of reliable parameters to objectively assess the degree of inflammation, imaging by whole body 18F-FDG PET/MR might help as a new approach.

METHOD AND MATERIALS

14 whole body 18F-FDG-PET/MR examinations were performed in 12 patients with IRF. T1 and T2 sequences were used for anatomical localization of FDG uptake and identification of morphological changes associated with IRF. Contrast enhanced-MRA was performed to judge changes of the vessel lumen. IRF tissue volume was calculated on MRI in cm3. FDG-uptake was assessed visually (using a 4-point scale) and quantitatively (maximal standardized uptake value [SUV max], target to background ratio [TBR]). Correlations between PET/MR findings (SUV max, TBR, visual score, IRF volume) and DAS (disease activity score), combining typical clinical symptoms for IRF, CRP/ESR/IL-6 levels and results of previous examinations by ultrasound, CT and MRI, were analyzed. Intended therapeutic management was documented before and after availability of PET/MR findings.

RESULTS

DAS classified 7 cases as having active disease and 7 as inactive. In contrast, PET/MR revealed active IRF in 10/14 cases and changed disease status according to DAS in 5 cases (36%), more specifically in 4 cases from inactive to active disease and active to inactive disease in 1 case. There was no association between DAS and the various PET/MR findings (p > 0.05). PET/MR showed vessel changes suggestive for active LVV in 3 cases. In addition, PET/MR imaging results had impact on therapeutic management in 6/14 cases (43%), in particular by starting or avoiding immunosuppressive therapy.

CONCLUSION

Whole body 18F-FDG-PET/MR may be considered as a useful approach for aiding in the management of patients with IRF.

CLINICAL RELEVANCE/APPLICATION

In IRF there is still a lack of reliable parameters to objectively assess the degree of inflammation and to guide therapy decisions. Imaging by whole body 18F-FDG PET/MR might help as a new approach.

SSM14-03 Glycosaminoglycan Chemical Exchange Saturation Transfer of Lumbar Intervertebral Discs in Patients with Spondyloarthritis

Wednesday, Dec. 2 3:20PM - 3:30PM Location: S504CD

Awards

Molecular Imaging Travel Award

Participants

Christoph Schleich, Dusseldorf, Germany (*Presenter*) Nothing to Disclose Anja Lutz, Dusseldorf, Germany (*Abstract Co-Author*) Nothing to Disclose Joel Aissa, Duesseldorf, Germany (*Abstract Co-Author*) Nothing to Disclose Philipp Sewerin, Dusseldorf, Germany (*Abstract Co-Author*) Nothing to Disclose Ruben Sengewein, Duesseldorf, Germany (*Abstract Co-Author*) Nothing to Disclose Benedikt Ostendorf, Dusseldorf, Germany (*Abstract Co-Author*) Nothing to Disclose Benjamin Schmitt, Vienna, Austria (*Abstract Co-Author*) Nothing to Disclose Gerald Antoch, MD, Duesseldorf, Germany (*Abstract Co-Author*) Nothing to Disclose Falk R. Miese, MD, Dusseldorf, Germany (*Abstract Co-Author*) Nothing to Disclose

PURPOSE

To assess glycosaminoglycan (GAG) content of lumbar intervertebral discs (IVD) in patients with spondyloarthritis (SpA) using glycosaminoglycan chemical exchange saturation transfer (gagCEST).

METHOD AND MATERIALS

Ninety lumbar intervertebral discs of nine patients with SpA and nine age-matched healthy controls (eight patients with ankylosing spondylitis; one patient with spondylitis related to inflammatory bowel disease; mean age: 44.1 ± 14.0 years; range: 27 - 72 years) were examined at a 3T MRI scanner in this prospective study. The MRI protocol included standard morphological, sagittal T2 weighted (T2w) images to assess Pfirrmann score of the five lumbar IVDs (L1 to S1) and biochemical imaging with gagCEST to calculate a region-of-interest analysis of nucleus pulposus (NP) and annulus fibrosus (AF). Prior to statistical testing of gagCEST effects (MTRasym values in %) in patients and controls, IVDs were classified according to the Pfirrmann score.

RESULTS

Significantly lower gagCEST values of NP and AF were found in SpA patients compared with healthy volunteers (NP: 1.41 % \pm 0.41 %, p = 0.001; 95%-confidence interval, CI [0.600% - 2.226 %]; AF: 1.19 % \pm 0.32 %, p < 0.001; CI [0.560 % - 1.822 %]) by comparing the differences of the means. Pooled non-degenerative IVDs (Pfirrmann 1 and 2) had significantly lower gagCEST effects in patients suffering from SpA compared with healthy controls in NP (p < 0.001; CI [1.176 % - 2.337 %]) and AF (p < 0.001; CI [0.858 % - 1.779 %]). No significant difference of MTRasym values was found in degenerative IVDs between patients and controls in NP (p = 0.204; CI [-0.504 % - 2.170 %]).

CONCLUSION

GagCEST analysis of morphologically non-degenerative IVDs (Pfirrmann score 1 and 2) in T2w images demonstrated significantly

lower GAG values in patients with spondyloarthritis in NP and AF possibly representing a depletion of GAG in spondyloarthritis in the absence of morphologic degeneration.

CLINICAL RELEVANCE/APPLICATION

GagCEST may be a powerful tool to access IVD composition in spondyloarthritis and to investigate therapy effects on GAG content in advanced studies.

SSM14-04 Preliminary Experience with 3T Time of Flight Simultaneous Cardiac PET/MRI in the Evaluation of Cardiac Sarcoidosis

Wednesday, Dec. 2 3:30PM - 3:40PM Location: S504CD

Awards

Trainee Research Prize - Fellow

Participants

Kate Hanneman, MD, Toronto, ON (*Presenter*) Nothing to Disclose Andrei Iagaru, MD, Stanford, CA (*Abstract Co-Author*) Research Grant, General Electric Company; Research Grant, Bayer AG Henry Guo, Stanford, CA (*Abstract Co-Author*) Nothing to Disclose Amir Barkhodari, Stanford, CA (*Abstract Co-Author*) Nothing to Disclose Mehran Jamali, Stanford, CA (*Abstract Co-Author*) Nothing to Disclose Dawn Holley, Stanford, CA (*Abstract Co-Author*) Nothing to Disclose Robert J. Herfkens, MD, Stanford, CA (*Abstract Co-Author*) Nothing to Disclose

PURPOSE

The aim of this study is to investigate the utility of simultaneous time of flight (TOF) cardiac PET/MRI in the evaluation of cardiac sarcoidosis.

METHOD AND MATERIALS

Six consecutive patients (50% male, 53.3±12.3 years) were prospectively recruited over a 3-month period for parallel assessment of suspected cardiac sarcoidosis by standard clinical evaluation and simultaneous PET/MRI. Five healthy volunteers were initially scanned for protocol optimization. Patients first underwent standard cardiac PET/CT (Discovery 600 or 690, GE Healthcare) after administration of 9.7±0.4 mCi of 18F FDG. This was followed by a cardiac PET/MRI using a simultaneous scanner with TOF and 3T (Signa, GE Healthcare). Participants were prepared with 8-hour dietary instructions in order to suppress physiologic myocardial glucose uptake. Cardiac MRI sequences included breath-hold, ECG-triggered cine SSFP, T2-weighted, T1-mapping (pre- and postcontrast), and delayed myocardial enhanced (DME). Three experienced readers performed image analysis using an independent workstation with dedicated post-processing software.

RESULTS

PET/CT was acquired with a delay of 95.8 ± 26.6 min, while PET/MRI had a delay of 195.5 ± 35.6 min from 18F FDG injection. Total scan time for PET/MRI was significantly longer than for PET/CT (75.8 ± 17.7 vs. 36.6 ± 6.3 min, p=0.016). PET from PET/CT was positive for cardiac sarcoidosis in 50% of patients, while PET from PET/MRI was positive for cardiac sarcoidosis in 100% of patients. LV measurements by MRI were: EDV (159.3 ± 3.5 mL), ESV (87.6 ± 50.0 mL), LVEF (47.3 ± 19.7 %), pre-contrast T1 (1455.9 ± 25.6 ms), post-contrast T1 (307.0 ± 63.6 ms) and extra-cellular volume (ECV) (38.5%). DME and T2 hyper-intensity were identified in 67% and 33% of patients, respectively. There was a significant difference in effective radiation dose (ED) between PET/CT and PET/MRI (p=0.007). ED from the CT component of the PET/CT exam alone was 4.6 ± 1.4 mSv.

CONCLUSION

Simultaneous cardiac PET/MRI is feasible achieving diagnostic image quality with the added benefit of radiation dose reduction in comparison to PET/CT.

CLINICAL RELEVANCE/APPLICATION

Simultaneous cardiac PET/MRI is feasible, and provides additional information over PET/CT, potentially reducing the number of exams for patients.

SSM14-05 Role of FDG PET/CT for the Detection of Renal Infections in Cases of Pyrexia of Unknown Origin

Wednesday, Dec. 2 3:40PM - 3:50PM Location: S504CD

Participants

Sikandar M. Shaikh, DMRD, Hyderabad, India (*Presenter*) Nothing to Disclose Hrushikesh Aurangabadkar, Hyderabad, India (*Abstract Co-Author*) Nothing to Disclose Madhur K. Srivastava SR, MBBS, Chennai, India (*Abstract Co-Author*) Nothing to Disclose

PURPOSE

Patients with pyrexia of unknown origin were evaluated by FDG PET/CT for the detection of renal infections

METHOD AND MATERIALS

26 patients underwent FDG PET/CT for the detection of infection foci involving the kidneys. Positive FDG PET/CT findings and pathological correlation served as the main outcome measures.

RESULTS

Of the 26 study patients, 18 (70.2%) had positive FDG PET/CT findings and a total of 24 major infection foci were identified. Five patients (24.6%) had at least two infection foci on FDG PET/CT scans. Two (53.8%) of the 3 patients with primary renal infections had concurrent multiple foci. seven patients (26.9%) had their treatments modified by FDG PET/CT results. Multivariate logistic regression analysis demonstrated that leucocyte count at diagnosis along with correlation with positive FDG PET/CT results. seven patients (26.0%) landed in hemodialysis during their hospital stay, and 6 of them had positive FDG PET/CT findings (P = 0.014). Positive FDG PET/CT results were an independent predictor of mortality (hazard ratio [HR]=3.896, 95% CI=1.039-14.613, P =

0.044).

CONCLUSION

Our results suggest that FDG PET/CT is clinically useful for detecting occult infection foci in renal infections. In this population, positive FDG PET/CT findings may lead to a significant change in clinical management and independently predict mortality.

CLINICAL RELEVANCE/APPLICATION

PET-CT IS HIGHLY SENSITIVE IN EVALUATING THE RENAL INFECTION IN CONTEXT OF PYREXIA OF UNKNOWN ORIGIN.

SSM14-06 Image Monitoring of Impaired Phagocytic Activity of Kupffer Cells and Liver Oxygen Saturation in a Mouse Cholangitis Model Using Sonazoid-Enhanced US and Photoacoustic Image

Wednesday, Dec. 2 3:50PM - 4:00PM Location: S504CD

Participants

Jung Hoon Kim, MD, Seoul, Korea, Republic Of (*Presenter*) Nothing to Disclose Seo-Youn Choi, MD, Bucheon, Korea, Republic Of (*Abstract Co-Author*) Nothing to Disclose Hyo Won Eun, MD, PhD, Seoul, Korea, Republic Of (*Abstract Co-Author*) Nothing to Disclose Seunghyun Lee, Seoul, Korea, Republic Of (*Abstract Co-Author*) Nothing to Disclose Joon Koo Han, MD, Seoul, Korea, Republic Of (*Abstract Co-Author*) Nothing to Disclose

PURPOSE

To investigate serial change of impaired phagocytic activity of Kupffer cells and liver Oxygen Saturation (sO2) in a mouse cholangitis model using sonazoid enhanced US (SEUS) and photoacoustic image (PI)

METHOD AND MATERIALS

Mouse cholangitis models were created by ligation of common bile duct (n=20, G1), left intrahepatic bile duct (n=19, G2-left and G2-right) and compared with control (n=14, G3). SEUS and PI were performed at 1, 2, and 4 weeks. PA images were collected at 750 and 850 nm and parametric maps of sO2 were generated. Serial change of echogenicity on the Kupffer phase and liver sO2were measured in each groups. Serial changes in each group were analyzed using one way ANOVA with Bonferroni's method. Kupffer cell fraction using CD68 immunohistochemistry stain was also compared with SEUS.

RESULTS

Serial change of sonazoid enhacement enhancement showed decreased in G1 ($15.1 + 8.6 \times 10-5$) and G2-left ($9.3+7.9 \times 10-5$) than G2-right ($248.8+253.3 \times 10-5$) and control ($153.7+34.7 \times 10-5$). However, Kupffer cell fraction showed increased in G1 (36.1+7.1%) and G2-left (26.8+5.1%) than G2-right (16.6+5.6%) and control (12.3+3.3%), suggesting impaired phagocytic activity of Kupffer cells. Liver sO2 showed decreased in G1 (24.0+8.0%) and G2-left (22.7+8.4%) than G2-right (39.1+12.0%) and control (41.7+8.1%).

CONCLUSION

SEUS and PI are useful for monitoring of serial change of impaired phagocytic activity of Kupffer cells and liver sO2 in a mouse cholangitis model.

CLINICAL RELEVANCE/APPLICATION

SEUS and PI are feasible to assess the serial change of phagocytic activity of Kupffer cells and liver sO2 in a mouse cholangitis model.

Emergency Radiology (Neurologic Emergencies)

Wednesday, Dec. 2 3:00PM - 4:00PM Location: S403B



AMA PRA Category 1 Credit ™: 1.00 ARRT Category A+ Credit: 1.00

Participants

Clint W. Sliker, MD, Ellicott City, MD (*Moderator*) Nothing to Disclose Savvas Nicolaou, MD, Vancouver, BC (*Moderator*) Institutional research agreement, Siemens AG

Sub-Events

SSM07-01 Utility of Repeat Head CT in Mild Traumatic Brain Injury (mTBI) Patients Presenting with Small Isolated Falcine or Tentorial Subdural Hematoma (SDH)

Wednesday, Dec. 2 3:00PM - 3:10PM Location: S403B

Participants

Kavi K. Devulapalli, MD, MPH, San Francisco, CA (*Presenter*) Nothing to Disclose
Alisa D. Gean, MD, San Francisco, CA (*Abstract Co-Author*) Medical Advisory Board, Samsung Electronics Co Ltd Speakers Bureau, Educational Symposium International Stockholder, Global Indemnity plc Spouse, Employee, Global Indemnity plc
Jared A. Narvid, MD, San Francisco, CA (*Abstract Co-Author*) Nothing to Disclose
Esther L. Yuh, MD, PhD, Stanford, CA (*Abstract Co-Author*) Nothing to Disclose
Bhavya Rehani, MD, San Francisco, CA (*Abstract Co-Author*) Nothing to Disclose
Michael C. Huang, MD, San Francisco, CA (*Abstract Co-Author*) Nothing to Disclose
David McCoy, San Francisco, CA (*Abstract Co-Author*) Nothing to Disclose
Alina Uzelac, MD, Mill Valley, CA (*Abstract Co-Author*) Nothing to Disclose
Jason F. Talbott, MD, PhD, San Francisco, CA (*Abstract Co-Author*) Nothing to Disclose

PURPOSE

In cases of mTBI with acute intracranial hemorrhage, serial head CT (hCT) scans to evaluate stability are routinely performed, even in cases of isolated small hemorrhages which are not easily accessible for surgical decompression. This practice has not been validated, and repeat exams frequently necessitate increased emergency room stay times, ICU monitoring, and additional exposure to ionizing radiation. The goal of this study is to evaluate clinical and imaging features of isolated falcine and tentorial SDH at presentation and short term follow-up.

METHOD AND MATERIALS

A retrospective analysis of all patients presenting to our Level 1 trauma center from January 2013 through March 2015 undergoing initial and short-term follow-up hCT with initial findings positive for isolated SDH along the falx and/or tentorium was performed. Patients with penetrating trauma, other sites of intracranial hemorrhage, brain contusion, or depressed skull fractures were excluded. Clinical information including gender, age and history of anticoagulation was obtained through review of electronic medical records.

RESULTS

90 patients met inclusion criteria (55 males; 35 females; average age 57.8 years). 63% of SDHs were falcine, 32% tentorial and 5% mixed. On average, isolated falcotentorial SDHs were small (mean thickness = 2.7mm; range 2-8mm), without significant mass effect, and decreased in size on follow-up hCT with an average follow-up time of 8.4 hours. Increase in SDH size was seen in 3 patients (3%) with average increase in SDH thickness of 3.3-mm. No new intracranial hemorrhages were seen on follow-up hCT. 2 of 3 patients with increase in SDH were anti-coagulated (average INR = 3.8) and the remaining patient had a depressed platelet count. In total, nine patients (10%) were anti-coagulated at presentation with mean INR=3.2 (range 2.1-4.9).

CONCLUSION

Isolated falcine and tentorial SDHs in mild TBI are small and rarely increase in size on short term followup hCT. Present data suggest repeat hCT in mTBI patients with isolated falcine or tentorial SDH who are not anti-coagulated is unnecessary for assessing stability of hemorrhage. In anti-coagulated patients and patients with low platelet counts, follow-up imaging is advisable.

CLINICAL RELEVANCE/APPLICATION

Isolated parafalcine and paratentorial SDH are common findings after trauma and often necessitate repeat imaging. This project may help guide clinical decision making with regards to repeat imaging.

SSM07-02 Traumatic Midline Subarachnoid Hemorrhages on Initial Computed Tomography as Markers of Severe Diffuse Axonal Injury

Wednesday, Dec. 2 3:10PM - 3:20PM Location: S403B

Awards

Trainee Research Prize - Fellow

Participants

Daddy Mata Mbemba, MD, PhD, Sendai, Japan (*Presenter*) Nothing to Disclose Shunji Mugikura, MD, PhD, Sendai, Japan (*Abstract Co-Author*) Nothing to Disclose Atsuhiro Nakagawa, Sendai, Japan (*Abstract Co-Author*) Nothing to Disclose Takaki Murata, MD, Sendai, Japan (*Abstract Co-Author*) Nothing to Disclose Yasuko Tatewaki, MD, Sendai, Japan (*Abstract Co-Author*) Nothing to Disclose Yumiko Kato, MD, Sendai, Japan (*Abstract Co-Author*) Nothing to Disclose Li Li, MD, PhD, Sendai, Japan (*Abstract Co-Author*) Nothing to Disclose Teiji Tominaga, Sendai, Japan (*Abstract Co-Author*) Nothing to Disclose Shoki Takahashi, MD, Aoba, Japan (*Abstract Co-Author*) Nothing to Disclose Kei Takase, MD, PhD, Sendai, Japan (*Abstract Co-Author*) Nothing to Disclose

PURPOSE

The presence of intraventricular hemorrhage (IVH) on initial CT (iCT) has been recently reported to predict diffuse axonal injury (DAI) located in the corpus callosum or brain stem (severe DAI) on subsequent MRI. We aimed to test the hypothesis that midline (interhemispheric and perimesencephalic) subarachnoid hemorrhages (SAH) commonly associated with IVH on iCT could have a similar clinical value in predicting severe DAI.

METHOD AND MATERIALS

Consecutive 270 head trauma patients who underwent iCT within 24 hours and MRI within 30 days were included. First, as potential CT predictors of DAI, we used the following 6 CT items included in Marshall or Rotterdam CT scores: status of basal cistern, status of midline shift, epidural hematoma, IVH, SAH, and volume of hemorrhagic mass. Next, SAH were searched at cerebral cortices, sylvian fissures, sylvian vallecula, cerebellar folia, interhemispheric fissure, and perimesencephalic cisterns and a 7-grade (0 to 6, 0 means no SAH) SAH severity score based on these locations was assigned to each patient. Based on MRI results, patients were divided in two groups of DAI positive and DAI negative, and were assigned a following DAI staging reported to be prognostic of functional outcome, stage 3 being the worst: stage 0: no DAI, 1: DAI in the lobar white matter or cerebellum, 2: DAI in the corpus callosum with or without stage 1 lesions, and 3: DAI in the brain stem with or without stages 1 or 2 lesions.

RESULTS

77 (28.5%) of 270 patients had DAI. Of the 6 CT items, IVH and SAH were independently associated with DAI (both P<0.05). Of the locations, the interhemispheric and perimesencephalic SAH were the independent predictors of DAI (both P<0.05). SAH score and DAI staging showed significant positive correlation (P<0.0001). SAH score in DAI stage 3 or stage 2 was significantly higher than that of DAI stage 0 (both, P <0.0001). No statistical significant difference was noted in SAH score between DAI stages 0 and 1. The presence of midline SAH on iCT had sensitivity of 60.7%, specificity of 81.8%, PPV of 43.6% and NPV of 90% in predicting severe DAI.

CONCLUSION

Midline SAH on iCT are makers of DAI, specifically severe DAI. Using them as markers could greatly reduce unnecessary MRI in head trauma patients

CLINICAL RELEVANCE/APPLICATION

Knowing that midline SAH on iCT has the same value as IVH in predicting severe DAI assists clinician to properly select head trauma patients who should undergo subsequent MRI.

SSM07-03 Delayed Intracranial Hemorrhage (ICH) in Patients Receiving Anti-coagulant or Prescription Antiplatelet (ACAP) Medication after Mild Blunt Trauma: Is Repeat hCT Necessary?

Wednesday, Dec. 2 3:20PM - 3:30PM Location: S403B

Participants

Kavi K. Devulapalli, MD, MPH, San Francisco, CA (Presenter) Nothing to Disclose

Alina Uzelac, MD, Mill Valley, CA (Abstract Co-Author) Nothing to Disclose

Esther L. Yuh, MD, PhD, Stanford, CA (Abstract Co-Author) Nothing to Disclose

David McCoy, San Francisco, CA (Abstract Co-Author) Nothing to Disclose

Alisa D. Gean, MD, San Francisco, CA (*Abstract Co-Author*) Medical Advisory Board, Samsung Electronics Co Ltd Speakers Bureau, Educational Symposium International Stockholder, Global Indemnity plc Spouse, Employee, Global Indemnity plc

Michael C. Huang, MD, San Francisco, CA (*Abstract Co-Author*) Nothing to Disclose

Jason F. Talbott, MD, PhD, San Francisco, CA (Abstract Co-Author) Data Safety Monitoring Board, StemCells, Inc

PURPOSE

Current literature is conflicted with respect to the risk of delayed intracranial hemorrhage (ICH) in patients undergoing ACAP medication after blunt head trauma. Short interval follow-up hCT after an initially negative hCT is routine practice at many institutions. Given the rise in patients on ACAP therapy, we sought to formally evaluate our institution's 6-hour repeat hCT protocol in this population who present with an initially negative hCT after blunt trauma.

METHOD AND MATERIALS

A retrospective query of our radiologic database was performed to identify all consecutive non-contrast hCT studies performed between January 2013 and November 2014 using search terms for generic and commercial names of ten common anticoagulation and prescription anti-platelet medications in addition to the general terms "anticoagulant", "anticoagulation" and "blood thinner." Studies were further screened on the basis of a prior CT within 24 hours, which was performed because of trauma and negative for intracranial traumatic pathology. Patients with indications for follow-up imaging other than ACAP use were excluded.

RESULTS

A total of 216 patients met inclusion criteria with only 2/216 (0.9%) developing delayed ICH. Both patients with delayed ICH were found to have trace volume subarachnoid hemorrhage in the ambient cistern, however without associated neurologic deficit or new symptoms. Both of these patients were receiving Coumadin anticoagulation with average INR of 2.5 at the time of admission and were subsequently treated to reverse their anticoagulation and discharged after short ICU observation without adverse event.

CONCLUSION

In our study, the incidence of delayed intracranial hemorrhage in patients receiving ACAP therapy was very small (<1%). The rare cases with delayed ICH were clinically silent. Present data build upon previous literature and lend further evidence that a short-interval follow-up CT among patients receiving ACAP therapy with an initially negative hCT after trauma may be unnecessary.

Head CT is commonly performed after blunt trauma. Results from this study may help to guide clinical deicision making regarding imaging in a subset of patients taking anti-coagulant or prescription anti-platelet medication.

SSM07-04 High-pitch Paranasal Sinus CT in Drunken Emergency Room Patients after Assault - Initial Results on Image Quality and Dose with Third-generation Dual-source CT

Wednesday, Dec. 2 3:30PM - 3:40PM Location: S403B

Participants

Claudia Frellesen, Frankfurt, Germany (*Abstract Co-Author*) Nothing to Disclose Patricia Dewes, MD, Frankfurt, Germany (*Presenter*) Nothing to Disclose Boris Schulz, MD, Frankfurt Am Main, Germany (*Abstract Co-Author*) Nothing to Disclose Jan-Erik Scholtz, MD, Frankfurt, Germany (*Abstract Co-Author*) Nothing to Disclose Josef Matthias Kerl, MD, Frankfurt, Germany (*Abstract Co-Author*) Research Consultant, Siemens AG Speakers Bureau, Siemens AG Thomas J. Vogl, MD, PhD, Frankfurt, Germany (*Abstract Co-Author*) Nothing to Disclose Ralf W. Bauer, MD, Frankfurt, Germany (*Abstract Co-Author*) Research Consultant, Siemens AG Speakers Bureau, Siemens AG

PURPOSE

Image quality benefits from high-pitch scanning in agitated patients by freezing patient motion. We compared image quality and exposure parameters in patients with suspected maxillofacial fractures on second- and third-generation dual-source CT (DSCT)

METHOD AND MATERIALS

4 groups with 30 patients each were compared according CTDIvol, DLP, acquisition time and subjective image quality. The first group was examined on a second-generation DSCT (Flash, Siemens) with fixed 120 kV/50 mAs, pitch 3.0. The other three groups were examined on a third-generation DSCT (Force, Siemens): group 1 with fixed 120 kV/50 mAs and pitch 2.2; group 3 and 4 with fixed 120kV and automated exposure control (AEC) with 50 ref.mAs and pitch factors of 2.2 and 3.0, respectively. Images in groups 2-4 were reconstructed with iterative reconstruction (ADMIRE), in group 1 with FBP

RESULTS

Median CTDIvol (2.76 vs. 2.66 vs. 0.66 vs. 0.69 mGy) and DLP (58 vs. 41 vs. 13 vs. 14 mGycm) were significant lower in group 3 and 4 scanned on the third-generation DSCT with AEC (-76%/-75% and -75%/74%; p < 0.0001) without significant difference among each other. Subjective image quality was rated best in group 2 followed by group 3, both with a pitch factor of 2.2 (average scores: 1.87/1.70 vs. 1.40/1.30 vs. 1.63/1.50 vs. 2.43/2.27). Due to strong high-pitch artefacts the subjective image quality of group 4 was inferior to all other groups. Median acquisition time was significant faster using third-generation DSCT (450 ms vs. 300 ms vs. 380 ms vs. 270 ms; p < 0.05).

CONCLUSION

Third-generation DSCT yields faster acquisition times and substantial radiation dose reduction using AEC. A pitch of 2.2 should be preferred since high-pitch artefacts are reduced. Although AEC was used, subjective image quality remains stable and reliable with iterative reconstruction

CLINICAL RELEVANCE/APPLICATION

Faster CT examination of agitated patients with suspected maxillofacial trauma with reduced radiation exposure and reliable image quality.

SSM07-06 Dual Energy in Noncontrast Head CT: Differentiation of Calcification from Acute Hemorrhage

Wednesday, Dec. 2 3:50PM - 4:00PM Location: S403B

Participants

Christopher A. Potter, MD, Boston, MA (*Presenter*) Nothing to Disclose Andrew Primak, PhD, Malvern, PA (*Abstract Co-Author*) Employee, Siemens AG Aaron D. Sodickson, MD, PhD, Wayland, MA (*Abstract Co-Author*) Research Grant, Siemens AG; Consultant, Bracco Group

PURPOSE

To evaluate whether a novel DECT postprocessing application that separates calcification from hemorrhage can reliably differentiate these materials in non-contrast head CT foci in an indeterminate Hounsfield Unit (HU) range.

METHOD AND MATERIALS

DECT acquisitions of noncontrast head CTs were performed in the Emergency Department on a 128x2 slice dual-energy scanner (Siemens FLASH, Forchheim Germany). All scans containing foci of intracranial calcification or hemorrhage of 50-85 HU were included. Foci were designated as calcium or hemorrhage based on typical morphology or confirmatory imaging. DECT acquisitions used tube voltages 100/Sn140 kVp and tube current modulation (CareDose4D) using reference mAs 300/300. Source images from each tube were reconstructed as 0.75 x 0.5 mm slices and used for postprocessing on thin-client server (Syngo via, version VA30). The Brain Hemorrhage 3-material decomposition application designed to differentiate iodine from hemorrhage was modified by changing the iodine dual energy ratio to the calcium ratio of 1.44. Dual energy regions of interest (ROI) were placed to measure HU and standard deviation (std) in the mixed high/low kVp image, and the corresponding virtual non-calcium (VNCa) and calcium-map (Ca) images. CTDIvol and DLP values were recorded.

RESULTS

10 foci each of calcification and hemorrhage were analyzed. Foci could not be differentiated based on mixed-image HUs (unpaired t-test p=0.24), with mean +/- std (range) of 63 +/- 7 (55-73) HU for hemorrhage and 68 +/- 12 (52-84) for calcification. VNCa and Ca images demonstrated excellent separation of hemorrhagic from calcified foci (both p<0.0001). Calculated HU due to calcium content was 4 +/- 10 (-7-26) HU in hemorrhages and 48 +/- 15 (28-72) in calcific foci. VNCa content was 58 +/- 12 (44-80) HU in hemorrhages and 20 +/- 7 (10-28) in calcific foci. A VNCa threshold value of greater than 35 HU correctly attributed all hemorrhage and calcium cases. X-ray tube output mean +/- std (range) values were CTDIvol 48 +/- 4 (40-54) mGy and DLP 842

CONCLUSION

DECT can reliably differentiate intracranial calcification from hemorrhage in a proof-of-principle cohort of indeterminate HU value foci where densities typically overlap.

CLINICAL RELEVANCE/APPLICATION

DECT shows promise in differentiating foci of hemorrhage from calcification in ranges where HU values overlap, which may be beneficial when HU values alone are not definitive.

Honored Educators

Presenters or authors on this event have been recognized as RSNA Honored Educators for participating in multiple qualifying educational activities. Honored Educators are invested in furthering the profession of radiology by delivering high-quality educational content in their field of study. Learn how you can become an honored educator by visiting the website at: https://www.rsna.org/Honored-Educator-Award/

Aaron D. Sodickson, MD, PhD - 2014 Honored Educator

Chest (Vascular/ Radiation Dose Reduction)

Wednesday, Dec. 2 3:00PM - 4:00PM Location: S404CD

СН СТ SQ

AMA PRA Category 1 Credit ™: 1.00 ARRT Category A+ Credit: 1.00

Participants

Edith M. Marom, MD, Ramat Gan, Israel (*Moderator*) Nothing to Disclose Brett W. Carter, MD, Houston, TX (*Moderator*) Author, Reed Elsevier; Consultant, St. Jude Medical, Inc; ;

Sub-Events

SSM05-01 Dual Energy Pulmonary CT Angiography with a 3rd Generation Dual Source CT System Using 5.4g of Iodine in Comparison to a Second Generation DSCT Scan with 32g of Iodine: A Feasibility Study

Wednesday, Dec. 2 3:00PM - 3:10PM Location: S404CD

Awards

Trainee Research Prize - Resident

Participants

Mathias Meyer, Mannheim, Germany (*Presenter*) Speaker, Siemens AG; Speaker, Bracco Group Holger Haubenreisser, Mannheim, Germany (*Abstract Co-Author*) Speaker, Siemens AG; Speaker, Bayer AG Sonja Sudarski, MD, Mannheim, Germany (*Abstract Co-Author*) Nothing to Disclose Stefan O. Schoenberg, MD, PhD, Mannheim, Germany (*Abstract Co-Author*) Institutional research agreement, Siemens AG Thomas Henzler, MD, Mannheim, Germany (*Abstract Co-Author*) Nothing to Disclose

PURPOSE

To compare objective and subjective image quality between a dual-energy (DE) CT pulmonary angiography (CTPA) protocol using a 5.4g of iodine load versus standard CTPA protocols using a 32g iodine load.

METHOD AND MATERIALS

This prospective IRB-approved study included 150 in-patients/emergency patients with suspected pulmonary embolism (78 male; mean age 65±17 years). Fifty patients who were examined on a 3rd generation dual-source CT (DSCT) with a newly optimized DE CTPA protocol had chronic renal insufficiency (estimated glomerular filtration rate <60ml/min/1.73mSquared) and thus received a low contrast media injection of 5.4g iodine. Each of these fifty patients were either examined with a standard CTPA protocol or a standard DE CTPA receiving an iodine load of 32g. For the DE CTPA virtual monochromatic spectral (VMS) datasets at 40-100keV were reconstructed. The optimal mean photon energy was determined, and subjective and objective image quality were evaluated and compared between these datasets. Comparisons between the groups were analyzed with two-way ANOVA or Wilcoxon-Rank-Sum Test depending on the distribution of the data.

RESULTS

For the main pulmonary arteries the 50keV and for the peripheral pulmonary arteries the 40keV dataset provided the highest contrast-to-noise-ratio (CNR) for both DE CTPA protocols, with significantly higher CNR values for the standard DE CTPA protocol (p<0.05). These 40/50keV VMS datasets resulted in significantly higher CNRs if compared to the standard CTPA protocol for both the main and peripheral pulmonary arteries, again for both DE CTPA protocols (p<0.05). Subjective image quality did not significantly differ for both DE CTPA protocols when compared to the standard CTPA protocol (p>0.05).

CONCLUSION

DE CTPA utilizing image reconstruction at 40/50keV allows for a significant reduction in iodine load while improving vascular signal intensity and maintaining CNR which is especially important in patients with chronic renal insufficiency.

CLINICAL RELEVANCE/APPLICATION

Dual-energy CTPA allows for reducing the contrast media amount by 83%, while maintaining diagnostic image quality. This is of particular importance in patients with chronic renal insufficiency

SSM05-02 Clinical Severity of Chronic Thromboembolic Pulmonary Hypertension: Assessment on Lung Perfused Blood Volume Images Acquired by Dual Energy CT

Wednesday, Dec. 2 3:10PM - 3:20PM Location: S404CD

Participants

Hidenobu Takagi, MD, Sendai, Japan (*Presenter*) Nothing to Disclose Hideki Ota, MD, PhD, Sendai, Japan (*Abstract Co-Author*) Nothing to Disclose Koichiro Sugimura, MD,PhD, Sendai, Japan (*Abstract Co-Author*) Nothing to Disclose Junya Tominaga, PhD, Sendai, Japan (*Abstract Co-Author*) Nothing to Disclose Hiroaki Shimokawa, MD, PhD, Sendai, Japan (*Abstract Co-Author*) Nothing to Disclose Kei Takase, MD, PhD, Sendai, Japan (*Abstract Co-Author*) Nothing to Disclose

PURPOSE

To evaluate whether the degree of perfusion defects assessed on lung perfused blood volume (LPBV) images acquired by dualenergy CT allows to estimate the clinical severity of chronic thromboembolic pulmonary hypertension (CTEPH). This Institutional Review Board-approved retrospective study included 39 consecutive patients with CTEPH (10 men, 29 women). LPBV was imaged with a second-generation dual-source CT scanner. Two radiologists independently scored the degree of perfusion defects in each lung segment according to the following criteria: score 0, no defect, score 1, defect in less than half of a segment, score 2, defect in more than half of a segment. In case of disagreement, final consensus was reached by mutual discussion. The LPBV defect score was defined as the sum of the scores of 18 lung segments.Pulmonary artery pressure (PAP), right ventricular pressure (RVP), pulmonary vascular resistance (PVR), cardiac output (CO) and cardiac index (CI) were recorded by right heart catheterization (RHC). Brain natriuretic peptide (BNP) and 6 minutes walk distance (6MWD) were also recorded.Interobserver agreement was calculated by weighted Cohen's kappa. Correlations between LPBV defect score and RHC-parameters, BNP and 6MWD were evaluated by Spearman's rho correlation coefficients. P < 0.05 was considered statistically significant.

RESULTS

Interobserver agreement for scoring perfusion defects on each segment was good ($\kappa = 0.79$, 95% confidence interval, 0.75, 0.83). All patients showed abnormal lung perfusion in bilateral lungs with the median LPBV defect score of 16 (range, 5-23). Positive correlation of LPBV defect score was found with mean PAP (rho = 0.50, P < 0.01), systolic PAP (rho = 0.55, P < 0.001), diastolic PAP (rho = 0.42, P < 0.01), PVR (rho = 0.57, P < 0.001), RVP (rho = 0.50, P < 0.01) and BNP (rho = 0.42, P < 0.01), a tendency of negative correlation with 6MWD (rho = -0.35, P = 0.08). No significant correlation was found with CO (rho = -0.22, P = 0.18) or CI (rho = -0.26, P = 0.11).

CONCLUSION

The LPBV defect score is significantly correlated with RHC- and clinical parameters, and may become a useful tool to estimate the severity of CTEPH.

CLINICAL RELEVANCE/APPLICATION

LPBV by dual-energy CT is useful for not only detecting abnormal findings of lung perfusion, but also for estimating the clinical severity in patients with CTEPH.

SSM05-03 Correlation between Pulmonary Emboli Characteristics and Perfusion Abnormalities in Material Decomposition Images of Dual Energy CT (DECT)

Wednesday, Dec. 2 3:20PM - 3:30PM Location: S404CD

Participants

Alexi Otrakji, MD, Boston, MA (*Presenter*) Nothing to Disclose Amita Sharma, MBBS, Boston, MA (*Abstract Co-Author*) Nothing to Disclose Efren J. Flores, MD, Boston, MA (*Abstract Co-Author*) Nothing to Disclose Jo-Anne O. Shepard, MD, Boston, MA (*Abstract Co-Author*) Nothing to Disclose Mannudeep K. Kalra, MD, Boston, MA (*Abstract Co-Author*) Nothing to Disclose Subba R. Digumarthy, MD, Boston, MA (*Abstract Co-Author*) Nothing to Disclose Shaunagh McDermott, FFR(RCSI), Boston, MA (*Abstract Co-Author*) Nothing to Disclose Azadeh Tabari, Boston, MA (*Abstract Co-Author*) Nothing to Disclose

PURPOSE

To assess relationship between iodine distribution abnormalities in pulmonary blood volume (PBV) images and type of pulmonary emboli (occlusive versus non-occlusive) in virtual monochromatic DECT images.

METHOD AND MATERIALS

Our study included 57 patients (mean age 59±15years, M:F 25:32, mean weight 77±19kg) who had pulmonary embolism on chest DECT. All CT exams were performed on single or dual source MDCT scanners capable of DECT. Virtual monochromatic (40-60keV), and PBV images were used for assessment. Images evaluated for enhancement in pulmonary arteries, the location of filling defects and their characteristics (occlusive vs non-occlusive). Pulmonary abnormalities were evaluated synchronously on virtual monochromatic and PBV images for location, shape, size, enhancement, and likely diagnosis. The presence of right heart strain (RHS) and diameter of pulmonary trunk were recorded. The CTDI vol, DLP were recorded. Data were analyzed using ANOVA and student's t-test.

RESULTS

Mean CTDI vol was 8±2 mGy (range:5-16). Mean pulmonary trunk diameter was 26±5 mm (15-44). Optimal/excellent enhancement in subsegmental pulmonary arteries was seen in 89% of cases. RHS was predicted in 40% of cases (23/57). Occlusive PEs (OPEs, present in 47/57 patients) was seen most commonly at segmental level (53%). Discordant pulmonary infarctions (characterized by PBV defects larger than size of radiographic opacity on lung window) were seen in 30% of cases, and were most often associated with segmental OPEs (28% of OPEs cases). Mismatched defects (defects seen on PBV without abnormality on lung window) were seen in 14% of cases, and were always associated with segmental OPEs (17% of total OPEs). Size-concordant infarctions and defects (size of PBV abnormality equal to radiographic abnormalities) were seen in 21% and 15% of OPEs cases, respectively. In total, 66% of total OPEs were associated with infarction or defects. Infarcts or PBV defects were noticed in 70% of expected RHS cases.

CONCLUSION

Presence of pulmonary infarction or perfusion defect on pulmonary blood volume images is a good predictor for presence of occlusive lobar or segmental pulmonary embolism as well as right heart strain.

CLINICAL RELEVANCE/APPLICATION

Presence of occlusive pulmonary emboli requires interpretation of PBV images to rule out any perfusion defects.

Honored Educators

Presenters or authors on this event have been recognized as RSNA Honored Educators for participating in multiple qualifying educational activities. Honored Educators are invested in furthering the profession of radiology by delivering high-quality educational content in their field of study. Learn how you can become an honored educator by visiting the website at:

Subba R. Digumarthy, MD - 2013 Honored Educator

SSM05-04 Do We Really Need Bolus Tracking for Chest CT Angiography?: Assessment of Fixed Delay Prolonged Blous (FDPB) Contrast Injection Protocol, for Optimal Vascular Enhancement

Wednesday, Dec. 2 3:30PM - 3:40PM Location: S404CD

Participants

Alexi Otrakji, MD, Boston, MA (*Presenter*) Nothing to Disclose Shaunagh McDermott, FFR(RCSI), Boston, MA (*Abstract Co-Author*) Nothing to Disclose Efren J. Flores, MD, Boston, MA (*Abstract Co-Author*) Nothing to Disclose Jo-Anne O. Shepard, MD, Boston, MA (*Abstract Co-Author*) Nothing to Disclose Mannudeep K. Kalra, MD, Boston, MA (*Abstract Co-Author*) Nothing to Disclose Subba R. Digumarthy, MD, Boston, MA (*Abstract Co-Author*) Nothing to Disclose

PURPOSE

To assess the feasibility of fixed delay prolonged bolus(FDPB) contrast injection during routine chest CT for evaluation of mediastinal and pulmonary vessels as compared to CT pulmonary angiography(CTPA) done with triggered bolus tracking(BT) techniques.

METHOD AND MATERIALS

Of the 100 patients included in our study, 50 patients underwent routine chest CT with FDPB(M:F 29:21, mean age 59±18 years, mean weight 77±15kg) and 50 weight-matched patients had CTPA using BT(4 cc/second, 370 mg%, 80ml), M:F 23:27, mean age 57±17 years, mean weight 77±15 kg. Patients weighing more than 90 kg and who got contrast injection via central venous catheter were excluded. The FDP injection involved administration of 25ml of contrast (370 mg%) at rate of 1ml/second followed by 55ml contrast at rate of 2.2ml/second with scanning at 57 second fixed delay. All CT scans were performed on (128-slice Siemens Definition Edge MDCT) using automatic kV selection technique(Care kV). All exams were assessed subjectively for vascular abnormalities (in pulmonary arteries, aorta, and heart), and artifacts. HU values in main pulmonary arteries and aorta, CTDI vol and DLP were recorded. Data were analyzed using student's t-test.

RESULTS

Mean CTDI vol was 5±1.3 mGy for FDPB. Mean HU for FDPB in main pulmonary artery and ascending aorta were 311 ± 79 and 305 ± 49 , respectively, with corresponding values of 371 ± 110 and 219 ± 88 for CTPA-BT. Optimal/excellent contrast enhancement at segmental level was seen in 92% of cases for FDPB compared to 86% for CTPA-BT examinations(p=0.9). The inability to rule out central pulmonary emboli was noticed in 3% of cases for FDPB and CTPA-BT. FDPB resulted in significantly superior enhancement in heart and thoracic aorta in all patients compared to CTPA-BT. Contrast streak artifacts were also substantially lower on FDPB than on CTPA-BT(p<0.001). For FDPB, 5% of cases revealed incidental pulmonary emboli compared to 9% of cases for CTPA-BT at segmental level.

CONCLUSION

Fixed delay prolonged contrast injection protocol can provide optimal contrast enhancement in pulmonary arteries, heart, and aorta compared to the bolus tracking technique. The prolonged injection results in substantially less artifacts.

CLINICAL RELEVANCE/APPLICATION

Fixed delay prolonged bolus of chest CT has the potential to be as the only chest contrast enhanced CT protocol for the evaluation of vascular and non-vascular chest abnormalities.

Honored Educators

Presenters or authors on this event have been recognized as RSNA Honored Educators for participating in multiple qualifying educational activities. Honored Educators are invested in furthering the profession of radiology by delivering high-quality educational content in their field of study. Learn how you can become an honored educator by visiting the website at: https://www.rsna.org/Honored-Educator-Award/

Subba R. Digumarthy, MD - 2013 Honored Educator

SSM05-05 Observer Performance at Varying Dose Levels and Reconstruction Methods for Detection of Indeterminate Pulmonary Nodules

Wednesday, Dec. 2 3:40PM - 3:50PM Location: S404CD

Participants

Joel G. Fletcher, MD, Rochester, MN (*Presenter*) Grant, Siemens AG; ; David L. Levin, MD, PhD, Rochester, MN (*Abstract Co-Author*) Nothing to Disclose Anne-Marie G. Sykes, MD, Rochester, MN (*Abstract Co-Author*) Nothing to Disclose Rebecca M. Lindell, MD, Rochester, MN (*Abstract Co-Author*) Nothing to Disclose Darin B. White, MD, Rochester, MN (*Abstract Co-Author*) Nothing to Disclose Ronald S. Kuzo, MD, Jacksonville, FL (*Abstract Co-Author*) Nothing to Disclose Lifeng Yu, PhD, Rochester, MN (*Abstract Co-Author*) Nothing to Disclose Maria Shiung, Rochester, MN (*Abstract Co-Author*) Nothing to Disclose Adam Bartley, Rochester, MN (*Abstract Co-Author*) Nothing to Disclose Shuai Leng, PhD, Rochester, MN (*Abstract Co-Author*) Nothing to Disclose David R. Holmes Iii, PhD, Rochester, MN (*Abstract Co-Author*) Nothing to Disclose Alicia Toledano, DSc, Washington, DC (*Abstract Co-Author*) President, Biostatistics Consulting, LLC Rickey Carter, PhD, Rochester, MN (*Abstract Co-Author*) Nothing to Disclose To estimate the ability to detect indeterminate pulmonary nodules \geq 5 mm (IPNs) at varying dose levels using standard filtered back projection (FBP) and iterative reconstruction (sinogram-affirmed iterative reconstruction; SAFIRE) using a two-stage study design.

METHOD AND MATERIALS

In stage 1, CT projection data from 44 chest CT exams performed using automatic exposure control [70 Quality ref. mAs (QRM)] were collected. IPNs were identified by two thoracic radiologists who did not participate in the reader study. Using a validated noise insertion tool to simulate reduced doses, 10 datasets were reconstructed for each patient (FBP and SAFIRE at 5 dose levels each (2.5, 5, 10, 30, and 70 QRM); 440 total cases). In each reading session, 3 thoracic radiologists randomly evaluated each patient's data once using thin 1 mm axial and MIP images. Using a dedicated computer workstation, readers tightly circumscribed all IPNs, gave a confidence score (0 - 100), and graded image quality. A successful interpretation was defined as \geq 2 readers localizing all "essential" IPNs (or no non-lesion localizations in negative cases), where an essential IPN was identified by the reference standard and \geq 2 readers at 70 QRM FBP. Sample size calculations (p0=0.8, p1=0.9, alpha=0.05 (one sided)) determined \geq 37 cases to pass through stage I. JAFROC analysis was also performed on a per-lesion basis using a non-inferiority limit of -0.1.

RESULTS

Dose levels of \geq 5 QRM (or 2.5 QRM using SAFIRE) met stage 1 criteria for correct interpretation. Using non-inferiority criteria, the JAFROC figure of merit was also non-inferior for all configurations except for 2.5 QRM FBP. At 5 QRM, pooled sensitivities and specificities were nearly identical between FBP and SAFIRE (FBP: 87% [95% CI: 70-95%] and 88% [74-95%], SAFIRE: 86% [69-94%] and 91% [75-97%]; respectively). Diagnostic image quality was greater for SAFIRE images at 10 - 70 QRM (p<0.05).

CONCLUSION

CT images reconstructed at dose levels corresponding to 5 - 30 QRM (and at 2.5 QRM when using SAFIRE) performed similar to 70 QRM FBP in this pilot study for detection of IPNs. Further study is needed to confirm this large potential for dose reduction.

CLINICAL RELEVANCE/APPLICATION

Whether or not iterative reconstruction is used, the radiation dose for screening or surveillance chest CT can be substantially lowered without compromising observer performance.

SSM05-06 The Usefulness of a Dictionary Learning Post-processing Technique for Improving Image Quality of Low-Dose Chest CT

Wednesday, Dec. 2 3:50PM - 4:00PM Location: S404CD

Participants

Yoshinori Kanii, MD, Tsu, Japan (*Presenter*) Nothing to Disclose Yasutaka Ichikawa, MD, Matsusaka, Japan (*Abstract Co-Author*) Nothing to Disclose Ryohei Nakayama, PhD, Kusatsu, Japan (*Abstract Co-Author*) Nothing to Disclose Motonori Nagata, MD, PhD, Tsu, Japan (*Abstract Co-Author*) Nothing to Disclose Masaki Ishida, MD, PhD, Tsu, Japan (*Abstract Co-Author*) Nothing to Disclose Kakuya Kitagawa, MD, PhD, Tsu, Japan (*Abstract Co-Author*) Nothing to Disclose Shuichi Murashima, MD, Tsu, Japan (*Abstract Co-Author*) Nothing to Disclose Hajime Sakuma, MD, Tsu, Japan (*Abstract Co-Author*) Nothing to Disclose Hajime Sakuma, MD, Tsu, Japan (*Abstract Co-Author*) Nothing to Disclose Grant, DAIICHI SANKYO Group; Departmental Research Grant, FUJIFILM Holdings Corporation; Departmental Research Grant, Nihon Medi-Physics Co, Ltd

PURPOSE

Low-dose CT is widely used for lung cancer screening. In low-dose conditions, however, CT images are prone to have increased noise and low-contrast detectability. Recently, our group developed a super-resolution (SR) technique based on a dictionary for enhancing image quality in MR angiography. The purpose of this study was to improve the image quality of low-dose CT by expanding the concept of the SR technique.

METHOD AND MATERIALS

Chest CT was acquired with 64-slice CT (Discovery CT750HD) by using a standard current of 200-300mA and a reduced current of 20mA in 12 patients who were referred for chest CT. We developed an image improvement method that consists of (1) generation of a dictionary representing the relationship between standard- and low-dose patches adopted from standard- and low-dose CT datasets, and (2) construction of high quality image from low-dose CT dataset by embedding optimal patches selected from the dictionary. For each patient, standard- and low-dose CT datasets in the remaining 11 patients were used to generate the dictionary. This procedure was repeated for all 12 patients. Image noise was evaluated as the standard deviation of CT intensity in the descending aorta. Qualitative assessment of image quality was performed for the mediastinum and lung by using a 5-point scale (5=excellent, 1=very poor) by two observers. In addition, image quality of abnormal lung structures (nodules or consolidation) were also assessed on a 5-point scale as well.

RESULTS

Image noise on low-dose CT was significantly reduced by using the dictionary learning method (20.4 ± 7.9 HU vs 48.5 ± 13.7 HU, p=0.0005). For image quality of the lung and mediastinum, low-dose CT generated by the dictionary learning method was rated significantly better than original low-dose CT (lung, score 2.8 ± 0.6 vs 1.9 ± 0.7 , p=0.0039; mediastinum, score 2.9 ± 0.8 vs 2.3 ± 0.8 , p=0.0078). Image quality of abnormal lung structures was also significantly improved by using the new technique (score 3.4 ± 0.6 vs 2.7 ± 0.6 , p=0.0273).

CONCLUSION

The dictionary learning post-processing method can provide significantly improved image quality and reduced image noise on lowdose chest CT.

CLINICAL RELEVANCE/APPLICATION

Substantial improvement of image quality can be achieved by using the dictionary learning-based method on low-dose chest CT, leading to more accurate interpretation, while minimizing radiation dose.

Physics (MRI III-Applications)

Wednesday, Dec. 2 3:00PM - 4:00PM Location: S404AB

MR PH

AMA PRA Category 1 Credit ™: 1.00 ARRT Category A+ Credit: .50

Participants

Gregory S. Karczmar, PhD, Chicago, IL (*Moderator*) Nothing to Disclose Chen Lin, PhD, Indianapolis, IN (*Moderator*) Nothing to Disclose

Sub-Events

SSM21-01 Skeletal Muscle Mitochondrial Capacity and Pi-to-ATP Exchange Rate Relate to Alkaline Pi Pool and PDE Concentration Measured at Rest by ³¹P-MRS at 7T

Wednesday, Dec. 2 3:00PM - 3:10PM Location: S404AB

Participants

Ladislav Valkovic, PhD, Vienna, Austria (*Presenter*) Nothing to Disclose Marjeta Tusek Jelenc, Vienna, Austria (*Abstract Co-Author*) Nothing to Disclose Barbara Ukropcova, Bratislava, Slovakia (*Abstract Co-Author*) Nothing to Disclose Wolfgang Bogner, MSc, Vienna, Austria (*Abstract Co-Author*) Nothing to Disclose Marek Chmelik, MS, Vienna, Austria (*Abstract Co-Author*) Nothing to Disclose Ivan Frollo, Bratislava, Slovakia (*Abstract Co-Author*) Nothing to Disclose Jozef Ukropec, Bratislava, Slovakia (*Abstract Co-Author*) Nothing to Disclose Siegfried Trattnig, MD, Vienna, Austria (*Abstract Co-Author*) Nothing to Disclose Martin Krssak, PhD, Vienna, Austria (*Abstract Co-Author*) Nothing to Disclose

PURPOSE

Dynamic phosphorus MR spectroscopy (31P-MRS) and saturation transfer (ST) are established methods for measurement of muscle mitochondrial capacity and ATP turnover-kinetics, associated with metabolic and cardiovascular disorders. However, as a complex experimental setup or advanced sequences are required, the use of static 31P-MR spectra, i.e., concentration of phosphodiesters ([PDE]) and moreover the alkaline Pi (Pi2), to obtain similar information, has been promoted recently. Therefore our aim was to assess the interrelations between parameters derived from static and dynamic 31P-MRS measurements at 7T.

METHOD AND MATERIALS

In total, data from thirty-seven subjects (25m/12f, a=32.9±7.3y) were analysed and divided into groups based on their physiological characteristics: obese sedentary subjects prior (ObSe) and after 3 months of training (ObAc), and lean subjects active on regular basis (LeAc). 31P-MRS was performed on a 7T MR system (Siemens Healthcare, Erlangen, Germany) equipped with a 1H/31P surface coil. The examination protocol was divided into three experiments: (i) acquisition of static spectra, for quantification of [PDE] and the Pi2/Pi1 ratio; (ii) ST experiment, for quantification of Pi-to-ATP reaction rate constant (kATP) and ATP flux (FATP); and (iii) dynamic examination, for quantification of mitochondrial capacity (Qmax). The physiological and 31P-MRS parameters were compared between the groups by a one-way ANOVA and a Tukey post-hoc test and their potential relations by a linear regression.

RESULTS

Group ObSe had significantly lower values of Qmax in comparison to the active groups. In addition, group LeAc had significantly lower PDE concentration and higher Pi2/Pi1 ratio when compared to the other groups. Apart from previously reported correlations between Qmax and FATP and between FATP and the [PDE], further significant correlations were found, i.e., Qmax correlated to Pi2/Pi1 and [PDE]; and Pi2/Pi1 correlated to kATP and [PDE].

CONCLUSION

Our investigation, performed on sedentary and active obese subjects as well as on lean active individuals, shows that resting measurements of Pi2/Pi1 ratio and [PDE] correlate with measures derived from dynamic and ST 31P-MRS measurements in skeletal muscle.

CLINICAL RELEVANCE/APPLICATION

Measurement of basal Pi2/Pi1 ratio and [PDE] at 7T might provide a surrogate marker of myocellular metabolism, alterations of which are connected to metabolic and cardiovascular disorders.

SSM21-02 In Vitro Assessment of Flow Patterns around Sub-prosthetic Pannus Tissue using PC-MRI

Wednesday, Dec. 2 3:10PM - 3:20PM Location: S404AB

Participants

Jihoon Kweon, PhD, Seoul, Korea, Republic Of (*Abstract Co-Author*) Nothing to Disclose Dong Hyun Yang, MD, Seoul, Korea, Republic Of (*Abstract Co-Author*) Nothing to Disclose Hojin Ha, Seoul, Korea, Republic Of (*Presenter*) Nothing to Disclose Guk-Bae Kim, Seoul, Korea, Republic Of (*Abstract Co-Author*) Nothing to Disclose Namkug Kim, PhD, Seoul, Korea, Republic Of (*Abstract Co-Author*) Stockholder, Coreline Soft, Inc Young-Hak Kim, Seoul, Korea, Republic Of (*Abstract Co-Author*) Nothing to Disclose

PURPOSE

Sub-prosthetic pannus overgrowth after aortic valve replacement (AVR) has been reported that may cause an aortic stenosis and a

high peak pressure gradient across the mechanical heart valve (MHV). However, clinical implications of the sub-prosthetic pannus have not been fully understood. The present study aims to investigate the hemodynamic effect of the pannus by applying phase contrast MRI to aorta phantoms with different pannus formations.

METHOD AND MATERIALS

A flow phantom was constructed by implementing a supra-annular mechanical valve (St. Jude 25 mm medical masters HP series) into an aorta model fabricated by 3D printer. Five different types of pannus models were alternately installed at the inlet of aorta model and the axial position of the pannus was the same as the hinge tip of the MHV. The effective orifice area (EOA) reduced by pannus models was $8.2\% \sim 47.66\%$, and the thickness of the modeled pannus was 3mm. Image acquisition was performed on 3T scanner (MAGNETOM Skyra, Siemens) using a gradient echo sequence. The velocity encoding range was set as 120cm/s and imaging matrix was 256×156 on a field of view of $160mm \times 97.5mm$. Repetition and echo times were 23ms and 3.16ms, respectively. Flow information on MR images was analyzed using customized-Matlab software.

RESULTS

The minimal pannus showed a negligible flow interference, maintaining almost planar symmetric flow pattern (maximum velocity 66.3cm/s). However, with larger single pannus, the peak velocity increases due to the reduced EOA (up to 11.2%) and the position of peak velocity was moved to between the leaflets. In the distal side of MHV, the flow was skewed toward the wall on the pannus side. For the paired pannus, peak flow was observed in the middle of flow area (26.8% increase) and the low velocity regions due to the leaflets were disappeared. For the largest pannus, the estimated pressure gradient using the averaged velocity of the far distal side (23cm/s) increased by 70.3% of the smallest one.

CONCLUSION

The EOA reduction due to the pannus formation caused a higher peak velocity in the distal side of MHV and thereby increased the pressure difference estimated from the peak velocity.

CLINICAL RELEVANCE/APPLICATION

Sub-prosthetic pannus after AVR may cause a high pressure gradient across the MHV.

SSM21-03 Magnetic Resonance Elastography and Ultrasound Shear Wave Speed Imaging for Assessment of Renal Allograft Function

Wednesday, Dec. 2 3:20PM - 3:30PM Location: S404AB

Participants

Stephan Marticorena Garcia, MD, Berlin, Germany (Presenter) Nothing to Disclose

Jing Guo, MD, PhD, Berlin, Germany (Abstract Co-Author) Nothing to Disclose

Bernd K. Hamm III, MD, Berlin, Germany (*Abstract Co-Author*) Research Consultant, Toshiba Corporation; Stockholder, Siemens AG; Stockholder, General Electric Company; Research Grant, Toshiba Corporation; Research Grant, Koninklijke Philips NV; Research Grant, Siemens AG; Research Grant, General Electric Company; Research Grant, Elbit Imaging Ltd; Research Grant, Bayer AG; Research Grant, Guerbet SA; Research Grant, Bracco Group; Research Grant, B. Braun Melsungen AG; Research Grant, KRAUTH medical KG; Research Grant, Boston Scientific Corporation; Equipment support, Elbit Imaging Ltd; Investigator, CMC Contrast AB Ingolf Sack, PhD, Berlin, Germany (*Abstract Co-Author*) Nothing to Disclose

Thomas Fischer, MD, Berlin, Germany (Abstract Co-Author) Speaker, Toshiba Corporation; Advisory Board, Toshiba Corporation

PURPOSE

Kidney transplant rejection is associated with viscoelastic tissue changes. The purpose of this study is to non-invasively assess the renal elasticity in kidney transplant recipients with magnetic resonance elastography (MRE) and ultrasound shear wave speed imaging (SSI).

METHOD AND MATERIALS

10 kidney transplant recipients (age range 27-51 years, 2 females) were included (mean transplant duration 63 ± 97 months). Among them, 3 patients have dysfunctional kidney (GFR <15 ml/min) with biopsy proven fibrosis. Recipients with normal renal function were identified by constant blood creatinine/GFR values, normal B-mode appearance and resistive index (RI), obtained during 6 months period before MRE/SSI. MRE (1.5 T scanner, Siemens) was performed with 7 slices (2.5 mm cubic voxel resolution) at 4 mechanical frequencies from 40 to 70 Hz. MRE data were processed giving $|G^*|$ (magnitude of the complex modulus) which relates to the shear stiffness of the kidney. In SSI (Aplio500, Toshiba), an ultrasonic burst was captured by a 14 MHz linear broadband transducer, and propagation speed reflecting tissue stiffness was compared to MRE results.

RESULTS

In combined cortex and medulla region, the group mean values of shear stiffness (MRE 6.12 ± 0.95 kPa) and wave speed (SSI: 3.1 ± 0.43 m/s) correlate very well with each other (r=0.76, p=0.01). In the same region, significant decrease of both stiffness and wave speed were observed in patients with dysfunctional kidney (MRE, functional: 6.09 ± 0.39 kPa vs. dysfunctional: 4.00 ± 0.79 kPa, p=0.012; SSI, functional: 3.44 ± 0.33 m/s vs. dysfunctional: 2.86 ± 0.33 m/s, p=0.019).

CONCLUSION

MRE and SSI are both sensitive in detecting renal allograft fibrosis.

CLINICAL RELEVANCE/APPLICATION

Mechanical properties obtained from both techniques could be used as biomarker for non-invasive assessment of renal allograft rejection.

SSM21-04 Time Effficient Estimation of Abdominal Fat Distribution in MRI

Wednesday, Dec. 2 3:30PM - 3:40PM Location: S404AB

Alexander Schaudinn, MD, Leipzig, Germany (*Abstract Co-Author*) Nothing to Disclose Nikita Garnov, Leipzig, Germany (*Abstract Co-Author*) Nothing to Disclose Thomas K. Kahn, MD, Leipzig, Germany (*Abstract Co-Author*) Nothing to Disclose Harald F. Busse, PhD, Leipzig, Germany (*Abstract Co-Author*) Nothing to Disclose

PURPOSE

To evaluate the prediction of abdimonpelvic visceral and subcutaneous adipose tissue (VAT, SAT) volume based on a single MRI slice.

METHOD AND MATERIALS

162 patients (Caucasians, mean BMI 35.6 kg/m², 43 males) were scanned at 1.5T (2 point Dixon, 50 slices of 10 mm thickness and 0.5 mm gap) and semiautomatic quantification of VAT and SAT volumes (V-VAT V-SAT) was performed. Fat areas at the level of 11 anatomical landmarks [levels of lumbar discs L1-L2 to L5-S1, umbilicus (UM) +/- 0,5,10 cm, femoral head] were used for estimation of VAT and SAT volumes (VE-VAT, VE-SAT). Statistical measures of agreement were the coefficient of determination R² of a linear regression through the origin as well as the standard deviations σ of the differences between measured and predicted volume.

RESULTS

Mean V-VAT and V-SAT were 3.6 and 15.4 L in females and 5.8 and 12.1 L in males. The optimum level of SAT volume prediction was at L5-S1 independent of sex and BMI (females: R²=0.82 and σ =1.4 L; males: R²=0.92 and σ =1.1L). Differences could be seen for VAT with the optimum level at L2-L3 for males (R²= 0.84 and σ =0.9 L) and less obese women (BMI < 35kg/m²; R²= 0.83 and σ =0.6 L) whereas more obese females (BMI > 35 kg/m²) showed an optimum at L5-S1 (R²= 0.69 and σ =0.8 L). Looking at a single slice position to quantify both SAT and VAT best results were detected at L4-L5 for females and L5-S1 for males.

CONCLUSION

Whole abdominopelvic SAT and VAT volumes can be reliably predicted from a single slice at the level of a BMI and sex-dependent anatomic landmark.

CLINICAL RELEVANCE/APPLICATION

This studys might be beneficial for standardization of VAT and SAT estimation in studies interested in obesity related risk factors.

SSM21-05 Non-Contrast 4D MR Myocardium Blood Flow

```
Wednesday, Dec. 2 3:40PM - 3:50PM Location: S404AB
```

Participants

Mitsue Miyazaki, PhD, Vernon Hills, IL (*Presenter*) Employee, Toshiba Corporation Xiangzhi Zhou, PhD, Oak Brook, IL (*Abstract Co-Author*) Employee, Toshiba Corporation Tsutomu Hoshino, Vernon Hills, IL (*Abstract Co-Author*) Employee, Toshiba Corporation Kenichi Yokoyama, MD, Mitaka-Shi, Japan (*Abstract Co-Author*) Nothing to Disclose Rieko Ishimura, MD, Tokyo, Japan (*Abstract Co-Author*) Nothing to Disclose Toshiaki Nitatori, MD, Tokyo, Japan (*Abstract Co-Author*) Nothing to Disclose

PURPOSE

To develop a non-contrast 4-dimensional time-spatial labeling inversion pulse (4D Time-SLIP) technique (3D acquisition and time) for investigation of myocardial blood flow on healthy volunteers without administration of contrast materials.

METHOD AND MATERIALS

The non-contrast 4D Time-SLIP technique was applied on eight healthy volunteers to image myocardium blood flow at 1.5T. The Time-SLIP sequence has a tag-on block with a non-selective inversion recovery (non-sel-IR) pulse and a spatially selective inversion recovery (sel-IR) and a tag-off block with only the non-sel-IR pulse. The tagging plane was placed at the proximal ascending aorta and imaging slab was placed at mid-ventricle. The complex subtraction between tag-on and tag-off is performed to depict only the tagged blood flowing into the myocardium with cancellation of background signal. For each inversion time (TI), tag-on and tag-off acquisitions with a 3D bSSFP readout was alternately acquired within a breath-hold. To achieve variable TI, the tagging pulses were triggered with variable delay time while the readout was placed at a fixed mid-diastolic phase in the second RR interval. As a result, each 3D tag-on and tag-off acquisition can be performed within 2 RR intervals, which can be repeated with was segmented for the visualization of myocardial signal changes caused by the tagged blood along the TI. The non-contrast perfusion curves were also generated to identify the perfusion peaks.

RESULTS

Both time-resolved 3D short axis images and perfusion curves were successfully obtained, where blood flow shows basal to apical directions. At the mid-ventricle, the blood flow reached peak about 200-400 ms after tagging the aortic root blood, and then blood signal returned to baseline. This observation of quick return to baseline is controversial to the results obtained from other non-contrast methods where the signal does not return to baseline.

CONCLUSION

The technique permits obtaining non-contrast 4D myocardium blood flow images and perfusion curves with high temporal resolution without administration of contrast materials.

CLINICAL RELEVANCE/APPLICATION

The 4D Time-SLIP technique permits obtaining non-contrast 4D myocardium blood flow images and perfusion curves with high temporal resolution without administration of contrast materials.

SSM21-06 Ultra-Fast Low Dose Dynamic Contrast Enhanced MRI for Prostate Cancer Diagnosis - A Preliminary Study

Participants Shiyang Wang, PhD, Chicago, IL (*Abstract Co-Author*) Nothing to Disclose Xiaobing Fan, PhD, Chicago, IL (*Abstract Co-Author*) Nothing to Disclose Federico Pineda, PhD, Chicago, IL (*Abstract Co-Author*) Nothing to Disclose Milica Medved, PhD, Chicago, IL (*Presenter*) Nothing to Disclose Ambereen Yousuf, MBBS, Chicago, IL (*Abstract Co-Author*) Nothing to Disclose Aytekin Oto, MD, Chicago, IL (*Abstract Co-Author*) Research Grant, Koninklijke Philips NV; ; ; Gregory S. Karczmar, PhD, Chicago, IL (*Abstract Co-Author*) Nothing to Disclose

PURPOSE

The aim of this study is to investigate the effectiveness of ultra-high temporal resolution (Ufast) dynamic contrast enhanced MRI (DCE), with a low dose of contrast media, for prostate cancer (PCa) diagnosis.

METHOD AND MATERIALS

Eleven men (age 40-69 years) who were scheduled for prostatectomy after MRI were enrolled. Ufast DCE MRI was performed on a Philips Achieva 3T scanner, with temporal resolution of 1.5 sec, slice thickness 3.5mm, 24 slices, in plane resolution 1.5x2.8 mm², before and for 15 sec after a low dose (LD) of contrast agent was (.015 mM/Kg; 15% of conventional dose). Following ultrafast imaging, a routine clinical DCE scan was performed pre- and post I.V. injection of 0.085 mM/kg of contrast media. A 'time of arrival' (TOA) map was calculated from the Ufast images, based on the time at which significant (25%) enhancement was detected in each pixel. The TOA ratio (rTOA) was defined as the percentage of voxels in each ROI significantly enhanced during the first 60 seconds. TOA and rTOA were compared in cancer (n=11), normal (n=10) and BPH (n=11) ROIs. Kruskal-Wallis Analysis of Variance (ANOVA) test and Welch two sample t-test were performed to compare results.

RESULTS

Enhancement in normal prostate was delayed by an average of 5.1 ± 1.6 sec compared with cancer, and enhancement of BPH was delayed by an average of 7.5 sec relative to cancer, where delays were calculated for each patient, then averaged over all patients. Average TOAs were 45.6 ± 4.4 sec, 48.3 ± 3.9 sec and 49.2 ± 4.1 sec in cancer, normal and BPH ROIs, respectively (where time of arrival was averaged over all patients). TOAs for cancer and BPH were significantly different (p=0.04). rTOAs were 0.77, 0.85 ± 0.3 and 0.94 ± 0.1 in patient groups with GS=6,7and 9, respectively.

CONCLUSION

Ufast imaging, with measurement of TOA and rTOA has the potential to differentiate PCa from BPHs, and may also be sensitive to cancer grade. In this study a very low dose was used in the Ufast protocol so that total dose (sum of the low dose and high dose used for conventional DCE scan) was acceptable. Enhancement due to the low dose was easily detectable, and may have advantages, including reduced non-linear enhancement effects. In future studies, a range of contrast agent doses will be tested.

CLINICAL RELEVANCE/APPLICATION

Ufast DCE-MRI has potential to increase diagnostic accuracy. Very low doses of contrast media are effective.

Honored Educators

Presenters or authors on this event have been recognized as RSNA Honored Educators for participating in multiple qualifying educational activities. Honored Educators are invested in furthering the profession of radiology by delivering high-quality educational content in their field of study. Learn how you can become an honored educator by visiting the website at: https://www.rsna.org/Honored-Educator-Award/

Aytekin Oto, MD - 2013 Honored Educator

Neuroradiology (Neurointerventional Radiology)

Wednesday, Dec. 2 3:00PM - 4:00PM Location: N227

NR IR

AMA PRA Category 1 Credit ™: 1.00 ARRT Category A+ Credit: 1.00

FDA Discussions may include off-label uses.

Participants

Colin P. Derdeyn, MD, Saint Louis, MO (*Moderator*) Consultant, Terumo Corporation; Consultant, Penumbra, Inc; Consultant, Silk Road Medical; Stock options, Pulse Therapeutics, Inc; ;

Albert J. Yoo, MD, Newton, MA (*Moderator*) Research Grant, Penumbra, Inc; Research Grant, Terumo Corporation; Research Consultant, Medtronic, Inc;

Sub-Events

SSM17-01 Recurrences May Occur More than Ten Years after Endovascular Treatment of Intracranial Aneurysms: A Prospective Cohort Study, a Systematic Review and Meta-Analysis

Wednesday, Dec. 2 3:00PM - 3:10PM Location: N227

Participants

Olivier Naggara, MD, Paris, France (*Presenter*) Nothing to Disclose Augustin Lecler, MD, Paris, France (*Abstract Co-Author*) Nothing to Disclose Jean Raymond, MD, Montreal, QC (*Abstract Co-Author*) Nothing to Disclose Christine Rodriguez, Paris, France (*Abstract Co-Author*) Nothing to Disclose Denis Trystram, MD, Paris, France (*Abstract Co-Author*) Nothing to Disclose Wagih Ben Hassen, Paris, France (*Abstract Co-Author*) Nothing to Disclose Jean-Francois Meder, MD, PhD, Paris, France (*Abstract Co-Author*) Nothing to Disclose Catherine Oppenheim, MD, PhD, Paris, France (*Abstract Co-Author*) Nothing to Disclose

PURPOSE

Our aim was to assess the 10-year efficacy of endovascular treatment (EVT) of intracranial aneurysm (IA) in terms of recurrence, assessed on long-term MR angiography (LT-MRA), and bleeding and de novo aneurysm formation. We also aimed to identify potential risk factors of aneurysm recurrence, including IA occlusion on 3-to 5-year MRA (MT-MRA), through a prospective study and a systematic review of the literature.

METHOD AND MATERIALS

We prospectively performed clinical examination and 3T MRA 10-years after EVT of IA in a single institution. Individual informed consent was obtained. In addition, the literature was searched using PubMed, EMBASE, and Cochrane databases to identify studies reporting bleeding and/or aneurysm recurrence rate in patients followed beyond 10-years after EVT. Univariate and multivariate subgroup analyses were performed to identify risk factors (MT-MRA results, aneurysm characteristics, retreatment within 5 years).

RESULTS

In the prospective study, among 129 aneurysms followed >10 years, 16 (12.4%) demonstrated sac recanalization between MT- and LT-MRA. Neck remnant on MT-MRA (Relative risk [RR]: 4.16, 99%Confident interval [99%CI]: 2.12-8.14) and retreatment within five years (RR: 4.67, 99%CI, 1.55-14.03) were risk factors for late recurrence. In the systematic review (15 cohorts, 2773 patients, 2902 aneurysms), bleeding rate, recurrent aneurysm, and de novo lesion were, respectively 0.7% (99%CI, 0.2-2.7%, I2: 0%, 694 aneurysms), 11.4% (99%CI, 7.0-18.0%, I2: 21.6%), and 4.1% (99%CI, 1.7-9.4%, I2: 54.1%). Incomplete initial treatment (RR: 7.08, 99%CI, 1.24-40.37, I2: 82.6%) and aneurysm size > 10 mm (RR: 4.37, 99%CI, 1.83-10.44, I2: 0%) were risk factors for late recurrence.

CONCLUSION

EVT of IA is effective in preventing long-term bleeding, but may be followed by recurrences in a significant proportion of cases, a finding that may justify following selected patients for ≥ 10 years, i.e. in patients with Raymond grade 2 classification on 3- to 5-year MRA or when aneurysm >10 mm.

CLINICAL RELEVANCE/APPLICATION

Long-term (> 10 years) MRA follow-up may be needed in patients with aneurysms larger than 10 mm, or in the case of grade 2 aneurysms at the end of standard midterm follow-up. De novo aneurysms may occur between 5 and 10 years after treatment in one in 25 patients.

SSM17-02 Does Recurrence Effect the Clinical Outcome after Endovascular Coiling of Ruptured Intracranial Aneurysms? - A Ten Year Retrospective Study

Wednesday, Dec. 2 3:10PM - 3:20PM Location: N227

Participants

Robert K. Moreland, MD, Ottawa, ON (*Presenter*) Nothing to Disclose Marlise P. dos Santos MSc, MD, Ottawa, ON (*Abstract Co-Author*) Nothing to Disclose Rafael Glikstein, Ottawa, ON (*Abstract Co-Author*) Nothing to Disclose

PURPOSE

To identify the factors associated with clinical outcome of coiling of ruptured intracranial aneurysms (RIA).

METHOD AND MATERIALS

Retrospective review of all patients with RIA treated with endovascular coil embolization at a active single centre between 2002-2013. Cases of flow-related (AVM, DAVF related) aneurysms, flow-diversion and parent artery occlusion were excluded. We identified patient, periprocedural, procedural and aneurysm characteristics associated with pre-discharge and long-term clinical outcome (modified Rankin Scale (mRS) 0-2 [favorable] versus 3-6 [unfavorable]). We used univariate Cox Proportional Hazards Model followed by multivariate regression analysis of covariates to identify risk factors associated with poor clinical outcome.

RESULTS

A total of 305 RIA in 302 patients (mean age of 55.3 years) met criteria, including 216(70.8%) females. The mean follow-up was 34.2 months. Preoperatively, 176 cases had a mRS of 0-2, and 129 had a mRS of 3-5.Complete/near-complete occlusion was achieved in 245(81.3%) of the RIA, and body residual in 60(19.7%). At discharge 11 patients (3.61%) had a clinically worse mRS, 59 (19.34%) improved, and 231 (77.05%) were unchanged. Our perioperative mortality (\leq 30 days) was 13.8%(42). Perioperative complications occurred in 18.4% of the cases. Postprocedure vasospasm occurred in 44.9% of the cases.Target maximum aneurysm size(<=7,>7) and aneurysm width (<=7,>7) had a significant effect on end clinical outcomes, while neurysm neck size(<=4,>4) and dome/neck ratio (<=2, >2) did not.Reoccurrence occurred 109 times (35.73%) after coiling, of which 40 (36.70%) underwent retreatment; the recoiling did not impact the clinical outcome. Mean time until retreatment was 15.7 months. Reoccurance post discharge was not associated with a worsening of clinical disability (HR 1.417 CI 95% 0.722-2.779). There were four rebleeds occurring on average 30.5 months post procedure.

CONCLUSION

In our practice from 2002-2013 the safety of coiling embolization of RIA was comparable to the available literature. Reoccurrence and baseline occlusion status did not influence clinical outcomes. The maximum aneurysm size and width impacted long term clinical results, while the neck size and dome/neck ratio did not.

CLINICAL RELEVANCE/APPLICATION

Reoccurance post ruptured aneurysm repair with endovascular coiling does not significantly impact end patient clinical outcome.

SSM17-03 Single Center Cereberal Aneurysm Treatment with FRED and PED Flow Divetrters; Initial Experience, Techniques and Comparative Outcomes

Wednesday, Dec. 2 3:20PM - 3:30PM Location: N227

Participants

Soheil Sabet, MD, Istanbul, Turkey (*Presenter*) Nothing to Disclose Nurten Andac, MD, Istanbul, Turkey (*Abstract Co-Author*) Nothing to Disclose Hacer Bal, MD, Istanbul, Turkey (*Abstract Co-Author*) Nothing to Disclose Feyyaz Baltacioglu, Istanbul, Turkey (*Abstract Co-Author*) Nothing to Disclose Gazanfer Ekinci, Istanbul, Turkey (*Abstract Co-Author*) Nothing to Disclose

PURPOSE

This retrospective study of the initial istitutional experience provides insight into technical challenges, clinical and radiographic outcomes, and complication rates during deployment and after the use of FRED (FREDTM, TUSTIN, CA.- MicroVention, Inc.) and PED (PEDTM, ev3; Plymouth, Minnesota) flow-diverting stents for cerebral aneurysms.

METHOD AND MATERIALS

Informed consent was obtained from all patients. We implanted 91 flow diversion devices, including 51 PED and 46 FRED with or without adjunctive intraaneurysmal embolization for treatment of a total of 95 aneurysms between February 2012-April 2015 in our institution (Forty FRED devices to treat 46 aneurysms in 35 cases and 51 Pipeline devices to treat 49 aneurysms in 36 cases.). All patients underwent ani-platelet therapy. Angiographic follow-up examinations were carried out in 50 patients (Thirty of PED and 20 of FRED cases.). Median clinical follow up period was 1,33 year :(1,81 year in PED and 0,85 year in FRED group).

RESULTS

The flow diverter was successfully deployed in 87 of 91 stents (95.6%). The complete or near-complete occlusion rate was 70% in PED and 95% in FRED cases who had angiographic follow ups. Postprocedural aneurysm hemorrhage and consequent subarachnoid bleeding occurred in 1 patients from PED group due to stent migration. Total mortality rate during study period was 0%. We experienced failure of PED expansion in two patients whereas only one early deployment of stent within normal segment of ICA occured in FRED group. We also encountered acute stent thrombosis within one hour of FRED deployment in one case. The stent was recanalized by deployment of a Solitaire AB (eV3[™], Irvine, CA, USA) stent and intraarterial Tirofiban infusion. During angiographic follow ups 1 case of each group showed evidence of asymptomatic in-stent stenosis.

CONCLUSION

Flow-diverting stents play an important role in the treatment of intracranial aneurysms. Considering our experience, easier delivery and implantation, retrievability owing to its different design and higher aneurysmal occlusion rate in FRED makes it more advantageous in treatment of cerebral aneurysms when compared with PED. The relative efficacy and morbidity of these treatment methods must be considered in the context of available alternate interventions.

CLINICAL RELEVANCE/APPLICATION

FRED flow diverter may be more advantageous in treatment of cerebral aneurysms when compared with PED.

SSM17-04 Prediction of Technical Endovascular Stent-Retriever Thrombectomy Outcome by Dynamic CT Angiography in Patients with Acute Ischemic Stroke

Wednesday, Dec. 2 3:30PM - 3:40PM Location: N227

Birgit B. Ertl-Wagner, MD, Munich, Germany (*Abstract Co-Author*) Nothing to Disclose Sebastian E. Beyer, Munich, Germany (*Abstract Co-Author*) Nothing to Disclose Wolfgang G. Kunz, MD, Munich, Germany (*Abstract Co-Author*) Nothing to Disclose Hendrik Janssen, MD, Dusseldorf, Germany (*Abstract Co-Author*) Nothing to Disclose Felix G. Meinel, MD, Munich, Germany (*Abstract Co-Author*) Nothing to Disclose Maximilian F. Reiser, MD, Munich, Germany (*Abstract Co-Author*) Nothing to Disclose

PURPOSE

The aim of this study was to determine the predictive value of three different dynamic CT angiography (dynCTA) parameters - occlusion length, collateralization extent, and time delay to maximum enhancement - for latest generation stent-retriever thrombectomy recanalization outcome in patients with acute ischemic stroke.

METHOD AND MATERIALS

In this IRB-approved study, subjects were selected from an initial cohort of 2059 consecutive patients who had undergone multiparametric CT including whole-brain CT perfusion (WB-CTP). We included all patients with (a) a complete occlusion of the M1-segment of the MCA or the carotid T and (b) subsequent intraarterial stent-retriever thrombectomy. dynCTA was reconstructed from WB-CTP raw datasets. Technical outcome of thrombectomy was scored using the modified Thrombolysis in Cerebral Infarction (mTICI) scale. Logistic regression analyses were performed to determine independent predictors of a favorable outcome (mTICI=3).

RESULTS

A total of 69 patients (mean age 68±14yrs, 46% male) were included for statistical analysis. mTICI scores after recanalization were as follows: mTICI=0: 5 patients, mTICI=1: 3 patients, mTICI=2a: 6 patients, mTICI=2b: 24; mTICI=3: 31 patients. In the regression analysis, a short occlusion length was an independent predictor of favorable technical outcome (OR: 0.41, p < 0.05). Both collateralization grade (OR: 1.00, p > 0.05) and time delay to peak enhancement (OR: 0.90, p > 0.05) failed to predict a favorable outcome.

CONCLUSION

A shorter occlusion length as assessed by dynCTA is associated with a better recanalization success, while collateralization grade and time delay of maximum enhancement distal to the occlusion failed to predict thrombectomy outcome.

CLINICAL RELEVANCE/APPLICATION

Large vessel occlusion length as determined by dynamic CT angiography is an independent predictor for the technical outcome of stent-retriever thrombectomy in patients with acute ischemic stroke and may be considered as a possible decicion-making parameter for patient selection.

SSM17-05 Should Informed Radiation Consent Exist for Neurovascular Interventional Radiology Procedures? The Patient Perspective

Wednesday, Dec. 2 3:40PM - 3:50PM Location: N227

Participants

Rebecca Zener, MD, London, ON (*Presenter*) Nothing to Disclose Peter B. Johnson, MBBS, Kingston 7, Jamaica (*Abstract Co-Author*) Nothing to Disclose Amol Mujoomdar, MD, London, ON (*Abstract Co-Author*) Speaker, Cook Group Incorporated; Speaker, Medtronic, Inc Sachin Pandey, MD, Dedham, MA (*Abstract Co-Author*) Nothing to Disclose

PURPOSE

Radiation exposure is inherent in neurovascular interventional radiology (IR). A potential exposure of 1 mSv has been suggested as a cutoff for provision of risk information, as it corresponds to a 1 in 10000 increased cancer risk. Informed consent requires disclosure of rare yet potentially significant risks, yet patient and non-radiologist physician knowledge of these risks is lacking. Neurovascular IR patient perception and knowledge of these risks remains unknown. The purpose of this study is to explore neurovascular IR patient perception of cancer-related radiation risk exposure and whether radiation consent is warranted.

METHOD AND MATERIALS

A multiple-choice survey was administered to 42 adult patients undergoing a non-emergent neurovascular IR procedure at a tertiary care centre. 67% of patients had previously undergone a neurovascular IR procedure. Statistical analysis of with Fisher Exact test was performed based on patient past neurovascular IR history (p<0.05).

RESULTS

Almost all subjects (90%) wanted to be informed if the radiation-related increased cancer risk was 1 in 100. Most (82%) wanted to be informed if the risk was moderate, 1 in 1000, or low, 1 in 10000 (70%). Only half of the patients were aware that they were exposed to radiation during their procedure, irrespective of previous neurovascular IR history. The majority (74%) believed that the ordering physician should be responsible for informing patients about radiation exposure. Most (85%) believed radiation consent should include radiation-related cancer risks, and that both verbal and written radiation consent should be obtained (74%). No significant difference was present based on past neurovascular IR history (p>0.05).

CONCLUSION

Neurovascular IR patient awareness of radiation exposure is suboptimal. Based on this survey, most patients want to discuss cancer-related radiation risks with the ordering physician in order to make informed decisions. This is potentially concerning as non-radiologist ordering physicians may not be as knowledgeable on radiation-related cancer risks. Neurointerventional radiologists should consider obtaining informed consent for procedures with anticipated doses of 1 mSv or greater.

CLINICAL RELEVANCE/APPLICATION

Neurovascular IR patients want to discuss cancer-related radiation exposure risk prior to undergoing an intervention in order to help them make an informed decision.

between Balloon Guide Catheter (BGC) and non-Balloon Guide Catheter (NBGC) in Acute Ischemic Stroke

Wednesday, Dec. 2 3:50PM - 4:00PM Location: N227

Participants

Aglae Velasco Gonzalez, MD, Muenster, Germany (*Presenter*) Nothing to Disclose Christian Stracke, Essen, Germany (*Abstract Co-Author*) Nothing to Disclose Shoma Berkemeyer, Muenster, Germany (*Abstract Co-Author*) Nothing to Disclose Boris Buerke, MD, Muenster, Germany (*Abstract Co-Author*) Nothing to Disclose Michael A. Stauder, Essen, Germany (*Abstract Co-Author*) Nothing to Disclose Christian Cnyrim, Muenster, Germany (*Abstract Co-Author*) Nothing to Disclose Wolfram Schwindt, MD, Muenster, Germany (*Abstract Co-Author*) Nothing to Disclose Thomas Niederstadt, MD, Muenster, Germany (*Abstract Co-Author*) Nothing to Disclose Walter L. Heindel, MD, Muenster, Germany (*Abstract Co-Author*) Nothing to Disclose Rene Chapot, MD, PhD, Essen, Germany (*Abstract Co-Author*) Nothing to Disclose

PURPOSE

The catheter system for mechanical thrombectomy (MT) with stent retrievers (SR) could be an important factor when it comes to successful and more rapid recanalization procedures. Multicenter retrospective data collection and comparative analysis were employed to assess the efficacy of intra-arterial mechanical thrombectomies carried out using the Balloon Guide Catheter (BGC) and the non-Balloon Guide Catheter (NBGC).

METHOD AND MATERIALS

170 consecutive patients with MCA or carotid terminus occlusions treated by SR with the BGC (N=90) or NBGC (N=80) at three stroke centers were analyzed retrospectively. Data on procedure duration, number of passes, initial and final angiographic findings were collected. The degree of vessel occlusion initially and post-intervention was defined as the Thrombolysis in Cerebral Infarction(mTICI) score. Successful revascularization was defined as a final mTICI score >=2b achieved upon conclusion of the procedure after <=3 passes. Adjuvant therapy was defined as intra-arterial thrombolysis, intracranial angioplasty, or stenting performed after a failed MT.

RESULTS

Successful recanalization (mTICI grade 3 or 2b accomplished within <=3 passes) was achieved with the BGC in 80 out of 90 thrombectomies (88.8%), significantly different from the successful recanalization rates achieved using the NBGC (67%;p<0.001). The one-pass-thrombectomy rate with BGC was significantly higher than for NBGC (62.2%vs.35%; p<0.001). The mean number of passes for a complete recanalization (mTICI3 or 2b) was 1.5 \pm 0.8 in the BGC group and 2.0 \pm 1.1 in the NBGC group. Recanalization procedure duration for a TICI3 or 2b was significantly shorter using the BGC (24.5 \pm 15.2 min) than the NBGC (53.2 \pm 37.8 min; p<=0.05). Intra-arterial thrombolysis, intracranial angioplasty, and stent placement after a failed MT were performed in 6.6% and 12.5% of the BGC and NBGC patients (BGC vs NBGC, p<=0.90).

CONCLUSION

The efficacy of mechanical thrombectomy with stent retrievers in acute ischemic stroke in the anterior circulation in terms of angiographic results and procedure duration was improved when performed in combination with BGC.

CLINICAL RELEVANCE/APPLICATION

Efficacy of mechanical thrombectomy with stent retrievers in acute ischemic stroke is improved when performed in combination with Ballon Guide Catheter.

Neuroradiology (Cerebral Ischemia and Hemorrhage)

Wednesday, Dec. 2 3:00PM - 4:00PM Location: N229



AMA PRA Category 1 Credit ™: 1.00 ARRT Category A+ Credit: 1.00

Participants

Ronald L. Wolf, MD, PhD, Philadelphia, PA (*Moderator*) Nothing to Disclose Jalal B. Andre, MD, Seattle, WA (*Moderator*) Research Grant, Koninklijke Philips NV; Consultant, Hobbitview, Inc; Research Grant, Toshiba Corporation;

Sub-Events

SSM19-01 Comparison of Iodinated Contrast Staining and Hyperacute Hemorrhage on MRI : Phantom Study

Wednesday, Dec. 2 3:00PM - 3:10PM Location: N229

Participants

Sung-Hye You, MD, Seoul, Korea, Republic Of (*Presenter*) Nothing to Disclose Kyu Ri Son, MD, Seoul, Korea, Republic Of (*Abstract Co-Author*) Nothing to Disclose Byung-Joon Kim, MD, Seoul, Korea, Republic Of (*Abstract Co-Author*) Nothing to Disclose Nam Joon Lee, Seoul, Korea, Republic Of (*Abstract Co-Author*) Nothing to Disclose Mina Song, MD, Seoul, Korea, Republic Of (*Abstract Co-Author*) Nothing to Disclose

PURPOSE

To evaluate the effect of diluted iodinated contrast agents with normal saline or blood on the magnetic resonance (MR) imaging, especially on T1 weighted image(T1WI), T2 weighted image (T2WI) and gradient echo image(GRE) for distinguishing contrast staining from hyperacute hemorrhage which could occur after intraarterial thrombolysis in the patient with acute stroke.

METHOD AND MATERIALS

On a 3.0T MRI, T1WI, T2WI and GRE images were scanned using the phantom with diluted five different kinds of non-ionic iodinated contrast agents with different concentration (0, 0.1, 0.4, 0.6, 1.2, 2, 2.4 M I mole/L). The contrast agents are diluted with normal saline or venous blood (which was sampled within 6 hours). We compared SI of the phantom visually, and quantitatively calculated T1- and T2-relaxation times.

RESULTS

Iodinated contrast agents showed T1 and T2 shortening effect. With increase in concentration of contrast agents, the effect of T1 and T2 shortening became more prominent. T2 shortening effect of the iodinated contrast agents was much weaker than that of the product of venous blood. Whereas diluted iodinated contrast agents with normal saline showed intermediate SI on GRE image, blood with/without iodinated contrast agents showed dark SI on GRE image.FIG Comparison of SI among the physiolotic saline, undiluted iodinated contrast agent with saline, contrast agent diluted with blood and undiluted blood itself on T2WI, T1WI and GRE image. Contrast agent mixed with blood or blood itself could be distinguished from diluted iodinated contrast agents at T2WI and GRE image.

CONCLUSION

By obtaining T2WI and GRE images, clinicians may be able to discriminate iodinated contrast staining from hyperacute hemorrhage in stroke patients receiving transarterial thrombolysis.

CLINICAL RELEVANCE/APPLICATION

By obtaining T2WI and GRE images, clinicians may be able to discriminate iodinated contrast staining from hyperacute hemorrhage in acute stroke patients after intrasarterial thrombolysis.

SSM19-02 Digital Subtraction Angiogram for Perimesencephalic Subarachnoid Hemorrhage: Is Once Enough? A Retrospective Study, Systematic Review and Meta-analysis

Wednesday, Dec. 2 3:10PM - 3:20PM Location: N229

Participants

Christopher A. Potter, MD, Boston, MA (*Presenter*) Nothing to Disclose Kathleen R. Fink, MD, Seattle, WA (*Abstract Co-Author*) Nothing to Disclose Amanda L. Ginn, BA, Seattle, WA (*Abstract Co-Author*) Nothing to Disclose David R. Haynor, MD, PhD, Seattle, WA (*Abstract Co-Author*) Nothing to Disclose

PURPOSE

Non-aneurysmal subarachnoid hemorrhage (NASAH) accounts for 15% of subarachnoid hemorrhage (SAH) cases. A subset of NASAH patients with perimesencephalic hemorrhage distribution (PM-NASAH) has a relatively benign clinical course. Identifying these patients on initial imaging can prevent exposure to the risks of multiple conventional angiograms. Previous studies demonstrating adequacy of a single initial digital subtraction angiogram (DSA) have been suggestive, but underpowered.

METHOD AND MATERIALS

Our institutional retrospective study included consecutive patients from 01/2000-12/2013 with noncontrast head CT within 48 hours positive for SAH, negative initial DSA and followup DSA within 10 days. 252 subjects were identified. Head CT images were reviewed and strictly classified per criteria of van Gijn. 131 subjects with PM-NASAH were identified. DSA reports and images were

reviewed. The medical record was reviewed, including condition at last follow up.Systematic review and meta-analysis using MEDLINE and electronic databases from database inception through 11/01/2014 identified studies documenting workup of patients with NASAH. Inclusion criteria were (a) consecutive patients, (b) head CT within 72h, (c) categorization of PM-NASAH as per Gijn et al, (d) initial negative DSA, (e) follow up DSA within 10 days. Exclusion criteria included cohort of less than 25 subjects. Data from 6 included studies were pooled. Methodology was assessed using the MOOSE guidelines for observational meta-analyses.

RESULTS

131 subjects from our institutional study were pooled with 298 subjects from 6 included studies. No aneurysm was seen on follow up DSA at our institution. 3 aneurysms were reported in the included studies. 2 of the 3 were reported in studies with cases that preceded current DSA technique. Diagnostic yield of subsequent DSA following initial negative DSA was 0.7% (95% CI, 0-1.4%), similar or less than the rate of DSA complication, reported from 0.3% to 2.6%.

CONCLUSION

In patients with SAH that strictly adheres to the PM-NASAH pattern, a single DSA essentially excludes a causative aneurysm. Subsequent DSA examinations are very unlikely to benefit and expose patients to unnecessary risk.

CLINICAL RELEVANCE/APPLICATION

Complications from SAH and hemorrhage recurrence in patients with PM-NASAH are rare. Reducing additive risk of multiple DSA examinations is essential in the preventing complications in a benign disease course.

SSM19-03 Dynamics of Cerebral Perfusion Deficits after Subarachnoid Hemorrhage - Predictive Value of an Early Incidence

Wednesday, Dec. 2 3:20PM - 3:30PM Location: N229

Participants

Christian Rubbert, MD, Dusseldorf, Germany (*Presenter*) Nothing to Disclose Rebecca May, MD, Dusseldorf, Germany (*Abstract Co-Author*) Nothing to Disclose Bernd Turowski, Duesseldorf, Germany (*Abstract Co-Author*) Nothing to Disclose

PURPOSE

Delayed cerebral ischemia (DCI) is the major contributor to reduced functional outcome after subarachnoid hemorrhage (SAH). Although the pathogenesis of DCI is not fully understood, limitations in microcirculation appear to be one of the main drivers. CT perfusion (CTP) imaging can indirectly measure microcirculation and is increasingly used in treatment decisions.Early changes in perfusion might be able to predict the risk for critical changes in perfusion after SAH and allow for further risk stratification. To this end, the value of early CTP imaging is retrospectively analyzed.

METHOD AND MATERIALS

Between 1/2006 and 6/2010 351 patients with an aneurysmal SAH underwent CTP imaging. According to local guidelines, CTP imaging is acquired within 1 day after aneurysm treatment (range 0-2d after SAH), 6-8d and 9-11d after SAH or when there is clinical suspicion for deterioration in brain perfusion. Inclusion criteria were 1) at least one early CTP exam <72h after SAH and 2) at least 3 CTP exams in total. 813 CTP exams of 166 patients (4.9 ± 1.8 exams/patient, aged 53.2 ± 12.4 , 65.1% female) were analyzed.Purpose-built software was used to automatically generate perfusion parameter maps, define a 1 cm wide circular ROI along the cortex and compute a running average over 10° every 2° for each parameter. The mean transit time (MTT) was evaluated. Critical changes in perfusion were defined as a mean MTT >=4.1s in a hemisphere according to prior work. Receiver-Operator-Characteristic analysis was performed to identify the MTT cutoff with the highest sensitivity and specificity in early CTP imaging to predict critical changes in perfusion in follow-up CTP imaging.

RESULTS

The optimal MTT cutoff was 3.58s (AUC 0.65). 88 of 166 patients (53%) had an early MTT >=3.58s. Critical changes in follow-up CTP imaging were observed in 67 of 166 patients (40.4%) and could be predicted with a sensitivity of 67.2% and specificity of 56.6%.

CONCLUSION

Critical changes in brain perfusion in follow-up CTP imaging can, to some degree, be predicted by early CTP imaging <72h after SAH. Further research is needed to improve the prediction model and include data on functional outcome. Given the potential disabilities due to DCI, a cutoff with a higher sensitivity and lower specificity may be of greater clinical value.

CLINICAL RELEVANCE/APPLICATION

Early CTP imaging might be used in the decision to escalate neuromonitoring.

SSM19-04 Diagnostic Yield of Cervical Spine MRI in the Setting of Angiogram-Negative Spontaneous Intracranial Subarachnoid Hemorrhage

Wednesday, Dec. 2 3:30PM - 3:40PM Location: N229

Participants Gelareh Sadigh, MD, Atlanta, GA (*Presenter*) Nothing to Disclose Chad A. Holder, MD, Atlanta, GA (*Abstract Co-Author*) Nothing to Disclose Jason W. Allen, MD, PhD, Atlanta, GA (*Abstract Co-Author*) Nothing to Disclose

PURPOSE

To assess the diagnostic yield of cervical spine (c-spine) magnetic resonance imaging (MRI) in identifying a structural cause for angiogram-negative spontaneous subarachnoid hemorrhage (SAH).

METHOD AND MATERIALS

Consecutive patients 18 years or older presenting with acute spontaneous (non-traumatic) intracranial SAH between February 2009

and October 2014 at two University Hospitals whose catheter angiography results did not reveal an etiology for the SAH, and who underwent c-spine MRI as part of the angiogram-negative SAH protocol, were eligible. Patients with acute intracerebral, subdural or epidural hematoma, parenchymal contusion, recent history of trauma, or previously known cervical vascular malformation were excluded. All patients underwent noncontrast head CT, CT angiography of the head and neck, and MRI of the brain and c-spine as part of the angiogram-negative SAH protocol. Radiology reports from c-spine MRI scans, interpreted by board-certified (CAQ) neuroradiologists, were retrospectively reviewed, with IRB approval.

RESULTS

232 patients met inclusion criteria (mean age 54 years; 50% male; 53% white; 26% African-American). 77% of patients presented to the hospital within 24 hours of experiencing symptoms. SAH was diagnosed by head CT in 97% of cases and by lumbar puncture in 3%. Of 135 patients with reported Hunt and Hess classification of SAH in the electronic medical record, 70% were scored 1, 4% scored 2, 18% scored 3, 7% scored 4, and 1% scored 5. Catheter angiography was performed within the first 4 days after admission in all cases (median of 12 hours). C-spine MRI was performed within the first 19 days after admission in all cases (median of 24 hours). In all 232 patients (100%), c-spine MRI was negative for an etiology to explain the SAH.

CONCLUSION

In our large retrospective series, c-spine MRI following angiogram-negative spontaneous SAH, specifically following a negative head and neck CTA, had no diagnostic yield and is not routinely needed.

CLINICAL RELEVANCE/APPLICATION

C-spine MRI following angiogram-negative SAH has very low to no diagnostic yield. Our data indicate that routine MRI for cervical sources of intracranial SAH after a negative angiogram is not warranted.

SSM19-05 Blood Brain Barrier Permeability Imaging Correlates with Cerebrospinal Fluid Matrix Metalloproteinase-2 (MMP-2) Levels in Aneurysmal Subarachnoid Hemorrhage

Wednesday, Dec. 2 3:40PM - 3:50PM Location: N229

Participants

Jana Ivanidze, MD, PhD, New York, NY (*Presenter*) Nothing to Disclose Omar N. Kallas, MD, New York, NY (*Abstract Co-Author*) Nothing to Disclose Ashley E. Giambrone, PhD, New York, NY (*Abstract Co-Author*) Nothing to Disclose Michael Lerario, New York, NY (*Abstract Co-Author*) Nothing to Disclose Alan Z. Segal, New York, NY (*Abstract Co-Author*) Nothing to Disclose Ajay Gupta, MD, New York, NY (*Abstract Co-Author*) Research Consultant, Biomedical Systems; Research support, General Electric Company Moonsoo Jin, New York, NY (*Abstract Co-Author*) Nothing to Disclose Pina C. Sanelli, MD, Manhasset, NY (*Abstract Co-Author*) Nothing to Disclose

PURPOSE

CT Perfusion (CTP) allows assessment of quantitative blood brain barrier permeability (BBBP) parameters, including PS (flow across the vessel wall to the extravascular extracellular space (EES)), Ktrans (plasma flow per unit tissue volume), and VE (EES volume). However, sensitivity has to date not been established in the clinical setting. Matrix metalloproteinase 2 (MMP-2) is a known molecular upregulator of BBBP. The purpose of our study was to correlate quantitative BBBP parameters on CTP with MMP-2 cerebrospinal fluid (CSF) protein levels in aneurysmal subarachnoid hemorrhage (SAH) patients to assess the ability of CTP to detect BBB dysfunction in the clinical setting.

METHOD AND MATERIALS

In this prospective IRB-approved study, 10 SAH patients underwent extended whole brain CTP with an axial shuttle mode protocol on day 0-3 after aneurysmal rupture. CTP data were post-processed into quantitative PS, Ktrans and VE maps using Olea Sphere software (Olea Medical, La Ciotat, France). Global mean values were calculated from standardized cortically based ROIs. CSF was collected via ventriculostomy catheter (placed for intracranial pressure management) within 24 hours of CTP. MMP-2 protein levels were measured in CSF supernatant using multiplex microbead immunoassay technology (Luminex Corp, Austin, TX). Spearman correlation analysis was performed to determine correlation between MMP-2 levels with each BBBP parameter.

RESULTS

Median patient age was 55 years, and the median modified Fisher score was 4. 80% of patients had hydrocephalus and 70% had global cerebral edema at presentation. There was a statistically significant positive correlation between MMP-2 CSF levels and PS (r = 0.6565; p = 0.0448), Ktrans (r = 0.8024; p = 0.0075), and VE (r = 0.7477; p = 0.0164), respectively.

CONCLUSION

Elevation of PS, Ktrans and VE indicates increased flow across the BBB into the EES, or increased BBBP. MMP-2 is an established indicator of BBBP. We demonstrate that elevated BBBP, as evaluated by CTP, correlates with elevated CSF levels of MMP-2 in patients with SAH, further establishing CTP as a promising tool to assess BBB dysfunction in the clinical setting.

CLINICAL RELEVANCE/APPLICATION

This preliminary study supports the clinical application of quantitative BBBP imaging with CTP. In SAH, where elevated BBBP has been shown to correlate with poor clinical outcomes, this application may become an important prognostic indicator in future studies.

SSM19-06 Preliminary Evaluation of Arterial Spin Labeling as a Method to Predict Clinically Significant Vasospasm Following Aneurysmal Subarachnoid Hemorrhage

Wednesday, Dec. 2 3:50PM - 4:00PM Location: N229

Participants

Jalal B. Andre, MD, Seattle, WA (*Presenter*) Research Grant, Koninklijke Philips NV; Consultant, Hobbitview, Inc; Research Grant, Toshiba Corporation;

Michael Levitt, MD, Seattle, WA (*Abstract Co-Author*) Research Grant, Koninklijke Philips NV Danial K. Hallam, MD, Seattle, WA (*Abstract Co-Author*) Nothing to Disclose Greg Zaharchuk, MD, PhD, Stanford, CA (*Abstract Co-Author*) Research Grant, General Electric Company; Daniel S. Hippe, MS, Seattle, WA (*Abstract Co-Author*) Research Grant, Koninklijke Philips NV; Research Grant, General Electric Company Basavaraj Ghodke, MD, Seattle, WA (*Abstract Co-Author*) Nothing to Disclose Laligam Sekhar, MD, Seattle, WA (*Abstract Co-Author*) Nothing to Disclose

Danny J. Wang, PhD, Los Angeles, CA (Abstract Co-Author) Research Grant, Siemens AG Research Grant, Biogen Idec Inc Shareholder, Translational MRI, LLC

Max Wintermark, MD, Lausanne, Switzerland (Abstract Co-Author) Advisory Board, General Electric Company;

Louis Kim, MD, Seattle, WA (Abstract Co-Author) Nothing to Disclose

Yoshimi Anzai, MD, Salt Lake Cty, UT (Abstract Co-Author) Nothing to Disclose

PURPOSE

To evaluate a multidelay, pseudocontinuous arterial spin labeling (MDpCASL)-based screening tool for the diagnosis of vasospasm (VSP) in patients with aneurysmal subarachnoid hemorrhage (aSAH).

METHOD AND MATERIALS

Patients with clinically suspected VSP after aSAH (based on clinical and/or Transcranial Doppler exam) underwent a 10-minute MDpCASL MRI en route to digital subtraction angiography (DSA) for endovascular VSP intervention. The multi-parametric MDpCASL sequence was performed with background suppression and 3-dimensional gradient- and spin-echo readout, at 4 postabel delays (=1.5/2/2.5/3s), and processed using an in-house post-processing pipeline to generate quantitative CBF maps. DSA images were independently reviewed by two blinded, expert neurointerventional readers at a PACS station for the presence, location and extent of VSP, and asked to provide treatment recommendations. Readers were then shown corresponding ASL images and asked how this information influenced treatment recommendations. ASL images were evaluated by a third, blinded expert reader with extensive ASL experience. DSA and ASL findings were aggregated into 5 major vascular territories per patient (anterior left and right, middle left and right and posterior) for comparison. Associations between DSA and ASL were analyzed using logistic regression based on generalized estimating equations to account for repeated measurements per patient.

RESULTS

Ten patients were studied. ASL perfusion deficits were significantly associated with spasm on DSA (p=0.002). ASL detected clinically significant perfusion deficits in nearly 31% of evaluated vascular territories, in which no significant (\geq 50%) DSA spasm was identified. 25% of territories with significant spasm had minimal perfusion deficits by ASL. Expert neurointerventionalists also agreed that having ASL images available prior to performing DSA would have changed treatment recommendations in 60% of cases. Blinded two-reader neurointerventional assessment of ASL images suggested that evaluation of ASL-derived CBF would have prevented 3 of 10 patients from undergoing an unnecessary DSA.

CONCLUSION

Perfusion information from MDpCASL prior to DSA may reduce unnecessary DSA in select patients and modify therapy in others, possibly improving patient triage and management.

CLINICAL RELEVANCE/APPLICATION

Obtaining MDpCASL prior to DSA may alter treatment in patients suspected of VSP following aSAH.

Honored Educators

Presenters or authors on this event have been recognized as RSNA Honored Educators for participating in multiple qualifying educational activities. Honored Educators are invested in furthering the profession of radiology by delivering high-quality educational content in their field of study. Learn how you can become an honored educator by visiting the website at: https://www.rsna.org/Honored-Educator-Award/

Yoshimi Anzai, MD - 2014 Honored Educator

ISP: Gastrointestinal (Pancreas Cystic Lesions)

Wednesday, Dec. 2 3:00PM - 4:00PM Location: E353C

GI CT MR

AMA PRA Category 1 Credit [™]: 1.00 ARRT Category A+ Credit: 1.00

Participants

Douglas S. Katz, MD, Mineola, NY (*Moderator*) Nothing to Disclose Desiree E. Morgan, MD, Birmingham, AL (*Moderator*) Research support, General Electric Company

Sub-Events

SSM10-01 Gastrointestinal Keynote Speaker: Update on the Management of Small Pancreatic Cysts

Wednesday, Dec. 2 3:00PM - 3:10PM Location: E353C

Participants Douglas S. Katz, MD, Mineola, NY (*Presenter*) Nothing to Disclose

Honored Educators

Presenters or authors on this event have been recognized as RSNA Honored Educators for participating in multiple qualifying educational activities. Honored Educators are invested in furthering the profession of radiology by delivering high-quality educational content in their field of study. Learn how you can become an honored educator by visiting the website at: https://www.rsna.org/Honored-Educator-Award/

Douglas S. Katz, MD - 2013 Honored Educator Douglas S. Katz, MD - 2015 Honored Educator

SSM10-03 Diffusion-Weighted MR Imaging in Distinguishing between Mucin-producing and Serous Pancreatic Cysts

Wednesday, Dec. 2 3:20PM - 3:30PM Location: E353C

Participants

Chiara Pozzessere, MD, Siena, Italy (*Presenter*) Nothing to Disclose Sandra L. Castanos Gutierrez, MD, Baltimore, MD (*Abstract Co-Author*) Nothing to Disclose Celia P. Corona-Villalobos, MD, Baltimore, MD (*Abstract Co-Author*) Nothing to Disclose Chunmiao Xu, MD, Baltimore, MD (*Abstract Co-Author*) Nothing to Disclose Ihab R. Kamel, MD, PhD, Baltimore, MD (*Abstract Co-Author*) Nothing to Disclose

PURPOSE

Pancreatic cysts detection has increased due to the widespread use of advanced cross-sectional imaging. Pancreatic cysts represent a wide spectrum of lesions varying from those with extremely low malignant potential, to those associated with cancer. Mucin-producing cysts have a malignant potential, whereas serous cysts are generally benign. An overlap between imaging features can be misleading, and in the indeterminate cases additional evaluations such as follow up, FNA and/or surgery are required. The aim of this study was to evaluate the feasibility and the reproducibility of diffusion-weighted imaging (DWI) in characterizing pancreatic cysts when standard imaging is not diagnostic.

METHOD AND MATERIALS

Forty-four pancreatic cysts (43 patients; 27 females; 16 males; mean age 47 years) underwent histological or cyst fluid analysis after MRI including DWI were retrospectively analyzed. Three blinded readers independently evaluated signal intensity (SI) and ADC. Intra-observer and inter-observer agreement were calculated. Fisher's exact test and Welch's t test were used to compare SI and ADC values respectively, to pathological results. Diagnostic accuracy of thresholds ADC was assessed by ROC analysis. A p value of less than 0.05 was considered statistically significant.

RESULTS

The mean ADC value of the mucin-producing cysts was $3.26 \times 10-3 \text{ mm2/sec}$, $3.27 \times 10-3 \text{ mm2/sec}$ and $3.35 \times 10-3 \text{ mm2/sec}$ for the three readers, respectively. The mean ADC value of the serous cysts was $2.86 \times 10-3 \text{ mm2/sec}$, $2.85 \times 10-3 \text{ mm2/sec}$ and $2.85 \times 10-3 \text{ mm2/sec}$ and $2.85 \times 10-3 \text{ mm2/sec}$ for the three readers, respectively. Difference in ADC values between the two cyst groups was 12.4%, 12.9% and 14.8% for the three readers, respectively (p<0.001). Intra-observer and inter-observer agreement were excellent. ROC analysis showed an area under the curve of 0.82 (CI, 0.69-0.94), 0.81 (CI, 0.67-0.94) and 0.85 (CI, 0.69-0.95) for the three readers, respectively. A threshold ADC of $3\times 10-3 \text{ mm2/sec}$ resulted in correct identification of cysts in 77-81% of cases, with sensitivity and specificity ranging between 84-88% and 66-72%, respectively.

CONCLUSION

DWI may be a helpful tool in distinguishing between mucin-producing and serous pancreatic cysts.

CLINICAL RELEVANCE/APPLICATION

ADC values may be used to differentiate between mucin-producing and serous cysts of the pancreas and could potentially reduce unnecessary invasive approaches to diagnosis or the need for follow up studies.

Honored Educators

Presenters or authors on this event have been recognized as RSNA Honored Educators for participating in multiple qualifying

educational activities. Honored Educators are invested in furthering the profession of radiology by delivering high-quality educational content in their field of study. Learn how you can become an honored educator by visiting the website at: https://www.rsna.org/Honored-Educator-Award/

Ihab R. Kamel, MD, PhD - 2015 Honored Educator

SSM10-04 Transabdominal Ultrasound of the Pancreas for Surveillance of Known Pancreatic Cystic Lesions

Wednesday, Dec. 2 3:30PM - 3:40PM Location: E353C

Participants

Maryellen R. Sun, MD, Boston, MA (*Presenter*) Research Grant, Glaxo SmithKline plc Corinne D. Strickland, MD, MS, Boston, MA (*Abstract Co-Author*) Shareholder, Thayer Medical Corporation Bahar Tamjeedi, MD, Montreal, QC (*Abstract Co-Author*) Nothing to Disclose Alexander Brook, PhD, Boston, MA (*Abstract Co-Author*) Spouse, Research Grant, Guerbet SA Olga R. Brook, MD, Boston, MA (*Abstract Co-Author*) Nothing to Disclose Robert A. Kane, MD, Boston, MA (*Abstract Co-Author*) Nothing to Disclose Koenraad J. Mortele, MD, Boston, MA (*Abstract Co-Author*) Nothing to Disclose Bettina Siewert, MD, Brookline, MA (*Abstract Co-Author*) Nothing to Disclose

PURPOSE

To assess the utility of transabdominal ultrasound in follow up evaluation of known pancreatic cystic lesions (PCL) using same-day MRI examinations as gold standard.

METHOD AND MATERIALS

In an IRB-approved, HIPAA-compliant study, patients with known PCL scheduled for MRI follow up underwent prospective transabdominal ultrasound of the pancreas on the same date as the MRI examination. PCL were measured in transverse (TR), anteroposterior (AP), and craniocaudad (CC) dimensions and the longest dimension obtainable in any plane. US was performed in blinded fashion to same date MR results. Detection rate of US was correlated with patient factors including weight, AP abdominal diameter, thickness of subcutaneous abdominal fat, location of cyst within pancreas, and size of cyst, using chi-squared and Wilcoxon rank sum tests. Size measurements of pancreatic cysts at US were compared with MR measurements. MR measurements were taken as gold standard for cyst size.

RESULTS

252 PCL were evaluated in 57 patients (39 females, 18 males, mean age 67 yrs (range, 39-86 yrs)). Mean maximum cyst diameter was 8.5 mm (range, 2-92 mm). PCL were identified at ultrasound in 100% (5/5) of cysts \geq 3 cm; 92% (12/13) of cysts \geq 2 and <3 cm; 78% (43/55) of cysts \geq 1 and <2 cm; 35% (27/78) of cysts \geq 5mm and <1 cm; and 16% (16/101) of cysts <5 mm. Measured max diameter at US differed from max diameter at MRI by a mean 0.7 mm (range, - 6 to +16 mm); cysts were under measured by US in 46% and over measured in 31% of maximum diameter measurements, respectively. US identified 47% (14/30) of cysts located in uncinate process, 53% (27/51) in head; 83% (10/12) in neck, 52% (35/67) in body, and 18% (17/93) in tail. There were statistically significant correlations between PCL visualization at US and maximum cyst size (p<0.001), patient weight (p=0.012), and AP abdominal diameter (p=0.0059); no significant correlation (p=0.43) between thickness of subcutaneous abdominal fat and cyst visualization at ultrasound was identified.

CONCLUSION

The vast majority of PCL can be visualized at follow up with transabdominal ultrasound. Frequency of detection varies strongly with lesion size, location, patient weight and abdominal diameter.

CLINICAL RELEVANCE/APPLICATION

Many pancreatic cystic lesions known to exist from prior imaging can be visualized and accurately measured at follow up with transabdominal ultrasound. Body habitus and cyst size and location correlate with success of ultrasound.

SSM10-05 Fate of Small Pancreatic Cysts (<3cm) after Long-term Follow-up: Analysis of Significant Radiologic Characteristics and Proposal of Follow-up Strategy

Wednesday, Dec. 2 3:40PM - 3:50PM Location: E353C

Participants

Heera Yoen, Seoul, Korea, Republic Of (*Presenter*) Nothing to Disclose Dong Ho Lee, MD, Seoul, Korea, Republic Of (*Abstract Co-Author*) Nothing to Disclose Su Joa Ahn, Seoul, Korea, Republic Of (*Abstract Co-Author*) Nothing to Disclose Jeong Hee Yoon, MD, Seoul, Korea, Republic Of (*Abstract Co-Author*) Nothing to Disclose Joon Koo Han, MD, Seoul, Korea, Republic Of (*Abstract Co-Author*) Nothing to Disclose

PURPOSE

To describe the natural history of small, incidental pancreatic cysts after long-term follow-up, with an emphasis on identifying indicators of indolent lesions.

METHOD AND MATERIALS

We retrospectively selected 95 patients with 150 cysts from our hospital database. Selection criteria included patients with pancreatic cysts<3cm in CT from 2003-2004, followed with CT or MR for greater than 5 years (mean 117.1±19.6 months), or received pancreatic surgery during the follow-up period. Two radiologists reviewed the initial CT and recorded size, location, shape, ductal communication, p-duct dilatation, calcification and presumptive radiologic diagnosis of each cyst. We then recorded the size change after the conclusion of follow-up period. For patients who underwent an operation, we compared the cysts' radiologic features with those of the patients who did not undergo an operation. Furthermore, for surgical patients, we compared the preliminary radiologic diagnosis with the pathologic results.

RESULTS

Among 95 patients with 150 cysts, 12 patients with 16 cysts underwent operations. Out of 134 cysts in 83 non-surgical patients, 49(36.6%) cysts didn't change in size, while 57(42.5%) increased, and 27(20.9%) decreased or vanished. Among increased 57 cysts, only 5 were larger than 3cm at the end of the follow-up period. The initial size of the cyst was significantly larger in the surgical group compared to the nonsurgical group(17.2 ± 7.3 mm vs 11.3 ± 5.5 mm, p<0.000). Reasons for surgery included malignancy(4/95, 4.21%), borderline IPMN(6/95, 6.31%) with 5 moderate and 1 low grade, and SCN with increasing size(2/95, 2.11%). Pleomorphic and clubbed shape were significant features for borderline and malignant cysts. No cysts<15 mm and without p-duct change showed a significant change in size in 3 years.

CONCLUSION

The incidence of malignancy was 4.21% in our group. However, the majority of small cysts remained less than 3cm after long-term follow-up. The initial size of cysts as well as the shape are important features for predicting the progress and potential for malignant transformation. Patients with initial cysts<15mm, without P-duct change, and non-pleomorphic or clubbed shape may be assessed at long term intervals without significant risk of malignancy.

CLINICAL RELEVANCE/APPLICATION

It is a feasible strategy to extend follow-up interval for cysts<15mm, without P-duct change, non-pleomorphic or clubbed shape, which could lead to reduce medical expenditure.

SSM10-06 The Diagnostic Performance of Transabdominal Ultrasonography for Incidental Pancreatic Cysts: Focus on the Effect of Prior Images, Size, and Location

Wednesday, Dec. 2 3:50PM - 4:00PM Location: E353C

Participants

Ju Hyun Jeon, Seoul, Korea, Republic Of (*Presenter*) Nothing to Disclose Jung Hoon Kim, MD, Seoul, Korea, Republic Of (*Abstract Co-Author*) Nothing to Disclose Ijin Joo, MD, Seoul, Korea, Republic Of (*Abstract Co-Author*) Nothing to Disclose Joon Koo Han, MD, Seoul, Korea, Republic Of (*Abstract Co-Author*) Nothing to Disclose

PURPOSE

To assess diagnostic performance of transabdominal ultrasonography (TAUS) for incidental pancreatic cysts with a focus on the effect of prior images, size, and location.

METHOD AND MATERIALS

1064 pancreatic cysts which were radiologically confirmed by contrast enhanced CT (n=795), MRI (n=21), CT and MRI (n=202), or endoscopic ultrasonography (EUS, n=46), were included in 938 patients who underwent TAUS. TAUS finding was analyzed based on the formal reports. One radiologist also retrospectively reviewed TAUS, CT, MR, and EUS images to determine the size, location, and detection rate of the pancreatic cyst before and after CT, MRI, or EUS. For statistical analysis, independent samples T-test and Chi-square test were applied.

RESULTS

Among 1064 pancreatic cysts, 107 cysts underwent TAUS before CT, MR, or EUS and 477 cysts underwent TAUS after prior study. 480 cysts underwent TAUS both before and after CT, MRI, or EUS. Overall 940 pancreatic cysts (88.3%) were delineated on TAUS.The detection rate of pancreatic cyst on TAUS before CT, MRI, or EUS was 49.2% (289/587), and the detection rate of pancreatic cyst on TAUS after CT, MRI, or EUS was 86.7% (830/957). In a group of patients who underwent TAUS both before and after CT, MRI, or EUS, the detection rate of pancreatic cyst on TAUS was increased after CT, MRI, or EUS (before; 40.0%, after; 85.2%, p=0.0001).The size of detected cysts (mean±SD, 15.5±9.2 mm) was larger than undetected cysts (mean±SD, 11.8±7.5 mm, p<0.0001) with significant difference. Undetected cysts on US were almost smaller than 2cm. The detection rate of TAUS before CT, MRI, and EUS in neck, body, head, tail, and uncinated process was 60.7%, 55.7%, 54.6%, 37.9%, and 27.5%. The detection rate of TAUS after CT, MRI, and EUS in neck, head, body, uncinated process, and tail was 95.6%, 91.4%, 91%, 87.6%, and 67.8%.

CONCLUSION

Transabdominal US is useful for detection of pancreatic cyst. The detection rate of TAUS was improved after CT, MRI, and EUS regardless the location.

CLINICAL RELEVANCE/APPLICATION

Transabdominal US is useful image modality for incidental pancreatic cysts; especially follow up after CT, MRI, and EUS.

Breast Imaging (Practice Issues)

Wednesday, Dec. 2 3:00PM - 4:00PM Location: E451A

BR

AMA PRA Category 1 Credit ™: 1.00 ARRT Category A+ Credit: 1.00

Participants

Mary S. Newell, MD, Atlanta, GA (*Moderator*) Nothing to Disclose Jiyon Lee, MD, New York, NY (*Moderator*) Nothing to Disclose

Sub-Events

SSM01-01 Evaluation and Outcomes of Patients Presenting with Focal Breast Pain

Wednesday, Dec. 2 3:00PM - 3:10PM Location: E451A

Participants

Wendi A. Owen, MD, Saint Louis, MO (*Presenter*) Nothing to Disclose Hilary A. Brazeal, MD, Saint Louis, MO (*Abstract Co-Author*) Nothing to Disclose Hillary L. Shaw, MD, Saint Louis, MO (*Abstract Co-Author*) Nothing to Disclose Susan O. Holley, MD, PhD, Saint Louis, MO (*Abstract Co-Author*) Research Consultant, Biomedical Systems

PURPOSE

1. Determine number/characteristics of breast cancers found in women undergoing imaging evaluation for focal breast pain.2. Determine the optimal imaging evaluation of focal breast pain.

METHOD AND MATERIALS

We performed a chart review of 4720 women who underwent imaging evaluation of focal breast pain from 2001-2013. Women ages 18 and over with breast pain isolated to a single focus, quadrant, or two separate foci were included. Exclusion criteria were concurrent symptoms (palpable lump, nipple discharge/retraction); recent trauma; breast surgery in the last 6 months; lactation; and personal history of breast cancer. 944 patients met criteria.We recorded the type of imaging work-up, whether there was a focal finding corresponding to their site of pain, type of finding described, BI-RADS[™] assessment, whether biopsy was performed, and pathologic outcomes. Subsequent imaging/clinical follow up was recorded.

RESULTS

Patients ranged in age from 18-90 (mean 47). Imaging evaluation consisted of sonogram (US) alone in 286 women, mammogram (MG) alone in 231 women, and both US/MG in 427 women. Mammographic parenchymal densities were 7% extremely; 41% heterogeneously; 43% scattered; 9% fatty. 111 women had an imaging finding at the site of pain, 99 of which were benign. 12 biopsies of corresponding findings were performed: 9 were benign (1 papilloma, 3 fibroadenomas, 5 other); 3 were malignant (1 invasive lobular, 1 invasive ductal, 1 ductal carcinoma in situ). The malignancies were diagnosed in three women, ages 56, 57, and 61. Two women had a family history of breast cancer. All three malignancies were seen on MG; 2 had an US correlate. At initial evaluation, 4 breast cancers were diagnosed remote from the site of pain. Follow up evaluation demonstrated subsequent breast cancers at the site of pain in 6 women, ranging from 1-10 years after initial presentation.

CONCLUSION

A corresponding imaging finding is seen in 11% of patients with focal breast pain. Neither breast density nor age correlates with focal breast pain. Focal breast pain rarely signifies malignancy (3/944 patients). No cancers were detected in women younger than 56; all cancers were visible on mammogram.

CLINICAL RELEVANCE/APPLICATION

Focal breast pain is common, but is rarely associated with malignancy (0.3% in our study). Optimal workup of focal pain may be guided by patient's age; targeted ultrasound may not be necessary if the mammogram is negative.

SSM01-02 Inter-observer Variability in Upgraded and Non-Upgraded BIRADS 3 Lesions and Common Reasons for Misclassification

Wednesday, Dec. 2 3:10PM - 3:20PM Location: E451A

Participants

Aya Michaels, MD, Boston, MA (*Presenter*) Nothing to Disclose Chris S. Chung, MD, Kensington, MD (*Abstract Co-Author*) Nothing to Disclose Elisabeth P. Frost, MD, Boston, MA (*Abstract Co-Author*) Nothing to Disclose Robyn L. Birdwell, MD, Boston, MA (*Abstract Co-Author*) Nothing to Disclose Catherine S. Giess, MD, Wellesley, MA (*Abstract Co-Author*) Nothing to Disclose

PURPOSE

To evaluate if mammographic lesions initially assessed as BIRADS 3 but upgraded during imaging surveillance had appropriate initial evaluation, and to determine possible factors in lesion misclassification.

METHOD AND MATERIALS

An IRB approved retrospective review of the mammography database from 1/1/04-12/31/08 identified 1188 screen detected lesions assessed as BIRADS 3 on diagnostic workup, 60 (5.1%) upgraded to BIRADS 4 or 5 during surveillance (cases). Cases were matched by lesion type, laterality, and year to 60 non-upgraded BIRADS 3 lesions (controls). Available studies were assessed separately by

2 blinded breast radiologists using the BIRADS lexicon, with only index lesion and patient age identified. Assessments were recorded and compared to the original prospective interpretation.

RESULTS

82 studies prospectively assessed as BIRADS 3 were available for blinded review, including 43 cases (8 malignancies) and 39 controls. The first reader assessed 18/82 (22.0%) as BIRADS 0, 13 cases, 5 controls; 35/82 (42.7%) as BIRADS 2, 11 cases, 24 controls; 7/82 (8.5%) BIRADS 3, 4 cases, 3 controls; 22/82 BIRADS 4, 15 cases, 7 controls. The second reader assessed 8/82 (9.8%) as BIRADS 0, 4 cases, 4 controls; 27 (32.9%) BIRADS 2, 11 cases, 16 controls; 33 (40.2%) BIRADS 3, 19 cases, 14 controls; 14 (17.0%) BIRADS 4, 9 cases, 5 controls. The two readers had the same BIRADS assessment on 34/82 (41.5%) exams. Of the 8 cancers, the first reader assessed 2 as BIRADS 0, 1 as BIRADS 2, 1 as BIRADS 3, and 4 as BIRADS 4; the second reader assessed 2 as BIRADS 3, and 2 as BIRADS 4. Reasons for BIRADS 0 assessment included incomplete mammographic views, lack of ultrasound for masses or asymmetries, and failure to include the lesion on follow up imaging. On blinded review, reasons for BIRADS 4 assessment included suspicious morphology or documented instability.

CONCLUSION

Many BIRADS 3 lesions were judged to have had incomplete diagnostic evaluation on blinded review. Lesions assigned to the BIRADS 3 category are, by definition, challenging to evaluate. There is a large amount of inter-observer variability in assessment of these challenging mammographic lesions.

CLINICAL RELEVANCE/APPLICATION

Internal practice audits of upgraded and non-upgraded BIRADS 3 lesions may improve consistency in interpretation as much interobserver variability exists in assessment of lesions as probably benign.

Honored Educators

Presenters or authors on this event have been recognized as RSNA Honored Educators for participating in multiple qualifying educational activities. Honored Educators are invested in furthering the profession of radiology by delivering high-quality educational content in their field of study. Learn how you can become an honored educator by visiting the website at: https://www.rsna.org/Honored-Educator-Award/

Catherine S. Giess, MD - 2015 Honored Educator Robyn L. Birdwell, MD - 2015 Honored Educator

SSM01-03 Patient Preferences and Understanding of the Breast Imager's Role in Performing and Communicating Biopsy Results

Wednesday, Dec. 2 3:20PM - 3:30PM Location: E451A

Participants

Jordana Phillips, MD, Boston, MA (*Presenter*) Nothing to Disclose Hannah Perry, MD,MS, Boston, MA (*Abstract Co-Author*) Nothing to Disclose Nancy Littlehale, Boston, MA (*Abstract Co-Author*) Nothing to Disclose Vandana M. Dialani, MD, Boston, MA (*Abstract Co-Author*) Nothing to Disclose Valerie J. Fein-Zachary, MD, Boston, MA (*Abstract Co-Author*) Nothing to Disclose Euguenia Karimova, MD, Memphis, TN (*Abstract Co-Author*) Nothing to Disclose Priscilla J. Slanetz, MD, MPH, Belmont, MA (*Abstract Co-Author*) Nothing to Disclose Shambhavi Venkataraman, MD, Boston, MA (*Abstract Co-Author*) Nothing to Disclose Richard E. Sharpe JR, MD, MBA, Denver, CO (*Abstract Co-Author*) Nothing to Disclose Tejas S. Mehta, MD, MPH, Boston, MA (*Abstract Co-Author*) Nothing to Disclose

PURPOSE

As the health care model transforms to a value-based system, radiologists may potentially add value by communicating biopsy results directly to patients. However, limited data is available in this area. Our purpose was to evaluate from whom patients want to hear results after image-guided breast biopsy procedures.

METHOD AND MATERIALS

An anonymous survey was offered to patients undergoing any image- guided breast biopsy before meeting the breast radiologist (BR) and after the procedure from March 16, 2015 - March 27, 2015 using SurveyMonkey, as part of a preliminary analysis. At our academic institution, the procedure team includes a technologist, radiology resident or breast imaging fellow, nurse practitioner, and attending BR.

RESULTS

27/41(66%) patients responded. 18/41(64%) thought the BR was a physician, 7/41(25%) a technologist, and 2/41(7%) were unsure. 27(100%) felt that the BR was an essential part of the breast care team. For normal results, before and after the procedure respectively, 14(52%) and 16(60%) wanted to hear from the ordering provider, 6(22%) and 5(19%) from the performing BR, 0(0%) and 1(4%) from anyone in breast imaging, and 7(26%) and 5(19%) from whoever would give results the soonest. (p=NS). For abnormal results, before and after the procedure respectively, 17(62%) and 22(82%) wanted to hear from the ordering provider, 6(22%) and 0(0%) from the performing BR, 0(0%) and 1(4%) from anyone in breast imaging, and 4(15%) and 4(15%) from whoever would give results the soonest (p<0.05).

CONCLUSION

Although patients perceive the BR to be an essential part of their care, most prefer to hear results from their ordering provider, especially if abnormal. Many patients did not know the BR was a physician, suggesting the need for better communication and further patient education.

CLINICAL RELEVANCE/APPLICATION

Although a BR may add value by giving biopsy results; patients prefer to hear from the ordering provider. Further study is needed to understand patient preferences and understanding of the BR role.

SSM01-04 Proteomics at Work: Can a Protein-based Blood Assay Help Detect Breast Cancer in Women Aged 25-75 with BI-RADS 3 or 4 Imaging Findings?

Wednesday, Dec. 2 3:30PM - 3:40PM Location: E451A

Participants

Ana P. Lourenco, MD, Providence, RI (*Presenter*) Nothing to Disclose David E. Reese, PhD, New York, NY (*Abstract Co-Author*) Employee, Provista Diagnostics, Inc Christa Corn, MD, Scottsdale, AZ (*Abstract Co-Author*) Employee, Provista Diagnostics, Inc Michael Silver, MS, Scottsdale, AZ (*Abstract Co-Author*) Employee, Provista Diagnostics, Inc Rao Mulpuri, Scottsdale, AZ (*Abstract Co-Author*) Employee, Provista Diagnostics, Inc Kasey Benson, PhD, Scottsdale, AZ (*Abstract Co-Author*) Employee, Provista Diagnostics, Inc Elias Letsios, Scottsdale, AZ (*Abstract Co-Author*) Employee, Provista Diagnostics, Inc

PURPOSE

To determine if a blood assay can improve breast cancer detection in patients ages 25-75 with BI-RADS 3 or 4 imaging findings.

METHOD AND MATERIALS

This IRB approved, HIPAA compliant prospective multi-center study enrolled patients aged 25-75 with BI-RADS 3 or 4 imaging findings. Informed consent was obtained. Eligible patients included women ages 25 - 75 with BI-RADS 3 or 4 imaging, no history of cancer and no prior breast biopsy in the last six months. Patients not undergoing biopsy had imaging follow-up at 6 months. Multiple algorithms for the detection of cancer were developed in the training set. These were validated and the data from the training was combined to perform a full prospective/ retrospective analysis to optimize model sensitivity and specificity.

RESULTS

508 patients were enrolled and randomized; 300 in the training set and 208 in the validation set. Serum protein biopmarkers (SPBs) and tumor associated autoantibodies (TAAbs) identified in prior proteomic screens were measured prior to biopsy. Pathology results were recorded for all patients undergoing biopsy, and imaging results were recorded for all patients undergoing 6 month follow-up imaging. Individual biomarker concentrations and patient data were evaluated using logistic regression models developed from prior studies. The most robust of these models utilized 5 SPBs together with 13 TAAbs to generate an initial sensitivity of 82.2%, specificity of 82.5%, PPV of 28.4% with a NPV of 97.5%. This model also produced an AUC of 0.8485 in a ROC analysis. 6-month follow-up is ongoing, and some patients presumed benign may be diagnosed with invasive cancer and/or DCIS at follow-up. Of the 508 BI-RADS 3 or 4 patients, 344 were biopsied resulting in the diagnosis of 51 malignancies (14.8%). By comparison, the protein based blood assay identified 148 patients to be biopsied and identified 42 malignancies (28.4%).

CONCLUSION

This multi-center study suggests that blood assays combining SPBs and TAAbs can differentiate benign from malignant breast disease in women aged 25-75 with BI-RADS 3 or 4 imaging findings with high sensitivity and negative predictive value.

CLINICAL RELEVANCE/APPLICATION

Blood assays that could distinguish benign from malignant breast disease may help decrease the number of benign breast biopsies performed, thus decreasing healthcare costs and patient morbidity.

SSM01-05 Focal Breast Pain: Does Breast Density Affect the Need for Ultrasound?

Wednesday, Dec. 2 3:40PM - 3:50PM Location: E451A

Participants

Michael W. Cho, MD, MPH, Durham, NC (*Presenter*) Nothing to Disclose Lars J. Grimm, MD, Durham, NC (*Abstract Co-Author*) Advisory Board, Medscape, LLC; Karen S. Johnson, MD, Durham, NC (*Abstract Co-Author*) Research Consultant, Siemens AG

PURPOSE

To evaluate the utility of ultrasound in women with focal breast pain who are categorized as low breast density (predominantly fatty and scattered fibroglandular) on digital mammography.

METHOD AND MATERIALS

This study retrospectively reviewed 2176 cases of breast pain imaged between 12/6/06 and 3/15/13. Of these, 248 met inclusion criteria for primary focal breast pain: women (mean age 53 years) with focal, non-axillary, non-radiating pain isolated to one quadrant. Women who were pregnant or lactating or who had associated symptoms of palpable lump, skin changes, history of trauma or infection were excluded. Digital mammogram and directed ultrasound were performed at initial presentation. Breast density, mammogram, ultrasound, biopsy findings (when applicable), and follow up imaging results (mean: 3.8 years, range: 2.0-8.1 years) were collected.

RESULTS

Fourteen percent (35/248) of cases demonstrated a lesion at the site of focal pain by directed ultrasound. Nine percent (23/248) of lesions were seen only by ultrasound and had no correlate on digital mammography. Lesions detected only by ultrasound (ultrasound-only lesions) occurred in women categorized in the following breast density categories on digital mammography: 0% predominantly fatty, 22% (5/23) scattered fibroglandular, 44% (10/23) heterogeneously dense, and 35% (8/23) extremely dense. Ultrasound-only lesions prompted four biopsies, which all resulted in benign histology. Additionally, 2% (4/248) of cases reported incidental ultrasound-only lesions, triggering either additional (benign) biopsies or a two year course of imaging follow up. At two-year follow-up, one patient developed breast cancer in the same quadrant as the site of primary focal pain, where no findings were initially detected by either digital mammography or ultrasonography. This occurred in a woman with heterogeneously dense breast tissue. No subsequent cases of breast cancer occurred in women with low breast density.

CONCLUSION

No cancers would have been missed by excluding directed ultrasound in the evaluation of focal breast pain in low breast density

women with a negative digital mammogram.

CLINICAL RELEVANCE/APPLICATION

Digital mammography alone without directed ultrasound appears to be a reasonable approach in evaluating primary focal breast pain in women whose breast density is categorized as either scattered fibroglandular or predominantly fatty.

SSM01-06 Is Ultrasound Effective in the Detection of Breast Cancer in Patients Presenting with Breast Pain?

Wednesday, Dec. 2 3:50PM - 4:00PM Location: E451A

Participants

Andrea X. Gallo, MD, Toronto, ON (*Presenter*) Nothing to Disclose Monali Warade, MD, MBBS, Toronto, ON (*Abstract Co-Author*) Nothing to Disclose Franklin Goldberg, MD, Toronto, ON (*Abstract Co-Author*) Nothing to Disclose Derek Muradali, MD, Toronto, ON (*Abstract Co-Author*) Nothing to Disclose

PURPOSE

The purpose of this study is to determine if the routine use of ultrasound is appropriate for cancer detection in patients presenting with breast pain.

METHOD AND MATERIALS

All consecutive patients presenting to our department with a sole complaint of breast pain, who underwent a breast ultrasound, over a 4 year period, were included in this IRB-approved retrospective study. Patients with a history of breast cancer or palpable lumps were excluded. Breast ultrasounds were performed by technologists with 7-12 years experience and reviewed by one of two fellowship trained radiologists with 20 -25 years experience. All follow up imaging and pathology reports were reviewed.

RESULTS

422 patients were entered into the study (mean age 45 years). After the initial ultrasound, 368/422 patients were classified as BI-RADS 1 or 2, 40/422 as BI-RADS 3, 5/422 as BI-RADS 0 and 9/422 as BI-RADS 4. Follow up imaging tests included 5 mammograms, 236 ultrasounds and 5 MRI's over a 56 month period. At total of 26 image guided biopsies (20 core biopsies, 7 fine needle aspiration biopsies) and 1 surgical biopsy were performed for final diagnosis. All cases were classified as benign as a final diagnosis. There were no cases of invasive or non-invasive breast cancer.

CONCLUSION

Our data suggests that the prevalence of breast cancer in patients presenting with breast pain as a sole complaint is low. Breast ultrasound also resulted in a substantial number of unnecessary follow up imaging tests, potentially resulting in more harm than benefit in this patient population.

CLINICAL RELEVANCE/APPLICATION

The use of breast ultrasound to detect breast cancer in patients with breast pain as the sole presenting symptom may result in more harm than benefit, as the prevalence of breast cancer in this population is low.

Breast Imaging (Ultrasound Advanced Applications)

Wednesday, Dec. 2 3:00PM - 4:00PM Location: E451B

BR US

AMA PRA Category 1 Credit ™: 1.00 ARRT Category A+ Credit: 1.00

FDA Discussions may include off-label uses.

Participants

Sughra Raza, MD, Boston, MA (*Moderator*) Nothing to Disclose Catherine S. Giess, MD, Wellesley, MA (*Moderator*) Nothing to Disclose

Sub-Events

SSM02-01 The Utility of Ultrasound Superb Microvascular Imaging for Evaluation of Vascularity in Solid Breast Masses: Comparison with Color and Power Doppler Imaging-Interobserver Variability and Diagnostic Performance

Wednesday, Dec. 2 3:00PM - 3:10PM Location: E451B

Participants

Ah Young Park, MD, Ansan, Korea, Republic Of (*Presenter*) Nothing to Disclose Bo Kyoung Seo, MD, PhD, Ansan, Korea, Republic Of (*Abstract Co-Author*) Nothing to Disclose Kyu Ran Cho, MD, PhD, Seoul, Korea, Republic Of (*Abstract Co-Author*) Nothing to Disclose Ok Hee Woo, MD, Seoul, Korea, Republic Of (*Abstract Co-Author*) Nothing to Disclose Kyoonsoon Jung, Anyang, Korea, Republic Of (*Abstract Co-Author*) Nothing to Disclose Jaehyung Cha, Seoul, Korea, Republic Of (*Abstract Co-Author*) Nothing to Disclose Seon Jeong Oh, MD, Ansan, Korea, Republic Of (*Abstract Co-Author*) Nothing to Disclose

PURPOSE

To investigate the utility of ultrasound Superb Microvascular Imaging (SMI) for evaluation of solid breast masses by comparing with conventional Doppler imaging.

METHOD AND MATERIALS

A total of 191 solid breast masses in consecutive 169 patients were prospectively evaluated with color Doppler (CDI), power Doppler (PDI) and SMI before core needle biopsy between February 2014 and March 2015. Three breast radiologists analyzed number, distribution (peripheral, central, or both), and morphology (dot, linear, branching or tortuous/penetrating) of vessels within the masses, and assessed BI-RADS categories on gray-scale images and all vascular images of each mass. These features were correlated with pathological results. We evaluated interobserver variability in imaging analyses with intraclass correlation and compared diagnostic performance between gray-scale imaging only and combined use of gray-scale and each vascular imaging, CDI, PDI, and SMI for discrimination between benign and malignant masses with receiver operating characteristic (ROC) curve analysis. In addition, we used Kruskal-Wallis test to determine whether three vascular imaging techniques had significant difference.

RESULTS

Pathological diagnoses revealed 92 cancers and 99 benign lesions. Interobserver variability was excellent in assessment of BI-RADS categories and analyses of vascular images (range of intraclass correlation coefficients, 0.86-0.98). SMI showed more number of vessels and more frequent central or both distribution and branching or tortuous/penetrating morphology than CDI and PDI (P<.0001). In the diagnostic performance, the area under the ROC curve (AUC) was the best in combined use of gray-scale and SMI (AUC=0.815) when compared with other modalities (AUC=0.774 for gray-scale only, 0.789 for combined use of gray-scale and CDI, and 0.791 for combined use of gray-scale and PDI and this was statistically significant (P<.0001).

CONCLUSION

SMI is superior to CDI or PDI in the demonstration and characterization of vascularity in solid breast masses. The combined use of gray-scale and SMI can improve the diagnostic performance for the differentiation of benign and malignant breast masses.

CLINICAL RELEVANCE/APPLICATION

SMI is a recommendable technique for evaluation of tumor vascularity in the breast and could be a supportive tool for the differentiation between benign and malignant breast masses.

SSM02-02 Shear Wave Elastography Assessed with Maximum Visual Color Stiffness in Breast Lesions: The Role as a Complementary Study on B-mode US

Wednesday, Dec. 2 3:10PM - 3:20PM Location: E451B

Participants

Shin Ho Kook, MD, Seoul, Korea, Republic Of (*Presenter*) Nothing to Disclose Seon Hyeong Choi, Seoul, Korea, Republic Of (*Abstract Co-Author*) Nothing to Disclose Yoon Jung Choi, Seoul, Korea, Republic Of (*Abstract Co-Author*) Nothing to Disclose Jung Eun Lee, Seoul, Korea, Republic Of (*Abstract Co-Author*) Nothing to Disclose Inyoung Youn, MD, Seoul, Korea, Republic Of (*Abstract Co-Author*) Nothing to Disclose

PURPOSE

To evaluate the diagnostic performance of shear-wave elastography (SWE) with maximum visual color elasticity assessment in addition to B-mode US and the value as a complementary study on B-mode US in breast lesions.

METHOD AND MATERIALS

From Jan 2011 to Dec 2013, 1621 lesions (1293 benign, 328 malignant) of 1561 patients (mean age, 50.5) who underwent B-mode US and SWE before biopsy were included. The size and BI-RADS final assessment of B-mode US features of each lesion were recorded. Color SWE was retrospectively assessed with maximum color stiffness, using the color scale. Two cut-off values as blue (<40kPs, group 1) or blue to green (<80kPs, group 2) were used as benign reference points to differentiate from malignant lesions. Diagnostic performance (sensitivity, specificity, PPV, NPV and diagnostic accuracy) of each B-mode US, color SWE, and combination of two modalities were statistically evaluated.And they were also evaluated according to the lesion size (<1cm, 1-2 cm, 2-3cm, 3cm <).

RESULTS

SWE with maximum visual color elasticity assessment showed improvement of 1.3 and 0.9% in specificity and 8.5 and 5.1% in PPV by adding color SWE on B-mode US in group 1 and 2 (p<0.001), without improvement of overall diagnostic accuracy. The sensitivity, specificity, PPV, NPV and diagnostic accuracy are as follows; 75.5%, 95.9%, 84.5%, 93% and 91.3% for B-mode only, and 38.3%, 97.2%, 93%, 61.9% and 68.2% in group 1, 52.8%, 96.8%, 89.6%, 79.7% and 81.7% in group 2 for combination of B-mode and color SWE respectively. Combination of B-Mode US and SWE results, according to the lesion size showed improvement of 1.1-1.8% in specificity and 5.1-17.8% in PPV in group 1 and 2. There was statistical significance in the lesions less than 2 cm in group 1 and 2 (p<0.001).

CONCLUSION

SWE with maximum visual color elasticity assessment added to B-mode US revealed improvement of specificity and PPV (P<0.001), without improvement of overall diagnostic accuracy. And it could be helpful as a complementary study to reduce the false positive diagnosis with confidence before making the decision of biopsy.

CLINICAL RELEVANCE/APPLICATION

B-mode US shows high sensitivity and relatively low specificity. SWE can decrease false positive by adding on B-mode US as a complementary tool with higher specificity and PPV than B-mode US

SSM02-03 Downclassification of Suspicious Breast Masses Using Opto-Acoustic Imaging

Wednesday, Dec. 2 3:20PM - 3:30PM Location: E451B

Participants

Erin I. Neuschler, MD, Chicago, IL (Presenter) Nothing to Disclose

A. Thomas Stavros, MD, San Antonio, TX (*Abstract Co-Author*) Advisor, Devicor Medical Products, Inc; Advisor, General Electric Company; Advisor, SonoCine, Inc; Owner, Ikonopedia, LLC; Medical Director, Seno Medical Instruments, Inc; Philip T. Lavin, PhD, Framingham, MA (*Abstract Co-Author*) Research Consultant, Seno Medical Instruments, Inc Michael J. Ulissey, MD, Auburn, WA (*Abstract Co-Author*) Consultant, Seno Medical Instruments, Inc; Stockholder, Tractus Company Limited

PURPOSE

Diagnostic specificity remains disappointingly low for methodologies optimized to achieve near 100% sensitivity. Seno Medical's opto-acoustic (OA) imaging fuses real time co-registered, interleaved laser optic and ultrasound imaging showing dual functional findings (hemoglobin de-oxygenation) and morphology (angiogenesis) for breast masses using a hand-held probe. A 100 subject pilot study, conducted as part of a larger pivotal study, was evaluated for the potential ability of OA to downgrade BI-RADS (BR) scores in benign masses, specifically whether masses originally scored BR 4a or 4b could be downgraded to either BR 3 or 2 and if masses coded BR 3 could be downgraded to 2.

METHOD AND MATERIALS

7 independent readers (IRs) and the expert radiologist (ER) trainer blindly assessed all 102 masses from the 100 pilot study cases using only OA without any knowledge of clinical data or outcome. There were 75 biopsied masses (39 benign, 36 malignant). Grayscale ultrasound images were taken with the OA device immediately prior to the OA exam. Later, the IRs assigned a BR score to these images, the internal ultrasound control (IUC). IRs were trained by the ER to identify and score three OA internal features and two OA external features for all masses. They were then immediately offered the results of two nomograms (that were calculated from their OA feature scores) to help predict the Probability of Malignancy (POM). A 2% or less POM was used as the threshold to define a mass that could be down classified to BR 3. A 0% POM was used to downgrade a mass to BR 2.

RESULTS

Using OA, the IRs were able to downgrade site-CDU classified BR 3 masses to BR 2 in 33% of cases, BR 4a masses to BR 2 or 3 in 53% of cases, and BR 4b masses to BR 3 or 2 in 33% of cases. Using OA, the IRs downgraded IUC-classified BR 3 masses to BR 2 in 43% of cases, BR 4a to either BR 3 or 2 in 43% of cases, and BR 4b masses to either BR 3 or 2 in 13% of cases. OA (IRs) had 97.6% sensitivity and 44.4% specificity.

CONCLUSION

Benign masses classified as BR 3, 4a and 4b could be potentially downgraded to BR 3 or 2 by using OA with the aid of nomograms. The multi-center 2097 subject pivotal study will allow for confirmation.

CLINICAL RELEVANCE/APPLICATION

Downgrading BR 3, 4a and 4b masses without missing cancers is an unmet need. If verified, these findings could prevent not only biopsies but multiple follow-up ultrasound exams over 2 years.

SSM02-04 Prediction of Invasive Breast Cancer Using Shear-wave Elastography in Patients with Biopsyconfirmed Ductal Carcinoma in Situ

Wednesday, Dec. 2 3:30PM - 3:40PM Location: E451B

Jung Min Chang, MD, Seoul, Korea, Republic Of (*Abstract Co-Author*) Nothing to Disclose Su Hyun Lee, MD,PhD, Seoul, Korea, Republic Of (*Abstract Co-Author*) Nothing to Disclose Sung Ui Shin, MD, Seoul, Korea, Republic Of (*Abstract Co-Author*) Nothing to Disclose Woo Kyung Moon, Seoul, Korea, Republic Of (*Abstract Co-Author*) Nothing to Disclose

PURPOSE

To investigate whether lesion stiffness measured by shear-wave elastography (SWE) could predict histologic upgrade of ductal carcinoma in situ (DCIS) confirmed by ultrasound (US)-guided core needle biopsy (CNB).

METHOD AND MATERIALS

This retrospective study was conducted with institutional review board approval, and informed consent was waived. From January 2012 to February 2015, database search revealed 120 biopsy-confirmed DCIS in patients (mean age 52.4 ± 9.8) who underwent B-mode US and SWE prior to surgery. Clinicopathologic results, B-mode findings, size on US, mean and maximum elasticity values on SWE were recorded. Three radiologists independently analyzed qualitative color scores on SWE images using 5 point scale. To identify the preoperative factors associated with upgrade to invasive cancer, B-mode US findings, SWE information, and clinical variables were analyzed using univariate and multivariate logistic regression analysis. Qualitative color scores assessed by individual radiologists were analyzed to identify correlation with clinicopathologic variables, lesion size, and findings on B-mode US using multiple linear regression analysis. Interobserver agreements among radiologists on qualitative color score were assessed using multi-rater kappa statistic.

RESULTS

The overall upgrade rate was 41.7% (50 of 120). Mean, maximum stiffness values, qualitative color scores, and lesion size showed significant differences in upgrade and non-upgrade groups. Multivariate logistic regression analysis revealed mean (P=0.012), maximum stiffness (P=0.039), and lesion size (P<0.001) were significantly correlated with histologic upgrade. In reader study, color scores were correlated with the histologic upgrade, mammographic density, and B-mode category in all three radiologists (P value <0.04). The overall interobsever agreement for elasticity score was excellent (κ = 0.814 -0.887).

CONCLUSION

Breast lesion stiffness measured by SWE could be helpful to predict the upgrade to invasive cancer in US-guided biopsy proven DCIS patients.

CLINICAL RELEVANCE/APPLICATION

For patients with DCIS confirmed by US-guided CNB, stiffness values on SWE can lead patient to undergo a proper one-step operation when surgical excision is performed.

SSM02-05 Is Contrast Enhanced Ultrasound as Good or Better than MRI in Evaluation of Breast Cancer Patients Receiving Neoadjuvant Chemotherapy?

Wednesday, Dec. 2 3:40PM - 3:50PM Location: E451B

Participants

Sandy C. Lee, MD, Los Angeles, CA (Presenter) Nothing to Disclose

Edward G. Grant, MD, Los Angeles, CA (*Abstract Co-Author*) Research Grant, General Electric Company ; Medical Advisory Board, Nuance Communications, Inc

Pulin A. Sheth, MD, Santa Monica, CA (Abstract Co-Author) Nothing to Disclose

Bhushan Desai, MBBS, MS, Los Angeles, CA (Abstract Co-Author) Nothing to Disclose

Steven Cen, PhD, Los Angeles, CA (*Abstract Co-Author*) Nothing to Disclose

Darryl Hwang, PhD, Los Angeles, CA (Abstract Co-Author) Nothing to Disclose

Mary W. Yamashita, MD, Los Angeles, CA (*Abstract Co-Author*) Nothing to Disclose

Linda Hovanessian-Larsen, MD, Los Angeles, CA (Abstract Co-Author) Nothing to Disclose

PURPOSE

The purpose of this pilot study is to evaluate the performance of Contrast Enhanced Ultrasound (CEUS) versus Contrast Enhanced MRI (CE-MRI) in monitoring treatment response in breast cancer (BC) patients receiving preoperative neoadjuvant chemotherapy (NAC) by comparing tumor visibility and size.

METHOD AND MATERIALS

We prospectively studied 18 women diagnosed with invasive BC and receiving NAC, who had CEUS and CE-MRI as part of their preoperative imaging to detect tumor response. Each woman had three CEUS scans and at least two CE-MRI scans: (1) baseline prior to initiating NAC, (2) 3 weeks after initiation of NAC, and (3) after completion of NAC prior to surgery. The breast imager interpreting the CEUS or the CE-MRI was blinded to results of the other study. The presence of a lesion, tumor size, percent necrosis, and peak intensity were recorded. Results of the two techniques were compared to each other and to the gold standard histopathology obtained at surgery. Spearman correlation and intraclass correlation with absolute agreement were used to evaluate the findings.

RESULTS

All 18 women have biopsy proven invasive ductal carcinoma. The mean size of enhancing tumor at baseline on CEUS is 3.4 cm (range 1.5-6.9 cm) and on CE-MRI is 4.3 cm (range 2.5-7.7 cm). The results demonstrate a strong correlation in tumor size between CEUS and CE-MRI r=0.87 (p<0.01). Intraclass correlation also shows good absolute agreement, icc=0.78 (p<0.01). When comparing percent tumor necrosis between CEUS vs. CE-MRI, there is 80% agreement (95% CI of 40%, 98%). Comparable quantitative parameters, namely "peak intensity (tumor - normal)" for CEUS and "peak enhancement at one minute" for CE-MRI, demonstrate correlation with r=0.46 (p=0.05). Trends suggest that CEUS has a better degree of correlation and agreement than CE-MRI with tumor size at surgical pathology.

CONCLUSION

CEUS is comparable to CE-MRI in evaluating treatment response of breast cancer in patients receiving NAC. In our pilot series, CEUS was found to be a valuable imaging modality for determining the tumor size, percent necrosis, and peak intensity, and is

comparable to the results of CE-MRI.

CLINICAL RELEVANCE/APPLICATION

Further investigation with a larger cohort may prove that CEUS can be a better, more cost effective method than CE-MRI in monitoring treatment response in breast cancer patients receiving NAC.

SSM02-06 Impact of Real-time MRI Navigated Ultrasound in Preoperative Breast Cancer Patients

Wednesday, Dec. 2 3:50PM - 4:00PM Location: E451B

Participants

Ah Young Park, MD, Ansan, Korea, Republic Of (*Presenter*) Nothing to Disclose Bo Kyoung Seo, MD, PhD, Ansan, Korea, Republic Of (*Abstract Co-Author*) Nothing to Disclose Kyu Ran Cho, MD, PhD, Seoul, Korea, Republic Of (*Abstract Co-Author*) Nothing to Disclose Ok Hee Woo, MD, Seoul, Korea, Republic Of (*Abstract Co-Author*) Nothing to Disclose Jaehyung Cha, Seoul, Korea, Republic Of (*Abstract Co-Author*) Nothing to Disclose

PURPOSE

To evaluate the utility of real-time MRI navigated ultrasound (US) for second-look examination in preoperative breast cancer patients.

METHOD AND MATERIALS

Between October 2013 and February 2015, 55 consecutive breast cancer patients who underwent second-look US examination with real-time MRI navigated US to identify MRI-detected lesions on preoperative evaluation were enrolled. Of a total of 67 breast lesions, 41 lesions were detected on conventional US, 23 were additionally detected on MRI navigated US, and the remaining two were not found. The detection rates of conventional US and MRI navigated US were compared with McNemar test. We evaluated clinical data (age and change of surgical plan), and US findings (background echotexture, distance from nipple, and mass characteristics) and MRI findings (size, depth, type, characteristics, and kinetics of lesions) based on the BI-RADS lexicon. We compared these features between two groups with student T test, chi-square, or Fisher's exact test; 41 lesions detected with both conventional US and MRI navigated US (Group 1) and 23 lesions detected with only MRI navigated US (Group 2).

RESULTS

The detection rates of conventional US and MRI navigated US were statistically different, 61.2% (41/67) vs 95.5% (65/67) (P<.0001). Hetergeneous background echotexture (69.6% [16/23] vs 34.1% [14/41], P=.012), isoechoic masses on US (65.2% [15/23] vs 7.3% [3/41], P<.0001), and deep location on MRI (26.1% [6/23] vs 14.6% [6/41], P=.041) were more common in Group 2. The proportion of change in surgical plan was higher in Group 2 although there was less statistical significance (43.5% [10/23] vs 22.0% [9/41], P=.071). In 10 patients with change of surgical plan in Group 2, four underwent mastectomy due to multicentric cancers and six underwent additional excision due to concurrent high-risk lesions.

CONCLUSION

Real-time MRI navigated US improves identification of MRI-detected lesions during second-look US examination for preoperative evaluation in breast cancer patients. Background echotexture, echo pattern of breast lesions, and lesion depth on MRI can affect the detection of breast lesions in second-look US examination.

CLINICAL RELEVANCE/APPLICATION

Real-time MRI navigated US is useful to identify breast lesions on second-look US examination for MRI-detected additional lesions in breast cancer patients, which can affect treatment plan.

Neuroradiology (Resting State Functional Brain Imaging)

Wednesday, Dec. 2 3:00PM - 4:00PM Location: N226

NR MR

AMA PRA Category 1 Credit [™]: 1.00 ARRT Category A+ Credit: 1.00

Participants

Haris I. Sair, MD, Baltimore, MD (*Moderator*) Research support, Carestream Health, Inc Joshua S. Shimony, MD, PhD, Saint Louis, MO (*Moderator*) Nothing to Disclose

Sub-Events

SSM18-01 Altered Brain Neural Activity in Sellar-Tumor Patients: A Resting-State fMRI Study

Wednesday, Dec. 2 3:00PM - 3:10PM Location: N226

Participants

Zhongyan Wang, Beijing, China (*Abstract Co-Author*) Nothing to Disclose Tianyi Qian, PhD, Beijing, China (*Abstract Co-Author*) Nothing to Disclose Binbin Sui, MD, Beijing, China (*Presenter*) Nothing to Disclose Peiyi Gao, MD, PhD, Beijing, China (*Abstract Co-Author*) Nothing to Disclose

PURPOSE

The purpose of the current study was to explore how brain neural activity changes with visual deprivation in patients with sellar tumors by measuring the pattern of low-frequency fluctuation $(0.1 \sim 0.01 \text{ Hz})$ of the BOLD signal.

METHOD AND MATERIALS

21 patients with sellar tumors and 21 sex-matched healthy volunteers participated in this study. The resting-state fMRI data were processed usingthe SPM8 MATLAB toolbox and DPARSF. The spontaneous brain neural activity was measured by calculating the amplitude of low-frequency fluctuations (ALFF), regional homogeneity (ReHo) and functional connectivity (FC) of BOLD (blood-oxygenation-level-dependent) signals. A two-sample t-test was performed to investigate the difference between the groups, thereafter computing the correlation coefficient between the patterns obtained from rs-fMRI of some regions and the tumor size, as expressed by its left-right radius.

RESULTS

The results of the group analysis showed that, compared to normal control subjects, patients with sellar tumors exhibited significantly decreased ALFF in the bilateral cuneus, left lingual gyrus and the right supplementary motor area (SMA). ALFF in bilateral lentiform nucleus has significantly increased (Fig.1). The sellar tumors showed decreased ReHo value in the bilateral cuneus, but increased ReHo value in the precuneus, the left insular, and left lentiform nucleus. The ReHo values in precuneus and insula are significantly correlated with the tumor radius in left-right direction (Fig.2)

CONCLUSION

The results of this study suggest that the function of the area response for high-level cognition function in visual network is less stable than primary visual cortex in the patient with sellar tumors. The decreased brain activity in the precuneus and other brain areas might reflect a maladjustment behavior caused by visual deprivation. The increased brain activity in the lenticular nucleus and insula might be related to a compensatory phenomenon. The results provide useful information for us to better understand how brain functional network change under the influence of visual deprivation.

CLINICAL RELEVANCE/APPLICATION

The value of the functional patterns in these areas could potentially be used for evaluating the recovery prognosis of visual function in the patients with sellar tumor.

SSM18-02 Changes of Brain Motor Functional Connectivity of Ischemic Stroke Patients in the Resting State after rTMS Treatments

Wednesday, Dec. 2 3:10PM - 3:20PM Location: N226

Participants

Jing Li, Beijing, China (*Presenter*) Nothing to Disclose Xuewei Zhang, Beijing, China (*Abstract Co-Author*) Nothing to Disclose Zhentao Zuo, Beijing, China (*Abstract Co-Author*) Nothing to Disclose Jie Lu, Beijing, China (*Abstract Co-Author*) Nothing to Disclose Yuzhou Guan, Beijing, China (*Abstract Co-Author*) Nothing to Disclose Wei-hong Zhang, MD, Baltimore, MD (*Abstract Co-Author*) Nothing to Disclose Yong Fan, PhD, Philadelphia, PA (*Abstract Co-Author*) Nothing to Disclose

PURPOSE

The study aimed to 1) investigate the resting-state functional connectivity (rsFC) changes of the ipsilesional primary motor cortex (M1) with the brain after acute stroke; 2) investigate the difference of rsFC of the ipsilesional M1 in stroke patients before and after high frequency repetitive Transcranial Magnetic Stimulation(rTMS) treatments.

METHOD AND MATERIALS

Nineteen patients with unilateral ischemic stroke and fourteen age- and gender-matched healthy volunteers were recruited. Five of

the patients achieved the rTMS treatment. Pearson correlation analysis between the time course of M1 and that of every voxel within the whole brain was performed for maps of correlation coefficients, which were Fisher's z-transformed and called as z-functional connectivity (z-FC) maps. Two sample t-tests were conducted to compare the z-FC maps between the patients and volunteers, and paired t-tests carried out between pre- and post-treatment groups. The Ethics Committee of hospital approved the study. All participants obtained written consent.

RESULTS

1) Compared with volunteers, the patients demonstrated decreased rsFC with the ipsilesional M1 and contralesional cerebellum, ipsilesional precentral gyrus, supplementary motor area(SMA) and precuneus. 2) The pre-treatment group showed higher rsFC of ipsilesional M1 with ipsilesional inferior temporal gyrus, while decreased ones with contralesional M1 and SMA. However, the post-treatment group showed higher rsFC of ipsilesional M1 with ipsilesional middle temporal gyrus, contralesional inferior temporal gyrus, middle frontal gyrus and precuneus, while decreased ones with the ipsilesional premotor cortex, M1, contralesional paracenteral lobe and M1. Higher rsFC was found in the ipsilesional M1 and contralesional frontal medial gyrus in the post-treatment groups. 3) The National Institutes of Health Stroke Scale (NIHSS) of the post-treatment group decreased (p<0.05) compared to pre-treatment group, while the Fugl-Meyer Assessment (FMA) and Barthel Index (BI) increased (p<0.05).

CONCLUSION

The areas mentioned above may play an crucial role in acute stroke and the rTMS may facilitate motor recovery in stroke patients.

CLINICAL RELEVANCE/APPLICATION

High frequency repetitive transcranial magnetic stimulation elicits cortical excitation. We localized it on the ipsilesional primary motor cortex to facilitate the motor recovery in stroke patients.

SSM18-04 The Similar Aberrant Spontaneous Brain Activity Related to Cognitive Impairment in Subcortical Stroke Patients: Using Two different Resting-state fMRI Analysis Methods

Wednesday, Dec. 2 3:30PM - 3:40PM Location: N226

Participants

Cheng-Yu Peng, Nanjing, China (*Presenter*) Nothing to Disclose Ying Cui, Nanjing, China (*Abstract Co-Author*) Nothing to Disclose Yun Jiao, PhD, Nanjing, China (*Abstract Co-Author*) Nothing to Disclose Shenghong Ju, MD, PhD, Nanjing, China (*Abstract Co-Author*) Nothing to Disclose Gao-Jun Teng, MD, Nanjing, China (*Abstract Co-Author*) Nothing to Disclose

PURPOSE

This study combined using two resting-state functional magnetic resonance imaging (rs-fMRI) analysis methods to investigate regional homogeneity (ReHo) and the amplitude of low frequency fluctuation (ALFF) changes in subcortical stroke patients and whether these changes were correlated with impaired cognitive performance.

METHOD AND MATERIALS

Subcortical stroke patients (n=30) and age-, sex-, and education-matched healthy controls subjects (n=30) underwent multimodality MRI examinations to calculate the ReHo and ALFF within the scope of the whole brain not limited in the DMN. In the process of data processing, the stroke patients were divided into two groups (the left- and right-sided lesion groups) by flipping the brain imaging, then, the two group results were compared with the controls respectively. Scores from neuropsychological tests were also obtained and compared between the two groups. The potential relationships between ALFF and ReHo values and cognitive performance were evaluated via partial correlation analysis.

RESULTS

The patients exhibited significant deficiencies in some cognitive domains (all P < 0.05). Compared with healthy controls, patients with stroke had significantly increased ALFF and ReHo values in the left inferior parietal lobule (IPL) consistently (Fig. 1). Moreover, the partial correlation results indicated that the ALFF values of the left IPL were positively correlated with the Digit Span Forwards Test scores (r = 0.427; P = 0.026) in the subcortical stroke patients.

CONCLUSION

The abnormalities of spontaneous brain activity reflected by ALFF and ReHo measurements in post-stroke patients may provide insights into the neurobiological consequences such as cognitive impairment no matter which side the lesions located in.

CLINICAL RELEVANCE/APPLICATION

ALFF and ReHo could be the important imaging biomarkers for the observation of neurobiological consequences in post-stroke patients no matter which side the lesions located in.

SSM18-05 Leveraging Microstructural White Matter Changes to Guide Investigation of Resting-state Functional Network Connectivity

Wednesday, Dec. 2 3:40PM - 3:50PM Location: N226

Participants

Susan Sotardi, MD, MS, Bronx, NY (*Presenter*) Nothing to Disclose Roman Fleysher, PhD, Bronx, NY (*Abstract Co-Author*) Nothing to Disclose Namhee Kim, PhD, Bronx, NY (*Abstract Co-Author*) Nothing to Disclose Michael Stockman, Bronx, NY (*Abstract Co-Author*) Nothing to Disclose Craig A. Branch, PhD, Bronx, NY (*Abstract Co-Author*) Nothing to Disclose Jeremy Smith, PhD, Bronx, NY (*Abstract Co-Author*) Nothing to Disclose David Gutman, MD, Bronx, NY (*Abstract Co-Author*) Nothing to Disclose Michael L. Lipton, MD, PhD, Bronx, NY (*Abstract Co-Author*) Nothing to Disclose Prior research has examined the relationship of diffusion measures of structural white matter integrity to cognitive outcomes. Additionally, resting-state functional connectivity (rs-FC) is correlated with behavioral outcomes. These parallel approaches have revealed important observations regarding the role of connectivity in brain disorders. However, the methodology is inherently limited by the essentially separate nature of structural and functional arms. We propose a method that uses abnormal structural integrity to guide investigation of rs-FC, in a cohort of patients with mild traumatic brain injury (mTBI).

METHOD AND MATERIALS

23 mTBI patients who presented to the emergency department within 48 hours of injury and 43 normal controls were recruited with IRB approval and gave informed consent. DTI and resting fMRI were performed at 3T. All individual FA maps were matched to the brain volume of a healthy volunteer for group analysis. A voxelwise t-test comparing mTBI and control subjects was used to identify regions of abnormally low FA. Regions of low FA were used as seeds for tractography with the entire cortex serving as the termination point. Gray matter regions thus reached then served as seed ROI for voxelwise analysis of rs-FC.

RESULTS

Multiple regions which showed low FA in mTBI subjects were identified. Using a region in the external capsule, tractography was used to delineate fiber tracts, (Figure1). The intersection of the fiber tract and frontal gray matter, which included the frontal eye field region, served as the seed for rs-FC analysis. Voxel-wise comparison of the correlation maps from the mTBI and control groups identified gray matter clusters where connectivity in mTBI subjects was stronger than in controls (Figure2).

CONCLUSION

Our results demonstrate a new approach to rs-FC analysis where diffusion tractography based on abnormal structural connectivity findings, is used to delineate cortical regions of interest for assessment of functional connectivity. The proposed method avoids the use of a priori seed ROI in rs-FC analysis to more directly interrogate the functional consequences of white matter injury.

CLINICAL RELEVANCE/APPLICATION

Our results demonstrate a new approach to resting state fMRI analysis where diffusion tractography, based on abnormal structural connectivity findings, is used to delineate cortical regions of interest for assessment of functional connectivity.

SSM18-06 Mutual Connectivity Analysis with Graph Theoretic Measures for Identifying Regions with Altered Functional Connectivity in HIV Infection

Wednesday, Dec. 2 3:50PM - 4:00PM Location: N226

Participants

Anas Z. Abidin, MS, Rochester, NY (*Presenter*) Nothing to Disclose Adora M. D' Souza, BEng, Rochester, NY (*Abstract Co-Author*) Nothing to Disclose Mahesh B. Nagarajan, PhD, Los Angeles, CA (*Abstract Co-Author*) Nothing to Disclose Xixi Wang, Rochester, NY (*Abstract Co-Author*) Nothing to Disclose Axel Wismueller, MD, PhD, Rochester, NY (*Abstract Co-Author*) Nothing to Disclose

PURPOSE

To quantify resting state fMRI (rsfMRI) functional connectivity profiles obtained from analyzing graph theoretic measures based on a novel Mutual Connectivity Analysis (MCA) framework, and to demonstrate the applicability of this approach for differentiating between HIV+ and HIV- subjects.

METHOD AND MATERIALS

A cohort of 25 age-matched subjects (13 HIV+, 12 HIV-, 21-68 yrs, 15M, 10F) underwent rsfMRI scanning (3T, TR=1650ms, 25 slices, 240 acquisitions). After standard preprocessing and registration, the datasets were parcellated into 116 regions using the Automated Anatomic Labeling (AAL) atlas. The average time series of each of these regions was computed and used with the MCA framework, resulting in a pairwise affinity matrix describing the nonlinear mutual predictability for each region pair. We used generalized radial basis function neural networks as nonlinear time-series predictors. The resulting network graph can be characterized using graph theoretic measures for global properties, such as assortativity, transitivity, global efficiency, or for local/regional properties, such as modularity, clustering coefficient, local efficiency. Whole-brain and region-specific measures were computed to test for differences between HIV+ and HIV- subject cohorts. Statistical analyses were performed using a non-parametric Kolmogorov-Smirnov test.

RESULTS

Modularity and clustering-coefficient values of nodes corresponding to regions of the parietal lobe and the right and left posterior cingulate gyrus showed significant differences (p<0.01) between HIV+ and HIV- subject cohorts. In contrast, no significant differences between cohorts were seen when using statistics characterizing the global properties of the whole-brain network.

CONCLUSION

Graph theoretic analysis of brain network properties using the MCA framework is a novel method that can identify changes in rsfMRI functional connectivity patterns in patients with HIV infection. Significant regional differences between HIV+ and HIV- subjects were demonstrated for several network measures. The corresponding brain regions are in agreement with the findings of other studies investigating the effects of HIV infection on the brain.

CLINICAL RELEVANCE/APPLICATION

The regional differences in functional connectivity profiles from rsfMRI captured by our approach can be used to develop clinical imaging biomarkers in patients with HIV-related cognitive impairment.

Vascular/Interventional (Advances in Transarterial Chemoembolization)

Wednesday, Dec. 2 3:00PM - 4:00PM Location: E351



AMA PRA Category 1 Credit ™: 1.00 ARRT Category A+ Credit: 1.00

Participants

Sarah B. White, MD,MS, Milwaukee, WI (*Moderator*) Nothing to Disclose Hyun S. Kim, MD, Atlanta, GA (*Moderator*) Nothing to Disclose

Sub-Events

SSM23-01 Transpulmonary Chemoembolization (TPCE) in Pulmonary Malignant Tumors: Evaluation of Treatment Response Using Parenchymal Blood Volume (PBV)

Wednesday, Dec. 2 3:00PM - 3:10PM Location: E351

Participants

Thomas J. Vogl, MD, PhD, Frankfurt, Germany (*Presenter*) Nothing to Disclose Thomas Lehnert, MD, Frankfurt Am Main, Germany (*Abstract Co-Author*) Nothing to Disclose Hanns Ackermann, Frankfurt On Main, Germany (*Abstract Co-Author*) Nothing to Disclose Marcus Hezel, BS, Frankfurt, Germany (*Abstract Co-Author*) Nothing to Disclose Nagy N. Naguib, MD, MSc, Frankfurt Am Main, Germany (*Abstract Co-Author*) Nothing to Disclose

PURPOSE

To evaluate initial experiences with the assessment of parenchymal blood volume (PBV) of pulmonary malignant tumors by using Carm CT for detecting early response to transpulmonary chemoembolization (TPCE) and clinical practicability.

METHOD AND MATERIALS

The study was approved by the institutional ethics committee. 21 patients (females: 15, males: 6; range: 41-77 years; mean: 56.77 years) were palliatively treated with TPCE. PBV and tumor diameter were analyzed and PBV maps were calculated from 3D-CTA data sets. Imaging was performed on a flat detector C-arm CT. Response groups were classified according to the RECIST criteria. Statistically significant differences were determined and PBV and diameter were correlated as parameters of response to treatment using the Pearson's regression analysis.

RESULTS

In a mean of 4.91 sessions the median diameter increased by 18.18% (p>0.05) and PBV was reduced by 39.62% (p>0.05). Functional and anatomical response per tumor was statistically significant (p \leq 0.05). Correlation coefficient was r=0.058. 2/41 tumors showed partial response, 31/41 tumors stable disease and 8/41 tumors progressive disease. Highest pre-treatment PBV values were measured in decreasing tumors (206.93 mL/L), lowest values in increasing tumors (60.17 mL/L; p>0.05). Lowest values also were measured in lung cancer (53.02 mL/L) vs. uterine leiomyosarcoma (103.31 ml/L) and renal cell cancer (113.14 mL/L; p \leq 0.05).

CONCLUSION

The assessment of PBV maps by using 3D-CTA image data should be easy to integrate into the clinical routine. PBV shows a stronger response to TPCE treatment than the measurement in diameter and should be considered as a response parameter for early detection.

CLINICAL RELEVANCE/APPLICATION

Parenchymal blood measurements allow optimization of TPCE treatment in pulmonary malignant tumors

SSM23-02 Chemosaturation with Percutaneous Hepatic Perfusion of Melphalan for Hepatic Metastases from Uveal Melanoma: Multiinstitutional Evaluation

Wednesday, Dec. 2 3:10PM - 3:20PM Location: E351

Participants

Thomas J. Vogl, MD, PhD, Frankfurt, Germany (Presenter) Nothing to Disclose

Silvia Koch, Frankfurt, Germany (Abstract Co-Author) Nothing to Disclose

Bernhard Gebauer, MD, Berlin, Germany (*Abstract Co-Author*) Research Consultant, C. R. Bard, Inc; Research Consultant, Sirtex Medical Ltd; Research Grant, C. R. Bard, Inc; Research Consultant, PAREXEL International Corporation;

Winfried A. Willinek, MD, Bonn, Germany (*Abstract Co-Author*) Speakers Bureau, Bayer AG Speakers Bureau, Bracco Group Speakers Bureau, General Electric Company Speakers Bureau, Koninklijke Philips NV Speakers Bureau, Lantheus Medical Imaging, Inc Advisory Board, General Electric Company Advisory Board, Lantheus Medical Imaging, Inc Advisory Board, Bayer AG

Roland D. Bruening, MD, Hamburg, Germany (*Abstract Co-Author*) Speakers Bureau, Bracco Group; Speakers Bureau, General Electric Company; Speakers Bureau, Koninklijke Philips NV; Speakers Bureau, Delcath Systems, Inc; Shareholder Delcath Systems, Inc; Alexander Enk, Heidelberg, Germany (*Abstract Co-Author*) Nothing to Disclose

PURPOSE

This multiinstitutional evaluation intends to retrospectively evaluate the results of the treatment of non-resectable hepatic metastases of uveal melanoma using percutaneous hepatic perfusion (PHP; Hepatic CHEMOSAT® Delivery System; Delcath Systems Inc., USA).

Between 2012 and 2014 fourteen patients with hepatic metastases of uveal melanoma received one to three sessions of Chemosaturation-PHP. Eleven patients were evaluated by means of RECIST criteria. Survival time analysis was performed. Adverse events and complications were registered.

RESULTS

Chemosaturation is well tolerated by the majority of all fourteen patients. After therapy seven patients developed leukopenia, six patients had thrombopenia and two patients showed neutropenia, infection and fever each.Out of the eleven patients evaluated by means of RECIST criteria, four patients (36%) showed PR, SD was observed in five patients (46%) and two patients (18%) had PD.Two patients underwent two further sessions. After the first session tumour response of one patient turned from SD to PR and returned to SD. The other patient's treatment response showed PR in all three sessions.Survival time of all patients ranged from 1.5 to 23 months (median OS 6.5 months) following first Chemosaturation.Time to progression of the two patients with PD was 6.2 months in one patient. The other patient died 1.6 months after evaluation.

CONCLUSION

Chemosaturation-PHP has been manifested as a potential treatment for patients with non-resectable hepatic metastases of uveal melanoma.

CLINICAL RELEVANCE/APPLICATION

Chemosaturation-PHP provides a good treatment option in patients with unresectable liver metastases from uveal melanoma.

SSM23-03 Quantitative Real-time Fluoroscopy Analysis on Measurement of the Hepatic Arterial Flow During Transcatheter Arterial Chemoembolization of Hepatocellular Carcinoma: Comparison with Quantitative Digital Subtraction Angiography Analysis

Wednesday, Dec. 2 3:20PM - 3:30PM Location: E351

Participants

Yi-Yang Lin, MD, Taipei City, Taiwan (*Presenter*) Research grant, Taipei Veterans General Hospital and Siemens, Grant No. T1100200.

Rheun-Chuan Lee, MD, Taipei, Taiwan (*Abstract Co-Author*) Nothing to Disclose Wan-Yuo Guo, MD, PhD, Taipei, Taiwan (*Abstract Co-Author*) Nothing to Disclose Cheng-Yen Chang, MD, Taipei, Taiwan (*Abstract Co-Author*) Nothing to Disclose

PURPOSE

To quantitatively measure the hemodynamic change of hepatic artery during transcatheter arterial chemoembolization (TACE) of hepatocellular carcinoma (HCC) by subtracted fluoroscopy quantitative color-coding analysis (f-QCA) and digital subtraction angiography quantitative color-coding analysis (d-QCA).

METHOD AND MATERIALS

This is a prospective study performed in a single medical institution from February 2014 to March 2015. Seventeen consecutive patients (mean 70.5 years old; male 12, female 5) underwent TACE with doxorubicin and Lipiodol emulsion or with microspheres for HCC. Patients were enrolled if superselective segmental TACE was technically feasible. The endpoint of TACE was sluggish antegrade arterial flow. Real-time subtracted fluoroscopic image and digital subtraction angiography image with a bolus injection were quantitatively analyzed. The f-QCA and d-QCA (syngo iFlow; Siemens) were used to determine the maximal density time (Tmax) of selected vessels. Relative Tmax (rTmax) was defined as the Tmax at the selected vessel minus the time of contrast medium spurting from the catheter tip. Imaging acquisition and injection protocols remained the same before and after TACE.

RESULTS

The pre- and post-TACE rTmax of the embolized segmental artery in f-QCA and d-QCA were $1.39 \pm .52s$, $2.28 \pm 1.09s$, p < .001 and $1.60 \pm .87$, $3.14 \pm 1.89s$, p < .001, respectively. The Pearson correlation of pre- and post-TACE rTmax of the embolized segmental artery between f-QCA and d-QCA were .65, p < .01 and .73, p < .001. The rTmax of the proximal lobar hepatic arteries and proper hepatic artery had no significant change before and after TACE in f-QCA and d-QCA.

CONCLUSION

The f-QCA is a fast and convenient method with lower radiation dose to quantify arterial flow change of embolized segmental artery during TACE. Flow quantification of embolized segmental artery by f-QCA has high correlation with that by d-QCA.

CLINICAL RELEVANCE/APPLICATION

The f-QCA is a fast and convenient method to evaluate arterial flow change during TACE. The f-QCA can potentially replace the d-QCA with lower radiation dose.

SSM23-04 Transarterial Chemoembolization for the Treatment of Advanced Hepatocellular Carcinoma: A Retrospective Cohort Study with 508 Patients

Wednesday, Dec. 2 3:30PM - 3:40PM Location: E351

Participants

Yan Zhao, MS, Baltimore, MD (*Presenter*) Nothing to Disclose Jae Ho Sohn, MD,MS, New Haven, CT (*Abstract Co-Author*) Nothing to Disclose Florian N. Fleckenstein, MS, New Haven, CT (*Abstract Co-Author*) Nothing to Disclose Sonia P. Sahu, New Haven, CT (*Abstract Co-Author*) Nothing to Disclose Rafael Duran, MD, Baltimore, MD (*Abstract Co-Author*) Nothing to Disclose Ruediger E. Schernthaner, MD, Vienna, Austria (*Abstract Co-Author*) Nothing to Disclose Howard Lee, New Haven, CT (*Abstract Co-Author*) Nothing to Disclose Li Zhao, New Haven, CT (*Abstract Co-Author*) Nothing to Disclose Susanne Smolka, New Haven, CT (*Abstract Co-Author*) Nothing to Disclose Ming De Lin, PhD, Cambridge, MA (*Abstract Co-Author*) Employee, Koninklijke Philips NV Jean-Francois H. Geschwind, MD, Westport, CT (*Abstract Co-Author*) Researcher, BTG International Ltd; Consultant, BTG International Ltd; Researcher, Koninklijke Philips NV; Consultant, Koninklijke Philips NV; Researcher, Guerbet SA; Consultant, Guerbet SA; Consultant, Terumo Corporation; Consultant, Threshold Pharmaceuticals, Inc; Consultant, PreScience Labs, LLC; Researcher, Boston Scientific Corporation; Consultant, Boston Scientific Corporation

PURPOSE

The efficacy and safety of transarterial chemoembolization (TACE) for Barcelona Clinic Liver Cancer (BCLC) class C remains controversial. We conducted a large retrospective study to summarize our available data about the treatment of TACE in advanced HCC patients over the last 15 years.

METHOD AND MATERIALS

Between November 1998 and December 2013, all advanced stage (BCLC C) HCC patients with Child-Pugh (A/B) and Eastern Cooperative Oncology Group score of 0-2 were consecutively enrolled. Cox proportional hazards model was used to examine risk factor association with survival. Risk scores for individual patients were calculated by combing the prognostic values with the corresponding regression coefficients. The concordance (c)-statistic [equivalent to the receiver operating characteristic (ROC) curve] was used to assess the validity of categorizing patients treated with TACE into two subgroups. Cut-off values were determined according to ROC curves.

RESULTS

Of the 508 patients, 79.3% were male and median patient age was 63 (range, 19-90). By multivariate analysis, extrahepatic metastasis (HR=2.19, 95%CI 1.44-2.46), AFP≥400ng/ml (HR=1.73, 95%CI 1.38-2.17), portal vein invasion (HR=1.62, 95%CI 1.3-2.02), Child-Pugh class B (HR=1.37, 95%CI 1.09-1.73) and number of tumor nodules >2 (HR=1.39, 95%CI 1.11-1.74) were significantly associated with survival. Risk scores (R) for individual patients were calculated by combining these five prognostic values with the corresponding regression coefficients. The c-statistic associate with the model in the prediction of 1 year, 2 year and 3 year survival was 0.74 (95%CI 0.69-0.78), 0.73 (95%CI 0.68-0.78) and 0.72 (95%CI 0.66-0.79), respectively. To achieve both the best sensitivity and specificity, we selected 5.5 as the cut-off value for R score. The Kaplan-Meier analysis showed that the median survival in the patients <5.5 was significantly longer than those >5.5 (21.6 vs. 6.9months, P<0.001).

CONCLUSION

TACE should be considered an effective therapy for select advanced HCC patients. We suggest modification of the BCLC stage C classification to improve staging of these patients.

CLINICAL RELEVANCE/APPLICATION

Select advanced stage (BCLC stage C) HCC patients with well-preserved liver function could benefit from TACE treatment.

SSM23-05 Feasibility of Flat-detector CT Perfusion Imaging in TACE for HCC: Implications for Treatment Planning and Response

Wednesday, Dec. 2 3:40PM - 3:50PM Location: E351

Participants

Rory O'Donohoe, MBBCh, Dublin, Ireland (*Presenter*) Nothing to Disclose Alexis M. Cahalane, MBBCh, Dublin 4, Ireland (*Abstract Co-Author*) Nothing to Disclose Aoife Hayes, Dublin, Ireland (*Abstract Co-Author*) Nothing to Disclose Olivia Connolly, Dublin, Ireland (*Abstract Co-Author*) Nothing to Disclose Jeffrey W. McCann, MBBCh, Dublin, Ireland (*Abstract Co-Author*) Nothing to Disclose Edmund Ronan Ryan, MBBCh, Dublin, Ireland (*Abstract Co-Author*) Nothing to Disclose

PURPOSE

Intra-procedural flat-detector CT perfusion imaging performed in the angiography suite at the time of TACE now allows assessment of tumor perfusion immediately before and after chemoembolization. This study examines the significance of areas of residual increased blood volume (indicating persistent tumor perfusion) immediately following TACE through comparison with the follow-up CT or MRI.

METHOD AND MATERIALS

Flat-detector CT perfusion imaging using syngo DynaPBV Body (Siemens Heathcare AG, Forcheim, Germany) is performed using rotational angiography before and after injection of a fixed small volume of dilute iodinated contrast via a microcatheter positioned either within the proper hepatic artery or more distally. Beginning in June 2014, nine chemoembolization procedures have been performed on seven patients using syngo DynaPBV for whom follow-up imaging is now available. We reviewed the post-chemoembolization DynaPBV images from these nine procedures and performed a direct comparison with the subsequent multiphase CT or MRI. We assessed for abnormally increased perfusion immediately following treatment and correlated this with the presence or absence of residual viable tumor on follow-up imaging.

RESULTS

In five treatments, residual abnormally increased perfusion was visible on the post treatment DynaPBV images and in all cases this correlated well with residual tumor on the follow-up CT or MRI. In two treatments, there was no residual abnormally increased perfusion which was confirmed as a complete treatment response on follow-up imaging studies. In two patients, both with lesions adjacent to the liver capsule, no abnormally increased perfusion was visible on DynaPBV, but hyperenhancing tumor was visible on follow-up imaging likely due to extra-hepatic supply via the inferior phrenic artery.

CONCLUSION

Our results show flat-detector CT perfusion imaging to be accurate in detecting residual disease at the end of the TACE procedure. Challenges exist with anomalous anatomy and lesions with extra-hepatic supply.

CLINICAL RELEVANCE/APPLICATION

Flat-detector CT perfusion imaging is accurate for detecting residual viable tumor at the end of the TACE procedure and may be useful in planning further treatments without the need for intervening imaging.

SSM23-06 Four-dimensional CT Navigation for Precise Chemoembolization of Hepatocellular Carcinoma

Wednesday, Dec. 2 3:50PM - 4:00PM Location: E351

Participants

Tianhao Su, MD, Beijing, China (*Presenter*) Nothing to Disclose Long Jin, Beijing, China (*Abstract Co-Author*) Nothing to Disclose Wen He, Beijing, China (*Abstract Co-Author*) Nothing to Disclose

PURPOSE

To describe and explore four-dimensional (4D) CT navigation prior to transarterial chemoembolization (TACE) for hepatocellular carcinoma (HCC).

METHOD AND MATERIALS

Contrast-enhanced computed tomographic imaging with volume helical shuttle (VHS) technique were prospective performed at a 64-row multidetector scanner before TACE in HCC patients. The whole liver region was selected for dynamic study of the tumor. A series of 16 phases images from pre-arterial to portal venous phase were collected and 4D CT images were reconstructed with 1.25-mm thickness on a commercial workstation. Radiologists analyzed the volumetric data, being free to use axial slices as well as postprocessing reconstruction algorithms (e.g., MIP and MPR). All 4D CT angiography (CTA) images in cine mode were compared with DSA in TACE, including anatomy of hepatic artery, tumor supplying arteries, tumor vessels, tumor staining. Embolization effect was also evaluated on DSA and follow-up CT.

RESULTS

The study included 46 independent HCC lesions in 38 patients. Normal hepatic artery anatomy was found in 24 cases (63.2%, according to Michels' classification) and variations in 14 cases (36.8%), which presented good hints for DSA selective hepatic arterial work. The diagnosis consistent rate was 100% between 4D CTA and DSA in showing the anatomy and variation of hepatic artery. 4D CTA noninvasively showed tumor supplying arteries (n = 41), tumor vessels (n = 36), and tumor staining (n = 42). DSA showed better tumor staining result and the visible rate of tumor staining in 4D CTA was 91.3% (42/46). However, 4D CTA had advantage in reproducibly delineating the three-dimension relationship between tumor and blood vessels while detecting tumor supplying arteries, especially for medium sized lesions lesions (diameter range from 3 to 7 cm). Since 4D CTA could dynamically show 3-5 levels of intrahepatic arterial branches, it provided a good navigation for effective superselective microcatheter placement. Upon 4D CT results, chemoembolization therapies were effectively performed. Successful lipiodol accumulations were achieved in specific region of liver.

CONCLUSION

Four-dimensional CT using VHS technique could be easy and helpful in evaluating hepatic artery anatomy and locating tumor supplying artery for interventional chemoembolization planning.

CLINICAL RELEVANCE/APPLICATION

Four-dimensional CT can be used as a planning and navigation tool for TACE in HCC.

ISP: Genitourinary (Intravenous Contrast Issues and CT Dose Reduction)

Wednesday, Dec. 2 3:00PM - 4:00PM Location: E352

CT GU SQ

AMA PRA Category 1 Credit ™: 1.00 ARRT Category A+ Credit: 1.00

Participants

Matthew S. Davenport, MD, Cincinnati, OH (*Moderator*) Book contract, Wolters Kluwer nv; Book contract, Reed Elsevier; Dean A. Nakamoto, MD, Beachwood, OH (*Moderator*) Research Grant, Galil Medical Ltd; Research agreement, Toshiba Corporation

Sub-Events

SSM11-01 Genitourinary Keynote Speaker: Safety and Efficacy of Corticosteroid Prophylaxis

Wednesday, Dec. 2 3:00PM - 3:10PM Location: E352

Participants

Matthew S. Davenport, MD, Cincinnati, OH (Presenter) Book contract, Wolters Kluwer nv; Book contract, Reed Elsevier;

SSM11-02 The Effect of IV Contrast on Renal Function in Patients on Metformin

Wednesday, Dec. 2 3:10PM - 3:20PM Location: E352

Participants

Cody W. McHargue, BA, San Francisco, CA (*Presenter*) Nothing to Disclose Arti D. Shah, MD, San Francisco, CA (*Abstract Co-Author*) Nothing to Disclose Judy Yee, MD, Clayton, CA (*Abstract Co-Author*) Research Grant, EchoPixel, Inc Priyanka Jha, MBBS, Sacramento, CA (*Abstract Co-Author*) Nothing to Disclose Isabel Allen, San Francisco, CA (*Abstract Co-Author*) Nothing to Disclose Donald Chau, BA, San Francisco, CA (*Abstract Co-Author*) Nothing to Disclose Robert Rushakoff, MD, San Francisco, CA (*Abstract Co-Author*) Nothing to Disclose

PURPOSE

Due to concerns of acute kidney injury and the theoretical risk of lactic acidosis with metformin, the Food and Drug Administration mandates that metformin be held for two days after intravenous (IV) contrast until renal function is checked and in an acceptable range. However, there is minimal evidence to support this practice. Further investigation is warranted.

METHOD AND MATERIALS

We conducted a retrospective cohort study of 130 adult outpatients at the San Francisco Veterans Affairs Medical Center to determine if there was a change in renal function in diabetic patients on metformin who underwent computed tomography (CT) scans with IV contrast between 2007-2014. Patients were excluded if immediately hospitalized after the CT scan. The generalized estimating equations method was used to determine whether IV contrast and pre-contrast creatinine (Cr; or pre-contrast estimated glomerular filtration rate [eGFR]) were associated with a change in Cr (or eGFR). Covariates included: age, gender, BMI, diabetes (DM) duration and HbA1c.

RESULTS

In our cohort, mean age was 67±10 years, 119 (91%) were male, 71 (55%) were Caucasian, and 63 (49%) were higher risk (precontrast eGFR <60 ml/min/1.73m2). Mean DM duration was 6.5±6.0 years and mean HbA1c was 7.1±1.3%. Mean pre- and postcontrast Cr were 1.13±0.25 mg/dL and 1.09±0.26 mg/dL; p=0.02 (overall t-test). Mean pre- and post-contrast eGFR were 72±24 ml/min/1.73m2 and 75±26 ml/min/1.73m2; p=0.006 (overall t-test). In fully-adjusted models, there was a significant decrease in Cr post-contrast: β -coefficient -0.24 (95% confidence interval [CI] -0.35 to -0.12), p<0.001. There was no significant change in eGFR post-contrast: β -coefficient -0.06 (95% CI -0.16 to 0.03), p=0.19. A subgroup analysis of patients with pre-contrast eGFR < 60 ml/min/1.73m2 showed similar results.

CONCLUSION

There is no evidence of deterioration in renal function in outpatients on metformin who receive IV contrast, even in a cohort with a large proportion of higher risk patients. Therefore, our results suggest that the current practice of holding metformin after IV contrast should be re-evaluated.

CLINICAL RELEVANCE/APPLICATION

The practice of holding metformin and checking Cr two days after IV contrast should be re-evaluated as there was no evidence to suggest a decline in renal function in a cohort with high risk patients.

SSM11-03 The Presence of a Solitary Kidney is not an Independent Risk Factor for Acute Kidney Injury Following Contrast-enhanced CT

Wednesday, Dec. 2 3:20PM - 3:30PM Location: E352

Participants

Jennifer S. McDonald, PhD, Rochester, MN (Abstract Co-Author) Research Grant, General Electric Company

Richard W. Katzberg, MD, Sacramento, CA (*Abstract Co-Author*) Research Grant, Siemens AG Research Grant, Bayer AG Investigator, Siemens AG Investigator, Bayer AG

Robert J. McDonald, MD, PhD, Rochester, MN (Presenter) Nothing to Disclose

Eric E. Williamson, MD, Rochester, MN (Abstract Co-Author) Research Grant, General Electric Company

David F. Kallmes, MD, Rochester, MN (Abstract Co-Author) Research support, Terumo Corporation Research support, Medtronic, Inc

Research support, Sequent Medical, Inc Research support, Benvenue Medical, Inc Consultant, General Electric Company Consultant, Medtronic, Inc Consultant, Johnson & Johnson

PURPOSE

To determine whether patients with a solitary kidney are at higher risk for contrast-induced acute kidney injury (AKI) than matched control bilateral kidney patients.

METHOD AND MATERIALS

This retrospective study was HIPAA compliant and approved by our Institutional Review Board. Adult patients with bilateral kidneys or a solitary kidney from unilateral nephrectomy who received a contrast-enhanced computerized tomography (CT) scan at our institution from January 2004 to August 2013 were identified. The effects of contrast exposure on the rate of AKI (defined as a rise in maximal observed serum creatinine (SCr) of either 1) > 0.5 mg/dL or 2) > 0.3 mg/dL or 50% over baseline within 24-72 hours of exposure), and 30-day post-scan emergent dialysis and death were determined following propensity score-based 1:3 matching of solitary and control bilateral kidney patients.

RESULTS

Propensity score matching yielded a cohort of 247 solitary kidney patients and 691 bilateral kidney patients. The rate of AKI was similar between the solitary and bilateral kidney groups [SCr > 0.5 mg/dL AKI definition odds ratio (OR) = 1.11 (95% confidence interval (CI) 0.65 - 1.86); p = 0.70; SCr > 0.3 mg/dL or 50% AKI definition OR = 0.96 (95% CI 0.41 - 2.07). p = 0.99]. The rate of emergent dialysis was rare and also similar between cohorts (OR = 1.87 (0.16-16.4), p=.61). Though the rate of mortality was higher in the solitary kidney group (OR = 1.70 (1.06-2.71), p=.0202), chart review found that no death was attributable to AKI.

CONCLUSION

This study did not detect any significant differences in the rate of AKI, dialysis, or death attributable to contrast-enhanced CT in patients with solitary versus bilateral kidneys.

CLINICAL RELEVANCE/APPLICATION

Contrast-enhanced CT protocols can be guided by image optimization, rather than contrast-induced nephropathy risk in solitary kidney patients.

SSM11-04 New Insights in the MRI Excretory Phase: The Use of Gd-EOB-DTPA for the Evaluation of the Excretory System

Wednesday, Dec. 2 3:30PM - 3:40PM Location: E352

Participants

Caterina Colantoni, MD, Milan, Italy (*Presenter*) Nothing to Disclose Antonio Esposito, MD, Milan, Italy (*Abstract Co-Author*) Nothing to Disclose Anna Palmisano, MD, Milan, Italy (*Abstract Co-Author*) Nothing to Disclose Francesco A. De Cobelli, MD, Milan, Italy (*Abstract Co-Author*) Nothing to Disclose Alessandro Del Maschio, MD, Milan, Italy (*Abstract Co-Author*) Nothing to Disclose

PURPOSE

Excretory MR urography is a useful complementary technique in many MR imaging studies of the abdomen to assess kidney excretion and the urinary collecting system. However, after the injection of a standard dose gadolinium-based contrast media, frequently, the collecting system is unassessable for T2* effect due to very high concentration of Gd in the urine. Aim of the present study was to compare the enhancement of the urinary collecting system after the injection of a single standard dose of Gd-based contrast media known for different renal excretion rates: Gadobutrol, Gadobenate dimeglumine, and Gd-EOB-DTPA.

METHOD AND MATERIALS

In 60 patients (pts) with normal creatinine clearance and without urinary tract dilatation, mean signal intensities (pixel values) of the renal pelvis and of the paravertebral muscles for the calculation of renal pelvis/skeletal muscle ratio, were evaluated on 3D fast T1-weighted gradient-echo sequences with fat suppression obtained during excretory phase after intravenous injection of 0.1 mmol/kg contrast media: 20pts were studied with Gadobutrol, 20pts with Gadobenate dimeglumine, and 20pts with Gd-EOB-DTPA, respectively. Urinary collecting system was considered assessable/not-assessable according to the presence of T2* effect.

RESULTS

The mean signal intensities of renal pelvis were 1954 \pm 1368.5 (pixel values) for Gadobutrol, 2488 \pm 843.8 for Gadobenate dimeglumine, and 3605 \pm 1025.3 for Gd-EOB-DTPA, respectively. The mean signal intensity ratio was 2.2 \pm 1.59 for Gadobutrol, 2.7 \pm 0.88 for Gadobenate dimeglumine, and 3.8 \pm 1.46 for Gd-EOB-DTPA. No significant differences were found between the mean signal intensity ratio of Gadobutrol and that of Gadobenate dimeglumine (p>0.05); significant differences were found between the mean signal intensity ratio of Gadobutrol and of Gd-EOB-DTPA (p<0.005), and that of Gadobenate dimeglumine and of Gd-EOB-DTPA (p<0.001). Urinary collecting system was considered not-assessable in 8/20pts for Gadobutrol, in 1/20pt for Gadobenate dimeglumine, and in 0/20pts for Gd-EOB-DTPA.

CONCLUSION

The urinary collecting system was considered assessable in all pts studied after injection of a standard dose of Gd-EOB-DTPA, and this could be due to the low urine excretion rate.

CLINICAL RELEVANCE/APPLICATION

The use of Gd-EOB-DTPA in the excretory MR urography can improve the assessability of the excretory system, with no evidence of $T2^*$ shortening effects.

SSM11-05 Feasibility and Image Quality of Reduced Dose CT Intravenous Pyelogram Using Model-Based Iterative Reconstruction in Patients with Hematuria

Participants Isabelle Boulay-Coletta, MD, Paris, France (*Abstract Co-Author*) Nothing to Disclose Linda N. Morimoto, MD, Stanford, CA (*Presenter*) Nothing to Disclose Dominik Fleischmann, MD, Palo Alto, CA (*Abstract Co-Author*) Research support, Siemens AG; Lior Molvin, Stanford, CA (*Abstract Co-Author*) Speakers Bureau, General Electric Company Lu Tian, Stanford, CA (*Abstract Co-Author*) Nothing to Disclose Juergen K. Willmann, MD, Stanford, CA (*Abstract Co-Author*) Research Consultant, Bracco Group; Research Consultant, Triple Ring Technologies, Inc; Research Grant, Siemens AG; Research Grant, Bracco Group; Research Grant, Koninklijke Philips NV; Research Grant, General Electric Company

PURPOSE

To evaluate the feasibility and image quality of Reduced Dose (RD) CT Intravenous Pyelogram (IVP) using Model-Based Iterative Reconstruction (MBIR) compared to Standard Dose (SD) CT IVP using Adaptive Statistical Iterative Reconstruction (ASIR) in patients referred for work-up of hematuria.

METHOD AND MATERIALS

In this IRB approved and HIPAA compliant study, 66 consecutive patients (44 males and 22 women; mean age, 62 years; mean BMI, 27 kg/m²) referred for a dual phase CT IVP (non-contrast and combined split-bolus nephrographic-excretory phase) were prospectively included and either imaged with SD CT IVP with 40% ASIR technique (n=34) or RD CT IVP with MBIR technique (n=32) on a 64-slice CT scanner (GE Discovery 750 HD). Quantitative measurements of image noise on both non-contrast and post-contrast imaging in addition to radiation dose and patients' BMI were recorded by one reader. Two independent, blinded readers assessed subjective image quality, including image noise, sharpness of the renal cortex and collecting system (calyces, renal pelvis, ureters, and bladder), presence of artifacts, and overall image quality impression on non-contrast and post-contrast images utilizing 4 or 5-point grading scales.

RESULTS

Both patient groups were not significantly different (26.8 +/- 7.8 kg/m² versus 27.5 +/- 4.8 kg/m²) in regards to BMI. Radiation dose was reduced by an average of 49% (p<0.01) on RD CT IVP (CTDI vol = 7.7 +/- 2.8 mGy) compared to SD CT IVP (CTDI vol = 15.1 +/- 4.8 mGy) on post-contrast imaging. Overall dose reduction averaged 36% with non-contrast and contrast-enhanced imaging (RD CT IVP CTDIvol =15.31 +/- 2.8 mGy versus SD CT IVP CTDI vol = 23.91 +/- 5.3 mGy). Overall image quality impression of the collecting system, artifacts, and image sharpness were not significantly different (p>0.05) between RD CT IVP and SD CT IVP. Subjective image noise was significantly lower (p<0.01) in RD CT IVP, which was also reflected by a quantitative reduction of image noise by an average of 44% (p<0.01) on non-contrast imaging and 37% (p<0.01) on post-contrast imaging.

CONCLUSION

RD CT IVP is feasible and allows for a substantial dose reduction compared to SD CT IVP protocol without compromising image quality.

CLINICAL RELEVANCE/APPLICATION

Introduction of iterative reconstruction algorithms which can be implemented with routine clinical CT IVP protocols to reduce radiation exposure while yielding diagnostic quality images.

SSM11-06 Reduced Radiation Dose with Iterative Reconstruction in 100 kVp CT Urography: With different Iodine Dosage

Wednesday, Dec. 2 3:50PM - 4:00PM Location: E352

Participants

Huihui Wang, MD, Beijing, China (*Presenter*) Nothing to Disclose Juan Hu, Kunming, China (*Abstract Co-Author*) Nothing to Disclose Xuedong Yang, Beijing, China (*Abstract Co-Author*) Nothing to Disclose Xiaoying Wang, MD, Beijing, China (*Abstract Co-Author*) Nothing to Disclose He Wang, MD, Beijing, China (*Abstract Co-Author*) Research Grant, General Electric Company Jian Jiang, MD, Beijing, China (*Abstract Co-Author*) Research Grant, General Electric Company

PURPOSE

To evaluate the image quality and radiation dose in CT urography at 100kVp with iterative reconstruction, combining a different iodine dosage.

METHOD AND MATERIALS

This study was approved by the institutional review board. From March to June 2012, 45 consecutive patients who underwent CTU for hematuria were divided into 3 groups: group A, 100kVp and 0.9mL/kg contrast material (CM) (9 men, 6 female; mean age 49.4 years; mean BMI 22.6kg/m2); group B, 100kVp and 1.1mL/kg CM (8 men,7 female; mean age 50.1years; mean BMI 22.6kg/m2); group C, 120kVp and 1.1mL/kg CM (13men, 2 female; mean age 58.5 years, mean BMI 23.5kg/m2). Automatic tube current was used in all groups. The 100kVp images (group A and B) were reconstructed with 80% adaptive statistical iterative reconstruction (ASiR), while filter back projection (FBP) for 120kVp images (group C). Urinary tract was divided into 11 segments, and mean CT values and contrast-to-noise ratio (CNR) of each segment in the excretory phase were measured respectively in 3 groups. The radiation dose in excretory phase was compared (volume computed tomography dose index, CTDIvol; size-specific dose estimate, SSDE and estimated effective dose, ED).

RESULTS

There were no significant differences among group A, B and C for age, BMI and transverse circumstance (all P>0.05). All examinations were considered to be of acceptable image quality and inter-observer agreement was good (K=0.717, P<0.001). There were no significant differences in mean attenuations of all urinary segments among 3 groups (P>0.05). Image noise was much less in group A and B (both P<0.001) than that of group C, but there was no significant difference between group A and B (P=0.934). CNRs in most segments were higher in group B than group C(P=0.001~0.062) and similar between group A and C(P=0.024~0.896), but there were no notable differences in CNRs between group A and B (P>0.05). Mean CTDIvol, SSDE and ED in excretory phase in

group A and B were significantly lower than those of group C(P<0.05). Iodine dosage was reduced by 18.2% in group A than group B and C.

CONCLUSION

Given subjective and objective image quality, CTU at 100 kVp with 80% ASiR resulted in reduction of radiation dose, and 0.9mL/kg CM (320mgI/ml) iodine dosage was workable.

CLINICAL RELEVANCE/APPLICATION

High radiation exposure and Contrast-Induced Nephropathy for CTU have drawn much attention and anxiety, 100kVp with 80% ASiR and 0.9mL/kg CM may offer a means of resolution.

Gastrointestinal (Loco-regional Therapy Liver Imaging)

Wednesday, Dec. 2 3:00PM - 4:00PM Location: E353A



AMA PRA Category 1 Credit ™: 1.00 ARRT Category A+ Credit: 1.00

Participants

Debra A. Gervais, MD, Chestnut Hill, MA (Moderator) Nothing to Disclose Steven S. Raman, MD, Santa Monica, CA (Moderator) Nothing to Disclose

Sub-Events

SSM08-01 Irreversible Electroporation in Patients with Hepatocellular Carcinoma: Immediate Versus Delayed **Findings on MR Imaging**

Wednesday, Dec. 2 3:00PM - 3:10PM Location: E353A

Participants

Guy E. Johnson, MD, Seattle, WA (Abstract Co-Author) Nothing to Disclose Matthew J. Kogut, MD, Seattle, WA (Abstract Co-Author) Nothing to Disclose James O. Park, MD, Seattle, WA (Abstract Co-Author) Nothing to Disclose Raymond S. Yeung, MD, Seattle, WA (Abstract Co-Author) Nothing to Disclose Daniel S. Hippe, MS, Seattle, WA (Abstract Co-Author) Research Grant, Koninklijke Philips NV; Research Grant, General Electric Company

Siddharth A. Padia, MD, Seattle, WA (Presenter) Nothing to Disclose

PURPOSE

Irreversible electroporation (IRE) is a non-thermal technique used to ablate soft tissue tumors. Our study assessed MR imaging appearance after IRE for the treatment of hepatocellular carcinoma (HCC).

METHOD AND MATERIALS

In this institutional review board-approved retrospective study with waiver of informed consent, twenty patients with HCC were treated with IRE over a 2.5 year period. Median patient age was 62, and 75% of patients had Child-Pugh A cirrhosis. Median tumor diameter was 2.0 cm (range 1.0-3.3 cm). Contrast-enhanced multiphase MR was performed on post-procedure day 1, 30, and every 90 days thereafter. Ablation zone sizes and signal intensities were compared between each time point for both T1- and T2weighted images. Trends in MR signal intensity and tumor dimensions over time were quantified using generalized linear models.

RESULTS

MR appearance of a treated tumor includes a zone of peripheral enhancement with centripetal filling on delayed post-contrast images. Compared to post-procedure day one, there is a decrease in enhancing ablation zone size of 28.9% (mean) every 90 days. There is a trend towards decreasing signal intensity of the peripheral ablation zone over time on both T2 (p=0.01) and contrastenhanced T1 weighted images (p<0.08). Conversely, the tumor itself typically demonstrates increased signal intensity over the same sequences.

CONCLUSION

IRE of HCC results in a large region of enhancement on immediate post-procedure MR, which involutes on follow-up imaging. This is associated with decreasing signal intensity of the peripheral ablation zone over time. This phenomenon may represent resolution of the reversible penumbra.

CLINICAL RELEVANCE/APPLICATION

1. Understanding of the standard MR imaging appearance after IRE can help guide future therapy and assess prognosis with respect to tumor response.2. The large area of enhancement seen after IRE may represent regions of reversible electroporation, which may be used to optimize treatment protocols or target localized drug delivery in future studies.

SSM08-02 Local Hepatic Tumor Control in Patients with HCC Undergoing Transarterial Lipiodol Embolisation **Followed by Microwave Ablation**

```
Wednesday, Dec. 2 3:10PM - 3:20PM Location: E353A
```

Participants

Roland M. Seidel, MD, Homburg, Germany (Presenter) Nothing to Disclose Alexander Massmann, MD, Homburg/Saar, Germany (Abstract Co-Author) Nothing to Disclose Peter Fries, MD, Homburg, Germany (Abstract Co-Author) Nothing to Disclose Guenther K. Schneider, MD, PhD, Homburg, Germany (Abstract Co-Author) Research Grant, Siemens AG; Speakers Bureau, Siemens AG; Speakers Bureau, Bracco Group; Research Grant, Bracco Group; Arno Buecker, MD, Homburg, Germany (Abstract Co-Author) Consultant, Medtronic, Inc Speaker, Medtronic, Inc Co-founder, Aachen Resonance GmbH Research Grant, Siemens AG

PURPOSE

To investigate local tumor control in patients with HCC undergoing lipiodol embolization and subsequent microwave ablation.

METHOD AND MATERIALS

25 patients with 35 HCC (mean size 23mm, SD 9mm) underwent superselective transarterial embolization with lipiodol. Subsequently

percutaneous CT guided microwave ablation of the tumors was performed using a 2,45 GHz generator (power output 80 to 120W) with cooled tip probes (Acculis , Angiodynamics, USA). All patients were investigated before therapy by unenhanced and dynamic contrast enhanced MR or CT; follow up was performed within 1, 3, 6 and more months after treatment. Treatment was rated as successful in case of a complete rim of necrosis surrounding the lesion and no further tumor growth. Patient data were evaluated retrospectively on a PACS workstation by two readers in consensus.

RESULTS

In 24 of 25 (96%) patients a complete ablation was diagnosed on the early follow up imaging. The patient rated with incomplete ablation presented tumor progression on follow up imaging. 1 patient initially rated as complete ablation presented lesion progression and underwent chemoembolization with no residual tumor up to 510 d after microwave ablation. Overall complete ablation rate per patient was 92% (23 of 25 patients) and 94% per lesion (33 of 35 lesions).

CONCLUSION

Microwave ablation in combination with lipiodol embolization for patients with HCC is a valuable therapeutic procedure for smaller hepatic tumors. Especially the targeting and embolizing potential of the retained lipiodol is likely to contribute to a more reliable tumor access and ablation effect .

CLINICAL RELEVANCE/APPLICATION

The treatment of smaller local HCC tumors becomes more and more an issue in the bridging to transplant situation and therefore minimal invasive percutaneous ablation techniques become attractive, since local tumor control is in the range of surgical treatments. This study demonstrates a reliable minimal invasive targeting and embolization technique in combination with microwave ablation for the enhancement of local tumor control.

SSM08-03 Analysis of a Series of Microwave Ablated Native HCCs: Which Parameters do Affect Outcome after Treatment?

Wednesday, Dec. 2 3:20PM - 3:30PM Location: E353A

Participants

Valentina Battaglia JR, MD, Pisa, Italy (*Presenter*) Nothing to Disclose Salvatore Mazzeo, MD, Pisa, Italy (*Abstract Co-Author*) Nothing to Disclose Carla Cappelli, MD,PhD, Pisa, Italy (*Abstract Co-Author*) Nothing to Disclose Rosa Cervelli, Pisa, Italy (*Abstract Co-Author*) Nothing to Disclose Piercarlo Rossi, MD, Pisa, Italy (*Abstract Co-Author*) Nothing to Disclose Carlo Bartolozzi, MD, Pisa, Italy (*Abstract Co-Author*) Nothing to Disclose

PURPOSE

To investigate the efficacy at 1 month after treatment of ultrasound-guided percutaneous microwave ablation (MWA) of series of native HCCs.

METHOD AND MATERIALS

From January 2013 to February 2015, 221 patients with a single HCC lesion were candidate for ultrasound-guided percutaneous MWA. Of them, 113 were excluded because of patients' habitus or limited US visibility of the lesion (42 and 71 patients respectively). Finally, our study included 108 patients who were treated with MWA for a single hepatic lesion. All lesions were classified on the basis of dimensions, location and venous vessel contiguity. A cooled shaft antenna of 16 or 14 Gauge was percutaneously inserted into the tumor under ultrasound guidance. Microwave emitting power and time of treatment were tailored to tumor size (ranging from 35 to 50W). Lesions were classified on the basis of dimensions (1.5cm to 2cm: 31/108; 2.1 to 3cm: 54/108; 3.1 to 4cm: 23/108), of location: centrohepatic, subcapsular, close to gallbladder, para-hilar and para-caval. Moreover, lesions were divided into subdiaphragmatic (23: yes; 86: no) and on the basis of proximity (<5mm) to vascular structures (59: yes; 49: no).In all cases, a CT evaluation performed 1 month after procedure was done. Tumor response after treatment was evaluated by means of mRECIST.Statistical analysis was performed by means of Chi-square test and bivariate correlation.

RESULTS

All neoplasm were ablated in a single session and no major complication occurred.At CT evaluation, 84 lesions showed a Complete Response, 23 Partial response and 1 lesion Stable Disease.Statistical analysis showed no significant relationship between complete response and tumor size, time of ablation or power applied. At bivariate analysis, tumor location and subdiaphragmatic position did correlate (p<0.0001) with lesions'response to treatment, independently from dimensions and technical parameters of power emission.

CONCLUSION

In our series, tumor size did not appear to impact complete ablation rates, whereas lesion localization represents the most important factor influencing tumor response.

CLINICAL RELEVANCE/APPLICATION

Lesions'characteristics might lead to formulate a grading on the basis of whom to predict tumor response after treatment.

SSM08-04 Local Treatment for Colorectal Cancer Liver Metastases, Comparison of Radiofrequency Ablation and Surgical Metastasectomy

Wednesday, Dec. 2 3:30PM - 3:40PM Location: E353A

Participants

Naik Vietti Violi, Lausanne, Switzerland (*Presenter*) Nothing to Disclose Alban L. Denys, MD, Lausanne, Switzerland (*Abstract Co-Author*) Nothing to Disclose Pierre E. Bize, MD, Lausanne, Switzerland (*Abstract Co-Author*) Nothing to Disclose Rafael Duran, MD, Baltimore, MD (*Abstract Co-Author*) Nothing to Disclose Nicolas Demartines, MD, Lausanne, Switzerland (*Abstract Co-Author*) Nothing to Disclose Nermin Halkic, Lausanne, Switzerland (*Abstract Co-Author*) Nothing to Disclose Jean-Francois Knebel, Lausanne, Switzerland (Abstract Co-Author) Nothing to Disclose

PURPOSE

To compare local recurrence rate of radiofrequency ablation (RFA) and surgical metastasectomy for colorectal cancer liver metastases from a surgical and radiological database of consecutive patients and to define the best candidates for each treatment.

METHOD AND MATERIALS

We analyzed, lesion by lesion, 121 metastases treated by metastastectomy (in 43 patients, median follow up 798 days) and 110 metastases treated by RFA (in 60 patients, median follow up 590 days). We compared rate of local recurrence (LR) and hepatic recurrence (HR) between the two groups. Predictive factors for recurrence (patients and primary tumor characteristics and metastasis data - size, depth in the liver (distance between metastasis and hepatic capsule), distance to vascular structures (all veins located within 10 mm to the metastasis were registered), pathological margins in case of surgery (R0/R1 status)), were analyzed by Chi square and logistic regression in uni and multivariate analysis.

RESULTS

We found no difference between the two groups for patients and primary tumor characteristics. Survival curves were similar between the two groups. Mean metastasis size was larger in metastectomy group than RFA group (18mm, range 2-90mm, standard error=0.11 and 15mm, range 3-55mm, standard error=0.06; p=0.03). Rate of LR and HR between the two groups were nearly statistically different in favor of RFA: LR was 19% for metastasectomy group and 10% for RFA group (p=0.06, delay: 245 and 289days, p=0.56), HR were 78.5% for metastasectomy and 66% for RFA (p=0.054, delay: 226 and 235days, p=0.81). R1 status and metastasis deepness were predictive factors for recurrence in the metastasectomy group (p=0.03 and p=0.02, respectively). Metastases deepness and proximity to vascular structure increased risk for R1 (p=0.04 and p<0.001, respectively). We found no predictive factor for recurrence in RFA group.

CONCLUSION

Pending proper selection (small lesions visible under imaging guidance), RFA tends to have a lower recurrence rate than metastasectomy. Lesions localized in depth in the liver parenchyma, close to large veins are at risk of local recurrence after metastasectomy.

CLINICAL RELEVANCE/APPLICATION

Metastasectomy and radiofrequency ablation are currently used for treatment of colorectal cancer liver metastasis aiming for total tumor ablation and sparing liver parenchyma. There is no study comparing results and risk of local recurrence between metastasectomy and RFA.

SSM08-05 Diagnostic Performance of DECT in the Assessment of Treated Zone Following Percutaneous Ablation in Renal Cell Cancer: Image Quality and Radiation Dose Considerations

Wednesday, Dec. 2 3:40PM - 3:50PM Location: E353A

Participants

Diana Murcia, MD, Boston, MA (*Presenter*) Nothing to Disclose Andrea Prochowski Iamurri, MD, Boston, MA (*Abstract Co-Author*) Nothing to Disclose Manuel Patino, MD, Boston, MA (*Abstract Co-Author*) Nothing to Disclose Ronald S. Arellano, MD, Boston, MA (*Abstract Co-Author*) Nothing to Disclose Dushyant V. Sahani, MD, Boston, MA (*Abstract Co-Author*) Research Grant, General Electric Company; Research Consultant, Allena Pharmaceuticals, Inc Avinash R. Kambadakone, MD, Boston, MA (*Abstract Co-Author*) Nothing to Disclose

PURPOSE

To determine the diagnostic performance of DECT in the evaluation of treated zone following percutaneous ablation of renal cell cancer (RCC) with assessment of value of iodine images (MD-I), image quality and radiation dose considerations.

METHOD AND MATERIALS

In this retrospective study, 26 patients (17 M, 9 F, mean age 69 years) with RCC treated with percutaneous ablation were included. The patients underwent contrast enhanced nephrographic phase dual energy CT scan with a single-source dual energy CT (750HD GE Healthcare, Milwaukee WI) as part of post ablation surveillance. In this cohort, 13 patients had single energy unenhanced scans. All the patients in this cohort had renal mass protocol single energy CT (SECT) at different time-points. Post processed subtraction, material density iodine (MD-I) and virtual unenhanced images were generated. Two blinded radiologists reviewed the SECT and DECT images in two separate sessions for ablation zone margin, presence of residual/recurrent tumor, image quality and presence of artifacts with a 5 point confidence score. The CTDI and DLP were recorded and compared between DECT series and SECT series.

RESULTS

A total of 28 RCC underwent percutaneous ablation. DECT with MD-I iodine images demonstrated higher specificity for detection of abnormal enhancement in the ablation zone suggesting residual tumor/recurrence compared to SECT (30% vs 91%). The image quality score for DECT (with MD-I) was higher compared to standard SECT images (5 vs 4.1 of SECT with p<0.05) with higher number of artifacts recorded in the subtraction images generated from standard non-contrast and contrast enhanced CT images (25% of cases). A single phase DECT had significant radiation dose reduction in comparison to dual phase SECT scans (736.11±231.6 mGy-cm vs 1596.5±450.2 mGy-cm; p<0.001) and the radiation dose considerations of nephrographic phase DECT and SECT were comparable (736.11±231.6 mGy-cm vs 609.5±169.1 mGy-cm; p=0.179)

CONCLUSION

DECT with iodine specific images improves diagnostic performance in the evaluation of ablation zone in RCC as compared to standard SECT images with significant reduction of radiation dose due to exclusion of non-contrast phase.

CLINICAL RELEVANCE/APPLICATION

Post ablation surveillance of treated zone in patients with RCC can present diagnostic challenges with the need for non-contrast

scans and subtraction images which increase the cumulative radiation dose and are affected by artifacts.

Honored Educators

Presenters or authors on this event have been recognized as RSNA Honored Educators for participating in multiple qualifying educational activities. Honored Educators are invested in furthering the profession of radiology by delivering high-quality educational content in their field of study. Learn how you can become an honored educator by visiting the website at: https://www.rsna.org/Honored-Educator-Award/

Dushyant V. Sahani, MD - 2012 Honored Educator Dushyant V. Sahani, MD - 2015 Honored Educator

SSM08-06 CT and MR Imaging Features to Predict Residual or Recurrent Hepatocellular Carcinoma after Transarterial or Percutaneous Treatment

Wednesday, Dec. 2 3:50PM - 4:00PM Location: E353A

Participants

Eric C. Ehman, MD, San Francisco, CA (*Presenter*) Nothing to Disclose Sarah Umetsu, MD, PhD, San Francisco, CA (*Abstract Co-Author*) Nothing to Disclose Nicholas Fidelman, MD, San Francisco, CA (*Abstract Co-Author*) Nothing to Disclose Linda Ferrell, MD, San Francisco, CA (*Abstract Co-Author*) Nothing to Disclose Michael A. Ohliger, MD, PhD, San Francisco, CA (*Abstract Co-Author*) Nothing to Disclose Benjamin M. Yeh, MD, San Francisco, CA (*Abstract Co-Author*) Nothing to Disclose Benjamin M. Yeh, MD, San Francisco, CA (*Abstract Co-Author*) Research Grant, General Electric Company; Author with royalties, Oxford University Press; Shareholder, Nextrast, Inc; Judy Yee, MD, San Francisco, CA (*Abstract Co-Author*) Research Grant, EchoPixel, Inc Thomas A. Hope, MD, San Francisco, CA (*Abstract Co-Author*) Advisory Committee, Guerbet SA; Research Grant, General Electric Company

PURPOSE

To determine which CT and MR features are most predictive of viable hepatocellular carcinoma (HCC) following percutaneous or transarterial therapy.

METHOD AND MATERIALS

Pathology reports for liver explants from 12/2012-7/2014 with CT or MR imaging performed within 90 days of transplant (45±28 days) were reviewed. Patients with a history of hepatocellular carcinoma and preoperative treatment including transarterial chemoembolization (TACE) or percutaneous ablation (radiofrequency, microwave, cryo, ethanol) were included. Each lesion was reviewed on the most recent pre-transplant imaging study and size, location and enhancement features recorded. Pathology slides were reviewed and the size of viable tumor nodule recorded (if present).

RESULTS

91 patients with 135 treated lesions were included. 88(65%) lesions were imaged with CT and 47(35%) with MR, including 89(66%) post-TACE, 24(18%) post-ablation, and 22(16%) post both TACE and ablation. At explant, 69(51%) of lesions showed viable tumor. 11/42(26%) of viable lesions at CT and 15/27(56%) at MR demonstrated nodular arterial enhancement (p=0.02). Washout was seen in 13/42(31%) of viable HCCs at CT and in 6/27(22%) at MR (p>0.05). Capsule appearance was seen in 2/42(5%) of viable lesions at CT and in 1/27(4%) at MR (p>0.05). Using each criteria to diagnose a study positive for recurrence, sensitivity and specificity were 38% and 92% for nodular enhancement, 28% and 94% for washout and 4% and 100% for capsule. Using any of the three criteria, overall sensitivity and specificity were 45% and 91%. Detection rate for nodular recurrence was 33% for lesions <1cm, 55% for lesions 1-2cm and 71% for lesions >2cm. Lesion detection by size was similar at CT and MR.

CONCLUSION

No single imaging finding was sensitive for viable HCC following treatment. Nodular arterial enhancement was the most frequently seen, and seen significantly more at MR than at CT. Washout was less frequently seen and seen equally at MR and CT. Capsule was rarely seen but when present always predicted recurrence. There is limited detection of lesions <1cm both at MR and CT and only marginal detection between 1-2cm.

CLINICAL RELEVANCE/APPLICATION

Post-treatment imaging is difficult to interpret and imaging features predictive of recurrent or residual disease are not well understood. Accurate diagnosis of viable tumor at post-treatment imaging is important to guide future therapy such as repeat TACE or ablation.

Gastrointestinal (Esophagus Imaging)

Wednesday, Dec. 2 3:00PM - 4:00PM Location: E353B



AMA PRA Category 1 Credit ™: 1.00 ARRT Category A+ Credit: 1.00

Participants

David J. Lomas, MD, Cambridge, United Kingdom (*Moderator*) Nothing to Disclose Lisa M. Ho, MD, Durham, NC (*Moderator*) Nothing to Disclose

Sub-Events

SSM09-01 Changes in Esophageal Dimensions during Continuous Swallowing in Healthy Adults as Detected by Magnetic Resonance Imaging

Wednesday, Dec. 2 3:00PM - 3:10PM Location: E353B

Participants

Sabarish Narayanasamy, MBBS,MD, Aligarh, India (*Presenter*) Nothing to Disclose Mehtab Ahmad, MBBS, Aligarh, India (*Abstract Co-Author*) Nothing to Disclose Mudit Arora, DMRD, Aligarh Ho, India (*Abstract Co-Author*) Nothing to Disclose Faisal Janal, MBBS, Aligarh, India (*Abstract Co-Author*) Nothing to Disclose Breethaa J. Selvamani, Aligarh, India (*Abstract Co-Author*) Nothing to Disclose Anusha Sundararajan, Loma Linda, CA (*Abstract Co-Author*) Nothing to Disclose

PURPOSE

This study was designed to quantify the degree of fluctuation in esophageal dimensions during continuous swallowing on Magnetic Resonance (MR) Imaging.

METHOD AND MATERIALS

30 healthy volunteers (25 males and 5 females, age range: 15-45 years) were chosen for the study. MR examination was done using a 1.5 tesla magnet. Initially, the esophagus was imaged in the resting state (Resting MR). Then, the volunteer was asked drink water continuously and another set of MR images were obtained (Swallowing MR). The thoracic esophagus was divided into three segments (upper, middle and lower) based on anatomical landmarks. Diameter and the wall thickness of the esophagus were measured in each segment and the cross sectional area (CSA) was calculated.

RESULTS

The esophageal CSA increased by twofold on swallowing MR scans as compared to the resting scans [Median(interquartile range) increase in CSA in upper segment - 117.3%(61-162.2), in middle segment - 87.7%(54.3-162.9) and in the lower segment - 122.1% (78.9 - 188.1)]. The anteroposterior and transverse diameters of the thoracic esophagus increased by about 60% as compared to the resting MR scans. The mean wall thickness of the thoracic esophagus was reduced by about 25% on swallowing MR as compared to resting scan.

CONCLUSION

Our study helps to define normal changes in esophageal dimensions during continuous swallowing. The lower third of the thoracic esophagus appears to be the most distensible segment.

CLINICAL RELEVANCE/APPLICATION

Swallowing MRI has been proposed as an experimental investigative modality for motility disorders of the esophagus and knowledge of the fluctuation in esophageal dimensions during swallowing might be of clinical utility.

SSM09-02 Differentiate Esophageal Cancer Stages with Spectral CT Imaging

Wednesday, Dec. 2 3:10PM - 3:20PM Location: E353B

Participants

Yang Chuangbo, MMed, Xianyang City, China (*Presenter*) Nothing to Disclose Yongjun Jia, MMed, Xianyang City, China (*Abstract Co-Author*) Nothing to Disclose Xirong Zhang, Xianyang, China (*Abstract Co-Author*) Nothing to Disclose Chenglong Ren, Shanxi, China (*Abstract Co-Author*) Nothing to Disclose Haifeng Duan, Xianyang City, China (*Abstract Co-Author*) Nothing to Disclose Taiping He, Xianyang, China (*Abstract Co-Author*) Nothing to Disclose Xiaoxia Chen, MMed, Xianyang City, China (*Abstract Co-Author*) Nothing to Disclose

PURPOSE

To explore the value of spectral CT imaging to differentiate esophageal cancer stages.

METHOD AND MATERIALS

67 patients with esophageal cancer diagnosed by esophagoscopy underwent plain and double-phase enhanced CT scan with spectral CT mode. Patients were divided into well-to-moderately differentiated and poorly differentiated squamous carcinoma groups. The iodine-based material decomposition (MD) images were generated and analyzed with GSI Viewer software to measure the iodine concentration (IC) in tumors. Normalized iodine concentration (NIC) was obtained by dividing tumor IC to that of aorta. Data from the two cancer groups were analyzed statistically by independent-samples t test and were correlated with pathological

RESULTS

There were 32 well-to-moderately differentiated(Picture 1) and 35 poorly differentiated(Picture 2) squamous carcinoma verified by pathology. IC values of the well-to-moderately differentiated squamous carcinoma in both the arterial phase (AP) $(2.66\pm1.07 \text{mg/ml})$ and venous phase (VP) $(2.12\pm0.94 \text{mg/ml})$ were lower than that of the poorly differentiated squamous carcinoma $(2.85\pm1.25 \text{mg/ml})$ and $2.57\pm1.06 \text{mg/ml}$, respectively). The NIC value of the well-to-moderately differentiated squamous carcinoma was also lower than that of the poorly differentiated squamous carcinoma was also lower than that of the poorly differentiated squamous carcinoma was also lower than that of the poorly differentiated squamous carcinoma: $0.12\pm0.05 \text{ vs}$. $0.13\pm0.06 \text{ in AP}$ and $0.42\pm0.13 \text{ vs}$. $0.61\pm0.18 \text{ in VP}$, respectively. Statistical differences of IC and NIC were found between the two groups in VP (both p<0.05) but not in AP (p>0.05).

CONCLUSION

There are correlation between the iodine concentration and normalized iodine concentration of esophageal cancers and their histological differentiation stages. IC and NIC parameters obtained in spectral CT for the esophageal cancer in the venous phase can be used as new indexes to differentiate esophageal cancer stages.

CLINICAL RELEVANCE/APPLICATION

Parameters such as normalized iodine concentration in esophageal cancer determined in spectral CT may be used to differentiate esophageal cancer stages.

SSM09-03 Diffusion-Weighted MRI in the Staging of Esophageal Cancer: Ready for Clinical Use? Prospective Comparison with EUS and MDCT

Wednesday, Dec. 2 3:20PM - 3:30PM Location: E353B

Participants

Francesco Giganti, MD, Milan, Italy (*Presenter*) Nothing to Disclose Paolo G. Arcidiacono, Milan, Italy (*Abstract Co-Author*) Nothing to Disclose Roberto Nicoletti, MD, Milan, Italy (*Abstract Co-Author*) Nothing to Disclose Elena Orsenigo, Milan, Italy (*Abstract Co-Author*) Nothing to Disclose Alessandro Del Maschio, MD, Milan, Italy (*Abstract Co-Author*) Nothing to Disclose Francesco A. De Cobelli, MD, Milan, Italy (*Abstract Co-Author*) Nothing to Disclose

PURPOSE

This pilot study was intended to prospectively compare the diagnostic performance of Diffusion-Weighted Magnetic Resonance Imaging (DW-MRI), Multidetector Computed Tomography (MDCT) and Endoscopic Ultrasonography (EUS) in the preoperative locoregional staging of esophageal cancer.

METHOD AND MATERIALS

This study was institutional review board-approved. Eighteen patients with biopsy proved esophageal or gastro-esophageal (Siewert I) tumor (9 directly treated with surgery and 9 addressed to chemo/radiotherapy before) underwent 1.5 T DW-MRI, 64channels MDCT and EUS before and after neoadjuvant treatment. All images were analyzed and staged blindly by dedicated operators according to the 7th TNM edition and two radiologists calculated indipendently the Apparent Diffusion Coefficient (ADC) from the initial scan. The results were then compared with histopathological findings. Statistical analysis included Spearman and intraclass correlation coefficients, Mann-Whitney U test and receiver operator characteristic curve analysis. After the population had been divided according to local invasion (T1-2 vs T3-4) and nodal involvement (N0 vs N+), sensitivity, specificity, accuracy, positive and negative predictive value were calculated and compared for each technique. Quantitative measurements from DWI were also analyzed.

RESULTS

For T staging, EUS showed the best sensitivity (100%) while MR showed the highest specificity (92%) and accuracy (83%). For N staging, MR and EUS showed the highest sensitivity (100%) but none of the three techniques showed adequate results for specificity. Overall, MR showed the highest accuracy (66%) for N stage. Mean pathological ADC was different between surgery-only and chemo/radiotherapy groups (1.90 vs 1.30 x 10-3 mm2/s, respectively; p=0.005), with an optimal cut off for local invasion of 1.33 x 10-3 mm2/s (p=0.05).

CONCLUSION

DW-MRI could improve the current preoperative staging workup for esophageal cancer, showing characteristic advantages for both staging and initial treatment decision-making.

CLINICAL RELEVANCE/APPLICATION

DW-MRI can be useful in the preoperative workup for esophageal cancer and could help to select appropriate treatments after initial staging.

SSM09-04 The Use of 3T Multiparametric MRI in the Staging of Esophageal Cancer (EC)

Wednesday, Dec. 2 3:30PM - 3:40PM Location: E353B

Participants

Daniela A. Cenzi, MD, Verona, Italy (*Presenter*) Nothing to Disclose Lisa Zantedeschi, MD, Verona, Italy (*Abstract Co-Author*) Nothing to Disclose Lucia Camera, Verona, Italy (*Abstract Co-Author*) Nothing to Disclose Giacomo Schenal, Verona, Italy (*Abstract Co-Author*) Nothing to Disclose Massimiliano Motton, MD, Verona, Italy (*Abstract Co-Author*) Nothing to Disclose Stefania Montemezzi, MD, Verona, Italy (*Abstract Co-Author*) Nothing to Disclose

PURPOSE

To evaluate diagnostic feasability of MP-MRI for the preoperative staging of EC and to assess its efficacy in discrimination between

responders and non-responders in those who underwent neoadjuvant treatment (NT).

METHOD AND MATERIALS

Between 2011 and January 2015, 36 patients with biopsy-proven EC underwent 3T MRI with the same approach: T2 weighted images, DWI and DCE sequences, with cardiac and respiratory gating. According to local invasion (T1-2 vs T3-4) and nodal involvement (N- vs N+), we identified 11 patients with organ confined lesion who underwent surgery: MR-staging results were compared with histopathological findings directly. 25 patients were addressed to NT and restaging MRI after treatment was compared to histological findings after surgery. Sensitivity (SE), specificity (SP), positive (PPV) and negative (NPV) predictive value and accuracy were calculated for the both groups. For NT group, changes in ACD and changes in DCE time intensity curve at MRI before and after treatment were calculated. 2 readers indipendently determined: pre-NT and post-NT ADC, percentage changes in ADC (Δ ADC), DCE time intensity curves and interobserver variability.

RESULTS

Surgery group: for T staging, SE was 98 %, SP 78 %, accuracy 90%; for N staging SE was 67 %, SP 60 %, accuracy 64%. NT group after NT: for T staging SE was 80 %, SP 85 %, PPV 67%, NPV 92%, accuracy 89% and 76%, 78%, 50%, 91% and 91% respectively for N staging.Responders showed lower pre-NT ADC (1.30 vs $1.80^{\text{A}} \sim 10-3 \text{mm2/s}$; P=0.002) and higher post-NT ADC (2.50 vs $1.64^{\text{A}} \sim 10-3 \text{mm2/s}$; P=0.001) than non-responders and ADC increased in responders (Δ ADC, 90.28 versus 11 %, respectively). A slight difference was observed in DCE curves but without a significant difference (p>0.05).Interobserver reproducibility was good both for surgery (k 0.68) and post-NT (k 0.86).

CONCLUSION

MR can correctly stage organ-confined lesions according to the high specificity (for the T stage) and to rightly assess pathological nodal involvement (for the N stage) thanks to the good SE. The ADC can be used to assess esophageal tumour response to NT treatment as a reliable expression of tumour regression.

CLINICAL RELEVANCE/APPLICATION

Preoperative staging in esophageal cancer is critical in order to prompt a surgical (T1-T2 stages without nodal involvement) or neoadjuvant therapy (T3-T4 stages with nodal involvement).

SSM09-05 Textural Analysis of Baseline 18F-FDG PET for Predicting Treatment Response and Prognosis in Patients with Locally Advanced Esophageal Cancer

Wednesday, Dec. 2 3:40PM - 3:50PM Location: E353B

Participants

Xiaorong Sun, Jinan, China (*Presenter*) Nothing to Disclose Lu Sun, Jinan, China (*Abstract Co-Author*) Nothing to Disclose Ligang Xing, Jinan, China (*Abstract Co-Author*) Nothing to Disclose

PURPOSE

Textural features on baseline 18F-FDG PET have shown the potential role in predicting treatment response in mixed stage esophageal cancer. This study is aim to investigate the value of this new technique for locally advanced esophageal squamous cell cancer (ESCC) receiving chemoradiotherapy.

METHOD AND MATERIALS

Under a waiver from IRB, 48 patients with newly diagnosed locally advanced ESCC who treated with concurrent chemoradiotherapy were retrospectively reviewed. Thirty-nine patients with early stage ESCC were included as control. All patients underwent pretreatment whole-body 18F-FDG PET/CT. Fifty-four texture indices describing global, local, and regional features were measured in addition to 5 conventional indices as standardized uptake values (SUVs, including maximum, peak, and mean SUV), metabolic volume (MV), and total lesion glycolysis (TLG). Patients were classified as responders (R, complete or partial response) and non-responders (NR, stable or progressive disease) according to RECIST1.1. Progression-free survival (PFS) and overall survival (OS) were recorded. The prognostic significance of parameters was examined using receiver-operating-characteristic curves, Kaplan-Meier analysis, and Cox regression analysis.

RESULTS

Both intratumor heterogeneity and mean/peak intensity of FDG uptake were significantly higher in locally advanced ESCC than those in early stage. Thirty-four texture indices, MV, and TLG showed the ability to differentiate R from NR. Nine texture indices showed higher sensitivity (76.7%~86.7%) and specificity (77.8%~94.4%) than MV (76.7% and 83.3%) and TLG (73.3% and 83.3%). Ten texture indices and MV were hazard factors of PFS and OS. Large-zone emphasis, one of the regional texture indices, was the only independent predictor of survival, with hazard ratio of 4.22 (95%CI:1.83~9.72) for PFS and 3.90 (1.74~8.79) for OS. None of the SUVs could predict treatment response and survival.

CONCLUSION

FDG PET texture indices provide better predictive information than conventional parameters for locally advanced ESCC.

CLINICAL RELEVANCE/APPLICATION

The clinical application of FDG PET texture analysis could be an important step in personalized treatment of esophageal cancer.

SSM09-06 CT Signs Can Predict Treatment Response and Long-Term Survival: A Study in Locally Advanced Esophageal Cancer with Preoperative Chemotherapy

Wednesday, Dec. 2 3:50PM - 4:00PM Location: E353B

Participants Xiao-Yan Zhang, Beijing, China (*Presenter*) Nothing to Disclose Xiaoting Li, Beijing, China (*Abstract Co-Author*) Nothing to Disclose Zhilong Wang, MD, Beijing, China (*Abstract Co-Author*) Nothing to Disclose Ying-Shi Sun, MD, PhD, Beijing, China (Abstract Co-Author) Nothing to Disclose

PURPOSE

Accurate prediction of treatment response and prognosis before surgery will allow prompt therapy adjustment. This study proposed to evaluate the efficacy of CT signs on treatment response and survival for advanced esophageal squamous cell carcinoma patients with preoperative chemotherapy.

METHOD AND MATERIALS

This study retrospectively enrolled 135 consecutive patients with preoperative chemotherapy from September 2005 to December 2011. Logistic regression model was conducted to evaluate the association between pathological response and CT signs. Overall survival(OS) and disease-free survival (DFS) were estimated using Kaplan-Meier method and Cox proportional hazards model was constructed to determine associations between CT signs after neoadjuvant chemotherapy and survival outcomes.

RESULTS

The logistic regression showed the total LN number(> 6) at baseline and the CT value change rate (\leq 17%) were significant for poor response; OR were 5.07 (95% CI, 1.86 to 13.81, P = 0.002) and 2.35 (95% CI, 1.05 to 5.23, P = 0.037), respectively. In Cox analyses, preoperative tumor thickness (> 10 mm), total LN number (>6), and short diameter of the largest LN (> 10 mm) were significant for OS, HR were 2.33(95% CI, 1.36 to 4, P = 0.002), 1.88(95% CI, 1.12 to 3.17, P = 0.017) and 1.87(95% CI, 1.07 to 3.28, P = 0.028), respectively; whereas only the short diameter of the largest LN was significant for DFS, HR was 2.36(95% CI, 1.23 to 4.54, P = 0.01).

CONCLUSION

CT signs can predict therapeutic efficacy and survival outcomes and provide an opportunity to offer additional treatment options before surgery.

CLINICAL RELEVANCE/APPLICATION

This study provided the first evidence that CT signs can predict survival outcomes and therapeutic efficacy of patients with esophageal cancer who received preoperative chemotherapy. Therefore, it is of great clinical significance to perform CT examinations before and after neo-adjuvant therapies in esophageal cancer patients. The CT images interpreted before surgery could provide important information about survival and response, which would improve individualized treatment programs.

ISP: Musculoskeletal (MRI Around Metal: Technique and Clinical Application)

Wednesday, Dec. 2 3:00PM - 4:00PM Location: E450A

MK MR

AMA PRA Category 1 Credit ™: 1.00 ARRT Category A+ Credit: 1.00

FDA Discussions may include off-label uses.

Participants

Hollis G. Potter, MD, New York, NY (*Moderator*) Research support, General Electric Company Siegfried Trattnig, MD, Vienna, Austria (*Moderator*) Nothing to Disclose

Sub-Events

SSM15-01 Musculoskeletal Keynote Speaker: MR Imaging Around Metal-Technique and Clinical Implementation

Wednesday, Dec. 2 3:00PM - 3:20PM Location: E450A

Participants

Hollis G. Potter, MD, New York, NY (Presenter) Research support, General Electric Company

SSM15-03 Particle Induced Synovitis on MRI and Correlation with Polyethylene Surface Damage at Retrieval Analysis

Wednesday, Dec. 2 3:20PM - 3:30PM Location: E450A

Awards

Trainee Research Prize - Fellow

Participants Angela E. Li, MBBS, MMed, New York, NY (*Presenter*) Nothing to Disclose Christine C. Johnson, MD, New York, NY (*Abstract Co-Author*) Nothing to Disclose Darryl B. Sneag, MD, Chestnut Hill, MA (*Abstract Co-Author*) Nothing to Disclose Chelsea N. Koch, BS, New York, NY (*Abstract Co-Author*) Nothing to Disclose Kara Fields, New York, NY (*Abstract Co-Author*) Nothing to Disclose Timothy M. Wright, PhD, New York, NY (*Abstract Co-Author*) Nothing to Disclose Theodore T. Miller, MD, New York, NY (*Abstract Co-Author*) Nothing to Disclose Douglas E. Padgett, MD, New York, NY (*Abstract Co-Author*) Consultant, Stryker Corporation; Hollis G. Potter, MD, New York, NY (*Abstract Co-Author*) Research support, General Electric Company

PURPOSE

To determine if a correlation exists between degree of polyethylene surface damage in total knee arthroplasty (TKA) tibial components and the severity of synovitis, osteolysis, and capsular thickness on MRI.

METHOD AND MATERIALS

With IRB approval, 62 patients who had an MRI within 1 year prior to revision arthroplasty were consecutively selected from our hospital registry of retrieved TKA implants. The MR images were retrospectively graded for particle induced synovitis based on the percentage of bulky hypertrophied synovium filling the joint. Capsular thickness and volume of osteolytic lesions were calculated. The articular surfaces of the retrieved tibial inserts were visually inspected, blinded to the MR appearances, and subjectively assigned damage scores by two independent observers using an established grading system. Inserts were graded for: deformation, embedded debris, scratching, burnishing, delamination, pitting, and abrasion. The MRI scores and measurements were compared to the articular surface damage scores using the Spearman correlation coefficient.

RESULTS

A positive correlation was found between the MRI grade of particle induced synovitis and the damage score (rs=0.423, p<0.01, or rs=0.450, p<0.01 when the synovitis grade was corrected for the degree of capsular distention). The volume of osteolytic lesions correlated with the damage score (rs=0.335, p<0.01). Capsular thickness did not correlate with damage scores (rs=-0.097, p=0.5). The synovitis grade strongly correlated with the volume of osteolytic lesions (rs=0.579, p<0.01). The length of implantation of the TKA correlated with both the synovitis grade and damage score (rs=0.396, p<0.01 and rs=0.487, p<0.01, respectively). The mean length of implantation was 6.7 years (range 1-30, SD 6.1 years).

CONCLUSION

Polyethylene surface damage in TKA correlates with the severity of particle-induced synovitis and volume of osteolytic lesions on MRI.

CLINICAL RELEVANCE/APPLICATION

The association between MRI findings and retrieval analysis of polyethylene damage suggests a link between wear debris and subsequent synovial reactions around failed TKAs.

SSM15-04 Metal Artifact Reduction (MAR) on a Sliding Gantry CT-scanner: Evaluation of a MAR Algorithm Based on Two Compartment Physical Modelling in Patients with Hip Implants

Johannes Boos, MD, Boston, MA (*Abstract Co-Author*) Nothing to Disclose Lino Sawicki, MD, Dusseldorf, Germany (*Abstract Co-Author*) Nothing to Disclose Rotem S. Lanzman, MD, Duesseldorf, Germany (*Abstract Co-Author*) Nothing to Disclose Christoph Schleich, Dusseldorf, Germany (*Abstract Co-Author*) Nothing to Disclose Gerald Antoch, MD, Duesseldorf, Germany (*Abstract Co-Author*) Nothing to Disclose Patric Kroepil, MD, Duesseldorf, Germany (*Presenter*) Nothing to Disclose

PURPOSE

The aim of this study was to evaluate the impact of a novel metal artifact reduction (MAR) algorithm on image quality compared to standard filtered back projection (FBP) on a CT scanner with sliding gantry in patients with metallic hip implants.

METHOD AND MATERIALS

Twenty two patients with 25 metallic hip implants were included in this retrospective study. All patients underwent abdominopelvic computed tomography on a 64 row scanner with sliding gantry (Definition AS+ sliding gantry, Siemens, Germany). Axial images were reconstructed using FBP and five increasing MAR levels (M30-34). Objective artifact reduction was assessed by ROI measurements in localization of the strongest artifact (SIart) and in osseous structures without artifacts (SInorm). Differences between both measurements served as a measure for objective artifact strength (OAS: SIart-SInorm). Two blinded, independent reader evaluated subjective IQ regarding metallic hardware, delineation of bone, adjacent muscle and pelvic organs on a five point scale (1: non diagnostic - 5: excellent IQ, no artifacts). In addition, new artifacts due to MAR were recorded.

RESULTS

OAS values were 153.2 ± 48.3 HU for M34; 261.0 ± 241.6 HU for M33; 328.7 ± 228.8 HU for M32; 393.2 ± 225.9 HU for M31; 446.8 ± 224.2 HU for M30 and 528.9 ± 227.7 HU for FBP. OAS values were significantly lower for M32-34 compared to FBP (p<0.05).Subjective image quality was 2.0 ± 0.2 for FBP, 2.3 ± 4.8 for M30, 2.6 ± 0.5 for M31, 3.0 ± 0.6 for M32, 3.5 ± 0.6 for M33 and 3.8 ± 0.4 for M34 (p<0.05 for M31-M34 vs. FBP, respectively). Increasing strength of the MAR level resulted in new artifacts in up to 16%.

CONCLUSION

The MAR algorithm leads to a significant reduction in artifacts from metallic hip implants. The highest MAR-level allows for the maximal artifact reduction but may also induce new artifacts.

CLINICAL RELEVANCE/APPLICATION

High levels of a MAR algorithm lead to a significant improvement of image quality in patients with hip implants.

SSM15-05 Contrast Enhanced MRI Adjacent to Metal Interfaces

Wednesday, Dec. 2 3:40PM - 3:50PM Location: E450A

Participants

Rajeev Mannem, MD, Milwaukee , WI (*Presenter*) Nothing to Disclose Suryanarayanan Kaushik, PhD, Milwaukee, WI (*Abstract Co-Author*) Nothing to Disclose Scott J. Erickson, MD, Milwaukee, WI (*Abstract Co-Author*) Nothing to Disclose Mark D. Hohenwalter, MD, Milwaukee, WI (*Abstract Co-Author*) Nothing to Disclose Kevin M. Koch, PhD, Waukesha, WI (*Abstract Co-Author*) Nothing to Disclose

PURPOSE

Metal-induced susceptibility artifacts in MRI can be greatly reduced using Three-Dimensional Multi-Spectral Imaging methods (3D-MSI). A variety of previous studies have demonstrated preliminary clinical utility of 3D-MSI (i.e. "MAVRIC SL" and "SEMAC/Advanced WARP") in assessing complications near metal implants. Here, we present preliminary analysis of 3D-MSI utility in contrastenhanced (CE) MRI at a field strength of 1.5T. Susceptibility-artifacts near metal implants introduce unique challenges to CE MRI. In particular, the hyperintense 'pileup' artifacts that are present in conventional fast/turbo spin-echo sequences often confound assessment of CE near metal implants. Use of T1w 3D-MSI for CE MRI reduces the footprint of these hyperintensity artifacts.

METHOD AND MATERIALS

MAVRIC SL 3D-MSI was implemented using modified pulse-sequencing software that allowed for shorter TR periods than the commercially available sequence. 3D-MSI images were acquired pre-and post contrast in at least one scan plane for each case. In addition conventional 2D-FSE images were acquired for each case for qualitative comparison of artifact reduction. Imaging data was acquired on a variety of implants including total hip-replacements, spinal fusion hardware, fixation screws, and support rods. All subjects were consented into a research study approved by the local ethics committee.

RESULTS

CE T1-weighted 3D-MSI at 1.5T enables uptake assessment in the immediate vicinity of metallic instrumentation. For assessments of painful total hip replacements CE aided in tissue differentiation in cases of adverse local tissue reaction. Contrast-enhanced 3D-MSI enabled improved assessments of early tumor recurrence. Assessment of failed back surgery syndrome also showed potential benefit from CE 3D-MSI, where contrast uptake in the immediate vicinity of pedicle screws was consistently observed. In addition, assessment epidural fibrosis and infection in the immediate vicinity of spinal hardware was enabled using contrast-enhanced 3D-MSI.

CONCLUSION

New 3D-MSI metal artifact reduction techniques can be used effectively to assess contrast uptake in the immediate vicinity of metallic hardware.

CLINICAL RELEVANCE/APPLICATION

These methods allow the freedom to assess common pathological conditions as if the hardware were absent and encourages future studies characterizing disease processes due to the hardware itself.

SSM15-06 Usefullness of Slice Encoding Metal Artifact Correction (SEMAC) for Reducing Metal Artifacts after Total Knee Arthroplasty

Participants

Miriam Reichert, MD, Mannheim, Germany (*Presenter*) Nothing to Disclose Michael Kostrzewa, MD, Mannheim, Germany (*Abstract Co-Author*) Nothing to Disclose Stefan O. Schoenberg, MD, PhD, Mannheim, Germany (*Abstract Co-Author*) Institutional research agreement, Siemens AG Ulrike I. Attenberger, MD, Mannheim, Germany (*Abstract Co-Author*) Research Consultant, Bayer AG

PURPOSE

To compare metal artifact reduction after total knee arthroplasty in MRI at 1.5 T using novel MRI sequence strategies.

METHOD AND MATERIALS

Two sequences were compared for the imaging of metal implants after total knee arthroplasty on a 1.5 T MR system: a slice encoding sequence for metal artifact correction (SEMAC) and a standard TSE sequence. 15 patients with titanium implants were evaluated. Degree of artifact reduction was assessed quantitatively and qualitatively by both, artifact measurements and a blinded read. The images were ranked by the following parameters: artifact size, distortion, and the ability to differentiate bone marrow, cortex and soft tissue. The images were also evaluated in respect of the visibility of crucial and collateral ligaments and the patellar tendon. The Insall-Salvati-Index was measured as well. The SEMAC technique was compared directly to the TSE standard sequence.

RESULTS

In comparison to standard sequences artifact size was 59% less utilizing SEMAC. In terms of bone marrow, bone cortex and soft tissue visualization SEMAC was ranked superior to the corresponding standard sequence. Distortion was less with SEMAC. For the evaluation of blur, the standard images were ranked superior to the corresponding SEMAC sequence. In terms of overall image quality, SEMAC was ranked superior to the standard sequence. For all terms of clinical relevance SEMAC was ranked superior to the corresponding standard sequence.

CONCLUSION

SEMAC effectively reduces artifacts caused by metallic implants after total knee arthroplasty relative to standard imaging.

CLINICAL RELEVANCE/APPLICATION

SEMAC sequences allow for better visualisation of crucial anatomic structures after total knee arthroplasty thus improving evaluation of postoperative result and detection of postoperative complications.

GU

IR

ISP: Vascular/Interventional (Gentiourinary Interventions-Treating Conditions of the Prostate and Uterus)

Wednesday, Dec. 2 3:00PM - 4:00PM Location: E450B

AMA PRA Category 1 Credit ™: 1.00 ARRT Category A+ Credit: 1.00

FDA Discussions may include off-label uses.

Participants

Sandeep Bagla, MD, Woodbridge, VA (*Moderator*) Consultant, Hansen Medical Inc; Consultant, NeuWave Medical, Inc; Consultant, CeloNova BioSciences, Inc; Consultant, Medtronic, Inc; Consultant, DFINE, Inc'; Consultant, Boston Scientific Charles T. Burke, MD, Chapel Hill, NC (*Moderator*) Nothing to Disclose

Sub-Events

SSM24-01 Evaluation of Changes in Quality of Life Related to Uterine Fibroid Embolization (UFE): Preliminary Results of the French SFICV EFUZEN Study

Wednesday, Dec. 2 3:00PM - 3:10PM Location: E450B

Participants

Helene Kovacsik, MD, PhD, Montpellier, France (*Abstract Co-Author*) Nothing to Disclose Sebastien Bommart, MD, Montpellier, France (*Abstract Co-Author*) Nothing to Disclose Marc R. Sapoval, MD, PhD, Paris CEDEX 15, France (*Abstract Co-Author*) Nothing to Disclose Denis Herbreteau, MD, Tours, France (*Presenter*) Nothing to Disclose Jean-Paul Beregi, MD, Nimes, France (*Abstract Co-Author*) Nothing to Disclose Jean-Michel Bartoli, MD, Marseille, France (*Abstract Co-Author*) Nothing to Disclose

PURPOSE

Main goal:- To evaluate quality of life before and one year after UFESecondary goals:- To determine impact of imaging findings (MRI data) before and 3-6months after UFE on changes in quality of life

METHOD AND MATERIALS

Study design: prospective, multicenter (25 centers) French observational studyPatients: 264 consecutive symptomatic women referred in the center for UFE using EmbozeneÒ (Celonova) particles. Methods:Clinical data: the quality of life score was calculated using the previously validated UFS-QOL by Spies, before and one year after UFE.Imaging data: MRI were performed before and 3-6 months after UFE. Data recorded were uterine and main fibroid volume, percentage of fibroid enhancement after injection of gadolinium. Impact of imaging data before and after UFE on QOL scores was searched.

RESULTS

189 patients (85.9%) showed monorrhagia at baseline. This was reduced to 39 patients (18%) at 1 year of follow up. 171 patients (78.1%) had pelvic pressure symptoms at baseline. This was reduced to 42 patients (19.4%) after 1 year of follow up.Complete QOL study was obtained in 192 women. Improvement of QOL score at one year after UFE a was found 183/203 (90.2%) for HRQL, 163/192 (84.9%) for Symptoms Severity. The probability of presenting a profuse bleeding was significantly reduced (by 62%) among patients with high reduction of fibroid volume (>=30%), as compared to patients with low fibroid volume reduction (<30%) (OR=0.38; 95%CI: [0.18;0.80]) (p = 0.011) The Impact of percentage of uterine volume or main fibroid reduction and decrease of fibroid enhancement on change in post embolization global UFS-QOL score was not established.

CONCLUSION

At one year post embolization, UFE improves significantly quality of life

CLINICAL RELEVANCE/APPLICATION

UFE is not only an effective technique but is also considered highly satisfactory by women

SSM24-02 Vascular/Interventional Keynote Speaker: Current Status of Prostate Artery Embolization as a Treatment for BPH

Wednesday, Dec. 2 3:10PM - 3:20PM Location: E450B

Participants

Sandeep Bagla, MD, Woodbridge, VA (*Presenter*) Consultant, Hansen Medical Inc; Consultant, NeuWave Medical, Inc; Consultant, CeloNova BioSciences, Inc; Consultant, Medtronic, Inc; Consultant, DFINE, Inc'; Consultant, Boston Scientific

SSM24-03 Percutaneous Ablation of Oligometastatic Prostate Cancer: Oncologic Outcomes and Safety

Wednesday, Dec. 2 3:20PM - 3:30PM Location: E450B

Participants

Andrew Erie, MD, Rochester, MN (*Presenter*) Nothing to Disclose Jonathan M. Morris, MD, Rochester, MN (*Abstract Co-Author*) Nothing to Disclose Brian T. Welch, MD, Rochester, MN (*Abstract Co-Author*) Nothing to Disclose Anil N. Kurup, MD, Rochester, MN (*Abstract Co-Author*) Nothing to Disclose Adam J. Weisbrod, MD, Rochester, MN (*Abstract Co-Author*) Nothing to Disclose Thomas D. Atwell, MD, Rochester, MN (*Abstract Co-Author*) Nothing to Disclose Grant D. Schmit, MD, Rochester, MN (*Abstract Co-Author*) Nothing to Disclose Eugene D. Kwon, MD, Rochester, MN (*Abstract Co-Author*) Nothing to Disclose Matthew R. Callstrom, MD, PhD, Rochester, MN (*Abstract Co-Author*) Research Grant, Thermedical, Inc Research Grant, General Electric Company Research Grant, Siemens AG Research Grant, Galil Medical Ltd

PURPOSE

To determine the oncologic outcomes and safety of percutaneous ablation in the treatment of oligometastatic prostate cancer.

METHOD AND MATERIALS

This is a retrospective, single-institution review of 31 patients with oligometastatic prostate cancer who underwent 43 percutaneous ablations of their limited (\leq 5) metastatic sites. Eight patients (26%) were antigen deprivation therapy-naïve (ADT-naïve) and received ablation with the purpose of delaying ADT. Twenty-three patients (74%) underwent ablation either because of resistance to systemic therapies or a more aggressive multimodal treatment approach was preferred. Study endpoints included procedural complications, local control, progression free survival (PFS), and androgen deprivation therapy-free survival (ADT-FS). ADT-FS was defined as the time between percutaneous ablation and the initiation of ADT.

RESULTS

Local control was achieved in 35 (81.4%) of 43 tumors with a median follow-up of 8 months (range, 3-60 mo) after ablation. Tumor recurrence was found in 8 (18.6%) of 43 tumors at a median follow-up of 6 months (range, 2-38 mo). Median prostate-specific antigen (PSA) measurements were significantly lower approximately 2 months after ablation compared to before ablation (0.27 ng/dl [range <0.01 to 7.7] and 1.5 ng/dl [range <0.01 to 72.0], respectively (p=0.02)). Estimated PFS rates for all patients at 6 and 12 months after ablation were 65% (95% CI, 44-80) and 45% (95% CI, 24-64), respectively. Of the 8 ADT-naïve patients who underwent ablation with purpose to delay ADT, all (100%) achieved local control and the ADT-FS at 12 months was approximately 70%. None of the ablations were associated with major complications.

CONCLUSION

Percutaneous ablation of oligometastatic prostate cancer appears safe, achieves acceptable local control rates, and can delay disease progression when used in combination with other therapies. Percutaneous ablation may be particularly valuable in ADT-naïve patients who do not tolerate or prefer to delay ADT.

CLINICAL RELEVANCE/APPLICATION

Percutaneous ablation can be used as part of a multimodal treatment approach for oligometastatic prostate cancer and can delay hormone therapy in ADT-naïve patients.

SSM24-04 Frequency of Penile and Rectal Collateral Flow from Prostatic Arteries during Prostatic Artery Embolization

Wednesday, Dec. 2 3:30PM - 3:40PM Location: E450B

Participants

Ari J. Isaacson, MD, Chapel Hill, NC (*Abstract Co-Author*) Advisory Board, BTG International Ltd Charles T. Burke, MD, Chapel Hill, NC (*Presenter*) Nothing to Disclose

PURPOSE

The most common mechanism of complication during prostatic artery embolization (PAE) is non-target embolization. Avoidance of branches supplying the bladder is commonly described. Less commonly discussed are intra-prostatic collaterals supplying the penis and rectum, although they are frequently seen during PAE. Because of the risks associated with non-target embolization as a result of these shunts, it would be beneficial to have an understanding of their incidence, as well as from what prostatic artery branches they arise. The purpose of this study was to retrospectively determine the frequency of rectal and penile collateral flow from each prostatic artery branch as seen during PAE.

METHOD AND MATERIALS

DSA images from PAEs performed between April 2013 and March 2015 were evaluated by two interventional radiologists experienced in performing PAE. A consensus determination was made about which arteries were catheterized (the anterolateral prostatic artery (ALPA), the posterolateral prostatic artery (PLPA) or a common trunk (CT) of the two) and about the presence of collateral flow to the arteries supplying the penis and/or the rectum from each catheterized artery. The overall incidence of such collaterals was calculated as well as the frequency in which they arose from each prostatic artery branch.

RESULTS

During 26 PAEs, 58 prostatic arteries were catheterized (36 ALPAs, 10 PLPAs and 12 CTs). Collateral flow to arteries supplying the penis or rectum was identified in 18/26 PAEs (69%). Flow to the penile arteries was seen in 13/36 (36%) ALPA catheterizations and in 5/12 (42%) CT catheterizations. Flow to rectal branches was seen in 8/10 (80%) PLPA catheterizations and in 4/12 (33%) CT catheterizations. No flow to penile branches was observed from a PLPA, nor was there flow to a rectal branch seen from an ALPA.

CONCLUSION

Shunting to the penis and/or rectum was present during the majority of PAEs. Collateral flow to the rectum from the PLPA or from a CT was seen quite frequently and collateral flow to the penis from an ALPA or CT was seen with moderate frequency during prostatic artery catheterization.

CLINICAL RELEVANCE/APPLICATION

Understanding the incidence of rectal and penile collateral pathways from the specific branches of the prostatic arteries will allow for greater detection of these findings during PAE in order to avoid complications.

SSM24-05 Prostate Cancer Treatment with Irreversible Electroporation (IRE): Experience, Safety and Efficacy after 4.5 Years in 222 Patients

Wednesday, Dec. 2 3:40PM - 3:50PM Location: E450B

Participants

Michael K. Stehling, MD, PhD, Offenbach, Germany (*Presenter*) Nothing to Disclose Enric Guenther, Dipl Phys, Frankfurt, Germany (*Abstract Co-Author*) Nothing to Disclose Nina Klein, MSc, Offenbach am Main, Germany (*Abstract Co-Author*) Nothing to Disclose Stephan Zapf, Frankfurt, Germany (*Abstract Co-Author*) Nothing to Disclose Ducksoo Kim, MD, Boston, MA (*Abstract Co-Author*) Nothing to Disclose Boris Rubinsky, PhD, Berkeley, CA (*Abstract Co-Author*) Nothing to Disclose

PURPOSE

Irreversible Electroporation (IRE) is a novel tissue ablation method. It selectively destroys cells whilst preserving tissue infrastructure and is hence an ideal method for focal prostate cancer (PCa) therapy. It preserves (or allows regeneration of) vital surrounding structures such as neurovascular bundle, inferior sphincter and rectum, thus minimizing the side-effects of PCa therapy, mainly being impotence and incontinence.

METHOD AND MATERIALS

We have employed IRE for the treatment of 222 patients with primary (stages T1-T4) and recurrent PCa after surgery (18/222), radiation therapy (4/222) and HIFU (3/222). All patients underwent mp-MRI prior to and after IRE (T2, diffusion, perfusion, in selected cases 1H spectroscopy). 44% of patients underwent additional 3D-transperineal biopsy before IRE. Treatment was carried out by rectal US-guided transperineal IRE-electrode insertion under general anesthesia and deep muscle relaxation. 161 patients had focal and 61 whole gland ablations. All patients had follow-ups with PSA and mp-MRI for documentation of local tumor control.

RESULTS

Initial tumor control was achieved in all patients. Within the follow-up period of up to 4y, the recurrence rates were 0/45 (Gleason <7), 4/103 (Gleason 7) and 5/54 (Gleason >7). There were no IRE-related complications and toxicity was extremely low: 16 patients reported a transient reduction of erectile function (EF) (recurred after 6-8m), 5 a permanent reduction and 2 a permanent loss of EF. There were no cases of IRE-related incontinence, even when the lower urinary sphincter was included in the treatment field; a partially included rectum also remained intact. Treatment was completed within 24h in all patients with a single overnight stay in the clinic. Patients had no wound pain.

CONCLUSION

IRE treatment of PCa is safe. In the short-term follow-up with MRI and PSA (maximum 4.5y) it is effective. Toxicity is significantly lower compared to other PCa treatments. Based on our data incontinence can be avoided altogether. MRI and 3D-biopsy are suitable for pre-treatment work-up and MRI for post-treatment follow-up. IRE has the potential to become an important tool for PCa therapy.

CLINICAL RELEVANCE/APPLICATION

IRE treatment is an alternative to the current treatment options for PCa, with much lower invasiveness and toxicity. It is effective in all stages of PCa and offers treatment options in advanced and recurrent PCa not amenable to other therapies.

SSM24-06 Phase II Clinical Trial for Evaluation of MRI-guided Laser Induced Interstitial Thermal Therapy (LITT) for Low-to-intermediate Risk Prostate Cancer

Wednesday, Dec. 2 3:50PM - 4:00PM Location: E450B

Participants

Aytekin Oto, MD, Chicago, IL (*Presenter*) Research Grant, Koninklijke Philips NV; ; ; Shiyang Wang, PhD, Chicago, IL (*Abstract Co-Author*) Nothing to Disclose Ambereen Yousuf, MBBS, Chicago, IL (*Abstract Co-Author*) Nothing to Disclose Sydeaka Watson, PhD, Chicago, IL (*Abstract Co-Author*) Nothing to Disclose Tatjana Antic, Chicago, IL (*Abstract Co-Author*) Nothing to Disclose Scott Eggener, Chicago, IL (*Abstract Co-Author*) Research Grant, Visualase, Inc Speakers Bureau, Johnson & Johnson

PURPOSE

To assess the oncologic efficacy and safety of MRI-guided laser-induced interstitial thermal therapy of biopsy confirmed and MRvisible prostate cancer.

METHOD AND MATERIALS

27 patients with biopsy proven low-to-intermediate risk prostate cancer underwent MRI-guided laser ablation of the cancer using Visualase laser ablation device. All patients had a pre-procedure endorectal MRI which showed suspicious foci concomitant with the positive sextant on TRUS-guided biopsy. The area of interest was targeted transperineally using 1.5 T Philips MRI scanner and Visualase ablation device. Ablation was monitored by real time MR thermometry using Visualase MRI thermometry software. Perioperative, early and late complications and adverse events were recorded. Follow-up was performed with 3-month MRI and MR-guided biopsy, 12-month MRI and TRUS guided biopsy and validated quality of life questionnaires to assess urinary and sexual function.

RESULTS

MRI-guided laser ablation of prostate cancer was successfully performed in all 27 patients without significant peri-procedural complications. All patients were discharged home the same day. Average duration of the procedure was 3 hours 17 minutes and average duration of a single laser ablation was 1 minute 22 seconds. Total number of ablations per patient ranged from 2-8, with a median of 4. The treatment created an identifiable hypovascular defect in all cases. Post procedure complications were minor and included urinary symptoms, perineal bruising and erectile dysfunction, all of which self- resolved. Validated quality of life urinary and sexual questionnaires obtained before and 12 months after the procedure did not reveal any significant differences ($p \ge 0.05$). 1/27 and 3/17 patients had residual cancer in the ablation zone at 3 months and 12 months respectively.

CONCLUSION

Short-term follow-up results of MRI-guided focal laser ablation for treatment of clinically localized, low-to-intermediate risk prostate cancer appear promising. It may offer a minimally invasive procedure for select patients that does not appreciably alter sexual or urinary function.

CLINICAL RELEVANCE/APPLICATION

Short-term results of our phase II trial show that MRI-guided focal laser ablation can be a safe and feasible option for treatment of low-to-intermediate risk prostate cancer.

Honored Educators

Presenters or authors on this event have been recognized as RSNA Honored Educators for participating in multiple qualifying educational activities. Honored Educators are invested in furthering the profession of radiology by delivering high-quality educational content in their field of study. Learn how you can become an honored educator by visiting the website at: https://www.rsna.org/Honored-Educator-Award/

Aytekin Oto, MD - 2013 Honored Educator

RSNA/ESR Emergency Symposium: General Principles, Pediatric and ENT Emergencies (An Interactive Session)

Wednesday, Dec. 2 3:30PM - 5:00PM Location: S402AB



AMA PRA Category 1 Credits ™: 1.50 ARRT Category A+ Credits: 1.50

Participants

Ronald J. Zagoria, MD, San Francisco, CA, (ron.zagoria@ucsf.edu) (*Moderator*) Nothing to Disclose Andras Palko, MD, PhD, Szeged, Hungary (*Moderator*) Medical Advisory Board, Affidea Group;

Sub-Events

```
MSSR44A Polytrauma
```

Participants

Ulrich Linsenmaler, MD, Munich, Germany (Presenter) Nothing to Disclose

LEARNING OBJECTIVES

1) Demonstrate general principles of diagnostic imaging in Emergency Radiology in traumatic and non-traumatic emergencies. 2) Analyze ethiology, background and management of common radiological emergencies. 3) Identify the role, indications and protocols for US, CR, MDCT in modern emergency radiology.

ABSTRACT

Multiple trauma / polytrauma remains the leading cause of death in a patient population below the age of 45 years. Modern Emergency Radiology plays today a key role in an interdisciplinary team guiding diagnosis and treatment in the initial clinical workup. This lecture will cover the following topics:To describe background, incidence and regional differences in patients with polytrauma / multiple trauma.To appreciate the clinical significance and to analyze critical triage criteria to undergo ER / shock room admission and concepts of initial clinical management (ATLS).To review imaging techniques and radiological management and logistic concepts for patients with polytrauma / multiple trauma within a clinical algorithm. To review the use of whole body computed tomography (WBCT), CTA as well as conventional radiography (CR) and ultrasound (US) in the initial work-up.To describe common and uncommon imaging findings.Image reading and data management, individualized CT protocols and outcome control.

MSSR44B Challenges of Imaging Pediatric Abdominal Emergencies

Participants

Susan D. John, MD, Houston, TX (Presenter) Nothing to Disclose

LEARNING OBJECTIVES

1) Understand the variations of pathology that cause abdominal pain and vomiting in infants and children. 2) Plan safe and effective imaging protocols using US, CT, and MRI. 3) Recognize pitfalls in the diagnosis of pediatric abdominal emergencies with imaging.

ABSTRACT

MSSR44C Imaging in ENT Emergencies

Participants

Diego B. Nunez JR, MD, MPH, New Haven, CT, (diego.nunez@yale.edu) (Presenter) Nothing to Disclose

LEARNING OBJECTIVES

1) Analyze imaging findings in patients presenting with acute head and neck conditions using a systematic spatial approach. 2) Demonstrate understanding of the role and indications of CT and MR in acute non-traumaric ENT case management. 3) Identify the extent of disease and recognize specific complications of cervicofacial infections.

ABSTRACT

Case-based Review of US (An Interactive Session)

Wednesday, Dec. 2 3:30PM - 5:00PM Location: S406A



AMA PRA Category 1 Credits ™: 1.50 ARRT Category A+ Credits: 1.50

Participants

Deborah J. Rubens, MD, Rochester, NY (Moderator) Nothing to Disclose

LEARNING OBJECTIVES

1) Recognize the diverse applications of ultrasound throughout the body and when it provides the optimal diagnostic imaging choice. 2) Understand the fundamental interpretive parameters of ultrasound contrast enhancement and its applications in the abdomen. 3) Know the important factors to consider when choosing ultrasound vs CT for image guided procedures and how to optimize ultrasound for technical success.

ABSTRACT

Ultrasound is a rapidly evolving imaging modality which has achieved widespread application throughout the body. In this course we will address the major anatomic areas of ultrasound use, including the abdominal and pelvic organs, superficial structures and the vascular system. Challenging imaging and clinical scenarios will be emphasized to include the participant in the decision-making process. Advanced cases and evolving technology will be highlighted, including the use of ultrasound contrast media as a problem solving tool, and the appropriate selection of procedures for US-guided intervention.

Active Handout: Deborah J. Rubens

http://abstract.rsna.org/uploads/2015/15002752/Active MSCU42.pdf

Sub-Events

MSCU42A Challenging Abdominal Cases

Participants

Oksana H. Baltarowich, MD, Philadelphia, PA (Presenter) Nothing to Disclose

LEARNING OBJECTIVES

View learning objectives under main course title.

ABSTRACT

View abstract under main course title.

MSCU42B Acute Pelvic Pain

Participants Leslie M. Scoutt, MD, New Haven, CT, (leslie.scoutt@yale.edu) (*Presenter*) Consultant, Koninklijke Philips NV

LEARNING OBJECTIVES

View learning objectives under main course title.

Honored Educators

Presenters or authors on this event have been recognized as RSNA Honored Educators for participating in multiple qualifying educational activities. Honored Educators are invested in furthering the profession of radiology by delivering high-quality educational content in their field of study. Learn how you can become an honored educator by visiting the website at: https://www.rsna.org/Honored-Educator-Award/

Leslie M. Scoutt, MD - 2014 Honored Educator

MSCU42C Superficial Ultrasound Imaging: Head to Toe

Participants Deborah J. Rubens, MD, Rochester, NY (*Presenter*) Nothing to Disclose

LEARNING OBJECTIVES

View learning objectives under main course title.

Essentials of Neuro Imaging

Wednesday, Dec. 2 3:30PM - 5:00PM Location: S100AB

HN NR

AMA PRA Category 1 Credits ™: 1.50 ARRT Category A+ Credits: 1.50

Participants

Sub-Events

MSES44A Cystic Neck Masses

Participants Barton F. Branstetter IV, MD, Pittsburgh, PA, (BFB1@pitt.edu) (*Presenter*) Nothing to Disclose

LEARNING OBJECTIVES

1) Categorize cystic neck masses in adults and children. 2) Indicate specific differentiting diagnostic criteria.

ABSTRACT

A nonenhancing, fluid-filled mass is a common finding on cross-sectional imaging of the neck. The location of the mass and its relationship to surrouding structures are critical for categorization of the mass and for providing a specific diagnosis. While congenital causes of cystic neck masses are often discussed, they are less frequent than infectious, developmental, or neoplastic causes. The purpose of this session is to review common and uncommon causes of cystic neck masses and to review the imaging characteristics that differentiate them. Potential pitfalls of imaging will be emphasized.

Active Handout:Barton F. Branstetter

http://abstract.rsna.org/uploads/2015/15001762/MSES44A.pdf

MSES44B Adult Orbital Neoplasms

Participants

Tanya J. Rath, MD, Pittsburgh, PA (Presenter) Nothing to Disclose

LEARNING OBJECTIVES

1) Understand the relevant compartmental anatomy of the orbit. 2) Differentiate the characteristic imaging features of benign and malignant adult orbital neoplasms. 3) Define the role of cross-sectional imaging in the management of orbital neoplasms. 4) Review non-neoplastic mimics of orbital neoplasms.

ABSTRACT

Cross-sectional imaging complements ophthalmologic examination in the evaluation of orbital neoplasms. A relevant succinct differential diagnosis for an orbital mass can be generated based on the morphology, location and extent of a lesion. MRI is critical for treatment planning by characterizing the orbital compartments involved and assessing for intracranial and perineural spread of disease. The purpose of this session is to review the characteristic imaging features of benign and malignant orbital neoplasms. Non-neoplastic processes that can mimic orbital neoplasms will also be discussed. Imaging findings that affect management will be emphasized.

Active Handout: Tanya Jaitley Rath

http://abstract.rsna.org/uploads/2015/15001763/MSES44B AA 12.2.15 FINAL RSNA ORBITS.pdf

MSES44C Imaging Dementia and Memory Loss

Participants

Meike W. Vernooij, MD, Rotterdam, Netherlands, (m.vernooij@erasmusmc.nl) (Presenter) Nothing to Disclose

LEARNING OBJECTIVES

1) Describe the minimum requirements for an MRI protocol to image patients suspected of dementia. 2) Read scans from a memory clinic in a standardized way, using available rating scales. 3) Construct a structured radiological report with useful recommendations for the referring clinician.

Active Handout: Meike Willemijn Vernooij

http://abstract.rsna.org/uploads/2015/15001764/MSES44C handouts_RSNA 2015_Meike Vernooij.pdf

ASRT@RSNA 2015: Prostate Cancer and MR Imaging: What Do We Want to See and How to Get It

Wednesday, Dec. 2 3:40PM - 4:40PM Location: N230



AMA PRA Category 1 Credit ™: 1.00 ARRT Category A+ Credit: 1.00

Participants

James Stirling, DCR, DMS, Middlesex, United Kingdom, (james.stirling@kcl.ac.uk) (Presenter) Nothing to Disclose

LEARNING OBJECTIVES

1) To learn the anatomy and comon pathology of the prostate gland. 2) To learn the factors and how to optimise prostate sequences eg. T1, T2 and STIR whole pelvis sequences, small field of view T2 axial, sagital and coronal sequences, diffusion weighted imaging, contrast enhanced T1 and T2* dynamic sequences. 3) To learn how different sequences are used with primary, secondary and metastatic prostate cancer. 4) To give a taste of hybid PET/MR 18F Choline imaging.

ABSTRACT

Over the last couple of years MRI of prostate cancer has moved from just T1 and T2 imaging to multi-parametric, multi-modality imaging. To produce high quality imaging, sequence parameter factors have to be optimized, balancing clinical requirements with patient comfort, total on-table time, scanner capabilities and limitations. The lecture will include prostatic anatomy and how different sequences can characterize benign and malignant disease. The talk will show the sequences that are needed and how to optimize them. This will include T2 small field of views, diffusion weighted imaging, T1 and T2* dynamic contrast enhanced sequences and intrinsic susceptibility weighted imaging. As prostate cancer develops and is treated the imaging protocols change. The protocols include surveillance and staging and then progress to recurrence and metastatic whole body imaging. MRI is now being complemented with PET in hybrid machines combining the strengths of both modalities. This lecture will show how MR imaging of malignant prostate disease changes as the disease progresses.

Controversy Session: Current USPSTF Lung Cancer Screening: Inclusive or Exclusive

Wednesday, Dec. 2 4:30PM - 6:00PM Location: S404AB

СН ОІ

AMA PRA Category 1 Credits ™: 1.50 ARRT Category A+ Credits: 1.50

Participants

Ella A. Kazerooni, MD, Ann Arbor, MI (Moderator) Nothing to Disclose

Sub-Events

SPSC45A USPSTF Lung Cancer Screening: Pro

Participants Ella A. Kazerooni, MD, Ann Arbor, MI (*Presenter*) Nothing to Disclose

LEARNING OBJECTIVES

1) List the major risk factors for lung cancer. 2) Describe the potential advantages of the inclusivity of USPSTF lung cancer screening eligibility criteria. 3) Understand the spectrum of lung cancer risk among patients meeting the USPSTF criteria. 4) Recognize how personalized risk assessment can facilitate shared decision making for patients meeting USPSTF criteria.

ABSTRACT

1. List the major risk factors for lung cancer.2. Describe the potential advantages of the inclusivity of USPSTF lung cancer screening eligibility criteria.3. Understand the spectrum of lung cancer risk among patients meeting the USPSTF criteria.4. Recognize how personalized risk assessment can facilitate shared decision making for patients meeting USPSTF criteria.

URL

Honored Educators

Presenters or authors on this event have been recognized as RSNA Honored Educators for participating in multiple qualifying educational activities. Honored Educators are invested in furthering the profession of radiology by delivering high-quality educational content in their field of study. Learn how you can become an honored educator by visiting the website at: https://www.rsna.org/Honored-Educator-Award/

Ella A. Kazerooni, MD - 2014 Honored Educator

SPSC45B USPSTF Lung Cancer Screening: Con

Participants

Doug Arenberg, Ann Arbor, MI, (darenber@umich.edu) (Presenter) Nothing to Disclose

LEARNING OBJECTIVES

1) Describe the rationale for the USPSTF lung cancer screening criteria. 2) Understand the importance of identifying risk among those referred for lung cacner screening. 3) Identify the impact of lung cancer risk on the balance of harms and benefits of lung cancer screening. 4) Describe the clinical and demographic traists that increase one's risk for lung cancer.

ABSTRACT

Controversy Session: Ultrasound versus CT for Suspected Renal Colic: Which Modality Rocks in the ER?

Wednesday, Dec. 2 4:30PM - 6:00PM Location: S404CD



AMA PRA Category 1 Credits ™: 1.50 ARRT Category A+ Credits: 1.50

Participants

Judy Yee, MD, San Francisco, CA (Moderator) Research Grant, EchoPixel, Inc Mitchell E. Tublin, MD, Pittsburgh, PA (Presenter) Nothing to Disclose Aaron D. Sodickson, MD, PhD, Wayland, MA, (asodickson@bwh.harvard.edu) (Presenter) Research Grant, Siemens AG; Consultant, Bracco Group

D. Mark Courtney, MD, MSc, Chicago, IL (Presenter) Nothing to Disclose

LEARNING OBJECTIVES

1) Describe the advantages of ultrasound and present a cost effective, rational algorithm for its use in the evaluation of ER patients with potential renal colic. 2) Understand the benefits of CT over ultrasound in ER imaging of suspected renal colic. 3) Understand the perspective and preferences of the ER physician for the workup of renal colic and the effect on clinical workflow.

Honored Educators

Presenters or authors on this event have been recognized as RSNA Honored Educators for participating in multiple qualifying educational activities. Honored Educators are invested in furthering the profession of radiology by delivering high-quality educational content in their field of study. Learn how you can become an honored educator by visiting the website at: https://www.rsna.org/Honored-Educator-Award/

Aaron D. Sodickson, MD, PhD - 2014 Honored Educator

Controversy Session: Concussion and Dementia: Will Football be the Tobacco of this Century?

Wednesday, Dec. 2 4:30PM - 6:00PM Location: E351

NR ER

AMA PRA Category 1 Credits ™: 1.50 ARRT Category A+ Credits: 1.50

Participants

Michael N. Brant-Zawadzki, MD, Newport Beach, CA (Moderator) Nothing to Disclose

LEARNING OBJECTIVES

1) Understand the functional as well pathophysiologic consequences of concussion. 2) Understand the overlap between chronic traumatic encephalopathy and Alzheimer's disease. 3) Understand the prevalence of chronic traumatic encephalopathy, its demographics, and distinguish those features from the more widely prevalent aspects of Alzheimer's dementia related disorders. 4) Properly understand the prognostic risk of contact sports as they relate to the prevalence of dementia in the population at large.

Sub-Events

SPSC42A CTE (Chronic Traumatic Encephalopathy) and Dementia: Causation?

Participants

Michael T. Modic, MD, Cleveland, OH (Presenter) Nothing to Disclose

LEARNING OBJECTIVES

View learning objectives under main course title.

SPSC42B Guilt by Association

Participants

William R. Shankle, MD, MS, Newport Beach, CA (Presenter) Nothing to Disclose

LEARNING OBJECTIVES

1) Understand the distinction between correlation and cause. 2) Understand how one can distinguish between a reported effect that is causal and one that is associational. 3) Apply this approach to Traumatic Brain Injury to examine the evidence of a causal vs. associative effect.

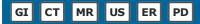
ABSTRACT

Guilt By AssociationWR Shankle, MS MD FACPTraumatic Brain Injury (TBI) is one condition where it seems intuitively obvious that brain trauma CAUSES brain dysfunction. In the past decade, methodological advances in computer science have led to the development of a mathematics called CAUSAL INFERENCE, that can be used to analyze risk factors and distinguish whether they are likely to CAUSE an outcome (e.g. brain dysfunction) or are simply ASSOCATED with the outcome's occurrence. This methodology combines probability theory with graph theory to accomplish this distinction. Causal Inference is very useful because it can analyze observational and other non-randomized studies. Interestingly, a search of the TBI literature identified no studies that have tested the assumption that TBI CAUSES brain dysfunction. One very useful causal inference method, called Targeted Maximum Likelihood Estimation, has been used in observational studies to minimize the chance that a causal effect is not detected due to some type of bias in the study. In simple terms, I will present how TMLE can be used to test the assumption that TBI causes brain dysfunction. Other risk factors, in which the question of causality is much less clear, can then be examined using TMLE with reference to what TMLE informs us about TBI.

URL

Controversy Session: US, CT, or MR Imaging in Possible Appendicitis in Children: Three Pegs and Often Only One Hole

Wednesday, Dec. 2 4:30PM - 6:00PM Location: E451A



AMA PRA Category 1 Credits ™: 1.50 ARRT Category A+ Credits: 1.50

Participants

Nancy R. Fefferman, MD, New York, NY, (nancy.fefferman@nyumc.org) (Moderator) Nothing to Disclose

LEARNING OBJECTIVES

Sub-Events

SPSC41A US

Participants

Nancy R. Fefferman, MD, New York, NY, (nancy.fefferman@nyumc.org) (Presenter) Nothing to Disclose

LEARNING OBJECTIVES

1) Describe the advantages, disadvantages and limitations of US as an effective imaging modality in the diagnosis of appendicitis in children. 2) Review the current literature addressing the diagnostic performance of US for pediatric appendicitis. 3) Discuss the role of US in the imaging evaluation of suspected appendicitis in children.

ABSTRACT

SPSC41B CT

Participants

Michael J. Callahan, MD, Boston, MA, (michael.callahan@childrens.harvard.edu) (Presenter) Nothing to Disclose

LEARNING OBJECTIVES

1) Highlight the advantages, disadvantages and versatility of computed tomography for the diagnosis of suspected acute appendicitis in children. 2) Describe published sensitivity and specificity values for computed tomography in the setting of suspected acute appendicitis in the pediatric population. 3) Explain the challenges and potential barriers for standardization of pediatric appendicitis clinical practice guidelines at academic and non-academic centers.

SPSC41C MR

Participants

R. Paul Guillerman, MD, Houston, TX, (rpguille@texaschildrens.org) (Presenter) Nothing to Disclose

LEARNING OBJECTIVES

1) Develop an MRI protocol for suspected pediatric appendicitis. 2) Estimate the diagnostic efficacy of MRI for suspected pediatric appendicitis. 3) Appraise how radiation-induced cancer risks and diagnostic performance characteristics influence the optimal selection of US, CT and MRI for suspected pediatric appendicitis.

RSNA Diagnosis Live™: Neuro and MSK

Wednesday, Dec. 2 4:30PM - 6:00PM Location: E451B



AMA PRA Category 1 Credits ™: 1.50 ARRT Category A+ Credits: 1.50

Participants

Paul J. Chang, MD, Chicago, IL, (pchang@radiology.bsd.uchicago.edu) (*Presenter*) Co-founder, Stentor/Koninklijke Philips NV; Researcher, Koninklijke Philips NV; Medical Advisory Board, lifeIMAGE Inc; Medical Advisory Board, Merge Healthcare Incorporated Gregory L. Katzman, MD, Chicago, IL (*Presenter*) Nothing to Disclose Neety Panu, MD, FRCPC, Thunder Bay, ON (*Presenter*) Nothing to Disclose

LEARNING OBJECTIVES

1) The participant will be introduced to a series of radiology case studies via an interactive team game approach designed to encourage "active" consumption of educational content. 2) The participant will be able to use their mobile wireless device (tablet, phone, laptop) to electronically respond to various imaging case challenges; participants will be able to monitor their individual and team performance in real time. 3) The attendee will receive a personalized self-assessment report via email that will review the case material presented during the session, along with individual and team performance. This interactive session will use RSNA Diagnosis Live™. Please bring your charged mobile wireless device (phone, tablet or laptop) to participate.

Controversy Session: Prostate Imaging: Just What MR Technique is Best?

Wednesday, Dec. 2 4:30PM - 6:00PM Location: E450A

GU MR

AMA PRA Category 1 Credits ™: 1.50 ARRT Category A+ Credits: 1.50

Participants

Rajan T. Gupta, MD, Durham, NC (Moderator) Consultant, Bayer AG; Speakers Bureau, Bayer AG; Consultant, Invivo Corporation

LEARNING OBJECTIVES

1) The goal of this session is to explore the different techniques that comprise high quality multiparametric MRI of the prostate. More specifically, we will deal with some of the key protocol questions that one must tackle in order to set up mpMRI in their own practice. Examples of the topics to be discussed include 1.5T vs. 3T imaging; endorectal coil vs. phased array body coil use; the optimal diffusion weighted metrics to be used to assess lesion aggressiveness, etc.; the changing role of dynamic contrast enhanced MRI in prostate imaging, especially in light of the recent release of PI-RADS version 2; and finally, the optimal techniques to evaluate for disease recurrence after therapy. The format of the session will be both didactic and interactive with audience participation.

Sub-Events

SPSC44A Introduction to Session and Overview of Multiparametric Prostate MRI

Participants

Rajan T. Gupta, MD, Durham, NC (Presenter) Consultant, Bayer AG; Speakers Bureau, Bayer AG; Consultant, Invivo Corporation

LEARNING OBJECTIVES

View learning objectives under main course title.

SPSC44B 1.5T vs 3T Imaging: Pros and Cons

Participants

Rajan T. Gupta, MD, Durham, NC (*Presenter*) Consultant, Bayer AG; Speakers Bureau, Bayer AG; Consultant, Invivo Corporation Francois Cornud, MD, Paris, France (*Presenter*) Nothing to Disclose

LEARNING OBJECTIVES

View learning objectives under main course title.

SPSC44C Diffusion Weighted Imaging

Participants Andrew B. Rosenkrantz, MD, New York, NY (*Presenter*) Nothing to Disclose

LEARNING OBJECTIVES

View learning objectives under main course title.

SPSC44D Dynamic Contrast Enhanced Imaging

Participants Sadhna Verma, MD, Cincinnati, OH (*Presenter*) Nothing to Disclose

LEARNING OBJECTIVES

View learning objectives under main course title.

Honored Educators

Presenters or authors on this event have been recognized as RSNA Honored Educators for participating in multiple qualifying educational activities. Honored Educators are invested in furthering the profession of radiology by delivering high-quality educational content in their field of study. Learn how you can become an honored educator by visiting the website at: https://www.rsna.org/Honored-Educator-Award/

Sadhna Verma, MD - 2013 Honored Educator

SPSC44E Imaging of Recurrence in Prostate Cancer

Participants Adam Froemming, MD, Rochester, MN (*Presenter*) Nothing to Disclose

LEARNING OBJECTIVES

View learning objectives under main course title.

Controversy Session: CT Perfusion (CTP) and Stroke: RIP?

Wednesday, Dec. 2 4:30PM - 6:00PM Location: S406B



AMA PRA Category 1 Credits ™: 1.50 ARRT Category A+ Credits: 1.50

Participants

Gordon K. Sze, MD, New Haven, CT (Moderator) Investigator, Remedy Pharmaceuticals, Inc

Sub-Events

SPSC43A CTP is Dead

Participants Ramon G. Gonzalez, MD, PhD, Boston, MA (*Presenter*) Nothing to Disclose

LEARNING OBJECTIVES

1) Understand the most important acute ischemic stroke physiology factors for patient outcomes and their relative importance. 2) Recognize the role of the ischemic core size in selecting patients with large vessel occlusion for endovascular therapy. 3) Review the animal literature on the use of CT perfusion for measuring the ischemic core and its value compared to diffusion MRI. 4) Recognize the source and magnitude of measurement error when using CTP including using the 95% confidence interval in ischemic core estimates in individual patients.

ABSTRACT

Recent trials have shown that intervention produces favorable outcomes when acute ischemic stroke patients are selected using CTP. Does that mean that CTP is adequate to decide whether an INDIVIDUAL patient should undergo treatment? The answer is "no". CTP is simply too imprecise to reliably measure the infarct core - the critical parameter for excluding from therapy patients who are at greatest risk of hemorrhagic complications, and are unlikely to benefit. Moreover, there is a more precise alternative, diffusion MRI.CTP measures hemodynamics, not tissue status. Hence, although a marker for irreversible injury absent timely reperfusion, CTP - which reflects a snapshot-in-time - is not a marker for treatment futility. Not surprisingly, validation studies in animal models are sparse and have not been reproduced. All published clinical data are consistent: CTP core estimates have high error. Although CTP may be adequate for selection of patients with small cores, where large measurement errors are of little consequence, the cost is exclusion of many with a high likelihood of treatment benefit8. CTP core-lesions segmented using automated software offer the illusion of quantitative accuracy that simply does not exist. CTP and DWI are different. The inherently poor signal-to-noise ratio (SNR) of post-processed CTP images is another fundamental weakness of the technique. Low SNR measurements may be useful if repeated and a mean calculated; this cannot be done for individual patients. That a strong linear correlation exists between CTP and DWI derived ischemic lesion volumes is not surprising, since both result from the same arterial occlusion. High correlation in a population, however, does not confer high measurement accuracy in an individual. As Bland and Altman pointed out almost 30 years ago, regression analyses are inappropriate to judge the validity of a quantitative clinical test. More appropriate are difference tests that establish the 95% confidence limits. As shown by Schaefer et al, a CBF core measurement of 70 ml could actually range from 11-to-124 ml within the 95% confidence limits; other papers in the CTP literature reveal similar variability. Although this large variability does not preclude using CTP to enroll patients into clinical trials, it does make such selection inherently less efficient compared to using "reference standard" DWI. Indeed, power calculations show that, for a simulated treatment study designed to detect a 20 ml improvement in final infarct volume, using CTP instead of DWI would require at least twice as many patients to reach significance. Given CTP's relative inaccuracy in delineating "core", what is the reason for the good outcome rate using a CTP-based selection strategy? The answer lies in its patient selection criteria. The successful trials used a highly conservative selection strategy, "cherry picking" the very best patients with very small cores who were likely to do well even with alteplase alone. Targeting small cores minimizes the effects of large measurement errors, at the cost of excluding many who might benefit. All agree that clinical trials have demonstrated that thrombolysis and thrombectomy are effective treatments for stroke caused by large vessel occlusion. All agree that identifying a target occlusion is important, and that measurement of the infarct-core is critical. The question centers on whether core measurement by CTP is sufficiently precise to be used for treatment selection in INDIVIDUAL patients? A wealth of theoretical, experimental, and clinical evidence suggests the answer is "no". Many argue that "CTP may be short of perfect, yet close enough." Would an internist accept a blood glucose or INR measurement with >50% error as "close enough"? No, she would not. Why, then, should stroke physicians accept a core measurement error of >50% as "close enough"? Clearly, they should not - especially when a more accurate alternative is readily available.Bland JM, Altman DG. Statistical methods for assessing agreement between two methods of clinical measurement. Lancet. 1986 Feb 8;1(8476):307-10.Schaefer PW, Souza L, Kamalian S, Hirsch JA, Yoo AJ, Kamalian S, Gonzalez RG, Lev MH. Limited reliability of computed tomographic perfusion acute infarct volume measurements compared with diffusion-weighted imaging in anterior circulation stroke. Stroke. 2015 Feb;46(2):419-24.

SPSC43B CTP is Underutilized

Participants

Max Wintermark, MD, Lausanne, Switzerland, (max.wintermark@gmail.com) (Presenter) Advisory Board, General Electric Company;

LEARNING OBJECTIVES

1) To review the indications of perfusion CT imaging in patients suspected of acute ischemic stroke.

ABSTRACT

Perfusion-CT is an imagig method used to assess the ischemic core and penumbra in acute stroke patients. A prospective multicenter study reported that an absolute cerebral blood volume (CBV) threshold reflected the ischemic core and that a relative mean transit time (MTT) threshold most accurately reflected the penumbra. However, in more recent and larger studies, relative cerebral blood flow (rCBF) was found to be more predictive of the ischemic core (nonviable tissue) than absolute CBV. There is a need for standardization of the PCT methods used to define the ischemic core and the penumbra.Determination of tissue viability based on imaging has the potential to individualize thrombolytic therapy and extend the therapeutic time window for some acute stroke patients. Although perfusion imaging has been incorporated into acute stroke imaging algorithms at some institutions, its clinical utility has not been proven.It is important to note that perfusion imaging has many applications beyond characterization of the penumbra and triage of patients to acute revascularization therapy. The negative results of the MR RESCUE trial do not negate these potential benefits. These applications include, but are not limited to: (1) improving the sensitivity and accuracy of stroke diagnosis (in some cases, a lesion on PCT leads to more careful scrutiny and identification of a vascular occlusion that was not evident prospectively, particularly in the M2 and more distal MCA branches), (2) excluding stroke mimics, (3) better assessment of the ischemic core and collateral flow, and (4) prediction of hemorrhagic transformation and malignant edema.

URL

RCC45

Practical Informatics for the Practicing Radiologist: Part One (In conjunction with the Society for Imaging Informatics in Medicine)

Wednesday, Dec. 2 4:30PM - 6:00PM Location: S501ABC

IN

AMA PRA Category 1 Credits ™: 1.50 ARRT Category A+ Credits: 1.50

Participants

LEARNING OBJECTIVES

1) Define and describe the fundamental components of imaging informatics in a very practical and easy-to-understand way. 2) Understand methods to minimize distraction and reporting time when using speech recognition and structured reporting. 3) Understand the history and basic principles of business analytics.

Sub-Events

RCC45A A Patient's Journey through Imaging Informatics

Participants

Marc D. Kohli, MD, San Francisco, CA (Presenter) Research Grant, Siemens AG

LEARNING OBJECTIVES

1) Describe the three major systems used in radiology departments and their function. 2) Provide details regarding the HL7 and DICOM standards including how they are important in radiology workflow. 3) Describe the function of an interface engine in a modern healthcare system.

ABSTRACT

Understanding how the basic systems in a radiology department interact to provide complete workflow is and important buildingblock for radiologists interested in informatics. This presentation will outline the RIS, PACS, and Voice recognition systems and illustrate how they interact as we follow a patient through the radiology department.

RCC45B Challenges in Enterprise Imaging

Participants

Alex Towbin, MD, Cincinnati, OH, (alexander.towbin@cchmc.org) (*Presenter*) Author, Reed Elsevier; Consultant, Reed Elsevier; Shareholder, Merge Healthcare Incorporated; Consultant, Guerbet SA; Grant, Guerbet SA

LEARNING OBJECTIVES

1) Describe the concept of an enterprise imaging archive. 2) Describe the differences between DICOM-based imaging and non-DICOM-based imaging. 3) Identify the unique challenges associated with incorporating non-DICOM images into an enterprise imaging archive.

ABSTRACT

Over the past 20 years, the field of radiology has built an impressive digital infrastructure, automating many portions of the imaging process from the time of order entry through image distribution. With the advent of small, low-cost, high quality digital cameras, other medical specialties have turned to imaging to visualize and document disorders yet, they have not implemented the same type of digital infrastructure as radiology. Today, thousands of medical images are obtained in hospitals each day. With the increasing reliance on imaging, there is a greater need to build systems and processes to obtain, store, and distribute these images across the enterprise so that health care providers can better care for their patients. Even though many of these problems have been solved in radiology, the solutions are not easily transferred to other specialties due to the differences in imaging hardware and the image acquisition workflow. The purpose of this talk is to describe the problems facing hospitals as they begin to build enterprise imaging archives and to discuss potential solutions to these problems.

Honored Educators

Presenters or authors on this event have been recognized as RSNA Honored Educators for participating in multiple qualifying educational activities. Honored Educators are invested in furthering the profession of radiology by delivering high-quality educational content in their field of study. Learn how you can become an honored educator by visiting the website at: https://www.rsna.org/Honored-Educator-Award/

Alex Towbin, MD - 2014 Honored Educator

RCC45C Breaching the Moat: Current Concepts in IT Security

Participants

James Whitfill, MD, Scottsdale, AZ (Presenter) President, Lumetis, LLC; Co-author, Hitachi, Ltd

LEARNING OBJECTIVES

1) Understand how the changing nature of security threats requires a new approach to security within the healthcare enterprise. 2) Understand how changes from HIPAA and HITECH affect managing breaches and leaks of PHI.

ABSTRACT

The role of security continues to be elevated as more organizations find themselves victims of hacking and breaches. Banks, retail organizations, insurers and even Children's Hospitals have all been victims of security breeches. While efficient workflow for healthcare providers remains a key focus of imaging informatics, the growing threats from international hacking require greater and greater focus by IT and Healthcare organizations. In response to these developments, an increasing regulatory burden exists to report and mitigate against such breeches. Managing both of these challenges will take increasing amounts of resources in the near future.